Ceramide and Reactive Oxygen Species (ROS) as signal transduction molecules in inflammation.

DARREN CHARLES PHILLIPS.
Doctor of Philosophy

ASTON UNIVERSITY.

January 2003.

Summary.

Reactive oxygen species (ROS) and the sphingolipid ceramide are each partly responsible for the intracellular signal transduction of a variety of physiological, pharmacological or environmental agents. Furthermore, the enhanced production of many of these agents, that utilise ROS and ceramide as signalling intermediates, is associated with the aetiologies of several vascular diseases (e.g. atherosclerosis) or disorders of inflammatory origin (e.g. rheumatoid arthritis; RA). Excessive monocyte recruitment and uncontrolled T cell activation are both strongly implicated in the chronic inflammatory responses that are associated with these pathologies. Therefore the aims of this thesis are (1) to further elucidate the cellular responses to modulations in intracellular ceramide/ROS levels in monocytes and T cells, in order to help resolve the mechanisms of progression of these diseases and (2) to examine both existing agents (methotrexate) and novel targets for possible therapeutic manipulation.

Utilising synthetic, short chain ceramide to mimic the cellular responses to fluctuations in natural endogenous ceramide or, stimulation of CD95 to induce ceramide formation, it is described here that ceramide targets and manipulates two discrete sites responsible for ROS generation, preceding the cellular responses of growth arrest in U937 monocytes and apoptosis in Jurkat T-cells. In both cell types, transient elevations in mitochondrial ROS generation were observed. However, the prominent redox altering effects appear to be the ceramide-mediated reduction in cytosolic peroxide, the magnitude of which dictates in part the cellular response in U937 monocytes, Jurkat T-cells and primary human peripheral blood resting or PHA-activated T-cells *in vitro*.

The application of synthetic ceramides to U937 monocytes for short (2 hours) or long (16 hours) treatment periods reduced the membrane expression of proteins associated with cell-cell interaction. Furthermore, ceramide treated U937 monocytes demonstrated reduced adhesion to 5 or 24 hour LPS activated human umbilical vein endothelial cells (HUVEC) but not resting HUVEC. Consequently it is hypothesised that the targeted treatment of monocytes from patients with cardiovascular diseases with short chain synthetic ceramide may reduce disease progression.

Herein, the anti-inflammatory and immunosuppressant drug, methotrexate, is described to require ROS production for the induction of cytostasis or cytotoxicity in U937 monocytes and Jurkat T-cells respectively. Further, ROS are critical for methotrexate to abrogate monocyte interaction with activated HUVEC *in vitro*.

The histological feature of RA of enhanced infiltration, survivability and hyporesponsiveness of T-cells within the diseased synovium has been suggested to arise from aberrant signalling. No difference in the concentrations of endogenous T-cell ceramide, the related lipid diacylglycerol (DAG) and cytosolic peroxide *ex vivo* was observed. TCR activation following PHA exposure *in vitro* for 72 hours did not induce maintained perturbations in DAG or ceramide in T-cells from RA patients or healthy individuals. However, T-cells from RA patients failed to upregulate cytosolic peroxide in response to PHA, unlike those from normals, despite expressing identical levels of the activation marker CD25. This inability to upregulate cytosolic peroxide may contribute to the T-cell pathology associated with RA by affecting the signalling capacity of redox sensitive biomolecules.

These data highlight the importance of two distinctive cellular pools of ROS in mediating complex biological events associated with inflammatory disease and suggest that modulation of cellular ceramides represents a novel therapeutic strategy to minimise monocyte recruitment.

Abbreviations.

A.A, antimycin A; AICAR, 5-amino-imidazole carboxamide ribonucleotide; AIF, apoptosis inducing factor; AP-1, activator protein-1; a.u, arbitrary units; BCECF-AM, 2'-7'-bis-2-carboxy-5-(6)-carboxyfluorescein-acetoxymethylester; A-SMase, acid sphingomyelinase; ASK-1, apoptosis-signal-regulated kinase-1, ATAF-2, activating transcription factor-2; bp, base pairs; BSA, bovine serum albumin; BSO, L-buthionine-[SR]-sulfoximine; BSS, buffered saline solution; bZIP, basic region leucine-zipper; CD-95L, CD-95 ligand; CAPK, ceramide activated protein kinase; CAPP, ceramide activated protein phosphatase; CoA, coenzyme A; cpm, counts per minute; DAG, diacylglycerol; DAGK, diacylglycerol kinase; DCF, 2', 7'-dichlorofluorescein; DCFH, non-fluorescent 2', 7'-dichlorofluorescein; DCFH-DA, 2', 7'-dichlorofluorescein diacetate; DD, death domain; DEM, diethyl malate; DHFR, dihydrofolate reductase; DIABLO, direct inhibitors of apoptosis proteins binding protein with low PI; DMSO, dimethyl sulfoxide; DNTB, 5,5'-dithio-bis (2-nitrobenzoic acid); EGM, endothelial growth medium; EPV, Epstein Barr virus; ER, endoplasmic reticulum; ERK, extracellular-signal-regulated-kinase; FADD, fas-associated death domain; FH2, dihydrofolate; FH4, tetrahydrofolate; FITC, fluorescein isothiocyanate; FS, forward scatter; GSH, glutathione; GSSG, oxidised glutathione; GSR; glutathione reductase; HPCV, half peak coefficient of variance; HPG, human cartilage proteoglycan; $HO_2\cdot$, hydroperoxy radical; HUVEC, human umbilical endothelial cells; IAP, inhibitors of apoptosis proteins; JNK, jun kinase; K, kinase; LPS, lipopolysaccharide; MPT, mitochondrial permeability transition; MAPK, mitogen activated protein kinase; MdX, median X; MNC, mononuclear cells; MoAb, monoclonal antibody; MPT, mitochondrial permeability transition; MTX, Methotrexate; MW, molecular weight; NAC, N-acetyl cysteine; NFκB, necrosis factor kappa B; NPD, Niemann Pick disease; NSD, neutral sphingomyelinase domain; NO, nitric oxide; N-SMase, neutral sphingomyelinase; OA, osteoarthritis; O_2, oxygen molecule; $O_2^{-}\cdot$; superoxide radical; $OH\cdot$, hydroxyl radical; PARP, poly (ADP-ribose) polymerase; PBL, peripheral blood lymphocytes; PBNNC, peripheral blood mononuclear cells; PBS, phosphate buffered saline; PC, phosphatidylcholine; PE, phycoerythrin; PG, prostaglandin; PHA, phytohemagglutinin; PI, propidium iodide; PI3K, phosphatidyl inositol-3-kinase; PKC, protein kinase C; PP2A,

phosphatase 2A; P/S, penicillin/streptomycin; PTP, protein tyrosine phosphatases; RA, rheumatoid arthritis; ROS, reactive oxygen species; RTPCR, reverse transcriptase polymerase chain reaction; SAPK, stress activated protein kinase; S1P, sphingosine 1-phosphate; SLE, systemic lupus erythematosus; SM, sphingomyelin; SMAC, second mitochondria-derived activator of caspase; SMase, sphingomyelinase; SOD, superoxide dismutase; SS, side scatter; T-cells, T-lymphocytes; TCR, T-cell receptor; TLC, thin layer chromatography; TM, transmembrane; TNFα, tumour necrosis factor alpha; TRADD, tumour necrosis factor receptor 1-associated death domain; TTFA, thenoyltrifluoroacetone, WT, wild type; $\Delta\Psi m$, mitochondrial transmembrane potential; e^-, electron; $[peroxide]_{cyt}$, cytosolic peroxide; $[peroxide]_m$, mitochondrial peroxide.

Acknowledgements.

I would like to thank my supervisor, Dr H.R. Griffiths, for her wisdom and encouragement and Dr G.D. Kitas, consultant rheumatologist at the Dudley NHS Trust of Hospitals, UK, for the selection of patients with RA according to the criteria of this study. A big thank you to Kevin Woollard for the culture of endothelial cells, and Kirsty Allen, who performed some of the experiments to determine mitochondrial peroxide production and cell viability. I am also grateful to Dr E.F. Adams and Dr. A. Vernallis for their helpful discussion.

Contents.

List of figures and tables.

Chapter 1.0: General Introduction.

This thesis has investigated the cellular responses to manipulations in the intracellular concentrations of the sphingolipid ceramide, and reactive oxygen species (ROS) in the context of immune cell function and the complex inter-relationship between these two molecules. This chapter introduces sphinoglipid metabolism, ROS formation and regulation of the redox state in the context of cell survival and death. Furthermore, their involvement in intracellular signal transduction in response to physiological or toxicological agents relevant to other signalling intermediates is discussed. It is consequently hypothesised that their aberrant signalling in T-cells and monocytes may contribute to the aetiologies of inflammatory diseases such as cardiovascular disease and rheumatoid arthritis (RA). The ensuing introductory sections of each chapter present a more detailed review of the current literature and theories with regards the interplay of ceramide with the redox state (Chapter 2), the interaction of immunological and circulatory cells with the endothelium in relation to cardiovascular disease (Chapter 3), aberrant T-lymphocyte intracellular signalling in RA (Chapter 4) and the mechanisms of action of the anti-inflammatory and immunosuppressive agent methotrexate (Chapter 5). Each introduction then presents the hypotheses to be investigated. These are followed by detailed descriptions of the methodologies used to address the questions posed, a results section describing the results obtained in detail and an in depth discussion of the findings in the context of the work of others. Chapter 6 discusses the key findings and conclusions of this thesis.

1.0 General introduction.

1.0.1 Apoptosis, necrosis and proliferation.

For normal tissue homeostasis, cells must be continuously lost in order to balance the effects of cell proliferation. An imbalance results in either disorders of cell accumulation or cell loss. Cell proliferation is a highly regulated process with numerous checks and balances, where various growth factors move cells from the resting G0 state of the cell cycle sequentially through the various phases (G1, S, G2, M). Each phase is regulated by the co-ordinate actions of kinases and proteases, stimulating transcription factors to initiate gene expression of proteins required for transition through each phase. The proliferative effects of growth factors and proto-oncogenes are negatively regulated by tumour suppressor genes (as reviewed in; Jones & Kazlauskas, 2001; Thompson, 1995).

To counteract cell growth, two morphologically distinct forms of cell death exist, necrosis and apoptosis, whose regulation is equally as complex as cell proliferation. Necrosis describes the morphology observed upon death due to severe or sudden injury such as that observed in ischaemia, sustained hyperthermia, or physical and chemical trauma. The mitochondria undergo a rapid loss in shape and homeostasis. The plasma membrane becomes the major site of damage, with dysregulation of osmotic potentials mediating cell swelling and eventually cell rupture. Cellular contents are thus released into the immediate surrounding tissue space, initialising an

inflammatory response (as reviewed in; Cohen, 1993). However, this form of cell death is not suggestive of any controlling role for the cell population size.

On the contrary, apoptosis represents cell death which is consistent with an active, inherently controlled phenomenon and plays an essential role in the regulation of cell number in both normal physiological and pathological conditions. Selected cells that have been produced to excess (e.g. during embryogenesis), developed improperly or have genetic damage are consequently eliminated (as reviewed in; Kerr *et al.*, 1972; Thompson, 1995). Apoptosis can be triggered by noxious agents, can appear spontaneously or in response to various known physiological stimuli (as reviewed in; Kerr *et al.*, 1972). The pathways mediating the activation of apoptosis differ according to cell type, but the final common pathways and morphologies appear to be very similar (as reviewed in; Cohen, 1993). During apoptosis, the integrity of the plasma membrane remains intact, enabling packaging of disintegrating organelles into membrane vesicles without leakage of toxic intracellular compounds. Consequently, there is no induction of an inflammatory response (as reviewed in; Kolenick & Krönke, 1998).

In vivo, two distinct phases of apoptosis are apparent. Initially, apoptotic bodies are formed which are then phagocytosed and degraded by neighbouring cells or macrophages without induction of inflammatory response (as reviewed in; Kerr *et al.*, 1972; Kolesnick & Krönke, 1998). On initiation of apoptosis *in vitro*, the cell shrinks, consequently the cytoplasmic organelles become tightly packed and there is evidence of clumping of chromatin. The cell undergoes zeiosis, whereby the cell membrane becomes ruffled and blebbed, with additional loss of mitochondrial

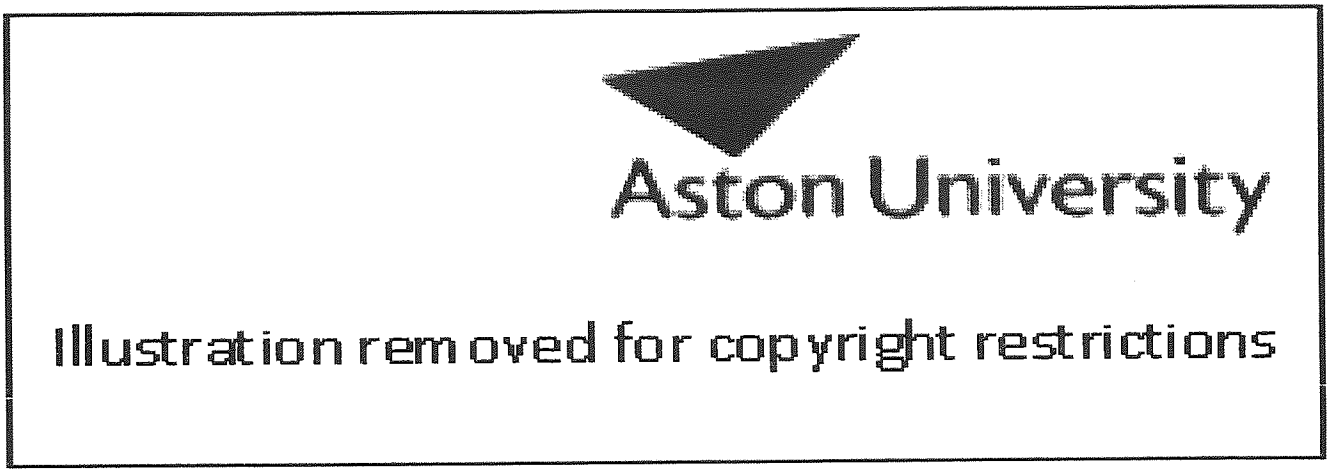

Figure 1.1. The stages of apoptosis in a lymphocyte as observed *in vitro*. The normal cell (a) has a sparse cytoplasm and heterogeneous nuclear chromatin. (b) The cell loses volume, consequently cytoplasmic organelles become tightly packed and there is clumping of nuclear chromatin. At this point, alterations in the plasma membrane signal phagocytosis. (c) Cell membrane becomes ruffled and blebbed, a process termed zeiosis. (d) Chromatin falls down into the crescents of the nuclear envelope, followed by collapses of the nucleus into a "black hole". (e) The nucleus now fragments, (e) leading to the break up of the cell into apoptotic bodies (as reviewed in; Cohen *et al.*, 1993).

function. It is at this point where *in vivo*, alterations in the cell membrane signal phagocytosis. The nucleus collapses into a "black hole," which often breaks up into small spheres accompanied by the formation of DNA into a ladder of regular sub-units due to random double strand breaks in the linker regions between nucleosomes. These DNA fragments are oligonucleosomal size, multiples of 180-200 base pairs (bp), where strand cleavage is mediated by Ca^{2+} and Mg^{2+} endonucleases. The cell may now break up into apoptotic bodies without spilling cellular contents and hence eliciting no provocation of inflammation (see Figure 1.1; Wylie, 1980; as reviewed in; Cohen, 1993).

Apoptosis, at the molecular level, can in fact be envisaged as occurring in three stages. Firstly, "initiation," which refers to events which cause entry into the common death pathway. Secondly, "sentencing" or "commitment" which encompasses the intracellular events that commit the cell irreversibly to the death process and finally, "execution." Here, effector molecules such as nucleases and proteases accomplish the overt changes associated with apoptotic death described above (Farschon *et al.*, 1997).

1.0.2 The TNF receptor superfamily.

The TNF receptor superfamily is comprised of 17 members, all of which share the common feature of a cysteine rich motif repeated 2-6 times in the extracellular domain. This family is divided in two according to two structural features. Both groups possess the ability to associate directly with signalling molecules such as proteins containing zinc finger motifs to induce proliferation, inflammation and cell death. Some members also possess an intracellular death domain (DD), which is believed to mediate transduction of an apoptotic signal (as reviewed in; Beutler & Bazzoni, 1998). It is this latter group to which TNF receptor and the lesser studied CD-95 (Fas/APO-1) receptor belong.

These two receptors are believed to undergo crosslinking or aggregation of subunits on association with their respective ligands. The ligand for the CD-95 receptor discovered in 1994 (Nagata, 1994), is simply termed the CD-95 ligand (CD-95L), and is a cell anchorage homologue to the TNF receptor ligand TNFα. TNFα is a 17kDa

protein produced primarily by macrophages (Aggarwal & Higuchi, 1997). In aqueous solutions, TNFα has been shown to exist as a native folded trimer with a high thermodynamic stability, only a small fraction existing as a monomer in solutions of physiological ionic strength. These trimers are capable of low stability aggregation and account for higher molecular weight oligomers of TNFα sometimes observed. Both CD-95 and TNF receptors are expressed in the membranes of virtually all somatic cells (as reviewed in; Pfizenmaier *et al.*, 1991; Sprang & Eck, 1991). However, the TNF receptor is not expressed in resting lymphocytes and a number of transformed B cells (Krammer *et al.*, 1994).

Binding and receptor crosslinking studies in a variety of cell lines have revealed the existence of two distinct TNF receptor subtypes, a 55kDa (p55TNF) and a 75kDa (p75TNF) subtype co-expressed on the surface of most cells (as reviewed in; Pfizenmaier *et al*, 1991). However, it is the p55TNF subtype which is predominantly expressed in most cell types, with the p75TNF receptor being found on immune and endothelial cells. Most TNF receptor mediated signalling appears to occur via the p55TNF receptor subtype and is associated with sphingomyelinase (SMase) activation, signalling via p75TNF receptor being highly restricted (Wiegmann *et al.*, 1994).

Both TNF receptor subtypes can be subdivided into 4 structural domains, a hydrophobic signal peptide, one extracellular cysteine rich domain, a single transmembrane (TM) domain and intracellular domain. The TNF receptor and structurally related CD-95 receptor are thus equipped to channel signals to the

cytoplasm and nucleus, thereby initialising profound alterations in the metabolic state and transcription programme of sensitive cells.

1.0.3 Ceramide and the sphingomyelin pathway.

The sphingomyelin (SM) pathway is a ubiquitous, evolutionary conserved signalling system, where several of the sphingolipid constituents, namely ceramide (N-acylsphingosine), sphingosine and sphingosine-1 phosphate (S1P), serve as second messengers in this pathway (see Figure 1.2). Sphingolipids constitute a large lipid group consisting of complexes of phospholipids and glycolipids, accounting for 10-15% of the total amount of phospholipids in cells. These are believed to be involved in cell proliferation, differentiation and apoptosis (as reviewed in; Okazaki *et al.*, 1998).

The SM pathway or cycle was first described by Okazaki *et al.*, (1989) and is shown in Figure 1.2. Thin layer chromatography (TLC) separation of sphingolipids following extraction from human leukaemic HL60 cells treated with 1α,25 dihydroxyvitamin D_3, revealed a 75% decrease in sphingomyelin levels when compared to controls within two hours of treatment, returning to normal levels within four hours. Accompanying alterations in sphingomyelin levels were comparable trends in the elevation of phosphocholine and ceramide, which imply both synthetic and metabolic enzymatic pathways.

Ceramide is generated mainly in cells as a result of two distinct classes of enzymes,

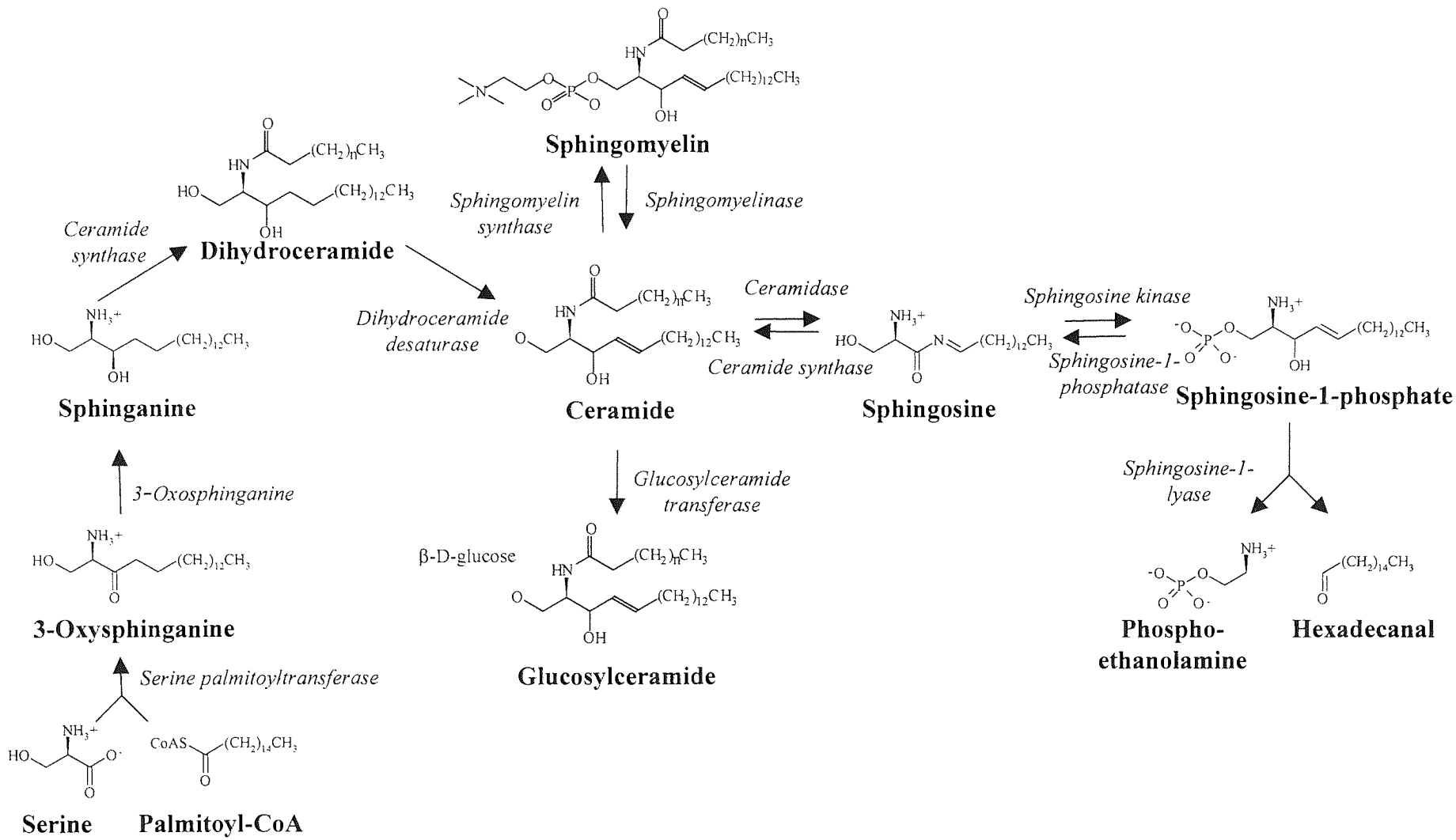

Figure 1.2. The sphingomyelin cycle. Shown are the various chemical structures of sphingolipids and the enzymes (*italics*) involved in their metabolism (adapted from; Mathias *et al.*, 1998; Okazaki *et al.*, 1998).

sphingomyelinases (SMase) and ceramide synthase, representing the metabolic and synthetic pathways respectively (Aggarwal & Higuchi, 1997). However, it should be appreciated that multiple enzymes exist that are capable of regulating ceramide concentrations (see Figure 1.2). Endogenous, natural ceramide consists of a sphingosine backbone, which is common to all sphingolipids and an esterified fatty acid acyl chain, which varies in both length and degree of saturatation. Ceramide synthesis *de novo* is mediated by condensation of serine and palmitoyl co enzyme A (CoA) to form 3-oxysphinganine, with subsequent reduction to sphinganine by NAD(P)H dependent reduction. Dihydroceramide is formed by acylation mediated by the action of the enzyme ceramide synthase (sphinganine-N-acyltransferase). Ceramide is finally produced by the action of the enzyme dihydroceramide desaturase (see Figure 1.2; as reviewed in; Peña *et al.*, 1997; Kolesnick & Krönke, 1998; Okazaki *et al.*, 1998). However, the most prominent form of ceramide accumulation involves the degradation of SM by the action of specific forms of phospholipase C, SMases, additionally yielding phosphorylcholine (See Figure 1.2). SM is distributed in virtually all subcellular membranes although it is particularly concentrated within the plasma membrane inner leaflet as reviewed in; Kolesnick & Krönke, 1998; Levade & Jeffrézou, 1999; Okazaki *et al.*, 1998). To date, seven isoforms of SMase have been described and distinguished by their sub-cellular location, pH optimum, cation dependence and role in cell regulation.

(i) The lysosomal acid SMase (A-SMase) which functions optimally at pH4.5-5.

(ii) The neutral and magnesium dependent SMase (N-SMase), optimum pH 7.4.

(iii) Zinc dependent and lysosomal A-SMase derived acid enzyme.

(iv) Magnesium independent N-SMase.

(v) Alkaline SMase.

(vi) Neutral and dithiothreitol (DTT) stimulated SMase.

(vii) N-SMase found within chromatin and rat liver nuclei.

Relatively little is known as to the biological activity of the latter five SMases. Human and murine ASMase have been cloned and determined to be the product of a single conserved gene (Horinouchi *et al.*, 1995), although alternative processing of the primary transcript allows for the prediction of multiple forms (Schuchman *et al.*, 1992, Schuchman, 1995). A-SMase is primarily found to reside in lysosomes or endosomes as low molecular weight (MW) forms, but is also detected in a higher MW soluble form in the cytosol and extracellular fluid. This is a reflection of post-transcriptional processing (as reviewed in; Basu & Kolesnick, 1998). Additionally, a putative plasma membrane microdomain termed calveolae, enriched in sphingolipids, may be significant for lipid mediated ASMase activation (Liu *et al.*, 1996).

N-SMases have not been characterised at the molecular level. Cells obtained from A-SMase knockout (-/-) mice and humans with Nieman Pick Disease (NPD), an inherited autosomal recessive disease resulting in a lysosomal SM storage disorder due to a deficiency in A-SMase activity, contain a normal level of N-SMase activity (Santana *et al.*, 1996; De Maria *et al.*, 1998), indicating N-SMase is a distinct gene product from that of A-SMase. The magnesium dependent and independent forms of N-SMase are localised within the membrane and cytosol respectively (as reviewed in; Basu & Kolesnick, 1998; Okazaki *et al.*, 1998). Under resting and stable conditions,

magnesium dependent N-SMase in cells remains as an inactive enzyme located in the outer membrane leaflet, negatively regulated by glutathione (GSH). Treatment of Molt 4 cells with the GSH synthesis inhibitor, L-butionine-[SR]-sulfoxamine (BSO), leads to a time dependent depletion of GSH accompanied by an increase in the hydrolysis of SM and increased production of ceramide (Liu & Hannun, 1997). Further, TNF stimulation of the same cell line results in GSH depletion, a consequent rise in N-SMase activity and ceramide production (Liu *et al.*, 1998). The redox regulation of ceramide production is discussed in more depth in Chapter 2.

In accord with most metabolic pathways, the cellular concentration of ceramide is regulated not only by its formation but also by its rate of removal by several classes of enzymes. Furthermore, many of these ceramide metabolites are signalling intermediates for a variety of extracellular agents in their own right and antagonise the signalling pathways and cellular responses mediated by ceramide. One of the metabolic pathways responsible for diacylglycerol (DAG) formation is via the action of phospatidylcholine specific phospholipase C from phospatidylcholine (PC; as reviewed in; Bielawska *et al.*, 2001; Goñi & Alonso, 1999). Initially DAG was thought to regulate ceramide generation via A-SMase, where SM is derived from PC hydrolysis by PC specific phospholipase C. This hypothesis was based upon the specificity of the xanthogenate D609, an inhibitor of PC-specific phospholipase C., and was found to prevent A-SMase activation induced by TNFα, IL-1 and CD95 (Cifone *et al.*, 1995; Liu & Anderson, 1995; Schütze *et al.*, 1992). However, induction of endogenous DAG production by bacterial phospholipase C or the pre-treatment with short chain 1,2 DAG, the protein kinase C (PKC) activation (phorbol ester, TPA) block both TNFα and ceramide mediated HL60 apoptosis.

Correspondingly, downregulation of PKC activity by the prolonged exposure to the TPA enhanced ceramide mediated apoptosis (Jarvis *et al.,* 1994a & b). Further, TPA and phosphatidylserine inhibited daunorubicin activation of SMase, ceramide generation and the associated apoptosis (Mansat-de Mas *et al.,* 1997) while TPA blocked ionising radiation induced apoptosis of primary bovine endothelial cells (Haimovitz-Friedman *et al.*, 1994). Elevations in endogenous natural DAG are largely associated with mitogenesis (as reviewed in; Ruvulo, 2001). SM synthesis results from the phosphocholine transfer from PC to ceramide, also yielding DAG, therefore sphingomyelin synthase (phosphocholine transferase) and SMase modulate ceramides and DAG. Additionally, ceramide can be deacylated by the action of ceramidase to generate sphingosine which can be further phosphorylated by sphingosine kinase to form S1P.

Sphingosine may act as a positive or negative regulator of proliferation, although its mitogenic effects are likely to be mediated by S1P. Indeed, it is proposed that S1P prevents apoptosis mediated by elevations in endogenous natural ceramide induced by the application of TNFα, CD95L, bacterial SMase and synthetic short chain ceramide (Cuvillier *et al.*, 1996, 1998). Furthermore, S1P exerts its inhibitory effects on ceramide mediated apoptosis upstream of the mitochondria since SIP it does not alter the expression of the mitochondria located anti-apoptotic protein family $Bcl\text{-}_2$. These S1P effects were also mimicked by stimulation of sphingosine kinase (see Figure 1.2) with phorbol ester. Additionally, inhibition of sphingosine kinase activity with dimethylsphingosine (DMS) enhances TNFα, CD95 and ceramide induced apoptosis (Cuvillier & Lavade, 2001). The existence of ceramide rheostats, one in partnership with S1P and the other with DAG, to produce a series of balances for

cellular regulation and the sensing of stimuli, makes studying the effects of an accumulation of endogenous ceramide mediated by external stimuli difficult. An appreciation that an elevation in cellular ceramide may not be the sole dictator of the response of a cell to stimuli, but rather, its combined effects and its ratio relative to other signalling metabolites should be considered. In this regard, cell type specific responses to external agents may be due to a differing basal ratio of ceramide:S1P:DAG rather than the sole modulation of one of these lipid species.

The kinetics of SM hydrolysis mediated by SMase and the consequent ceramide accumulation are complex and variable. A considerable amount of contradictory evidence exists with regards the kinetics even when observed within the same cell lines following treatment with the same concentration of stimuli. This picture is further complicated by the different experimental approaches used to quantify ceramide. However, attempts have been made to ascribe a particular ceramide source to the kinetics of its formation. Following TNFα, CD-95, LPS, ionising irradiation or pharmacological agent exposure of a variety of cell types, ceramide has been reported to accumulate rapidly and transiently within seconds to several minutes. This has been attributed to A-SMase (Cifone *et al.*, 1993; Gulbins *et al.*, 1995; Karasavvas & Zakeri, 1999; Mackichan & DeFranco, 1999; Modur *et al.*, 1996; Schütze *et al.*, 1992; Schwandner *et al.*, 1998; Wiegmann *et al.*, 1994). Acute ceramide elevations however are only of modest magnitude, 20-60% above basal levels and may reflect ceramide metabolism to other sphingolipid species (see Figure 1.2). This hypothesis is reflected upon the TNFα exposure of human umbilical endothelial cells (HUVEC), where the loss of SM is greater than the accumulation of ceramide (Modur *et al.*, 1996).

The role of A-SMase as a functional active enzyme responsible for cellular responses to external agents is cast into doubt by differing observations of SM hydrolysis and consequent ceramide formation in cells obtained from either A-SMase -/- mice or those derived from patients with NPD. While human skin NPD fibroblasts undergo apoptosis in response to TNFα or IL-1 treatment that was associated with SM hydrolysis and consequent ceramide formation (Andrieu *et al.*, 1994), TNFα treatment of mouse embryonic fibroblasts derived from A-SMase -/- mice did not induce SM hydrolysis and ceramide formation (Zumbansen & Stoffel, 1997). A-SMase -/- mice exposed to radiation expressed defects in ceramide generation and apoptosis *in vivo* compared to wild type (WT) mice. These observations were most evident within the lung and were reflected albeit to a lesser degree within the thymus and spleen (Santana *et al.*, 1996). Findings of defective ceramide signalling and apoptosis in response to radiation exposure were also seen in lymphoblast cell lines derived from human NPD patients utilising Epstein Barr virus (EBV) transformed normal human lymphoblasts as controls. Restoration of A-SMase activity within NPD lymphoblasts by the retroviral gene transfer of A-SMase cDNA induced a normal ceramide response to radiation preceding cell death (Santana *et al.*, 1996). Similarly, EBV transformed NPD lymphoid B-cells fail to respond to CD95 stimulation with A-SMase activity resulting in inefficient apoptosis and the failure to accumulate the ceramide lipid target GD3 ganglioside. Mannose receptor mediated transfer of A-SMase into NPD lymphoblasts rescued CD95 induced A-SMase activation, GD3 ganglioside accumulation and apoptosis. Similarly, the addition of synthetic short chain ceramides to NPD lymphoblasts, effectively bypassing A-SMase induced apoptosis (De Maria *et al.*, 1998). However, contradictory observations were reported by Boesen-de Cock *et al.*, (1998), who reported the EBV

transformed NPD B cells readily undergo CD95 induced apoptosis which was associated with a slow sustained accumulation in endogenous ceramide and did not require A-SMase since the retrovirus gene transfer of A-SMase cDNA did not enhance the kinetics of CD95 mediated apoptosis or ceramide formation.

Further scepticism against the involvement of A-SMase in the rapid elevation of intracellular ceramide derives from its cytosolic location within lysosomes or endosomes (as reviewed in; Hoffman & Dixit, 1998). Indeed, in contrast to fluorescently tagged or short chain ceramides, endogenous, natural ceramide is unable to escape lysosomal compartments. How ceramide is then able to physically interact with downstream organelles or biomolecules is unclear (as reviewed in; Levade & Jeffrézou, 1999). However Grassmé *et al.*, (2001a & b), utilising confocol microscopy, scanning electron microscopy and flow cytometry, proposed a novel mechanism whereby upon CD95 stimulation, A-SMase translocates to the plasma membrane and localises to rafts rich in its sphingolipid substrate. This permits the formation of ceramide rich domains within the plasma membrane and allows CD95 induced apoptosis. Fibroblast or lymphocytes deficient in A-SMase did not accumulate ceramide in the plasma membrane and did not undergo apoptosis. These authors propose that ceramide accumulation in response to CD95 stimulation via the action of A-SMase is required to alter the membrane fluidity, thereby clustering the CD95 receptor in lipid rafts which permits interaction with downstream effector proteins and enables efficient transduction of the apoptotic signal. In support of this, cells defective in ceramidase, an enzyme responsible for metabolic conversion of ceramide (see Figure 1.2) showed strongly enhanced CD95 receptor clustering.

However, others have not observed this rapid, acute and transient ceramide response to TNFα or CD-95L treatment (Boesen de Cock *et al.*, 1998; Gamard *et al.*, 1997; Watts *et al.*, 1997; Watts *et al.*, 1999). Indeed, inhibition of ceramidase and glycosyltransferase to prevent removal of the subtle and early changes in ceramide levels, does not reveal any ceramide accumulation following CD-95L exposure of Jurkat T-cells (Tepper *et al.*, 1997). An intermediate and reversible accumulation of ceramide between 10 minutes and 4 hours post stimulation has been described for IL-1, TNFα, 1α,25 dihydroxyvitamin D_3, NGF and several neurotrophins (Hannun, 1996; Jaffrézou *et al.*, 1998; Karasavvas & Zakeri, 1999; Tepper *et al.*, 1997). Following CD-95 receptor stimulation of Jurkat T-cells, a primary increase in intracellular ceramide levels has been observed at 3-4 hours (7 fold above basal levels at 8 hours) paralleling the onset of apoptosis measured by nuclear fragmentation (Tepper *et al.*, 1997). Applying an HPLC method for measurement of endogenous ceramide accumulation, the ceramide species involved has been identified to be mainly C_{16} or C_{18}. Similar observations are described by Watts *et al.*, (1999) using ionising mass spectrometry, where U937 cells were treated with TNFα plus the protein synthesis inhibitor cycloheximide, demonstrated an accumulation of ceramide species with fatty acyl chain lengths greater than 14 carbon atoms at 2 hours post treatment. Taken together, this evidence suggests that the elevations in endogenous ceramide with intermediate kinetics, 10 minutes to 4 hours post treatment are associated with the hydrolysis of SM by N-SMase (Tepper *et al.*, 1997). Magnesium dependent N-SMases are membrane associated and therefore are ideally localised for direct interactions with receptors (as reviewed in; Basu & Kolesnick, 1998; Okazaki *et al.*, 1998).

A third, late, prolonged and persistent accumulation of intracellular ceramide has been described over several hours for U937s exposed to C_6-ceramide, TNFα, CD95L, γ-radiation, etoposide, vincristine and daunorubicin, reaching 400% above basal levels at 24 hours TNF incubation. In some cases this elevation has been shown to precede the appearance of cell death while in others, it occurs before maximal apoptosis induction (Bose *et al.*, 1995; Boland *et al.*, 1997; Dbaibo *et al.*, 2001; Tepper *et al.*, 1997, 1999; Zhang *et al.*, 1996). The ceramide synthesis inhibitor fumonsin B1 reduces ceramide accumulation by 50% in U937 monocytes after 24 hours stimulation with TNFα or daunorubicin but did not prevent the phasic ceramide accumulation by these agents observed 0-4 hours post-treatment (Jaffrézou *et al.*, 1998). Fumonsin B1 also reduced the late ceramide accumulation by 75% in P388 murine leukaemia cells treated with daunorubicin (Bose *et al.*, 1995), 60% in MCF-7 cells and 40% in L929 murine fibrosarcoma cells, and reduced the loss of adhesion to culture plates due to apoptosis by approximately 10 and 40% respectively following TNFα treatment for 24 hours (Dbaibo *et al.*, 2001). However, fumonsin B1 did not confer any protection in either MCF-7 or L929 cells from cell death after 72 hours of TNFα exposure (Dbaibo *et al.*, 2001). Furthermore, where high doses of anthracyclines induce necrosis, ceramide synthase activity is reported (Jaffrézou *et al.*, 1996). Collectively, these results imply a significant contribution of *de novo* synthesis for the late elevations of ceramide levels, where the percentage of newly synthesised ceramide and the contribution to the total death process is cell type dependent. Ceramide synthesised via this pathway is presumably formed within the endoplasmic reticulum (ER), the subcellular location of ceramide synthase. However, Karasavvas & Zakeri, (1999) describe increasing ceramide levels 1 hour post treatment with TNFα, 30 minutes before U937 monocyte cell death detected by

agarose gel electrophoresis of DNA fragmentation, but is later than the TNFα mediated commitment to cell death. Similarly, TNFα in the presence of the protein inhibitor cycloheximide induced biochemical evidence of apoptosis in U937 monocytes within 1 hour of exposure, before elevations in ceramide (Watts *et al.*, 1999). This has led to the opinion by some authors that the late persistent ceramide elevations may be, at least in part, produced as of a consequence of apoptosis (Sillence & Allan, 1997; Tepper *et al.*, 1997, 1999) representing dysregulation of normal ceramide metabolic processes in dying cells rather than the cause. Jaffrézou *et al.*, (1998) suggest that late ceramide accumulation mediated by ceramide synthase, is required to ensure self destruction, a positive feedback phenomena or amplification of the apoptotic process.

Together, the kinetic data described suggest that early to intermediate elevations in intracellular ceramide levels above are mediated by the SMases. Any autoregulation of intracellular ceramide level is likely to occur within these two periods, the early to intermediate phase. The rapid rise in ceramide concentration is fundamental in its role as a receptor mediated signal transduction molecule.

SM hydrolysis mediated by A-SMase and N-Smase and the ensuing activation of multiple protein targets has led some to propose that the source of ceramide formation mediates the different cellular responses observed to occur upon induction of ceramide accumulation by TNFα, IL-1 CD95 or pharmacological agents. Kolesnick and Krönke, (1998) proposed that ceramide formation due to A-SMase activation is associated with cell death via the Jun kinase (JNK)/ stress activated protein kinase (SAPK) pathway associated with NFκB nuclear translocation whereas N-SMase

results in extracellular-signal-regulated-kinase (ERK) pathway activation resulting in proliferation and pro-inflammatory effects with no cross talk between the two sources (Schütze *et al.*, 1992; Weigmann *et al.*, 1994; see Figure 1.3). However, in the human breast carcinoma cell line MCF-7, N-SMase activity mediating the formation of endogenous ceramide is associated with the induction of TNFα induced cell death (Liu *et al.*, 1998). The degree and persistence in the elevation of intracellular ceramide levels may gauge the extent of cell damage leading the cell to execute varying degrees of programmed cell death. The observations that different agents induce varying kinetics of endogenous ceramide formation, utilising various combinations of enzymes located at different cellular locations, probably via alternative signal transduction pathways is indicative of compartmentalisation. Selecting one compartment over another may lead to the initiation of distinct biological processes. Indeed, Watts *et al.*, (1999) observed different subspecies of ceramide, which vary in fatty acyl chain length, accumulate following exposure of U937s to TNFα compared to those mediated by Anisomycin and geranylgeraniol. Dobrowsky *et al.*, (1993) reported different potencies for various synthetic short chain ceramide analogues in activating the natural ceramide protein target ceramide activated protein phosphatase (CAPP) ABαC heterodimer. A potency order of C_{10}->C_6->C_2-ceramide was observed, implying the more hydrophobic the analogue the more efficient CAPP activation. Conversely, a potency order of C_2->C_6-ceramide is observed in the release of cytochrome C (cyt.C) from mitochondria (Ghafourifar *et al.*, 1999) and C_{16}-ceramide, a natural product, is more potent as an activator of c-Raf in rat renal mesangial cells than other shorter chain ceramides (Huwilier *et al.*, 1996). Consequently, ceramide subspecies may activate specific transduction pathways and determine one cellular outcome over another. Decreases in the steady state

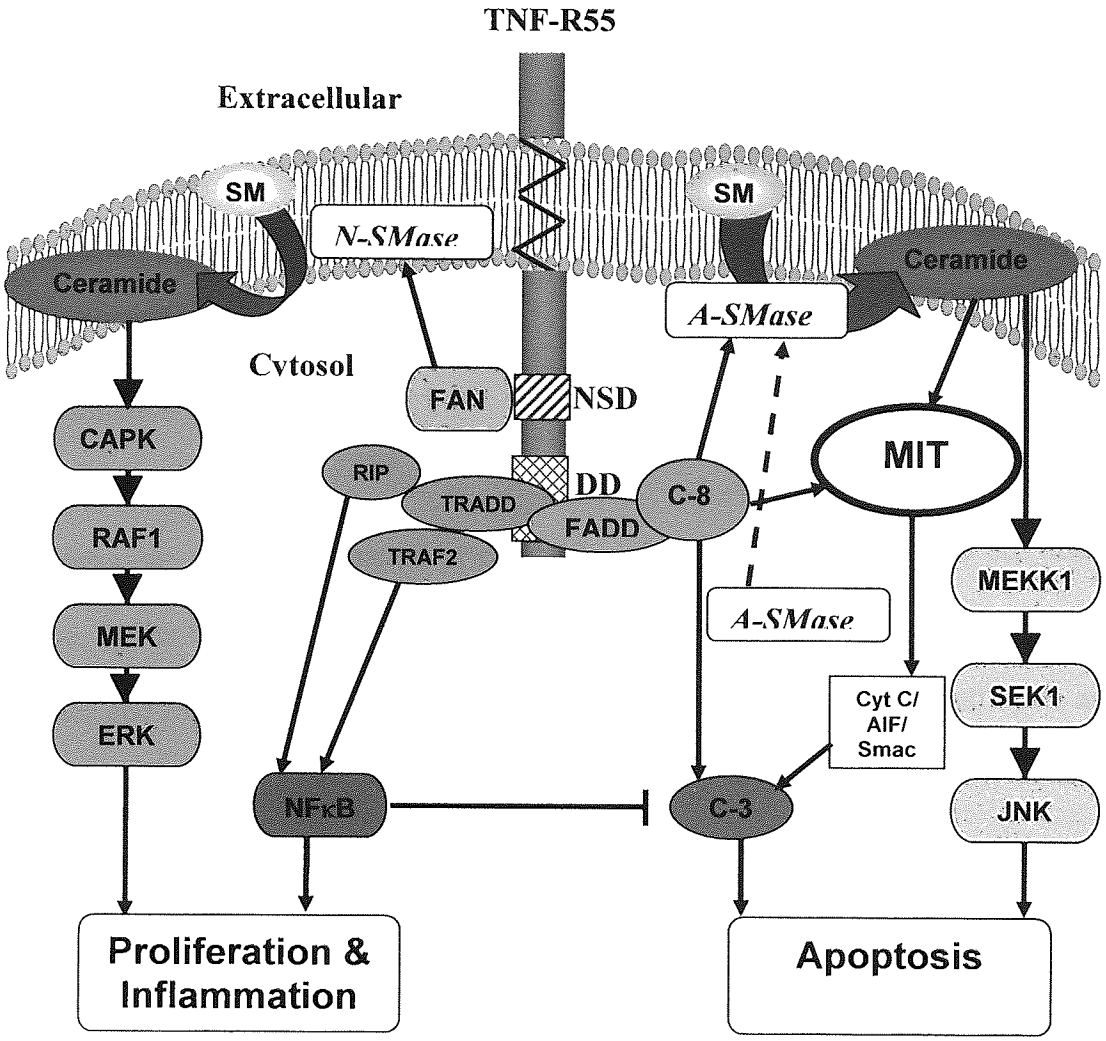

Figure 1.3. Proposed mechanism for TNF-induced signalling. Activation of the 55kDa TNF receptor initiates an apoptotic signal by the binding of FADD (Fas-associated death domain) to the death domain (DD) of the cytosolic tail. Caspase-8 (C-8) is then recruited to this adaptor protein that initiates activation of a caspase cascade leading to apoptosis via mitochondria dependent or independent pathways. C-8 activation may also lead to the migration of acid sphingomyelinase (A-SMase) from the cytosol to the sphingomyelin (SM) rich plasma membrane and catalyses its metabolism to ceramide. Ceramide generated here induces disruption of the mitochondrial membrane potential and the formation of pores promoting the release of the pro-apoptotic factors cytochrome c (cyt C), apoptosis inducing factor (AIF) and second mitochondria-derived activator of caspase (Smac). Additionally, ceramide formed by the action of A-SMase also activates the JNK/SAPK pathway. Both the JNK/SAPK pathway and mitochondrial pro-apoptotic factors induce apoptosis via the activation of caspase-3 (C-3). Alternatively, TNF stimulation can mediate a proliferative response by the linking of the adaptor protein FAN to the neutral sphingomyelinase (N-SMase) domain (NSD) situated proximal to the DD of the TNF receptor. Consequent activation of membrane associated N-SMase catalyses the conversion of SM to ceramide which in turn stimulates ceramide-activated protein kinase (CAPK), and thus the sequential phosphorylation of Raf-1 and ERK to induce proliferation. In addition, TRADD may link to both RIP and/or TRAF2 to induce NFκB activation, capable of suppressing C-3 and inducing proliferation. Adapted from Kolesnick & Krönke, (1998).

intracellular ceramide levels have been shown to lead to growth arrest and an undifferentiated cell phenotype (as reviewed in; Sharma & Shi, 1999). However, elevations of ceramide levels have been identified to act as a second messenger in activating a variety of cell functions including proliferation (Adam *et al.*, 1996), apoptosis (Schwandner *et al.*, 1998), necrosis (Goossens *et al.*, 1995), and differentiation (Ragg *et al.*, 1998).

The described pleiotropic nature of ceramide seems to be dictated by its enzymatic source, by its implicated association with a variety of receptors and agents, by the kinetics and magnitude of formation, in addition to cell type, phase of cell cycle and engagement of various downstream effector systems and organelles. All of these variables play a role in determining the final cellular outcome. Elevations of intracellular ceramide in response to a specific agent in one cell type, mediating a specific cellular outcome, is therefore not directly applicable to other cell types exposed to the same agent.

1.0.4 Putative involvement of ceramides in signalling cascades.

Signalling cascades frequently comprise of a series of protein kinases that are sequentially phosphorylated and hence activated, leading to propagation of a signal from the cell surface to the specific targets within the cytoplasm. The final target is often the nucleus, via transcription factors.

The most prominent transcription factors responsible for the effects of TNFα are NFκB (p105) and activator protein-1 (AP-1), which mediate induction of many genes central to the inflammatory process and immune response. NFκB consists of two subunits, p65/RelA and p50. The heterodimer is complexed to the inhibitory IκB (36kDa) protein in the unstimulated cytosol. Activation of NFκB requires the signal induced phosphorylation of IκB, followed by its conjugation with ubiquitin leading to its degradation by the proteosome (as reviewed in; Baeuerle & Baltimore, 1996; Eder, 1997). IKK (Erk-1 kinase) phosphorylates IκB following TNF/TRAFF/NIK sequential activation (Mercurio *et al.*, 1997). Liberated NFκB translocates to the nucleus to activate gene transcription by binding to the nucleotide sequence 5'-GGGACTTCC-3 (as reviwed in; Baeuerle & Henkel, 1994; Eder, 1997). Genes encoding transcription factors (AP-1, IRF-1, and NFGMa) are induced by TNF and may consequently lead to a secondary phase of protein expression. Other TNF responsive genes include those encoding secreted factors such as cytokines and enzymes, cell surface receptors and the proto-oncogenes c-myc, c-fos and c-jun (as reviewed in; Pfizenmaier *et al.*, 1991). AP-1 belongs to the basic region leucine zipper (bZip) group of DNA binding proteins and is a heterodimer of Jun and Fos family subunits. Consequently, the transcription factor is regulated by activation of c-jun and c-fos genes and requires MAPK mediated phosphorylation of both its subunits for activation. CD-95L and C_6-ceramide are capable of induction of another transcription factor GADD153/CHOP, although its function is unknown (Brenner *et al.*, 1997).

The involvement of ceramide as a mediator of NFκB activation is somewhat controversial with as many reports describing this lipid as essential as there are

reporting its total absence. Schütze *et al.,* (1992) first suggested that TNF induced NFκB translocation via ceramide which was formed specifically by the action of A-SMase rather than by N-SMase. Further, stable membrane expression of the 55kDa TNF receptor with truncated DD in murine pre-B cell line 70Z/3 (thereby preventing A-SMase activation and ceramide accumulation) did not activate NFκB unlike cells expressing the wild type receptor (Wiegmann *et al.*, 1994). The application of bacterial SMase to NIH-3T3 fibroblasts led to kappa B dependent activation of the chloramphenicol acetyltransferase (CAT) reporter gene in a similar manner to TNFα (Lozano *et al.*, 1994). In U937 monocytes, TNFα (Chan & Aggarwal, 1994) and low concentrations of synthetic ceramides rapidly activated NFκB via the intermediate PKCζ to induce proliferation, whereas at higher ceramide doses, PKCζ was not activated and consequently nuclear NFκB was absent. This process perhaps represents a process by which mitogenic stimulation can be interrupted (Müller *et al.*, 1995). However, in primary murine embryonic fibroblasts deficient in A-SMase and NPD skin fibroblasts following TNFα binding to its receptor, NFκB was activated in the same manner as wild type cells (Gamard *et al.*, 1997; Zumbansen & Stoffel, 1997). Further, in the parental fibroblasts, TNFα induced neither A-SMase nor N-SMase activity with no ceramide generation, while in HUVEC, TNFα induced NFκB activation independently of ceramide generation (Modur *et al.*, 1996; Zumbansen & Stoffel, 1997). Additionally, bacterial SMase or C_2-/C_6-ceramide did not activate NFκB translocation and IκB degradation in Jurkat T-cells. Rather, in studies utilising low concentrations of the phorbol ester PMA to activate NFκB, short chain synthetic ceramides actually abrogated this effect (Gamard *et al.*, 1997). Similarly, in HL60 cells, TNFα, but not bacterial SMase or C_2-ceramide, stimulated an NFκB reporter gene (Westwick *et al.*, 1995). Boland & O'Neill, (1998) proposed an alternative

mechanism to explain this disparity in ceramide mediated NFκB activation. These authors showed that C_2-ceramide failed to drive κB linked CAT reporter gene expression in Jurkat T-cells or HL-60 cells. However, EMSA showed a dose response activation of NFκB made of predominantly the p50 subunit in contrast to TNF treated cells where both the p50 and P65/RelA subunits were observed. This led to the hypothesis that suggestion that ceramide induces processing of the p105 to p50 mediating p50 homodimer activation whereas TNFα induced immediate κB degradation with later ensuing p105 processing (Boland & O'Neill, 1998).

The mitogen activated protein kinase (MAPK) family cascade have been implicated as playing a key role in mediating the cellular outcome in response to several stressing agents that induce endogenous ceramide formation including TNFα, CD-95L, ionising radiation, UV light, H_2O_2 and heat or synthetic short chain ceramides (Brenner *et al.*, 1997; Cuvillier *et al.*, 1996; Verheij *et al.*, 1996) and consist of 3 separate pathways, the JNK/SAPK cascade, the ERK cascade and the p38 cascade (as reviewed in: Basu & Kolesnick, 1998). The JNK/SAPK pathway is evolutionarily conserved, the cellular outcome as a result of it activation being context dependent, with apoptosis, cell proliferation and differentiation being observed. A simple model involves the sequential activation pathway of MEKK1, SEK1 and JNK/SAPK eventually leading to c-Jun phosphorylation. The upstream pathway of JNK/SAPK however is poorly understood, with numerous upstream protein activators identified. X-rays (10Gy), H_2O_2, UV-C, heat shock, TNFα, C_2-ceramide and bacterial SMase all induce a concentration dependent increase in SAPK/JNK activation in U937 cells and bovine endothelial cells resulting in apoptosis (Verheij *et al.*, 1996). Upstream activators include the apoptosis-signal-regulated kinase-1 (ASK-1), which signals

JNK/SAPK via MKK4 following TNF receptor stimulation. Dominant negative mutant ASK-1 blocks TNFα mediated apoptosis (as reviewed; Basu &Kolesnick, 1998; Kolesnick & Krönke, 1998). Alternatively, the cascade may couple to the adaptor protein DAXX, which associates with the death domain of the activated CD-95 receptor (Yang *et al.*, 1997). Expression of dominant negative p21 Ras or the small G-protein Rac1 in Jurkat T-cells completely inhibits C_2-/C_6-ceramide and CD-95L induced JNK/SAPK or p38 activation and apoptosis, but not CD-95 induced ceramide accumulation. This suggests both these small G proteins are downstream of intracellular ceramide accumulation and activate JNK/SAPK to induce apoptosis (Brenner *et al.*, 1997; Gulbins *et al.*, 1995), presenting a pathway that is paradoxical to the general consensus of Ras involvement in cell survival, proliferation and differentiation. The JNK/SAPK and p38 pathways also activate the transcription factor GADD153/CHOP following C_6-ceramide or CD-95L exposure of Jurkat T-cells. Prevention of GADD153 phosphorylation also abrogates CD95L and C_6-ceramide induced JNK/SAPL and p38 activation, suggesting they regulate the activity of this transcription factor (Brenner *et al.*, 1997). Expression of dominant negative c-Jun (TAM67) or a dominant negative kinase inactive construct in U937 cells inhibited JNK/SAPK activity and apoptosis due to C_2-ceramide or H_2O_2 exposure (Verheij *et al.*, 1996). However, inhibition of p38 in addition to JNK/SAPK was required to prevent both CD-95L and ceramide mediated apoptosis in Jurkat T-cells (Brenner *et al.*, 1997). Modur *et al.*, (1996) suggest that TNFα exposure of HUVECs leads to the activation of two signalling cascades, ceramide dependent and independent. Additionally, JNK pathway phosphorylates the transcriptional activation domain of ATF2, ELK-1 and cJun, alternatively, NFAT4 phosphorylation decreases its transcriptional activity. It should also be appreciated that the cellular

response to activation of the JNK pathway is cell type and context specific, with growth and differentiation being observed in addition to the induction of apoptosis described here. It is likely that different upstream protein mediators determin the cellular response to JNK activation (as reviewed in; Basu & Kolesnick, 1998; Kolesnick and Krönke, 1998).

Transient expression of dominant negative MEK-1 mutant in U937 cells, to inhibit signal transduction via ERK-1, does not affect short chain ceramide, H_2O_2, UV, ionising radiation, TNFα or CD95L induced apoptosis, and therefore signalling via this cascade is not required for ceramide induced apoptosis (Verheij *et al.*, 1996). To further the above observations, S1P was observed to stimulate ERK-1 cascade, counteracting or inhibiting JNK/SAPK mediated apoptosis following TNFα or synthetic short chain ceramide exposure of U937 cells, without affecting ceramide levels suggesting transmodulatory inactivation. However, TNFα was unable to inhibit ERK activated by S1P. Blockade of the ERK pathway with the selective inhibitor PD098059 removed the cytoprotective effect of S1P on the TNF mediated activation of JNK/SAPK. The described evidence is indicative of a dynamic balance between lipid metabolites from the SM cycle and their ability to activate opposing kinase cascades and determine life or death of the cell (Cuvillier *et al.*, 1996). TNFα via N-SMase or bacterial SMase application to HUVEC initiates proliferation and inflammatory gene expression by inducing autophosphorylation of the proline-directed serine/threonine specific ceramide activated protein kinase (CAPK). This protein consequently activates the ERK-1 cascade via Raf-1 to phosphorylate and activate transcription factor C/EBPβ, inducing elevated IL-6 and IL-8 expression (as reviewed in; Peña *et al.*, 1997). In HUVEC, where TNF induced a small increase in

ceramide, 20-30% above basal levels, protein expression was not enhanced, but initiated ERK cascade activation via Raf-1 and was mimicked by exogenously applied SMase that induced comparable elevations in ceramide. However, unlike TNFα, SMase induced ceramide accumulation did not activate NFκB, p38 or JNK suggesting that TNF receptor stimulation generates two signals in endothelial cells, Raf-1 and ERK cascade activation via a ceramide dependent pathway, and NFκB, p38 or JNK by a ceramide independent route (Modur *et al.*, 1996). Similarly, IL-1 induced ceramide formation in rat renal messangial cells leading to CAPK induced ERK activation (Huwillier *et al.*, 1996).

Activation of the phosphatidyl inositol pathway has been implicated in mediating proliferation of confluent rat 2 fibroblasts following C_2-ceramide, SMase or TNFα exposure; Phosphatidyl inositol-3-kinase (PI3K) activity increased 3-6 fold over basal levels following treatment with C_2-ceramide within 10 minutes, an effect seen within 20 minutes with TNFα or SMase exposure, leading to ERK kinase activation. Using the tyrosine kinase inhibitor genestein or fibroblasts expressing a dominant negative p21Ras mutant, complete inhibition of C_2-ceramide or bacterial SMase mediated PI_3K activation, or 70% of that mediated by TNFα has been observed. It can thus be concluded that ceramide may mediate in part the proliferative effects of TNFα, where activity is dependent on a tyrosine kinase and Ras_{GTP}, although this cytokine clearly activates an additional proliferative signal transduction pathway independent of ceramide and Raf-1. Conversely, C_2-ceramide induced proliferation depends absolutely on Ras_{GTP} (Hanna *et al.*, 1999). Opposing observations have been described by Zundel & Giaccia, (1998), who described that UVC and ionising radiation lead to ceramide generation, downregulating PI3K by 10-30% inhibiting

Akt and the subsequent phosphorylation of the pro-apoptotic factor Bad to mediate apoptosis of rat-1 MyC-ER cells. NPD fibroblasts deficient in A-SMase activity did not decrease PI3K activity and induce apoptosis in response to UVC and ionising radiation. Bypassing ceramide generation by the application of C_2-ceramide restored PI3K and Akt inactivation leading to apoptosis. In addition, expression of constitutively active forms of PI3K or Akt inhibited apoptosis induced by C_2-ceramide. These observations suggest that ceramide induces apoptosis by downregulating proliferative pathways, as well as upregulating the activation of apoptotic pathways (Zundel & Giaccia, 1998).

The conflicting evidence with regards kinetics of ceramide generation following TNFα or CD-95L exposure described in Section 1.0.3 has been attempted to be explained by the recruitment of various proteins to different domains of the intracellular C-terminal tail of these ligands respective receptors. Differing kinetics of ceramide formation are attributed to either N-SMase or A-SMase activity as observed in the nuclei free lysates of U937 cells exposed to TNFα for various time periods. P55TNF receptor mutants truncated by 32, 42, 52 or 81 amino acids were defective in A-SMase activation and also displayed loss of function phenotype to PC-PLC or $NF_{\kappa}B$ induction, but all retained their N-SMase activity, indicating that the domain responsible for N-SMase activation is N-terminal to residue 345 (Weigmann *et al.*, 1994). This region is termed the N-SMase domain (NSD) spanning 11 amino acids (Adam *et al.*, 1996). The WD repeat adaptor protein FAN binds to this region to activate N-SMase (Adam-Klages *et al.*, 1996). Ceramide produced via N-SMase triggers CAPK phosphorylation leading to initialisation of Erk-1 cascade and eventually increases intracellular PLA2 (Wiegmann *et al.*, 1994). Overexpression of

TRAFF or RIP does not activate A-SMase but induces NFκB activation (Schwandner *et al.,* 1998). The A-SMase domain, C-terminal to the NSD consists of a 75 amino acid region termed the death domain. Deletion of the death domain abolish TNF receptor induced apoptosis. Consequently, it is concluded that only ceramide produced via A-SMase mediates apoptosis, with a requirement for $NF_{\kappa}B$ (Wiegmann *et al.*, 1994; Adam-Klages *et al.*, 1996). Deletions in the death domain of the CD-95 receptor also abolish CD95L mediated apoptosis with inhibition of A-SMase (Hanna *et al.*, 1999). Despite producing the same lipid messenger, there is no apparent cross talk between the two ceramide sources. The death domain of the TNF and CD-95 receptors is a protein interaction domain, a conformational shift presumably leading to propagation of ligand modulated signal. The 34kDa, zinc finger protein TRADD (TNF receptor 1-associated death domain) associates with the p55TNF receptor death domain, in turn, FADD/MORT-1 (Fas-associated death domain) may bind to TRADD. In the case of CD-95 receptor stimulation, TRADD does not associate with the activated receptor, instead direct FADD receptor association occurs. FADD contains a protein/protein interaction domain in addition to death domain and can be consequently bind to ICE/ced-3-like protease FLICE/MACH-1 (caspase 8/a) to mediate an apoptotic response without the need for ceramide or other second messengers. Cotransfection of a crmA construct blocked caspase-8 overexpression induced apoptosis, whereas pharmacological inhibition of caspase-3 also inhibited TNFα induced apoptosis and A-SMase activity (Schwandner *et al.*, 1998). However, overexpression of dominant negative FADD was shown to block ligand induced ceramide generation and apoptosis, where ceramide analogues restored the apoptotic response. Signalling of the TNF receptor and CD-95 receptor via their respective death domains can mediate apoptotic signals that are ceramide dependent or

independent (as reviewed in; Beutler & Bazonni, 1998; Haimovitz-Friedman *et al.*, 1997; Kolesnick & Krönke). Activation of FLICE by these two cytokine receptors highlights a possible site of convergence of apoptotic signals (see Figure 1.3).

Downstream protein targets for endogenous ceramide identified through the application of short chain ceramides or agents which induce its formation include CAPP, proposed to be a phosphatase 2A (PP2A) family protease member (Chalfant *et al.*, 1999; Dobrowski *et al.*, 1993; N'Cho & Brahmi, 1999; Ruvolo, *et al.*, 1999), PKC ζ (Huwillier *et al.*, 1996; Müller *et al.*, 1995), the guanine nucleotide exchange factor Vav, potentially linking ceramide signalling to p21Ras (Gulbins *et al.*, 1995; Lozano *et al.*, 1994) and specific protein complexes that form the mitochondrial electron transport chain (Esposti & McLennan, 1998; Garcia-Ruiz *et al.*, 1997; Gudz *et al.*, 1997; Quillet-Mary *et al.*, 1997) potentially modulating cellular respiration and reactive oxygen species (ROS) production.

1.0.5 Reactive oxygen species (ROS) production: sources, effects and their influence on the redox state.

ROS are produced at a high rate in all mammalian cells as a by product of normal mitochondrial aerobic metabolism, the electron transport system (or respiratory chain) consuming 85-95% of O_2 utilisation by reducing it to water and generating energy necessary to synthesise ATP from ADP as a result of oxidative phosphorylation (as reviewed in; Fernández-Checa *et al.*, 1998) according to the equation

$$O_2 + 4e^- + 4H^+ \rightarrow 2H_2O$$

The continuous production of ROS results from approximately 1-2% of the O_2 consumed under normal conditions due to electron leakage. ROS comprise of oxygen moieties with unpaired electrons, for example the hydroxyl radical (OH·) and the superoxide radical ($O_2^{-}\cdot$), or moieties that have the ability to abstract electrons from other molecules such as H_2O_2 and HOCl. Additionally, ground state diatomic oxygen molecule (O_2) is itself a radical, with 2 unpaired electrons, each located in a π antibonding orbital. ROS are derived from specific segments of the electron transport chain, mainly the ubiquinone site at complex III, which catalyses the single electron transfer required for the conversion of O_2 to $O_2^{-}\cdot$, and at complex I from NADPH cytochrome P450 oxidase. The resulting $O_2^{-}\cdot$ can consequently produce other ROS. O_2 acts as the terminal electron acceptor for oxidative phosphorylation at complex IV (as reviewed in; Buttke & Sandstrom, 1994; Halliwell & Gutteridge, 1990). The electron transport chain consists of 5 protein complexes. Complexes I and II collect electrons from NADPH and succinate respectively and pass them to unbiquinone which is subsequently oxidised by ubiquinone cyochrome c oxidoreductase (complex III) and cytochrome c oxidase (complex IV). Excluding complex II, these complexes couple electron flow to proton pumping and the ensuing proton motive force is utilised by complex V (GoF1 H^+ ATP synthase) to form ATP from ADP. Each complex consists of different subunits where complexes I-IV have multiple redox active prosthetic groups. Ubiquinone (Co-enzyme Q) is the only non-protein component of the electron transport chain, capturing one or two electrons, thereby forming ubiquinol (hydroquinone). Since ubiquinone is not tightly bound to proteins,

it may play a strategic role as a mobile carrier of electrons, transferring them to cytochrome c and this is termed the Q cycle. In turn, cytochrome c shuttles electrons from complex III to Complex IV of the electron transport chain (see Figure 1.4). The electron transport chain is also found within the endoplasmic reticulum (ER), where the reduced form of NADPH cytochrome P450 reductase leaks electrons to O_2 reducing it to $O_2^{-}\cdot$ while nuclear membranes also contain an electron transport chain (as reviewed in; Cross & James, 1991).

As the requirement for energy increases, so does the amount of $O_2^{-}\cdot$ produced as a consequence of leakage from the electron transport chain due to enhanced metabolism. However, $O_2^{-}\cdot$ is not lipid soluble and does not mediate lipid peroxidation but can be toxic especially via the interaction with proteins that contain iron sulphur centres such as succinate dehydrogenase, mitochondrial NADPH-ubiquione oxidoreductase and aconitase. In aqueous solutions, $O_2^{-}\cdot$ is extensively hydrated and much less reactive, undergoing a dismutation reaction at physiological pH catalysed by the enzyme superoxide dismutase (SOD) according to the equation

$$2\ O_2^{-}\cdot + 2H^{+} \rightarrow H_2O_2 + O_2$$

which is the sum of the two equations

$$O_2^{-}\cdot + H^{+} \rightarrow HO_2\cdot$$

$$HO_2\cdot + O_2^{-}\cdot + H^{+} \rightarrow H_2O_2 + O_2$$

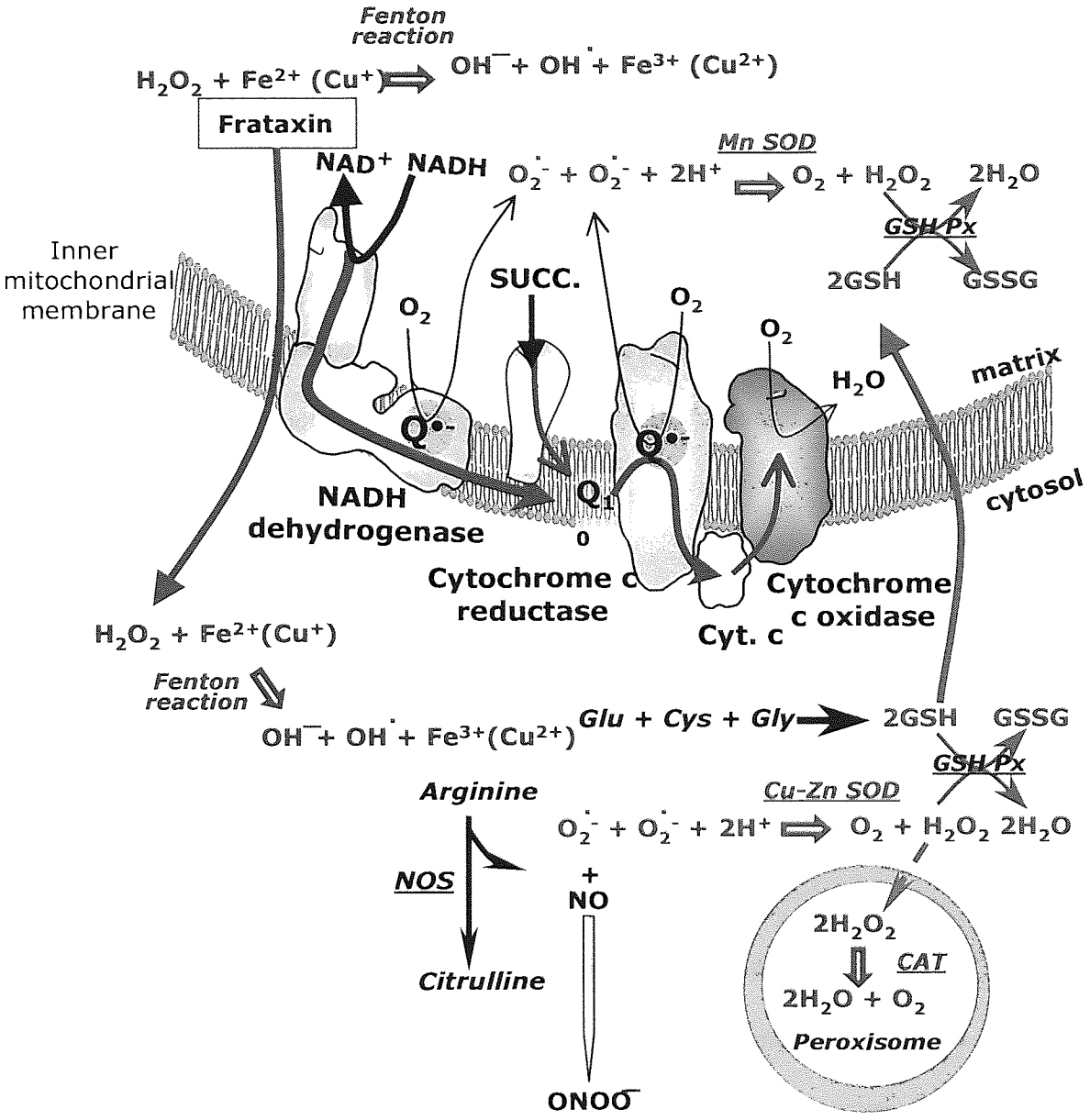

Figure 1.4. Putative sites of reactive oxygen species (ROS) formation and their associated detoxification pathways. Shown is a simplified schematic of the various components of the mitochondrial electron transport chain and sites of ROS production. Abbreviations used; Catalase, CAT; Copper/Zinc superoxide dismutase, Cu-ZnSOD; glutathione, GSH; oxidised glutathione, GSSH; glutathione peroxidase, GSH Px; manganese superoxide dismutasse, MnSOD; nitric oxide synthase, NOS; Superoxide dismutase ,SOD; Adapted from Jackson *et al.*, (2002).

SOD catalyses this reaction 4 fold, but at the expense of producing the ROS, H_2O_2. H_2O_2 itself is relatively stable and has limited reactivity, but can freely diffuse across biological membranes which $O_2^{-}\cdot$ can only do so slowly, unless an anion channel is present as in the erythrocyte membrane or vascular endothelial cells. However, due to the ease of diffusion, H_2O_2 may lead to the production of more free radical species in the presence of catalytic metal ions. Similarly H_2O_2 generated within the cell can continuously traverse across membranes to the extracellular fluid and be constantly lost due to the action of catalase (as reviewed in; Evans *et al.*, 1997; Halliwell & Gutteridge, 1990; Raha & Robinson, 2000).

The moderate reactivity of $O_2^{-}\cdot$ or H_2O_2 in an aqueous solution makes it unlikely that damage observed from oxidative insult by these ROS can be directly attributed to their presence alone. Any damage may be due to their conversion to more reactive species (as reviewed in; Evans *et al.*, 1997).

The hydroperoxy radical ($HO_2\cdot$) is produced by the protonation of $O_2^{-}\cdot$, but at physiological pH, only 0.025% of $O_2^{-}\cdot$ exists as $HO_2\cdot$ and therefore its role as a cytotoxic molecule in biological systems is doubtful. However, it may be an important damaging species in acidic compartments (as reviewed in; Evans *et al.*, 1997).

The hydroxyl radical ($OH\cdot$) is formed by the degradation of H_2O_2 in the presence of catalytic metal ions. It is highly reactive and therefore reacts close to its site of formation eliciting site-specific damage. The biological implications for the specificity of $OH\cdot$ formation are profound. The major determinant of the actual

toxicity of H_2O_2 may be the availability or location of metal ion catalysts for OH· formation by the Häber-Weis reaction according to the general equation

$$M^{n+} + H_2O_2 \rightarrow M^{n+1} + OH\cdot + OH^-$$

Where M^{n+} equals a metal ion, for example copper (I), or, when equal to Iron (II) is termed the Fenton reaction. Consequently, OH· generated by this mechanism in free solution attacks targets randomly and would produce damage of different degrees and nature to that of OH· formation at a site of bound metal ions. Reactions of OH· with susceptible biological molecules can produce another radical species with lower reactivity, which may induce further oxidative reactions by diffusing away from the site of formation and attacking specific biomolecules initiating an oxidation chain reaction. The formation of OH· observed in systems generating $O_2^{-}\cdot$ is inhibited by catalase or SOD. The catalase effect not being surprising as OH· formation is due to the metal ion catalysed splitting of H_2O_2. It remains to be determined whether apoptosis is, at least in part triggered by H_2O_2, or by the formation of the more highly reactive OH· (as reviewed in; Halliwell & Gutteridge, 1990)

Nitric oxide (NO) is a lipophilic molecule with a half life of between 6 and 30 seconds under anaerobic conditions. Its reaction with O_2 forms nitrogen dioxide which rapidly dispoportionates to nitrite and nitrate in aqueous solutions of neutral pH. The potential for NO to react with biological targets is poor owing to its short half life and propensity to react with O_2. However, the simultaneous production of NO and $O_2^{-}\cdot$ within close vicinity to one-another leads to their rapid reaction to produce the potent oxidising and highly diffusible products peroxynitrite and

peroxynitrous acid (see Figure 1.4). Peroxynitrite is itself short lived, but displays far more reactivity than either of its precursors or H_2O_2 readily reacting with proteins, non-protein thiol groups and non-ionised sulfhydryls (as reviewed in; Evans *et al.*, 1997; Murphy *et al.*, 1998).

While the electron transport chain of the mitochondria and those of the ER and nucleus have been described in detail here, other sources of ROS exist within the cell. These include, the NADPH oxidase system located within the plasma membrane and is particularly prevalent within leukocytes. Here NADPH acts as an electron donor, converting molecular oxygen to $O_2^{-}\cdot$ according to the equation

$$NADPH + H^{+} \rightarrow NADP^{+} + H^{+} + O_2^{-}\cdot$$

followed by the dismutation of $O_2^{-}\cdot$ to H_2O_2 as described earlier. Additionally, ROS are formed from hypoxanthine/xanthine oxidase, lipoxygenase, cyclooxygenase and the recently reported gamma-glutamyltranspeptidase systems (as reviewed in; Gabbita *et al.*, 2000; Sauer *et al.*, 2001).

ROS readily react with cellular macromolecules either damaging them directly or setting in motion a chain reaction, where a free radical is passed from one macromolecule to another resulting in extensive damage to cellular structures such as membranes (as reviewed in; Buttke & Sandstrom, 1994). Consequently, cells possess valuable defence systems to cope including the enzymes catalase, SOD, glutathione peroxidase (GSH Px) and thioredoxin (Thx) reductase. Tocopherols, carotenoids and ascorbic acid are able to block free radical chain reactions, while lactoferrin,

transferrin and caeruloplasmin are a group of agents which sequester transition metals involved in catalytic formation of ROS (as reviewed in; Buttke & Sandstrom, 1994).

In humans there are 3 forms of SOD; cytosolic CuZn SOD, MnSOD localised to the mitochondrial matrix and extracellular SOD. $O_2^{-}\cdot$ produced at the cytosolic side of the inner mitochondria membrane can be converted to H_2O_2 by cytosolic CuZnSOD. MnSOD scavenges $O_2^{-}\cdot$ essentially produced at the matrix side of the inner mitochondria membrane within the matrix (see Figure 1.4). Removal of MnSOD leads to the enhanced production of $O_2^{-}\cdot$ and other species. Where the overexpression of CuZnSOD was hypothesised to enhanced life expectancy of mice, $O_2^{-}\cdot$ was detoxified with the consequence of elevating peroxide products to mediate toxicity. Consequently CuZnSOD overexpressing mice showed no increased life expectancy but were more susceptible to infection and radiation. In transgenic drosphila, enhancement of life expectancy was only observed when CuZnSOD overexpression was accompanied by elevated catalase expression to detoxify H_2O_2 (as cited in; Raha & Robinson, 2000).

While catalase represents a method of cellular detoxification of H_2O_2 to H_2O and O_2 when this species diffuses into peroxisomes (see Figure 1.4), the primary route for the detoxification of H_2O_2 is via the oxidation of the thiol glutathione (GSH) within the GSH redox cycle catalysed by the enzyme GSH Px. As a result, oxidised GSH (GSSG) is formed. Rejuvenation of GSH regenerated from GSSG by the energy dependent process at the expense of NADPH is catalysed by the enzyme GSH reductase (GSH Rx; see Figures 1.4 & 1.5). A small concentration of the total cytosolic pool is sequestered in the mitochondria by the action of carrier mediated

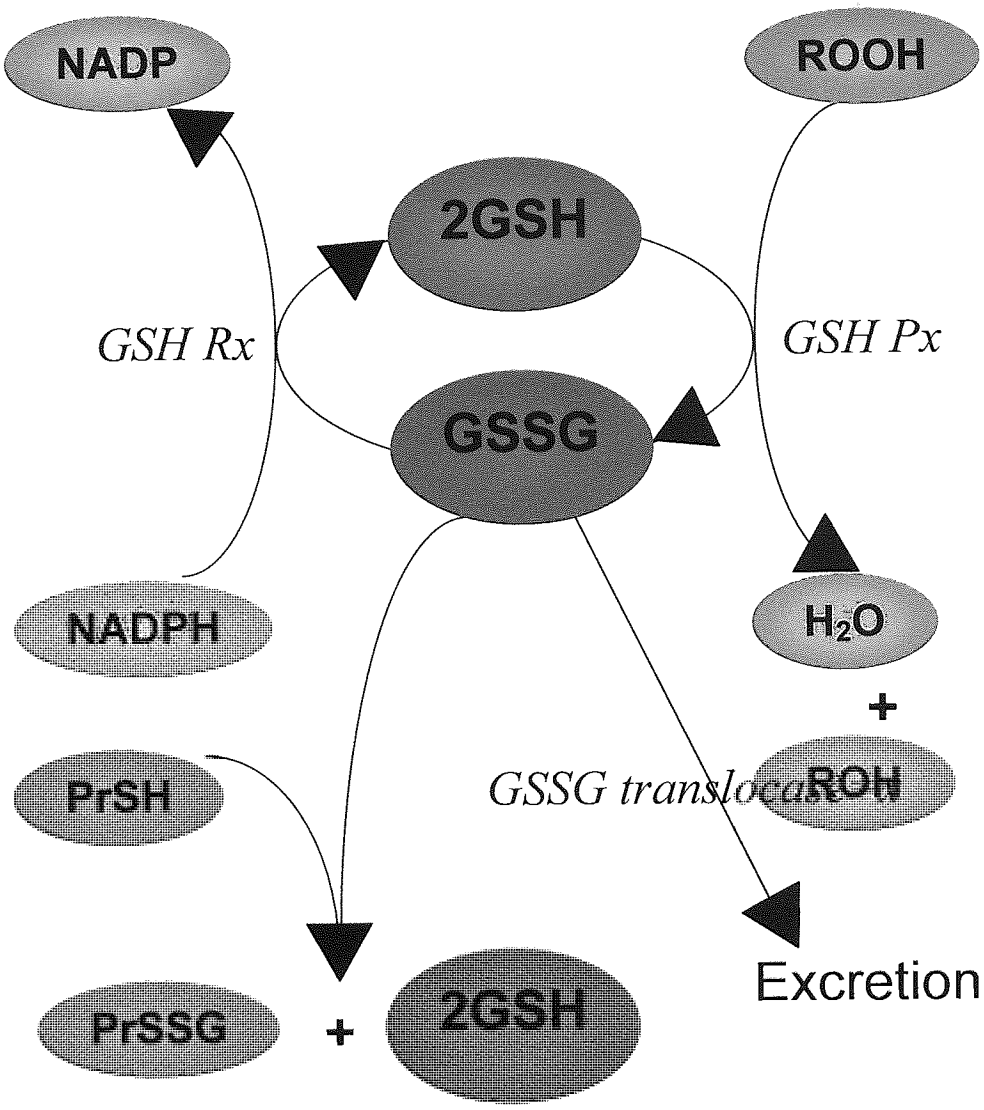

Figure 1.5. The glutathione redox cycle: The effects of hydroperoxides (ROOH) on cellular glutathione (GSH). The detoxification of ROOH to water and an alcohol moiety is catalysed by the enzyme GSH peroxidase (GSH Px) at the expense of GSH generating glutathione disulfide (GSSG). GSSG can be removed by several pathways; (a) the cellular excretion of GSSG catalysed by the membrane bound enzyme GSSG translocase, (b) coupling to proteins (PrSH) to generate a GSH-protein mixed disulphide (PrSSG) with the concomitant re-generation of GSH or (c) recycling to GSH via an energy dependent process requiring NADPH expenditure which is catalysed by GSH reductase (GSH Rx; adapted from Evans *et al.*, 1997).

transport from the cytosol to the matrix. The GSH redox cycle ensures that H_2O_2 production is kept to low levels thereby minimising the participation of this molecule in the Häber-Weiss reaction and the consequent formation of OH·. Concentrations of peroxide that exceeds the redox capacity of the GSG redox cycle result in the production of GSSG to exceed its reduction by GSH Rx. The resulting accumulation of GSSG can be detrimental primarily due to the enhancement in the formation of mixed disulfides with protein thiols leading to impaired protein function. Secondly, excessive GSSG can be exported to the extracellular environment leading to GSH depletion (see Figure 1.5), although ROS may compromise this export. Augmentation of the cellular GSH content serves to increase the detoxification of peroxide and prevent damage (as reviewed in; Evans *et al.*, 1997).

Thx is a small 12-kDa protein processing both thiol reducing and free radical scavenging properties. This protein contains a conserved catalytic region consisting of the amino acids Trp-Cys-Gly-Pro-Cys-Lys. The two cysteine molecules can form a reversible disulphide bridge upon oxidation, acting as a hydrogen donor due to NADPH-dependent disulphide oxidoreductase activity to reduce exposed disulphide bridges of oxidised proteins. Thx reductase, a selenoenzyme reduces oxidised Thx utilising NADPH as a hydrogen donor. Thus Thx displays dithiol to disulphide exchange activity (as reviewed in; Gabbita *et al.*, 2000; Raha & Robinson, 2000).

Oxidative overload mediated by physical or chemical trauma results in disturbances of the described defence systems leading to their saturation or destruction. Consequently, there is gross cellular damage and a number of pathological processes are induced, including lipid peroxidation, loss of Ca^{2+} homeostasis and alterations in

metabolic pathways (as reviewed in; Clutton, 1997). The detection of lipid peroxidation is often used to support the involvement of free radicals in toxicology and pathophysiology associated with human disease (as reviewed in; Halliwell & Gutteridge, 1990). Lipid peroxidation describes the process whereby multiple carbon double bonds of polyunsaturated fatty acids are subject to attack initiated by hydrogen primarily by $OH\cdot$ but not by $O_2^{-}\cdot$. As a consequence conjugated diene is formed which rapidly reacts with O_2 to form the peroxy radical $ROO\cdot$. This molecule is capable of abstracting $H\cdot$ from other fatty acids to initiate an autocatalytic free radical chain reaction.

Although extreme, non-physiological concentrations of oxidants or oxidant signalling agents cause necrosis, the majority of recent evidence is suggestive of a role for ROS and oxidative stress in the propagation of the apoptotic signal mediated by various stimuli, acting as signalling molecules or as initiators of damage themselves (as reviewed in; Gabbita *et al.*, 2001; Jacobson *et al.*, 1996). However, the involvement of ROS as signalling intermediates in T-cell proliferation appears to be rather more precarious and it is likely that rather than acting as direct signalling intermediates, they contribute to alterations in the cellular redox state thereby altering the function of intracellular proteins and transcription factors to subsequent stimuli thus manipulating gene expression. In the presence of mononuclear cells (MNC), PMA mediated the production of ROS within T-cells, which was enhanced by co-stimulation with the Ca^{2+} ionophore A23187 or anti-CD3 MoAb and was associated with enhanced IL-2 release and proliferation. Similarly, anti CD3 MoAb synergised with PMA to induce T-cell proliferation and IL-2 release prior to ROS production. However, a 100 fold higher dose of ascorbic acid was required to prevent

proliferation and IL-2 generation than was required to totally ameliorate ROS production. Furthermore, while CD28 stimulation mediated a small rise in ROS production it did not synergise with PMA dependent IL-2 secretion or proliferation. In addition, while anti-CD3 MoAb synergised with PMA to enhance proliferation and IL-2 secretion in isolated T-cells *in vitro*, ROS production was not upregulated. This data implies an input from signal from accessory cells is required for efficient T-cell activation. It is likely that monocytes provide CD2 stimulation via the ligand CD58, however, while inducing ROS production in the presence or absence of anti-CD3 MoAb, CD2 stimulation inhibited proliferation and IL-2 release (Tatla *et al.*, 1999).

1.0.6 Mitochondrial involvement in apoptosis.

Mitochondria have a dual function, as suppliers of energy required for cell viability, and as key players in stress by inducing changes in redox potentials, direct oxidative effects and protease activation. The mitochondria is a major intracellular organelle whose function is compromised in apoptosis and it is thus not surprising that it plays a critical central role as a determinant of cell survival. The mitochondrial permeability transition (MPT) appears to control apoptosis. MPT is a candidate for the central "executioner," allowing convergence of a variety of diverse apoptotic signals into one downstream event to mediate the morphology observed when a cell is described as apoptotic (as reviewed in; Fernández-Checa *et al.*, 1998). The term refers to the opening of large pores within the mitochondrial inner membrane permitting the free diffusion of substances with a molecular weight of less than 1.5kDa. Consequently, the equilibrium of ions and respiratory substrates between the

cytosol and mitochondrial matrix transcends into loss in the mitochondrial transmembrane potential ($\Delta\Psi m$). The reduction in $\Delta\Psi m$ is responsible for a defect in the maturation of mitochondrial proteins synthesised in the cytoplasm, cessation of mitochondrial translation and uncoupling of oxidative phosphorylation coupled with GSSG depletion (as reviewed in; Mignote & Vayssiere, 1998). $\Delta\Psi m$ may mark the point of no return in the apoptosis signal transduction and it is only after $\Delta\Psi m$ has fallen are mitochondrial ROS generated (Zamzami *et al.,* 1995). MPT leads to the release of three mitochondrial pro-apoptotic factors: the 15kDa cytochrome c (Susin *et al.*, 1997) which acts together with other cytosolic factors to induce apoptosis, the 50kDa protease presumed to be the protein apoptosis inducing factor (AIF), which may be an individual inducer of apoptosis and Smac (second mitochondria-derived activator of caspase) or DIABLO (direct IAP binding protein with low PI) which bind to inhibitors of apoptosis proteins (IAP) preventing the sequestration of capases (Cuvillier & Levade, 2001; Du *et al.*, 2000). AIF liberated from the mitochondria undergoing MPT may enagage in self-amplification, and further exacerbate MPT therefore locking the cell in an irreversible state of apoptosis. The application of purified AIF to isolated nuclei induces DNA fragmentation, indicating AIF is capable of inducing nuclear apoptosis without the need for signalling intermediates, although it is capable of activating caspase-3 directly or via caspases-6 and –7 (Susin *et al.*, 1997). Although cytochrome c is loosely attached to the inner mitochondrial membrane, the mechanism of release to propagate an apoptotic signal is unknown. Once within the cytosol, cytochrome c activates caspase-3 (as reviewed in; Mignote & Vayssiere, 1998). Rather than mediating cyochrome c release, Cai & Jones (1998) speculate that $O_2^{-}\cdot$ is formed due to cytochrome c loss. Release of cytochrome c into

the cytosol is proposed to produces a gap between complexes III and IV of the e-transport chain leading to electron leakage (as reviewed in; Cai & Jones, 1998).

There is a wealth of data implicating the mitochondria as central sites for the induction of ROS generation and subsequent alteration in the cellular redox state mediated by physiological, pharmacological or environmental stimuli. There is an essential requirement for mitochondrial ROS generation in the apoptotic response to TNFα treatment directly observed following enhanced fluorescence of oxidant sensitive probes or the amelioration of apoptosis by anti-oxidants, scavengers of free radical species or metal ion chelators (Goossens *et al.*, 1995; Schulze-Osthoff *et al.*, 1992). Murine L929 cells and U937 monocytes deficient in mitochondria respiration are resistant to the induction of apoptosis by TNFα associated with an inability to generate ROS (Schulze-Osthoff *et al.*, 1993; Zamzami *et al.*, 1995). Furthermore, where electron flow through the respiratory chain is prevented by inhibitors of complexes I and II, TNFα induced ROS production and apoptosis was reduced (Schulze-Osthoff *et al.*, 1992; Hennet *et al.*, 1993).

1.0.7 The role of caspases in apoptosis.

Caspase activation is a requirement for the induction of the apoptotic signal mediated by a variety of agents (Cuvillier *et al.*, 1998; Genestier *et al.*, 1998b; Schwandner *et al.*, 1998; Tepper *et al.*, 1999). It is the general consensus that caspases are divided into two groups. Activator/initiator caspases, for example caspases-2, -8, -9 and –10 are proposed to couple to the cytoplasmic domains of the TNF receptor family (see

figure 1.3; as reviewed in; Harmovitz-Friedman *et al.*,1997; Mathias *et al.*, 1998). These caspases have a large pro-domain containing motifs for protein-protein interactions (as reviewed in; Green & Kroemer, 1998). Effector or executioner caspases, for example caspase-3/CPP32, -6 and –7/mch3, act distal in this signalling cascade, often downstream of the mitochondria (Genestier *et al.*, 1998b), and target a variety of substrates including the DNA repairing enzyme poly (ADP-ribose) polymerase (PARP; 116kDa) cleaving it to its 89kDa fragment, and nuclear lamins. Lamin degradation is required for packaging of condensed chromatin into apoptotic bodies (as reviewed in; Green & Kroemer, 1998). Often cleavage of either of these two proteins is used as a marker for induction of apoptosis.

TNFα or CD-95L exposure of Jurkat T-cells induces caspase-8/FLICE recruitment to FADD (Genestier *et al.*, 1998b) which is associated with these receptors death domain (DD). It is proposed that caspase-8 recruitment links the TNF and CD95 receptors to A-SMase to induce ceramide formation, or sequential activation of a caspase cascade. This caspase cascade is proposed to signal either via the mitochondria or independently of the mitochondria to induce apoptosis (see Figure 1.3; as reviewed in; Kolesnick & Krönke, 1998). Caspase mediated alterations in mitochondria structure and function that is associated with apoptosis is independent of $Bcl\text{-}_2$ (Susin *et al.*, 1997). Purified caspases from CD95L treated cells induced MPT, mitochondrial swelling, $\Delta\Psi m$ loss and AIF release of isolated mitochondria (Susin *et al.*, 1997). Caspase-8 activation is inhibited by the cow pox virus product and potent caspase inhibitor cytokine response modifier A (CrmA) and the pan caspase inhibitor zVAD-fmk and as a consequence prevents ceramide accumulation and ensuing apoptosis in response to CD95L or TNFα (Cuvillier *et al.*, 1998; Dbaibo

et al., 1997; Genestier *et al.*, 1998b; Tepper *et al.*, 1999). However, zVAD-fmk does not inhibit etoposide or ionising radiation induced apoptosis or ceramide generation (Tepper *et al.*, 1999). Further, zVAD-fmk does not prevent loss in $\Delta\Psi m$ induced by synthetic ceramide. Caspase-3 inhibition with the inhibitor Ac-DEVD.CHO ameliorates both TNFα and CD95L induced apoptosis with no effect on A-SMase and consequent ceramide generation. Further caspases-1 and –3 do not inhibit the reduction of $\Delta\Psi m$ or NADPH loss in response to CD95L or C_2-cerammide, etoposide or ionising radiation (Genestier *et al.*, 1998b; Petit *et al.*, 2001; Schwandner *et al.*, 1998; Susin *et al.*, 1997; Tepper *et al.*, 1998, 1999) suggesting they are positioned downstream of the mitochondria in the apoptotic signalling cascades. Caspase-9 activation, positioned downstream of the mitochondria is proposed to induce ceramide accumulation in response to etoposide or ionising radiation and does not require caspase-3. Conversely, caspase-9 is only partially activated by CD95L (Tepper *et al.*, 1999). It is likely that the mitochondria act as an intermediate between the initiator and executioner caspases. In line with the SIP ceramide rheostat theory, S1P generated via a PKC mediated activation of sphingosine kinase, is also able to block caspase-3, -6 and –7 activation and suppress apoptosis, although S1P does not inactivate caspase-8. Therefore, the proliferative sphingolipid S1P may balance the apoptotic effects induced by ceramide generation downstream of initiator caspases, but upstream of execution caspases (Cuvillier *et al.*, 1998).

1.0.8 Bcl-$_2$: a regulator of apoptosis at the level of the mitochondrion.

The Bcl-$_2$ family member consist of both pro-apoptotic, e.g. Bcl-$_2$, Bcl-x_l and anti-apoptotic proteins, e.g. Bax, Bad, which are differentially regulated yet share sequence homology. The prototypic member, Bcl-$_2$, is the most widely studied and was initially discovered as the gene abnormally expressed due to the t(14-18) translocation associated with lymphoma leading to the blockade of apoptosis induction. Sequence analysis of Bcl-$_2$ family members reveals a shared hydrophobic amino acid motif at the C-terminus which is responsible for membrane localisation. Bcl-$_2$ itself is specifically localised to the mitochondria, close to the site of ROS generation via the electron transport chain (as reviewed in; Evans *et al.*, 1997; Green & Kroemer, 1998; Voehringer & Meyn, 2000). Hockenbury *et al.*, (1993) first suggested that Bcl-$_2$ functions in an anti-oxidant like manner. Bcl-$_2$ overexpression protected cells from H_2O_2 and menadione, an inducer of intracellular $O_2^{-}\cdot$, induced cell death, but did not prevent the elevation in cyanide resistant oxygen consumption generated by menadione. Bcl-$_2$ overexpression did not affect e- transport through the respiratory chain followed by an oximeter, with no effect on oxidative phosphorylation since ATP and NAD^+ levels remained unaltered. Furthermore, dexamethasone induced cell death and lipid peroxidation prevented by Bcl-$_2$, but does not suppress ROS production (Hockenbery *et al.*, 1993). Bcl-$_2$ expression actively enhanced the basal levels of H_2O_2, which in turn induced an elevation in the intracellular levels of antioxidants. As a consequence, the larger increase in ROS induced by TNFα or synthetic ceramides was prevented and inhibited apoptosis. It is proposed that the elevation in basal ROS generation derives from increased levels of NADPH present in Bcl-$_2$ expressing cells and maintains iron sulphur clusters of

mitochondria redox enzymes such as those at complex I in a reduced steady state. In Bcl-$_2$ expressing cells, the ROS generated in response to TNFα or synthetic ceramide was lower than that induced in parental cells (Esposti *et al.*, 1999). Not surprisingly due to its mitochondrial location, Bcl-$_2$ expression does not affect endogenous ceramide formation in response to the chemotherapeutic agent vincristine in ALL-697 leukaemia cells (Zhang *et al.*, 1996), TNFα or the topoisomerase inhibitor captothecin in MCF-7 breast carcinoma cells (El-Assad *et al.*, 1998). Apoptosis mediated by synthetic short chain ceramides in ALL-697 and Daudi human B-lymphoma cells is prevented by Bcl-$_2$ overexpression but does not affect ceramide induced *Rb* dephosphorylation and the ensuing G0/G1 growth arrest in Molt-4 cells (Esposti *et al.*, 1999; Zhang *et al.*, 1996). Bcl-$_2$ expression also inhibits the mitochondrial alterations associated with apoptosis such as cytochrome c release, loss of $\Delta\Psi$m, PMT formation and loss of NADPH (Petit *et al.*, 2001; Zamzami *et al.*, 1996) and activation of the downstream execution caspase-3 by TNFα (El-Assad *et al.*, 1998). Furthermore, HeLa cells overexpressing Bcl-$_2$ show reduced GSH efflux (Meredith *et al.*, 1998).

Unlike Bcl-$_2$ expression, the anti-apoptotic factor Bcl-x$_l$ inhibits TNFα induced apoptosis, by prevention of ceramide accumulation and caspase-8 activation, therefore is situated upstream of ceramide formation and caspase-8 recruitment to the DD of the 55kDa TNF receptor. Further, the addition of short chain synthetic ceramides bypasses the Bcl-x$_l$ anti-apoptotic effect (El-Assad *et al.*, 1998). This data is suggestive that at least in human MCF-7 breast carcinoma cells, Bcl-$_2$ and Bcl-x$_l$ are not interchangeable. In addition to redox regulatory properties, Bcl-$_2$ family of proteins have been proposed to function as docking proteins, existing as homo- or

heterodimers whereby the interaction with pro- and anti-apoptotic members is critical in determining cellular fate. Wang *et al.*, (1996) reported that the small G-protein Raf-1, a kinase involved in proliferative signalling, can be translocated to the mitochondria initiating signalling that phosphorylates and inactivates Bad, dissociating it from $Bcl\text{-}_2$. In the absence of phosphorylation, Bad induces apoptosis by forming heterodimers with $BCL\text{-}x_l$ and $Bcl\text{-}_2$ and concomitant Bad homodimers. Alternatively, $BCl\text{-}_2$ family member have been proposed to form functional channels when added to synthetic membranes in vitro. It is proposed that Bax translocates from the cytosol to the mitochondria where it forms pores permitting the release of cytochrome c. $Bcl\text{-}_2$ and $Bcl\text{-}x_l$ may form small conductance channels in mitochondria membranes to counteract the effect of Bax, maintiaining electrical homeostasis and membrane integrity or, alternatively prevents pore formation by Bax (as reviewed in; Voehringer & Meyn, 2000). Therefore, pro-apoptotic family members are ubiquitously expressed and cell survival requires their continuous inhibition.

1.0.9 Inflammatory disease.

Cells of the circulatory and immune system are distributed through the body as non-adherent cells via the blood and lymphatic system, and migrate through the endothelium as adherent cells. The rapid transition between adherent and non-adherent states is of key importance to the immunological function of these cells. In the presence of foreign bodies, pathogens and antigens or at sites of injury, cells of the immune system congregate in the lymphoid organs, or cross endothelium and

basement membranes to accumulate at the site of infection. This process requires the up-regulation of cell adhesion, but under conditions of vascular and inflammatory disease becomes deregulated due to chronic stimulation. Enhanced recruitment to the endothelium, and subsequently migration into subendothelial tissues is a characteristic trait of diseases such as atherosclerosis, RA and inflammatory lung disease (as reviewed in; Lum & Roebuck, 2001; Ross, 1999; Springer 1990). The enhancement of adhesion at specific sites of the vascular system particular to the disease type is associated with an elevated activation status of the endothelial cells and circulatory cells, mediated by the pro-longed exposure to oxidants, cytokines such as IL-1α, IL-1β, TNFα and chemokines. Each is capable of enhancing the expression of other pro-inflammatory cytokines in an autocrine and paracrine manner thereby forming a positive feedback loop of inflammation leading to the escalation in the severity of disease and deterioration of human health (as reviewed in; Feldman & Maini, 1999; Koybayashi *et al.*, 1999; Odeh *et al.*, 1997). The physical means by which cell-cell interaction occurs is governed by the association of adhesion molecules expressed upon the vascular endothelium and their counter receptors present on the surface of leukocytes. The number and conformation of these molecules is dictated by the activation state of the cell in which they are expressed and therefore, regulated by the presence of cytokines and oxidants. Elevated levels of adhesion molecules are allied with atherosclerosis (Davis *et al.*, 1993; O'Brien *et al.*, 1993, 1996;) and rheumatoid arthritis (RA; Koch *et al.*, 1991; Lioté *et al.*, 1996; Saki *et al.*, 1992; Veale *et al.*, 1993). Consequently, the development of pharmacological agents that reduce the expression of proteins associated with adhesion either on circulatory cells or the endothelium, disrupt the cytokine/oxidant feedback loop, or

agents that directly inhibit cell-cell interaction is of primary importance for the clinical management of inflammatory diseases of vascular origin.

One of the hallmarks of RA is the increased infiltration of leukocytes from the synovial capillary system into the synovium of infected joints where 30% of the accumulating leukocytes are T-cells. In addition to the enhanced infiltration, the persistence and hyporesponsiveness of the synovial T-cells contribute to the histology of increased cellularity (as reviewed in; Arend, 1997; Feldman, 2001). This aetiology is indicative of an inability to apoptose, despite a T-cell phenotype that is suggestive of apoptosis (Salmon *et al.*, 1997) and therefore is symptomatic of a defect in the intracellular signalling pathways that mediate the cellular response of apoptosis. Indeed, unstimulated T-cells from BALB/c mice with proteoglycan (PG) induced arthritis constitutively express Fas-like IL-1β-converting enzyme-inhibitory protein (FLIP) which impairs activation of the execution capases –3 and –8 (Zhang *et al.*, 2001), while peripheral blood T-cells from RA patients show a reduced ability to mobilise $[Ca^{2+}]$ from intracellular stores compared to normal peripheral blood T-cells upon T-cell receptor (TCR) activation (Carruthers *et al.*, 1996). Furthermore, freshly isolated synovial T-cells from patients with RA express enhanced levels of the anti-apoptotic protein Bcl-x_l, which was associated with the lack of apoptosis observed within the synovium compared to those from gout patients, where significant synovial apoptosis was apparent (Salmon *et al.*, 1997).

A second histological feature of RA is synovial hyperplasia, whereby the synovial lining of affected joints undergoes expansion due to the accumulation of infiltrating cells and enhanced proliferation of fibroblast-like or macrophage-like synoviocytes.

The numerous cell types contained within the RA synovium contribute to its potent pro-inflammatory environment, generating numerous cytokines and growth factors, which eventually induce bone and cartilage damage resulting in loss of joint function (as reviewed in; Feldman *et al.*, 1996; Cunnane *et al.*, 1998). The prognosis of this debilitating disease is one of pain, severe functional decline as the disease spreads to involve multiple joints, an inability to work and premature death from infection, hematopoietic malignancies, cardiovascular disease, renal disease or treatment related complications (as reviewed in; Odeh, 1997). The first and second line treatment of RA only partially control the disease once established. Initial treatments involve non-steroidal anti-inflammatory drugs, and if symptoms fail to be alleviated, second line treatment evolves. Drugs used in the second line treatment of RA are often termed as disease modifying or remission inducing drugs, and include gold compounds, D-penicillamine, quinilones, sulfasalazine, and methotrexate (MTX). MTX represents one of the most effective agents, although its mechanisms of anti-inflammatory and immuosuppressive action, and thus control of the progression of RA, are ill understood. Current opinion regarding the mechanism of MTX action stem from its antagonism of dihydrofolate reductase (DHFR) to inhibit DNA synthesis and hence cell proliferation, and/or from its ability to induce the production of the natural anti-inflammatory agent adenosine (Genestier *et al.*, 1998a; Paillot *et al.*, 1998; da Silva *et al.*, 1995; as reviewed in; Allison, 2000; Genestier *et al.*, 2000). Initially, toxicity limited the use of this compound, however, it was noticed that the toxic effects early after MTX administration resembled that of folate-deficiency due to inhibition of DHFR. Subsequent co-administration of folic acid was observed to reduce toxicity without compromising MTX efficacy. Toxicities associated with the use of MTX include those of the liver, pulmonary system, may induce malignancies by

synergising with other carcinogenic compounds, teratogenecity and haematological toxicity, therefore continuous patient monitoring is required when this agent is prescribed (as reviewed in; Alarcón, 2000; Bondeson, 1997). Furthermore, long-term studies of RA patients treated with MTX describe that clinical improvement plateaus after six months treatment (Kremer & Phelps, 1992) and may be due to the development of resistance to MTX. Indeed, *in vitro* studies utilising the immortalised human T-cell line, Jurkat T-cell, show that long-term culture induces a decrease in MTX uptake and a reduction in DHFR gene copy number (Hall *et al.*, 1997). The limitations of MTX (and other disease modifying drugs) for inducing long-term remission in RA exemplify the need to improve the present therapeutic regimens available either through the prevention of resistance to MTXs action or increasing its clinical efficacy without enhancing toxicity. A useful strategy to achieving this aim is to improve the understanding as to the mechanisms of action of MTX and other disease modifying drugs.

1.0.10 Hypothesis and aims.

The discussed evidence, mainly obtained from immortalised cell lines, describing a putative involvement of ceramide and ROS in the intracellular signalling cascades of circulatory cells of the immune system in response to physiological stimuli such as cytokines and growth factors is suggestive of their involvement in the pathophysiology of various inflammatory diseases. Furthermore, it is likely that the signalling capabilities of both endogenous ceramide and ROS are intimately related in that both are capable of regulating one another's formation and as a consequence,

manipulating signal transduction, gene expression and cellular response to various extracellular agents of physiological or pharmacological origins. Initially, the purpose of this work is to clarify the interplay between ceramide, intracellular ROS production and the redox state in mediating differential cellular responses *in vitro*. The enhanced recruitment of cells of the circulatory system to various tissues via interaction with the inflamed endothelium, and epithelium is regarded to be of primary importance in the development of multiple immune diseases including RA, atherosclerosis and acute and chronic respiratory lung disease. This pathology is associated with enhanced levels of pro-inflammatory cytokines and oxidative stress. The effects of altering the intracellular levels of ceramide and the redox state of leukocytes on their adherence to inflamed endothelium *in vitro* will be evaluated.

One of the hallmarks of the complex aetiology associated with RA is the enhanced cellularity of the synovium of diseased joints. A major cell type contributing to this histology are T-lymphocytes (T-cells), supplying approximately 30% of the total number of cells infiltrating the RA synovium. Their consequent persistence and hyporesponsivness to stimulation, despite their accumulation in a pro-apoptotic environment, is suggestive of a defect in the signal transduction to physiological agents. *In vitro* studies have emphasised both ceramide and ROS to be of particular importance in mediating the intracellular signals of extracellular stimuli of both mitogenic, pro-inflammatory and apoptotic origin, such as by those mediated by TCR, TNF or CD95 receptor stimulation. It is hypothesised that accumulation of T-cells within the RA synovial joint arises from altered endogenous levels of ceramide, its lipid metabolites and ROS. Furthermore, the hyporesponsiveness of these cells is proposed to be due to an inability to appropriately manipulate the levels of these

signalling intermediates in response to stimulation. Therefore, the purpose of this work is to examine the endogenous concentrations of both ceramide, a related metabolite DAG and ROS from T-cells obtained from patients diagnosed with RA according to the American College of Rheumatology criteria 1987 (Arnet *et al.*, 1988) compared to normal T-cells from consenting apparently healthy donors *ex vivo*. Further, the effect of TCR stimulation by phytohaematoglutinnin (PHA) exposure to RA T-cells *in vitro* on endogenous ceramide, DAG and ROS will be compared to those of normal T-cells.

The use of MTX in the second line treatment of RA is limited by the development of resistance that prevents continuation of the initial disease remission observed and associated toxicity. The mechanism by which MTX achieves radiological progression in RA is not completely understood. At present, its anti-inflammatory and immunosuppressive actions are thought to be mediated by growth suppression and the generation of the anti-inflammatory agent adenosine. The contribution of perturbations in the redox state to the mechanisms of MTX action has not been described. It is hypothesised that the generation of ROS is essential to the anti-inflammatory and immunosuppressive actions of MTX.

Chapter 2.0: Ceramide induced redox alterations.

This chapter summarises the current literature concerning the interrelationship between ceramides and the cellular redox state. Evidence is presented for the regulation of ceramide formation from sphingomyelin via the redox state through the action of N-SMase, and further, enhanced ROS formation following targeting of synthetic short chain ceramides to the mitochondria. Conflicting data demonstrating a lack of ROS involvement downstream of ceramides is also discussed. Consequently, the viability of ceramides induced ROS formation is questioned. The experiments presented here attempts to resolve the controversy behind redox involvement in ceramides signalling and suggest that ceramides differentially manipulates the cellular redox state within independent subcellular compartments. The methods section in this chapter gives a detailed description of the theories behind the major experimental procedures utilised throughout the thesis and subsequent methodologies from proceeding chapters are cross referenced to this.

2.1 Introduction.

The sphingolipid ceramide has been identified as an important, but not exclusive, signalling intermediate in the induction of cellular responses to a variety of agents. These include both physiological, e.g. TNFα (Gamard *et al.*, 1997; Liu *et al.*, 1998; Obeid *et al.*, 1993; Verheij *et al.*, 1996), interleukin-1β (IL-1β; Andrieu *et al.*, 1994; Huwiler *et al.*, 1996), CD-95 (APO-1/Fas; Cifone *et al.*, 1993; Gamard *et al.*, 1997; Gulbins *et al.*, 1995; Tepper *et al.*, 1997) and toxicological agents, e.g. hydrogen peroxide (H_2O_2), heat shock, UV light, ionising radiation (Santana *et al.*, 1996; Verheij *et al.*, 1996), anticancer drugs (Boland *et al.*, 1997; Bose *et al.*, 1995; Herr *et al.*, 1997; Mansat-de Mas *et al.*, 1999) or the bacterial endotoxin LPS (MacKichan & DeFranco, 1999). Ceramide accumulation in response to extracellular agents appears to be driven either by the action of sphingomyelinases (SMase), catalysing the hydrolysis of sphingomyelin to ceramide (Cifone *et al.*, 1993; Liu *et al.*, 1998; Santana *et al.*, 1996; Wiegmann *et al.*, 1994) or through *de novo* ceramide generation via ceramide synthase (Boland *et al.*, 1997; Bose *et al.*, 1995). Downstream events, which vary according to cell type and stimulus, include apoptosis and proliferation, following activation of intracellular signalling cascades.

The application of cell permeable, synthetic ceramides or bacterial sphingomyelinase to a variety of cell types is able to induce the apoptotic (Herr *et al.*, 1997; Liu *et al.*, 1998; Mansat-de Mas *et al.*, 1999; Verheij *et al.*, 1996) and proliferative (Hanna *et al.*, 1999) responses supporting a cell type specific signalling role. Cell cycle arrest by dephosphorylation of the retinoblastoma gene product (Dbaibo *et al.*, 1995;

Jayadev *et al.*, 1995; MacKichan & DeFranco, 1999 Zhang *et al.*, 1996), differentiation (Ragg *et al.*, 1998), and senescence (Venable *et al.*, 1995) have also been observed upon cell treatment with synthetic ceramide. Further, synthetic ceramides activate protein targets such as the transcription factor NFκB (Müller *et al.*, 1995; Wiegmann *et al.*, 1994), PKCζ (Müller *et al.*, 1995), Ras (Gulbins *et al.*, 1995; Hanna *et al.*, 1999; Oh *et al.*, 1998), phosphatidyl inositol (PI) 3-kinase (Hanna *et al.*, 1999, Zundel & Giaccia, 1998), and the signalling cascades JNK/SAPK (Gulbins *et al.*, 1995; Verheij *et al.*, 1996) and ERK (Modur *et al.,* 1996) in a cell type dependent fashion. An important target for ceramide is the electron transport chain within mitochondria, where the ubiquinone pool is a critical target for production of ROS (as reviewed in; Andreieu-Abadie *et al.*, 2001).

ROS such as hydrogen peroxide (H_2O_2), participate in signal transduction, acting as second messengers to external signals where an increase in the intracellular levels of ROS can affect the activity of specific protein kinases and phosphatases (Dröge, *et al.,* 1994; Knebel *et al.*, 1996). Indeed, low concentrations of H_2O_2 induce apoptosis, activating the JNK signalling pathway (Verheij *et al.*, 1996) and NFκB (Hennet *et al.,* 1993; Um *et al.*, 1996). The application of various antioxidants, ROS scavengers and iron chelators protects against apoptosis induced by CD-95 (Um *et al.*, 1996), TNFα (Cossarizza *et al.*, 1995; Goossens *et al.*, 1995; Hennet *et al.,* 1993; Wong *et al.*, 1989; Yamauchi *et al.*, 1989) or chemotherapeutic agents (Mansat-de Mas *et al.*, 1999).

Considering that the endogenous cellular ceramide and ROS levels are elevated in response to similar if not the same external stimuli, and that the external application

of synthetic ceramides or the ROS, H_2O_2, induces the activation of common downstream protein targets, evidence is therefore suggestive that ROS and ceramide are intimately related. Indeed, recent observations are suggestive of a ROS association with ceramide at two levels; firstly, in regulation of ceramide metabolism and secondly as a putative mediator of ceramide signalling following disruption of the mitochondrial electron transport chain.

The intracellular antioxidant glutathione (GSH) reversibly inhibits the activity of neutral sphingomyelinase (N-SMase) but not A-SMase. Depletion of GSH by the application of L-buthionine-(SR)-sulfoximine (BSO) to Molt-4 human leukaemia cells induced a time dependent increase in SM hydrolysis accompanied by an elevation in intracellular ceramide associated with GSH loss (Liu & Hannun, 1997). Consequently, an alteration in cellular GSH levels by ROS may influence the cellular ceramide levels by loss of N-SMase regulation. Furthermore, in the breast carcinoma cell line MCF-7, where GSH depletion also promoted N-SMase activity, TNFα reduced the intracellular level of GSH followed by an elevation in the endogenous ceramide levels and SM hydrolysis resulting in cell death. Pre-treatment with GSH or NAC ameliorated the TNFα-induced SM hydrolysis, ceramide generation and apoptosis. Here, the application of bacterial SMase or short chain, synthetic ceramides did not alter the total cellular GSH levels. Furthermore, NAC or GSH pre-treatment did not protect MCF-7 cells from C_6-ceramide or bacterial SMase induced apoptosis. In light of these observations, it was suggested that TNFα induced GSH depletion occurs upstream of N-SMase inhibition and ceramide generation (Liu *et al.*, 1998). One could speculate that the elevation in endogenous ceramide levels observed in U937 monocytes following exposure to H_2O_2 (Verhiej *et al.*, 1996) is due

to the removal of the inhibitory role of GSH over N-SMase. Overall, these studies highlight the existence of a redox dependent and independent pathway in the regulation of ceramide generation involving N-SMase and A-SMase respectively.

The mitochondria act as a convergence point for multiple signals of internal or external sources. As well as supplying energy to maintain cellular metabolism, this organelle is a major player in dictating the cellular stress response to stimuli by inducing changes in the redox potential of the cell, directing oxidative signalling and transducing upstream signals via the release of mitochondrial proteins. The mitochondria is a major organelle whose function is compromised during apoptosis and thus it is not surprising that it plays a critical central role as a determinant of cell survival and sensor of stress.

It is well established that the induction of apoptosis in various cells by TNFα requires, in part, the generation of ROS either as signal transduction molecules or inducers of direct cellular damage. TNFα exposure of various murine tumorgenic cell lines induces evidence of oxidative damage where $[GSH]_i$ is elevated coupled with enhanced oxidised GSH (GSSG), the formation of thymine glycols in DNA (Zimmerman *et al.*, 1989; Yamauchi *et al.*, 1989) and lipid peroxidation in rat mesangial cells (Böhler *et al.*, 2000). In addition, iron chelators such as desferroxamine, o-Phenanthroline or 2, 2' bipyrodine, anti-oxidants such as NAC, GSH, BHA or BHT, and MnSOD or catalase provide protection from TNF induced cell death (Cossarizza *et al.*, 1995; Liu *et al.*, 1998; Schulze-Osthoff *et al.*, 1992; Wong *et al.*, 1989; Yamauchi *et al.*, 1989).

ROS are produced at various sites within the cell, although the primary source appears to be via leakage of electrons from the mitochondrial electron transport chain during ATP production, as required for normal aerobic respiration, following the single electron transfer to molecular oxygen forming $O_2\cdot^-$ at complexes I and II. Its metabolism to other ROS and free radicals of various reactivities may mediate differential damage to proteins and lipids, or alter their function at various distances from the source of ROS production (as reviewed in; Buttke & Sandstrom, 1994; Evans *et al.*, 1997; Fernández-Checa *et al.,* 1998). To counteract the deleterious effects of ROS and free radical production as a consequence of electron leakage from normal respiration or to reduce the effects following their excessive production, the cell possesses several mechanisms for their detoxification (see Section 1.0.5; as reviewed in Evans *et al.*, 1997; Raha & Robinson, 2000). It is when the detoxification mechanisms become deregulated or exhausted that the full effects of ROS and free radicals became apparent. It is therefore the balance between detoxification pathways and ROS production which dictates a cellular response. Subtle shifts in the balance between pro- and antioxidant states of the cell could consequently alter gene expression via activation of redox sensitive transcription factors. Indeed, degeneration of mitochondrial ultrastructure and sequential dysregulation of its function precedes pronounced damage to other intracellular organelles and cell shrinkage. TNFα treatment of L929 cells lead to enhanced lucigenin fluorescence indicating elevated superoxide production. Electron flow analysis reveals TNFα to rapidly inhibit the mitochondria in its ability to oxidise succinate and NADH linked substrates at complex I and II. Inhibition of complex III of the mitochondria electron transport chain with antimycin A (A.A), preventing the flow of electrons from ubiquinone to cytochrome C potentiates the action of TNFα in

inducing superoxide formation and apoptosis whereas inhibition of complex I and II with amytal or thenoyltrifluoroacetone (TTFA) respectively inhibits TNF cytotoxicity and superoxide generation with only minor effects at complex IV (Schulze-Osthoff *et al.*, 1992; Hennet *et al.*, 1993). Collectively, these results are suggestive that TNF, via a signalling intermediate, targets the mitochondria to induce ROS production. Further, L929 cells lacking mitochondrial DNA to create mitochondrial respiratory deficient cells are resistant to the apoptotic effects of TNFα which is attributed to their inability to generate mitochondrial ROS (Schulze-Osthoff *et al.*, 1993). However, mitochondrial respiratory deficient U937 monocytes undergo apoptosis, albeit at a slower rate than respiratory competent U937 monocytes in response to TNFα treatment. Here, respiratory deficient cells manifest early $\Delta\Psi m$ loss, as normal U937s, preceding DNA fragmentation despite reduced ROS formation indicating that loss of mitochondrial function with or without ROS formation can induce apoptosis (Zimmerman *et al.*, 1995). Direct evidence for the enhancement of mitochondrial ROS production was obtained utilising the mitochondrial selective peroxide sensitive dye DHR123, where TNFα induced elevated fluorescence prior to cellular collapse. Blocking of GSH synthase or reductase did not affect ROS production in response to TNFα treatment, however depletion of both cytosolic and mitochondrial GSH lead to a 20 fold increase in ROS production in response to TNFα (Goossens *et al.*, 1995).

Corresponding to the putative role of ceramide as an intermediate in the propagation of TNF signalling, direct effects on the mitochondria have been reported by several authors utilising synthetic, short chain ceramides. Exposure of isolated rat liver mitochondria to C_2-ceramide induced marked swelling (de Gannes *et al.*, 1998)

although these observations were disputed by Garcia-Ruiz *et al.*, (1997). Exposure of U937 monocytes to high concentrations of C_6-ceramide led to a significant elevation in ROS production within 1 hour and increased further up to 3 hours post-stimulation, with the ensuing apoptosis inhibited by the anti-oxidants NAC and PDTC. Where U937 monocytes were mitochondria deficient, no elevation in ROS production was recorded. In a similar manner to the effects on ROS production by TNFα, complex I and II inhibitors rotenone or TTFA reduced ROS generation and apoptosis respectively, whereas A.A potentiated these two ceramide mediated events. It was consequently concluded that ceramide targets the mitochondrial electron transport chain distal to complexes I and II and before ubiquinone pool of complex III (Quillet-Mary *et al.*, 1997). Similar observations were described following treatment of isolated rat liver mitochondria with low concentrations of C_2-ceramide, where depletion of matrix GSH potentiated the C_2-ceramide mediated ROS generation. However, these effects were biphasic, since doses exceeding 5μM did not induce ROS production (Garcia-Ruiz *et al.*, 1997). Furthermore, the activity of purified complex III was inhibited in a concentration dependent manner by up to 93% in the presence of 20μM C_2-cermamide. These observations were reflected in HL60 cells that possessed reduced complex III activity after treatment with C_2-ceramide (Gudz *et al.*, 1997). More specifically, it is proposed that it is centre "o" of complex III of the electron transport chain, one of two Q reactions sites, with which ceramide interacts (Esposti & McLennan, 1998). The cytoplasmic region of complex III acts as a docking site for cytochrome c, by perturbing its conformation, ceramide not only enhances ROS formation but prevents cytochrome c shuttling. As a consequence, cytochrome C is released into the cytosol to act in a signalling capacity leading to caspase 3 activation and PARP cleavage (Amarante-Mendes *et al.*, 1998; Tepper *et*

al., 1997; Zang *et al.*, 1997). Conversely, Cai & Jones, (1998) speculate that superoxide is formed as a result of cytochrome C release and not as a cause. Cytochrome C shuttles electrons from complex III to complex IV, where O_2 is consumed. Ghafourifar *et al.*, (1999) hypothesise that ceramide directly interacts with high affinity for oxidised rather than reduced cytochrome c leading to its rejection from the mitochondria. The resulting gap in the arrangement of the mitochondrial electron transport chain between complexes III and IV leads to enhanced electron leakage.

A rather more confusing picture exists with regards the TNF superfamily member CD95 and its ability to induce redox alterations. Jurkat T-cells treated with CD95L induced an elevation in superoxide anion generation, as detected by flow cytometric evaluation of the emitted fluorescence of cells loaded with the superoxide sensitive dye hydroethidine, which was associated with loss of GSH (Petit *et al.*, 2001). Using chemiluminescence methodology various B and T lymphoid cell lines induced ROS production within 20 seconds of CD95L exposure which was maximal after 5-10 minutes, and declined thereafter. The NADPH oxidase inhibitor diphenylene iodonium prevented ROS generation suggesting that CD95 induces ROS generation via stimulation of the oxidase system (Suzuki *et al.*, 1998; Suzuki & Ono, 1999). These observations are supported from data obtained from the HL60 variant HL-525 where NAC and GSH inhibited CD95L induced apoptosis, but was not associated with the elevation in endogenous ceramide. However, TNF induced apoptosis in HL-60 cells was inhibited by the ceramide synthase inhibitor fumonsin B1 but was relatively unaffected by NAC or GSH pre-treatment (Laouer *et al.*, 1999). Normal human peripheral blood monocytes also responded to CD95L treatment with ROS

formation and apoptosis, both of which were inhibitable by antioxidants (Um *et al.*, 1996). Furthermore, neuroglioma cells overexpressing Cu or ZnMnSOD showed marked attenuation of CD95 induced apoptosis, whereas catalase treatment inhibited CD95 induced apoptosis of normal neurogliomas (Jayanthi *et al.*, 1999). However, A.A, rotenone or menadione did not affect CD95L induced apoptosis of Jurkat T-cells suggesting that mitochondrial ROS production is not a key event in CD95 induced apoptosis (Dumont *et al.*, 1999). Additionally, L929 cells expressing the CD95 receptor underwent CD95 induced apoptosis that was not inhibited by anti-oxidants (Hug *et al.*, 1994; Schulze-Osthoff *et al.*, 1994).

While the use of specific antagonists to the electron transport chain in whole cells treated with synthetic short chain ceramides support those data obtained from isolated mitochondria, equating these observations to specific cellular effects is more controversial. Uptake and partitioning studies of short chain synthetic ceramides show that when cells *in vitro* at a concentration of $2x10^6$/ml – $10x10^6$/ml are treated with concentrations of 1-20μM ceramide, the cellular concentration is similar to the observed alterations in endogenous ceramide. Further, given the propensity of ceramide to partition into biological membranes, consideration as to the concentration of membrane bound lipids rather than the bulk molar concentration of lipid in solution is required. For example, application of 20μM C_2-ceramide to a cellular suspension of $2x10^6$/ml will result in twice the membrane concentration if half the concentration of cells were used (as reviewed in; Hannun & Luberto, 2000). Where elevations in ROS production are described in response to short chain synthetic ceramides, these are achieved with a relatively high concentration of membrane lipid (Petit *et al.*, 2001; Quillet-Mary *et al.*, 1997) and occur in cells that already exhibit

signs of apoptosis (Esposti *et al.*, 1999) implying they occur as a consequence rather than a cause. Further, the use of antioxidants to detoxify the harmful ceramide induced production of ROS and ensuing apoptosis are inconsistent. U937 monocytes or MCF-7 breast carcinoma cell lines are not protected from short chain ceramide induced cell death by pre-treatment with the anti-oxidants GSH and NAC (Lee & Um, 1999; Liu *et al.*, 1998) whereas catalase antagonised the lethality of C_2-ceramide in WEHI 231 B cells (Fang *et al.*, 1995). Additionally, in U937 monocytes, C_2-ceramide did not enhance the fluorescence of the cytosolic peroxide sensitive dye DCF (Lee & Um, 1999). What is more, it is difficult to understand how enhancement of ceramide either at the plasma membrane or within lysosomal compartments is able to access the mitochondria. Indeed, natural ceramide formed or introduced into lysosomal or endosomal compartments appear to be unable to escape (Chatelut *et al.*, 1998).

Clearly, the extent of the interrelationship between ceramide and ROS production, and the potential for mediating diverse outcomes including proliferation, growth arrest and apoptosis remain unclear. It is hypothesised that the differences in the cellular responses to elevations in the intracellular ceramide levels reported by several authors is related to differential redox altering properties. Consequently, the effects of C_2- or C_6-ceramide on the cell cycle using two cell models, the acute T-cell leukaemia line, Jurkat T-cell, and human monocytic cell line, U937, in the context of mitochondrial peroxide production, the effect on cytosolic peroxide and cellular glutathione were examined. The observations obtained from cell lines were compared with those of primary human cells of identical lineage. Further, the redox altering properties of the proposed mediator of ceramide accumulation in leukocytes,

CD95L, was also investigated. In light of the data presented here, it is reasoned that the elevation of the cellular ceramide concentration in response to CD95L induces the differential disruption of the cellular redox state at multiple distinct sites, the extent of which contributes to the cellular response.

2.2 Materials and methods.

2.2.1 Materials.

All reagents were obtained from Sigma Chemical Company (Poole, UK), solvents were from Fisher (Loughborough, UK) and all gases from BOC Ltd (Guildford, UK) unless otherwise stated. RPMI 1640, foetal bovine serum and penicillin (1000U/ml)/streptomycin (10,000μg/ml; P/S) were purchased from GibcoBRL (Paisley, UK). Human monoclonal anti-human CD95 (Fas/APO-1) antibody were from R&D Systems (Abingdon, UK). C_2-ceramide (N-acetyl-sphingosine), C_6-ceramide (N-hexanoyl-sphingosine), and (±)-1,2-dioleoylglycerol (18:1; diacylglycerol) were obtained from Biomol Research Laboratories (Plymouth Meeting, PA, USA). *Escherichia coli* diacylglycerol kinase (DAGK) and n-octyl-β-D-glycopyranoside were purchased from Calbiochem (Nottingham, UK). [γ^{32}P] ATP was purchased from Amersham Life Science Ltd. (Little Charford, UK) and dihydrorhodamine 123 from Molecular Probes Europe BV (Leiden, The Netherlands).

The required H_2O_2 concentrations were prepared by freshly diluting an 8.8M H_2O_2 stock solution with sterile distilled water. 2', 7',-dichlorofluoroescein diacetate (DCFH-DA) and dihydrorhodamine 123 (DHR-123) were dissolved in dimethyl sulfoxide (DMSO) to stock solutions of 75mM and 10mM respectively. Subsequent dilutions were made with serum free RPMI 1640. The antioxidants N-acetylcysteine (NAC) and glutathione (GSH) were made up in serum free RPMI 1640. In the ROS

assays, the final cellular concentration of DMSO employed did not exceed 0.1%. Monoclonal anti-human CD95 (Fas/APO-1) antibody or LPS were reconstituted in sterile phosphate buffered saline (PBS; 0.01M Na_2HPO_4, 0.002M KH_2PO_4, 0.003M KCl, 0.137M NaCl; pH 7.4) containing 0.1% fraction V bovine serum albumin (BSA; Sigma, Poole, UK) to a concentration of 10μg/ml, 500μg/ml and 1mg/ml respectively, further dilutions being made in PBS/0.1% BSA. C_2-/C_6-ceramide were dissolved in anhydrous DMSO to a stock solution of 20mM. Subsequent dilutions were made in 1mM fatty acid free BSA.

2.2.2 Cell culture and stimulation.

The acute human T-cell leukaemia cell line, Jurkat and the human monocytic cell line, U937 (both kindly provided by Dr Alison Goodall, University of Leicester) were maintained in RPMI 1640 media, supplemented with 10% heat inactivated foetal calf serum and 1% penicillin/streptomycin. Cells were incubated at 37°C in a humidified atmosphere of 5% CO_2 and 95% air. The number of viable cells per ml was determined by trypan blue exclusion using an improved Neubauer haemocytometer (Weber Scientific International Ltd., Teddington, UK). Cells at a concentration of $2x10^6$/ml were serum starved for 4 hours in the described incubator conditions prior to treatment. Where indicated, cells were treated with H_2O_2, CD95, or C_2-/C_6-ceramide for the times and concentrations noted, incubations at 37°C in a humidified 5% CO_2/95% air incubator. To investigate the role of reactive oxygen species (ROS) in the cellular responses to the above agents, cell suspensions were pre-treated for 4 hours with 10mM NAC or GSH. Stimulation was discontinued by removing cells

suspensions from culture vessels, centrifuging at 1000xg (Eppendorf centrifuge 5415D, Hamburg, Germany) for 5 minutes and washing twice with 1ml of ice cold PBS prior to further experimental manipulation.

Individual additions to cells suspensions did not exceed 1% of the total volume and were dispersed with gentle mixing by pipette. Control experiments were conducted under identical conditions as tests, employing vehicle treatment.

2.2.3 Preparation of mononuclear cells from peripheral whole blood.

Peripheral blood mononuclear cells (PBMNC) were isolated by density gradient centrifugation using Lymphoprep^{TM} (Nycomed Pharma AS, Oslo, Norway) to obtain low platelet number (Romari *et al.*, 1996). Briefly, 40mls of venous blood was obtained from consenting adults into 10% sodium citrate (4% w/v) to prevent coagulation. Here, heparin was not used since it is known to interfere with platelet function. Further manipulation of the blood was conducted under aseptic conditions. All containers were washed with SigmaCote (Sigma, Poole, UK) and allowed to dry at least 30 minutes before use, to prevent activation and adherence of monocytes. Blood was diluted with PBS containing 0.1% BSA (w/v) in the ratio 2:5 into 50ml conical tubes (Orange Scientific, Braine-l'Alleud, Belgium). Diluted blood was gently layered onto the top of 15mls of Lymphoprep^{TM}. Tubes were centrifuged at 160xg for 15 minutes at 20°C. The top 15mls of the supernatant was removed by aspiration to eliminate platelets. Tubes were then re-centrifuged at 350xg for 20 minutes at 20°C. PBMNC appeared as a 'fluffy' band between the plasma

Lymphoprep™ interface. The PBMNC were collected by suction using a Pasteur pipette and transferred to 15ml conical falcon tubes (Orange Scientific, Braine-l'Alleud, Belgium). The cell suspensions were diluted 1:1 with PBS/0.1% BSA and washed three times with PBS/0.1% BSA by centrifugation at 225xg for 8 minutes at 4°C. PBMNC were resuspended to a concentration of $1x10^7$ per 150µl of PBS/0.1% BSA.

2.2.4 T-lymphocyte purification by negative isolation.

T-lymphocytes were purified from washed PBMNC utilising Dynal T-cell Negative isolation kit (Dynal A.S., Oslo, Norway). T-cells were negatively isolated from the washed PBMNC sample by depletion of magnetic bead captured B-lymphocytes, natural killer cells, monocytes, activated T-cells and granulocytes.

For each $1x10^7$ PBMNC, 20µl of heat inactivated foetal calf serum was added to inhibit non-specific Ab binding, followed by 20µl of antibody mix solution (containing the mouse monoclonal antibodies for CD14, CD16a, CD16b, CD56 and HLA Class II DR/DP and bind to all cells within the PBMN except resting T-lymphocytes). The PBMNC solution was incubated at 4°C with rotation for 10 minutes. Cell suspensions were diluted by the addition of 1ml of PBS/0.1%BSA per $1x10^7$ PBMNC and centrifuged at 500xg for 8 minutes at 4°C. Supernatants were removed and discarded and the cell pellet resuspended in 0.9mls of PBS/0.1%BSA per $1x10^7$ PBMNC. The cells with bound antibody were then captured by Depletion Dynabeads® (Dynal A.S. Oslo, Norway) and removed by magnetism.

Depletion Dynabeads® were resuspended prior to the transferral of 100µl of beads per $1x10^7$ PBMNC into microfuge tubes. Depletion Dynabeads® are uniform, supramagnetic, polystyrene beads coated with an Fc specific human IgG4 antibody against mouse IgG. Microfuge tubes were then placed into a Dynal magnetic particle collector (MPC; Dynal A.S. Oslo, Norway) for one minute to allow beads to migrate to the surface of the tube in contact with the magnet. The solution was allowed to clear, the fluid removed and discarded without disturbing the beads. Tubes were removed from the MPC and the beads resuspended in 1ml of PBS/0.1% BSA to wash. The tube was returned to the MPC for 1 minute before removal of the buffer. The Dynabeads® were resuspended in their original volume of PBS/0.1%BSA.

Washed Dynabeads® were added to the PBMNC suspension (100µl/10^7 cells) and incubated at room temperature with rotation for 15 minutes. Rosettes of PBMNC-Dynabeads® were resuspended by aspiration and the volume increased by the addition of 1ml of PBS/0.1% BSA per $1x10^7$ PBMNC. Tubes were then placed in the MPC for 2 minutes at room temperature to allow magnetic bead associated cells to accumulate at the face of the magnet. The clear supernatant containing resting T-lymphocytes was carefully transferred to a fresh conical falcon tube and the cell concentration determined using an improved Neubauer haemocytometer (Weber Scientific International Ltd., Teddington, UK). T-cell purity and monocyte contamination was evaluated by flow cytometry as described in Method *2.2.8 Immunofluorescence of peripheral blood lymphocytes.*

2.2.5 Culture of purified peripheral whole blood resting T-lymphocytes.

PBS/0.1% BSA washed PBL were pelleted by centrifugation at 225xg for 8 minutes. The supernatants were carefully removed so not to disturb the cell pellet and discarded. The cells were resuspended in RPMI 1640 supplemented with 20% heat inactivated FCS and 1% P/S at a concentration of $2x10^6$/ml and cultured in 6 well plates or T25 culture flasks (Orange Scientific, Braine-l'Alleud, Belgium). For activation of PBL, phytohaematoglutinin (PHA; Sigma, Poole, Dorset, UK) in PBS/0.1%BSA was added to a final concentration of $10\mu g/2x10^6$ cells (Carlens *et al.*, 2000). Both resting and activated T-cells were cultured for 72 hours at 37°C in a humidified 95% air, 5% CO_2 atmosphere. Activation of cultured PBL was determined by the level of membrane expressed CD25 (IL-2 receptor; Hemler *et al.*, 1984) within the CD3 population and assessed by flow cytometry as described in Method *2.2.8 Immunofluorescence of peripheral blood lymphocytes.* Resting and activated PBL concentrations were adjusted to $1x10^6$/ml in serum free RPMI 1640 as described for the culture and stimulation of Jurkat T-cells and U937 monocytes prior to treatment with C_2-/C_6-ceramide (see Method *2.2.2 Cell culture and stimulation*).

2.2.6 Flow cytometry.

Flow cytometric analysis was performed on an EPICS® XL-MCL flow cytometer (Beckman-Coulter, Miami, USA). The excitation source was an air cooled argon ion laser emitting a 488nm beam at 15mW. Linearity was monitored monthly using Immuno-Brite (Beckman-Coulter, Miami, USA). Prior to analysis of samples, the

optical alignment and fluidic system verified using Flow Check Fluorespheres™ (Beckman-Coulter, Miami, USA). The fluorescence peak position and half peak co-efficient of variance (HPCV) of fluorescence detectors (FL) and forward scatter detector (FS) were observed, and ensured to be within the laboratory standards.

2.2.7 Colour compensation for multiple fluorescence analysis by flow cytometry.

The Coulter Epics XL-MCL is equipped with 4 fluorescent channels, which collect light within the specific wavelengths of 505-545nm (FL1), 560-590nm, (FL2), 605-635nm (FL3) and 660-690nm (FL4). This allows analysis of several fluorescent probes simultaneously. However, fluorescent probes and fluorescently tagged antibodies possess emission spectra covering a range of wavelengths which may be wider than that band width covered by a specific fluorescent detector. Consequently, fluorescence overspills into neighbouring channels. When several fluorecent probes are used, channel overspill produces elevated levels of fluorescence in neighbouring channels and hence false data is obtained. This problem is overcome by selecting fluorochromes with minimal spectral overlap, for example using 2 probes one whose peak fluorescent lies in the range detected by the FL1 detector and the second by the FL4 detector. Spectral overlap may be further minimised by electronic colour compensation. Essentially, fluorescently tagged antibodies, which bind to antigens with high membrane expression, are selected. Antigens with weak membrane expression are not used since the regions of positivity are difficult to define and fluorescent overspill into neighbouring channels minimal. Regions of background, negative fluorescence of cells are established utilising the corresponding monoclonal

isotype negative controls. For 3-way colour compensation, combinations of isotype monoclonal negative controls for 2 of the FL detectors with one positive fluorescently tagged antibodes are systematically analysed. Positive fluorescence overspilling into neighbouring FL detector is electronically corrected to fall in the negative region previously established.

3-way colour compensation for the detectors FL1, FL2 and FL4 were established on the monocytic cell line U937 using the antibodies; mouse monoclonal anti-human CD95 antigen FITC conjugated (clone B-G34; Diaclone, Besançon Cedex, France), mouse monoclonal anti-human CD31 antigen PE conjugated (CD31-PE; B-B38; Diaclone, Besançon Cedex, France) and mouse anti-human CD14 antigen RPE-Cy5 conjugated (CD14-Cy5; clone TuK4; Serotec Ltd, Kiddlington, UK). 2-way colour compensation for the FL1 and FL2 detectors was established using either U937 monocytes or Jurkat T-cells with the antibodies mouse monoclonal anti-human CD14 antigen FITC conjugated (CD14-FITC; clone B-A8; Diaclone, Besançon Cedex, France) and CD31-PE, and CD95-FITC and mouse monoclonal anti-human CD3 antigen PE conjugated (CD3-PE; clone B-B11; Diaclone, Besançon Cedex, France) respectively.

In brief, untreated PBS washed cells were incubated in the dark on ice for 30 minutes with a saturating concentration (>10µl per 10^6 cells) of antibodies and/or isotype negative controls in the combinations described in Table 2.1. Cells were then fixed by the addition of 250µl of 4% formaldehyde, vortexed and incubated in the dark for 15 minutes at room temperature. Samples were diluted by the addition of 200µl of isoton (Beckman Coulter, Miami, FL, USA), brief mixing and a further minimum

a

	Tube number				
Conjugated fluorescent probe	*1*	*2*	*3*	*4*	*5*
Ab-FITC (FL1)	x	✓	x	x	✓
Ab-PE (FL2)	x	x	✓	x	✓
Ab-Cy5 (FL4)	x	x	x	✓	✓
-ve- FITC (FL1)	✓	x	✓	✓	x
-ve-PE (FL2)	✓	✓	x	✓	x
-ve-Cy5 (FL4)	✓	✓	✓	x	x

b

	Tube number			
Conjugated fluorescent probe	*1*	*2*	*3*	*4*
Ab-FITC (FL1)	x	✓	x	✓
Ab-PE (FL2)	x	x	✓	✓
-ve- FITC (FL1)	✓	x	✓	x
-ve-PE (FL2)	✓	✓	x	x

Table 2.1. Combinations of fluorescently tagged probes required for the determination of three-way colour compensation (a) and two-way colour compentsation (b). Saturating concentrations (>10µl/10^6 cells) of the indicated (✓) antibodies (Ab) or isotype negative controls (-ve) were added to PBS washed cells and incubated in the dark at room temperature for 30 minutes. Samples were then fixed with 4% formaldehyde and then diluted by the addition of isoton prior to flow cytometric adjustment for overlapping emission spectra.

incubation of 10 minutes in the dark at room temperature. For 3-way colour compensation, a flow cytometry protocol containing the dual parameter histograms of FS versus side scatter (SS), log integral FL1 versus log integral FL2, log integral FL1 versus log integral FL4 and log integral FL2 versus log integral FL4 were established. For 2-way colour compensation, histograms containing the log integral FL4 detector were omitted. Background fluorescence was established using cell suspensions

labelled with isotype negative controls (Tube 1; see Table 2.1) with 1% positive analysis selected on the histograms of fluorescence. The remaining tubes were then systematically analysed and positive fluorescence overspilling into the established negative regions electronically corrected.

2.2.8 Immunofluorescence of peripheral blood lymphocytes.

The percentage of $CD3^+$ peripheral blood T-lymphocytes (PBL) and their percentage activation by the appearance of CD25 (IL-2α receptor)$^+$ $CD3^+$ T-lymphocytes was evaluated following the negative isolation procedure by flow cytometry. The purity of extracted PBL was assessed by the percentage of $CD3^+$ PBL in the whole sample and mononcyte contamination evaluated by the presence of $CD14^+$ cells.

Purified PBL *ex vivo* or following 72 hour culture were treated with 10µl of antibody per 10^6 cells. Samples were incubated at room temperature in the dark for 30 minutes. The antibodies used were the mouse monoclonal anti-human CD3 antigen PE conjugated (clone B-B11, Diaclone), mouse monoclonal anti-human CD25 antigen FITC conjugated (clone B-F2; Diaclone) and the mouse mononclonal anti-human CD14 antigen RPE-Cy5 conjugated (clone TuK4; Serotec Ltd, Kidlington, UK). For each sample, isotype negative controls of the monoclonal antibodies were used to establish background fluorescence. These were the mouse monoclonal negative control IgG1 FITC conjugated (clone B-Z1), mouse monoclonal negative control IgG1 PE conjugated (clone B-Z1) both from Diaclone Research (Besançon Cedex, France) and mouse monoclonal negative control IgG1 PE-Cy5 conjugated

(Serotec). To the whole blood samples, 250µl of Optilyse C (Beckman Coulter, Miami, USA) was added to lyse red blood cells and fix PBMNC. PBMNC and purified PBL were fixed in 250µl of 4% formaldehyde solution. Samples were then vortexed vigorously and incubated in the dark for a further 15 minutes followed by the addition of 200µl of Isoton (Beckman Coulter). Samples were again vortexed and incubated in the dark, at room temperature for a minimum of 10 minutes. Samples were on occasion stored in the dark at 4°C for up to 24 hours without adversely affecting results. Samples were then analysed by flow cytometry utilising 3-way colour compensation as previously described and corrected for background fluorescence detected with isotype negative controls for the primary monoclonal antibodies. A minimum of 10,000 PBL were analysed per sample using the following gating strategy: PBL were gated according to FS and SS properties and the percentage $CD3^+$ cells evaluated on a single parameter histogram of log FL2 (CD3 PE) versus count. The percentage activation of $CD3^+$ PBL was evaluated on a dual parameter histogram of log FL2 (CD3 PE) versus log FL1 (CD25 FITC). The purity of PBL extracted was assessed as the percentage of $CD3^+$ cells on an ungated histogram of SS versus log FL2 (CD3 PE). Monocyte contamination was determined on an ungated histogram of log FL4 (CD14 PE-Cy5) versus count and expressed as a percentage.

2.2.9 Flow cytometric DNA cell cycle analysis.

Determination of nuclear DNA content reveals information on the cell cycle. This can be used to give information as to the effects of agents on the cell cycle and also

apoptosis. The DNA intercalating fluorescent dye propidium iodide (PI) binds specifically and stoichiometrically to nucleic acids, where fluorescence is enhanced on binding. However, PI is not cell permeable and hence, prior to DNA staining, cells are lysed to isolate nucleoids. Flow cytometric evaluation of nucleoid associated PI fluorescence permits quantification of both stages of the cell cycle and apoptosis.

A quiescent or resting cell, which is not growing or progressing through the cell cycle, is referred to as being in the G0 state. After cell division is triggered by exposure to various cytokines, growth factors or mitogens, the cell enters the G1 phase of the cell cycle, where the amount of mRNA increases and proteins required for DNA replication are synthesised. New synthesis of DNA marks the entry of the cell into the synthetic phase (S-phase) where the DNA content of the cell increases until it doubles that of G0/G1 cells. The cell is now considered to be in the G2 phase of the cell cycle and DNA synthesis is terminated. Finally the cell enters the mitotic phase (M), to divide into two daughter cells which revert to G1 phase for sustained cell division, or G0 phase (Ormerod, 1999; as reviewed in; Thompson, 1995). Since cells in the G2/M phase of the cell cycle have double the DNA of those in the G0/G1 phase, according to stoichiometry, G2/M nucleoids stained with PI have double the fluorescence of those in the G0/G1 phase. PI stained nucleoids in the S phase contain DNA and hence fluorescence which is intermediate of G0/G1 and G2/M (See Figure 2.1). As previously described, DNA fragmentation represents a biochemical and morphological feature of apoptosis. Fragmented DNA binds less fluorochrome due to its smaller size (Wylie, 1980; as reviewed in; Cohen, 1993). This produces a decrease in fluorescence in comparison to aneuploid DNA, appearing to the left of the

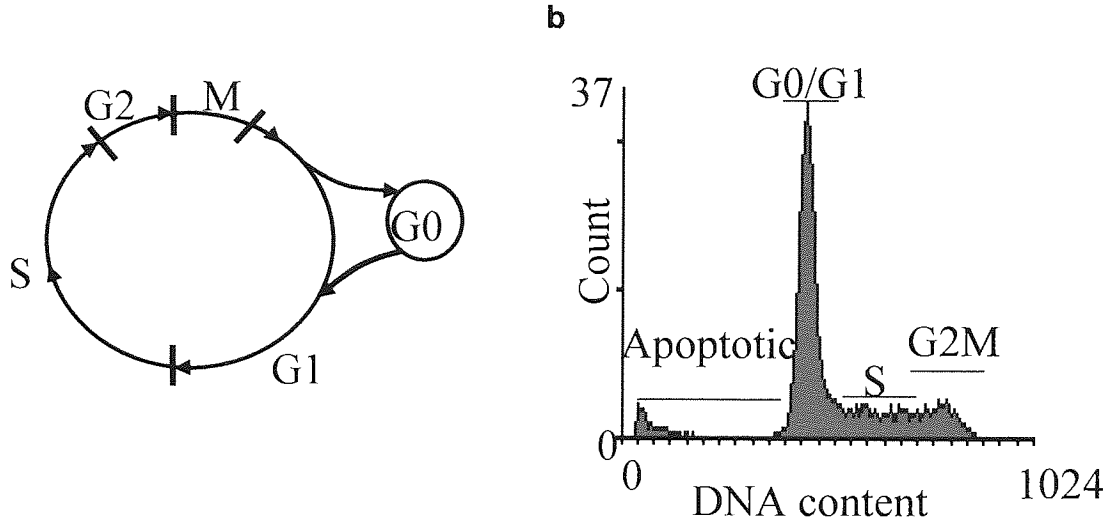

Figure 2.1. The cell cycle. (a) A simplified schematic of the various phases of the cell cycle. G0 represents cells in the resting or quiescent state, which upon stimulation by growth factors, cytokines or mitogens enter the G1 phase. The synthesis of DNA marks entry into the synthetic (S) phase, where the amount of DNA increases until it has doubled at which point the cell enters the G2 phase. DNA synthesis is terminated and the cell undergoes mitosis (M), dividing into 2 daughter cells, which remain in the G1 phase for sustained cell division re-enter the G0 phase. (b) A flow cytometric DNA cell cycle histogram showing the corresponding phases of the cell cycle.

G0/G1 peak and the cellular DNA content is termed subdiploid or hypoploid (See Figure 2.1).

The amount of subdiploid DNA increases as the degree of fragmentation increases due to apoptotic insult. The fluorescence produced can be quantified by flow cytometry (Nicolleti *et al.*, 1991). Briefly, PBS washed cells were centrifuged at 100xg (Eppendorf centrifuge 5415D, Hamburg, Germany) for 5 minutes, the supernatant removed and the resulting cell pellet resuspended in 1ml hypotonic fluorochrome solution (50μg/ml PI in 0.1% sodium citrate and 0.1% Triton x-100) to extract and stain nucleoids (Nicoletti *et al.*, 1991). Samples were incubated in the dark at 4°C for 14-24 hours prior to flow cytometric cell cycle analysis.

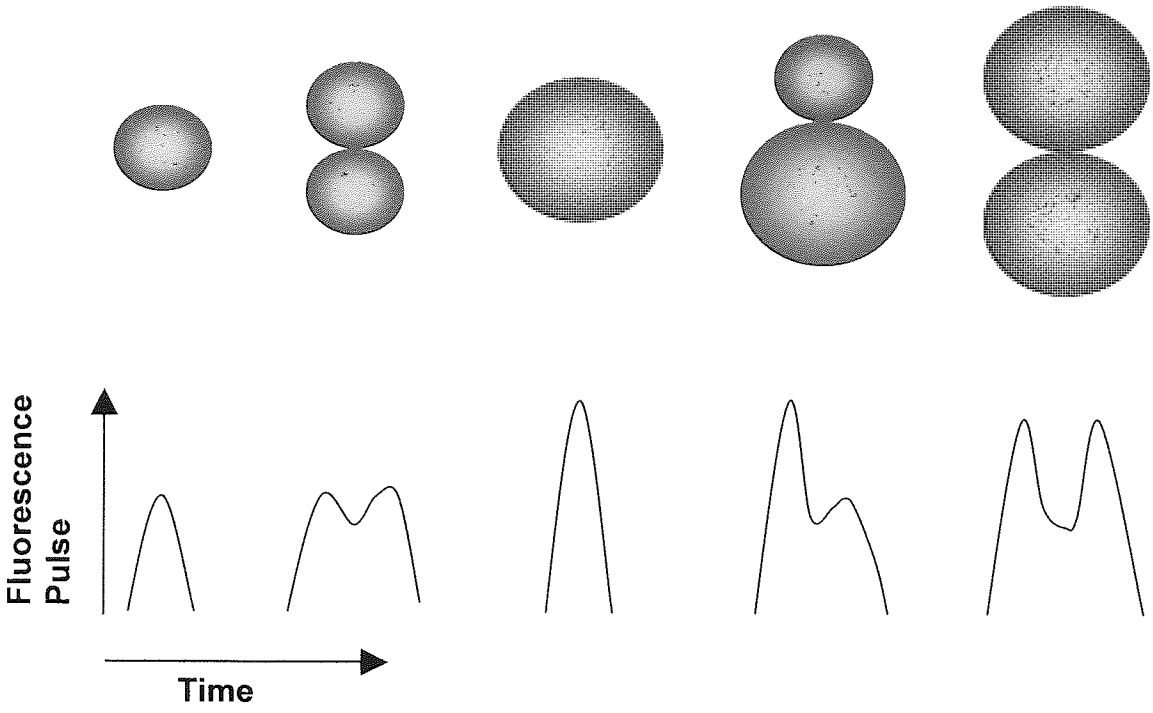

Figure 2.2. Differentiation of aggregates of nucleoids on the basis of differing peak and integral fluorescence intensities. The shape of the fluorescence pulse generated as a function of time upon nucleoid excitation by a 488nm Argon laser. Single nucleoids are distinguished from doublets according to the integral and peak of the fluorescence pulse. Green spheres represent G0/G1 nucleoids and red spheres represent nucleoids in the G2/M phase of the cell cycle (adapted from Ormerod, 1999).

PI fluorescence of individual nuclei was measured by flow cytometry. PI intercalated nuclei were excited by a 488nm Argon laser at a low flow rate. FS and SS of the nuclei were simultaneously measured in addition to peak and integral linear red fluorescence (FL3, bandwidth 605nm-635nm). Since nucleoids in the G2M phase of the cell cycle contain double the DNA of those in the G0/G1 phase of the cell cycle and hence according to stoichiometry, twice the dye content, doublets of PI intercalated nucleoids in the G0/G1 phase will have the same integral fluorescence as a single PI stained nucleoid in the G2M phase. Consequently, a false number of cells in the G2M phase of the cell cycle may be quantified. However, the peak

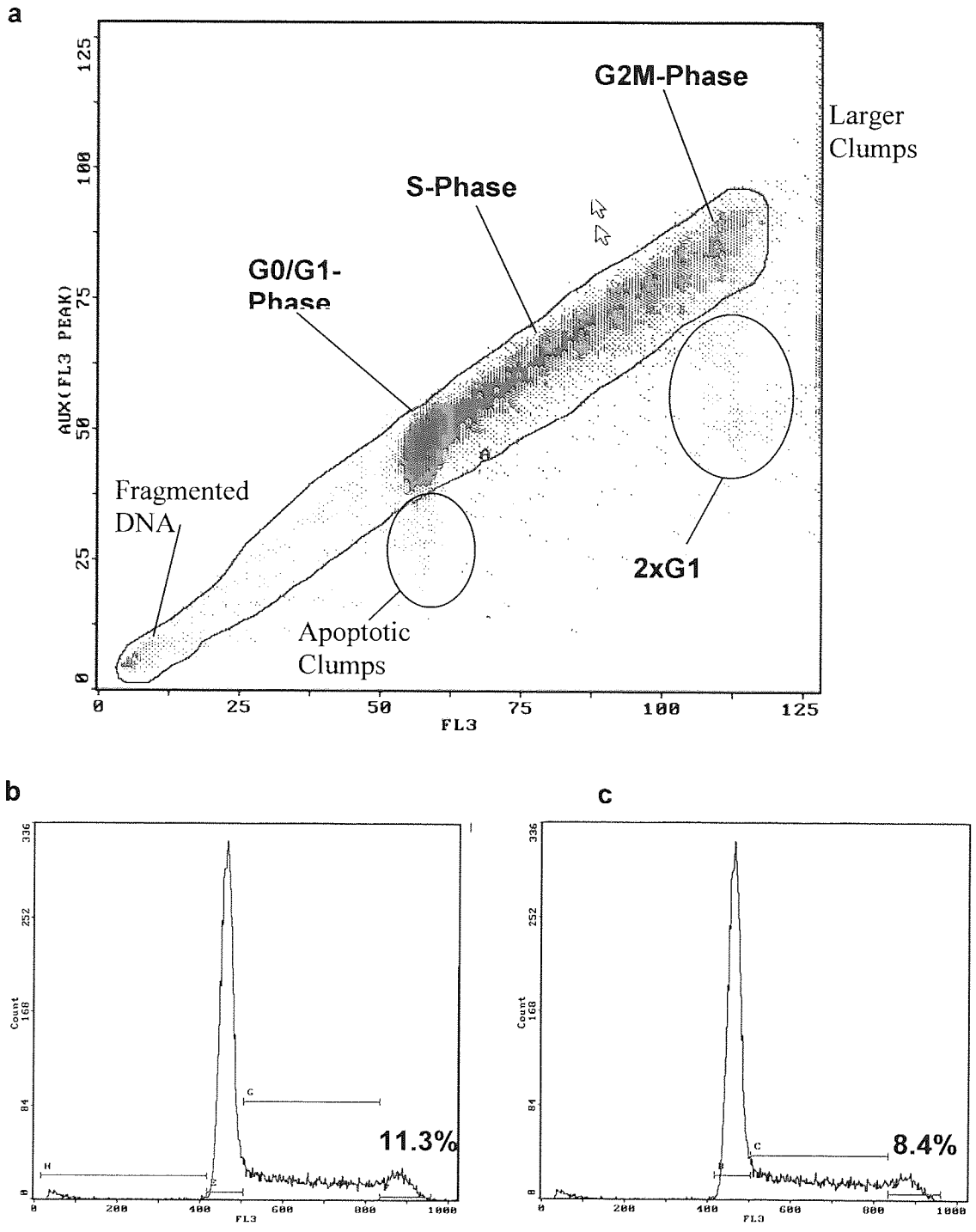

Figure 2.3. The exclusion of aggregates from flow cytometric analysis of DNA cell cycles. (a) Histogram of FL3 (integral) versus Aux FL3 peak fluorescence of propidium iodide (PI) stained nucleoids. Single nucleoids are contained within gate A. Excluded aggregates are marked. (b) Ungated DNA cell cycle histogram, containing single nucleoids and aggregates. (c) The same DNA cell cycle limited to contain only the single nucleooids within gate A. Percentages shown represent the percentage of nucleoids within the G2M-phase of the cell cycle (adapted from Ormerod, 1999).

fluorescence of doublets of G1 phase nucleoids is half that of G2M phase nucleoids (Ormerod, 1999; See Figure 2.2). Therefore, clumps of nuclei were eliminated by appropriate gating on a dual parameter histogram of peak FL3 versus integral FL3 (See Figure 2.3). This principle applies to nucleoids in all phases of the cell cycle.

Optimal incubation periods for cell lysis and PI DNA staining, their effect on DNA damage and quality of the DNA cell cycle obtained were pre-determined experimentally by evaluating the half peak co-efficient of variance (HPCV) of the G0/G1 and S phases of the cell cycle non-treated Jurkat T-cells (Data not shown). Histograms of high quality possess low HPCVs (Ormerod, 1999). Cell cycles were then analysed by flow cytometry with the following modifications. Control, vehicle treated samples were fixed so that the position of the G0/G1 peak was at channel 460 ± 14 on a gated histogram of linear integral FL3 versus count, with discriminator set at channel 24 to exclude excessive debris and machine noise from analysis. These settings were established experimentally (Data not shown). For each analysis, 20,000 events were recorded on the gated histogram of linear integral FL3 versus count. Nucleoid staining and extraction was considered to be optimal when the HPCV of the G0/G1 peak was within the predetermined range 4 ± 0.87 (Data not shown) and analysis of the S-phase CV by MultiCycle™ for Windows DNA cell cycle analysis software (Phoenix Flow Systems, San Diego, U.S.A.) was considered average to good. DNA cell cycles of control, vehicle treated samples which fell outside these criteria were rejected on the basis of poor staining.

The effects of the described agents on the various phases of the cell cycles were quantified. The percentage of apoptotic nuclei was determined by quantifying the

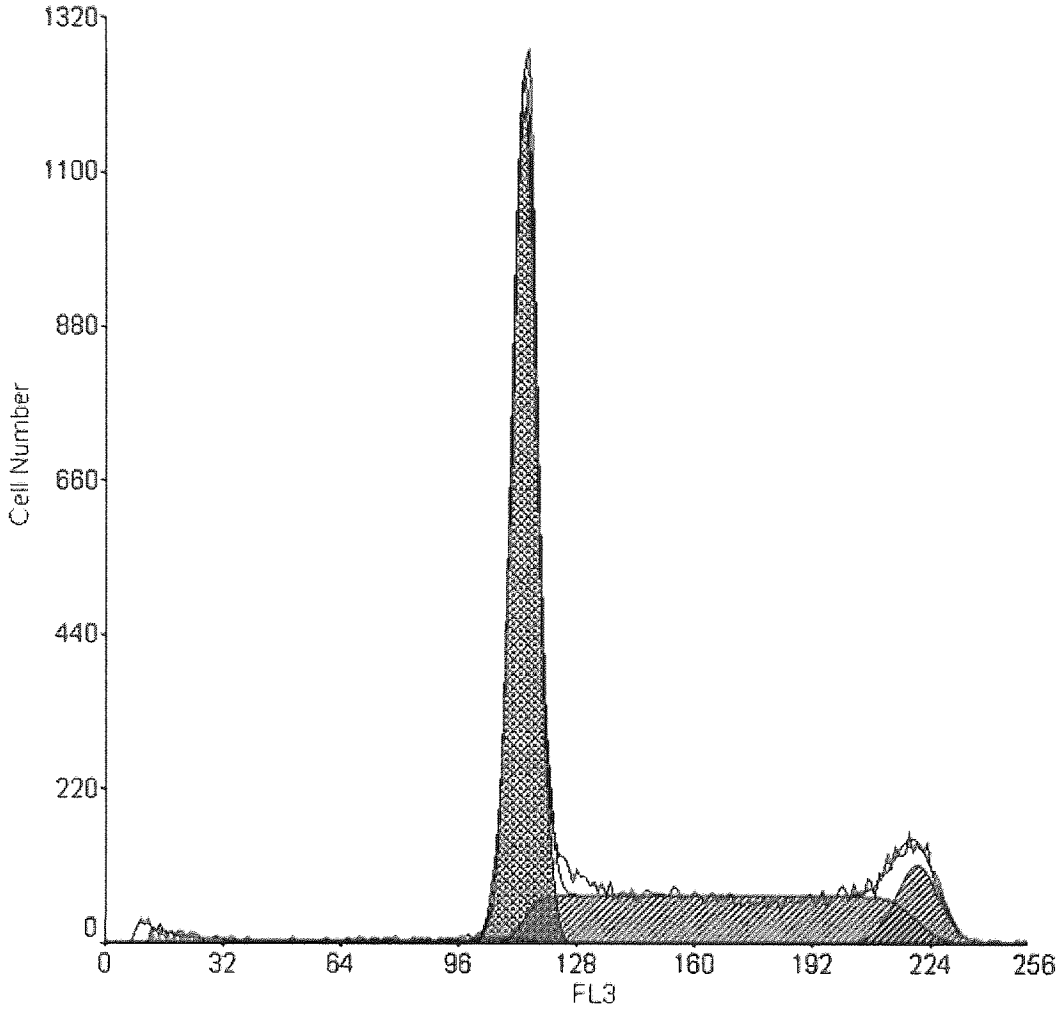

Figure 2.4. Analysis of individual phases of the cell cycle by MultiCycle™ for Windows. The number of nucleoids in the G0/G1 (blue) or G2M phases (red) of the cell cycle is estimated mathematically by fitting gaussian curves to their distributions. S phase (green) content is calculated by linear regression of the midpoints between the the G0/G1 and G2/M peaks.

number of hypoploid (subdiploid) nuclei. Values were then expressed as a percentage of actual apoptosis or percentage of specific apoptosis according to the formula specific apoptosis = (T-C)/(100-C)x100, where T equals the percentage of apoptotic events from treated cells, and C equals the percentage of apoptotic control cells (Genestier *et al.*, 1998b). Metabolically active cells which progress through the S and G2/M phases at an elevated rate present difficulties for accurate determination of DNA content due to the overlapping phases of the cell cycle. Consequently

MultiCycle^{TM} for Windows was used to evaluate the G0/G1, S-, and G2M phases of the cell cycle. This fits Gaussian curves to the GO/G1 and G2/M phases and approximates the proportion of nucleoids in the S-phase by linear regression of the midpoints between the G0/G1 and G2/M peaks (See Figure 2.4).

2.2.10. Flow cytometric assay for cytosolic peroxide production.

The effects of both pharmacological and physiological agents on intracellular peroxide levels was monitored following exposure of cells to numerous agents utilising flow cytometry. 2', 7,'-dichlorofluoroescein diacetate (DCFH-DA) is a stable non-polar, non-fluorescent compound, which freely diffuses across selectively permeable membranes. Intracellular DCFH-DA is activated by intracellular esterases to hydrolyse the acetate groups forming the non-fluorescent 2', 7'-dichlorofluorescein (DCFH), effectively trapping the compound within the cell. In the presence of cytosolic peroxide ($[peroxide]_{cyt}$) R-OOH, DCFH acts as a substrate which is rapidly oxidised to the highly fluorescent 2',7'-dichlorofluorescein (DCF). DCF is excited at 488nm, and emits fluorescence within the range 505-545nm, and hence can be measured by flow cytometry (See Figure 2.5; Bass *et al.*, 1983). DCFH is not oxidised by $O_2^{\cdot-}$ (Royal & Ischiropoulos, 1993; Zhu *et al*, 1993; Carter *et al.*, 1994; Hempel *et al.*, 1999) although it may react with peroxynitrite ($ONOO^-$), and nitric oxide ($NO^{\cdot}$); Lokesh & Cunningham, 1986; Crow, 1997; Hempel *et al.*, 1999). Flow cytometric analysis has advantages over standard spectrofluorometric techniques for the evaluation of intracellular ROS levels, allowing quantitative examination of large

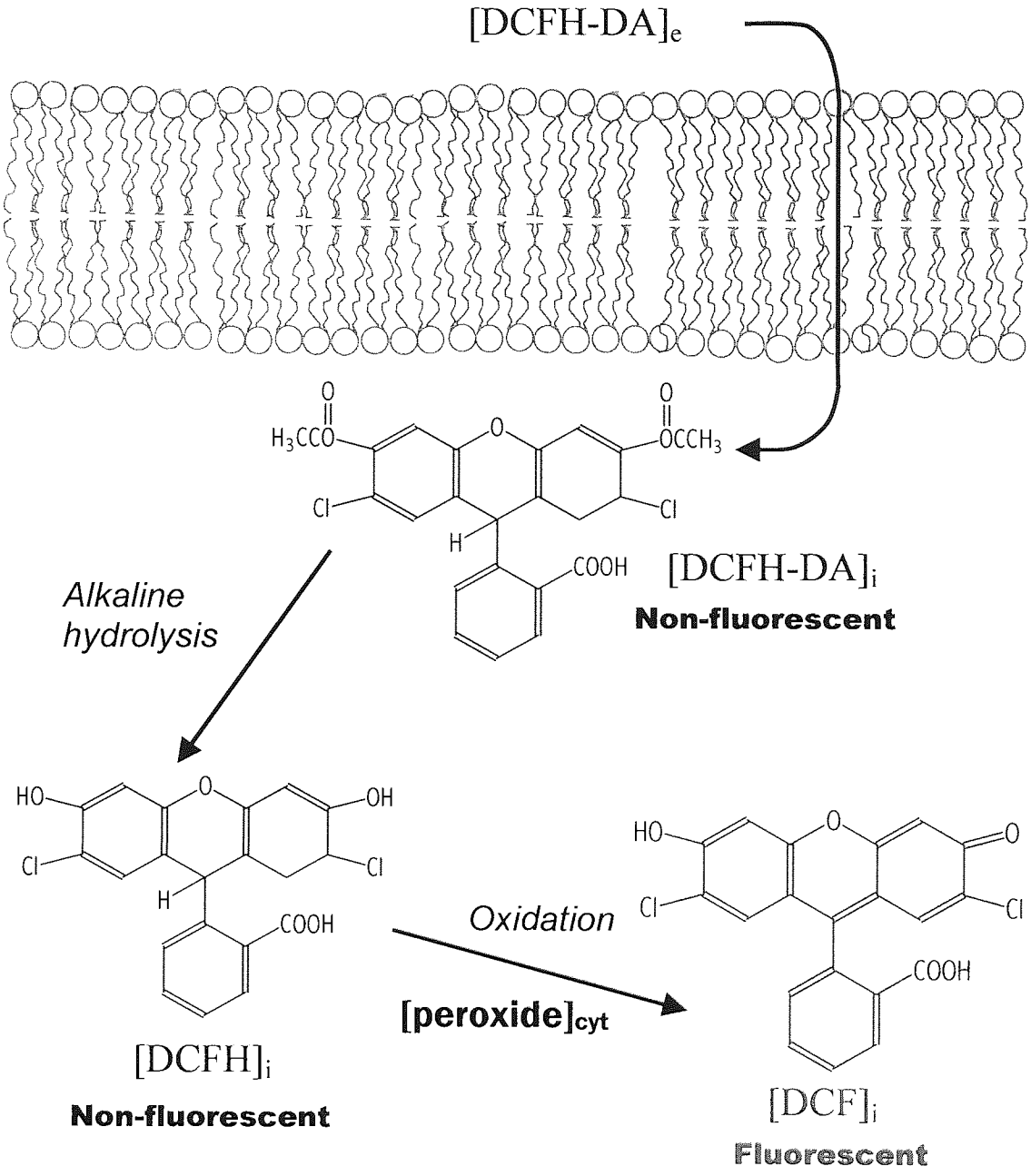

Figure 2.5. Mechanism of action of the peroxide sensitive probe 2',7'-dichlorofluorescein diacetate (DCFH-DA). DCFH-DA enters the intracellular compartment by diffusion where it is immediately hydrolysed by intracellular esterases to form the non-fluorescent pre-cursor dichlorofluorescein (DCFH). DCFH is a polar molecule therefore processes poor membrane permeability and is essentially trapped within the cytosol. In the presence of cytosolic peroxides ($[peroxide]_{cyt}$), DCFH is oxidised to fluorescent isomer, DCF. When excited at 488nm, DCF emits green light detectable by flow cytometry within the bandwidth 505-545nm (FL1).

numbers of individual cells rather than measuring mean responses of a total population (Bass *et al.*, 1983).

A procedure adapted from Bass *et al.*, (1983) was used to measure $[peroxide]_{cyt}$ levels by flow cytometry. Briefly, to optimise, systematic variations in 2',7', dichlorofluorescein (DCFH-DA) concentration (1-50μg/ml), DCFH-DA pre-incubation period (5-240 minutes), co-incubation of DCFH-DA and H_2O_2 (0-300μM; 0-60 minutes) and incubation system were evaluated experimentally. Immediately following agent/DCFH-DA incubation, cell treatments were analysed by flow cytometry. Measurements of forward scatter, side scatter and log FL1 fluorescence (green light, band width 505nm-545nm.) were recorded. Cells were gated to exclude debris, clumped cells or machine noise. 10,000 cells were examined from each sample on a histogram of count versus log FL1.

Applying the optimised conditions for the use of DCFH-DA for the detection of $[peroxide]_{cyt}$ by flow cytometry, the standard assay was as follows. $2x10^6$/ml of viable cells were incubated for 10 minutes with 50μM DCFH-DA after which cells were treated with varying concentrations and incubation periods with CD95 or C_2-/C_6-ceramide. The total incubation period with 50μM DCFH-DA did not exceed 40 minutes. Cell treatments for longer than 40 minutes were incubated with 50μM DCFH-DA for the last 40 minutes prior to analysis. Immediately following agent/DCFDA incubation, cell treatments were analysed by flow cytometry.

2.2.11 Flow cytometric analysis of mitochondrial peroxide production.

Mitochondrial ROS production was analysed utilising the mitochondrial specific properties of the brightly fluorescent probe rhodamine 123. Its precursor, dihydrorhodamine 123 (DHR-123) is uncharged and non-fluorescent, passively diffusing across membranes where it is converted to rhodamine 123 by intracellular esterases. This cationic cyanine dye accumulates in the electrically negative compartments such as the mitochondria. The large surface area of the mitochondrial matrix binds large amounts of the dye. Like DCFH-DA, rhodamine 123 reacts with peroxide rather than superoxide to produce a fluorescent compound excitable at 488nm and emits light at 515nm detectable by flow cytometry (Rothe *et al.*, 1991).

To detect mitochondrial peroxide ($[peroxide]_m$) production induced by C_2-/C_6-ceramide (0-20μM/$2x10^6$ cells) exposure of Jurkat T-cells or U937 monocytes, 10μl of DHR-123 (1mg/ml; Molecular Probes Europe BV Leiden, The Netherlands) was added to 0.5ml of $2x10^6$/ml of cell suspension thirty minutes prior to the termination of the treatment period. Cell suspensions were gently dispersed by pipette and samples returned to the incubator (Dumont *et al.*, 1999). As a positive control, cells were treated with antimycin A (AA; 1-25μM) for 1 hour. AA inhibits complex III of the mitochondrial electron transport chain, preventing electron shuffling from ubiquinone to cytochrome c_1 resulting in the increased generation of the superoxide anions. Dismutation of superoxide anions catalysed by Mn-superoxide dismutase induces the generation of hydrogen peroxide (Garcia-Ruiz *et al.*, 1997). After the full incubation period, samples were analysed immediately by flow cytometry (Beckman-Coulter, Miami, USA) for rhodamine-123 fluorescence. The viable population was

determined on a histogram of FS v SS and the rhodamine-123 fluorescence of 10,000 viable cells analysed on a histogram of log fluorescence (FL1, band width 505nm-545nm) versus count. The median X (MdX) rhodamine fluorescence of vehicle controls ($R123MdX_{control}$) was adjusted to lie at the third log decade of the x-axis and the MdX of test samples ($R123MdX_{test}$) compared. The change in rhodamine-123 fluorecence ($\Delta R123MdX$) of test cells from controls was determined according to the formula $\Delta R123MdX = R123MdX_{test} - R123MdX_{control}$.

2.2.12 Flow cytometric analysis of cell viability.

To establish the contribution of necrosis in addition to that of apoptosis in the induction of cell death, flow cytometry may be used to analyse the cellular exclusion of fluorescent dyes. Cells undergoing necrosis lose the integrity of their plasma membrane permitting the release of intracellular material (as reviewed in; Cohen, 1993). However, this also permits the entry of cationic, polar dyes into the cell such as trypan blue, PI and ethidium bromide. Consequently, necrotic cells in the presence of a polar dye for a short period of time, display high dye uptake. Early apoptotic cells show an uptake of dye which is much lower than that observed with necrotic cells, whereas healthy, viable cells show no dye uptake. When this dye is fluorescent, such as PI, it is possible to distinguish via flow cytometry cells that are healthy (PI negative), apoptotic (PI weak) and necrotic (PI strong) on the basis of the fluorescence contained with individual cells (Yeh *et al.*, 1981). These cell populations can be further distinguished from each other by combination with the cells forward scatter properties. When a cell dies via necrosis, its FS and SS

properties are increased due to swelling of the cell. However, the morphology of apoptosis is characterised by shrinking of the cell causing the cytoplasm to compact (; as reviewed in; Wylie, 1980). This can be visualised by flow cytometry as a decrease in the cells FS properties with an associated increase in SS properties. A dual parameter histogram of FS versus log integral FL3 (PI) of the PI incubated cell sample enables the separation of cells into a healthy, normal sized, low PI population; a necrotic population displaying elevated FS and PI properties and an apoptotic population possessing low FS and low PI fluorescence (Mangan *et al.*, 1991).

PBS washed cells were centrifuged (Eppendorf centrifuge 5415D, Hamburg, Germany) at 1000xg for 5 minutes, the supernatant removed and discarded. The cell pellet was resuspended in 1ml of PI (25μg) in PBS/0.1% BSA per 10^6 cells. Samples were incubated at room temperature in the dark, for 15 minutes and then analysed immediately by flow cytometry. The PI fluorescence of individual cells were analysed on an ungated dual parameter histogram of FS against log integral FL3 (PI, red fluorescence; 560-590nm) and the percentage of normal, apoptotic and early or late necrotic cells in a given cell sample quantified.

2.2.13 Analysis of $[peroxide]_{cyt}$ levels of mononuclear cells from peripheral whole blood.

Human blood was collected from consenting normal volunteers into tubes washed with SigmaCote (Sigma, Poole, Dorset, UK), to minimalise monocyte activation and adherence to plasticware, containing sodium citrate solution (4% w/v) at 10% of the

total volume of blood to be collected. Blood (200µl) was treated with C_2-/C_6-ceramide, for 1 hour in a water bath at 37°C with gentle horizontal shaking. Concentrations were pre-determined from the responses achieved from cell lines *in vitro*. At T_{end} –10 minutes, DCFH-DA added to give a final concentration of 50µM, and samples returned to the waterbath. At the end of agent treatment period, blood was stained with antibodies at a saturating concentration of greater than 10µl of antibody per 100µl of blood. Samples were then incubated on ice for a further 30 minutes. To identify monocytes and T-cells, the antibodies used were mouse monoclonal anti-human CD3 antigen PE conjugated (clone B-B11, Diaclone) and mouse monoclonal anti-human CD14 RPE-Cy5 conjugated (Clone TuK4; Serotec) respectively. 3-way colour compensation to account for overlapping emission spectra of the fluorescent-tagged antibodies and DCF was applied. Red blood cells were lysed and the mononuclear cell (MNC) population fixed with Optilyse C (Beckman Coulter, Miami, USA). Samples were vortexed vigorously and incubated in the dark at room temperature for 15 minutes. This process does not cause damage to the fixed MNC membranes. Cell suspensions were then diluted 1:1 with Isoton (Beckman Coulter, Miami, USA), vortexed vigorously for a second time and incubated in the dark at room temperature for a further 10 minutes. Cell suspensions were immediately analysed by flow cytometry. Individual peripheral blood MNC (PBMNC) populations were identified and gated according to their FS and SS properties. Histograms of log FL2 (CD3 PE) versus SS and log FL4 (CD14 RPE-Cy5) versus SS were used to gate $CD3^+$ lymphocytes and $CD14^+$ monocytes respectively. The DCF fluorescence of $CD3^+$ T-lymphocytes and $CD14^+$ monocytes were analysed on separate single parameter histograms of log integral FL1 (DCF) versus count. The median fluorescence (MdX) intensity of each sample was

recorded. A minimum of 25,000 $CD3^+$ T-lymphocytes and 10,000 $CD14^+$ monocytes were analysed per sample.

2.2.14 DTNB-GSSG-reductase recycling assay for glutathione.

This was done according to the method of Tietze (1969). The recycling assay quantifies spectrophotometrically both GSH and GSSG utilising the selectivity of GSSG-reductase for its substrate GSSG, and the sensitivity of DTNB (5' 5'-dithiobis(2-nitrobenzoic acid); Ellman's reagent) to reduction by GSH. DTNB reacts with GSH to form GSSG and, with stoichiometry, the highly fluorescent 5-thio-2-nitrobenzoic acid (TNB) anion (1 and 2). GSSG produced as a product of the reaction, or cellular GSSG, is converted back to GSH by the action of glutathione reductase (GSH) coupled to NADPH (3). The rate of TNB^- formation is followed at 410nm and is proportional to the sum of GSH and GSSG. Cellular GSSG content was not analysed owing to the potential for artefactual oxidation of GSH during sampling and collection (Griffiths *et al.*, 2002).

$$GSH + DTNB \rightarrow GS\text{-}TNB + TNB^- + H^+ \quad (1)$$

$$GS\text{-}TNB + GSH \rightarrow GSSG + TNB^- + H^+ \quad (2)$$

$$GSSG + NADPH + H+ \rightarrow 2GSH + NADP^+ \quad (3)$$

Briefly, a 100µl aliquot of PBS washed cell samples was removed for protein determination. Cell suspensions were pelleted by centrifugation (Eppendorf centrifuge 5415D, Hamburg, Germany) at 1000xg for 5 minutes and the supernatants

removed. Cell pellets were resuspended in 30µl PBS, 16.6µl 100% 5-sulfasalicyclic acid dihydrate (SSA) and 453.4µl stock buffer (125mM dibasic sodium phosphate; 6.3mM EDTA, disodium salt; pH 7.5). Samples were vortexed vigorously and centrifuged at 15,000xg (Eppendorf centrifuge 5415D, Hamburg, Germany) for 5 minutes to liberate protein. Supernatants were transferred to fresh microfuge tubes and stored on ice until analysis.

GSH standards were made up as shown in Table 2.2 to give the same SSA concentration as the test samples since SSA shows some inhibition of GSR action. To each well of a 96 well flat bottomed plate (Orange Scientific) 50µl of 6.43mM DNTB and 150µl daily buffer (60µM NADPH in stock buffer) was added using a multichannel pipette. GSH standards (25µl) and test samples (25µl) were added to the appropriate wells, using a fresh pipette tip for each sample.

Concentration	*GSH (µl)*	*SSA (µl)*	*Stock buffer (µl)*
0µM	0	33.3	966
10µM	0.1	33.3	966
20µM	0.2	33.3	966
30µM	0.3	33.3	966
40µM	0.4	33.3	966
60µM	0.6	33.3	966

Table 2.2. Preparation of glutathione (GSH; reduced form) standards in 1% SSA and stock buffer. The plate was incubated at 37°C in the dark for three minutes, after which 25µl of GSR was added to each well to initiate the reaction and the absorbance analysed immediately at 410nm. Further readings were taken at +1 and +5 minutes. Samples were stored at -70°C for reanalysis if necessary. Optical densities (OD) were calculated by subtracting values at time zero from those at +1 and +5 minutes. The test sample values were converted to ng of GSH using a calibration curve constructed from the change OD of the GSH standards. Total cellular GSH content was expressed per mg of cellular protein. All solutions were freshly prepared on the day of the assay.

The plate was incubated at 37°C in the dark for three minutes, after which 25µl of GSR was added to each well to initiate the reaction and the absorbance analysed immediately at 410nm. Further readings were taken at +1 and +5 minutes. Samples were stored at -70°C for reanalysis if necessary. Optical densities (OD) were calculated by subtracting values at time zero from those at +1 and +5 minutes. The test sample values were converted to nmoles of GSH using a calibration curve constructed from the change OD of the GSH standards. Total cellular GSH content was expressed per mg of cellular protein. All solutions were freshly prepared on the day of the assay.

2.2.15 Protein determination.

Protein standards (0, 1, 2, 3, 4 and 6µl; Sigma, Poole, Dorset, UK) and 10µl of test samples were aliquoted in quadruplicate into the separate wells of a labelled 96 well, flat bottomed plate (Orange Scientific). Pre-mixed BCA solution (200µl) was added to each well using a multichannel pipette. The plate was incubated in the dark at 37°C for 30 minutes, followed by a further 10 minutes at room temperature. The plate was then analysed by a Dynex MRX 1.13 micro plate reader (Dynex Technologies (UK) Ltd, Billinghurst, West Sussex, UK) at 570nm. The protein content of cell samples was obtained from a calibration curve constructed from the OD of the standards.

2.2.16 Cellular lipid determination.

To determine intracellular ceramide and diacylglycerol (DAG) levels, the DAG kinase (DAGK) assay has been used. This utilises a standard protocol for the extraction of lipids (Bligh & Dyer, 1959) followed by the use of the enzyme DAGK to catalyse the transfer of the γ phosphate groups of ATP to the 3' hydroxyl group of DAG and 1'hydroxyl group of ceramide. Consequently, phosphatidic acid (DAG-3-phosphate) and ceramide 1-phosphate are produced respectively (See Figure 2.6). The phosphoryl transfer mechanism uses [γ-^{32}P] ATP as a substrate to generate a quantifiable radiolabelled product, which is separated from other non-radiolabelled lipids by thin layer chromatography (TLC). Radiolabelled ceramide 1-phosphate is identified by comparison to that of a co-chromatographed known concentration of pure ceramide 1-phosphate, or from autoradiography. Ceramide 1-phosphate is identified by radiography and then scraped from TLC plates into scintillation vials and the radioactivity expressed in terms of counts per minute (cpm).

Ceramide conversion to ceramide 1-phosphate does not follow Michaelis Menten kinetics as the concentration of DAG in the reaction mixture is in excess, as is the substrate [γ-^{32}P] ATP. Therefore, ceramide 1-phosphate formation is unaffected byfactors influencing K_m and V_{max}. To validate the assay, a standard curve of biological ceramide (Type III ceramide; Sigma, Poole, UK) that encompasses the concentration range of ceramide expected in cellular samples is produced. The mass of ceramide-1-phosphate from each standard, based on the cpm of ceramide-1-phosphate and specific activity of [γ-^{32}P] ATP, should have a conversion of greater than 90%. The slope of the standard curve will then be used to determine the amount

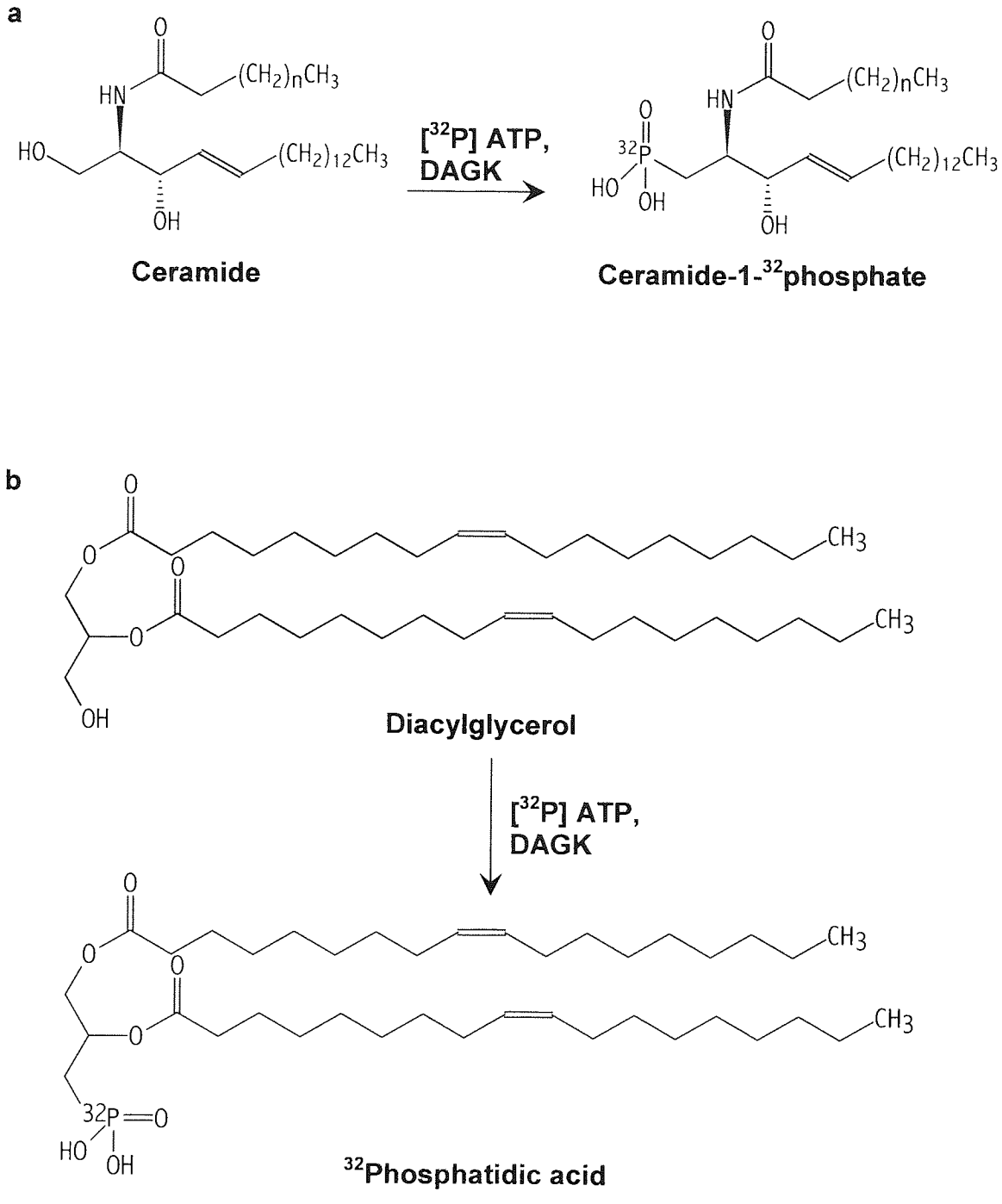

Figure 2.6. Enzymatic method for the radiolabelling of (a) Ceramide or (b) Diacyl glycerol (DAG; (±) –1, 2-Dioleoylglycerol (18:1). The enzyme *sn*-1,2-Diacylglycerol kinase (DAGK) catalyses the transfer of the γ ^{32}phosphate groups of ATP to the 1'hydroxyl group of ceramide and 3' hydroxyl group of DAG to form Ceramide-1-^{32}Phospate and ^{32}Phosphatidic acid respectively. Radiolabelled lipids can be separated from other lipids by thin layer chromatography, identified by autoradiography and consequently quantified by scintillation counting.

of ceramide in each sample. Variation in the extent of conversion of ceramide-1-phosphate was monitored using an internal standard that has a fatty acid carbon chain length significantly different from endogenous ceramide, C_6-ceramide (Bligh & Dyer, 1959; Perry & Hannun, 1999).

2.2.17 Lipid extraction.

PBS washed cells ($2x10^6$/ml) were pelleted by centrifugation at 1000xg for 5 minutes at 4°C (Eppendorf centrifuge 5415D, Hamburg, Germany). Supernatants were carefully removed by pipette and discarded. Cell pellets were resuspended in 750µl of premixed methanol:chloroform (2:1, v/v) and vortexed vigorously until an even suspension was gained. Sterile, distilled water (200µl) was then added to each sample and the suspension vortexed for a second time. Samples were incubated for 14-16hrs at 4°C to extract lipids. Occasionally, premature phase break was observed, which can hinder lipid extraction. This was corrected by the addition of 125µl of methanol (Bligh & Dyer, 1959).

At the end of this incubation period, cell samples were centrifuged at 2000xg (Eppendorf centrifuge 5415D, Hamburg, Germany) for 5 minutes to pellet cellular debris. Supernatants were carefully transferred to fresh, appropriately labelled microfuge tubes without disturbing pelleted cellular debris. Cellular debris was discarded. To each tube, 250µl of chloroform and 250µl of sterile water were added with vigorous mixing by vortex between additions. Samples were incubated at room temperature for 30 minutes to allow phase break of the liquid material into a lower,

organic phase and upper, aqueous phase. Microfuge tubes were then centrifuged at 2000xg (Eppendorf centrifuge 5415D, Hamburg, Germany) for 5 minutes to obtain clean separation of phases. The lower, organic phase was transferred by pipette to fresh microfuge tubes, ensuring that no aqueous phase was collected (Bligh & Dyer, 1959). Mild alkaline hydrolysis of the lipid extractions, which is often used to remove glycerolipids, was not employed, since diacylglycerol is sensitive to this procedure (Perry & Hannun, 1999).

2.2.18 Ceramide and Diacylglycerol quantification.

Ceramide and DAG were quantified by the diacylglycerol kinase (DAGK) assay (Preiss *et al.*, 1986; Dressler & Kolesnick, 1990; Perry & Hannun, 1999). For the construction of standard curves, type III ceramide (from bovine brain; Sigma, Poole, UK) was prepared in chloroform in the range 0, 160, 320, 640, 1280 and 2560 pmol and (±) 1-, 2-dioleoylglycerol (18:1; DAG; Biomol, Plymouth Meeting, PA, USA) was also prepared in chloroform in the range 0, 80, 160, 320, 640 and 1280 pmol. Organic samples containing extracted lipid and ceramide/DAG standards were dried under N_2. The resulting dried lipids were then resuspended in 20µl of 7.5% octyl-β-D-glycopyranoside, 5mM cardiolipin in 1mM diethlenetriaminepentaacetic acid (pH 7.0) by vortexing vigorously and bath sonication (50/60Hz, Ultrawave, Cardiff, UK) for 3 minutes. Lipid suspensions were incubated at room temperature for 30 minutes.

On completion of incubation period, 50µl of 2x reaction buffer (100mM imidazole HCl, pH 6.6; 100mM LiCl; 25mM $MgCl_2$; 2mM EGTA, pH 6.6), 19.4µl of dilution

buffer (10mM imadazole, pH 6.6; 1mM diethlenetriaminepentaacetic acid), 0.2μl of freshly prepared 1M dithiothreitol and 5μl of non-lyophilised *sn* 1,2-DAGK (1μg/ml) from E. *coli* (Calbiochem, Nottingham, UK) were added to each sample. The transfer of radioactive phosphate to ceramide/DAG by DAGK was initiated by the addition, 10μl of 10mM [γ-^{32}P]-ATP (1μCi/sample; Amersham Pharmacia Biotech UK Ltd, Little Chalfort, UK) to each sample, which was immediately mixed by vortex. The reaction was allowed to proceed for 30 minutes, after which, 750μl of premixed chloroform:methanol (2:1, v/v) was added to stop the reaction. Further additions of 150μl of sterile, distilled H_2O_2, 250μl of chlorofom and 250μl of 1% perchloric acid were made to each sample with intermediate vortexing (Bligh & Dyer, 1959; Perry & Hannun, 1999). Clean separation of organic and aqueous phases was ensured by centrifugation at 2000xg (Eppendorf centrifuge 5415D, Hamburg, Germany) for 5 minutes. The lower organic phase was carefully transferred to fresh microfuge tubes, ensuring no carryover of the aqueous phase. The aqueous phase contained approximately 90% of the radiation and was appropriately discarded. The organic phase, contained extracted radiolabelled lipids, was dried under a steady stream of dry N_2 gas and the resulting dried lipids resuspended in 50μl of 5% methanol in chloroform.

2.2.19 Separation of lipids by thin layer chromatography (TLC).

Scored silica pre-coated TLC plates (10x25cm, 0.25mm thickness, Merk, Poole, UK) were activated by running in 200mls of acetone in a TLC tank (Sigma, Poole, UK). Plates were then air dried immediately for 30 minutes. 20μl of lipid sample, in 5%

methanol in chloroform, was spotted in 5µl aliquots per lane using a fresh, glass capillary tube (Sigma, Poole, Dorset, UK) for each sample, 2.5cm from the base of the TLC plate. Each aliquot was dried with direct warm air before the next, so to concentrate each sample.

Well mixed chloroform:acetone:methanol:acetic acid:H_2O_2 (100:40;30;20;10, v/v/v/v/v; 200mls) was placed in a TLC tank. A large sheet of chromatography paper (Whatman 3MM Chr) was added to the tank to aid atmospheric saturation and the lid applied. The tank was allowed to saturate for 30 minutes prior to careful lowering of the spotted TLC plate in to the tank and the lid closed. The solvent front was allowed to migrate 15mm from the top of the TLC plate and was halted by removal of the TLC plate from the tank. The TLC plate was again air dried for 30 minutes.

2.2.20 Identification and quantification of ceramide 1-phosphate and phosphatidic acid.

Migration of phosphatadic acid/ceramide 1-phosphate standards or those extracted from cell samples was determined by autoradiography. Briefly, chromatographed TLC plates were exposured to Biomax™ imaging film (13x18cm, Eastman Kodak Co., New York, USA) for 14-16 hrs in the dark at -80°C with Biomax™ low energy intensifying screen (20.3x25.4cm, Eastman Kodak Co., New York, USA). Films were developed, and the positions of radioactive spots corresponding to ceramide-1-^{32}phosphate and ^{32}phosphatidic acid for the standards and each sample were identified.

The radioactive spot from each sample corresponding to ceramide 1-phosphate and phospatidic acid were scraped into separate scintilation vials, to which 5mls of OptiPhase"HiSafe" 3 scintilation fluid (Wallac Oy, Turku, Finland) was added. Counting was performed on a Canberra Packard 1900TR liquid scintillation analyser (Pangbourne, UK).

The mass of ceramide and DAG extracted from each cell sample was obtained from the standard curve and standardised as the lipid concentration per 10^6 cells. The assay was analysed for complete phosphorylation by calculating the linearity, r^2, of the standard curve. The efficiency of the assay was evaluated from the standard curve and a known concentration of C_6-ceramide. Cellular ceramide and DAG levels were adjusted according to the % efficiency of conversion.

2.3 Results.

Exposure of Jurkat T-cells to 20μM C_2-/C_6-ceramide induced a rapid, time dependent elevation in the percentage of specific apoptosis, not observed at lower synthetic ceramide concentrations (1-10μM; see Figures 2.7a & b). C_2-ceramide (20μM) induced an apoptotic cellular response, which was greater in magnitude, with more rapid kinetics than that observed with 20μM C_6-ceramide. Apoptosis was first observed at 2hrs post stimulation with 20μM C_2-ceramide ($p<0.05$) and 4hrs post treatment upon Jurkat exposure to 20μM C_6-ceramide ($p<0.05$). Maximum apoptotic response of approximately 55% and 40% were observed following 12hrs treatment with 20μM C_2- or C_6-ceramide respectively. Treatment of Jurkat T-cells for longer periods of up to 36 hours with 20μM C_2-/C_6-ceramide did not further increase the percentage of specific apoptosis ($p>0.05$; see Figures 2.7a & b). The percentage of actual apoptosis observed in Jurkat T-cells following 36 hours treatment with 20μM C_2-/C_6-ceramide rose to approximately 80% compared to 20% in vehicle treated controls, where the elevated levels of apoptosis in controls may be attributed to serum starvation (Data not shown). The trend for protection against apoptosis observed at 36 hours treatment of Jurkat T-cells with 1-10μM C_2-C_6-ceramide was not significant ($p>0.05$; see Figures 2.7a & b). FS and the uptake of the membrane impermeant dye, PI, by Jurkat T-cells was not significantly affected by 10μM C_2-/C_6-ceramide exposure for treatment times of up to 16 hours ($p>0.05$; see Figure 2.8a & b). Similarly, no alteration in FS or PI uptake was observed in Jurkat T-cells treated for up to 4 hours with 20μM C_2-/C_6-ceramide ($p>0.05$; see Figures 2.8a & b). However, on increasing the incubation period to 16 hours, a sub-population of C_2-/C_6-ceramide

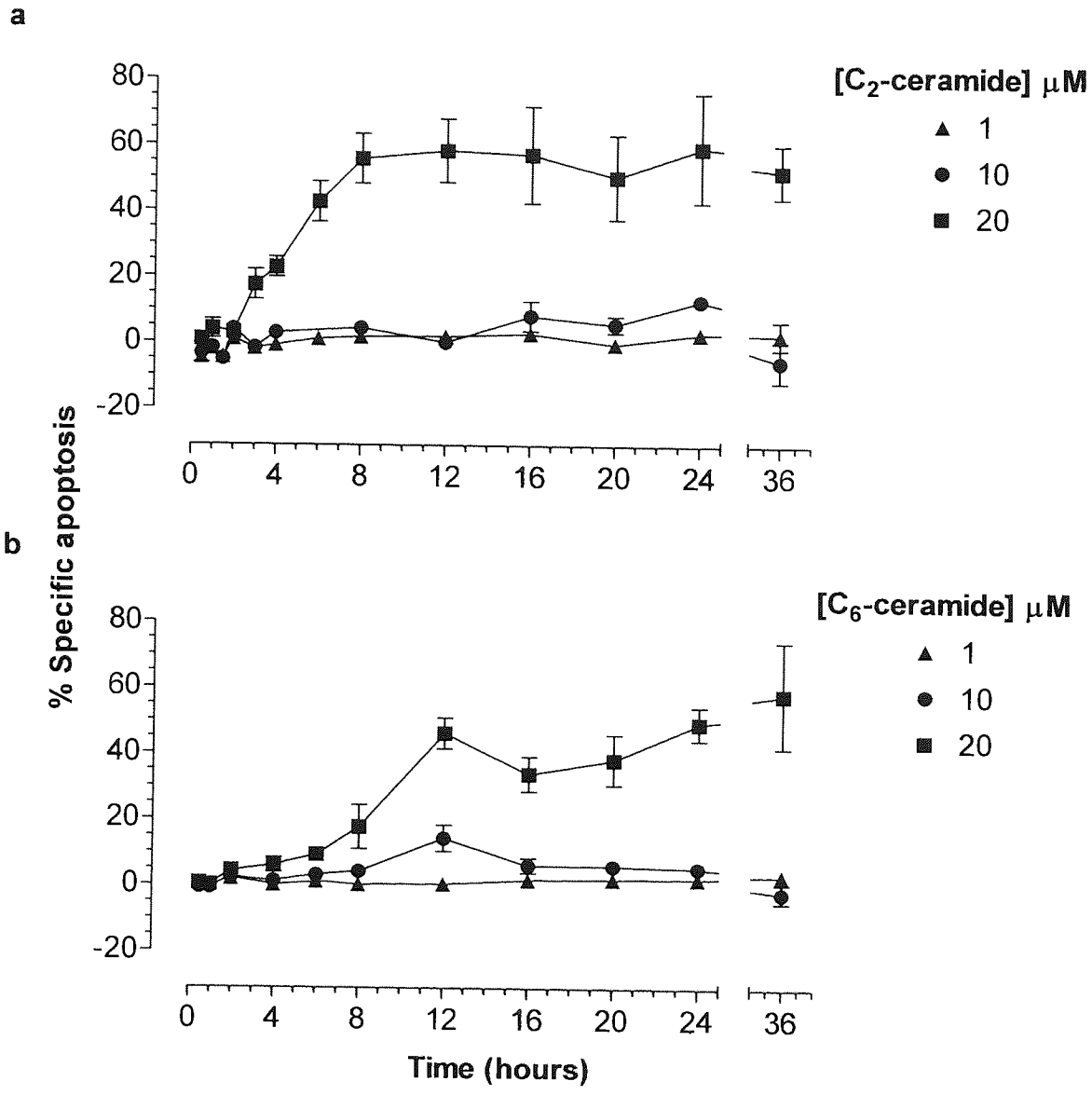

Figure 2.7. Short chain synthetic ceramides induce time- and concentration-dependent increases in apoptosis in Jurkat T-cells. Jurkat T-cells ($2x10^6$/ml) were serum starved for 4 hours prior to the addition of (a) C_2- or (b) C_6 (0-20μM) for 0-36 hours. Incubations were performed at 37°C in a 95% air, 5% CO_2 humidified atmosphere and terminated by washing the cells twice with ice cold PBS. Cell pellets were resuspended in 1ml of hypotonic fluorochrome solution and incubated in the dark at 4°C overnight prior to DNA cell cycle analysis by flow cytometry. The sub-diploid DNA content of 20,000 nucleoids from each sample was analysed. The data are presented as the mean ± s.e.m of at least 7 individual experiments, expressed as the percentage specific apoptosis according to the formula specific apoptosis = (T-C)/(100-C) x100, where T equals the percentage of apoptotic events from treated cells, and C equals the percentage of apoptotic events from control cells.

a

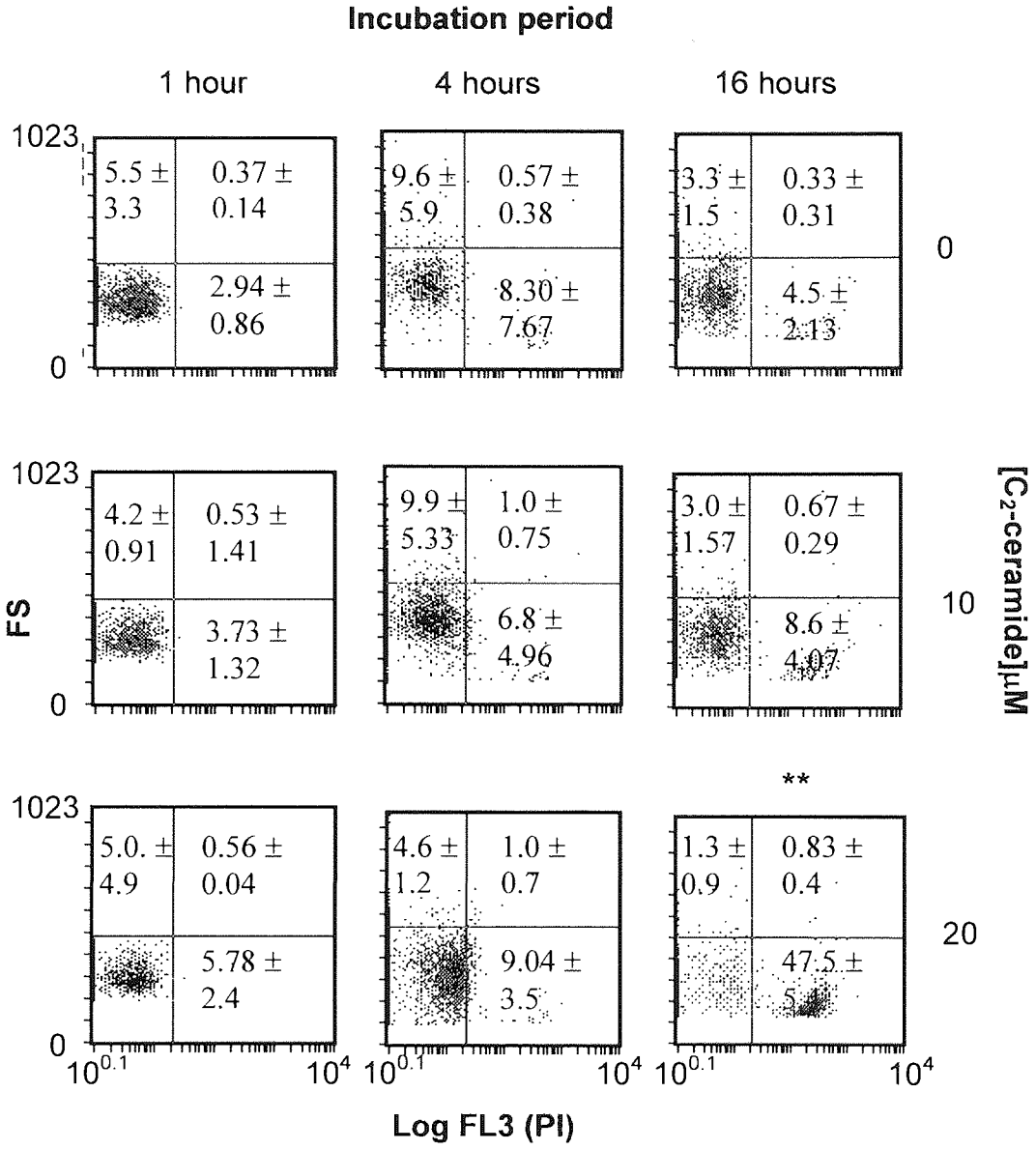
Incubation period
1 hour
4 hours
16 hours
1023
0
5.5 ± 3.3
0.37 ± 0.14
2.94 ± 0.86
9.6 ± 5.9
0.57 ± 0.38
8.30 ± 7.67
3.3 ± 1.5
0.33 ± 0.31
4.5 ± 2.13
0
4.2 ± 0.91
0.53 ± 1.41
3.73 ± 1.32
9.9 ± 5.33
1.0 ± 0.75
6.8 ± 4.96
3.0 ± 1.57
0.67 ± 0.29
8.6 ± 4.07
10
**
5.0. ± 4.9
0.56 ± 0.04
5.78 ± 2.4
4.6 ± 1.2
1.0 ± 0.7
9.04 ± 3.5
1.3 ± 0.9
0.83 ± 0.4
47.5 ± 5.4
20
FS
[C2-ceramide]μM
10^0.1
10^4
Log FL3 (PI)

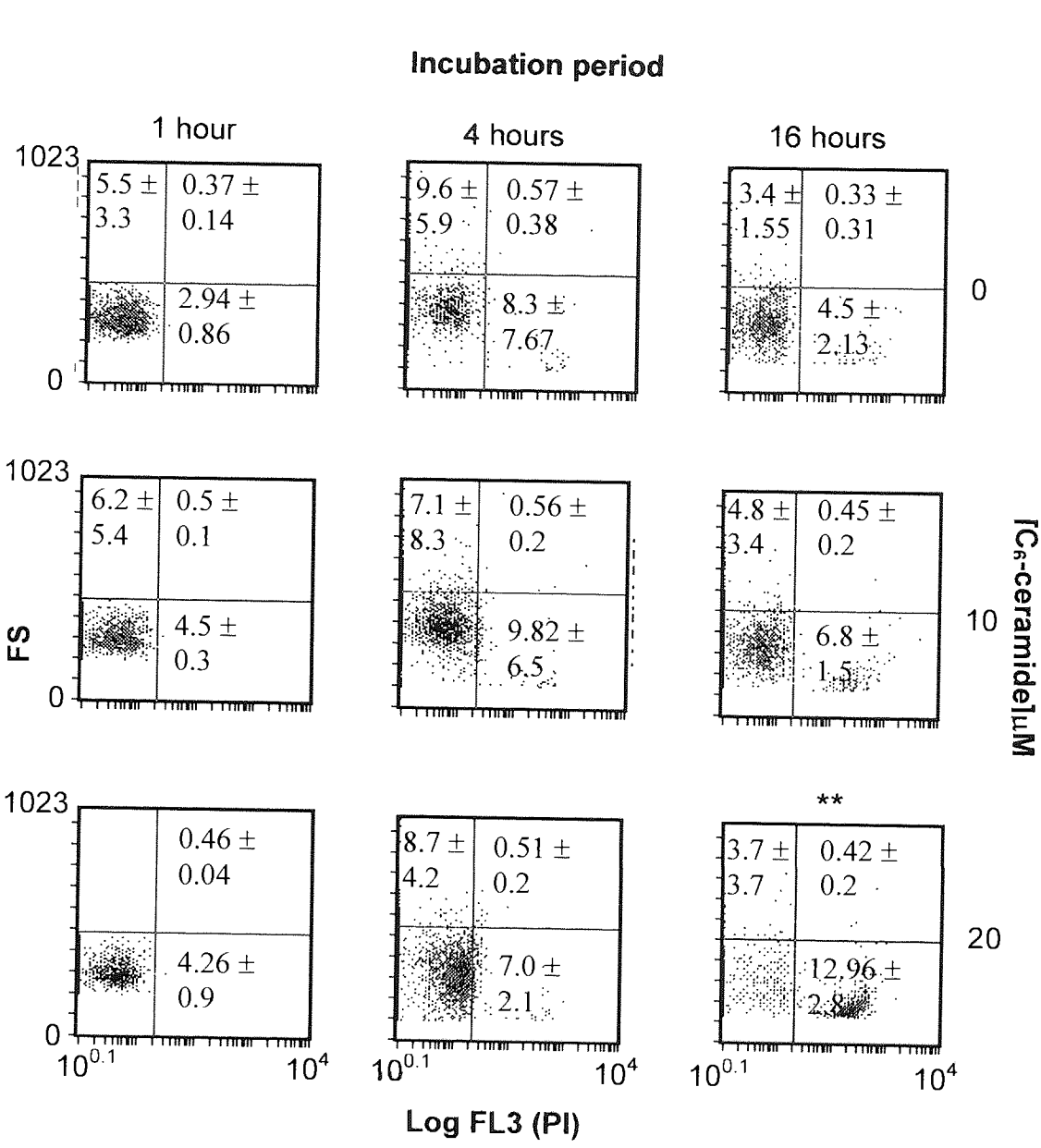

Figure 2.8. C_2-/C_6ceramide induces time and concentration dependent loss in Jurkat T-cell membrane permeability. Jurkat T-cells ($2x10^6$/ml) were serum starved for 4 hours prior to the addition of C_2- (a) or C_6-ceramide (b) 0-20μM for 0-16 hours. Incubations were performed at 37°C in a 95% air, 5% CO_2 humidified atmosphere and terminated by washing the cells twice with ice cold PBS. Cell pellets were resuspended in 1ml of PI solution (25μg/ml in PBS containing 0.1% BSA) and incubated in the dark at room temperature for 15 minutes. Cell samples were analysed immediately by flow cytometry for PI uptake on a dual parameter histogram of log FL3 (propidium iodide, PI) versus forward scatter (FS) as described in method 2.2.12. Flow cytometry histograms shown are representational of 3 individual experiments. Data are expressed as the percentage of cells in each quadrant as the mean ± s.d of 3 individual experiments and test samples analysed for statistical significance from control by one-way ANOVA followed by Dunnett's multiple comparison test where ** ($p<0.01$) represents significant difference from control.

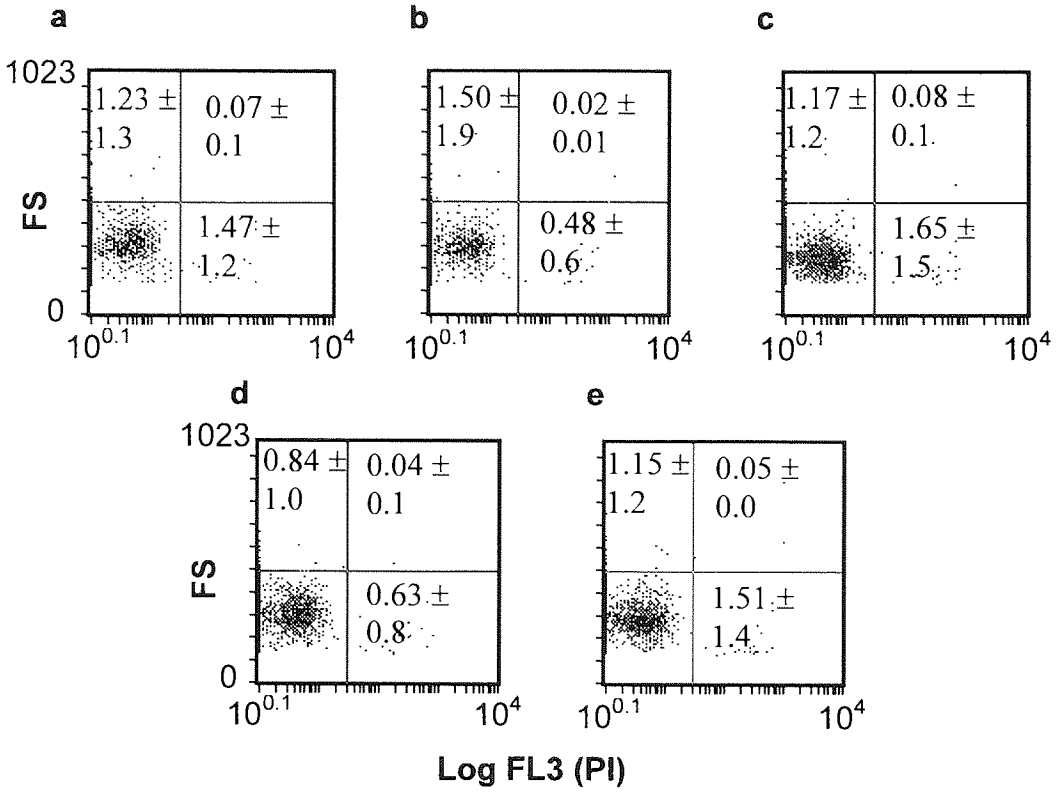

Figure 2.9. U937 monocyte viability is not compromised by C_2-/C_6-ceramide. U937 monocytes ($2x10^6$/ml) were serum starved for 4 hours prior to the addition of vehicle control (a), 10μM C_2-ceramide (b), 20μM C_2-ceramide (c), 10μM C_6-ceramide (d) or 20μM C_6-ceramide (e) for 16 hours. Incubations were performed at 37°C in a 95% air, 5% CO_2 humidified atmosphere and terminated by washing the cells twice with ice cold PBS. Cell pellets were resuspended in 1ml of PI solution (25μg/ml in PBS containing 0.1% BSA) and incubated in the dark at room temperature for 15 minutes. Cell samples were analysed immediately by flow cytometry for PI uptake on a dual parameter histogram of log FL3 (propidium iodide, PI) versus forward scatter (FS) as described in method 2.2.12. Flow cytometry histograms shown are representational of 3 individual experiments. Data are expressed as the percentage of cells in each quadrant as the mean ± s.d of 3 individual experiments and test samples analysed for statistical significance from control by one-way ANOVA followed by Dunnett's multiple comparison test.

(20μM) Jurkat T-cells possessed a significant reduction in FS properties corresponding with an elevation in PI uptake ($p<0.01$; see Figures 2.8a & b). No significant elevation in FS properties were showed in Jurkat T-cells at all incubation periods (0-16 hours) with 20μM C_2-/C_6- ($p>0.05$ for each ceramide species, see Figures 2.8a & b).

Unlike Jurkat T-cells, exposure of the human monocytic cell line U937 to either C_2- or C_6-ceramide (0-20μM) for up to 36 hours induced no evidence of DNA fragmentation when analysed by flow cytometric DNA cell cycle analysis ($p>0.05$). Furthermore, no significant alterations in FS or PI uptake were observed in U937 monocytes treated with C_2-/C_6-ceramide (0-20μM) at incubations up to 16 hours ($p>0.05$; see Figure 2.9). Instead, flow cytometric DNA cell cycle analysis revealed that ceramide exposure induced an accumulation of nuclei in the G0/G1 phase of the cell cycle when compared to vehicle treated controls. This was first evident following 16 hrs treatment of U937s with 20μM C_2-/C_6-ceramide ($p<0.05$; see Figures 2.10a & b), but was also observed at 20hrs incubation with 10μM C_6 ceramide ($p<0.05$; see Figure 2.10b). Vehicle treated, control U937 monocytes also showed, albeit to a lesser extent, a time dependent elevation in the percentage of nucleoids in the G0/G1 phase of the cell cycle from approximately 45% at 8 hours to approximately 55% at 16-24 hours post-stimulation (see Figures 2.10a & b). Extending the treatment period to 36 hours induced a significant reduction in the percentage G0/G1 content of vehicle treated control U937 monocytes compared to 24 hours treatment (mean percentage ± s.e.m; 40.35 ± 2.732, n=10 compared to 62.30 ± 2.004 n=6; $p<0.001$; see Figures 2.10a, b, 2.11a & b). This was associated with a significant elevation in the actual apoptosis in 36 hours treated controls versus 24

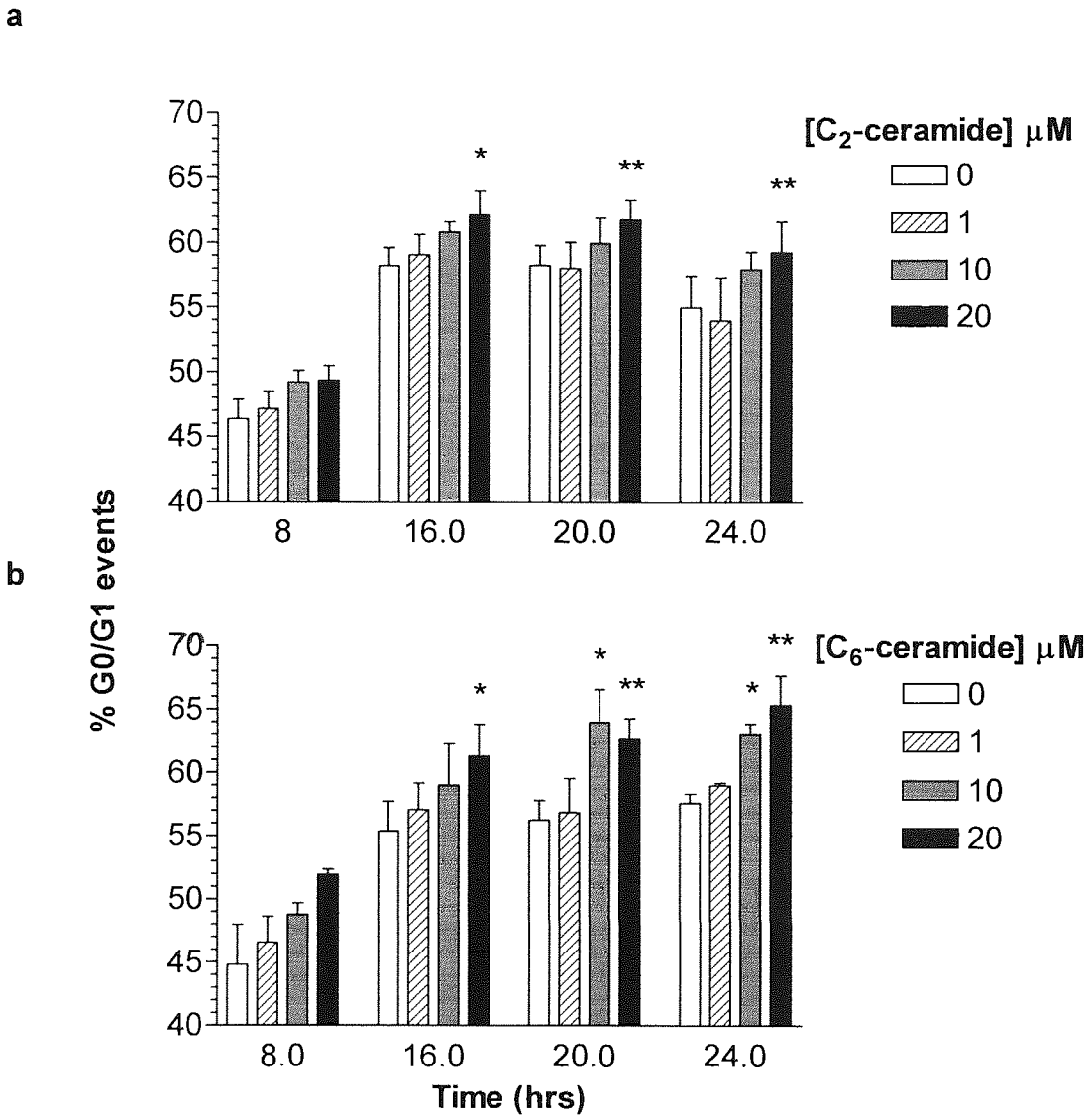

Figure 2.10. Short chain synthetic ceramides induce growth arrest in U937s. U937s ($2x10^6$/ml) were serum starved in RPMI 1640 for 4 hours prior to the addition 0-20μM C_2-ceramide (a) or C_6-ceramide (b) and incubated in a humidified 5% CO_2, 95% air atmosphere at 37°C for 8, 16, 20 or 24 hours. Cell pellets were resuspended in 1ml of hypotonic fluorochrome solution as described in materials and methods prior to DNA cell cycle analysis by flow cytometry. 20,000 nucleoids were counted per sample. The percentage G0/G1 content of DNA cell cycles were quantified using MultiCycle™ for Windows (Phoenix Flow Systems, San Diego, U.S.A.). The data are presented as the arithmetic mean percents ± s.e.m of 5 individual experiments. * indicate $p<0.05$ or ** indicate $p<0.01$ compared to vehicle treatment by one way ANOVA followed by Dunnett's multiple comparison test.

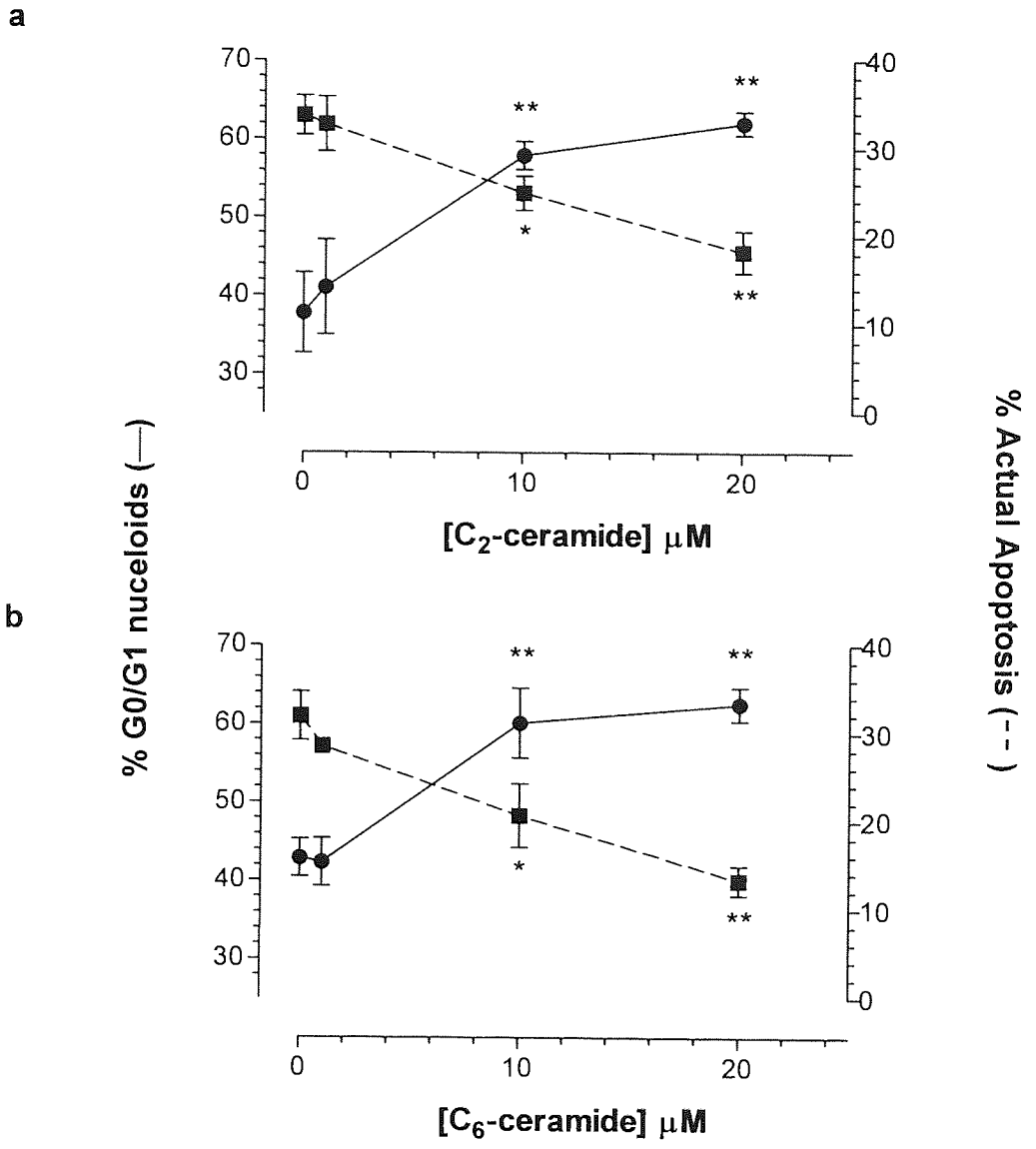

Figure 2.11. Synthetic ceramides protect against apoptosis induced by serum withdrawal. U937s ($2x10^6$/ml) were serum starved in RPMI 1640 for 4 hours prior to the addition 0-20μM C_2-ceramide (a) or C_6-ceramide (b) and incubated in a humidified 5% CO_2, 95% air atmosphere at 37°C for 36 hours. Cell pellets were resuspended in 1ml of hypotonic fluorochrome solution as described in materials and methods prior to DNA cell cycle analysis by flow cytometry. 20,000 nucleoids were counted per sample and the sub-diploid DNA content recorded to represent the percentage actual apoptosis (■). The percentage G0/G1 content of DNA cell cycles (●) was quantified using MultiCycle™ for Windows (Phoenix Flow Systems, San Diego, U.S.A.). The data are presented as the arithmetic mean percents ± s.e.m of 3 individual experiments. * indicate $p<0.05$ or ** indicate $p<0.01$ compared to vehicle treatment by one way ANOVA followed by Dunnett's multiple comparison test.

hour treated controls (mean percentage ± s.e.m.; 32.9 ± 1.633, n=6 compared to 6.47 ± 1.42 n=5; $p<0.001$). Low dose C_2-/C_6-ceramide (1μM) exposure for 36 hours did not significantly affect either the percentage of nucleoids in the G0/G1 phase of the cell cycle ($p>0.05$) nor the percentage of actual apoptosis compared to that observed in vehicle treated control U937 monocytes ($p>0.05$; see Figures 2.11a & b). Monocytes treated with either 10 or 20μM C_2/-C_6-ceramide for 36 hours possessed significantly elevated G0/G1 DNA content compared to vehicle controls ($p<0.01$ for each ceramide species). There was no significant difference between 10 and 20μM ceramide treatment with either species ($p>0.05$). The G0/G1 content remained elevated to statistically identical levels to that of U937 monocytes treated with 10 or 20μM C_2-/C_6-ceramide for 24 hours ($p<0.05$). Correspondingly, the synthetic ceramide treatment of U937 monocytes induced a dose dependent inhibition of actual apoptosis. C_2/-C_6-ceramide (10μM) treatment for 36 hours significantly inhibited the appearance of actual apoptosis by approximately 10% ($p<0.05$) and 12% ($p<0.05$) respectively. Greater protection against actual apoptosis by 16% ($p<0.01$) and 18% ($p<0.01$) was seen following 20μM C_2- and C_6-ceramide respectively (see Figure 2.11a & b). The inhibition of actual apoptosis induced by 36 hour C_2- and C_6-ceramide exposure was not significantly different at either concentration 10μM ($p>0.05$) and 20μM ($p>0.05$).

During the first 16 hours of Jurkat T-cell or U937 monocyte exposure to C_2-/C_6-ceramide, the presence of mitochondrial peroxide ($[peroxide]_m$) was monitored by flow cytometry, analysing the fluorescence emission distribution of cells co-exposed to the peroxide sensitive dye DHR123. As a positive control both U937 monocytes and Jurkat T-cells were exposed to A.A, a complex III inhibitor of the electron

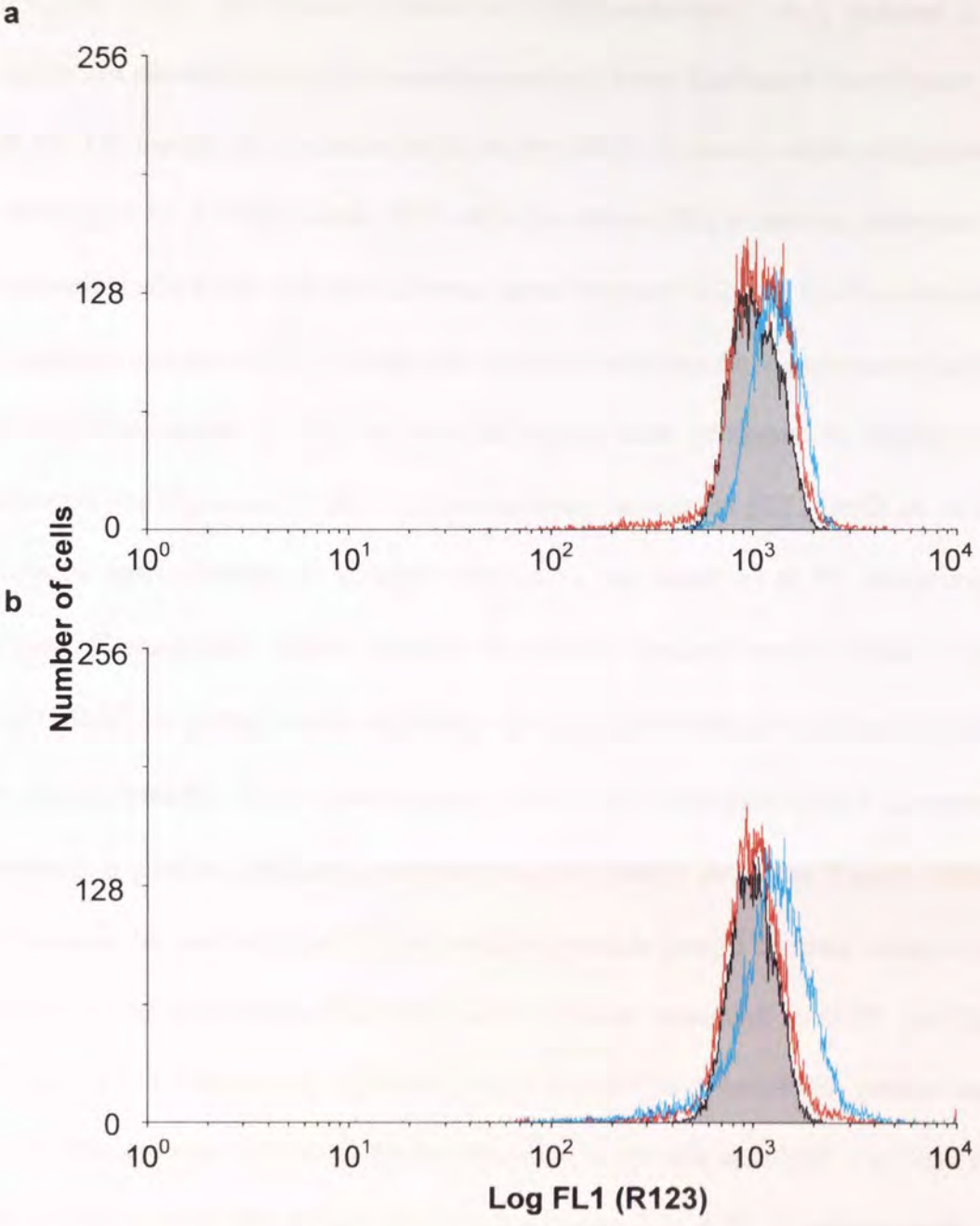

Figure 2.12. Increase in R123 fluorescence in response to antimycin A. Concentration dependent effects of antimycin A (A.A) induced oxidation of rhodamine 123 (R123). Briefly, $2x10^6$/ml (0.5mls) of U937 monocytes (a) or Jurkat T-cells (b) were serum starved for 4 hours in RPMI 1640 prior to the addition of 0-25μM AA for 2 hours. Thirty minutes prior to the termination of treatment periods, 10μl of dihydrorhodamine 123 (DHR123; 1mg/ml) was added to each sample. At the end of the incubation periods, cell samples were washed twice with ice cold PBS and the viable cell population analysed by flow cytometry for rhodamine 123 (R123) fluorescence as described in method 2.2.11. Shown are typical R123 emission spectra of U937 monocytes (a) or Jurkat T-cells (b) treated with either vehicle (black outline), 10μM (red) or 25μM (blue) AA.

transport chain and known inducer of ROS production. A.A induced a dose dependent elevation in R123 fluorescence after 2 hours incubation (see Figures 2.12a & b). The median fluorescence (MdX) of the DHR123 treated viable cell population, determined by forward scatter (FS) and side scatter (SS) properties, increased with immediate effect and with rapid kinetics upon exposure to 20μM C_2-/C_6-ceramide. A significant increase in R123 MdX was recorded after one hour exposure to all doses of C_2-/C_6-ceramide ($p<0.05$) in both cell types when compared to vehicle treated controls (see Figures 2.13 & 2.14). A maximum increase in ΔR123MdX of Jurkat T-cells of approximately 25 arbitrary units (a.u) was observed at 1hr treatment with 20μM C_2-ceramide, which returned to vehicle control levels within 4 hours. ΔR123MdX of Jurkat T-cells exposed to 20μM C_2-ceramide for 16 hours fell further to approximately –60 a.u (see Figure 2.14a). The analogue, 20μM C_6-ceramide, induced a similar significant elevation in ΔR123MdX in Jurkat T-cells following incubation for one hour ($p<0.01$) returning to vehicle treated controls within 4 hours ($p>0.05$) and remaining at this level after 16 hours treatment ($p>0.05$; see Figures 2.13a). R123 fluorescence of Jurkat T-cells exposed to ceramide for greater than 16 hours was not measured as no further alteration in specific apoptosis was observed at these longer incubation periods ($p>0.05$; see Figure 2.7a & b). A non-apoptotic dose of C_2-/C_6-ceramide (10μM; $p>0.05$; see Figure 2.7a & b) caused significant elevations in ΔR123MdX to approximately 10 a.u ($p<0.01$) and 18 a.u respectively ($p<0.01$) in Jurkat T-cells after 1 hour, which were significantly less than the elevations mediated by higher concentrations of either species ($p<0.05$). ΔR123MdX returned to baseline after 4 hours treatment of Jurkat T-cells with 10μM ($p>0.05$) and remained identical to vehicle control treated cells for the remainer of the experimental period ($p>0.05$; see Figures 2.13a & 2.14b). The elevation in DHR123 fluorescence

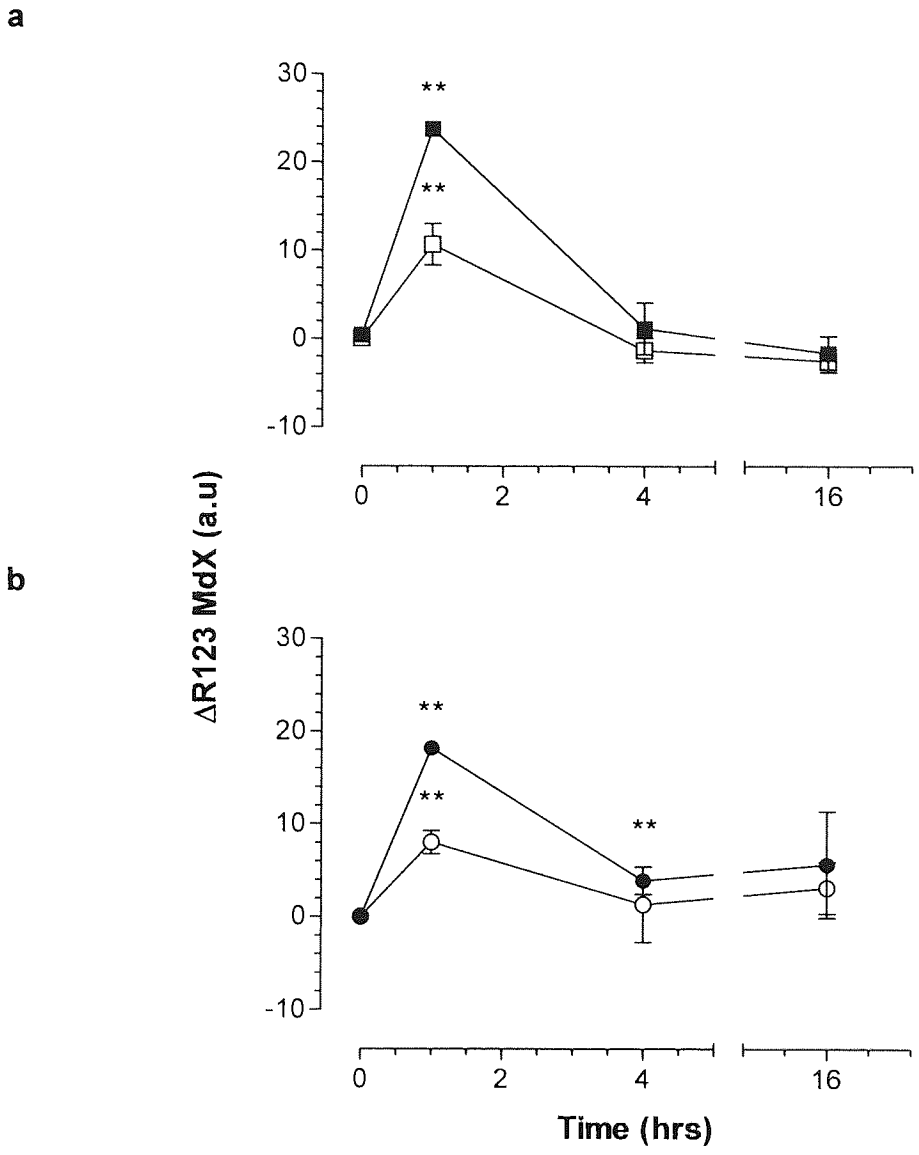

Figure 2.13. C_6-ceramide induces a transient elevation in mitochondrial peroxide production in Jurkat T-cell and U937 monocytes: kinetics for the C_6-ceramide dependent oxidation of rhodamine 123 (R123). Jurkat T-cells (solid fill) and U937 monocytes (open; 0.5mls; $2x10^6$/ml) were serum starved for 4 hours in RPMI 1640 prior to the addition of (a) 20μM or (b) 10μM C_6-ceramide for 0-16 hours, with vehicle treatment as controls. Thirty minutes prior to the termination of treatment periods, 10μl of dihydrorhodamine 123 (DHR123; 1mg/ml) was added to each sample. At the end of the incubation periods, cell samples were washed twice with ice cold PBS and the viable cell population analysed by flow cytometry for R123 fluorescence as described in method 2.2.11. The median R123 (MdR123) fluorescence of 10,000 viable cells per sample were recorded and the difference in MdR123 of test samples from control samples (ΔR123) calculated. All incubations were performed in a humidified 95% air, 5% CO_2 atmosphere at 37°C. Data are presented as the mean ± S.D. of 3 individual experiments, where ** ($p<0.01$) represents significant difference from controls by one way ANOVA followed by Dunnett's multiple comparison test. Arbitrary units, a.u

of U937 monocytes treated for one hour with either dose of C_2-/C_6-ceramide was significantly lower than that observed in Jurkat T-cells ($p<0.05$; see Figures 2.13a, 2.13b, 2.14a & b). This small increase in R123 fluorescence corresponds to the adaptive stress response of growth arrest observed in U937 monocytes treated with synthetic ceramide rather than the larger increase in R123 fluorescence associated with apoptosis seen in Jurkat T-cells (see Figures 2.7a, b, 2.10a & b). ΔR123MdX in U937s exposed to C_2-/C_6-ceramide for 1 hour was dose dependent, where 10μM of either species induced an increase in ΔR123MdX to approximately 6 a.u (see Figures 2.13b & 2.14b), which was of lower magnitude than that observed with 20μM C_2-/C_6-ceramide (9 a.u; $p<0.05$; see Figures 2.13a & 2.14b). At 4 hours post-treatment with the higher concentrations of C_2-/C_6-ceramide (20μM), U937 ΔR123MdX returned to baseline ($p<0.05$) and remained at this level for the remainder of the experimental period ($p<0.05$; see Figure 2.13a & 2.14b). The ΔR123MdX induced by lower concentrations of synthetic ceramides (10μM) in U937 monocytes remained elevated above baseline after 4 hours treatment ($p<0.05$) and in the case of C_6-ceramide, remained elevated at 16 hours post-treatment ($p<0.01$; see Figures 2.13b and 2.14b).

To further evaluate the effect of synthetic, short chain ceramide's on the overall redox state of the cell, the presence of cellular glutathione (GSH) was monitored using the DTNB dependent recycling assay of Tietze, (1969). The total cellular GSH levels were expressed per mg of protein since treatment of Jurkat T-cells or U937 monocytes with all doses of C_2-/C_6-ceramide did not significantly affect protein levels (see Figures 2.15a & b). The mean total cellular GSH levels of Jurkat T-cells or U937 monocytes decreased with immediate effect and with rapid kinetics upon exposure to 10μM or 20μM C_2-/C_6-ceramide. The first significant loss of GSH was

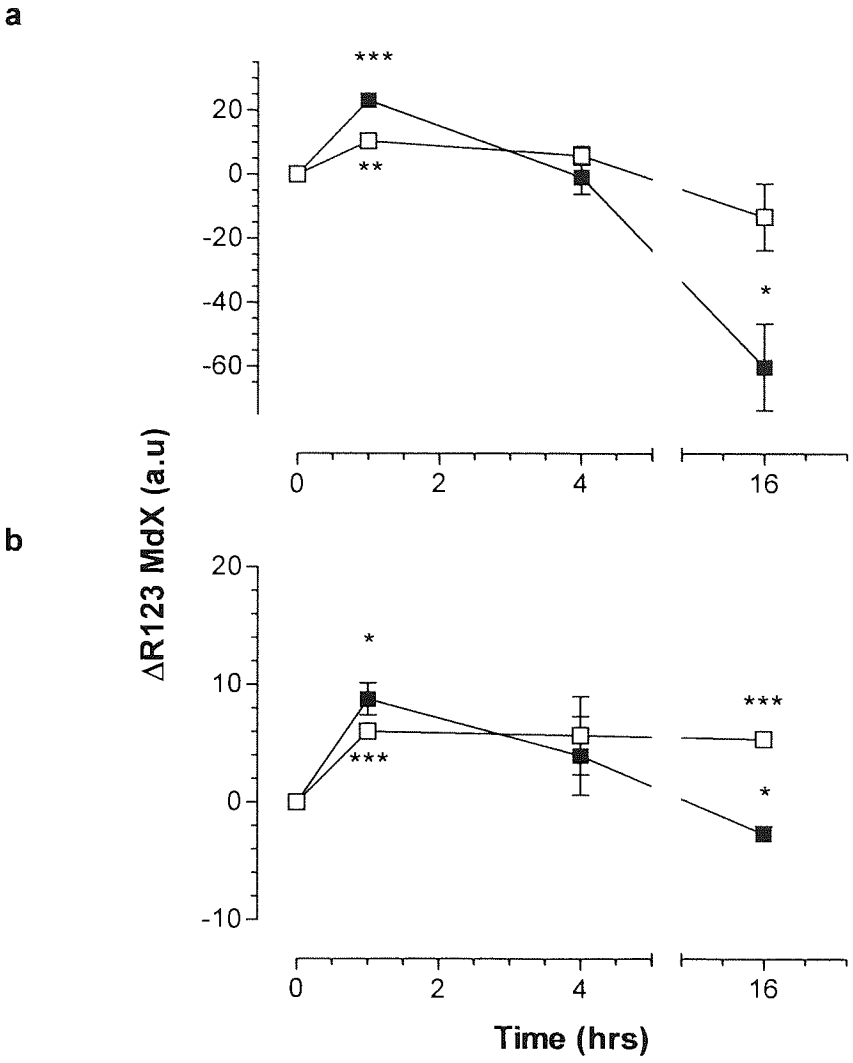

Figure 2.14. C_2-ceramide induces a transient elevation in mitochondrial peroxide production in Jurkat T-cell and U937 monocytes: kinetics for the C_2-ceramide dependent oxidation of rhodamine 123 (R123). Jurkat T-cells (a) and U937 monocytes (b; 0.5mls; $2x10^6$/ml) were serum starved for 4 hours in RPMI 1640 prior to the addition of 20μM (■) or 10μM (□) C_2-ceramide for 0-16 hours, with vehicle treatment as controls. Thirty minutes prior to the termination of treatment periods, 10μl of dihydrorhodamine 123 (DHR123; 1mg/ml) was added to each sample. At the end of the incubation periods, cell samples were washed twice with ice cold PBS and the viable cell population analysed by flow cytometry for R123 fluorescence as described in method 2.2.11. The median R123 (MdR123) fluorescence of 10,000 viable cells per sample were recorded and the difference in MdR123 of test samples from control samples (ΔR123) calculated. All incubations were performed in a humidified 95% air, 5% CO_2 atmosphere at 37°C. Data are presented as the mean ± S.D. of 3 individual experiments, where * ($p<0.05$), ** ($p<0.01$) and *** ($p<0.001$) represents significant difference from controls by one way ANOVA followed by Dunnett's multiple comparison test. Arbitrary units, a.u

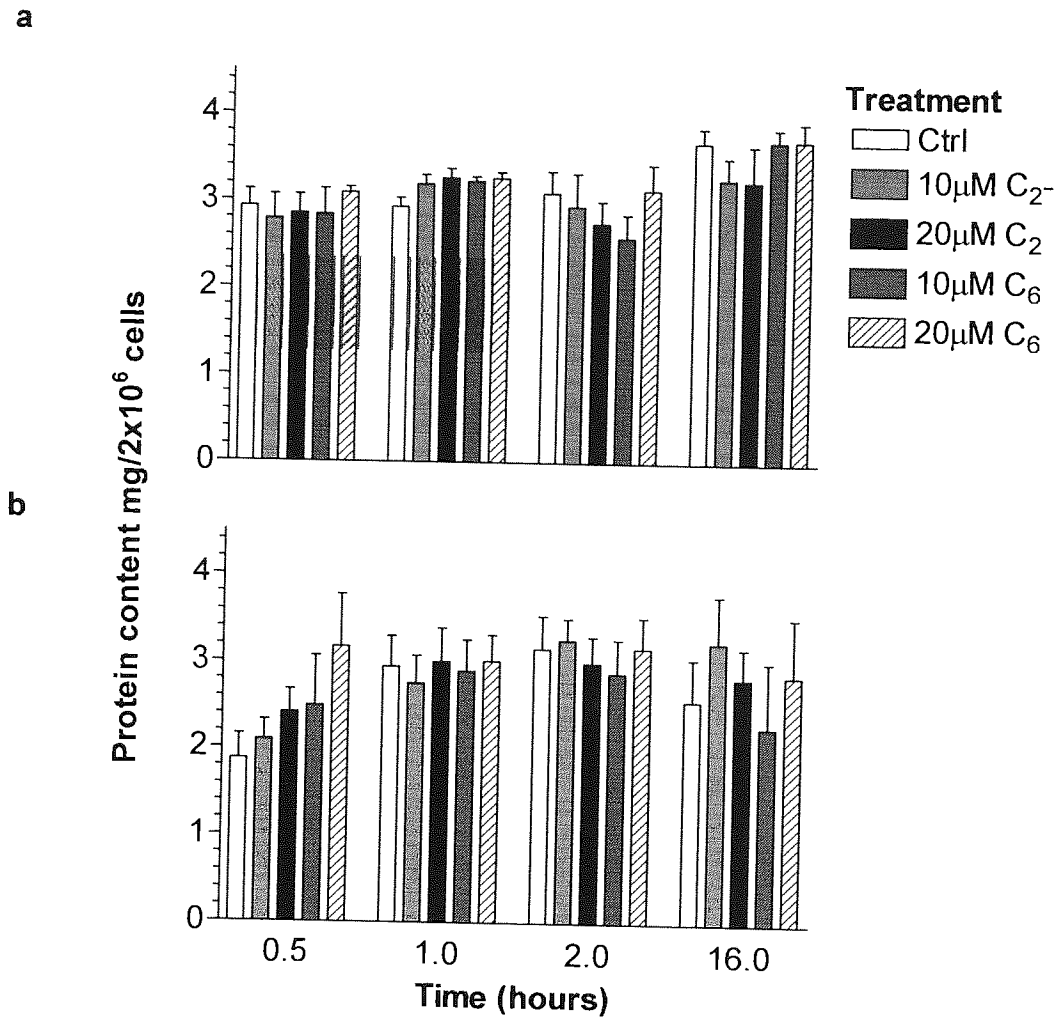

Figure 2.15. Jurkat T-cell and U937 monocyte protein content is not affected by C_2-/C_6-ceramide treatment. Jurkat T-cells (a) or U937 monocytes (b; $2x10^6$/ml) were serum starved in RMPI 1640 for 4 hours prior to the addition of C_2-/C_6-ceramide (0-20μM) for 0-4 hours (a) or 0-16 hours (b). At the end of the treatment period, cells were washed twice with ice cold PBS. The total protein content was analysed by the bichinonic acid assay and quantified against a standard curve of known protein concentrations as described in method 2.2.15. Data represents the mean ± s.e.m of 4 individual experiments analysed in quadruplicate. Statistical analysis was performed by one-way ANOVA followed by Tukey's post hoc test.

recorded after 30 minutes Jurkat T-cell exposure to 20μM C_2-ceramide ($p<0.01$) or 1 hour post-stimulation with C_6-ceramide ($p<0.05$) when compared to vehicle treated controls. A maximum decrease in GSH of Jurkat T-cells of approximately 55% for C_6- and total loss for 20μM C_2-ceramide was observed after 4 hours exposure (see Figures 2.16a & b). Over time, the effect was dose-dependent, with lower concentrations (10μM) of C_2-/C_6-ceramide eliciting a reduction in the total cellular GSH at 30 minutes ($p<0.01$) and 1 hour ($p<0.05$) respectively, followed by a return to control GSH levels equivalent to vehicle treated Jurkat T-cells after 2 and 4 hours treatment ($p>0.05$; see Figures 2.16a & b).

Exposure of the human monocytic cell line U937 to either C_2- or C_6-ceramide induced a time dependent, transient loss of total cellular GSH. U937 monocytes treated with 20μM C_6-ceramide for 30 minutes significantly reduced GSH levels to approximately 75% of controls ($p<0.01$) and remained at this level for up to 2 hours post-treatment ($p<0.01$). A lower concentration of 10μM C_6-ceramide also decreased GSH levels to 75%, but with delayed kinetics, and was first observed after 1 hour treatment ($p<0.01$; see Figure 2.17b). C_2-ceramide induced an identical reduction in the total U937 monocyte GSH levels, however, these losses occurred after 1 and 2 hours with 20μM ($p<0.01$) and 10μM ($p<0.01$) C_2-ceramide respectively (see Figure 2.17a). The cellular GSH pool of U937 monocytes treated with either concentration of C_6-ceramide and 20μM C_2-ceramide showed complete recovery after 4 hours treatment ($p>0.05$) and remained at control levels for the remainder of the experimental period ($p>0.05$). U937 monocytes treated with 10μM C_2-ceramide showed recovery of GSH levels to that of controls after 16 hours treatment ($p>0.05$; see Figures 2.17a & b). The total cellular GSH concentration of control U937

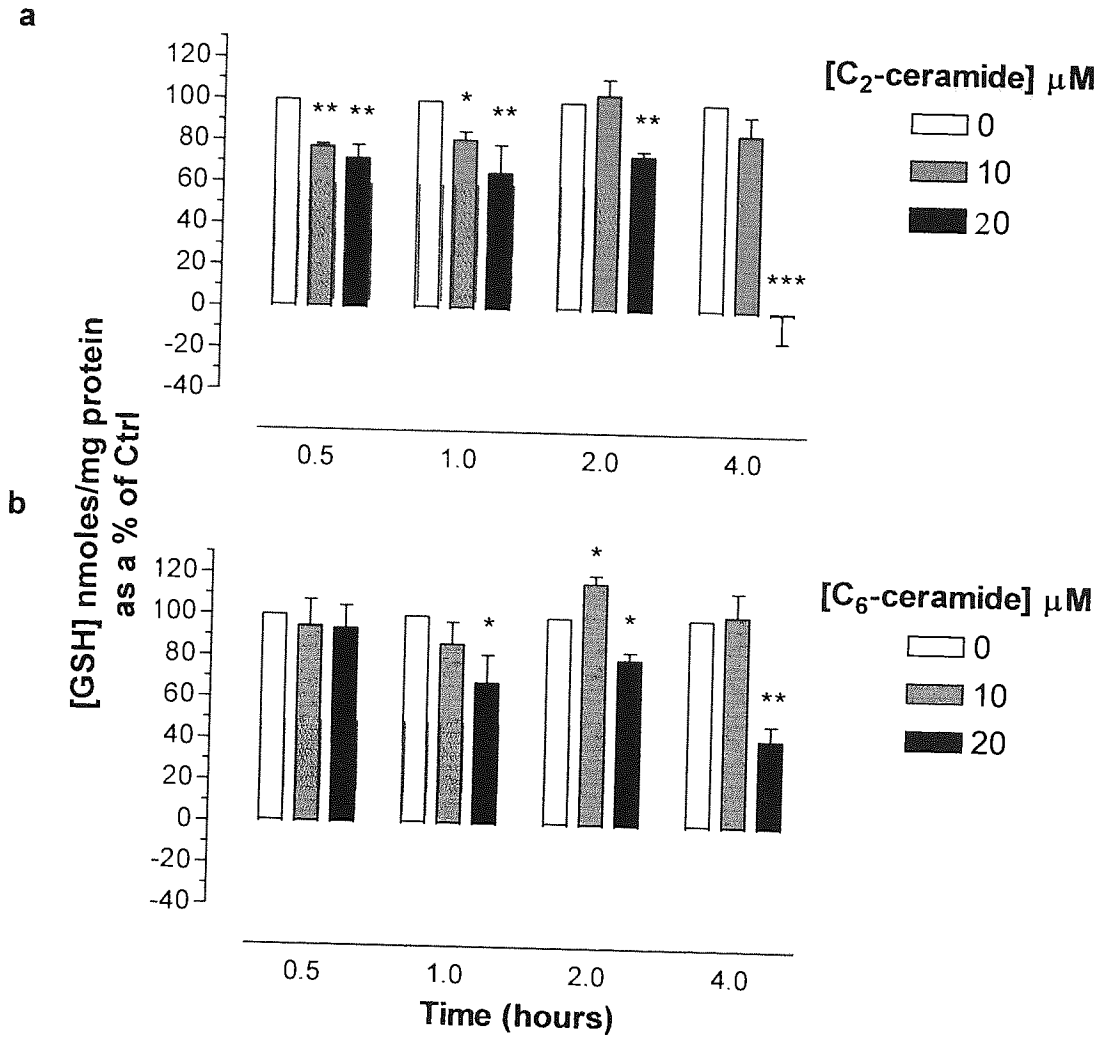

Figure 2.16. The effects of synthetic ceramides on Jurkat T-cell total cellular glutathione levels. Jurkat T-cells ($2x10^6$/ml) were serum starved for 4 hours prior to the addition of 0, 10 or 20μM C_2- (a) or C_6-ceramide (b) for 0.5, 1, 2 or 4 hours. At the end of the treatment period, cells were washed twice with ice cold PBS. The total glutathione (GSH) content was analysed by spectrophotometric determination of reduced DNTB using a GSSG recycling assay and quantified against a standard curve of known GSH concentrations as described in method 2.2.14. Data represents the mean GSH content per mg of cellular protein ± s.e.m of 4 individual experiments analysed in quadruplicate and expressed as a percentage of control. Statistical analysis was performed by one-way ANOVA followed by Tukeys' post hoc test where * ($p<0.05$), ** ($p<0.01$) or *** ($p<0.001$) was considered significant from vehicle control treatments.

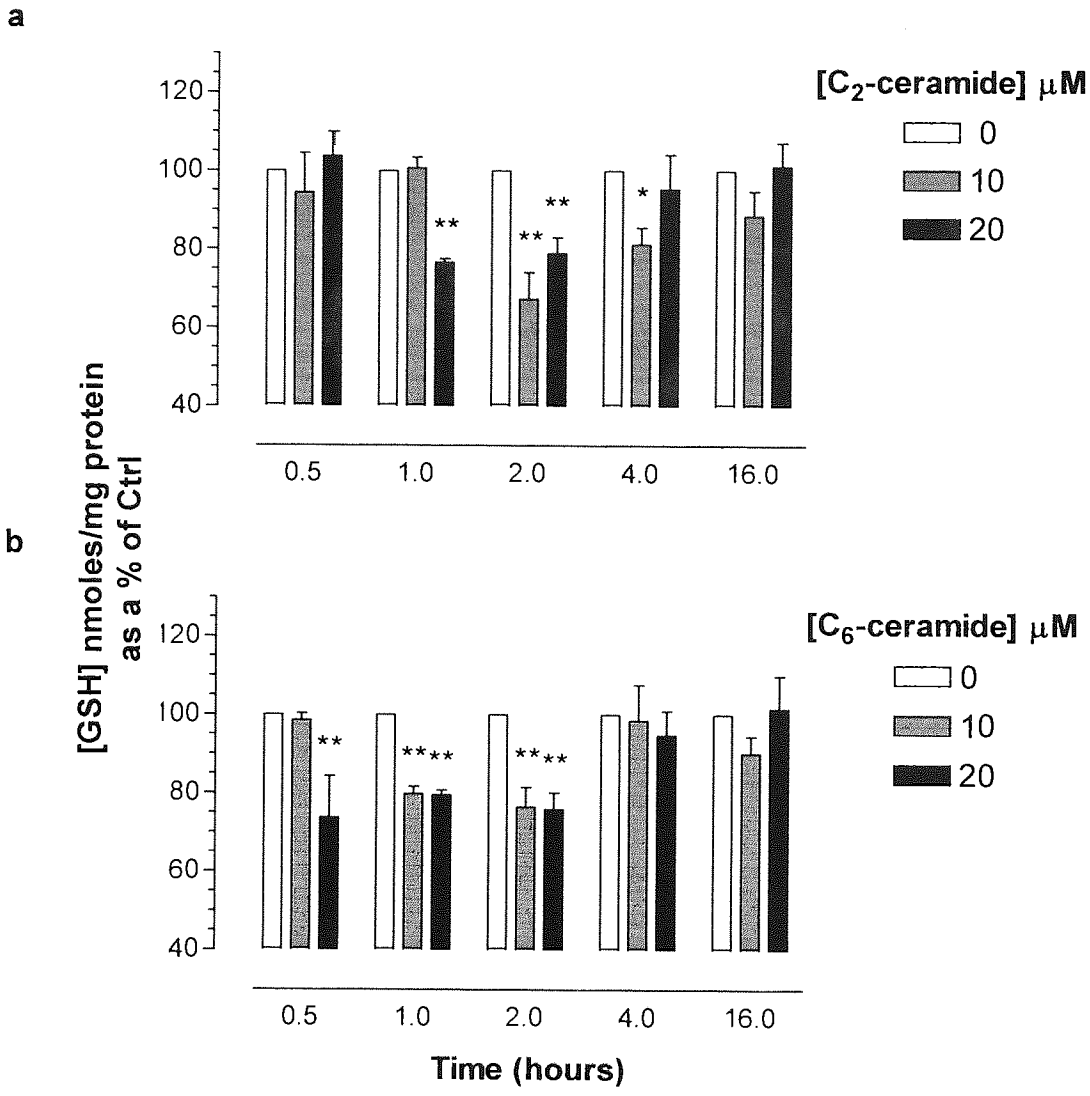

Figure 2.17. Synthetic ceramides induce transient alterations in the total cellular glutathione levels of monocytes. U937 monocytes ($2x10^6$/ml) were serum starved for 4 hours prior to the addition of 0, 10 or 20μM C_2- (a) or C_6-ceramide (b) for 0.5, 1, 2, 4 or 16 hours. At the end of the treatment period, cells were washed twice with ice cold PBS. The total glutathione (GSH) content was analysed by spectrophotometric determination of reduced DNTB using a GSSG recycling assay and quantified against a standard curve of known GSH concentrations as described in method 2.2.14. Data represents the mean GSH content per mg of cellular protein ± s.e.m of 4 individual experiments analysed in quadruplicate and expressed as a percentage of control. Statistical analysis was performed by one-way ANOVA followed by Tukeys' post hoc test where * ($p<0.05$) or ** ($p<0.01$) was considered significant from vehicle control treatments.

monocytes (mean ± s.d; = 31.18 ± 1.479 nmoles of GSH/mg protein, n=6) was significantly greater than that of Jurkat T-cells (mean ± s.d; 10.95 ± 2.103 nmoles of GSH/mg protein, n=6; $p<0.01$).

During the first 8 hours of Jurkat T-cell exposure to C_2-/C_6-ceramide, the presence of $[peroxide]_{cyt}$ was monitored by flow cytometry determining the fluorescence emission of DCF from cells co-exposed to the peroxide sensitive dye DCFH-DA. The median fluorescence (MdX) of the DCFH-DA treated viable cell population, determined by FS and SS properties, decreased with immediate effect and with rapid kinetics upon exposure to 20μM C_2-/C_6-ceramide. The first significant decreases in DCF MdX were observed at 15 minutes and 20 minutes Jurkat T-cell exposure to 20μM C_2- or C_6-ceramide respectively ($p<0.05$) when compared to vehicle treated controls. A maximum decrease in ΔDCF MdX of Jurkat T-cells of approximately -60 arbitrary units (a.u) was observed at 4 hours treatment with 20μM C_2-ceramide and 8 hours incubation with 20μM C6-ceramide (see Figure 2.18a). DCF fluorescence of cells exposed to 20μM C_2-/C_6-ceramide for greater than 8 hours was not measured as no further alteration in specific apoptosis were observed at these longer incubation periods. ΔDCF MdX induced by 16 hours Jurkat T-cell treatment with 10μM C_2-/C_6-ceramide fell significantly to approximately -35 a.u ($p<0.01$) and -25 a.u ($p<0.01$; see Figure 2.18a) respectively without the appearance of apoptosis ($p>0.05$; see Figures 2.7a & b). Similar alterations in ΔDCF MdX of Jurkat T-cells treated with 20μM C_2-/C_6-ceramide were observed after 45-60 minutes (see Figure 2.18a) and this was not associated with the appearance of apoptosis at this time point ($p>0.05$; see Figures 2.7a & b).

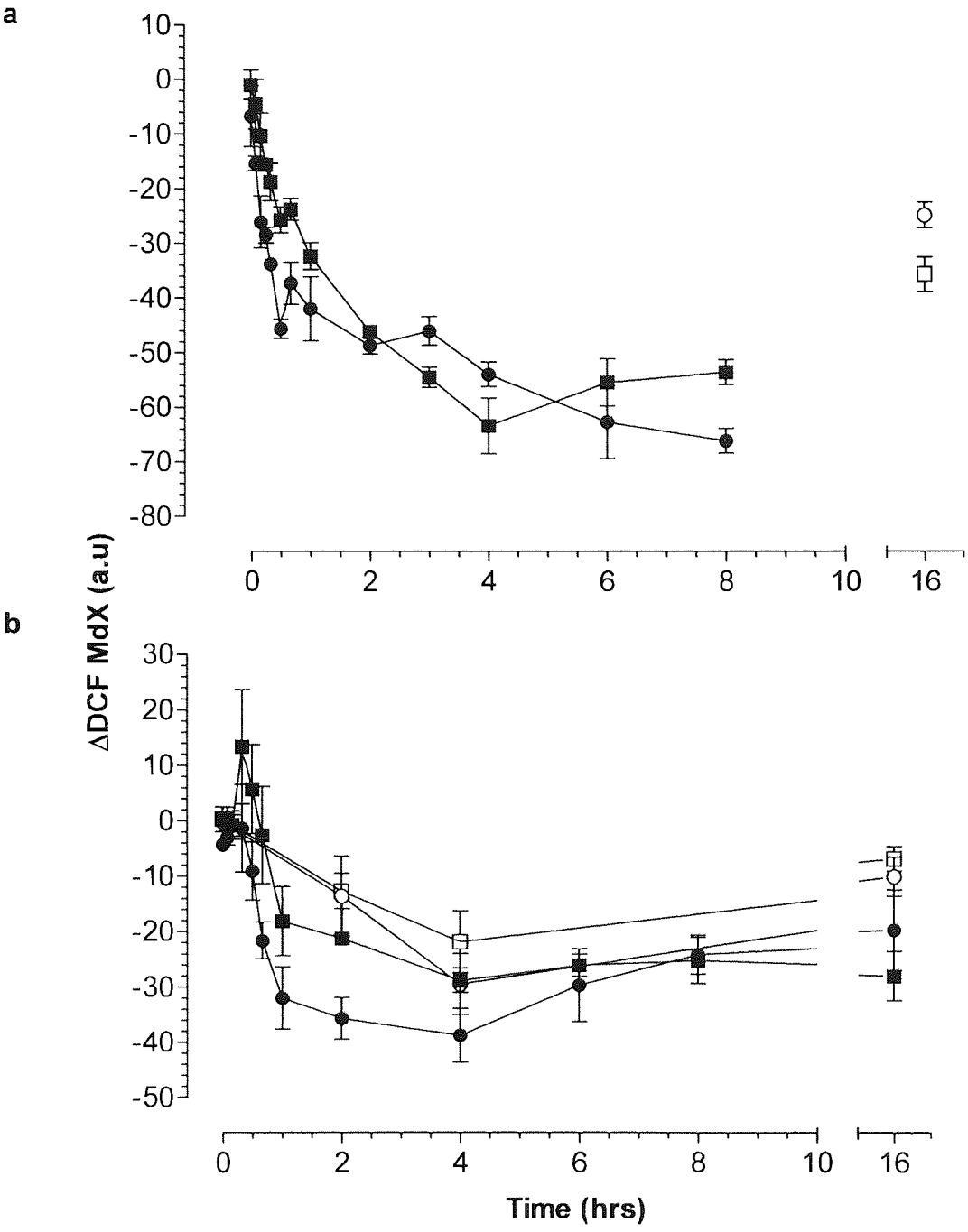

Figure 2.18. Loss of endogenous, cytosolic peroxide from Jurkat T-cells and U937 monocytes following treatment with synthetic ceramides: kinetics for the impaired oxidation of DCFH to DCF. Jurkat T-cells (a) or U937 monocytes (b; $2x10^6$/ml) were serum starved for 4 hours prior to the addition of 20μM C_2-ceramide (■), 20μM C_6-ceramide (●), 10μM C_2-ceramide (□) or 10μM C_6-ceramide (○). Cells were treated with 50μM DCFH-DA as described in method 2.2.10. At the end of the treatment periods, cell samples were analysed immediately for DCF fluorescence by flow cytometry. The median X (MdX) DCF fluorescence of 10,000 cells was analysed per sample. ΔDCF MdX represents the difference in MdX DCF of C_n-ceramide treated cells from that of vehicle treated cells for each time point. All incubations were performed at 37°C in a humidified, 5% CO_2, 95% air, 5% CO_2 atmosphere. The data are presented as the arithmetic mean ± s.e.m of at least 5 individual experiments. Arbitrary units, a.u.

No alteration in the intracellular H_2O_2 concentration, monitored by flow cytometry of U937s exposed to DCFH-DA, was observed for the first 40 minutes of 20μM C_2-ceramide and 30 minutes of 20μM C_6-ceramide exposure when compared to vehicle treated control cells (see Figure 2.18b). ΔDCF MdX then rapidly decreased to a minimum of approximately -40 and -25 a.u. in C_6- and C_2-ceramide treated U937s respectively within 4hrs, which in the case of C_6-ceramide treated U937s rose to -25 a.u. on increasing the treatment period to 8 hours (see Figure 2.18b). ΔDCF MdX remained at –25 a.u after 16 hours incubation with 20μM C_2-/C_6-ceramide. At lower concentrations (10μM), C_2-/C_6-ceramide decreased DCF fluorescence compared to control with slower kinetics than that observed with higher doses (20μM). The decrease in ΔDCF MdX observed in U937 monocytes following 10μM C_2-/C_6-ceramide treatment was of significantly lower magnitude than that recorded upon 20μM C_2-/C_6-ceramide treatment for all time points examined (2, 4 and 16 hours, $p<0.05$; see Figure 2.18b). The described data implies that the magnitude of loss of DCF fluorescence confers the cellular response to synthetic ceramide, a mild loss induces the accumulation of nucleoids in the G0/G1 phase of the cell cycle whereas a decrease in DCF fluorescence of greater magnitude bestows the fragmentation of DNA. One would assume that lowering the peroxide capacity of the cell would on the exposure of synthetic ceramides, induce an apoptotic response in U937 monocytes rather than growth arrest. Pre-treatment of U937 monocytes with either of the anti-oxidants NAC or GSH significantly prevented the accumulation of nucleoids in the G0/G1 phase of the cell cycle mediated by 16 hours exposure to 20μM C_2-($p<0.001$) or C_6-ceramide ($p<0.01$). There was no significant difference between the inhibitory effects of NAC or GSH on synthetic ceramide mediated G0/G1 nucleoid accumulation ($p<0.05$). The percentage nucleoids in the G0/G1 phase of vehicle

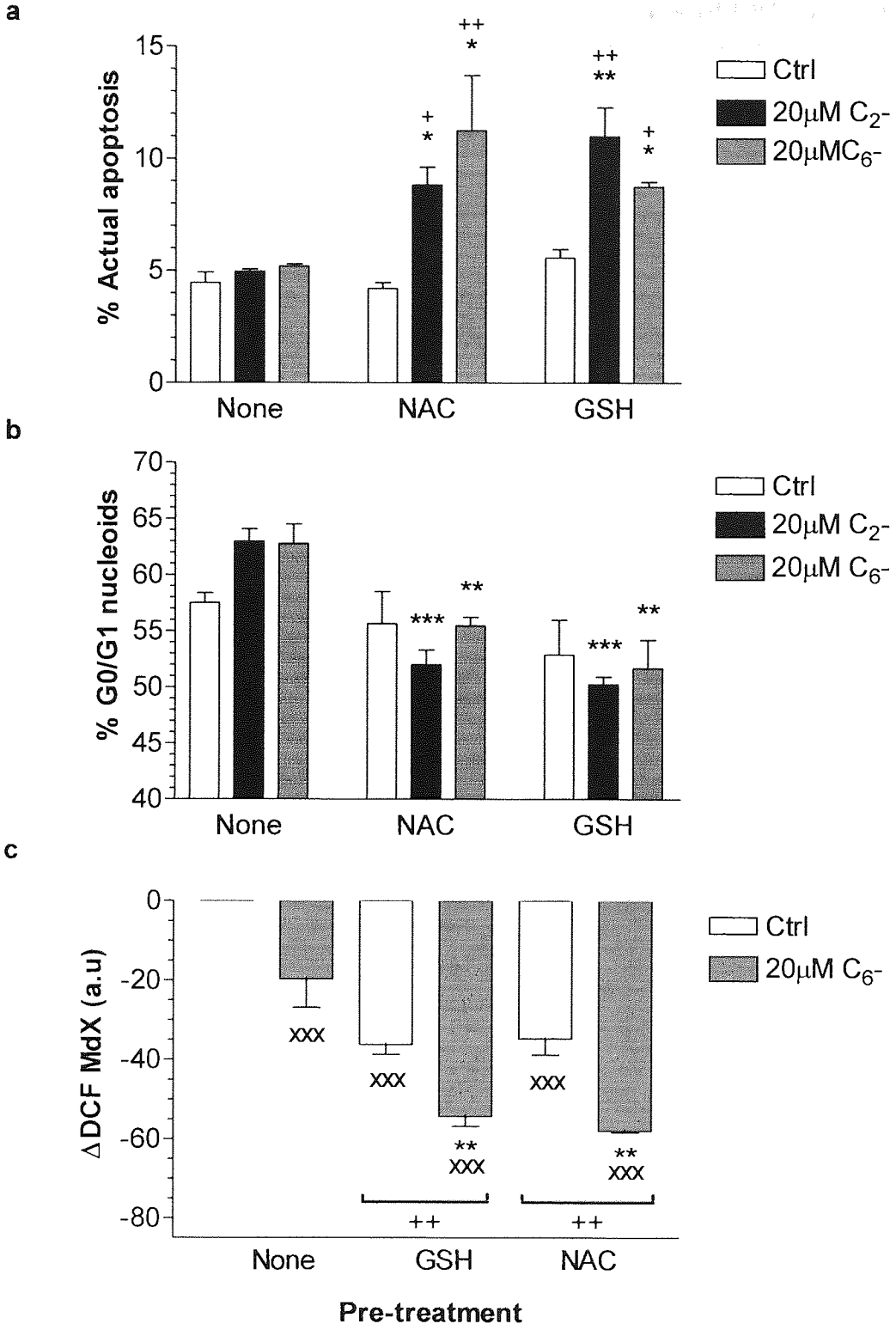
a
% Actual apoptosis
15
10
5
0
None
NAC
GSH
Ctrl
20μM C2-
20μMC6-
b
% G0/G1 nucleoids
70
65
60
55
50
45
40
None
NAC
GSH
Ctrl
20μM C2-
20μM C6-
c
ΔDCF MdX (a.u)
0
-20
-40
-60
-80
None
GSH
NAC
Pre-treatment
Ctrl
20μM C6-

Figure 2.19. Anti-oxidants drive synthetic ceramide treated U937 monocytes into apoptosis rather than growth arrest. U937s ($2x10^6$/ml) were serum starved in RPMI 1640 for 4 hours with or without 10mM N-acetylcysteine (NAC) or 10mM glutathione (GSH) prior to the addition 20μM C_2-/C_6-ceramide for 16 hours. Incubations were performed in a humidified 5% CO_2, 95% air atmosphere at 37°C for 36 hours. Cell pellets were resuspended in 1ml of hypotonic fluorochrome solution as described in materials and methods prior to DNA cell cycle analysis by flow cytometry. 20,000 nucleoids were counted per samples and the sub-diploid DNA content recorded to represent the percentage actual apoptosis (a). The percentage G0/G1 content of DNA cell cycles (b) was quantified using MultiCycle™ for Windows (Phoenix Flow Systems, San Diego, U.S.A.). The data are presented as the arithmetic mean percentage ± s.e.m of 3 individual experiments. * ($p<0.05$), ** ($p<0.01$) or *** ($p<0.001$) indicate significant difference of samples pre-treated with NAC or GSH compared to no pre-treatment by one way ANOVA followed by Tukey's multiple comparison test. For analysis of cytosolic peroxide (c), 50μM DCFH-DA was added to each sample at 40 minutes prior to the end of the incubation period. At 16 hours, cell samples were analysed immediately for DCF fluorescence by flow cytometry as described in methods 2.2.10. The median X (MdX) DCF fluorescence of 10,000 cells was analysed per sample. ΔDCF MdX represents the difference in MdX DCF of C_n-ceramide treated cells from that of vehicle treated cells for each time point. The data are presented as the arithmetic mean percents ± s.e.m of 3 individual experiments. ** ($p<0.01$) indicate significant difference between samples treated with 20μM C_6-ceramide with GSH or NAC pre-treatment compared to no pre-treatment, xxx ($p<0.001$) represents significant difference of test samples from control treated cells with no pre-treatment and ++ ($p<0.01$) indicates significant difference between samples test and control samples both pre-treated with NAC or GSH compared to one way ANOVA followed by Dunnett's multiple comparison test.

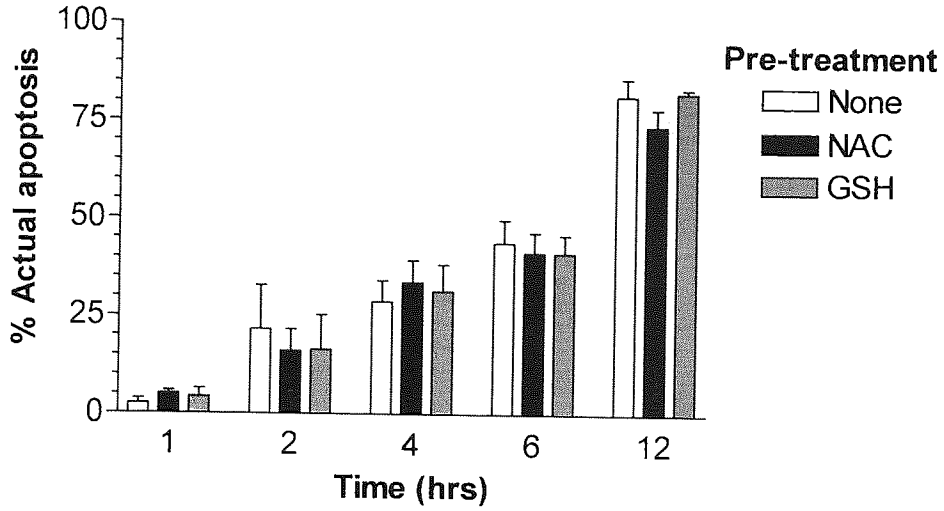

Figure 2.20. Anti-oxidants do not protect Jurkat T-cells from ceramide mediated apoptosis. Jurkat T-cells ($2x10^6$/ml) were serum starved in RPMI 1640 for 4 hours with or without 10mM N-acetylcysteine (NAC) or 10mM glutathione (GSH) prior to the addition 20μM C_2-ceramide for 1 to 12 hours. Incubations were performed in a humidified 5% CO_2, 95% air atmosphere at 37°C for 36 hours. Experiments were terminated by washing with ice cold PBS. Cell pellets were resuspended in 1ml of hypotonic fluorochrome solution as described in materials and methods prior to DNA cell cycle analysis by flow cytometry. 20,000 nucleoids were counted per sample. The data are presented as the arithmetic mean percents ± s.e.m of 5 individual experiments. Data was analysed for significant difference of samples pre-treated with NAC or GSH compared to no pre-treatment by one way ANOVA followed by Tukey's multiple comparison test.

treated controls were not affected by pre-treatment with NAC ($p>0.05$) or GSH ($p>0.05$; see Figure 2.19b). Prevention of synthetic ceramide mediated accumulation of nucleoids in the G0/G1 phase of the cell cycle was accompanied by the appearance of sub-diploid DNA. C_2-/C_6-ceramide (20μM) significantly increased the appearance of sub-diploid DNA of U937 monocytes pre-treated with either NAC or GSH compared to no pre-treatment ($p<0.05$). There was no significant difference in the percentage of actual apoptosis induced by either species in the presence of anti-oxidant ($p>0.05$). Furthermore, there was no difference in the degree of apoptosis induced by synthetic ceramides in the presence of either anti-oxidant ($p>0.05$). The percentage of actual apoptosis in control treated U937 monocytes was identical regardless of the nature of the antioxidant pre-treatment ($p>0.05$; see Figure 2.19a).

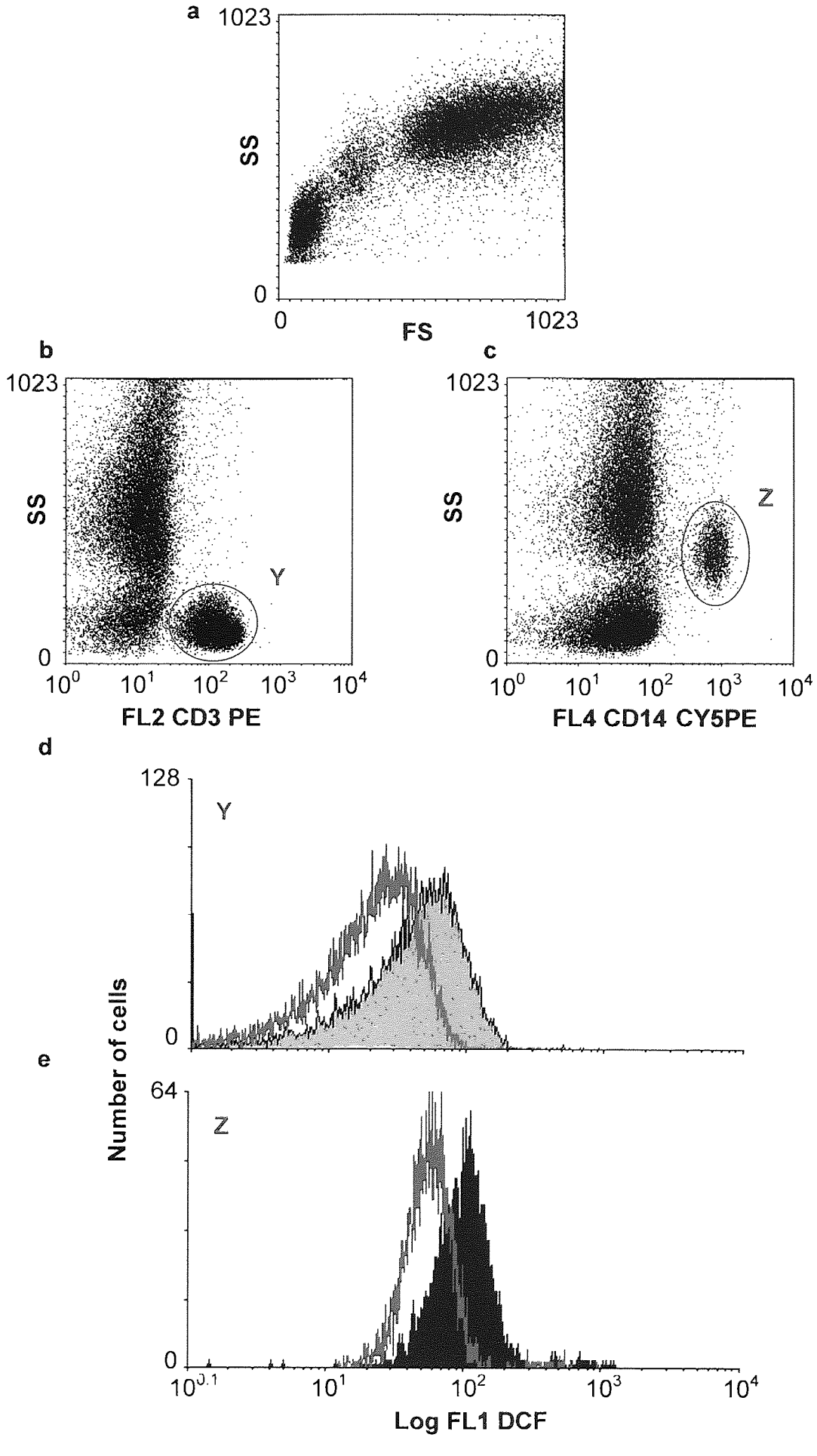
a
1023
SS
0
0
FS
1023
b
1023
SS
Y
0
10^0 10^1 10^2 10^3 10^4
FL2 CD3 PE
c
1023
SS
Z
0
10^0 10^1 10^2 10^3 10^4
FL4 CD14 CY5PE
d
128
Y
0
e
64
Z
0
$10^{0.1}$ 10^1 10^2 10^3 10^4
Log FL1 DCF
Number of cells

Figure 2.21. Treatment of whole blood with C_6-ceramide reduces the cytosolic peroxide concentration of $CD3^+$ T-lymphocytes and $CD14^+$ monocytes. Venous blood was obtained from healthy consenting adult humans and treated with 20μM C_6-ceramide for 2 hours at 37°C with rotation. Reactions were terminated by incubation on ice with simultaneous treatment with the fluorescently tagged monoclonal antibodies CD3-PE and CD14-Cy5PE, and 50μM DCFH-DA for 30 minutes. Red blood cells were lysed and leukocytes fixed as described in method 2.2.13. Samples were analysed by flow cytometry and the DCF fluorescence of the $CD3^+$ population and $CD14^+$ population quantified. Shown are typical flow cytometry histograms of (a) the leukocyte populations differentiated by forward scatter (FS) and side scatter (SS) properties, (b) CD3-PE (FL2) versus SS, the highly fluorescent $CD3^+$ cell population isolated and gated 'Y', (c) CD14-CY5PE (FL4) versus SS, the highly fluorescent $CD14^+$ cell population isolated and gated 'Z', (d) DCF (FL1) versus count of the gated $CD3^+$ population 'Y' and (e) DCF (FL1) versus count of the gated $CD14^+$ population 'Z'. Grey and black fill represent the DCF fluorescence of $CD3^+$ and $CD14^+$ populations respectively from vehicle treated whole blood, red and blue outlines represent the DCF fluorescence obtained from whole blood treated with 20μM C_6-ceramide. Results are representational of 3 independent experiments.

The maximal decreases in ΔDCF MdX of U937s monocytes treated with 20μM C_2- or C_6-ceramide were significantly less than those achieved in Jurkat T-cells ($p<0.01$ for either species). Pre-treatment of U937 monocytes with the anti-oxidants GSH or NAC significantly reduced ΔDCF to approximately –35a.u ($p<0.001$) after 16 hours vehicle treatment. On addition of 20μM C_6-ceramide to NAC or GSH pre-treated U937 monocytes, ΔDCF decreased further to approximately –55a.u, and was significantly lower than U937s pre-treated with NAC or GSH alone ($p<0.01$; see Figure 19c). The pre-treatment of Jurkat T-cells with either of the antioxidants NAC or GSH did not increase the kinetics or the magnitude of apoptosis induced by C_2-ceramide (see Figure 2.20).

Whole blood was treated with 20μM C_6-ceramide for 2 hours with rotation at 37°C and the effects on $[peroxide]_{cyt}$ of $CD3^+$ T-lymphocytes and $CD14^+$ monocytes evaluated by 3-colour flow cytometry with appropriate colour compensation previously established with fluorescently tagged MoAb corresponding to strongly expressed antigens (see Method 2.2.7). Reactions were terminated by incubation on ice for 30 minutes following treatment with 50μM DCFH-DA, 10μl/10^6 cells of anti-CD3-PE MoAb and anti-CD14-CY5PE MoAb. RBC were lysed and leukocytes fixed prior to analysis by flow cytometry. Lymphocytes, monocyte and granulocytes can be differentiated approximately from each other on a basis of their FS and SS properties (see Figure 2.21a). However, cell populations of different linerage overlap and to aid their differentiation, the $CD3^+$ T-lymphocytes and $CD14^+$ monocyte populations were identified according to elevated PE (FL2) and CY5PE (FL4) fluorescence respectively on dual parameter histograms of FL2/FL4 versus SS. These populations were individually gated and the DCF fluorescence of $CD3^+$ and

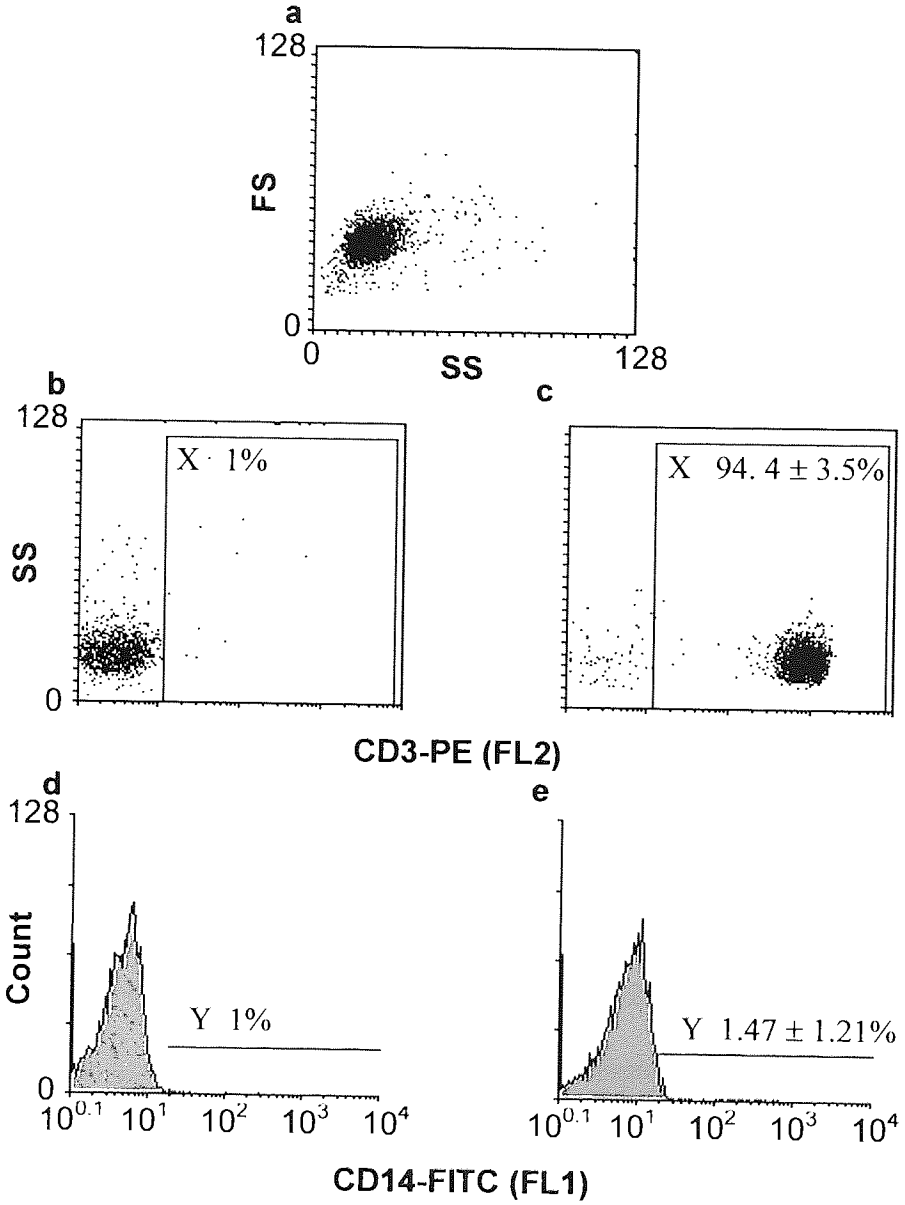

Figure 2.22. Resting T-lymphocyte purity with low monocyte contamination. Resting T-lymphocytes were extracted from venous blood of consenting adults using density centrifugation over lymphoprep™ followed by negative isolation employing magnetic beads (Dynal) as described in method 2.2.4. T-cell purity and monocyte contamination were determined by quantifying the percentage of $CD3^+$ and $CD14^+$ cells respectively by flow cytometry. Cells were labelled with CD3-PE and CD14-FITC for 30 minutes on ice in the dark and fixed as described in method 2.2.8. Samples were analysed by two colour flow cytometry utilising pre-determined colour compensation parameters. The viable T-cell population was located on a histogram of side scatter (SS) versus forward scatter (FS; a). T-cell purity was quantified on dual parameter histograms of CD3-PE (FL2) versus SS (b & c). Monocyte contamination was analysed on single parameter histograms of CD14-FITC (FL1) versus count (d & e). Background fluorescence was determined with samples stained with isotype negative controls conjugated to PE (b) or FITC (d) and regions of positive analysis identified to contain 1% positive cells as Y and X respectively. The percentage fluorescence of 10,000 cells were analysed per sample. Shown are representative histograms. Numbers represent the mean percentage of $CD3^+$ or $CD14^+$ cells ± s.d of 40 experiments.

$CD14^+$ populations analysed on a single parameter histogram of FL1 versus count (see Figures 2.21b & c). The DCF fluorescence of $CD3^+$ T-cells and $CD14^+$ monocytes displayed reduced $[peroxide]_{cyt}$ following the treatment of whole blood with 20μM C_6-ceramide when compared to vehicle treated whole blood T-cells or monocytes (see Figures 2.21d & e).

To further substantiate the observations of reduced $[peroxide]_{cyt}$ in response to short chain ceramides obtained in immortalised cell lines and whole blood, primary, resting T-cells were extracted from venous whole blood from consenting individuals by density centrifugation over Lymphoprep™ and purified using negative isolation by magnetic bead methodologies (Dynal). Flow cytometry revealed the purified cell samples to be a homogenous population as defined by SS versus FS properties (see Figure 2.22a). Purity was assessed by flow cytometry as the percentage of $CD3^+$ T-cells and was always greater than 94% (see Figure 2.22b & c). Monocytic contamination was quantified simultaneously as the percentage of cells expressing the antigen CD14 and was always less than 1.5% (see Figures 2.22d & e). T-cells were then cultured in RPMI 1640 in the presence or absence of 10μg/ml of PHA to induce activation. T-cell activation was assessed as the percentage of $CD3^+CD25^+$ T-cells. Flow cytometry histograms of SS versus FS showed an increase in size of T-cells which was coupled with a significant elevation in $CD3^+CD25^+$ levels to 43.62 ± 15.39 % positive T-cells (mean ± s.d; n=22) upon activation with PHA for 3 days compared to 2.605 ± 2.082 for resting T-cells (mean ± s.d; n=22; $p<0.001$). Primary activated or resting human T-cells were then treated in an identical fashion as described for Jurkat T-cells. A limiting factor in performing the necessary

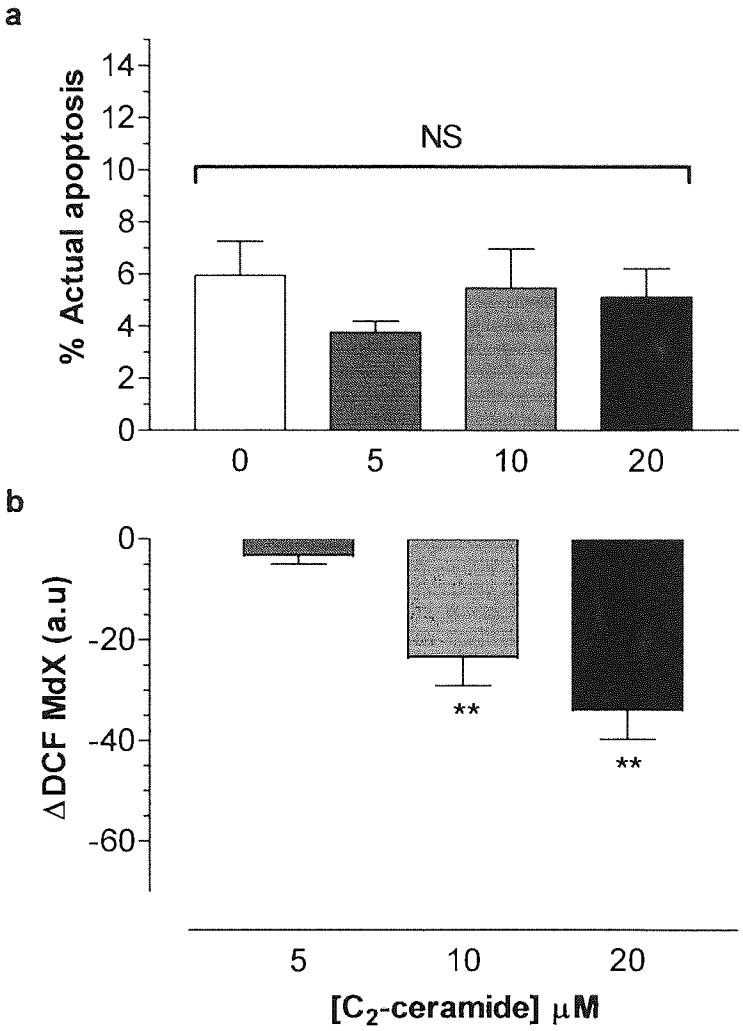

Figure 2.23. Synthetic short chain ceramides induce cytosolic peroxide loss in resting human T-lymphocytes prior to the appearance of DNA fragmentation. Primary human peripheral blood T-lymphocytes were extracted by density centrifugation and purified by negative isolation. T-cells were cultured for 3 days in RPMI 1640 (10% FCS, 1% P/S) at a concentration of $2x10^6$/ml. T-cells ($1x10^6$/ml) were then serum starved in RMPI 1640 for 4 hours prior to exposure to C_2-ceramide (0-20μM) for 6 hours. (a) For the quantification of apoptosis, samples were resuspended in hypotonic fluorochrome solution and incubated overnight in the dark at 4°C prior to DNA cell cycle analysis by flow cytometry as described in method 2.2.9. The percentage actual apoptosis was calculated from the sub-diploid content of 20,000 nucleoids per sample. For analysis of cytosolic peroxide levels (b), 40 minutes before termination of incubation period, cell samples were loaded with 50μM of DCFH-DA. At the end of the treatment period, samples were analysed immediately for DCF fluorescence by flow cytometry as described in method 2.2.10 and the median X (MdX) of 10,000 cells were recorded. ΔDCF represents the change in DCF MdX of test samples from vehicle controls. The data are presented as the arithmetic mean ± s.d of at least 3 individual experiments. All cell culture and treatments were performed at 37°C in a humidified 95% air, 5% CO_2 atmosphere. Statistical analysis was performed by one way ANOVA followed by Dunnett's post *hoc* test analysis, where ** ($p<0.01$) represents significant difference from controls. Arbitrary units, a.u. NS represents no significant difference between vehicle treated controls and tests.

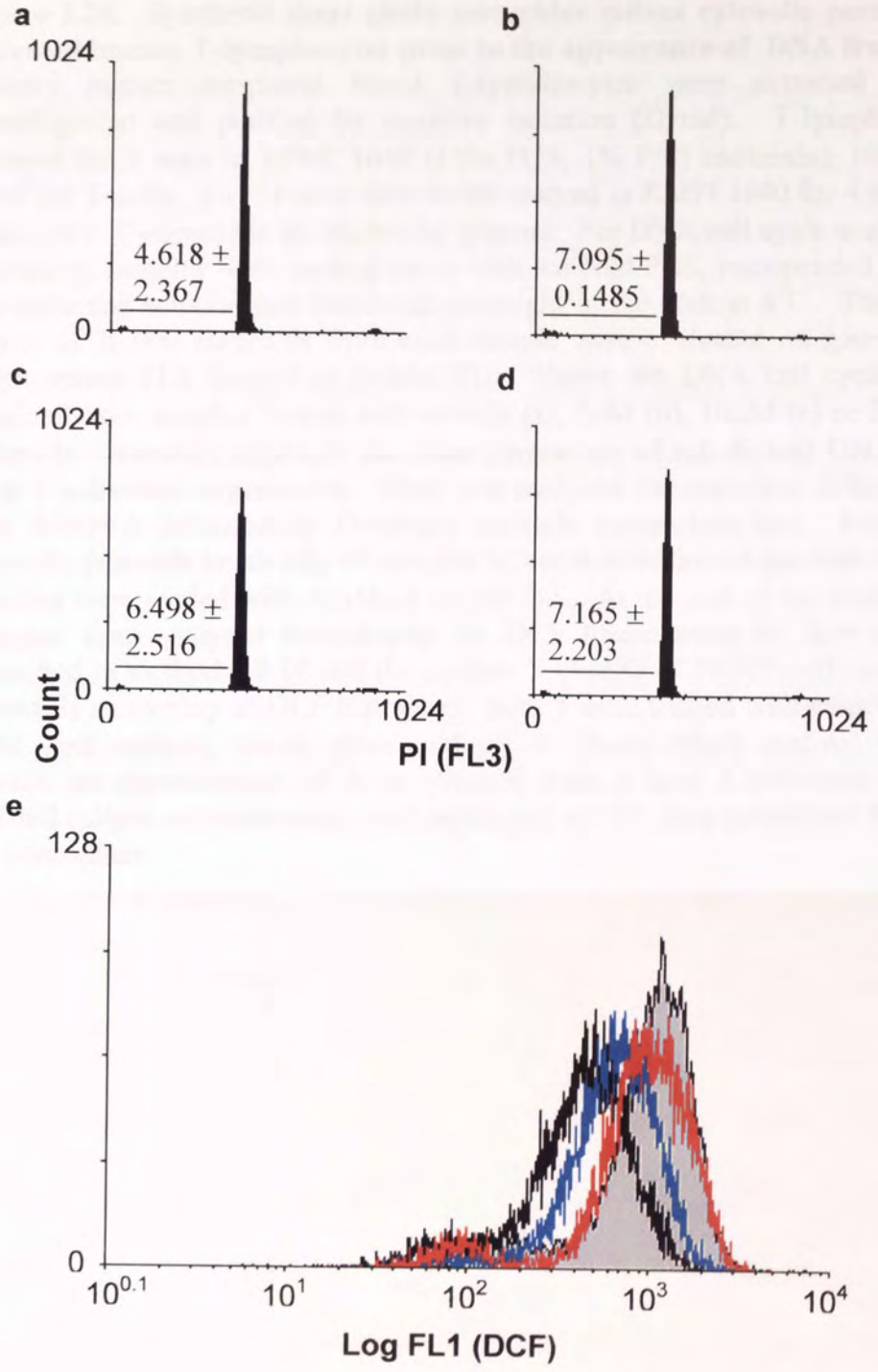
a
1024
4.618 ±
2.367
0
b
7.095 ±
0.1485
c
1024
6.498 ±
2.516
0
0
1024
Count
d
7.165 ±
2.203
0
1024
PI (FL3)
e
128
0
$10^{0.1}$
10^{1}
10^{2}
10^{3}
10^{4}
Log FL1 (DCF)

Figure 2.24. Synthetic short chain ceramides induce cytosolic peroxide loss in activated human T-lymphocytes prior to the appearance of DNA fragmentation. Primary human peripheral blood T-lymphocytes were extracted by density centrifugation and purified by negative isolation (Dynal). T-lymphocytes were cultured for 3 days in RPMI 1640 (10% FCS, 1% P/S) containing 10μg PHA per $2x10^6$/ml T-cells. T-cells were then serum starved in RMPI 1640 for 4 hours prior to exposure to C_2-ceramide (0-20μM) for 6 hours. For DNA cell cycle analysis by flow cytometry, samples were washed twice with ice cold PBS, resuspended in hypotonic fluorochrome solution and incubated overnight in the dark at 4°C. The sub-diploid region of 20,000 nucleoids from each sample were evaluated on gated histograms count versus FL3 (propidum iodide; PI). Shown are DNA cell cycle histograms obtained from samples treated with vehicle (a), 5μM (b), 10μM (c) or 20μM (d) C_2-ceramide. Numbers represent the mean percentage of sub-diploid DNA ± s.d of at least 3 individual experiments. Data was analysed for statistical difference by one way ANOVA followed by Dunnett's multiple comparison test. For analysis of cytosolic peroxide levels (d), 40 minutes before termination of incubation period, cell samples were loaded with 50μM of DCFH-DA. At the end of the treatment period, samples were analysed immediately for DCF fluorescence by flow cytometry as described in method 2.2.10 and the median X (MdX) of 10,000 cells were recorded. Shown is an overlay of DCF histograms from T-cells treated with vehicle (solid fill), 5μM (red outline), 10μM (blue outline) or 20μM (black outline) C_2-ceramide. Results are representative of those obtained from at least 3 individual experiments. All cell culture and treatments were performed at 37°C in a humidified 5% CO_2, 95% air atmosphere.

experiments was the number of T-cells obtained from 40mls of blood, typically $10x10^6$/ml, and consequently for experimental purposes half the concentration of cells, $1x10^6$/ml, was used. Following 6 hours treatment with 0-20μM C_2-ceramide, DNA cell cycle analysis by flow cytometry revealed no significant accumulation of sub-diploid DNA in either resting ($p>0.05$; see Figure 2.23a) or activated ($p>0.05$) primary T-cells (see Figure 2.24a-d). Quantification of DCF fluorescence at this time point showed C_2-ceramide to induce a concentration dependent decrease in DCF in both resting and activated T-cells (see Figures 2.13b & 2.14e) which was initially significant at a concentration of 5μM C_2-ceramide in both cell types ($p<0.05$). On extending the incubation to 24 hours, C_2-ceramide induced a dose dependent increase in the appearance of sub-diploid DNA in activated T-cells, which was first significant at a concentration of 10μM inducing approximately 21% DNA fragmentation ($p<0.05$) and at 20μM C_2-ceramide 28% ($p<0.01$; see Figure 2.25a-d). Following 24 hours treatment of activated T-cells with 5μM C_2-ceramide DCF fluorescence was significantly reduced to approximately -10 a.u from vehicle treated controls ($p<0.05$) with no significant evidence of sub-diploid DNA ($p>0.05$) at this time point (see Figure 2.20e). The DCF fluorescence of the viable activated T-cell population, 24 hours post-treatment with 10μM or 20μM C_2-ceramide were approximately –40 a.u and –50 a.u respectively identical to the loss of DCF fluorescence observed afters 6 hours treatment ($p>0.05$ for both concentrations; see Figures 2.24e & 2.25e). Likewise, in resting T-cells, at 24 hours post-treatment, the extent of DNA fragmentation was identical to that observed in activated T-cells for each concentration of C_2-ceramide ($p>0.05$ for each dose; see Figure 2.26a-d). DNA cell cycle analysis of PHA activated T-cells revealed the appearance of S-phase and G2M phase nucleoids, however, following treatment with 20μM C_2-ceramide for 24 hours

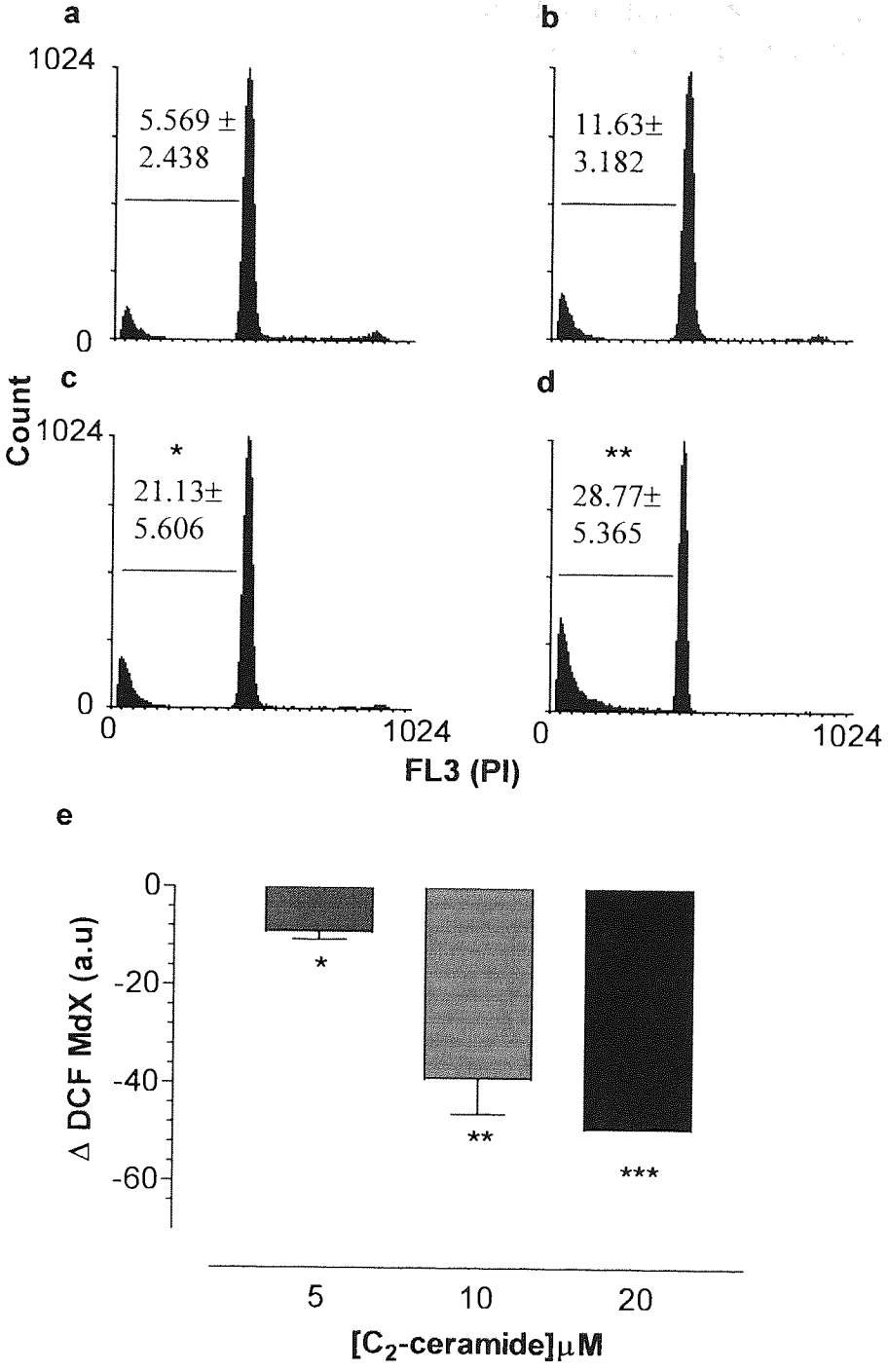
a
b
c
d
e
1024
0
5.569 ± 2.438
11.63± 3.182
21.13± 5.606
28.77± 5.365
*
**
Count
FL3 (PI)
1024
0
Δ DCF MdX (a.u)
0
-20
-40
-60
5
10
20
[C2-ceramide]μM
***

Figure 2.25. Synthetic short chain ceramides induce DNA fragmentation associated with loss in cytosolic peroxide in primary activated T-cells. Primary human peripheral blood T-lymphocytes were extracted by density centrifugation and purified by negative isolation (Dynal). T-lymphocytes were cultured for 3 days in RPMI 1640 (10% FCS, 1% P/S) containing 10μg/ml PHA per $2x10^6$ T-cells. T-cells ($1x10^6$/ml) were then serum starved in RMPI 1640 for 4 hours prior to exposure to C_2-ceramide (0-20μM) for 24 hours. For DNA cell cycle analysis by flow cytometry, samples were washed twice with ice cold PBS, resuspended in hypotonic fluorochrome solution and incubated overnight in the dark at 4°C. The sub-diploid region of 20,000 nucleoids from each sample were evaluated on gated histograms count versus FL3 (propidum iodide; PI). Shown are DNA cell cycle histograms obtained from samples treated with vehicle (a), 5μM (b), 10μM (c) or 20μM (d) C_2-ceramide. Numbers represent the mean percentage of sub-diploid DNA ± s.d. of at least 3 individual experiments. (e) For analysis of cytosolic peroxide levels, 40 minutes before termination of incubation period, cell samples were loaded with 50μM of DCFH-DA. At the end of the treatment period, samples were analysed immediately for DCF fluorescence by flow cytometry as described in method 2.2.10 and the median X (MdX) of 10,000 cells were recorded. ΔDCF represents the difference in MdX of tests from vehicle controls. Data are presented as the mean ± s.d. of at least 3 individual experiments where * ($p<0.05$), ** ($p<0.01$) and *** ($p<0.001$) represents significant deviation from controls by one way ANOVA followed by Dunnett's multiple comparison test. Arbitrary units, a.u. All cell culture and treatments were performed at 37°C in a humidified 95% air, 5% CO_2 atmosphere.

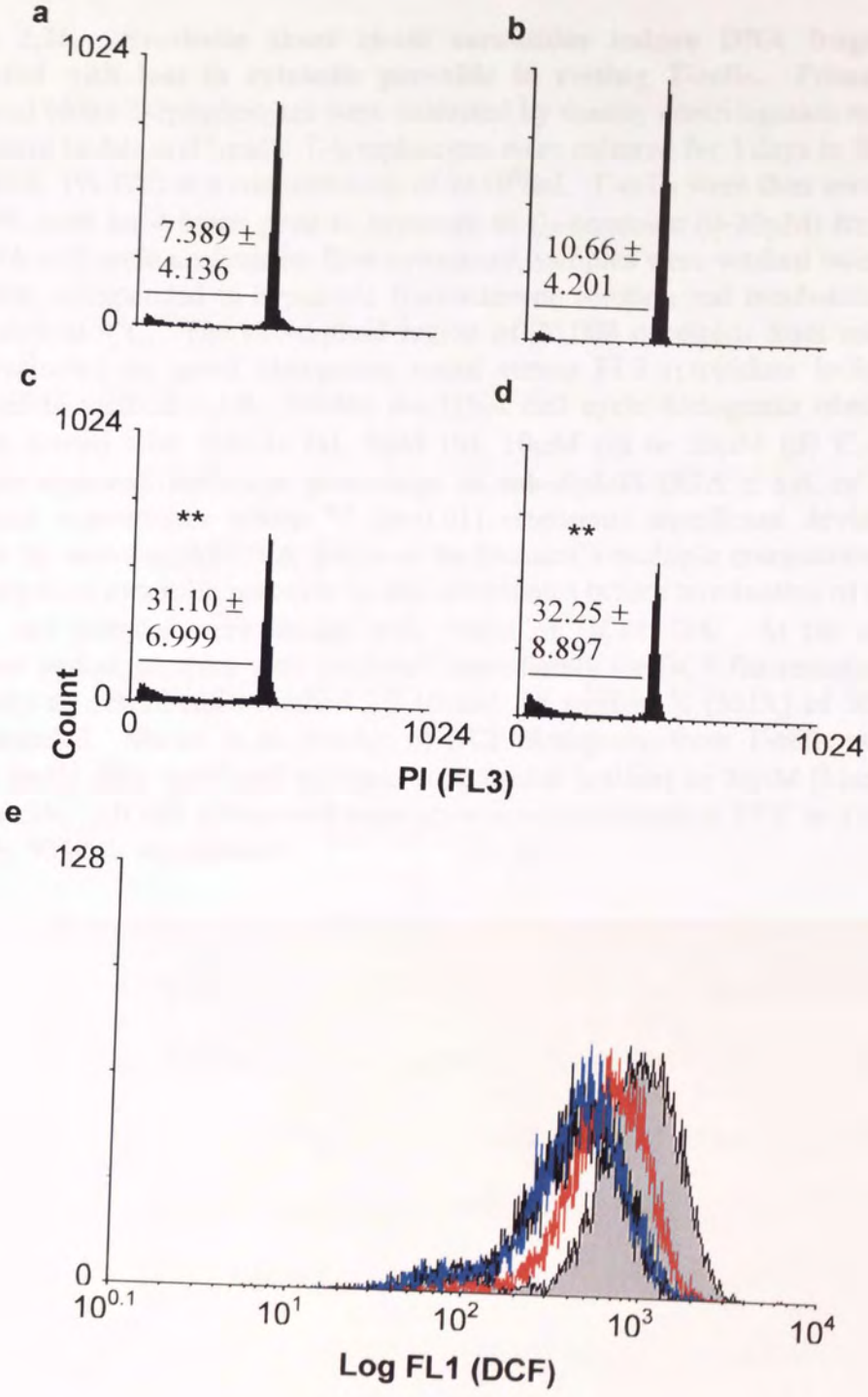
a
1024
7.389 ±
4.136
0
b
10.66 ±
4.201
c
1024
**
31.10 ±
6.999
Count
0
0
1024
d
**
32.25 ±
8.897
0
1024
PI (FL3)
e
128
0
$10^{0.1}$
10^{1}
10^{2}
10^{3}
10^{4}
Log FL1 (DCF)

Figure 2.26. Synthetic short chain ceramides induce DNA fragmentation associated with loss in cytosolic peroxide in resting T-cells. Primary human peripheral blood T-lymphocytes were extracted by density centrifugation and purified by negative isolation (Dynal). T-lymphocytes were cultured for 3 days in RPMI 1640 (10% FCS, 1% P/S) at a concentration of $2x10^6$/ml. T-cells were then serum starved in RMPI 1640 for 4 hours prior to exposure to C_2-ceramide (0-20μM) for 24 hours. For DNA cell cycle analysis by flow cytometry, samples were washed twice with ice cold PBS, resuspended in hypotonic fluorochrome solution and incubated overnight in the dark at 4°C. The sub-diploid region of 20,000 nuceloids from each sample were evaluated on gated histograms count versus FL3 (propidum iodide; PI) as described in method 2.2.9. Shown are DNA cell cycle histograms obtained from samples treated with vehicle (a), 5μM (b), 10μM (c) or 20μM (d) C_2-ceramide. Numbers represent the mean percentage of sub-diploid DNA ± s.d. of at least 3 individual experiments where ** ($p<0.01$) represents significant deviation from controls by one-way ANOVA followed by Dunnett's multiple comparison test. (e) For analysis of cytosolic peroxide levels, 40 minutes before termination of incubation period, cell samples were loaded with 50μM of DCFH-DA. At the end of the treatment period, samples were analysed immediately for DCF fluorescence by flow cytometry as described in method 2.2.10 and the median X (MdX) of 10,000 cells were recorded. Shown is an overlay of DCF histograms from T-cells treated with vehicle (solid fill), 5μM (red outline), 10μM (blue outline) or 20μM (black outline) C_2-ceramide. All cell culture and treatments were performed at 37°C in a humidified 5% CO_2, 95% air atmosphere.

these phases were absent. As expected, resting T-cells possessed no evidence of DNA in the S-phase or G2M phase of the cell cycle (see Figures 2.24a-d, 2.25a-d & 2.26a-d).

Treatment of Jurkat T-cells with CD95L induced a time and dose dependent elevation in apoptosis. Specific apoptosis was initially observed after 4 hours exposure to 1μg/ml ($p<0.05$) and 5μg/ml ($p<0.05$) of CD95L. These concentrations of CD95L mediated maximal elevation in the percentage of specific apoptosis of approximately 70% after 12 ($p<0.01$) and 16 hours ($p<0.01$) respectively, after which a plateau was observed. Incubations of Jurkat T-cells with these concentrations of CD95L did not induce further alterations in the percentage of specific apoptosis following 16 hours treatment ($p>0.05$). There was no significant difference in the maximal percentage specific apoptosis induced by 1μg/ml and 5μg/ml CD95L ($p>0.05$). Treatment of Jurkat T-cells with 100ng/ml of CD95L failed to induce any significant elevation in the percentage of specific apoptosis ($p<0.05$) for up to 16 hours. Intermediate concentrations of CD95L (250ng/ml and 500ng/ml) also induced significant time dependent elevations in the specific apoptosis, which were maximal after 16 hours (20%) and 36 hours (55%) respectively and significantly different to the maximal apoptotic response of 70% induced by higher concentrations of CD95L ($p<0.001$; see Figure 2.27).

The effect of a maximal (1μg/ml) and sub-maximal apoptotic dose of CD95L on endogenous, intracellular levels of ceramide ($[ceramide]_i$) was evaluated by the DAGK assay. The concentration range of $[ceramide]_i$ alterations expected in response to extracellular stimuli were used to construct a standard curve from which

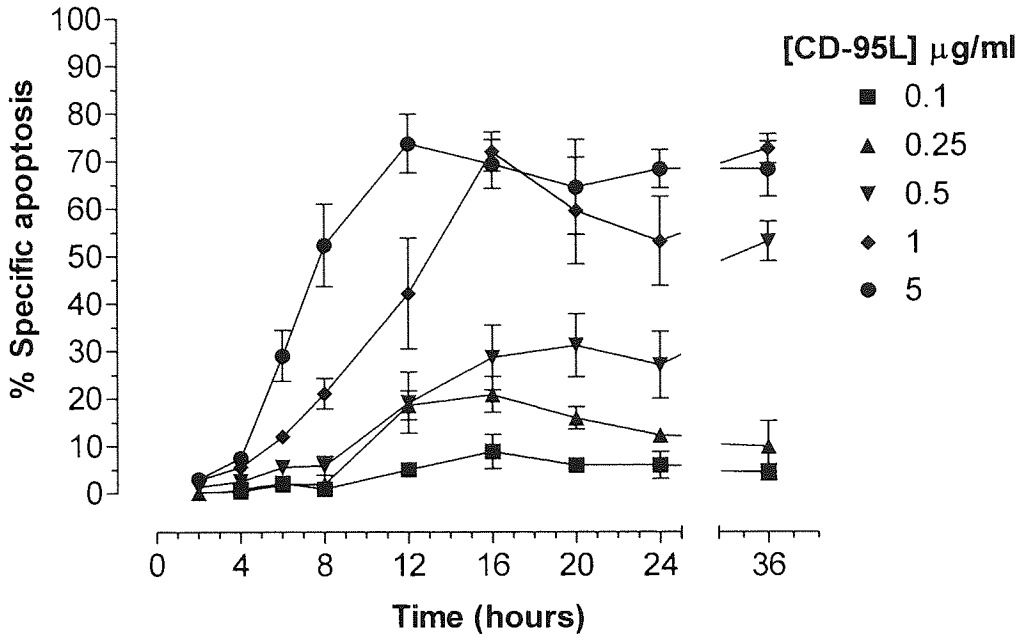

Figure 2.27: CD95 induced time- and concentration- dependent apoptosis in Jurkat T-cells. Jurkat T-cells ($2x10^6$/ml) were serum starved for 4 hours prior to the addition of CD95 ligand (CD95L; 0-5µg/ml) for 0-36 hours. Incubations were performed at 37°C in a 95% air, 5% CO_2 humidified atmosphere and terminated by washing the cells twice with ice cold PBS. Cell pellets were resuspended in 1ml of hypotonic fluorochrome solution and incubated in the dark at 4°C overnight prior to DNA cell cycle analysis by flow cytometry. The sub-diploid DNA content of 20,000 nucleoids from each sample was analysed as described in method 2.2.9. The data are presented as the mean ± s.e.m of 5 individual experiments, expressed as the percentage specific apoptosis according to the formula specific apoptosis = (T-C)/(100-C) x100, where T equals the percentage of apoptotic events from treated cells, and C equals the percentage of apoptotic events from control cells.

unknown ceramide levels are quantified. Shown in Figure 2.28a is an autoradiogram obtained following radiolabelling of ceramide in the concentration range 0 2,560pmoles. Over this range, the standard curve of ceramide (pmoles) versus cpm was linear where r^2 was always greater than 0.9 (see Figure 2.28b). Performing the DAGK assay upon 640pmoles of C_6-ceramide and quantifying the concentration of C_6-ceramide from the standard curve determined the labelling efficiency in each experiment, which was always greater than 90%.

CD95L induced a transient elevation in endogenous ceramide levels in a

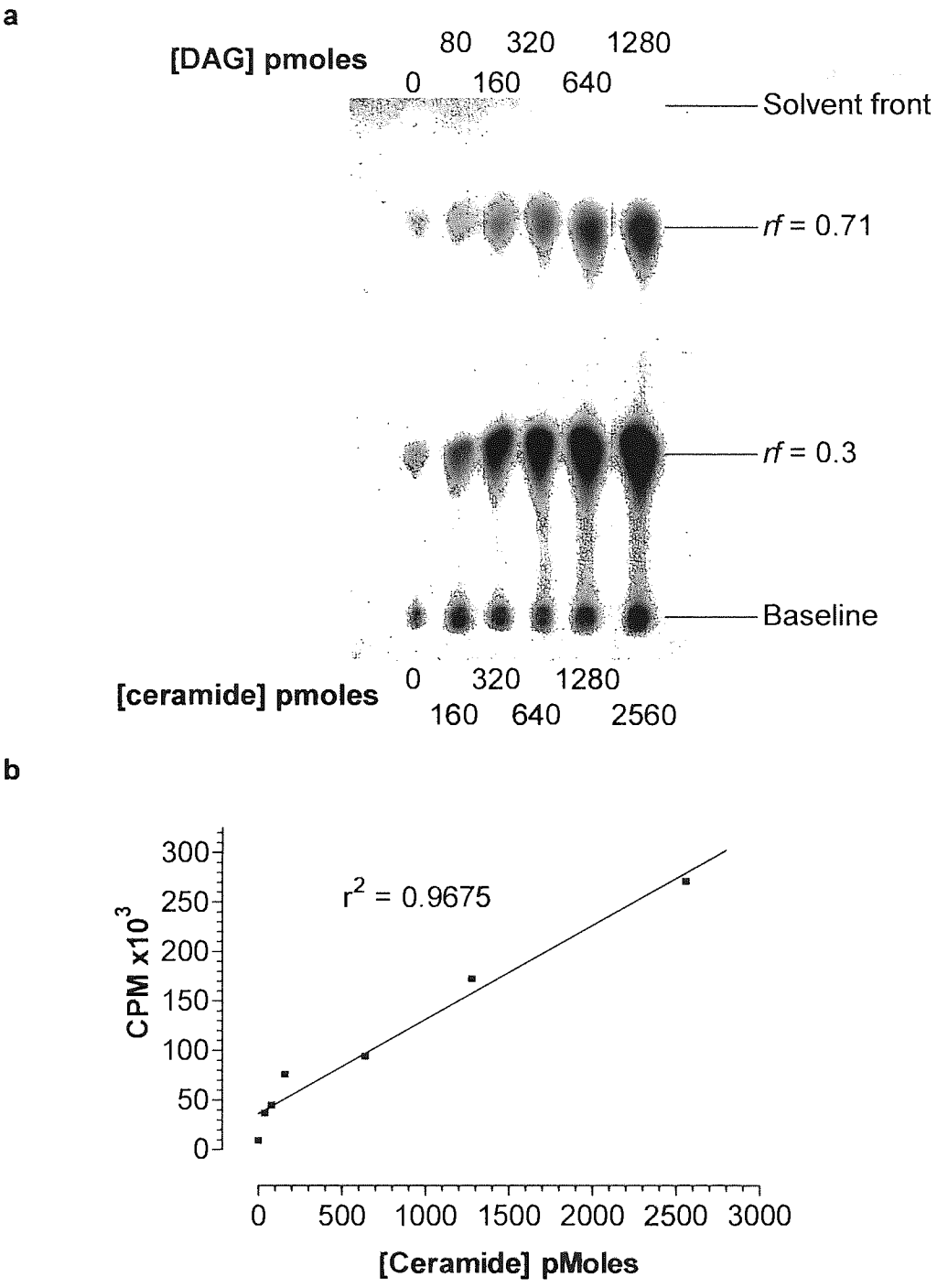

Figure 2.28. Standard curve for the labelling of long chain endogenous ceramide with γ^{32}P by the DAGK assay. Endogenous ceramide and diacylglycerol (DAG) in the concentration range of 0-2560 pmoles and 0-1280 pmoles respectively were labelled with 2μCi of γ^{32}P[ATP] by the DAGK assay as described in methods 2.2.16-20. Lipids were separated by thin layer chromatography. Ceramide 1-phosphate and phosphatadic acid were visualised by autoradiography and *rf* values determined. Shown is a typical autoradiogram of ceramide standards and DAG standards indicating rf values (a). Ceramide spots were scraped from TLC plates and the counts per minute (cpm) quantified by scintillation counting. A standard curve of [ceramide] pmoles versus cpm was constructed and the correlation coefficient (r^2) determined by GraphPad Prism (b). Unknown cellular ceramide concentrations per 10^6 cells were consequently quantified.

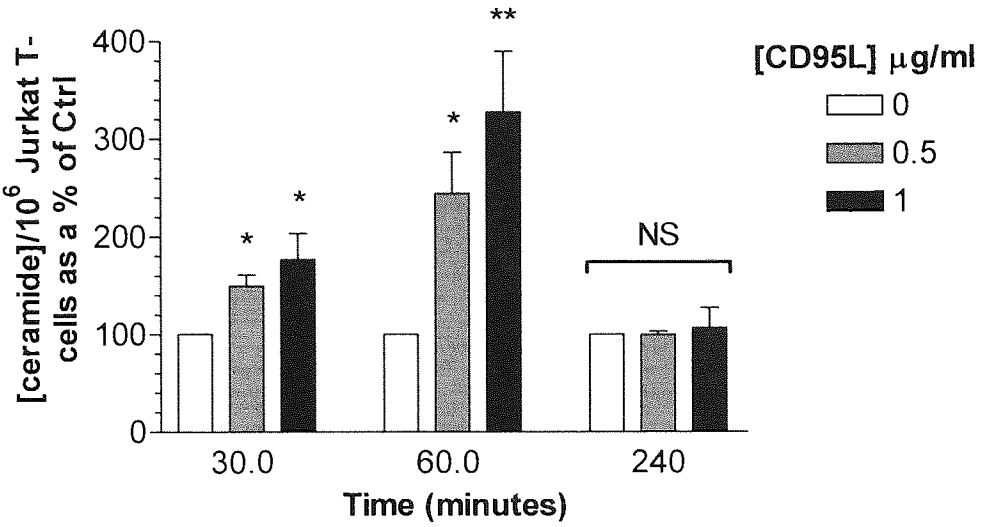

Figure 2.29. CD95L induces the accumulation of endogenous ceramide in Jurkat T-cells. Jurkat T-cells ($2x10^6$/ml) were serum starved in RMPI 1640 for 4 hours prior to treatment with 0, 500ng/ml or 1µg/ml CD95L. Incubations were performed in a humidified 5% CO_2, 95% air atmosphere at 37°C and were terminated by washing cells twice with ice cold PBS. Lipids were extracted and endogenous ceramide quantified against a standard curve of known ceramide concentrations by the DAGK assay as described in method 2.2.16-20. Results are presented as the mean of 3 experiments analysed in duplicate. Statistical analysis was performed by one way ANOVA followed by Dunnett's multiple comparison where * ($p<0.05$) and ** ($p<0.01$) were considered significantly different from controls. NS, not significant.

concentration dependent fashion. $[ceramide]_i$ increased significantly to approximately 150% ($p<0.05$) and 180% ($p<0.05$) of control levels following 30 minutes treatment with 0.5 and 1µg/ml CD95L. On increasing the incubation period to 1 hour, $[ceramide]_i$ was elevated further to approximately 240% ($p<0.05$) and 320% of control ($p<0.01$) by 0.5 and 1µg/ml CD95L respectively. After 4 hours exposure to either 0.5 or 1µg/ml CD95L $[ceramide]_i$ returned to that of control levels ($p>0.05$ for both concentrations; see Figure 2.29).

Since CD95L mediated an elevation in the intracellular signal transduction molecule ceramide, and considering our observations of reduced $[peroxide]_{cyt}$ in Jurkat T-cells in response to synthetic ceramide, the effects of CD95L on $[peroxide]_{cyt}$ in Jurkat T-

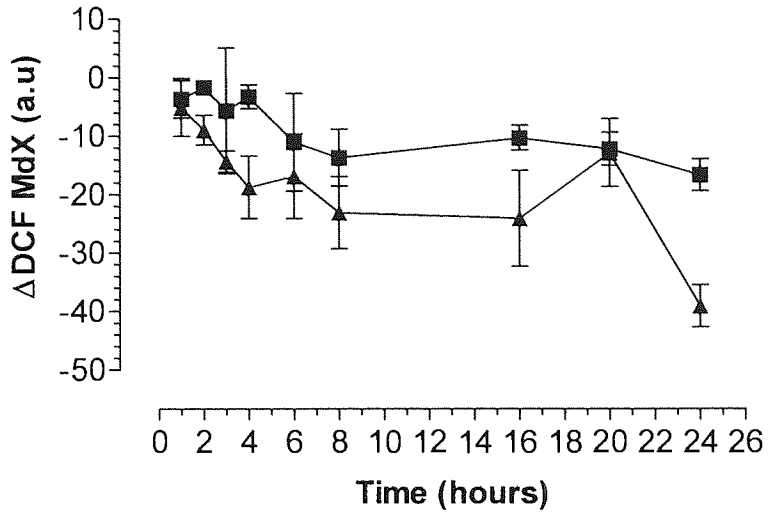

Figure 2.30. Loss of endogenous, cytosolic peroxide from Jurkat T-cells following treatment with CD95L: kinetics for the impaired oxidation of DCFH to DCF. Jurkat T-cells ($2x10^6$/ml) were serum starved for 4 hours prior to the addition of vehicle, 500ng/ml (■) or 1μg/ml (▲) CD95L. Cells were treated with 50μM DCFH-DA as described in method 2.2.10. At the end of the treatment periods, cell samples were analysed immediately for DCF fluorescence by flow cytometry. The median X (MdX) DCF fluorescence of 10,000 cells was analysed per sample. ΔDCF MdX represents the difference in MdX DCF of CD95L treated cells from that of vehicle treated cells for each time point. All incubations were performed at 37°C in a humidified, 5% CO_2, 95% air. The data are presented as the arithmetic mean ± s.e.m of at least 5 individual experiments. Arbitrary units, a.u.

cells were consequently examined. CD95L exposure of Jurkat T-cells mediated a decrease in DCF fluorescence. ΔDCF MdX was significantly reduced after 2 hours treatment with 1μg/ml ($p<0.01$) and 6 hours following 500ng/ml CD95L ($p<0.05$; see Figure 2.30), which was prior to any significant observations of apoptosis ($p>0.05$ for both concentrations; see Figure 2.27) and after the accumulation of intracellular ceramide in response to either concentration of CD95L (see Figure 2.29). The reduction in ΔDCF MdX occurred with faster kinetics and was of greater magnitude following Jurkat T-cell treatment with 1μg/ml of CD95L than that observed following treatment with 500ng/ml CD95L. The decrease in ΔDCF MdX following CD95L exposure reached a plateau after 4 and 8 hours treatment with 1μg/ml and 500ng/ml respectively (see Figure 2.30).

2.4 Discussion.

Determination of the cellular responses to short chain synthetic ceramides has highlighted further the pleotropic nature of the intracellular signalling molecule ceramide. Cellular treatment with synthetic, membrane permeable ceramides induces an alteration in the redox state at two sites, the extent and kinetics of which are associated with discrete, cellular responses. The functional consequence of these observations has application towards the development of novel therapeutic regimens in the treatment of several inflammatory diseases.

Jurkat T-cells exposed to synthetic, short chain ceramides showed a time dependent elevation in the appearance of fragmented DNA, a marker for apoptosis, as described previously by numerous authors (Cifone *et al.*, 1993; Obeid *et al.*, 1993; Liu *et al.*, 1998; Tepper *et al.*, 1997; Gulbins *et al.*, 1995; Mansat-de Mas *et al.*, 1999; Zhang *et al.*, 1996). This was maximal at 8 hours post-treatment with either C_2- or C_6-ceramide (20μM). At 16 hours post-treatment, this was associated with the formation of a sub-population of Jurkat T-cells displaying a reduction in cell size coupled with the loss of membrane permeability evaluated by flow cytometric analysis of the cellular uptake of the membrane impermeable dye PI as the cells enter late apoptosis or secondary necrosis. The appearance of apoptosis was preceded by an early increase in the $[peroxide]_m$ concentration upon Jurkat T-cell exposure to exogenous ceramide which decreased to baseline before the maximum apoptotic effect. C_2-ceramide (20μM) mediated a similar elevation in $[peroxide]_m$ in Jurkat T-cells after 1 hours treatment to that of 20μM C_6-ceramide, despite inducing an apoptotic response

which was greater in magnitude and with faster kinetics, implying that $[peroxide]_m$ is not the only intracellular signal involved in ceramide induced apoptosis. Non-apoptotic concentrations of C_2-/C_6-ceramide also enhanced $[peroxide]_m$ in Jurkat T-cells, and in a manner similar to pro-apoptotic ceramide concentrations, $[peroxide]_m$ returned to baseline after extended treatment periods.

Unlike Jurkat T-cells, exposure of U937s to synthetic ceramide induced an accumulation of nucleoids in the G0/G1 phase of the cell cycle, which is indicative of cell cycle arrest (Jayadev *et al.*, 1995; Dbaibo *et al.*, 1995; Ragg *et al.*, 1998) but was not as pronounced as described previously (Ragg *et al.*, 1998). The observation of growth arrest occurred after 16 hours incubation with 20μM C_2-/C_6-ceramide, later than the onset of apoptosis in Jurkat T-cells and was persistent for up to 36 hours. This may be attributed to an increase in $[peroxide]_m$, which was of smaller magnitude than that seen in apoptosis mediating an adaptive response rather a deleterious one. As in Jurkat T-cells, an initial increase of $[peroxide]_m$ occurred at 1 hour post C_2- or C_6-ceramide, and returned to baseline within 4 hours. Furthermore, cell size and membrane permeability remained unaltered by ceramide treatment, indicating no induction of necrosis. U937 monocytes have been described to undergo apoptosis upon exposure to concentrations of ceramide in excess of 20μM (Mansat-de Mas *et al.*, 1999; Quillet-Mary *et al.*, 1997; Zamzami *et al.*, 1995) and it is likely that the magnitude of changes in $[peroxide]_m$ occurs with differing kinetics to that associated with growth arrest. This principle is confirmed by the observation that synthetic ceramides which mediate growth arrest or apoptosis in U937 monocytes and Jurkat T-cell respectively, induce a greater elevation in $[peroxide]_{mit}$ than those which mediate no cellular response. The reported massive elevation in ROS production by

Quillet-Mary *et al.*, (1997) that was associated with apoptosis of U937 monocytes was achieved at a cellular concentration of $5x10^5$/ml in the presence of 25μM C_6-ceramide, a five fold greater dose per cell than utilised here. The cellular effects of high ceramide concentrations have not been examined since ceramide metabolites may initiate activation of opposing signal transduction pathways. Additionally, the experiments were designed to achieve intracellular concentrations that are within the order of magnitude of endogenous ceramide fluctuations achieved when administered at a concentration of 1-20μM to $2x10^6$/ml – $10x10^6$/ml of cells (as reviewed in; Hannun & Luberto, 2000). The transient nature of the ceramide mediated disturbances of $[peroxide]_m$ are probably due to their metabolism at the cellular or mitochondrial level, indeed, ceramidase, which converts ceramide to sphingosine, is located within the mitochondrial matrix at a similar site to the electron transport chain.

To solely observe the effects of ceramide, cells were treated in serum free media, hence removing opposing proliferative signals induced by serum. These conditions favour a reduction in cell growth, as observed by the gradual time dependent increase of nucleoids in the G0/G1 phase of control U937 monocytes. Longer incubations (36 hours) resulted in the appearance of apoptosis due to growth factor withdrawal by serum deprivation. Elevated endogenous ceramide levels have been reported following serum starvation in Molt-4 human leukaemia cells. However, this was initially apparent after 24 hours and coincided the appearance of fragmented DNA (Jayadev *et al.*, 1995).

Since the elevation in $[peroxide]_m$ occurs before any observations of a cellular response, this alteration in redox state may be contributing factor to the cell type specific response to ceramide rather than a result of the cellular response. The magnitude of enhanced $[peroxide]_m$ upon synthetic ceramide treatment may in part influence the activation state of redox sensitive signalling intermediates and consequently the cellular outcome to synthetic ceramide exposure.

Cell type specific alterations in the $[peroxide]_i$ upon ceramide exposure may be influenced by the constitutive intracellular antioxidant levels. The action of N-SMase is negatively regulated by GSH in human leukaemia Molt-4 cells, GSH inhibition mediating an elevation in N-SMase activity and endogenous ceramide levels (Liu *et al.*, 1998, Liu & Hannun, 1997). It is plausible that ceramide may manipulate these intrinsic levels, probably via the activation of one of its several protein targets (Gulbins *et al.*, 1995; Hanna *et al.*, 1999; Müller *et al.*, 1995; Wiegmann *et al.*, 1994; Oh *et al.*, 1998) or kinase signalling cascades (Gulbins *et al.*, 1995; Hanna *et al.*, 1999; MacKichan & DeFranco., 1999; Modur *et al.*, 1996;Verheij *et al.*, 1993; Zundel & Giaccia, 1998) rather than directly. However, previous studies showed that glutathione levels remained unchanged when MCF7 cells were treated with bacterial SMase or C_6-ceramide at concentrations that induced apoptosis (Liu *et al.*, 1998), although SMase activity was reduced in GSH peroxidase over-expressing cells (Gouazé *et al.*, 2001). In contrast, it is observed here that significant loss of glutathione from Jurkat T cells and U937 monocytes occurs prior to evidence of apoptosis or growth arrest respectively, demonstrating that dramatic flux in redox state precedes these stress responses. This reduction in total cellular GSH corresponded well with the appearance of enhanced $[peroxide]_m$ production. Since

the assay employed to measure cellular GSH evaluates both GSH and oxidised GSH (GSSG), a reduction in total cellular GSH implies loss of GSH through either the energy dependent export of excess GSSG into the extracellular space or formation of mixed disulfides with proteins (as reviewed in; Evans *et al.*, 1997). Where ceramide treatment mediated a growth arrest response in U937 monocytes, or at low doses, a non-apoptotic response in Jurkat T-cells, GSH levels returned to that of controls. $[peroxide]_m$ production to non-apoptotic C_2-/C_6-ceramide doses were smaller than that observed in an ensuing apoptotic response and may be attributed to efficient detoxification of peroxide by GSH and consequent cessation of GSSG production. Where U937 monocyte apoptosis has been described by others to be mediated by concentrations of synthetic ceramides in excess of 20μM (Mansat-de Mas *et al.*, 1999; Quillet-Mary *et al.*, 1997; Zamzami *et al.*, 1995) it could be predicted that the total loss of GSH would occur due to excessive $[peroxide]_m$, a similar response to that observed in Jurkat T-cell. Export of GSSG is halted prior to the total depletion of the GSH pool enabling restoration of GSH by the action of GSR. Total cellular GSH levels remained lower than that of controls in response to apoptotic concentrations of C_2-/C_6-ceramide (20μM), and were totally lost after C_2-ceramide treatment, -possibly due to the larger quantity of $[peroxide]_m$ produced. The total loss in GSH mediated by 20μM C_2-ceramide corresponds with a greater apoptotic efficacy for C_2- than for the C_6- species at the same concentration. It is plausible that the apoptotic response to synthetic ceramides may be amplified by the release of endogenous ceramide following depletion of GSH, whose levels negatively regulate the action of N-SMase (Liu & Hannun, 1997). In U937 monocytes, HL60s and normal skin fibroblasts, C_2-/C_6-ceramide treatment led to N-SMase activation, SM hydrolysis and, as a consequence, ceramide production within 10 minutes. Further, a prolonged and

persistent accumulation of up to 400% of control endogenous ceramide levels were detectable at 24 hours that was inhibited by 50% by fumonsin B1 pre-treatment (Jaffrézou *et al.*, 1998). A more recent study describes no N-SMase or A-SMase activity in A549 cells, MCF7 or HL60s in response to 20μM C_6-ceramide, but induced endogenous ceramide accumulation via the action ceramide synthase. However, labelling of C_6-ceramide with [3-^{3}H-sph]D-*erythro*- or N-[1-^{14}C-N-hexanoyl]D-*erythro*-C_6-ceramide to tag the sphingosine backbone or fatty acid acyl chain respectively, revealed that the generation of endogenous ceramide in response to synthetic ceramide was due to the biochemical recycling of the sphingosine backbone via deacylation and reacylation. This process was inhibited by fumonsin B1 (Orgetman *et al.*, 2002).

Moreover, the amplitude of $[peroxide]_m$ production in response to concentrations of synthetic ceramides which induce apoptosis may reflect the intrinsic, endogenous levels of antioxidant present within the cell. Indeed U937 monocytes, possess three times the concentration of total cellular glutathione than Jurkat T-cells and hence may reduce $[peroxide]_m$ levels to those which mediate a non-deleterious response rather than the terminal cellular response of apoptosis associated with a larger production of peroxide. The decrease in GSH in U937 monocytes may not be sufficient to remove the inhibitory effect on N-SMase unlike that observed in Jurkat T-cells. The importance of GSH is highlighted further by the observation of elevated H_2O_2 production in GSH depleted mitochondria treated with C_2-ceramide (García-Ruiz *et al.*, 1997). If it is the greater intrinsic level of antioxidants present in U937 monocytes compared with Jurkat T-cells which confers growth arrest rather than apoptosis by detoxification of $[peroxide]_m$, the part or total depletion of GSH by pre-

incubation of U937 monocytes with diethylmalate (DEM), which reacts with free sulphydryl groups, prior to synthetic ceramide treatment (20μM) may induce apoptosis rather than growth arrest. Alternatively, GSH depletion may be achieved by inhibition of GSH synthesis or reductase with buthionine sulfoximine (BSO) or 1,3-bis(2-chloroethyl)-1-nitrosourea (BCNU) respectively. These observations confirm previous work using genetic variants of mouse epidermal tumour cells, which varied in susceptibility to ceramide and also endogenous glutathione levels, the decrease in cellular redox potential appeared to determine susceptibility to ceramide-dependent killing pathways (Davis *et al.*, 2000). For further consideration, different cell types may possess different basal levels of the various enzymes responsible for ceramide accumulation. In view of the implied regulation of N-SMase by GSH (Liu & Hannun 1997; Lui *et al.*, 1998) and the observations that the total cellular GSH content of U937 monocytes is almost 3 fold higher than Jurkat T-cells, it is possible that there is a greater degree of negative regulation in U937 monocytes with the consequence of lower endogenous ceramide levels than in Jurkat T-cells. The significance of this may affect the cellular response of exogenously applied synthetic ceramide. Similarly, the ratio of ceramide with its metabolites from the sphingomyelin cycle, such as sphingosine 1-phosphate which has been implicated in a proliferative response and inhibits both C_2-ceramide and CD95L mediated apoptosis (Cuvillier *et al.*, 1996, 1998), may also dictate the cellular response to exogenously applied short chain ceramides.

While this study characterises the effects of ceramide on $[peroxide]_m$ generation, analysis of total cellular GSH has been undertaken here and perturbations of GSH pools within subcellular organelles have not been investigated. The mitochondria

possesses its own GSH store which arises via an ATP dependent carrier which translocates cytosolic GSH into the mitochondria matrix from the cytosol (Garcia-Ruiz *et al.*, 1995). It may be of interest to further characterise the transient alterations in $[peroxide]_m$ in respect to mitochondrial GSH levels within U937 monocytes and Jurkat T-cells in response to synthetic ceramide treatment. The mitochondria is considered to be an early target in TNFα mediated apoptosis, since morphological studies reveal them to swell with a reduced number of cristea, which is associated with abrogation of mitochondrial respiration (Schulze-Osthoff *et al.*, 1992). Similar observations have been described in isolated rat liver mitochondria in response to C_2-ceramide treatment (de Gannes *et al.*, 1998). Furthermore, treatment of L929 murine fibrocarcinoma cells with TNFα, which utilises ceramide as a signal transduction molecule, induces an elevation in $[peroxide]_m$ which was not affected by depletion of cytoslic GSH only. However, depletion of cytosolic and mitochondrial GSH with DEM led to a 20 fold elevation in $[peroxide]_m$ production. These results suggest that it is the mitochondrial GSH and not cytoplasmic GSH which acts as the major scavengers of $[peroxide]_m$ (Goossens *et al* 1995).

The close kinetic relationship between elevations in $[peroxide]_m$ and loss of total cellular GSH makes it difficult to determine which is the cause of the other. Enhanced $[peroxide]_m$ production and decreased total cellular GSH levels are likely to be related and it has been implied here that peroxide production precedes alteration in GSH levels. Paradoxically, synthetic ceramide mediated depletion of total cellular GSH may be necessary for initial increases in $[peroxide]_m$ (Tan *et al.*, 1998). GSH efflux may be one of the steps which mediates apoptosis. Ghibelli *et al.*, (1998) have described that prevention of carrier mediated GSH export with methionine or

cystathionine rescued cells from apoptosis and once removed, prevented proliferation. Controversially, the experiments described herein have shown that pre-treatment of Jurkat T-cells or U937s with either of the anti-oxidants GSH or NAC does not protect against synthetic ceramide mediated Jurkat T-cell apoptosis, and additionally drive ceramide treated U937 monocytes into apoptosis implying a more complex scenario of redox alterations in the cellular responses to synthetic ceramides. Other anti-oxidant defence systems and their role in controlling peroxide production in response to ceramide have not been examined here. Over expression of the 12kDa thiol thioredoxin (Wong *et al.*, 1989) or, the mitochondrial matrix associated enzyme MnSOD inhibit TNF mediated apoptosis (Manna *et al.*, 1999). Furthermore, incubation of primary rat hepatocytes with exogenously applied bacterial SMase or cell permeable ceramide leads to an increase in MnSOD activity (Pahan *et al.*, 1999). Clearly, these and the roles of catalase and CuSOD in ceramide mediated cellular and redox responses require attention.

Ceramide has been identified as a second messenger in response to a variety of extracellular stimuli (Andrieu *et al.*, 1994; Bose *et al.*, 1995; Boland *et al.*, 1997; Cifone *et al.*, 1993; Gamard *et al.*, 1997; Gulbins *et al.*, 1995; Herr *et al.*, 1997; Huwiler *et al.*, 1996; Liu *et al.*, 1998; MacKichan & DeFranco, 1999; Mansat-de Mas *et al.*, 1999; Obeid *et al.*, 1993; Santana *et al.*, 1996; Tepper *et al.*, 1997; Verheih *et al.*, 1996) and the mitochondria is likely to be a primary target for its actions (Esposti & McLennan, 1998;García-Ruiz *et al.*, 1997; Ghafouifar *et al.*, 1999; Zamzami *et al.*, 1995). Over expression of the mitochondrial anti-apoptotic proto-oncogene $Bcl\text{-}_2$ in U937 cells or isolated mitochondria, inhibits the structural and biochemical events associated with this organelle in ceramide induced apoptosis (Ghafourifar *et al.*,

1999; Susin *et al.*, 1997; Zamzami *et al.*, 1995). Pre-treatment of U937 monocytes or isolated mitochondria with the complex I or complex II inhibitors rotenone or trifluroacetone (TFA) respectively inhibits peroxide production whereas inhibition of complex III with AA enhanced peroxide generation mediated by ceramide (Quillet-Mary *et al.*, 1997; Garcia Ruiz *et al.*, 1997; Gudz *et al.*, 1997) and TNFα (Schulze-Osthoff *et al.*, 1992). As expected, TFA or rotenone inhibited ceramide or TNFα induced apoptosis in U937 monocytes or L929 cells respectively, whereas AA potentiated apoptosis (Quillet-Mary *et al.*, 1997; Schulze-Osthoff *et al*, 1992). Further, direct interaction of ceramide with the mitochondrial respiratory chain at complex III has been described as the source of ROS generation (Esposti & McLennan, 1998; García-Ruiz *et al.*, 1997; Gudz *et al.*, 1997; Quillet-Mary *et al.*, 1997), although others believe this to be as a consequence of cytochrome c release (Cai & Jones, 1998; Ghafourifar *et al.*, 1999). Indeed, following 6 hours treatment of Molt 4 or HL60 cells with C_6- or C_2-ceramide respectively an increase in cytosolic cytochrome c was reported (Amarante-Mendes *et al.*, 1998; Zhang *et al.*, 1997). Ghafourifar *et al.*, (1999) hypothesised that ceramide has a high affinity for oxidised cytochrome c rather than reduced cytochrome c, which changes its physical properties leading to its release from the mitochondria and an associated decrease in mitochondrial respiration. The observations described here of an increase in $[peroxide]_m$ upon cellular ceramide treatment support the observations of Garcia-Ruiz *et al*, (1997) who showed that doses of C_2-ceramide (0.25-50μM) induced a dose dependent bi-functional effect on H_2O_2 production from isolated rat liver mitochondria. Incubation of isolated mitochondria with low doses of C_2-ceramide (0.25-5μM) for 1 hour induced the production of H_2O_2. This was also observed in primary rat hepatocytes with no alteration in cell viability. However, at higher doses,

no alteration in H_2O_2 production was observed after 1 hour incubation (García-Ruiz *et al.*, 1997). Taken together, it is possible that following exposure to a concentration of ceramide the amount of ROS generated at the mitochondria is increased and via interaction with complexes I and II of the electron transport chain, is increased and is associated with an alteration in the antioxidant capacity of the cell (see Figure 2.31). It is likely that the synergistic magnitude of these two events contributes to the induction of a cellular response (as reviewed in; Gabbita *et al.*, 2000). The balance between ROS production at the mitochondria and the intrinsic antioxidant capacity of the cell modulates in part the cellular outcome to ceramide.

The redox state of the cell is liable to affect protein-protein interaction and consequently gene transcription. Considering that H_2O_2 activates the transcription factor NFκB (Dumont *et al.*, 1999; Schreck *et al.*, 1992), an elevation in the $[peroxide]_m$ by exogenously applied synthetic ceramides at high concentrations promotes NFκB and AP-1 activation which has been associated with apoptosis in U937 monocytes (Quillet-Mary *et al.*, 1997). The cell type specific effects of ceramide are demonstrated further by the conflicting report of exogenously applied bacterial SMase or short chain, synthetic ceramides inability to induce NFκB translocation and IκB degradation in Jurkat T-cells. Further, synthetic ceramides actually inhibited phorbol ester (PMA, PKC activator) induced activation of NFκB in Jurkat T-cells (Gamard *et al.*, 1997). Whether the ceramide mediated elevation in $[peroxide]_m$ observed here can promote extra-mitochondrial signalling or mediates mitochondrial DNA mutation (mitDNA) requires further investigation (see Figure 2.31). The excessive intracellular accumulation of GSSG may impair the function of protein tyrosine phosphatases (PTP) via interaction with cysteine thiols. PTP are of

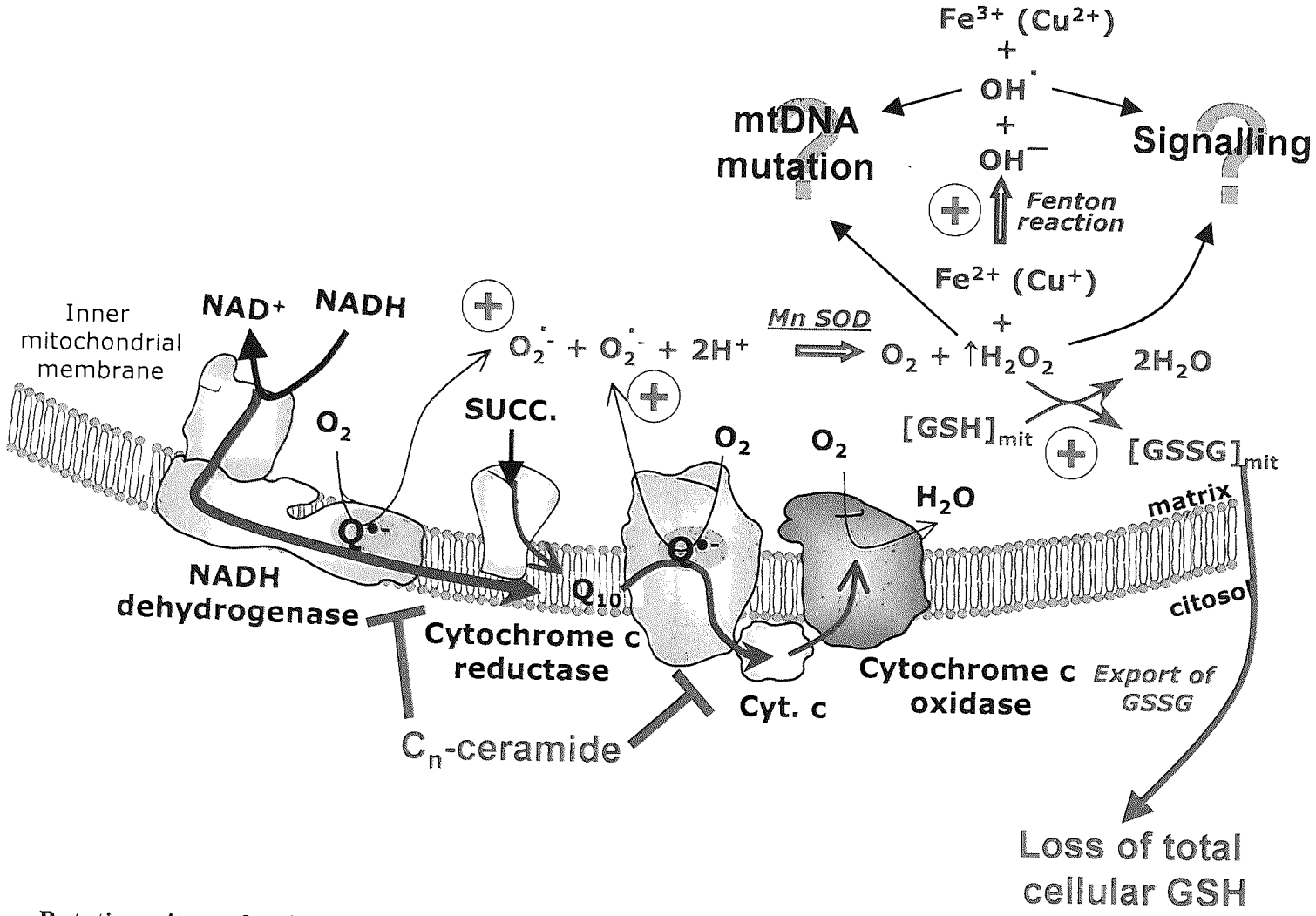

Figure 2.31. Putative sites of mitochondrial peroxide formation in response to synthetic short chain ceramides and the consequence of their formation. Shown is a simplified schematic of the various components of the mitochondrial electron transport chain, sites of reactive oxygen species (ROS) production and the effect of C_n-ceramides on their production. Superoxide dismutase ,SOD; glutathione, GSH; oxidised glutathione, GSSH; superoxide, $O_2^{\cdot -}$; manganese superoxide dismutasse, MnSOD; mitochondrial DNA, mitDNA;. Adapted from Jackson *et al.*, (2002).

primary importance in mitogenesis, cell adhesion, cell differentiation, oncogenic transformation and apoptosis, regulating protein tyrosine kinase activity (as reviewed in; Gabbita *et al.*, 2000), and modification of their activity by oxidants may modulate the cell cycle. However, short and long chain synthetic ceramides have been shown to activate the protein phosphatases PP2A *in vitro* (Dobrowsky *et al.*, 1993; Ruvolo *et al.*, 1999) and isolated PP1 (Chalfant *et al.*, 1999) respectively, although the PP2A inhibitor okadaic acid did not block C_2-ceramide inhibition of complex III in isolated rat heart mitochondria (Gudz *et al.*, 1999).

If the excessive production of $[peroxide]_m$ were the sole mediator of apoptosis or growth arrest, then a beneficial effect might be expected by pre-treatment of Jurkat T-cells of U937 monocytes respectively with anti-oxidants. However, the antioxidants NAC or GSH failed to abrogate synthetic ceramide mediated apoptosis at any time point as reported by others (Lee & Um, 1999; Liu *et al.*, 1998), although catalase protected WEHI 231 B cells from the lethality of C_2-ceramide (Fang *et al.*, 1995) probably indicating some cell type specificity in synthetic ceramide mediated redox alterations. Surprisingly in U937 monocytes NAC and GSH inhibited synthetic ceramide induced G0/G1 growth arrest by driving ceramide treated cells into apoptosis as indicated by the presence of fragmented DNA. In effect, antioxidants transform the cellular response of U937 monocytes to ceramide exposure from cytostatic to cytotoxic. Further, and contrary to the observation of ceramide mediated transient elevations in $[peroxide]_m$, analysis of $[peroxide]_{cyt}$ utilising the peroxide sensitive dye DCFH-DA revealed an overall loss prior to the appearance of DNA fragmentation or G0/G1 growth arrest in Jurkat T-cells and U937 monocytes respectively. Utilising planar phospholipid membranes, Siskind & Combini (2000)

described the formation of large stable pores by short and long chain ceramides, and applying mathematical models, it was proposed that 5 or more ceramide molecules form a polar centre which can accommodate water and solutes, and it is these which contribute to the apoptotic response (Siskind & Combini, 2000). Presumably, the same number of pores would of formed in Jurkat T-cells as in U937 monocytes that are exposed to the same concentration of synthetic ceramides, yet different cellular responses are achieved indicating a more complex scenario. The apparent loss of $[peroxide]_{cyt}$ was not due to the leakage of DCFH-DA from the cytosolic environment since cells remained viable as indicated by the minimal uptake of the membrane impermeable dye PI throughout the DCF analysis period. Although 20μM C_2-/C_6-ceramide induced a population of Jurkat T-cells with high PI uptake and reduced cell size after 16 hours treatment, $[peroxide]_{cyt}$ was not evaluated as these cells had undergone secondary necrosis. Lower concentrations of synthetic ceramide (10μM), which did not compromise membrane viability following 16 hours treatment, showed reduced $[peroxide]_{cyt}$ which was not to a level associated with apoptosis. The magnitude and kinetics of $[peroxide]_{cyt}$ loss may be the true dictator of the cellular responses to synthetic ceramides. An apoptotic response in Jurkat T-cells to C_2-/C_6-ceramide was preceded by an immediate, almost exponential like reduction in $[peroxide]_{cyt}$. In contrast, where growth arrest was observed in U937 monocytes, the decrease in $[peroxide]_{cyt}$ was initially delayed, and fell approximately 40 minutes post-treatment. Additionally, the maximal loss if $[peroxide]_{cyt}$ was of lower magnitude than that observed in Jurkat T-cell apoptosis. It is therefore of no surprise that reducing the intracellular peroxide levels of U937 monocytes by pre-treatment with anti-oxidants, which were not in themselves toxic, permits $[peroxide]_{cyt}$ to fall upon ceramide treatment to a level which confers apoptosis. By driving U937

monocytes into growth arrest through a reduction in $[peroxide]_{cyt}$ of lesser magnitude, protection from apoptosis is conferred. These observations of reduced fluorescence of DCF in U937 monocytes following synthetic ceramide treatment are in direct contrast to those of Mansat-de Mas *et al.*, (1999) who observed elevated fluorescence of a DCFH-DA analogue, C2938, within 20 minutes C_6-ceramide treatment that returned to baseline after 30 minutes, whereas Lee & Um, (1999) described no alteration in DCF fluorescence following U937 exposure to C_2-ceramide. Growth factor withdrawal via serum deprivation in confluent mouse proximal tubular cells lead to the production of superoxide radicals that were associated with apoptosis, both observations inhibited by the application of catalase or the iron chelator deferoxamine (DFO; Lieberthal *et al.*, 1998). In this experimental system, the decrease in $[peroxide]_{cyt}$ induced by synthetic ceramide application to U937 monocytes may prevent apoptosis due to serum deprivation by limiting the levels of ROS produced to those that are non-deleterious. Furthermore, the application of C_2-ceramide to CTLL-2 T-lymphocytes blocked cell cycle progression, caused the down regulation of the anti-apoptotic factors Bcl-x_L induced by IL-2, and promoted apoptosis mediated by IL-2 deprivation (Flores *et al.*, 1998). As discussed, the elevation in peroxide production in response to synthetic ceramide treatment as reported by others (Quillet-Mary *et al.*, 1997) may be due to the relatively larger concentration of synthetic ceramide per 10^6 cells utilised, which in effect, masks other cellular redox alterations.

The biochemical and molecular processes that lead to cellular responses to various agents analysed in immortalised cell lines are often criticised as they are continually cycling and possess higher metabolic rates. It was therefore of importance to study the cellular and redox effects of synthetic short chain ceramides on normal, primary

human cells. The observation of reduced $[peroxide]_{cyt}$ in $CD3^+$ T-cells and $CD14^+$ monocytes in whole blood treated with C_2-/C_6-ceramide and in purified resting T-cells or PHA activated T-cells *in vitro* prior to the observation of apoptosis supports and is in agreement with those data obtained from cell lines. The C_2-ceramide effects on $[peroxide]_{cyt}$ observed in cell lines are representational of those that occur in primary cells. The ability of C_2-ceramide to induce apoptosis which was preceded by loss in $[peroxide]_{cyt}$ was independent of activation state and phase of the cell cycle, where identical levels of $[peroxide]_{cyt}$ loss and DNA fragmentation were observed in resting and PHA activated T-cells. Resting T-cells possessed only DNA that was in the G0/G1 phase of the cell cycle whereas PHA activated T-cells displayed the appearance of a small number of S-phase and G2M phase DNA, indicating progression through the cell cycle. Furthermore, the lack of difference between the degree of apoptosis induced by C_2-ceramide in resting and PHA activated T-cells implies that RNA, DNA nucleotide-sugar and lipid synthesis is not required. In contrast, under identical culture conditions and treatments, Mengabas *et al.*, (1999) reported that C_2-ceramide killed normal human T-lymphocytes via a non-apoptotic mechanism that was prevented by PHA activation. In the data described, the membrane permeability of resting and activated primary human T-cells treated with C_2-ceramide (0-20μM) was not compromised at 6 hours post-treatment when analysed for uptake of the membrane impermeable dye PI by flow cytometry indicating that necrosis did not contribute to the death process. The effects of C_2-/C_6-ceramide on primary monocytes requires elucidation, although the observed effects on the $CD14^+$ monocytes of $[peroxide]_{cyt}$ loss following treatment of whole blood was similar to that of U937 monocytes.

The site of $[peroxide]_{cyt}$ loss remains elusive and requires further investigation. The mitochondria is a primary site for ROS production and we have described transient $[peroxide]_m$ production in response to synthetic ceramide probably via the electron transport chain. However, it is not the exclusive site for ROS production. In the cytosol, hypoxanthine/xanthine oxidase, NADPH-oxygenase and cyclo-oxygenase are sources of ROS production. The electron transport chain is also functional at the E.R, which like the mitochondria, generate superoxide from electron leakage of NADPH cytochrome P450 reductase (as reviewed in; Cross & Jones, 1991). It is plausible that ceramide may inhibit ROS production at one of these sites with an overall effect of reducing $[peroxide]_{cyt}$. However, a more intriguing whilst speculative target, is the NADPH oxidase present within the plasma membrane which is responsible for superoxide generation in leukocytes. Here, NADPH acts as the electron donor and converts molecular oxygen to superoxide according to the equation,

$$NADPH + H^+ \rightarrow NADP^+ + 2H^+ + 2O_2^{\cdot -}$$

with the dismutation of superoxide to H_2O_2 (as reviewed in Gabbita *et al.*, 2000).

$$2O_2^{\cdot -} + 2H^+ \rightarrow H_2O_2 + O_2$$

In resting cells, the outer leaflet of the plasma membrane contains the majority of SM displaying low fluidity, an intrinsic property of SM (Patra *et al.*, 1999). Upon SM hydrolysis, ceramide is generated in association with the release of cholesterol increasing membrane of fluidity and the lateral mobility of membrane constituents

(Chatterjee, 1994; Ridgeway *et al.*, 1998). Given the amphipathic nature of ceramide and its propensity to partition into lipid bilayers, it is reasonable to hypothesise that an accumulation of ceramide may modulate NADPH oxidase activity. Indeed in model membranes, ceramide aggregates spontaneously (Huang *et al.*, 1996) initially forming small microdomains that possess the propensity to fuse (Holopainen *et al.*, 1998). Furthermore the formation of ceramide rich domains has been reported to lead to enzyme activation such as phospholipase A2 (Huang *et al.*, 1996; 1998), aggregation of membrane receptors (Boniface *et al.*, 1998; Grassmé *et al.*, 2001a, & b, 2002; Graziadei *et al.*, 1990; Monks *et al.*, 1998; Natoli *et al.*, 1998; Rosenman *et al.*, 1993) or may provide a milieu for segregation of specific proteins. However, the role of these non-mitochondrial sources of ROS in apoptosis is unknown.

As a consequence of cell impermeability of natural ceramide, the cellular responses and targets of inducers of endogenous ceramide production are often analysed with synthetic ceramide. The difference in the structure between short and long chain ceramide make it likely that they induce differential effects on the lipid membrane structure and thereby different biological effects. Indeed, short chain ceramides inhibit PLA2 activity, while long chain ceramides potentiate this activity (Huang *et al.*, 1998). In an attempt to analyse the effects of intrinsic endogenous ceramide generation on $[peroxide]_{cyt}$, Jurkat T-cells were treated with the known inducer of ceramide accumulation, CD95L (Cifone *et al.*, 1993; Gulbins *et al.*, 1995; Tepper *et al.*, 1997). Herein, Jurkat T-cell treatment with CD95L leads to an accumulation of ceramide within 30 minutes, which rose further at 1 hour. This was followed by a reduction in $[peroxide]_{cyt}$ prior to the appearance of apoptosis and in contrast to the elevation in DCF fluorescence reported in IL-1β/TNFα activated peripheral blood

monocytes (PBM) prior to apoptosis induced by CD95L exposure (Um *et al*,. 1996). These opposing observations are likely to be owing to differences in cell lineage. Whilst the extent of apoptosis induced by 1μg/ml or 0.5μg/ml CD95L was similar to that mediated by 20μM C_2-/C_6-ceramide, the magnitude reduction in $[peroxide]_{cyt}$ generation was less and gradual. These discrepancies may exist due to differences in the degree of saturation and length of fatty acid chain between endogenous and short chain ceramides. Additionally, CD95L induced apoptosis in Jurkat T-cells is in part induced by ceramide independent signals involving caspase-8 recruitment to the DISC domain of activated CD95 receptor leading to autocatalytic activation of pro-apoptotic caspase cascade (Cuvillier *et al.*, 1998).

There is much debate as to the source of ceramide generation and the kinetics of its production, where differential observations are frequently cell type dependent. It is probable that *de novo* synthesis of ceramide is not involved in CD95 mediated Jurkat T-cell apoptosis as the activation of this enzyme is associated with a late accumulation of this sphingolipid, where it maybe a commitment step to ensure or further commit to cell death (Tepper *et al.*, 1997) or a consequence of cell death due to loss of cellular homeostasis (Watts *et al.*, 1997). In this thesis ceramide accumulation occurred within 30 minutes of CD95L exposure implying the involvement of either or both N-Smase or A-Smase associated with an intermediate or rapid rise respectively (Cifone *et al.*, 1993; De Maria *et al.*, 1997, 1998;Gamard *et al.*, 1997; Sawada *et al.*, 2002; Tepper *et al.*, 1999). However, there is significant controversy regarding their location. A specific criticism against the role of A-Smase in the rapid rise in endogenous ceramide, which often occurs within minutes of receptor stimulation in some cell types (Cifone *et al.*, 1993; Genestier *et al.*, 1998b;

Gulbins *et al.*, 1995), is that it primarily resides in lysosomes (as reviewed in; Hoffman & Dixit, 1998) which raises the question that if A-SMase is responsible for the rapid hydrolysis of SM to ceramide in response to CD95 receptor stimulation, how is the signal translocated with such rapid kinetics? Utilising two experimental approaches, Ségui *et al.*, (2000) suggested that endosomal/lysosomal ceramide is not involved in cytokine-induced apoptosis; Firstly, the selective introduction of natural ceramide into acidic organelles of the cell did not result in apoptosis. Furthermore, utilising SV40 transformed fibroblasts from a patient with Farbers disease, an autosomal recessive, lysosomal storage disorder characterised by an accumulation of ceramide as a result of a deficiency in the activity of lysosomal ceramidase, the apoptotic response to TNFα/CD95L exposure was not different from normal fibroblasts. Additionally, apoptosis was preceded by a comparable accumulation in ceramide (Ségui *et al.*, (2000). Liu & Anderson (1995) were the first to suggest that Zn-independent A-SMase and not N-SMase is localised to caveolae within fibroblasts. Recently, Gressmé *et al.*, (2001a & b) have suggested a novel mechanism involving CD95 receptor activation coupled with A-SMase and ceramide generation. It is suggested than an initial interaction of CD95L with a limited number of CD95 receptors leads to a transient and weak activation that is insufficient to trigger apoptosis, but is able to mediate A-SMase translocation from the cytosol to the outer membrane leaflet to co-liase with its substrate SM. As a consequence, ceramide is generated forming ceramide rich microdomains, which possesses the ability to fuse to form ceramide rich rafts leading to clustering of receptors (Gressmé *et al.*, 2001a & b; Holopainen *et al.*, 1998). Cells deficient in acid ceramidase, which metabolises ceramide thereby negatively regulating ceramide action, strongly enhanced CD95 receptor clustering. The recent development of a fluorescently tagged MoAb to

ceramide, 15B4, has revealed ceramide not to be present in resting cells, but locates to areas of CD95 receptors and A-SMase clusters on CD95L treated B-cells, which later underwent apoptosis. Additionally A-SMase deficient B-cells did not undergo CD95 receptor mediated apoptosis; this response was restored on the addition of C_{16}-ceramide (Gressmé *et al.*, 2001a & b). It has been suggested that accumulation of ceramide rich domains in membranes requiring cytoskeleton alterations (Brown & London, 1998), may disrupt or activate membrane associated enzymes, energy producing centres or proteins to reduce $[peroxide]_{cyt}$.

It is described that synthetic ceramides can target the mitochondria to mediate a transient elevation in $[peroxide]_m$ generation. Whether short chain ceramides are able to translocate to the mitochondria due to their relatively greater water solubility compared to long chain ceramides, or via a signalling intermediate such as GD3 ganglioside (De Maria *et al.*, 1998) or PTP, which was observed at elevated levels in the mitochondria isolated from HL60 cells treated with 10μM C_2-ceramide for 3 hours when compared to those from control cells (Ruvolo *et al.*, 1999), has not been investigated. It is also of interest to determine whether the endogenous ceramide generated in response to CD95L exposure of Jurkat T-cells translocates to the mitochondria to induce transient alterations in $[peroxide]_m$ via direct interaction with complex III of the electron transport chain as described for synthetic ceramides (Esposti & McLennan, 1998; García-Ruiz *et al.*, 1997; Gudz *et al.*, 1997; Quillet-Mary *et al.*, 1997) or via a target of ceramide accumulation in response to CD95L such as the lipid GD3 ganglioside (DeMaria *et al.*, 1997, 1998) or PTP (N'cho & Brahmi, 1999). However, A.A, rotenone or menadione did not affect CD95L induced apoptosis of Jurkat T-cells (Dumont *et al.*, 1999). Further, Bcl_2 hyperexpression in

Jurkat T-cells inhibits the mitochondrial perpetuations of $\Delta\Psi m$ collapse and AIF release associated with apoptosis induced by oxidants and ceramide, but does not interfere with that induced by CD95L (Susin *et al.*, 1997). Like synthetic ceramides, the treatment of Jurkat T-cells with CD95L was capable of reducing total cellular GSH, although this was only investigated after the appearance of fragmented DNA and may be as of a consequence of apoptosis rather than as a result of excessive $[peroxide]_m$ production. Further, ceramide may be potentially be generated in the mitochondria or ER where the enzyme ceramide synthase resides, but not SMases (as reviewed in; Levade, & Jaffrézou, 1999). It remains to be determined whether extracellular agents that target the mitochondria to induce ROS formation do so by generating *de novo* synthesis of ceramide within this organelle.

The observations of decreased $[peroxide]_{cyt}$ in response to CD95L or synthetic ceramide support those of Gamard *et al.*, (1997) who observed that CD95L induced apoptosis of Jurkat T-cells which followed an elevation in endogenous $[ceramide]_i$ but did not activate the redox sensitive transcription factor NFκB. In contrast, the related cytokine, TNFα, induced apoptosis with NFκB activation that was independent of ceramide accumulation. Further, it was hypothesised that ceramide accumulation may participate in negative feedback regulation of NFκB since synthetic ceramide prevented activation of this transcription factors by the PKC activator PMA (Gamard *et al.*, 1997). Where CD95L was described to induce apoptosis via an anti-oxidant inhibitable pathway, ceramide was not involved (Laouar *et al.*, 1999). Furthermore, CD95L mediated apoptosis of Jurkat T-cells was inhibited by calcytolin A, a potent inhibitor of Ser/Thr phosphatases 1 and 2A in the nM range

and okadaic acid in the μM range (N'cho & Brahmi, 1999) supporting the role for protein phosphatases in ceramide mediated apoptosis.

The opposing observations of differential redox events in the cellular response to an elevation in ceramide, whether this is due to the application of synthetic ceramide or inducers of endogenous ceramide, helps to clarify the controversy and conflicting reports of the cellular responses and targets of ceramide. More importantly, the data presented here indicates the existence of discrete redox sensitive entities targeted and manipulated by ceramide to produce independent responses. Short chain ceramide manipulates the intracellular redox state through mitochondrial and non-mitochondrial pathways. $[peroxide]_m$ generation may be important in parallel or as a potentiator to ceramide induced loss of $[peroxide]_{cyt}$. The loss of $[peroxide]_{cyt}$ in response to short chain ceramides in the immortalised cell lines of U937 monocytes and Jurkat T-cells has been translated to that in of primary human cells of identical lineage. Furthermore, it has been hypothesised that ceramide targets may be manipulated by the redox effects of ceramide at distinct sites, although further investigations are required to address these theories. Whether the described effects on the redox state are representational of the various species of endogenous ceramide, which vary in their fatty acid acyl chain length and degree of saturation, requires further examination rather than the co-incidental observations supplied here. Long chain natural ceramides are poorly soluble in the aqueous environment, and this prevents the cellular accumulation of an effective concentration. Recently Ji *et al.*, 1995 and Chalfant *et al.*, 1999 described that a mixture of long chain ceramides with 2% dodecane gave a final reaction mixture of 0.02% dodecane and up to 15μM of long chain ceramide. Use of long chain ceramides in the experiment systems utilised

here may help to resolve the putative involvement of endogenous cellular ceramide in the redox altering properties of various external agents and their subsequent cellular effects.

Chapter 3.0: Consequences of ceramide and anti-oxidants on monocyte-endothelial cell interactions.

Herein, a detailed description of the multistep paradigm of circulatory cell interaction with the vascular endothelium under normal and various pathological conditions is provided. Evidence suggestive of ceramides and ROS as intracellular mediators that enhance leukocyte endothelial cell interaction in response to physiological stimuli is discussed. However, from the key finding of chapter 2 that synthetic ceramides reduce the leukocyte $[peroxide]_{cyt}$ of leukocytes, it is controversially hypothesised that ceramide treatment would abrogate this circulatory cell adhesion to the endothelium. This may therefore provide a rationale for therapeutic intervention using targeted ceramides in the treatment of inflammatory disease of vascular origin. The discussion of the data presented supports this theory with additional consideration of ceramide induced biophysical perturbations and consequences for cellular physiology.

3.1 Introduction.

The vascular endothelium represents a primary site in the pathophysiology of several vascular diseases and disorders of inflammatory origins. Monocyte adhesion and transmigration across resting endothelial cells occurs at very low rates, however, an early observation in the development of atherosclerotic lesions is the enhanced recruitment of monocytes into subendothelial segments of arteries which ultimately leads to foam cell formation (as reviewed in; Lum & Roebuck, 2001; Ridley *et al.*, 2001; Ross, 1999; Springer, 1990). An elevation in adhesion molecules expressed on the endothelium in RA is associated with the augmented homing of leukocytes to inflamed synovial tissue compartments (as reviewed in Mojcik & Shevach, 1997). Additionally, monocytes isolated from the whole blood of patients with RA possess elevated adherence to fibronectin and resting or IL-1β activated endothelial cells (Lioté *et al.*, 1996). The appearance of monocytes within the synovium of rheumatoids is followed by their differentiation into tissue macrophages and type A synoviocytes whereas type B synoviocytes form fibroblasts (as reviewed in; Cutolo *et al.*, 1993; Carlos & Harlan, 1994; Müller-Ladner *et al.*, 1998).

Observations *in vivo* and in dynamic systems *in vitro* have lead to the proposition of a multistep paradigm for adhesion involving the homing of and rolling of leukocytes across the endothelium and matrix components. Leukocytes become activated by the endothelium leading to their arrest followed by their firm adhesion and eventually the extravasation (diapedisis/transmigration) though the endothelial cell layer in to the extracellular matrix (see Figure 3.1). This complex sequence of cell to cell

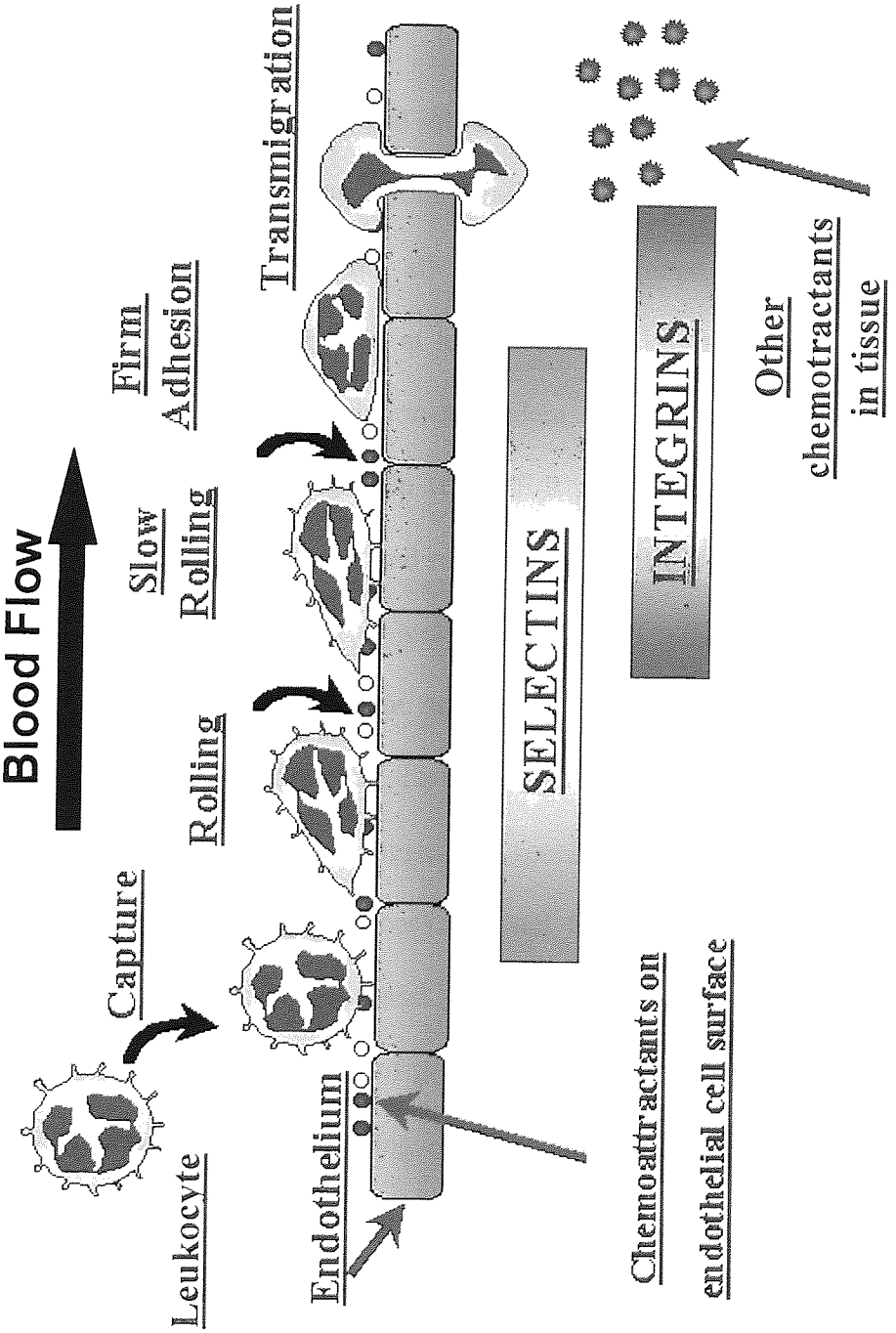

Figure 3.1. The multistep paradigm of leukocyte adhesion to the endothelium of blood vessels.

interactions are mediated by the engagement and detachment of receptors and counter receptors each present on circulatory leukocytes and endothelial cells. Each phase of the multistep paradigm of adhesion has been dissected to involve the interaction of specific receptors and their counter receptors (as reviewed in von Andrian & Mackay, 2000; Madri & Graesser, 2000; Springer, 1990, 1994).

Selectins initiate tethering and rolling of leukocytes to the endothelium and recognise sialyl Lewis X containing carbohydrate determinant on counter receptors. L-selectin (CD62L) is expressed on all leukocytes except a subpopulation of memory lymphocytes and recognises at least 2 mucin-like molecules on human endothelial cells, CD34 and glycosylation-dependent cell adhesion molecule-1 (GlyCAM-1). Conversely, E- and P-selectin (CD62E/P respectively) are present on the luminal surface of endothelial cells and recognise distinct but related structures expressed on the membranes of circulatory leukocytes. The CD62E/P ligands are carbohydrates O-linked to specific mucin like molecules rich in the serine and threonine and are heavily glycoslyated. The disulfide like dimer P-selectin glycoprotein ligand-1 (PSGL-1) is, as the name suggests, a specific ligand for P-selectin. Once tethered, CD62L is shed, a vital process required for leukocyte rolling. Metalloproteinase inhibitors prevent shedding and slow rolling. (as reviewed in; Madri & Graesser, 2000). The integrin family of glycoproteins consist of more than 20 non-covalently bound heterodimers consisting of an α and β chain expressed on the surface of leukocytes and it is their association with the immunoglobulin gene superfamily of receptors expressed on a variety of tissues including endothelial cells and epithelial cells which is primarily responsible for firm adhesion and diapedesis. These include intracellular adhesion molecule-1 (ICAM-1/CD54) ICAM-2 (CD102), ICAM-3

(CD50) which bind various combinations of the β2 integrins, vascular cell adhesion molecule-1 (VCAM-1/CD106) binds to very late antigen 4 (VLA4/CD29CD49D/α4β1) and fibronectin (CS-1). Mucosal addressin cell adhesion molecule-1 (MAdCAM-1) possesses a dual function in binding both the integrin LPAM-1 (CD49dCD-/α4β7) and L-selectin. LPAM-1 also has a weak affinity for VCAM-1. Antagonists to CD62L decreased rolling leukocytes and the subsequent number of firmly adhered leukocytes, whereas MoAb to CD18 only reduced the number of firmly adhered leukocytes suggesting that L-selectin acts at a step prior to the involvement of integrins (von Andrian *et al.*, 1991; Ley *et al.*, 1991). Transfection of resting endothelial cells with an adenovirus carrying VCAM-1 showed VCAM-1 alone could support lymphocyte adhesion, but not rolling or transmigration, whereas monocytes roll, show firm adhesion and transmigration (Gerszten *et al.*, 1996; 1998). The immunoglobulin family member PECAM-1 (CD31) is expressed on the surface of both leukocytes and endothelial cells, and is involved in homophilic and homotypic interaction with an unknown ligand, although the later is controversial. Engagement of this molecule is largely associated with diapedesis. The interactions of various classes of adhesion molecules expressed on leukocytes and endothelial cells are summarised in Figure 3.2. The multistep adhesion hypothesis allows simple interpretation of a complex scenario and it should be appreciated that the steps are overlapping rather than sequential, and the importance of each class of adhesion molecules involved in each stage can differ depending on the type of leukocyte adhering. In addition to processing a functional property, engagement of adhesion receptors may modulate integrin affinity and expression, protease induction and activation, and surface organisation via

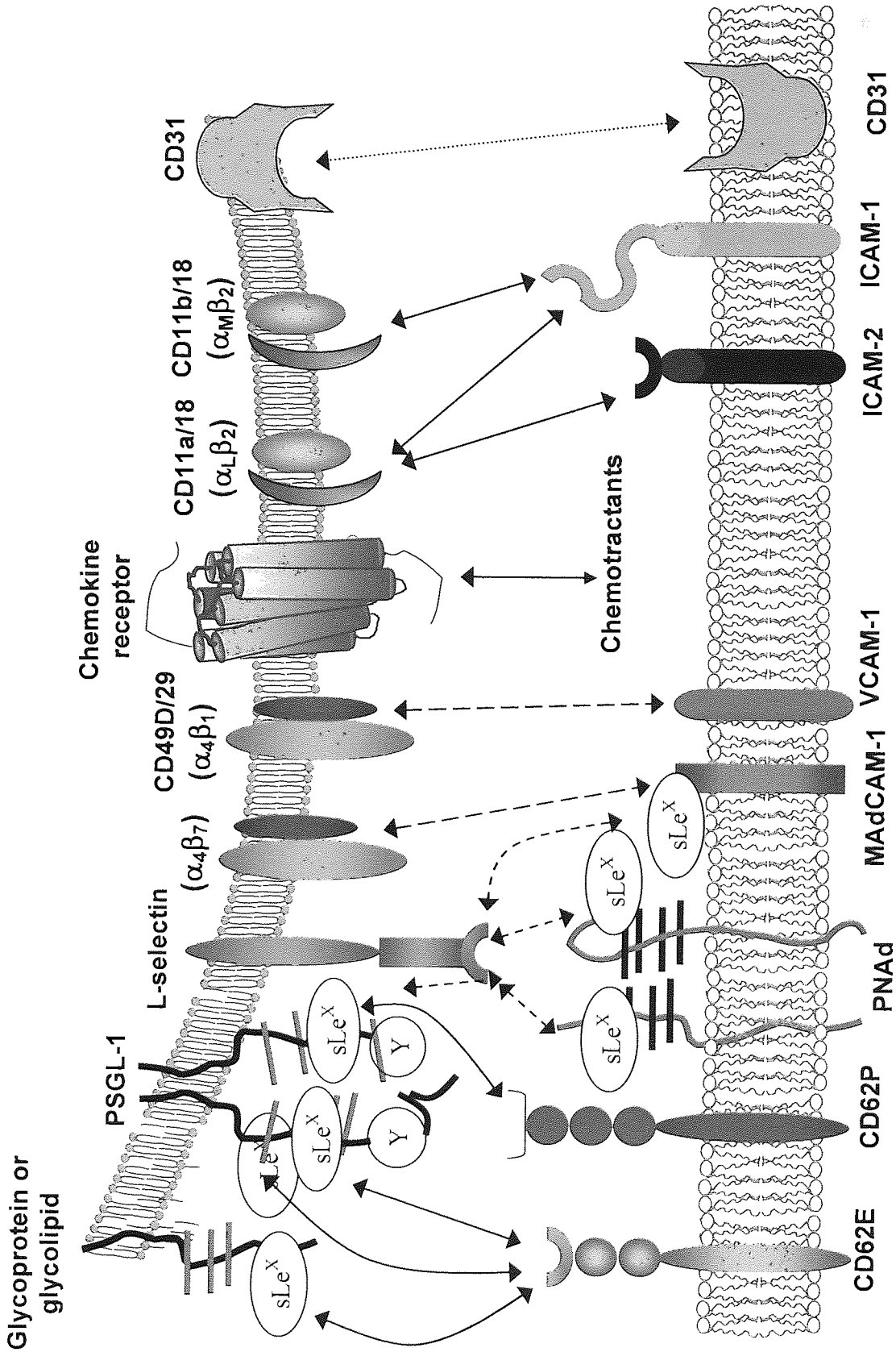
Glycoprotein or glycolipid
PSGL-1
L-selectin
CD49D/29 ($\alpha_4\beta_1$)
($\alpha_4\beta_7$)
Chemokine receptor
CD11a/18 ($\alpha_L\beta_2$)
CD11b/18 ($\alpha_M\beta_2$)
CD31
Chemotractants
ICAM-2
ICAM-1
CD31
VCAM-1
MAdCAM-1
PNAd
CD62P
CD62E
sLe^X
Y

Figure 3.2. Adhesion molecule interactions. Shown are the main players in leukocyte-endothelial cell interaction. L-selectin (CD69L) and P-selectin (CD69P) are believed to be the molecules primarily involved in the tethering of leukocytes and endothelial cells and recognise sulphated sialy-Lewis^x (sLe^x)-like sugars termed peripheral-node addressin (PNAd). L-selectin is also able to interact with other ligands expressed on the inflamed endothelium and with glycoprotein ligand 1 (PSGL-1) on adherent leukocytes. For PSGL-1 binding to L-/P-selectin an sLe^x molecule needs to be close to the N-terminus containing sulphated tyrosines (Y). E-selectin may also interact with PSGL-1, but does not require tyrosine sulfation or bind with other sLe^x-bearing glycoconjugates. E-selectin (CD62E) and the α_4 integrins are predominantly involved in rolling, but do also participate in tethering. Leukocytes respond to chemotractants released from endothelial cells and leukocytes via 7 transmembrane chemokine receptors. CD31 is expressed on the membrane surfaces of both leukocytes and endothelial cells and is involved in homophilic interaction. CD11a/18 interacts with both intracellular adhesion molecule (ICAM) -1 and –2 while CD11b binds only to ICAM-1. CD49D is able to bind to only vascular adhesion molecule (VCAM)-1 on resting endothelial cells and also mucosal addressin-cell adhesion molecule type 1 (MAdCAM-1) on the activated endothelium. Not shown are the interactions between ICAM-3 expressed on endothelial cells and interacts with CD11a/18 and CD11c/CD18. CD11a/18 is also able to bind with ICAM-1 and –2. CD11b/18 and CD11c/18 may bind to fibrinogen whereas CD29/49d binds to alternatively spliced CS-1 peptide at the extracellular matrix glycoprotein fibronectin. Adapted from von Andrian & Mackay, 2000).

intracellular signalling (Reedquist *et al.*, 2000; as reviewed in; Madri & Graesser, 2000; Newman, 1997).

Chemotaxis is the process of cell migration from a region of low chemokine concentration to that of high chemokine concentration. The role of chemokines in the circulation to mediate chemotaxis is widely debated since chemokines are typically soluble molecules generated by virtually all cells, but especially by activated endothelial and epithelial cells or leukocytes, and would diffuse away or rapidly be removed by the blood stream from the site of highest concentration. However, some chemokines are retained at their site of production by non-covalent interaction with molecules at inflammatory sites and are observed *in vivo* to contribute to monocyte migration in synovial fluid and the lung (as reviewed in; von Andrian & Mackay, 2000; Springer, 1994).

Chemokine receptors are typical G-protein coupled receptor (GPCR) possessing 7 trans-membrane domains and are expressed on leukocytes. As well as directing leukocytes to sites of inflammation, chemokines stimulate strong integrin mediated adhesion via chemokine receptors and as a pre-requisite for their action, they require the initial tethering of cells via selectins. This has been demonstrated *in vitro* utilising phospholipid bilayers expressing ICAM-1 and CD62P where neutrophils tether and subsequently roll in the presence of chemokines. Chemokines did not enhance adhesion on phospholipid bilayers that contained CD62P only. Additionally, chemokine receptor activation stimulates degranulation, shape change actin polymerisation and respiratory burst (as reviewed in; von Andrian & Mackay, 2000; Madri & Graesser, 2000; Springer, 1994).

The combination of adhesion molecules expressed at the surface of both leukocytes and at tissues such as those lined by endothelial cells is thought to determine the specificity of cell interaction. Elevated leukocyte adhesion is as a response to endothelial cell activation by cytokines such as IL-1α, TNFα, IFNγ or the bacterial product LPS. There is an abundance of evidence for a role of multiple pro-inflammatory cytokines in the pathogenesis of inflammatory diseases such as RA and atherosclerosis where there is aetiology of increased leukocyte adhesion. There are numerous reports of elevated TNFα levels in the serum and synovial fluid of patient with RA where its importance is elevated due to its propensity to activate the gene expression of other pro-inflammatory cytokines such as IL-1, IL-6 and IL-8 in an autocrine and paracrine fashion, and what's more, positively amplify its own production (as reviewed in; Feldman & Maini, 1999; Kobayashi *et al.*, 1999; Odeh *et al.*, 1997). Monocytes isolated from the whole blood of RA patients display elevated production of IL-1β and IL-6 when compared to monocytes from normals. However, IL-6 treatment of human umbilical vein endothelial cells (HUVEC) did not enhance monocyte adhesion (Lioté *et al.*, 1996). Both ICAM-1 (Muller *et al.*, 1992) and ICAM-2 are constitutively expressed on endothelial cells, but only ICAM-1 can be upregulated transcriptionally via NFκB nuclear translocation (Chen *et al.*, 2001; Kalogeris *et al.*, 1999; Roebuck & Finnegan, 1999) leading to high expression at the membrane surface following treatment with LPS, phorbol esters or inflammatory cytokines (Lane *et al.*, 1989; Kalogeris *et al.*, 1999; Pober *et al.*, 1986; Tosi *et al.*, 1992), while the literature reports mixed observations concerning the constitutive levels of VCAM-1; Korlipara *et al.*, (1996) and Muller *et al.*, (1992) report no constitutive expression whereas Meerschaert & Furie, (1994) describe low levels which are sufficient for adhesion. Adhesion of monocytes to unactivated HUVEC via

CD18 independent process was inhibited by Ab against the CD29 or CD49d (Chuluyan & Issekutz, 1993) implying the presence of the counter receptor VCAM-1. Upon activation with LPS or TNFα for 4 hours, VCAM-1 mRNA and protein expression is elevated in HUVEC but not human umbilical arterial endothelial cells (HUAEC; Kalogeris *et al.*, 1999). CD31 is expressed on the endothelial lateral cell border where greater than 85 % reside (Muller *et al.*, 1993), and mediates homotypic as well as heterotypic adhesion. Its engagement is largely associated with leukocyte transmigration through the intracellular junctions of activated and resting endothelial cells. Indeed, anti-CD31 Ab does not block chemotaxis of neutrophils or monocytes nor prevent their adhesion. However, CD31 interaction between monocytes and endothelial cells is not the only method of transmigration since this process was not completely prevented by blocking Ab to CD31 or Fab fragments to CD31 (Muller *et al.*, 1993). Indeed, monocyte chemotactic factor-induced migration across the unactivated or activated endothelium requires CD18 and CD29CD49d (VLA4) on the monocyte and VCAM-1 as a counter receptor on the endothelium, but not ICAM-1 or CD62E. MoAb to CD29 and CD49d were more potent at reducing chemotactic induced monocyte migration than MoAb against VCAM-1 due to binding to other counter receptors on HUVEC such as CS-1 present on unactivated and activated endothelial cells (Chuluyan & Issekutz, 1993) and on the extracellular matrix glycoprotein fibronectin (Wayner *et al.*, 1989). CD62P is stored in pre-formed Wiebel Palade bodies of endothelial cells and is rapidly mobilised to the plasma membrane to bind monocytes and neutrophils in response to inflammation. CD62E is induced on vascular endothelial cells upon IL-1, LPS or TNFα induced activation and requires *de novo* mRNA and protein synthesis (as reviewed in; Madri & Graesser, 2000; Springer, 1994).

There are multiple pieces of evidence that implicate ICAM-1 interactions in monocyte/arterial adhesion during the development of atherosclerosis and allied vascular diseases. Increased ICAM-1 expression has been correlated with the increased infiltration of monocytes to inflammatory sites (Nakashima *et al.*, 1998; Poston *et al.*, 1992; as reviewed; Ross, 1999) where loss of ICAM-1 or inhibition of its expression decreases atherosclerotic lesion formation in animal models (Collins *et al.*, 2000; Nageh *et al.*, 1997; Nie *et al.*, 1997). Endothelial cells are also the major source of soluble ICAM-1 found in rheumatoid synovial tissue (Krenn *et al.*, 1997). Elevated ICAM-1 and VCAM-1 levels are found on the atherosclerotic lesions (Davies *et al.*, 1993; O'Brien *et al.*, 1993, 1996). The abdominal aortic surface of normal rats displayed almost no ICAM-1 expression but was massively elevated along lesion prone areas near the ostia of branching arteries of atherogenic rats with diet induced hypercholesterolemia (Watanabe & Fan, 1998). In contrast, rabbits on an atherogenic diet for one week focally expressed CD62P and VCAM-1 in the ascending aorta or lesion prone areas before the appearance of macrophages (Li *et al.*, 1993; Sakai *et al.*, 1992). CD62E and ICAM-1 are highly expressed by synovial capillary endothelial cells in rheumatoid inflammatory synovitis (Koch *et al.*, 1995; Veale *et al.*, 1993). On the other hand, monocytes isolated from peripheral whole blood of humans with RA displayed elevated expression of CD11b compared with monocytes isolated from normals which was associated with their enhanced adhesion to fibronectin or resting and IL-1β stimulated endothelial cells *in vitro* (Lioté *et al.*, 1996). Additionally, macrophages from synovial fluid and tissue possess enhanced levels of CD18 and CD29 (Allen *et al.*, 1989; El-Gabalawy *et al.*, 1996; Koch *et al.*, 1995).

However, *in vitro* observations have revealed that the population of endothelial adhesion molecules that is upregulated and the extent to which each becomes more highly expressed is agent specific where different pro-inflammatory agents stimulate diverse signalling pathways in endothelial cells. IFNγ activation of HUVEC does not support CD18 independent chemokine induced monocyte transmigration unlike LPS, TNFα or IL-1α (Chuluyan & Issekutz, 1993). Monocyte adhesion to mouse aortic endothelial cells (MAEC) is upregulated by the atherogenic plasma protein oxidised low density lipoprotein (LDL) and TNFα. However, exposure of MEAC obtained from ICAM-1 -/-mice to high concentrations of TNF mediates monocyte adhesion not observed following ICAM -/- MAEC treatment with oxidised LDL (Kevil *et al.*, 2001). Consequently the activating agent that is associated with a specific inflammatory disease may differentiate between the recruitment of one specific leukocyte subtype over another. However, inflammatory states are often associated with the upregulation at the mRNA and protein level of multiple cytokines and chemokines rather than a single agent (Lioté *et al.*, 1996; as reviewed in; Feldmann & Maini, 1999; Koybayashi *et al.*, 1999; Odeh *et al.*, 1997). There are no reports of the effects of endothelial cell activation and consequent leukocyte adhesion induced by multiple agents *in vitro*. Furthermore, observations *in vitro* suggest that the pro-inflammatory exposure period can effect adhesion molecule expression, where their surface expression up and down regulates as a function of time (Woollard *et al.*, 2002). Pharmacological manipulation to prevent adhesion to and migration of leukocytes across tissues and basal lateral membranes is of clinical importance. What is more, the therapeutic approach essentially requires a reduction in the membrane expression of, or the inhibition of the interaction of, multiple adhesion molecules expressed either on endothelial cells, tissues or circulator cells.

At low levels, ROS function as intracellular signalling molecules regulating cellular activity at multiple sites, altering the structure and function of proteins, whereas at higher concentrations they induce direct cellular and tissue injury (see Chapter 2). Oxidative stress plays an important role in the vascular dysfunction observed in inflammation. Depending on their reactivity, the effects ROS are apparent at the source of formation, at other intracellular organelles or may diffuse through cellular membranes to act in a paracrine fashion (as reviewed in; Cai & Harrison, 2000; Lum & Roebuck, 2001; Napoli *et al.*, 2001).

ROS are generated at sites of inflammation and remain at the inflammatory location together with cytokines and growth factors such as TNFα, IL-1β and INFγ, and chemokines. These molecules are involved in a positive feedback loop involving their increased generation to amplify the inflammatory response. The prolonged and excessive exposure of the endothelium and leukocytes to oxidants, cytokines and chemokines increases cellular activation. Infusion of hypoxanthine/xanthine oxidase or H_2O_2 into the rate mesenteric circulation leads to an increase in leukocyte rolling, adhesion and migration (Gaboury *et al.*, 1994; Scalia & Lefer, 1998). Further, oxidants increase PMN adhesion to the endothelium that was associated with elevated ICAM-1 mRNA and protein expression on endothelial cells. Ab against ICAM-1 inhibited oxidant induced PMN adhesion (Lo *et al.*, 1993; Sellak *et al.*, 1994) while anti CD31 Ab inhibits transmigration of HL60 cells across endothelial cells *in vitro* induced by the oxidant tert-butylhydroperoxide (Rattan *et al.*, 1997). The addition of catalase also reduced the adhesion of PMN to H_2O_2 activated HUVEC (Lo *et al.*, 1993). Alternatively, oxidative stress can be induced by redox imbalance and can mediate transcription dependent and independent endothelial membrane expression of

various adhesion molecules suggesting that oxidative stress can induce acute and chronic phases of leukocyte adhesion to the endothelium. In fact, modulating the GSH/GSSG ratio in endothelial cells produces a biphasic effect on PMN adhesion (Kokura *et al.*, 1999).

Endothelial cell activation *in vitro* with the cytokines IL-1 and IFNγ leads to a dose and time dependent increase in $O_2\cdot^-$ (Matsubara & Ziff, 1986) whereas TNFα induced elevated fluorescence of the peroxide sensitive dye DCF. Here, inhibition of complex I of the mitochondrial electron transport chain with TTFA or rotenone inhibited ROS formation while complex III inhibition with A.A potentiated. However, the TNF induced elevation in endothelial cell ROS production was not affected by inhibition of the ROS producing sites NADPH oxidase or xanthine oxidase. Further, the NO or cyclo-oxygenase pathways were not involved. Collectively these observations suggest that the TNFα activation of endothelial cells involves the redox signalling via the mitochondria only (Corda *et al.*, 2001). ROS production via endothelial cell NADPH oxidase is essential for lymphocyte migration but not required for adhesion. Inhibitors of NADPH oxidase blocked migration by greater than 65% with no effect on firm adhesion and prevented VCAM-1 mediated actin re-organisation. Furthermore, VCAM-1 activation directly induces ROS production not seen upon CD31 activation where catalase inhibited migration. ROS induce the formation of gaps between endothelial cells, cell shape change and re-organisation of actin filaments necessary to maintain cell structure and are likely to be the basis for increased endothelial cell permeability (Mathney *et al.*, 2000; as reviewed in; Lum & Roebuck, 2001).

While plenty of attention has focussed on ROS formation and their subsequent signalling properties with regards the endothelium, less has been ascribed to the effects of the redox state in leukocytes. H_2O_2 treatment of PBMN induced an elevation in CD11b and CD18 which was allied to enhanced adhesion to resting or TNFα activated HAEC. Similar results were obtained following PBMN exposure to xanthine and xanthine oxidase to mediate free radical production. However, treatment of PBMN with H_2O_2 and desferroxamine to chelate Fe^{2+} and prevent the formation of OH· radicals via the Häber Weiss reaction, did not alter the elevation in the adhesion of monocytes treated with only H_2O_2. Further, the addition of Fe^{3+}-NTA to H_2O_2 treated monocytes to generate OH· was not additive to the enhanced adhesion mediated by H_2O_2 on its own. It was reasoned that OH· radicals do not contribute peroxide mediated monocyte adhesion (Fraticelli *et al.*, 1996). This study suggests that the exposure of leukocytes to oxidants may promote their interaction with endothelial cells via a peroxide sensitive up-regulation in the membrane expression of monocyte adhesion molecules or their stabilisation in an active conformation. Conversely, it is likely that decreasing the oxidation state of the leukocytes may reduce the efficacy by which they adhere to resting or activated endothelial cells. Adherence of PBN to matrix proteins or the endothelium primes PMN for a massive respiratory burst lasting 1-3 hours in response to TNFα and the chemotactic peptide fMLP (Nathan, 1987). Inhibition of xanthine oxidase, cytochrome P450 or NOS production in lymphocytes did not affect lymphocyte migration. However treating lymphocytes with the tyrosine kinase inhibitor herbimycin A, calmodulin inhibitor phenoxybenzamine or the PI3-kinase inhibitor wortmanin decreased lymphocyte migration, suggesting intracellular signalling within leukocytes is required for migration (Mathney *et al.*, 2000). Various signalling pathways are ROS sensitive,

these include MAPK cascade, PKC, various protein tyrosine kinases and the sphingolipid pathway (see Chapter 2). Additionally, numerous transcription factors, such as NFκB and AP-1, which modulate adhesion molecule gene expression are redox regulated and are activated by the described signalling pathways following stimulation with pro-inflammatory cytokines (Kalogeris *et al.*, 1999). NFκB nuclear translocation is initiated by the pro-inflammatory cytokines TNFα and IL-1α in leukocytes and endothelial cells via a redox sensitive pathway. Anti-oxidants such as NAC or pyrrolidine dithiocarbamate (PDTC) inhibit NFκB activation by TNFα, IL-1α H_2O_2 or phorbol ester in both leukocytes and endothelial cells (Rahman *et al.*, 1999; Roebuck *et al.*, 1995; Schreck *et al.*, 1992). Alternatively, GSH depletion with either diamide or BSO alters the redox state leading to oxidative stress and inhibition of NFκB and AP-1 (Kokura *et al.*, 1999; Rokutan *et al.*, 1998).

Consequently, emphasis on the development of pharmacological agents geared to reduce inflammation by preventing leukocyte-endothelium/epithelial/tissue interactions should be focused on modulating the redox state in the local environment and at the intracellular level. In Chapter 2, it is described how the exposure of U937 monocytes to synthetic short chain ceramides reduces the $[peroxide]_{cyt}$ which was coupled to their mild arrest in G0/G1 phase of the cell cycle without the induction of cell death by necrosis or apoptosis. Therefore, it is proposed that the treatment of U937 monocytes with synthetic short chain ceramides, through lowering the $[peroxide]_{cyt}$, will modulate their adhesion to endothelial cells *in vitro*.

3.2 Materials and methods.

3.2.1 Materials.

All reagents were obtained from Sigma Chemical Company (Poole, UK), solvents were from Fisher (Loughborough, UK) and all gases from BOC Ltd (Guildford, UK) unless otherwise stated. RPMI 1640, foetal bovine serum, Hanks balanced salt solution (HBSS), gentamicin and penicillin (1000u/ml)/streptomycin (10,000µg/ml) were purchased from GibcoBRL (Paisley, UK). Endothelial Growth Medium (EGM) was from BioWhittaker (Wokingham, UK) C_2-ceramide (N-acetyl-sphingosine) and C_6-ceramide (N-hexanoyl-sphingosine) were obtained from Biomol Research Laboratories (Plymouth Meeting, PA, USA).

The antioxidants N-acetylcysteine (NAC) and glutathione (GSH) were made up in serum free RPMI 1640. C_2-/C_6-ceramide were dissolved in anhydrous DMSO to a stock solution of 20mM. Subsequent dilutions were made in 1mM fatty acid free BSA.

3.2.2 Cell culture and stimulation.

U937 monocytes were cultured and treated as described in Method 2.2.2.

3.2.3 Endothelial cell culture.

Endothelial cells were isolated from freshly obtained human umbilical cords of greater than 7" in length from consenting patients (see Appendix). Ethical approval was granted from the Birmingham Local Research Ethics Committee, Birmingham Woman's Hospital, Edgbaston, Birmingham, UK (See Appendix). The cord was stored in a sterile container containing Hanks buffered saline solution (HBSS) supplemented with gentamicin (10mg/ml; GibcoBRL Paisley, UK) at 4°C until manipulation.

Handling of the umbilical cord was performed from here on under sterile conditions. The cord vein was cannulated with a blunt, hubless 16-gauge needle (Becton-Dickinson, Oxford, UK) and secured in place with surgical silk thread (EP1, UB5/0; Davis & Geck, Gosport, UK). Blood was washed from the interior of the umbilical vein by slow perfusion with 20mls of HBSS supplemented with gentamicin (10mg/ml) and the cord allowed to drain. The other end of the umbilical cord vein was then cannulated with a second blunt, hubless 16 gauge needle and secured in place as described. HBSS (20mls) was infused into the vein to wash out any gentamicin, and once again, the HBSS was allowed to drain from the cord. The vein of the cord was filled with 0.1% collagenase in PBS to remove endothelial cells from the vein and the cannulas closed. The cord was wrapped firstly in cellophane and then foil, and incubated at 37°C for a maximum of 20 minutes so to prevent undesirable disruption of underlying structures (Jaffe *at al.*, 1973).

Subsequently, collagenase/endothelial cell suspension was eluted from the umbilical cord vein by perfusion with a further 20mls of HBSS. The eluate was collected into a 30ml universal (Bibby Sterilin Ltd, Stone, UK) and centrifuged at 100xg (Sigma benchtop centrifuge Type 1-13, rotor # 12027, Osterode am Harz, Germany) for 5 minutes to pellet the endothelial cells. The supernatant was removed and discarded, and the remaining cell pellet resuspended in 5mls of medium 199 (M199; Sigma, Poole, UK) containing 10mM HEPES, 20 % FCS and 1% P/S. The cell suspension was transferred to a T75 culture flask (Orange Scientific, Braine-l'Alleud, Belgium) and incubated in a 37°C, 95% air, 5% CO_2 humidified atmosphere.

After 24hrs, media was removed from the culture flask to eliminate any dead and contaminating suspension cells. Cells were washed gently with EGM (BioWhittaker, Wokingham, UK) supplemented with EGM® BulletKit® (BioWhittaker, Wokingham, UK) and re-cultured under the described incubator conditions in the presence of 5mls of EGM (+EGM® BulletKit®) until confluence. The cell cultures were fed every 2-3 days with a complete change of media. Morphologies were examined routinely by light microscopy (CK2-TR, Olympus, Tokoyo, Japan).

When confluent, medium was aspirated from each flask and cells were washed with HBSS to remove FCS. HUVEC were passaged by trypsin isolation. Briefly, 5mls of trypsin (0.05% Trypsin, 0.53mM EDTA-4Na; Bibco BRL, Paisley, UK) was added to washed HUVEC and incubated at 37°C for no more than 5 minutes. Any loosely adherent cells were removed by agitation. 5mls of EGM (+EGM® BulletKit®) was added to each flask to neutralise trypsin and the cell suspension transferred to 30ml universals (Bibby Sterilin Ltd, Stone, UK). Flasks were washed with 5mls of EGM

(+EGM® BulletKit®) and the remaining cell suspension was added to the universal. Cells were sedimented at 100xg in a Sigma benchtop centrifuge Type 1-13, rotor # 12027, (Osterode am Harz, Germany) for 5 minutes. The supernatant was removed and HUVEC resuspended in EGM (+EGM® BulletKit®). HUVEC were counted by light microscopy (CK2-TR, Olympus, Tokoyo, Japan) using an improved Neubauer haemocytometer (Weber Scientific International Ltd., Teddington, UK). For the adhesion assay, HUVEC were seeded in 24 well plates (Orange Scientific, Braine-l'Alleud, Belgium) at a concentration of $1x10^5$/ml, 1ml per well and incubated under the described incubator conditions until confluent, with complete media changes every 2-3 days.

3.2.4 Adhesion assay.

The adhesion of U937 monocytes (treated or controls) to endothelial cells in a static system was measured using the method of Weber *et al.*, (1996) by fluorescence determination of the dye of 2', 7'-bis-2-carboxyethyl-5-(6)-carboxyfluorescein-acetoxymethylester (BCECF-AM; Sigma, Poole, UK) as described by De Clerck *et al.*, (1994) and Moy *et al.*, (1993). BCECF-AM is non-fluorescent and membrane permeable permitting non-invasive loading of cells. Once contained within the intracellular compartment, BCECF-AM is converted by the action of intracellular esterases to the fluorescent BCECF, which is retained within cells due to its four or five negative charges at pH 7-8.

Confluent, homogenous HUVEC monolayers in 24 well plates were washed and cultured in 1ml per well of EGM (EGM® BulletKit®), and LPS (1μg/ml) added for 0, 5 or 24 hours at 37°C, in a 5% CO_2, 95% air humidified atmosphere. At the end of the LPS incubation period, media was removed from each well and adherent cells washed three times with M199 (10% FCS, 1% P/S) prior to the addition of 1ml of monocyte suspensions in M199.

Treated U937 monocytes were transferred to 15ml conical tubes (Orange Scientific) washed twice in ice cold PBS and resuspended in M199. Cell number was adjusted to $5x10^6$/ml using an improved Neubauer haemocytometer (Weber Scientific International Ltd., Teddington, UK) and labelled with 1μg/ml of 2', 7'-bis-2-carboxyethyl-5-(6)-carboxyfluorescein-acetoxymethylester (BCECF-AM, 1mg/ml) for 30 minutes in the dark at room temperature (RT). Dye loading was terminated by ten-fold dilution with HBSS and sedimentation of U937 monocytes at 100xg (Labfuge 400R, Heraeus Instruments, rotor, # 8179, Kendo laboratory products, Bishops Stortford, Hertfordshire, UK) for 5 minutes. The supernatant was removed and discarded. U937 monocytes were resuspended in M199 (10% FCS, 1% P/S) to a concentration of $0.5x10^6$/ml. Each monocyte treatment (1ml) was added in to individual HUVEC monolayers in duplicate and incubated for 30minutes, under the described culture conditions.

Non-adherent cells were removed by centrifugation of inverted plates for 5 minutes at 40xg (Labfuge 400R, Heraeus Instruments, rotor, # 8177, Kendo laboratory products, Bishops Stortford, Hertfordshire, UK). Adhered cells were lysed with 1ml of lysis buffer (0.1% Triton X; 0.1M Tris, pH 8.8) for 30 minutes in the dark at RT. Lysed

cells were then pipetted into 96 well plates and fluorescence measured at an excitation of 485nm and emission of 535nm on a dual-scanning microplate spectrofluorometer (Spectramax GeminiXS, Molecular Devices, Sunnyvale, USA) utilising the cut out filter at 520nm.

Test samples were calibrated against a standard curve of vehicle treated U937 monocytes, at concentrations of $5x10^4$, $1.25x10^5$, $2.5x10^5$ and $5x10^5$ dye loaded with BCECF-AM, lysed and fluorescence analysed as described above.

3.2.5 Analysis of monocyte adhesion molecule expression.

PBS washed treated U937 monocytes were divided into two tubes for immunofluorescence staining. Cells in one tube were labelled with combinations of the mouse monoclonal antibodies conjugated to PE and FITC described in Table 3.1 at saturating concentrations of greater than 10µl per 10^6 cells. The second tube was treated with the appropriate isotype negative controls at identical concentrations. These were the mouse monoclonal negative control IgG1 FITC conjugated (clone B-Z1) and mouse monoclonal negative control IgG1 PE conjugated (clone B-Z1) both from Diaclone Research (Besançon Cedex, France). Samples were incubated in the dark on ice for 30 minutes. Cells were then fixed by the addition of 250µl of 4% formaldehyde and vortexed vigorously. Tubes were incubated for 15 minutes at room temperature before sample dilution by the addition of 200µl of PBS. Samples were vortexed for a second time and re-incubated at room temperature for at least 10 minutes.

Antigen	*Source*	*Species*	*Clone*	*Fluorescent Tag*
CD11a	Mouse	Human IgG1	B-B15	PE
CD11b	Mouse	Human IgG1	ICRF-44	PE
CD18	Mouse	Human IgG1	MEM 48	FITC
CD31	Mouse	Human IgG1	B-B38	PE
CD29	Mouse	Human IgG1	B-F5	FITC
CD49d	Mouse	Human IgG1	44H6	FITC
CD62L	Mouse	Human IgG1	BF-12	PE

Table 3.1: Characteristics of the fluorescent conjugated antibodies used to determine the membrane expression of antigens involved in cell-cell adhesion by flow cytometry. Antibodies were purchased from Diaclone Research, Besançon Cedex, France or from Serotec Ltd, Kidlington, UK. Abbreviations are as follows, fluorescein iothiocyante (FITC), phycoerythrin (PE) and intracellular adhesion molecule-1 (ICAM-1).

All samples were analysed by an EPICS® XL-MCL flow cytometer utilising 2-way colour compensation as described in Method 2.2.7. The U937 monocyte population was located according to a histogram of FS versus SS properties and gated to exclude debris and aggregates. The fluorescence of the gated cell population was analysed on single parameter histograms of log FL2 (PE) versus count, log (FITC) versus count and dual parameter histograms of Log FL1 versus Log FL2. Background fluorescence of each sample was established utilising cells stained with isotype negative control antibodies. Positive regions were established to contain 1% of the negatively stained cells. The percentage of positive cells and their median fluorescence (MdX) intensity was recorded for all samples. At least 10,000 cells were analysed per sample.

3.3 Results.

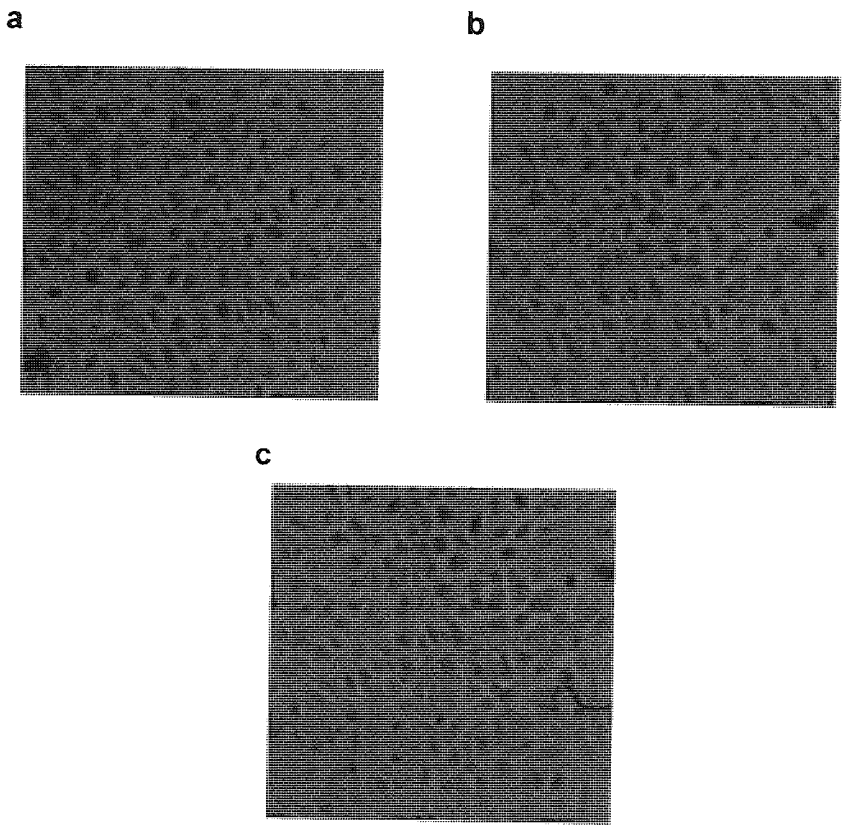

Figure 3.3. Endothelial cells isolated form the veins of human umbilical cords when cultured display a cobblestone-like morphology which is not affected by LPS treatment. Endothelial cells were isolated from the veins of human umbilical cords from consenting patients by collagenase digestion. HUVEC were cultured as described in method. Confluent HUVEC monolayers in 24 well plates were washed and re-cultured in endothelial growth media (EGM®, BioWhittaker) supplemented with EGM® BulletKit® (BioWhittaker) and 1μg/ml LPS added for 0 (a), 5 (b) or 24 hours prior to examination by light microscopy (CK2-TR, Olympus) at a magnification of 250x.

Endothelial cells were isolated from the umbilical vein of human umbilical cords by collagenase digestion. The cells were grown in 75cm^2 tissue culture flasks until confluence. Inspection of HUVEC cultures by light microscopy revealed a homogenous population free from contamination by fibroblasts and smooth muscle cells. Cultures were considered confluent when the tissue culture flask surface was

totally obscured by HUVEC monolayers displaying the characteristic 'cobble stone' morphology (see Figure 3.3). HUVEC were cultured for up to three passages and for use in adhesion assays, cultured in 24 well plates until confluence. LPS (1μg/ml) treatment for 24, 5 or 0 hours did not alter HUVEC morphology (see Figure 3.3).

Synthetic ceramide treatment of U937 monocytes at a concentration of 10-20μM for 16 hours did not affect their adhesion to resting, 0 hours LPS (1μg/ml) treatment, HUVEC ($p>0.05$; see Figure 3.4a). However, 20μM C_2- or C_6-ceramide treatment of U937 monocytes for 16 hours significantly reduced their adherence to HUVEC activated with LPS (1μg/ml) for 5 hours by approximately 45% of vehicle treated U937 monocytes ($p<0.001$) with no significant difference between synthetic ceramide species ($p>0.05$; see Figure 3.4b). Following 10μM C_6-ceramide treatment, the adherence of U937 monocytes was reduced to 80% of control monocytes ($p<0.05$). Further, the adherence of U937 monocytes treated with 20μM C_2-/C_6-ceramide or 10μM C_6-ceramide to 24 hours LPS (1μg/ml) HUVEC was significantly decreased to approximately 40 % of that of vehicle control treated monocytes ($p<0.001$) which was not affected by concentration or species of synthetic ceramide ($p>0.05$; see Figure 3.4c).

To evaluate the possible mechanism by which synthetic ceramide may abrogate monocyte adhesion to endothelial cells, the effects of synthetic ceramides on the monocytic membrane expression of integrins and selectins associated with endothelial cell interactions was analysed by flow cytometry. U937 monocytes constitutively expressed ICAM (CD54), CD11a, CD49and CD29 weakly, and CD11b, CD18, and CD62L more strongly (see Figure 3.5a-d). U937 monocytes

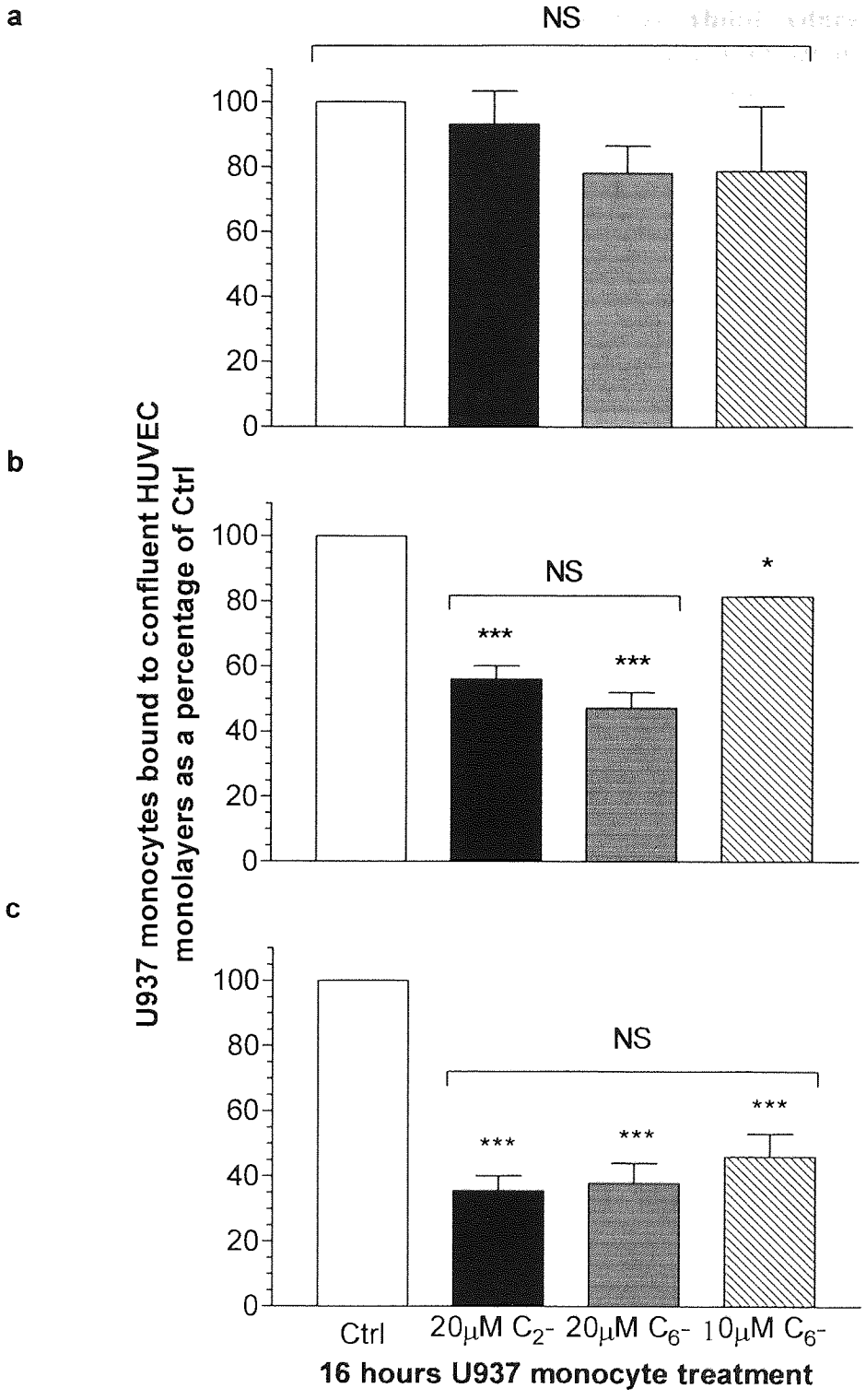
a
b
c
NS
NS
NS
*
***
***
***
***
***
100
80
60
40
20
0
U937 monocytes bound to confluent HUVEC monolayers as a percentage of Ctrl
Ctrl
20μM C2-
20μM C6-
10μM C6-
16 hours U937 monocyte treatment

Figure 3.4. Synthetic ceramide treated monocytes exhibit reduced adhesion to LPS activated HUVEC. U937 monocytes ($2x10^6$/ml) were serum starved for 4 hours in RPMI 1640 prior to C_2-/C_6-ceramide treatment. Treatments were terminated by centrifugation and washing resulting cell pellets twice with ice cold PBS. Cells ($5x10^6$/ml) were loaded with 1μg/ml of BCECF-AM for 30 minutes in the dark. Cells were then washed and resuspended in M199 to a concentration of $0.5x10^6$/ml. Confluent HUVEC monolayers in 24 well plates were treated with 1μg/ml LPS for 0 (a), 5 (b) or 24 (c) hours. HUVEC were washed twice prior to the addition of treated monocyte suspensions in duplicate for 30 minutes under the described incubator conditions. Their adherence was quantified against a standard curve of vehicle treated monocytes and expressed as a percentage of controls. The results are presented as the mean ± s.d of at least 4 individual experiments where * ($p<0.05$) and *** ($p<0.001$) represent significant difference from controls by one-way ANOVA with Tukey's post *hoc* test analysis or students T-test.

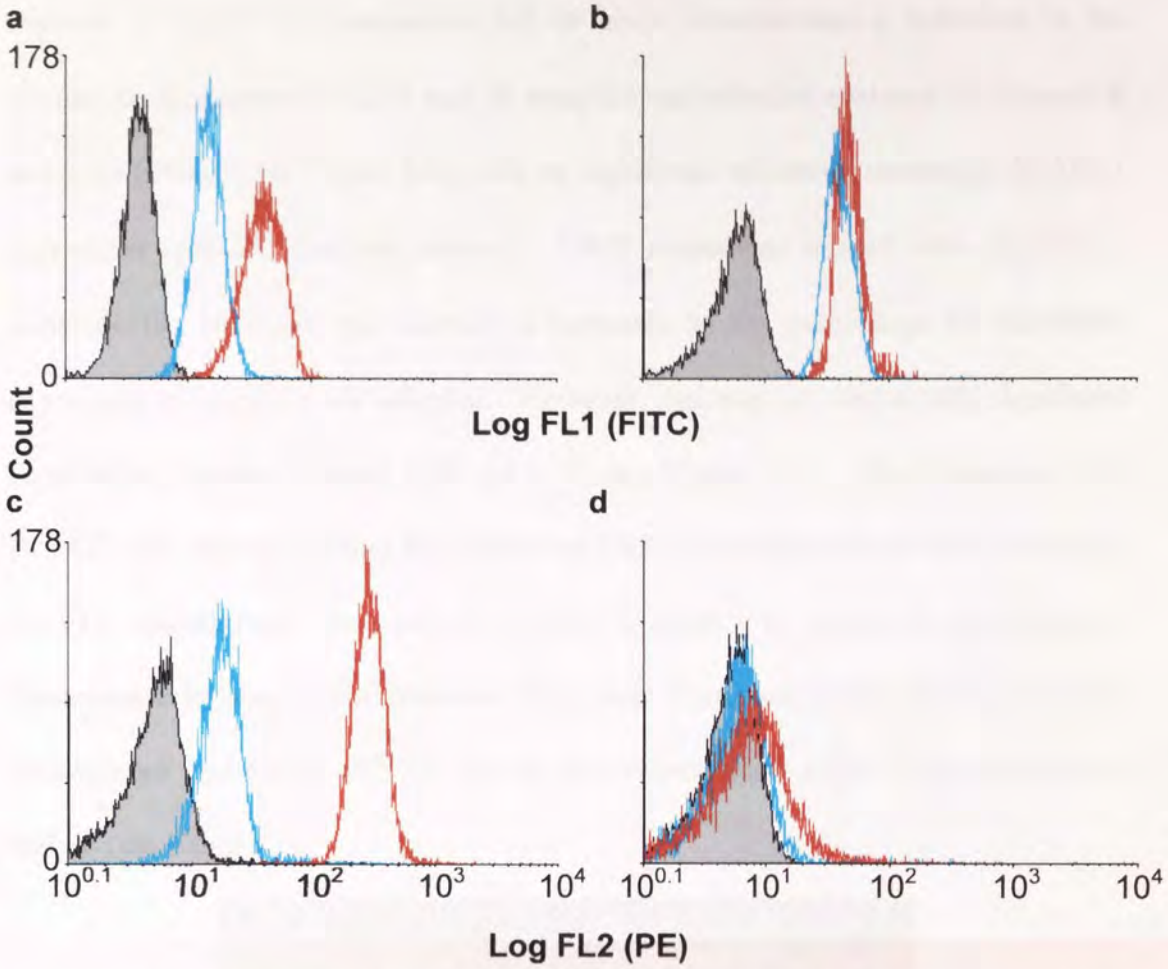

Figure 3.5. U937 monocyte basal membrane expression of proteins associated with adhesion. U937 monocytes ($2x10^6$/ml) were incubated in serum free RMPI 1640 for 4 hours in a humidified 95% air, 5%CO_2 atmosphere at 37°C. Cell samples were labelled with saturating concentrations of monoclonal antibodies (MoAb) conjugated to FITC or PE in combination, or to determine background fluorescence isotype negative controls, on ice for 30 minutes in the dark. Samples were then fixed as described in materials and methods and analysed by flow cytometry corrected for colour compensation. The viable U937 population was identified according to forward scatter and side scatter properties, and the median X (MdX) fluorescence of 10,000 cells quantified on single parameter histograms of FL1/FL2 versus count. Background fluorescence and regions for positive fluorescence were determined by analysing the fluorescence emitted from samples labelled with isotype negative controls (solid grey fill). The MoAb used were (a) ICAM-1 (blue) and CD18 (red), (b) CD29 (blue) and CD49D (red), (c) CD62L (blue) and CD31 (red),and (d) CD11a (blue) and CD11b (red).

exposed to 20μM C_2-/C_6-ceramide for 16 hours demonstrated a reduction in the membrane expression of CD31 and all integrins and selectins analysed by between 8 and 15% ($p<0.05$; see Figure 3.6), with no significant effects on monocytic ICAM-1 expression ($p>0.05$; data not shown). U937 monocytes treated with 10μM C_6-ceramide for 16 hours also showed a reduction in the percentage of membrane expression of integrins and selectins. However, this was not statistically significant from vehicle control treated cells ($p>0.05$; see Figure 3.6). The fluorescent dye BCECF-AM used to quantify the number of U937 monocytes which have adhered to HUVEC monolayers, was analysed by flow cytometry to assess for quenching of fluorescence by short chain synthetic ceramides. C_2-/C_6-ceramide did not affect the fluorescence emitted by BCECF-AM at 505-545nm upon argon laser excitation at 488nm (see Table 3.1).

Treatment	*Mean MdX ± St Dev*	*Significant Difference from Ctrl*
Ctrl	12.35 ± 2.192	-
C_2-	13.65 ± 1.626	No
C_6-	14.5 ± 1.723	No

Table 3.2. Synthetic ceramides do not interfere with the fluorescence emitted from BCECF-AM in U937 monocytes. U937 monocytes ($2x10^6$/ml) were serum starved for 4 hours in RPMI 1640 prior to 0 or 20μM C_2-/C_6-ceramide treatment for 16 hours at 37°C in a humidified 5% CO_2, 95% air atmosphere. Treatments were terminated by centrifugation and the resulting cell pellets washed twice with ice cold PBS. Cells ($5x10^6$/ml) were loaded with 1μg/ml of BCECF-AM for 30 minutes in the dark. Cells were then washed and resuspended in M199 to a concentration of $0.5x10^6$/ml and the fluorescence of the viable U937 monocyte population, as determined by forward scatter (FS) and side scatter (SS) properties, analysed by flow cytometry on a single parameter histogram of Log FL1 versus count. 10,000 cells were analysed per sample and the median x (MdX) of the fluorescence peak recorded. Results are presented as the arithmetic mean of 3 individual experiments and analysed for statistical difference by one way ANOVA followed by Dunnets' multiple comparison tests where $p<0.05$ was considered significantly different from vehicle treated control cells.

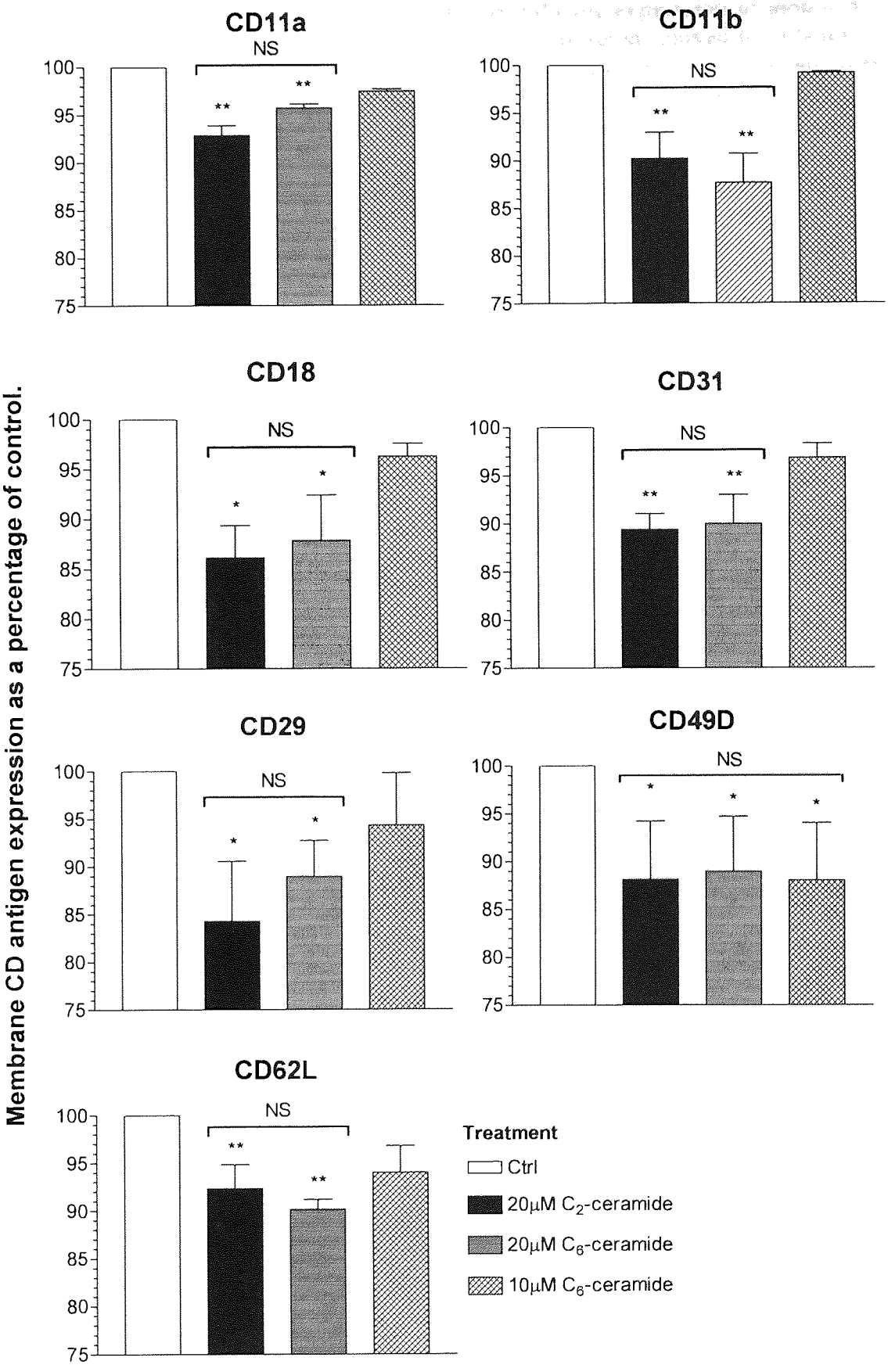
CD11a
CD11b
CD18
CD31
CD29
CD49D
CD62L
NS
Membrane CD antigen expression as a percentage of control.
100
95
90
85
80
75
Treatment
Ctrl
20μM C2-ceramide
20μM C6-ceramide
10μM C6-ceramide

Figure 3.6. Synthetic ceramides reduce the membrane expression of monocytic adhesion molecules. U937 monocytes ($2x10^6$/ml) were serum starved for 4 hours in RPMI 1640 prior to 16 hours 10/20μM C_2-/C_6-ceramide treatment. Treatments were terminated by centrifugation and the resulting cell pellets washed twice with ice cold PBS. Cells were treated with >10μl of fluorescently tagged mouse IgG1 monoclonal antibody (MoAb) or isotype negative control per 10^6 cells for 30 minutes on ice, in the dark and fixed as described in method 3.2.5. Samples were then analysed by flow cytometry. Background fluorescence of each sample was established utilising cells stained with isotype negative controls. Positive regions were defined to contain 1% of the negatively stained cells. Samples were then analysed for MoAb membrane expression and the median X of the fluorescent peak recorded. The membrane expression of CD11a, CD11b, CD18, CD31, CD29, CD49D and CD62L were evaluated. At least 10,000 cells were analysed per sample. The results are presented as the mean ± s.d of at least 4 individual experiments where * ($p<0.05$) and ** ($p<0.01$) represent significant difference from controls by one-way ANOVA with Tukeys' post *hoc* test analysis or Students T-test. NS, not significant.

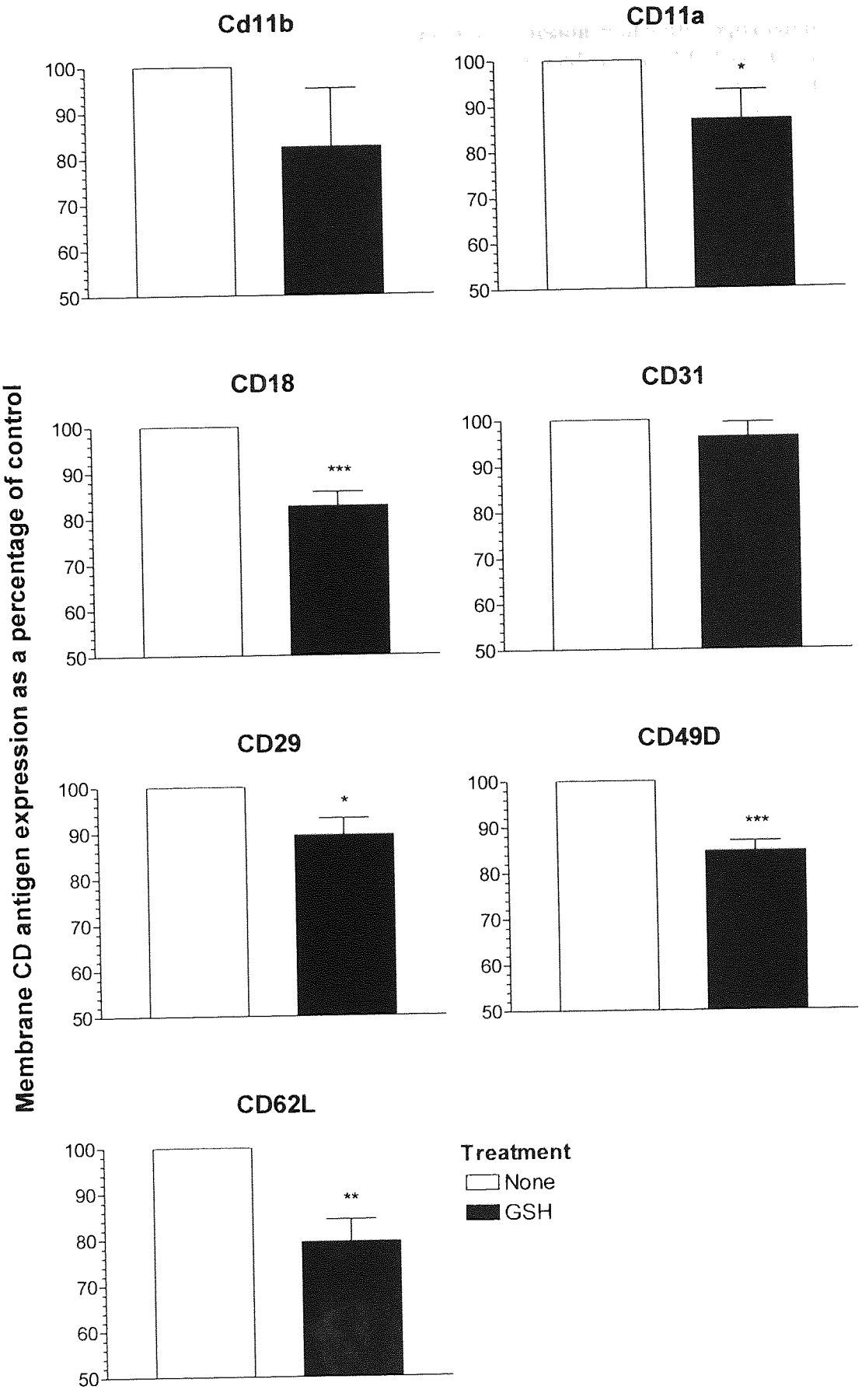
Cd11b
CD11a
CD18
CD31
CD29
CD49D
CD62L
Membrane CD antigen expression as a percentage of control
100
90
80
70
60
50
*
***
**
Treatment
None
GSH

Figure 3.7. Selective reduction in U937 monocyte adhesion molecule expression by glutathione. U937 monocytes ($2x10^6$/ml) were re-suspended in RPMI 1640 for 4 hours prior to the addition of 10mM glutathione (GSH) or vehicle for 16 hours at 37°C in a humidified 95% air, 5% CO_2 atmosphere. Incubations were terminated by washing cell samples twice with ice cold PBS. Samples were labelled with fluorescently tagged monoclonal antibodies for the antigens indicated or isotype negative controls and analysed by flow cytometry as described in method 3.2.5. Background fluorescence and regions of positive analysis were evaluated with samples stained with isotype negative controls. The median fluorescence value of each antibody was recorded from 10,000 viable cells per sample. Data is presented as the mean ± s.d of 3 individual experiments where * ($p<0.05$), ** ($p<0.01$) and *** ($p<0.001$) represent significant difference form controls by students T-test.

The treatment of U937 monocytes with short chain synthetic ceramides produces a reduction in $[peroxide]_{cyt}$ (see Chapter 2), which can be allied to an antioxidant-like effect. Consequently, as a positive antioxidant control, the effect of the antioxidant GSH on U937 monocyte with regards their membrane expression of integrins and selectins, and subsequently their adhesion to resting and LPS activated HUVEC was examined. GSH treatment of U937 monocytes for 16 hours induced a significant decrease in CD11a ($p<0.05$) and CD29 ($p<0.05$) to approximately 85% of controls, CD62L ($p<0.01$), CD49d ($p<0.001$) and CD18 ($p<0.001$) to approximately 80% of control treated cells. The surface expression of CD31 and CD11b were reduced compared to controls, but not significantly ($p>0.05$ for either protein; see Figure 3.7). The treatment of U937 monocytes with GSH for 16 hours significantly reduced their adhesion to 5 hours ($p<0.05$) and 24 hours ($p<0.01$) LPS (1μg/ml) activated HUVEC when compared to vehicle treated U937 monocytes. GSH treatment of U937 monocytes did not show significant alteration in their adhesion to resting HUVEC compared to control treated U937 monocytes. Additionally, vehicle treated U937 monocytes displayed elevated adhesion to 5 hours activated HUVEC compared to both resting ($p<0.05$) and 24 hours LPS activated HUVEC ($p<0.05$). Vehicle treated control U937 monocytes bound to resting and 24 hours activated HUVEC to the same level ($p>0.05$; see Figure 3.8).

To assess whether the reduction in monocyte adhesion to activated HUVEC and the decrease in membrane expression of adhesion molecules following long term synthetic ceramide were evident after short exposure periods, U937 monocytes were treated with 20μM C_6-ceramide for 2 hours and the effects on adhesion evaluated. C_6-ceramide (20μM) treated monocytes displayed reduced adhesion to HUVEC,

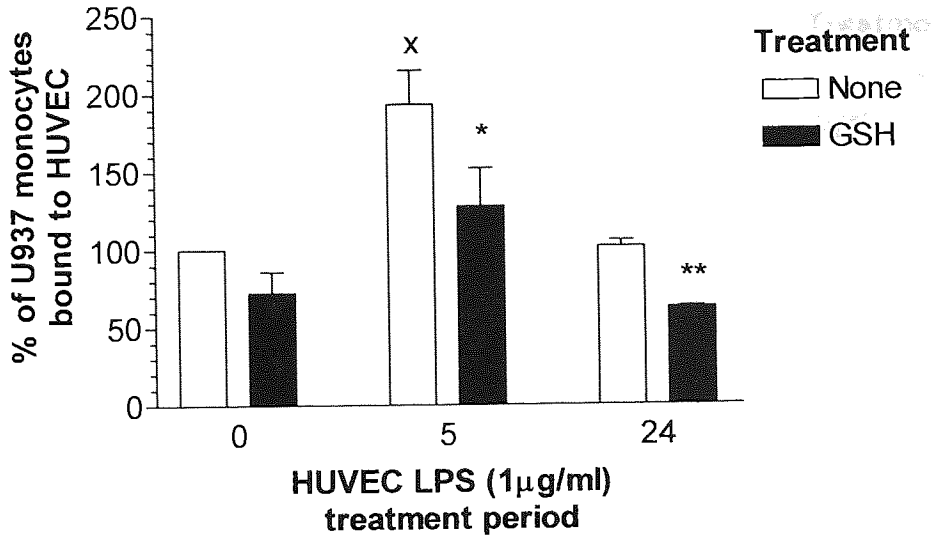

Figure 3.8. GSH treatment of U937 monocytes reduces their adhesion to activated endothelial cells. U937 monocytes ($2x10^6$/ml) were serum starved for 4 hours in RPMI 1640 prior to 10mM glutathione (GSH) treatment. Treatments were terminated by centrifugation and washing resulting cell pellets twice with ice cold PBS. Cells ($5x10^6$/ml) were loaded with 1μg/ml of BCECF-AM for 30 minutes in the dark. Cells were then washed and re-suspended in M199 to a concentration of $0.5x10^6$/ml. Confluent HUVEC monolayers in 24 well plates were treated with 1μg/ml LPS for 0 5 or 24 hours. HUVEC were washed twice prior to the addition of treated monocyte suspensions in duplicate for 30 minutes under the described incubator conditions. Their adherence was quantified against a standard curve of vehicle treated monocytes and expressed as a percentage of control treated U937 monocytes adhered to 0 LPS hours activated HUVEC. The results are presented as the mean percentage ± s.d of 3 individual experiments in replicates of 9, where * ($p<0.05$) and ** ($p<0.01$) represent significant difference of GSH treated U937 monocytes from controls for each activation period by students T-test or, x ($p<0.05$) represents significant difference from the adherence of control treated monocytes to 0 hours LPS activated HUVEC by one way ANOVA followed by Dunnett's multiple comparison test.

irrespective of the LPS (1μg/ml) treatment period ($p<0.001$). Increasing the HUVEC (1μg/ml) activation period significantly exacerbated the magnitude of inhibition of monocyte-endothelial cell interaction induced by C_6-ceramide (20μM) treatment ($p<0.001$; see Figures 3.4 & 3.9). Further, U937 monocyte treatment with 20μM C_2-/C_6-ceramide for 2 hours reduced the membrane expression of the integrins CD11b and CD49D, and the immunoglobulin CD31 by approximately 15-20% of control cells ($p<0.01$; see Figure 3.10). The membrane expression of CD29 was reduced by

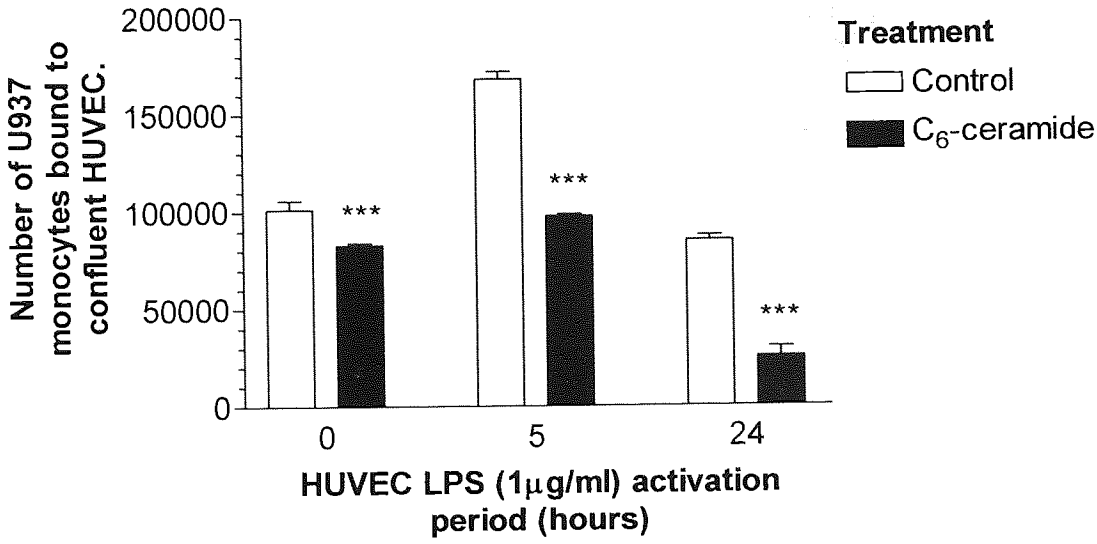

Figure 3.9. Short term exposure of monocytes to C_6-ceramide inhibits their adhesion to HUVEC. U937 monocytes ($2x10^6$/ml) were serum starved for 4 hours in RPMI 1640 prior to vehicle or 20μM C_6-ceramide treatment for 2 hours. Treatments were terminated by centrifugation and resulting cell pellets washed twice with ice cold PBS. Cells ($5x10^6$/ml) were loaded with 1μg/ml of BCECF-AM for 30 minutes in the dark. Cells were then washed and resuspended in M199 to a concentration of $0.5x10^6$/ml. Confluent HUVEC monolayers in 24 well plates were treated with 1μg/ml LPS for 0, 5 or 24 hours. HUVEC were washed twice prior to the addition of treated monocyte suspensions in duplicate for 30 minutes under the described incubator conditions. Their adherence was quantified against a standard curve of vehicle treated mononcytes. The results are presented as the mean ± s.d of two experiment in replicates of 9, where *** ($p<0.001$) represents significant difference from controls by students T-test.

approximately 8% ($p<0.05$; see Figure 3.10). U937 monocytes treated with 10μM of C_6-ceramide for 2 hours did not significantly alter the membrane expression of CD11b, CD29, CD49D ($p>0.05$; see Figure 3.10).

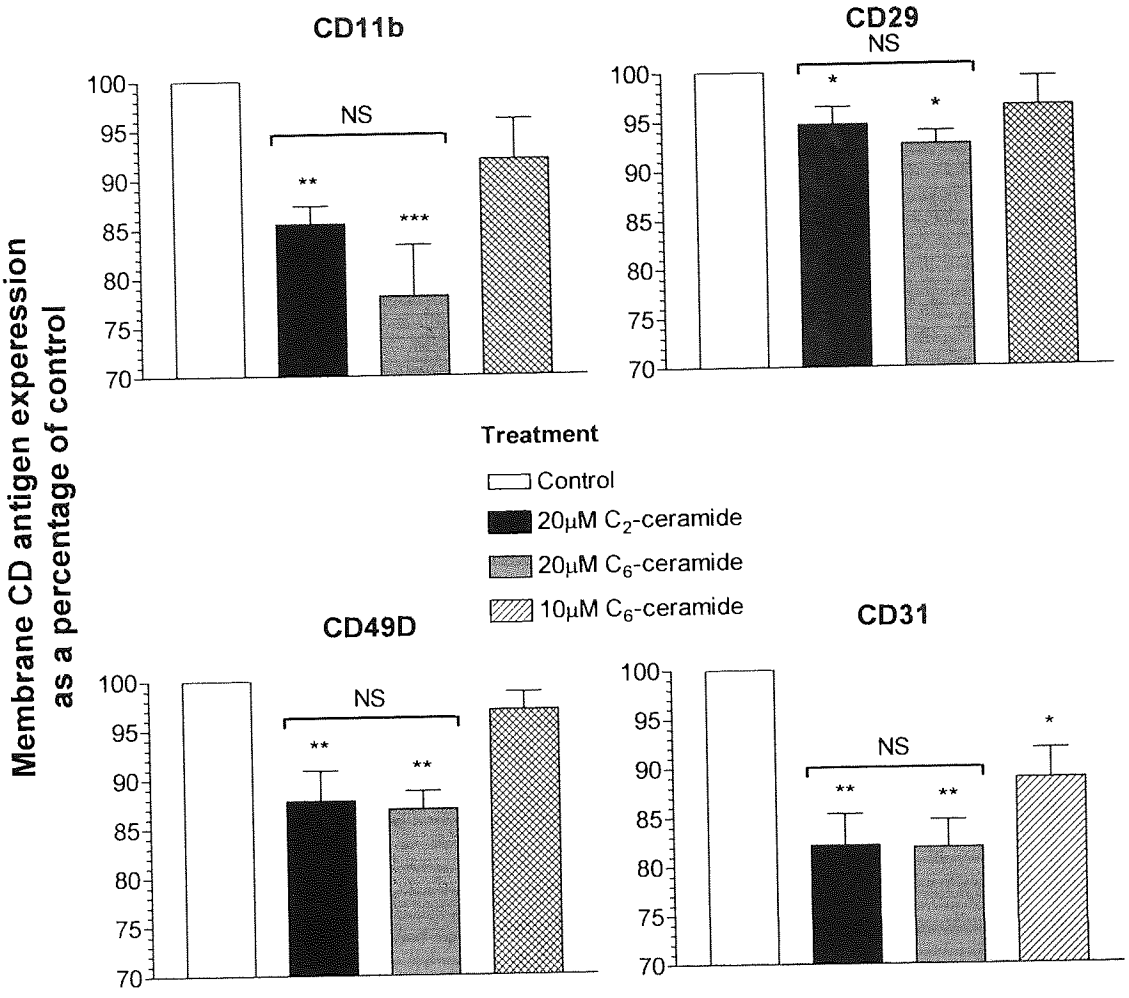

Figure 3.10. Short term treatments of monocytes with synthetic ceramides reduces the membrane expression of proteins associated with adhesion. U937 monocytes ($2x10^6$/ml) were serum starved for 4 hours in RPMI 1640 prior to 10/20μM C_2-/C_6-ceramide treatment for 2hours. Treatments were terminated by centrifugation and the resulting cell pellets washed twice with ice cold PBS. Cells were treated with >10μl of fluorescently tagged mouse IgG1 monoclonal antibody (MoAb) or isotype negative control per 10^6 cells for 30 minutes on ice, in the dark and fixed as described in method 3.2.5. Samples were then analysed by flow cytometry. Background fluorescence of each sample was established utilising cells stained with isotype negative controls. Positive regions were defined to contain 1% of the negatively stained cells. Samples were then analysed for MoAb membrane expression and the median X of the fluorescent peak recorded. The membrane expression of CD11b, CD29, CD49D, and CD31 were evaluated. At least 10,000 cells were analysed per sample. The results are presented as the mean ± s.d of 4 individual experiments where * ($p<0.05$) and ** ($p<0.01$) represent significant difference from controls by one-way ANOVA with Tukey's post *hoc* test analysis or Students T-test. NS, not significant.

3.4 Discussion.

As discussed in Chapter 2, the treatment of U937 monocytes with C_2-/C_6-ceramide induced a time and concentration dependent decrease in $[peroxide]_{cyt}$ which is associated with the adaptive cellular response of mild growth arrest. Additionally, the viability of U937 monocytes treated with synthetic, short chain ceramides was not compromised. It is the ceramide mediated decrease in $[peroxide]_{cyt}$ which appears to be the primary determinant of the cellular response rather than the elevation in $[peroxide]_m$ also described here (see Chapter 2) and by others (García-Ruiz *et al.*, 1997; Quillet-Mary *et al.*, 1997). Rather than pursue to define further biochemical consequences of the ceramide induced reduction in $[peroxide]_{cyt}$ the functional consequences of this monocyte response in the context of inflammation utilising an *in vitro* model of adhesion were evaluated.

The pathophysiology of several vascular and inflammatory diseases is characterised by the increased recruitment and adhesion of monocytes to inflamed tissues. A primary histological feature of RA is synovial hyperplasia, characterised by an increase in the number of inflammatory mononuclear cells into the synovial intima of the intraarticular space. Monocyte adhesion to the endothelium is a critical step in this process and is preceded by monocyte migration between endothelial cells through the sub-endothelial matrix into the inflamed synovium. This is followed by monocyte differentiation into tissue macrophages and type A synoviocytes (Cutolo *et al.*, 1993; as reviewed in; Carlos & Harlan, 1994; Müller-Ladner *et al.*, 1998). Furthermore, monocytes isolated from the peripheral whole blood of RA patients possess enhanced

adherence to fibronectin and resting or IL-1β activated HUVEC compared to monocytes from normals (Lioté *et al.*, 1996). Monocyte-endothelial cell interactions and the subsequent monocyte migration into the sub-endothelial space are critical processes required for the induction of atherosclerotic lesions in atherogenesis that ultimately leads to foam cell formation and the secretion of matrix metalloproteases capable of degrading the extracellular matrix (Herrmann *et al.*, 2001; as reviewed in Huo & Ley, 2001; Lum & Roebuck, 2001; Springer, 1990, 1994; von Andrian & Mackay, 2000). Similarly, in acute and chronic inflammatory lung disease, monocyte adhesion is followed by their emigration into the alveolar compartment additionally crossing vascular and alveolar epithelial cells (Rosseau *et al.*, 2000).

To represent the endothelium, endothelial cells were isolated and purified from the vein of human umbilical cords. Most observations of adhesion are performed using endothelial cells from venous rather than arterial sources. Further, treatment of human aortic endothelial cells (HAEC) with TNFα or LPS does not stimulate U937 monocyte adhesion, unlike that observed in HUVEC and has been ascribed to the inability of HEAC to up-regulate VCAM-1 (Kalogeris *et al.*, 1999). It is therefore hypothesised that the venous endothelium is more predisposed to inflammation than the arterial endothelium. Therefore, this study has addressed the effects of ceramide treatment of monocytes with regards interaction with endothelial cell from a venous source. For the adhesion assays, HUVEC of passage 3 or lower were grown to confluence in 24 well plates and U937 monocytes treated with or without C_2-/C_6-ceramide applied for 30 minutes. The number of monocytes adhered were then quantified utilising a fluorescence methodology (De Clerk *et al.*, 1994) as described in materials and methods. This *in vitro* system is a recognised model for studying the

adhesion of isolated circulatory cells to the endothelium (Kalogeris *et al.*, 1999; Weber *et al.*, 1995, 1996) and was optimised by colleagues within this laboratory (Woollard *et al.*, 2002). U937 monocytes have previously been shown to be an adequate model for studying monocyte-endothelial cell interactions (Cybulsky & Gimbrone Jr., 1991; Kallogeris *et al.*, 1999;). To simulate different inflammatory states of the endothelium, confluent HUVEC monolayers were activated with 1μg/ml of LPS for 0, 5 or 24 hours. These treatments did not compromise the cobblestone morphology associated with confluency. Sub-confluent HUVEC monolayers possess different adhesion qualities than those of confluent morphology. Further, long term culture (72 hours) of HUVEC with TNFα or IFN-γ induces elongations and the formation of gaps between HUVEC that affect the basal level of adhesion (Korlipara *et al.*, 1996) hence these studies were restricted to a maximal HUVEC activation period of 24 hours.

ROS are recognised as propagators and mediators of inflammatory responses and as propagators of cell adhesion where oxidants and oxygen free radicals are capable of modulating the expression of leukocyte and endothelial cell adhesion molecules (Fraticelli *et al.*, 1996; Gaboury *et al.*, 1994; Lo *et al.*, 1993; Sellack *et al.*, 1994). The ceramide treatment of U937 monocytes reduced their adhesion to activated endothelial cells which is associated with the reduced membrane expression of all integrins, selectins and immunoglobulins analysed and supports the earlier work demonstrating a reduction in monocyte $[peroxide]_{cyt}$. Whilst these data agree with the hypothesis, one could argue that ceramide would be expected to be pro-inflammatory given its role as a signal transduction molecule of pro-inflammatory cytokines such as IL-1β or TNFα and agents such as LPS or H_2O_2 (Andrieu *et al.*, 1994; Gamard *et al.*,

1997; Huwiler *et al.*, 1996; MacKichan & DeFranco, 1999; Obeid *et al.*, 1993; Verheij *et al.*, 1996). Furthermore many of these agents are reported to modulate and enhance the membrane expression of antigens allied to leukocyte-endothelial cell interactions therefore, contrary to the observations here, an elevation in monocyte adhesion to endothelial cells may be predicted.

Following the long term treatment of U937 monocytes with either C_2-/C_6-ceramide, the reduction in adhesion observed was dependent upon the activation state of HUVEC. Synthetic ceramide monocytes treated for 16 hours, when compared to vehicle treated controls, did not display any efficacy in reducing adhesion to 0 hours LPS activated HUVEC. When the LPS treatment of HUVEC was extended to 5 and then 24 hours, the adherence of monocyte treated with C_2-/C_6-ceramide for 16 hours was reduced to 50% and 35% of control U937 monocytes. The percentage inhibition of monocyte adherence bestowed by ceramide treatment was independent of the species.

Long term treatment of U937 monocytes with 10μM of C_6-ceramide was less effective 20μM C_6-ceramide at decreasing monocyte adhesion after 5 hours LPS HUVEC activation, but displayed an equivalent efficacy to inhibit U937 monocyte adhesion at 24 hours. These differential results are correlated with the magnitude of the decrease in $[peroxide]_{cyt}$ induced by synthetic ceramide treatment, where 20μM C_2-/C_6-ceramide reduced $[peroxide]_{cyt}$ to a greater extent than that of 10μM C_6-ceramide. Likewise, the reduction in integrin and selectin membrane expression was of greater magnitude following 16 hours 20μM C_2-/C_6-ceramide than that observed following 10μM ceramide. U937 monocytes treated with 20μM C_6-ceramide for 2

hours possess lower $[peroxide]_{cyt}$ content than those treated with the same dose for 16 hours (see Chapter 2) and corresponding with the hypothesis that it is the lower $[peroxide]_{cyt}$ levels which mediate the reduction in monocyte adherence to endothelial cells, U937 monocytes treated for 2 hours displayed a lower level of adhesion. Furthermore, 20μM C_6-ceramide caused greater reduction of the membrane expression of CD31, CD11b and CD49D of U937 monocytes after 2 hours exposure than after 16 hours. It is likely that this is also the case regarding CD62L, CD29, CD11a and CD18 following short term ceramide treatment. Low dose C_6-ceramide (10μM) treatment for 2 hours, which did not cause a significant reduction in $[peroxide]_{cyt}$ (see Chapter 2), as expected did not reduce CD31, CD11b nor CD49D membrane expression. Consequently, the effect of 2 hour 10μM C_6-ceramide treatment on monocytes-HUVEC interaction was not evaluated. Additionally the effect on monocyte-endothelial cell interactions were not evaluated where monocytes were treated with 20μM C_2-ceramide since an identical reduction in CD49D, CD11b and CD31 were observed to that mediated by 20μM C_6-ceramide and both species were equal in their efficacy at reducing monocye adhesion to HUVEC following 16 hours treatment. Given that the anti-adhesive properties of monocytes treated with synthetic ceramides is apparent after 2 hours, this cannot be attributed to growth arrest, which was first significant after 16 hours C_2-/C_6-ceramide treatment (see Chapter 2). In support of these observations that ceramide treatment of monocytes reduces their adhesion to activated HUVEC, are studies of ceramide in platelets, which display reduced aggregation following C_2-ceramide treatment (Simon & Gear, 1998). Further, it has been shown that C_2-ceramide induced slight inhibition of ADP-induced platelet aggregation despite not mediating any effect on thrombin-induced aggregation (Hannun *et al.*, 1987).

A criticism levelled at these results is that the reduction in membrane expression of a single integrin or selectin is small. However, it is likely that the collective response of all of these molecules, which individually each display a small decrease in expression which is responsible for the large reduction in U937 monocyte adhesion to activated HUVEC.

Treatment of U937 monocytes with GSH reduced their adhesion to 0 hour, 5 hour and 24 hours LPS (1μg/ml) activated HUVEC, although not to the same extent as that observed with 20μM C_2/C_6-ceramide. This difference may reflect the selective effect of GSH on the membrane expression of monocyte adhesion molecules. GSH treatment of U937 monocytes did not reduce CD11b or CD31, but significantly lowered the membrane expression of CD11a, CD18, CD29, CD49d, CD31, and CD62L. With the exception of ICAM-1, short chain ceramides were capable of reducing the monocytic membrane expression of all molecules analysed. Quite clearly, in the treatment of U937 monocytes, synthetic ceramide possess some anti-oxidant-like properties, although the greater inhibition of adhesion induced by ceramide treatment, with multiple effects on adhesion molecule membrane expression, point towards additional mechanisms to those of an antioxidant pathway. In support of redox regulation in the leukocyte membrane expression of molecules associated with adhesion, and consequently their interaction with endothelial cells, H_2O_2 treatment, or xanthine oxidase generated $O_2^{\cdot -}$ increased CD11b and CD18 expression of human PBN and as a result their adhesion to HEAC. MnSOD or catalase inhibited these effects (Fratacelli *et al.*, 1996). Further, infusion of hypoxanthine/xanthine oxidase or H_2O_2 into the rat mesenteric circulation lead to an increase in leukocyte rolling, adhesion and migration (Gaboury *et al.*, 1994; Scalia &

Lefer, 1998). The above considerations warrant studies on the effects of synthetic ceramide as an inhibitor of oxidant induced monocyte adherence to endothelial cells.

The decrease in $[peroxide]_{cyt}$ may therefore reduce the membrane expression of monocytic integrins and selectins, which as a consequence is one of the mechanism by which ceramide treated monocytes display reduced adhesion when compared to vehicle control treated monocytes. For further consideration, as discussed in Chapter 2, ceramide possesses the ability to fuse into phospholipid bilayers where it aggregates to form small microdomains, which aggregate into ceramide rich lipid rafts (Huang *et al.*, 1996). As a consequence, synthetic ceramides disrupt lipid composition and induce cytoskeleton alterations (Brown & London, 1998) without altering the membrane concentration of natural metabolites producing an increase in membrane fluidity and lateral mobility of membrane constituents (Chatterjee *et al.*, 1994; Ridgeway *et al.*, 1998; Simon & Gear, 1998). The accumulation of natural endogenous ceramide into lipid rafts has been reported to mediate CD95 (Grassmé *et al.*, 2001a & b) and CD40 (Grassmé *et al.*, 2002) receptor clustering in human lymphocytes. Conversely, the tyrosine phosphatase CD45 is excluded from rafts (Cheng *et al.*, 1999; Janes *et al.*, 1999). The functional consequences of receptor clustering induced by alteration in the lipid composition of membranes have not been examined. The spatial separation of the subunits of integrin adhesion molecules expressed upon monocytes following synthetic short chain ceramide treatment may contribute to reducing their adherence to the activated endothelial cells. Secondly, ceramide rich rafts may prevent apical clustering of integrins and selectins on the binding surface of monocytes thereby inhibiting endothelial cell interaction. Alternatively, the formation of ceramide rich rafts may cluster the integrins and

selectins thereby directly alter their function. Similarly, it has been described recently that caveolin 1 recruitment to receptor complexes is ceramide dependent and inhibits phospatidylinositol 3-kinase activity (Zundel *et al.*, 2000). Conformational changes in CD11a/CD18 and CD11b/CD18 following activation are suggested from studies utilising MoAb or Fab fragments that react with these integrins only after activation (Diamond & Springer, 1993; Landis *et al.*, 1993; Springer *et al.*, 1990). Whether the application of synthetic ceramides to monocytes can prevent the transition of integrins to an active conformation to upregulate adhesion warrants investigation.

The majority of work undertaken to reduce leukocyte adhesion, with a view to application in pathophysiological conditions, has focussed on blocking leukocyte-endothelial cell interaction using Ab to specific molecules present either on leukocytes or the endothelium. However, the roles of adhesion molecules in each stage of the multistep paradigm of adhesion are not mutually exclusive. Furthermore loss of function of one mode of leukocyte-endothelial cell interaction can be compensated for, in some cases, by another. For example, the effects of anti-CD18 or anti-CD29/CD49d are negligible unless in combination at inhibiting monocyte transendothelial migration (Meerschaert & Furie, 1994).

In addition to integrins and selectins, monocytes also express at their membranes the carbohydrate ligands glycoprotein/gycolipids and P-selectin glycoprotein ligand-1 (PSGL-1) for interaction with E- and P-selectin (CD62E/P) respectively expressed on the apical surface of endothelial cells. In concert with L-selectin (CD62L), CD62E and CD62P are responsible for initial leukocyte tethering. Like adhesion molecules,

chemokine receptors can be up-regulated or lost from the monocyte surface, and bind to chemokines secreted from virtually all cells. In excess of 50 chemokines exist which can trigger, amplify (Fratachelli *et al.*, 1996) or direct leukocytes into and within the extracellular matrix. The monocyte chemotractant protein-1 (MCP-1) is a secreted protein and member of the β-chemokine family, and as it name suggests, possesses powerful chemotactic activity for monocytes (as reviewed in; Springer, 1994; von Andrian & Mackay, 2000; Watanabe & Fan, 1998). If the membrane expression or conformational state of chemokine receptor for MCP-1, glycoproteins/glycolipids and PSGL-1, or indeed, if their function is influenced by the lipid ratio in phospholipid bilayers, then it is likely that short chain ceramide treatment of monocytes may disrupt their influence on monocyte-endothelial cell interactions. If the reduction in $[peroxide]_{cyt}$ observed following C_2-/C_6-ceramide is NADPH oxidase dependent the synthetic ceramide treatment of monocytes may inhibit the consequences of respiratory burst following chemokine receptor activation (as reviewed in; Madri & Graesser, 2000).

It can be envisaged that reducing the membrane expression of multiple molecules in concert with conformational changes and protein re-organisation within the plasma, may disrupt the multistep paradigm of leukocyte-endothelial adhesion. Ceramide treatment of monocytes may reduce initial tethering to the endothelium due to reduced CD62L expression. Any monocytes that tether will possess a reduced ability to firmly adhere and transmigrate into the extracellular space due to diminished CD11a/18, CD11b/CD18, CD49D/29 and CD31 membrane expression, and consequently flow back into the circulation (see Figure 3.11). Since ceramide treatment did not significantly reduce adhesion to the non-activated endothelium, it is

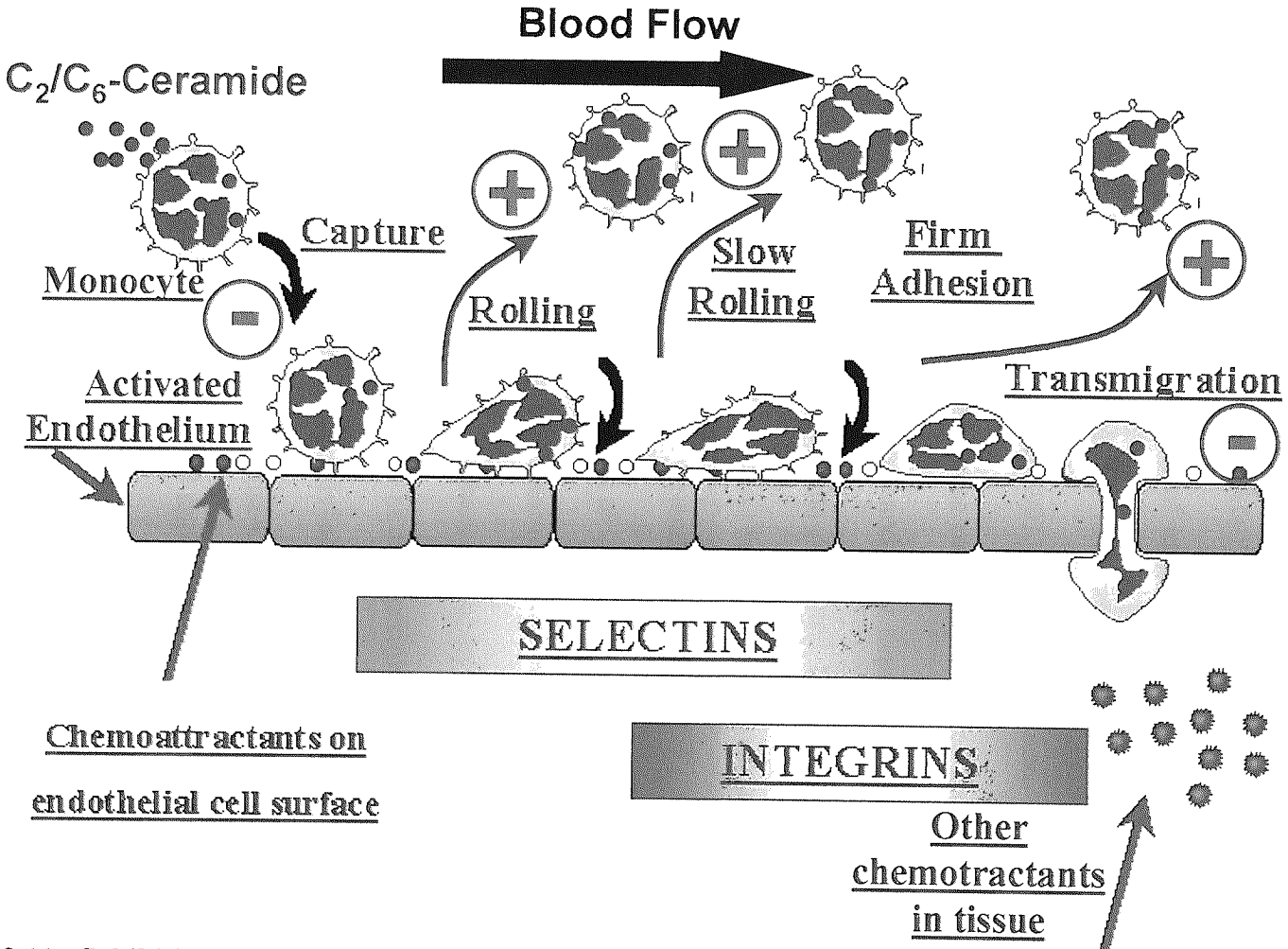

Figure 3.11. Inhibition of the multistep paradigm of adhesion by the synthetic ceramide treatment of monocytes – application to inflammatory disorders. The pathogenesis of several inflammatory disorders of vascular origin are characterised by the increased recruitment, tethering, rolling, firm adhesion and transmigration of monocytes to the activated endothelium. It is proposed that the treatment of monocytes with synthetic ceramides inhibits (-) this multistep interaction with the activated endothelium promoting (+) monocyte re-entry into the flowing blood stream and in the case of atherosclerosis, reducing plaque formation.

possible that the low level of constitutive monocyte adherence and migration to the resting endothelium may remain unaltered.

Further investigation is required to confirm this hypothesis utilising primary human monocytes under conditions of flow and shear stress *in vitro* and consequently *in vivo*. There are concerns that leukocyte-endothelial interactions observed within a static system do not reflect those of inflammation *in vivo* where cell surfaces must resist shear flow forces from blood. Integrins and selectins function differently under these conditions (Spertini *et al.*, 1991, 1992) and *in vitro* studies by Tsuboi *et al.*, (1995) have shown that shear stress reversibly elevates the endothelial cell surface expression of ICAM-1 in a force and time dependent manner with no change in VCAM-1. Nevertheless, the results presented here are encouraging and act as a platform for studies taking into account pressures exerted by shear flow. Furthermore, analysis of monocyte-endothelial cell interaction in a dynamic system will enable dissection of the effects of ceramide treatment of monocytes in each stage of the multistep paradigm of adhesion. Studies preformed within this laboratory (unpublished results) and that of others (Cybulsky & Gimbrone Jr, 1991; Kalogeris *et al.*, 1999) confirm that primary human peripheral blood monocytes and U937 monocytes possess identical levels of adhesion to resting or activated HUVEC monolayers. Further, where low dose C_2-/C_6-ceramide have been described to reduce $[peroxide]_{cyt}$ without induction of apoptosis in the immortalised Jurkat T-cell and primary human resting or activated T-lymphocytes *in vitro* (see Chapter 2), the effect on their adhesion to endothelial cells or other circulatory cells warrants investigation. However, it should be appreciated that different mechanisms exist for the lymphocyte paradigm of adhesion compared to monocytes. By transfecting the resting

endothelium with adenovirus carrying VCAM-1, Gerszten *et al.*, (1996, 1998) showed VCAM-1 alone supported lymphocyte rolling but not firm adhesion nor transmigration, whilst monocyte rolling, firm adhesion and transmigration was supported under these conditions.

The majority of reports addressing monocyte-endothelial cell adhesion during inflammation focus on the inflammatory response of the endothelium rather than the effects of pro-inflammatory mediators on monocytes. Studies within this laboratory have shown that the adherence of monocytes to 24 hour LPS activated HUVEC is significantly up-regulated following monocyte exposure to physiologically relevant concentrations of the prototypic acute phase serum protein C-reactive protein (CRP; Woollard *et al.*, 2002; in press). Similarly, H_2O_2 treatment of PMNs increases their adherence to resting and 4 hours TNF activated HEAC (Fratacelli *et al.*, 1996) while chemokines increase CD11b/CD18 on neutrophils (Springer *et al.*, 1990). An intriguing question not answered here which requires addressing is; can ceramide treatment reduce the adherence of monocytes treated with agents that are pro-inflammatory by preventing the increased expression of adhesion molecules? Further, monocytes isolated from the whole blood of patients with RA possess elevated CD11b expression compared to those isolated from normal. This correlated with their elevated adhesion to fibronectin or resting and IL-1β activated HUVEC compared to normal monocytes (Lioté *et al.*, 1996). Similarly, monocytes isolated from human patients who smoke, a recognised major risk factor in atherogenesis, posses elevated surface expression of CD11b/CD18 that was associated with elevated adhesion to resting HUVEC (Weber *et al.*, 1996). Other studies have shown that macrophages from the synovial fluid and tissue possess enhanced CD18 and CD29

(Allen *et al.*, 1989; El-Gabalawy *et al.*, 1996; Koch *et al.*, 1995). Subsequently, the targeted ceramide treatment to monocytes in humans with inflammatory diseases could reduce the aetiology of increased monocyte recruitment to endothelial/epithelial cell barriers or other tissue membranes, and slow or prevent disease progression?

The effect of LPS treatment over time upon the HUVEC surface expression of P-/E-selectin, ICAM, VCAM or glycoproteins has not been investigated. Following HUVEC activation for 5 hours with LPS, untreated U937 monocytes possessed a 1.75 fold increase in adherence over U937 monocytes adhering to resting HUVEC. Similar observations were reported by Kalogeris *et al.*, (1999) following 4 hours activation with TNFα/LPS which correlated with the up-regulation in the HUVEC surface expression of ICAM-1, E-selectin and VCAM-1 (Kalogeris *et al.*, 1999). Both ICAM-1 (Muller *et al.*, 1992) and ICAM-2 are constitutively expressed on endothelial cells, but only ICAM-1 can be upregulated transcriptionally (Roebuck & Finnegan, 1999), while the literature reports mixed observations concerning the constitutive levels of VCAM-1. Korlipara *et al.*, (1996) and Muller *et al.*, (1992) report no constitutive expression whereas Meerschaert & Furie, (1994) describe low levels which are sufficient for adhesion. Additionally resting HUVEC do not express CD62E (Muller *et al.*, 1992). Extending the LPS activation of HUVEC to 24 hours saw non-treated U937 monocytes adhere with the same magnitude as those following 0 hours activation and may reflect down regulation of these HUVEC adhesion molecules. Since the ceramide treatment of U937 monocytes reduced their adhesion to HUVEC which were activated for 24 hours but not 0 hours, this is likely to reflect the fact that HUVEC possess different populations of adhesion molecules on activation. The up-regulation of surface expression of adhesion molecules restricted

to HUVEC is dependent on the type and strength of inflammatory stimulus. Utilising a genetic approach to determine the contribution of ICAM-1 in mediating monocyte adhesion to mouse aortic endothelial cells (MAEC), stimulation of MAEC with oxidised LDL induced an increase in monocyte adhesion not observed in ICAM-1 -/- MAEC, whereas high doses of TNFα induced monocyte adhesion to ICAM-1 -/- MAEC (Kevil *et al.*, 2001). Under these conditions, TNFα mediated an ICAM-1 independent adhesion and these studies highlight that oxidised LDL, TNFα and other pro-inflammatory agents stimulate different signalling pathways in endothelial cells resulting in the agent specific modification of endothelial cell adhesion molecules (Kevil *et al.*, 2001). This is confirmed by studies showing that IFNγ activation of HUVEC does not support CD18 independent chemotaxin induced monocyte transmigration unlike LPS, TNFα or IL-1α (Chuluyan & Issekutz, 1993). Since short chain ceramides are capable of reducing the surface expression of most adhesion molecules involved in monocyte adhesion, reducing their interaction with inflamed tissues and cell surfaces is likely to be less dependent of the population of counter receptors expressed at these sites, and thus independent of the source of their up-regulation.

The β2 integrins primarily mediate cell-cell interactions, however the β1 integrin of CD29/CD49d participates not only in cell-cell interaction but also matrix-cell interaction via VCAM-1 and the alternatively spliced connecting segment-1 (CS-1) region of the matrix protein fibronectin (Wayner *et al.*, 1989; Komoriya *et al.*, 1991). In human coronary artery atherosclerotic plaques, expression of CD62E, ICAM-1 and VCAM-1 in the plaque neovasculature is 2 fold greater than that of the arterial luminal endothelium and is associated with an elevated leukocyte density (O'Brien *et*

al., 1996). Additionally, high levels of CD62E and ICAM-1 are expressed on the synovial endothelial capillary cells in RA inflammatory synovitis (Koch *et al.*, 1995; Veale *et al.*, 1993). The observations of reduced monocyte membrane expression of selectins and integrins reported here following ceramide exposure are indicate that synthetic short chain ceramide treatment would reduce monocyte adhesion to the arterial endothelium, tissue matrix and atherosclerotic plaques.

While elevated leukocyte-endothelial cell interactions are primary consequences of a host of inflammatory diseases, leukocyte extravasion following adherence to the endothelium is a vital armoury in the host defence system against infection. What remains to be determined is whether the ceramide treatment of monocytes interferes with the immune response to infection, their differentiation into macrophages and the ability of these macrophages to induce a respiratory burst in response to pathogens.

Irrespective of the biochemical and molecular mechanisms which mediate the decreased adhesion of ceramide treated monocytes for endothelial cells, a novel therapeutic application for these observations lies in the host of inflammatory disorders whose aetiology are characterised by the increased adherence of leukocytes to endothelial/epithelial cell walls, or synovial tissue. The targeted ceramide treatment of monocytes or other leukocytes at concentrations that do not confer apoptosis may inhibit inflammation by two mechanisms. Firstly, by reducing the $[peroxide]_{cyt}$ of monocytes, synthetic short chain ceramides may not necessarily break, but rather reduce the amplification loop associated with whereby elevated levels of local oxidative stress increase cytokine production from both circulatory

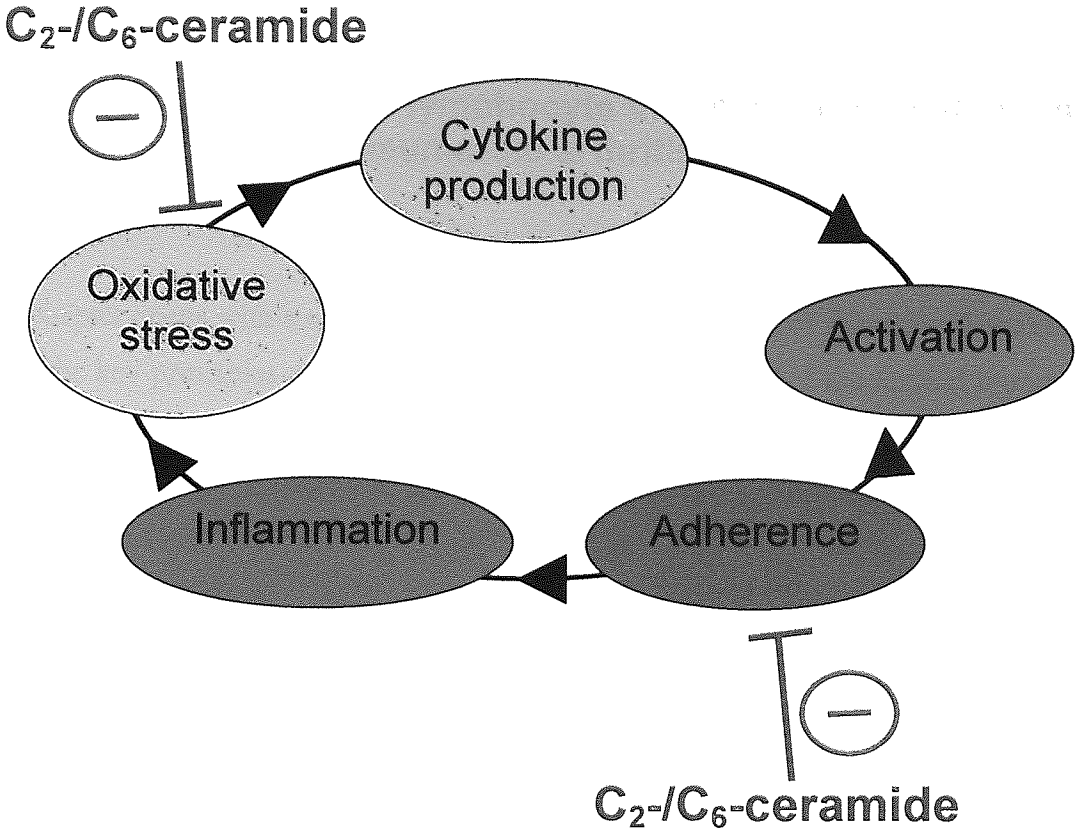

Figure 3.12. Monocytic treatment with short chain synthetic ceramides may disrupt the amplification loop of inflammation. The oxidative stress associated with inflammation is mediated by the increased formation of reactive oxygen species (ROS) from various cell types affecting vascular reactivity. Exposure of cells to ROS leads to the production and secretion of growth factors and cytokines. Together with ROS, these lead to cellular activation the promotion of cell adhesion and propagation of the inflammatory response, closing the positive feedback loop to increase the local oxidative stress. It is proposed that by the targeted treatment of monocytes with C_2-/C_6-ceramide, this amplification loop maybe inhibited (-) at 2 sites; (i) At the intracellular level, reduction in $[peroxide]_{cyt}$ in monocytes by treatment C_2-/C_6-ceramide may reduce the incidence of oxidative stress in the inflammation locus. (ii) Inhibition of cell-cell interaction at the inflammatory site.

cells and endothelial/epithelial cells, and increase cell adhesion (see Figure 3.12). Additionally, monocytes treated with synthetic ceramide show lower efficacy of adherence to the inflamed tissues due to the reduce membrane expression of cell adhesion molecules (see Figure 3.11) and/or their conformational changes, potentially reducing or slowing the appearance of atherosclerotic plaque formation in cardiovascular disease, synovial hyperplasia in RA, and acute and chronic respiratory lung disease.

Chapter 4.0: Aberrant T lymphocyte intracellular signalling in rheumatoid arthritis.

This chapter opens with a summary of the histological features of rheumatoid arthritis (RA), the key principles of T-cell function in the maintenance of the normal immune response and their reduced activity in RA. The central differences between diseased and healthy T-cell phenotypes, protein expression and signalling in response to physiological stimuli is discussed. The evidence for ROS, DAG and ceramide acting as aberrant signalling molecules which may contribute to RA T-cell pathology is then debated in the context of the results obtained from the study of these signalling intermediates in resting and PHA activated T-cells from RA patients and normals.

4.1 Introduction.

There are many forms of rheumatic disease where the most debilitating, RA, is an autoimmune disease of synovial joints associated with chronic inflammation, followed by cartilage and bone destruction with a prevalence in 1% of the worlds population (as reviewed in; Feldman, 2001). The pathological progression of RA is characterised by two histological features; (i) the development of the inflammatory pannus, an aggressive tumour-like expansion of the synovium as a result of synovial hyperplasia and (ii) elevated infiltration of inflammatory leukocytes into the synovial fluid and lining, both processes leading to neovascularisation and, bone and cartilage destruction. The synovial intima lines the intra-articular space and is normally 1-2 cells thick which in RA, through proliferation or increased adherence of infiltrating leukocytes, becomes up to 20 cells thick, mainly consisting of fibroblast-like cells (type B synoviocytes) and macrophage-like cells (type A synoviocytes) with lymphoid aggregates. This aetiology of enhanced cellularity is suggestive of an elevation in the recruitment of leukocytes into the synovium and/or an imbalance between proliferation and death of multiple different cell types, where there are excessive signals that induce proliferation, defects in the signal that mediates apoptosis or a combination of both. Neovascularisation is a complex process involving endothelial cell division, the selective degradation of vascular basement membranes and surrounding extracellular matrix induced by VEGF, IL-1, TNFα, IL-8 and FGF that enhance the expression of degradative enzymes. Bone destruction is mediated by osteoclasts. Osteoclastogenesis is promoted by cells found within inflammatory bone lesions and is enhanced by pro-inflammatory cytokines. Cartilage

is a highly resilient and compressed hypocellular tissue consisting of a matrix of a dense network of collagen type II cells and hydrophilic macromolecular complex of the proteoglycan aggrecan. Aggrecan cleavage is the first step in cartilage destruction by members of the ADAMTs (a disintegrin and metalloproteinase with thrombospodin type I motif) family (as reviewed in; Arend, 1997; Feldman, 2001; Koch *et al.*, 1995; Sewell & Trentham, 1993).

T-cells are critical players in the regulation of immune responses and are responsible for the effector responses of the immune system. The T-cell population is sub-divided according to various operational and phenotypic parameters. T-helper (Th) cells are assigned to one of 3 sub-sets, Th0, Th1 and Th2, a classification that is based up on cytokine production. Largely, Th1 cells are considered responsible for cell mediated effector mechanisms whereas Th2 cells are implicated in Ab production. There is however considerable overlap in T-cell function. Cells that possess both Th1- and Th2-like cells properties have been assigned to the Th0 classification. Immune responses require the interaction of multiple cell types where T-cells serve to regulate the cell- and Ab-mediated action, events which cannot be considered as separate entities. (as reviewed in; Hickling, 1998). Mechanisms for the maintenance of immune homeostasis are essential for normal immune function. The global T-lymphocyte population is tightly regulated where stringent control exists to prevent clonal outgrowth while allowing certain effector cells to establish T cell memory. The normal immune response to pathogens initiates transient cell proliferation followed by elimination of expanded clones specific for pathogens. The immune system is therefore in a constant state of flux, where dysfunction in the mechanisms for expansion and elimination of activated cells may contribute to the development of

autoimmune disease. Cytokines, co-stimulation by antigen presenting cells and TCR stimulus strength may regulate the decision of peripheral blood lymphocytes to live or die. In the periphery, the T-cell receptor (TCR) mediated activation of T-cells induces either the primary activation of resting T-cells, which in the absence of co-stimulatory signals may induce anergy (a state of immune unresponsivness) or apoptosis of activated T-cells unless they are rescued by additional signals (as reviewed in Krammer *et al.*, 1994).

The T-cell response in RA is abnormally reduced and consequently they show persistence within the joints of RA patients. 30% of cells infiltrating the RA synovium are T-cells and are chiefly small non-cycling $CD4^+$ T-cells where 5-20% express T-cell activation markers possessing mainly the Th1 pattern of cytokine production (Dolhain *et al.*, 1996; as reviewed in; Feldman, 2001). However, the mechanisms that permit T-cell survival within the synovium are ill understood and observations *in vitro* or *in vivo* are often contradictory. Evidence is accumulating to suggest dysfunctional signal transduction of extracellular signals, since synovial T-cells respond poorly to mitogenic and antigen stimulation suggesting they are hyporesponsive (Salmon & Gaston, 1995). Indeed murine models of the RA allied disease systemic lupus erythematosus (SLE) is produced by a monogenic germline defect that prevents CD95 signal transduction. Mice displaying the *Gld* or *Lpr* mice which lack CD95L and CD95 develop lymphadenopathy and autoimmune disease as a result of a failure to clear an unusual class of CD4, CD8, TCR positive cells (as reviewed in; Nagata, 1998; Nagata & Suda, 1995).

The majority of rheumatoid synovial T-cells are highly differentiated, $CD45RB^{dull}$, $CD45RO^{bright}$ with high CD95 expression, a phenotype suggesting susceptibility to apoptosis, whereas those obtained from gout patients are $CD45RB^{bright}$ (Matthews *et al.*, 1993; Salmon *et al.* 1997). CD95 is expressed on 40-60% of $CD3^+$ T-cells in the synovium, although other authors report this expression to be higher, where RTPCR revealed CD95 to be overexpressed (Samida *et al.*, 1997; Cantwell *et al.*, 1997). However, T-cells in the RA synovium showed no evidence of T-cell apoptosis unlike those observed in crystal arthritis, OA, or the normal synovium. This suggests that factors present in the RA synovium selectively support T-cell survival, although apoptosis of fibroblasts and macrophages is apparent. Further, RA synovial T-cells undergo spontaneous apoptosis upon culture which can be rescued upon addition of IL-2Rγ chain signalling cytokines (Firestein *et al.*, 1995; Salmon *et al.*, 1997) although the $CD4^+$ T-cell subset characterised by a defect in CD28 expression associated with RA are resistant to apoptosis upon growth factor withdrawal. This $CD4^+CD28^-$ subset frequently expands *in vivo* where they are not affected by clonal exhaustion and persist for years (Goronzy *et al.*, 1994; Schirmer *et al.*, 1998). Freshly isolated synovial T-cells and monocytes from human patients with RA have enhanced susceptibility to CD95L induced apoptosis *in vitro* when compared to those from OA patients. The majority of these rheumatoid T-cells that are susceptible to CD95L possess a phenotype of $CD3^+$, $CD4^+$ $CD45^+$ RO^+, a major population responsible for chronic inflammation (Hasunuma *et al.*, 1996; Hoa *et al.*, 1996). Further, synovial T-cells undergo apoptosis to a significantly higher degree than those from PBL from the same patient or those from age matched normals (Cantwell *et al.*, 1997). However, despite autoreactive T-cells expressing both CD95 and CD95L, they are not eliminated by CD95-CD95L interaction. It has been proposed that the

enhanced concentration of soluble CD95 detected in the RA synovium compared to that compared to that observed in the OA synovium, binds to CD95L to prevent cell-cell interaction to induce CD95-mediated T-cell apoptosis (Hasunuma *et al.*, 1997). However, these observation are contentious, as immunoblots have reported no soluble inhibitor of CD95 in synovial fluid. Additionally, little if any CD95L was detected at the mRNA and protein level in RA synovial T-cells. Nevertheless, these cells, RA PBL and RA synovial MNC could be induced to express CD95L by treatment with anti CD3 MoAb to crosslink the TCR, phorbol ester or the calcium ionophore ionomycin. Such treatment induced CD95L expression on the surface of RA synovial T-cells or PBL as effectively as on normal donor T-cells (Cantwell *et al.*, 1997). Proteoglycan (PG)-induced arthritis in BALB/c mice, brought on by human cartilage PG (HPG) immunisation, produces a novel model of RA that shows similar radiological progression as that seen in humans. Naïve T-cell from unimmunised mice displayed low levels of the activation marker CD25 and CD95. In order to express high levels of CD95 these cells required stimulation with CD3 and CD28 *in vitro*, while for membrane expression of CD95L, repeated TCR stimulation was necessary. Highly activated $CD4^+$ T-cells from both HPG immunised BALB/c and B6 mice, which were resistant to PG induced RA, possess equal membrane expression of CD95 and CD95L. However, $CD4^+$ T-cells from BALB/c mice that develop RA, fail to undergo TCR induced apoptosis leading to an accumulation of autoreactive Th1 cells in the periphery which may contribute to autoimmune disease. Conversely, $CD4^+$ T-cells from HPG immunised B6 mice undergo apoptosis following CD3 stimulation which is inhibitable by blocking CD95-CD95L interactions and is symptomatic of an essential requirement for CD95 and its signalling system (Zhang *et al.*, 2001). Overall, these results are indicative of

defective CD95 signalling in $CD4^+$ T-cells from the RA murine model rather than differences in CD95 or CD95L expression.

Examination of the intracellular apoptotic signalling cascade revealed that Fas-like IL-1β-converting enzyme-inhibitory protein (FLIP), which impairs activation of pro-apoptotic caspase-3 and –8 at the death inducing signalling complex (DISC), was constitutively expressed in unstimulated cells from B6 or BALB/c mice. Upon HPG-immunisation of B6 mice, FLIP expression disappeared but remained unchanged in HPG-immunised BALB/c mice. Consistent with this observation caspase-3 and –8 showed reduced cleavage. Further, higher amounts of FLIP were associated with the DISC in $CD4^+$ T-cells from HPG immunised BALB/c mice displaying RA than those in HPG-immunised B6 mice without RA despite identical levels of CD95 ligation (Zhang *et al.*, 2001), lending further support to the hypothesis that aberrant intracellular signalling of T-cells contributes to their accumulation within the RA joint.

The link between cytokines and autoimmune diseases is not fully understood and the question remains as to whether cytokines are of primary importance as inducers of inflammatory disease or act as a consequence of the initial development. The balance between pro- and anti-inflammatory cytokines within the periphery and synovium may influence cell death or survival, although a recent study described that the concentration of cytokines within the synovium of RA patients does not correlate with the number of inflammatory cells (Wagner *et al.*, 1997). Fibroblasts and macrophage derived cytokines such as IL-1α, IL-1, IL-2, IL-6, GM-CSF and TNFα are present in abundance in the RA synovium and may sustain the Th1 phenotype that

is associated with RA. However, cytokines derived from T-cells such as IL-2, IL-4 or IFN-γ are present in relatively low concentrations (as reviewed in Cunnane *et al.*, 1998). Many of these pro-inflammatory cytokines are involved in the self amplification of their own production or other pro-inflammatory cytokines (Gracie *et al.*, 1999). IL-18 is novel cytokine with pleiotropic activities, critical not only for the development of Th1 responses by inducing proliferation and upregulating INFγ, TNFα and GM-CSG production (Gracie *et al.*, 1999; Kohno & Kurimoto, 1998; Okamura *et al.*, 1998) but also for the enhancement of T-cell and natural killer cell cytotoxicity (Takeda *et al.*, 1998). Elevated IL-18 mRNA and protein expression is reported within the synovial tissue of RA patients compared with OA synovial tissue. Correspondingly enhanced IL-18 receptor expression was detected on synovial lymphocytes and macrophages from rheumatoids when compared with osteos (Gracie *et al.*, 1999). Administration of IL-18 to collagen/incomplete Freund's adjuvant-immunised DBA/1 mice induced the development of an erosive inflammatory disease suggesting IL-18 is pro-inflammatory *in vivo* (Gracie *et al.*, 1999). Furthermore, expression of the pro-apoptotic proteases ICH-IL and CPP32 is reduced *in vitro* by treatment of RA synovial cells with TNFα or IL-1β (Wakisaka *et al.*, 1998).

The secretion of cytokines with anti-inflammatory properties is a physiological mechanism to re-address the pro-inflammatory environment within the RA synovium. IL-4 and IL-10 act by quite different mechanisms. IL-4 has been shown to increase levels of the IL-1 receptor agonist (ra) released from macrophages and monocytes of RA patients. IL-4 increases the degradation of cytokine mRNA whereas IL-10 inhibits the activation of the transcription factor NFκB to reduce cytokine production. Further, IL-10 can down regulate TNF, IFNγ and granulocyte-macrophage colony-

stimulating factor (GM-CSF). By inhibiting a variety of macrophage functions, IL-10 is thought to mediate natural suppression of the evolution of RA, especially through a reduction in MHC class II expression thereby blocking cytokine production. TGF-β also possesses anti-inflammatory properties particularly by antagonising IL-1 induced T-cell proliferation by decreasing the expression of IL-1 antigen and increasing the production of IL-1ra in macrophages (as reviewed in Cunane *et al.*, 1998).

Blockade of NFκB in human rheumatoid synovial cultures using adenovirus overexpressing IκBα reduced the synovial production of TNFα by approximately 70%. A reduction in the production of other pro-inflammatory cytokines and metalloproteinases, without affecting the production of the anti-inflammatory cytokines IL-10 or IL-1ra, has also been reported (as reviewed in; Makarov *et al.*, 2001). In the synovium of rats with streptococcal cell wall (SCW) induced arthritis, a model of human RA, NFκB was found to be activated, which was not associated with the normal rat synovium. Further, the intra-articular administration of proteasomal inhibitors or the adenovirus gene transfer of an inhibitor of IκBα enhanced the incidence of apoptosis within the synovium of rats with SCW or pristane induced arthritis but not that of normal rats. Employing a liposomal delivery system, the intra-articular administration of NFκB decoy oligodeoxynucleotides significantly inhibited the severity of recurrent SCW in the joint of administration. Surprisingly, the severity of arthritis in untreated, contralateral joints of SCW rats was also inhibited indicating systemic therapeutic effects of local treatment (Miagkov *et al.*, 1998).

Ohshima *et al.*, (2000) hypothesise that the low level of apoptosis observed within the RA synovium is due to the inhibition of CD95 mediated apoptosis by the presence of TNFα. RA synovial T-cells in culture readily undergo apoptosis in response to CD95. However, this effect is ameliorated dose dependently by the addition of TNFα within the concentration range expected within the RA synovium but not by the pro-inflammatory cytokines IL-1 or IL-6. The pro-apoptotic actions of CD95 were restored by the incubation of an anti-TNFα Ab (cA2; Ohshima *et al.*, 2000). Similarly, IL-1β and TNFα which were not in themselves pro-apoptotic, rendered synovial-like fibroblasts refractory to CD95 mediated apoptosis *in vitro*. CD95 mediate apoptosis of synovial cells was not inhibited by IL-6 or IL-18 (Wakisaka *et al.*, 1998). The effects of TNF induced inhibition of T-cell apoptosis were neither through the down regulation of CD95 membrane expression nor through alterations in Bcl-$_2$ expression since these remained unaltered following TNFα treatment. It is proposed that the CD95 and TNF signalling pathways share a common intermediate (Ohshima *et al.*, 2000). However, at a 100 fold higher concentration, TNFα induced apoptosis of cultured RA synovial T-cells (Firestein *et al.*, 1995) rather than the inhibition of apoptosis described by Ohshima *et al.*, (2000). Furthermore, PHA stimulation of peripheral blood T-cells from patients with RA showed a reduced $[Ca^{2+}]_i$ signal compared to PBL from normals; a defect which is believed to contribute to the hyporesponsivness of RA T-cells and their inability to undergo apoptosis (Carruthers *et al.*, 1996). RA synovial cells express more Bcl-$_2$ and Bcl-x *in vivo* than those from OA patients where Bcl-x_l is overexpressed indicating an enhanced tendency for survival in RA than in OA. Further, the RA synovial lining does not express CPP32 or ICH-IL proteases in contrast to OA synovial fibroblasts (Wakisaka *et al.*, 1998).

RA patients possess a subset of $CD4^+CD28^-$ T-cells whose expansion and persistence *in vivo* without clonal exhaustion is believed to be due to an altered apoptotic response; despite expressing identical levels of the proteins Bax or Bcl-$_2$ in $CD4^+CD28^+$ T-cells, immunoblots and flow cytometry revealed that $CD4^+CD28^-$ T-cells expressed higher amounts of Bcl-$_2$ which was independent of IL-1. This dysfunction in survival protein expression may induce clonal outgrowth of autoreactive T-cells that contributes to the RA pathology. Indeed, applying *in situ* end labelling of genomic DNA isolated from RA patients, macrophages and some fibroblasts were positive for DNA strand breaks whereas T-cells obtained from synovial tissue lymphoid aggregates were negative and were associated with high Bcl-$_2$ expression (Firestein *et al.*, 1995). Salmon *et al.*, 1997 described that synovial T-cells cultured in fibroblast condition media expressed low amounts of Bcl-$_2$ but high amounts of Bcl-x_l, a similar phenotype to freshly isolated synovial T-cells, with no observations of apoptosis whereas T-cells from gout patients displayed significant evidence of apoptosis allied to low Bcl-x_l. However, these observations are limited due to the lack of evidence from non-diseased individuals.

The rheumatoid synovium appears to be an anti-apoptotic environment where multiple factors *in vivo* may mediate the downregulation of pro-apoptotic signalling intermediates while enhancing the expression of anti-apoptotic proteins to decrease the incidence of apoptosis that is an evident histological feature of the RA synovium. Identification of defective biochemical and molecular processes associated with this pathology may allow treatment of this disease through resolution of rational therapeutic design. The relative ratio of pro- and anti-apoptotic intracellular

signalling intermediates may determine the sensitivity of RA cells to apoptosis inducing agents.

ROS and free radical species are generated at sites of inflammation and injury, where at high concentrations they cause direct cell injury and death. Furthermore, their excessive production can lead to the oxidation of biological macromolecules such as DNA, protein, carbohydrates and lipids. Free radicals can be passed from one macromolecule to another setting in motion a chain reaction leading to extensive cellular damage. Concentration and duration of ROS exposure is critical to the mechanism of damage. Since the various ROS and free radicals have differing reactivities and diffusion rates, their damaging effects are seen at varying distances from their production source. Hydrogen peroxide is lipophilic and can readily traverse biological membranes and transfer oxidising potentials to cellular targets distinct from the site of generation. The charge of the ROS constrains many species to specific compartments. For example, superoxide generated in the extracellular environment can only access the cytosol via anion channels or via conversion to lipophillic species. The concentration, type and rate of formation of ROS and free radicals in addition to the oxidation of biological macromolecules contribute to the pathophysiology of oxidative stress. Alternatively, reducing the ability of the cell to detoxify ROS by depletion of the antioxidant defence system can induce oxidative stress. However, the enhanced gene expression of proteins or their activities involved in the antioxidant defence system is a marker of enhanced ROS production in an attempt by individual cells or tissues to cope with the elevated incidence of oxidative stress (as reviewed in; Evans *et al.*, 1997; Raha & Robinson, 2000; see Chapter 1).

Several factors are involved in the development of oxidative stress within the joint of RA patients including elevated pressure in the synovial cavity, reduced capillary density, vascular changes and enhanced synovial tissue metabolic rate. Locally activated leukocytes also produce ROS (as reviewed in; Hallliwell, 1995). PBL and urine from RA patients contain significantly elevated levels of the excreted pro-mitogenic 8-oxohydroxyguanosine, a product of oxidative DNA damage indicating genotoxic damage (Bashir *et al.*, 1993; Hassan *et al.*, 2001; Jikimoto *et al.*, 2001). In addition, lipid peroxidation products, and both CuSOD and MnSOD activity in whole blood were significantly elevated in patients with RA compared to normals. This was also associated with reduced amount of non-protein thiols and serum transferrin levels (Ostrakhovitch & Afanas'ev, 2001; Taraza *et al.*, 1997; Taysi *et al.*, 2002). In comparison to normals, PBN SOD activity was reduced in RA while "loose" iron in the plasmalemma of neutrophils and monocytes was enhanced (Ostrakhovitch & Afanas'ev, 2001). Serum from RA patients contains 50% less GSH and GSR than that of normals with a 45% reduction in GSH Px, while GST activity is enhanced 3 fold (Hassan *et al.*, 2001). Plasma thioredoxin (Trx) levels are enhanced in RA patients compared to normals reflecting a systemic effect of chronic inflammation. Further, the Trx levels within the synovium were greater than those of non-RA patients and the plasma Trx concentration of rheumatoids suggesting local production at the site of inflammation, which subsequently seeps into the systemic circulation (Jikimoto *et al.*, 2001; Maurice *et al.*, 1997). Furthermore, plasma Trx levels were greater in severe RA than in patients with mild or inactive RA as determined by the Lansbury index (Jikimoto *et al.*, 2001).

Utilising the chemiluminescence of the superoxide sensitive and mitochondria selective probe lucigenin, monocytes and neutrophils from RA patients were shown to possess enhanced superoxide levels than those of non rheumatiods. This enhanced concentration of ROS correlated with the plasma TNFα concentration (Miesel *et al.*, 1996). Neutrophils and monocytes isolated from the peripheral whole blood of patients with RA display elevated spontaneous free radical production compared to normals as measured by luminol and lucigenin chemiluminescence. This elevated chemiluminescence observed in RA monocytes was repressed by the complex III inhibitor A.A and complex I inhibitor rotenone, but these agents had little effect on the spontaneous free radical production from normal monocytes (Ostrakhovitch & Afanas'ev, 2001). Collectively, these observations are suggestive that mitochondrial ROS formation in RA monocytes and neutrophils contribute to RA pathology. SOD and the natural non-toxic bioflavanoid rutin (vitamin P) inhibited the enhanced chemilumescence observed in RA neutrophils which was only weakly inhibited by the hydroxyl radical scavenger mannitol or the iron chelator desferrioxamine (DF) and slightly enhanced by catalase. These findings indicate that the major free radical species produced by circulatory neutrophils is superoxide. However, there was no difference between the free radical production of PMA activated neutrophils *in vitro* from normals and RA, although the free radical production was three fold greater than that observed in monocytes which reflected differences in their NADPH activities (Ostrakhovitch & Afanas'ev, 2001). Ostrakhovitch & Afanas'ev, (2001) described that in addition to NADPH oxidase activity, RA neutrophil superoxide formation was inhibited by approximately 50% in the presence of NO synthase inhibitor NMMA, and was slightly enhanced by L-arginine suggesting the involvement of NO synthase. However, this study did not comment on the role of

NO synthase in the production of superoxide in normal neutrophils, although NO synthase in RA neutrophils generated enhanced amounts of peroxynitrite than in normal neutrophils as followed by NMMA-inhibited DHR oxidation (Ostrakhovitch & Afanas'ev, 2001).

In addition to causing direct cellular and biological macromolecule damage, at lower concentrations there is a plethora of evidence for ROS to participate in an intracellular signalling capacity for a diverse range of external stimuli of physiological, pharmacological or environmental source (Cossarizza *et al.,* 1995; Mansat-de Mas *et al.,* 1999; Schulze-Osthoff *et al.*, 1992; Verheij *et al.*, 1996). The direct application of ROS or agents that induce their formation can directly affect the activity of various intracellular kinases, phosphatases, transcription factors and caspases (Dröge *et al.*, 1994; Knebel *et al.*, 1996; Manna *et al.*, 1999; Schulze-Osthoff *et al.*, 1994; see Chapter 2). TNFα has been observed in various immortalised cell lines to possess various redox altering properties including enhancement $[GSH]_i$, GSSG and lipid peroxidation (Böhler *et al.*, 2000; Yamauchi *et al.*, 1989; Zimmerman *et al.*, 1989). The exposure of the murine fibrosarcoma cell line L9292 to TNFα induced an enhancement in the fluorescence of mitochondrial specific, peroxide sensitive probe DHR123, indicating the involvement of the mitochondria in the generation of ROS in response to TNFα stimulation (Goossens *et al.*, 1995). Furthermore, iron chelators, antioxidants and free radical scavengers specifically inhibit TNFα and IL-1β induced apoptosis (Cossarizza *et al.*, 1995; Liu *et al.*, 1998; Schulze-Osthoff *et al.*, 1992; Wong *et al.,* 1989; Yamauchi *et al.*, 1989). The overexpression of MnSOD in the human breast carcinoma MCF-7 cell line prevented TNFα induced activation of the redox sensitive transcription factors NFκB

and AP-1, the former being associated with prevention of IκB degradation and NFκB dependent gene expression. MnSOD overexpression also prevented MEK and JNK activation suggesting they are downstream of TNFα induced ROS production. Furthermore, MnSOD suppressed TNFα induced caspase-3 activation; an enzyme essential for TNFα induced apoptosis (Manna *et al.*, 1999). However, ROS involvement as an intracellular signalling intermediate following CD95 activation is contentious, where various authors have reported ROS independent and dependent mechanisms in CD95-induced apoptosis (Dumont *et al.*, 1999;Hug *et al.*, 1994; Jayanthi *et al.*, 1999; Laouar *et al.*, 1999; Petit *et al.*, 2001; Schulze-Osthoff *et al.*, 1994; Suzuki *et al.*, 1998; Suzuki & Ono, 1999). Controversially, it is reported in this thesis that CD95L treatment of Jurkat T-cells, in agreement with a role for ceramide signalling involvement, reduces the $[peroxide]_{cyt}$ (see Chapter 2).

As discussed (see Chapters 1 & 2), ceramide has been identified as a signalling intermediate in response to the cellular stimulation by pro-inflammatory cytokines associated with RA, namely IL-1β, TNFα and CD95L. The accumulation of endogenous ceramide is largely associated with an ensuing apoptotic response, although proliferation and growth arrest have also been reported. The cellular redox state has been implicated as playing an essential role in the regulation of one of the three enzymes responsible for ceramide production, N-SMase. Cellular GSH is believed to be negatively regulate N-SMase, where GSH depletion leads to N-SMase activity and ceramide accumulation. Further, TNFα reduced the intracellular level of GSH enhancing N-SMase activity and SM hydrolysis associated with elevated levels of endogenous ceramide (Liu & Hannun, 197; Liu *et al.*, 1998). In addition to the redox regulation of ceramide metabolism, it has been discussed here (see Chapter 2)

and by others through the use of short chain synthetic ceramides or the application of agents that mediate the accumulation of endogenous ceramide, that an intracellular accumulation in this sphingolipid can modulate ROS production at the mitochondria (de Gannes *et al.*, 1998; Garcia-Ruiz *et al.*, 1997; Gudz *et al.*, 1997; Quillet-Mary *et al.*, 1997) and another undefined site (see Chapter 2).

A closely related lipid to ceramide, DAG, has been recognised to directly antagonise the effects of ceramide. Like ceramide, DAG is a neutral hydrophobic lipid with similar physical properties (see Chapter 1; as reviewed in; Hannun & Luberto, 2000). Diglycerides constitute the primary structure for all naturally occurring glycerolipids that possess differing compositions of saturated and unsaturated fatty acids. DAG are glycerol derivatives where two hydroxyl groups have been substituted by fatty acids through ester bond formation (see Chapter 1). The physiologically relevant species is 1,2-diacyl-*sn*-glycerol although which isomer is physiologically active is unclear. Most often physiological DAG possesses two different fatty acid chains. The one found at the *sn*-1 position tends to be saturated and the other unsaturated (as reviewed in; Goñi & Alonso, 1999).

DAG is proposed to act as a positive mitogenic stimulus, which is opposed by endogenous ceramide. Indeed their production lies at opposite ends of a long and complex metabolic pathway, where their regulation appears to be simultaneously regulated albeit in opposing directions (see Figure 4.1; as reviewed in; Ruvulo, 2001). DAG is actually a minor component of cellular membranes, constituting 1-2 mol%, although transformed cells have up to a 10 fold greater membrane concentration likely to be functioning at a threshold for protein activation. Due to its localisation,

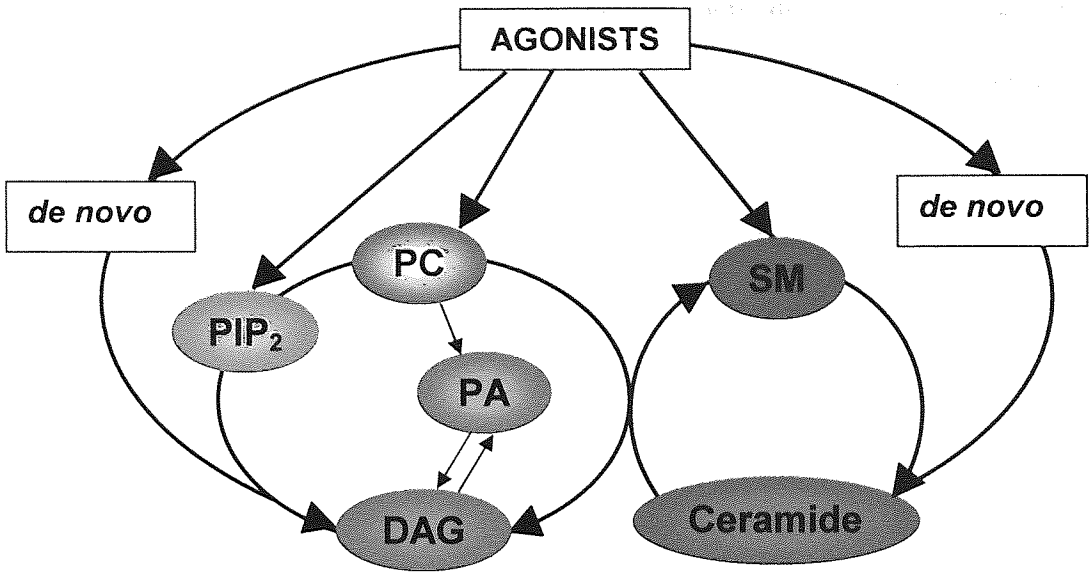

Figure 4.1. Simplified schematic of the metabolic interrelationship between ceramide and diacylglycerol. Abbreviations used; DAG, diacylglycerol; PA, phospatidic acid; PC, phospatidylcholine; PIP_2, phophatidylinositol bisphosphate; SM, sphingomyelin (adapted from; Bielawska *et al.*, 2001; Kanoh *et al.*, 1993).

DAG modifies the activity of intrinsic or extrinsic membrane related enzymes, or soluble proteins which translocate form the cytosol to the membrane to associate with their substrates. An elevation in DAG levels occurs as a result of specific agonist-receptor interactions at the cell surface where the kinetics of DAG formation appears to be cell type and agent specific. DAG may be derived from phosphatidylinositol through PI specific phospholipase C hydrolysis. These are usually polyunsaturated of the type 1 stearyl-2-arachidonoyl-*sn*-glycerol. Saturated, mono- or bi-unsaturated DAG's are derived from either phosphatidylcholine (PC) via the action of PC-phospholipase C or the combined action of phospholipase D and phospatidate phosphatase. Thirdly, DAG may be formed following the activation of a de novo pathway of glycerol lipid synthesis (see Figure 4.1; as reviewed in; Bielawska *et al.*, 2001; Goñi & Alonso, 1999).

Although cell type dependent, ceramide largely activates signal transduction pathways associated with apoptosis whereas DAG activates classical and novel forms of protein kinase C (PKC), and phospholipases which are allied with cell survival (as reviewed in; Goñi & Alonso, 1999). These two classes of DAG targets represent the most studied and it should be appreciated that these are not exclusive. The ensuing activation of PKC stimulates a cascade of other signalling intermediates by transferring phosphoryl groups to other proteins such as MAPK. In cohort with DAG induced PKC activation, an elevation in $[Ca^{2+}]$ is observed following TCR stimulation (as reviewed in; Altman *et al.*, 1992; Berridge, 1997). DAG enhances the activity of phospholipases A2 and C. These are members of a heterogenous group of enzymes that hydrolyse glycerophospholipids and also lead to the formation of a soluble form of DAG (as reviewed in; Goñi & Alonso, 1999).

The enhancement of DAG levels following protein tyrosine kinase activation induced by TCR stimulation is a widely accepted pathway for the induction of T-cell proliferation and immune response (as reviewed in; Altman *et al.*, 1992; Berridge, 1997), however, the involvement of ceramide in TCR signalling is contentious. Jurkat T-cells treated with C_2-ceramide for 4 hours downregluate the TCR receptor while lower concentrations upregulate TCR expression by 10-15% in freshly isolated human T-cells. CD8 ligation in resting and activated primary murine T-cells and in Jurkat T-cells leads to A-SMase activation resulting in a rapid and transient rise in endogenous ceramide. In the presence of anti-CD3 MoAb, exogenously applied A-SMase or C_6-ceramide enhanced T-cell proliferation (as cited in; Adam *et al.*, 2002). In contrast, inhibition of proliferation has been reported by others (Mengubas *et al.*, 1999; O'Byrne & Sanson, 2000).

Rather than a simple elevation in one of these lipids to induce an apoptotic or proliferative response, it is hypothesised that it is the ratio or balance between the two that is the key to dictating cell fate to external stimuli which utilise them as signalling intermediates. Indeed, Flores *et al.,* (2000) showed that in the activated human T-lymphocyte cell line Kit 225, the addition of IL-2 to induce proliferation was preceded by an elevation in DAG levels with a concomitant reduction in endogenous ceramide, the DAG:ceramide ratio increased. Conversely, upon IL-2 withdrawal to induce mild apoptosis, an increase in the endogenous ceramide levels was observed which was associated with a reduction in cellular DAG content, i.e., the DAG:ceramide ratio was reduced. This pattern was reflected in the DAG and ceramide precursors phospatidylcholine and SM respectively (Flores *et al.*, 2000). The signal transduction pathways involving lipid metabolism during T-cell activation are unclear and the possible contribution of ceramide and DAG to the enhanced survivability of T-cells in rheumatoid arthritis remains unstudied. Indeed, intracellular signalling of the DAG target Ca^{2+} is defective in PHA induced activation of peripheral whole blood T-cells from patients with RA (Carruthers *et al.*, 1996).

Collectively, the pathology of RA is suggestive of enhanced oxidative stress within the periphery and synovium. Additionally, individual cells possess elevated ROS production which is reminiscent of an altered redox state with the consequence of defective intracellular lipid signalling. It is hypothesised that the inability of T-cells to undergo apoptosis and as a result, persist within the synovial joint to contribute to the chronic inflammation associated with RA, is due to a dysfunction in the capacity of T-cells to transduce proliferative and or apoptotic signals in response to external

stimuli. ROS, ceramide and DAG have been identified to be of significant importance in mediating the intracellular response to apoptotic and proliferative agents, many of which are associated with the pathology of RA. It is proposed that defects in the endogenous levels of ROS production, ceramide and DAG contribute to the enhanced survivability of T-cells in RA. To address this hypothesis, cytosolic peroxide ($[peroxide]_{cyt}$), endogenous ceramide and endogenous DAG were quantified immediately after T-cell isolation from peripheral whole blood, or following culture of resting or *in vitro* activated T-cells.

4.2 Materials and Methods.

4.2.1 Patients.

Venous blood was obtained from consenting patients (see Appendix) with RA. All patients were evaluated and diagnosed by Dr. G.D. Kitas, consultant rheumatologist at the Dudley NHS Trust of Hospitals, UK, as having RA according to the criteria of the American College of Rheumatology (Arnet *et al.*, 1988). Ethical approval was granted from Dudley Local Research Committee (See Appendix). Patients on disease modifying anti-rheumatic drugs were excluded. Laboratory markers of inflammation – the erythrocyte sedimentation rate (ESR) and C-reactive protein (CRP) were noted. As controls, venous blood was obtained from consenting volunteers who did not meet any of the criteria for the diagnosis of RA as depicted by the American College of Rheumatology (Arnet *et al.*, 1988) and matched for sex and age with no statistical difference between the two groups.

4.2.2 T-cell isolation and culture.

Peripheral blood mononuclear cells (PBMNC) were isolated by density gradient centrifugation over Lymphoprep^{TM} (Nycomed Pharma AS, Oslo, Norway) and the resting T-cells purified by negative isolation employing magnetic beads (Dynal A.S., Oslo, Norway) as described in Methods 2.2.3 & 2.2.4. For *ex vivo* examination, T-cells were analysed for $[peroxide]_{cyt}$ and lipid content immediately following

isolation. Additionally, resting T-cells were cultured for 72 hours in RMPI 1640 supplemented with 10% FCS and 1% P/S with or without 10μg of PHA per $2x10^6$ /ml T-cells to activate as described in Method 2.2.5. Prior to further experimental manipulation, T-cells in culture were washed twice with serum free RPMI 1640.

4.2.3 Assessment of T-cell purity, activation and contamination.

Immediately following T-cell isolation, cell suspension were analysed for T-cell purity and monocyte contamination according to the percentage of $CD3^+$ and $CD14^+$ cells by flow cytometry (Hickling, 1998) according to Method 2.2.8. The activation of 72 hour cultured resting or PHA activated PBL was determined by flow cytometric evaluation of the membrane expression of CD25 (IL-2 receptor; Hemler *et al.*, 1984) within the $CD3^+$ T-cell population as described Method 2.2.8.

4.2.4 Quantification of endogenous T-cell ceramide and DAG content.

Lipids from resting, PHA-activated, or *ex vivo* T-cells ($1x10^6$/ml) were extracted according to the method of Bligh & Dyer, (1959) and the concentration of ceramide and DAG quantified by the DAGK assay as described in Methods 2.2.16 – 20.

4.2.5 Evaluation of T-cell [peroxide]$_{cyt}$.

The [peroxide]$_{cyt}$ of primary human T-cells was determined utilising a modified version of the standard [peroxide]$_{cyt}$ assay utilising the fluorescence generated from Jurkat T-cells loaded with DCFH-DA as a standard reference point. Jurkat T-cells, resting, PHA-activated or *ex vivo* T-cells ($1x10^6$/ml) were resuspended in serum free RPMI 1640 and loaded with 50μM of DCFH-DA for 40 minutes under the conditions previously determined (see Method 2.2.10). At the end of the DCFH-DA incubation period, the MdX DCF fluorescence of the viable Jurkat T-cell population was analysed by flow cytometry and set to channel 100. Subsequent analysis of the viable resting, activated and *ex vivo* T-cells DCF fluorescence was made against the Jurkat T-cell DCF standard. The MdX DCF value of 10,000 cells from each sample was recorded.

4.3 Results.

Resting T-cells were isolated from the peripheral whole blood of patients diagnosed with RA and those from consenting, apparently healthy individuals. The mean age of the RA group was 56 ± 16 years (mean ± s.d; n = 13) and 47 ± 12 years (n = 11) for the normal group. The yield of resting T-cells isolated from 40mls of peripheral whole blood of rheumatoids ($8.016 \times 10^6 \pm 4.387$, n = 13) was equivalent to those from normals ($9.15 \times 10^6 \pm 6.53$, n = 11). T-cell purity and monocyte contamination was evaluated by flow cytometric evaluation of the percentage of $CD3^+$ and $CD14^+$cells within each sample. The average percentage of $CD3^+$ was 95.52 ± 4.12 (mean ± s.d; n = 13) in RA patients and 97.42 ± 2.6 (n = 11) in normals with a mean percentage of 1.05 ± 1.39 (n = 11) and 0.813 ± 0.976 (n = 13) $CD14^+$ monocytes in each group respectively. As a marker of T-cell activation, the membrane expression of CD25 was analysed. The percentage of T-cell CD25 expression immediately following isolation was 4.49 ± 4.11 (n =13) in rheumatoids and 2.59 ± 2.60 (n = 11) in normals. Following culture for 3 days in RMPI 1640 supplemented with 10% FCS and 1% P/S in the presence of 10μg/ml PHA there was a significant elevation in the membrane expression of CD25 to 55.35 ± 19.18 (n = 13) compared to 2.57 ± 2.72 (n =13) in RA T-cells cultured without PHA ($p<0.0001$). Normal T-cell CD25 expression was upregulated to the same extent upon culture with PHA as observed in RA T-cells, from 2.09 ± 0.84 (n =11) in resting T-cells to 46.86 ± 18.46 (n = 11) $p<0.0001$) in activated T-cells. Cytosolic peroxide ($[peroxide]_{cyt}$), endogenous ceramide and DAG were then quantified directly after isolation for *ex vivo* examination, the effects of

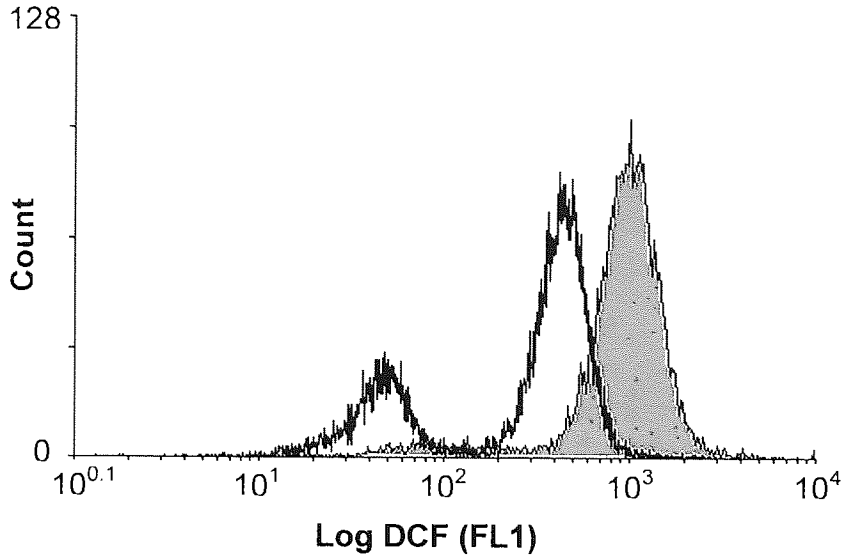

Figure 4.2. Jurkat T-cell reference for the analysis of DCF fluorescence from primary T-cells. Jurkat T-cell ($1x10^6$/ml) were resuspended in serum free RPMI 1640 and incubated with 50μM DCFH-DA for 40 minutes in a 95% air, 5% CO_2 humidified atmosphere. At the end of the incubation period, the viable cell population, determined by forward scatter and side scatter properties, was analysed for DCF fluorescence on a single parameter histogram of FL1 (DCF) versus count. The median X (MdX) DCF fluorescence was set to 100 (grey fill). Primary T-cells ($1x10^6$/ml; no fill) were then loaded with 50μM DCFH-DA for 40 minutes in the described incubator conditions and analysed against the reference Jurkat T-cell DCF fluorescence. The MdX of 10,000 cells was recorded for each sample.

activation were observed after 3 days of stimulation *in vitro* with 10μg/ml of PHA utilising non-stimulated, resting T-cells in identical culture conditions as controls.

To standardise the flow cytometric evaluation of DCF fluorescence in primary T-cell population Jurkat T-cells ($1x10^6$/ml) were loaded with 50μM DCFH-DA for 40 minutes. At the end of this incubation period, the DCF fluorescence of the immortalised cell line Jurkat T-cell was analysed immediately by flow cytometry. The MdX of the Jurkat T-cell DCF fluorescence peak was set to channel 100 and acted as a reference point for consequent evaluation of DCF fluorescence in primary T-cells (see Figure 4.2).

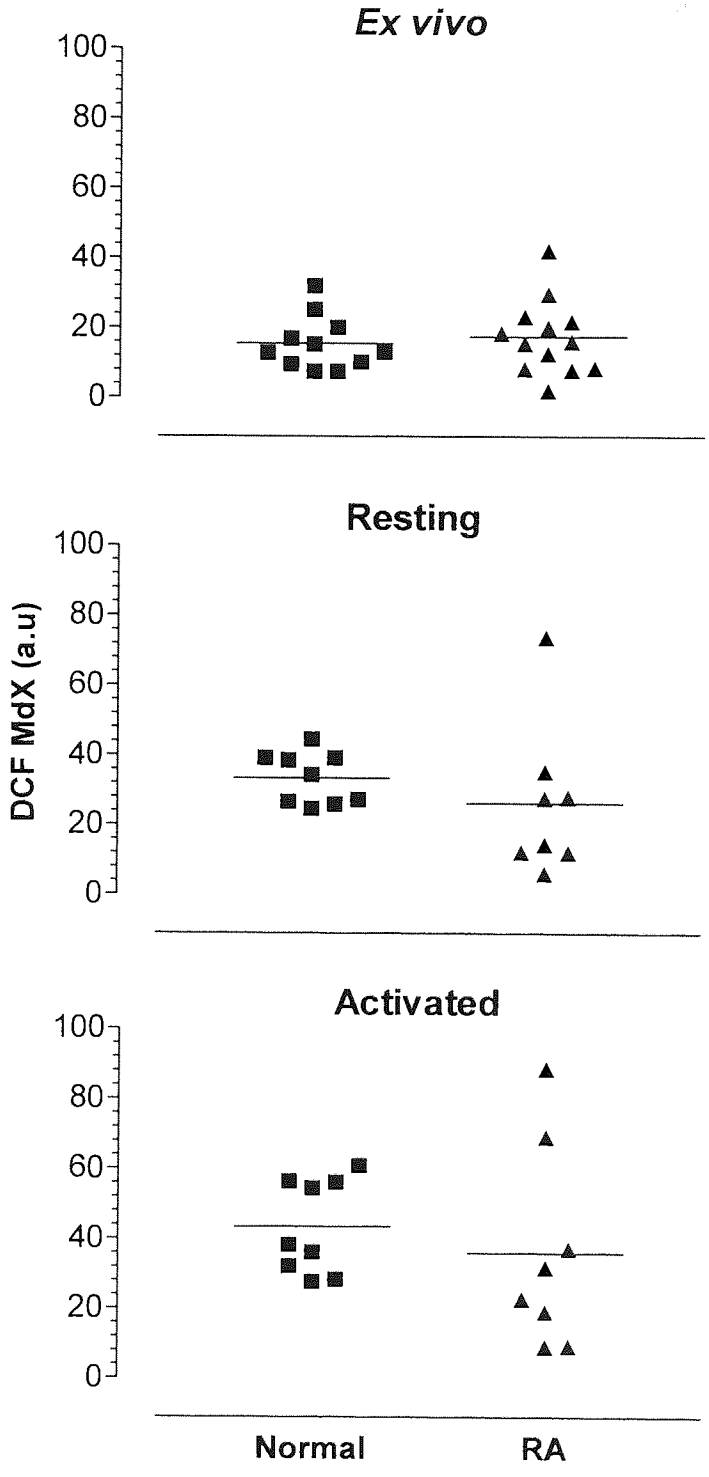
Ex vivo
100
80
60
40
20
0
Resting
DCF MdX (a.u)
Activated
Normal
RA

Figure 4.3. The cytosolic peroxide concentration of T-lymphocytes from peripheral whole blood of rheumatoids does not differ to that of normals. Resting $CD3^+$ T-lymphocytes were isolated and purified from the venous blood from normal healthy volunteers or individuals with rheumatoid arthritis (RA) as described in methods 4.2.2 and 4.2.3. To examine the cytosolic peroxide concentration $[peroxide]_{cyt}$, T-cells were resuspended in serum free RPMI 1640 and incubated for 40 minutes with 50μM DCFH-DA. At the end of the incubation period, the viable T-cell population determined by forward scatter and side scatter parameters, were analysed by flow cytometry for DCF fluorescence on a single parameter histogram of log FL1 flourescence versus count. Recordings were made against a standard DCF fluorescence of Jurkat T-cells treated identically as controls and set to a DCF MdX channel of 100 as described in method 4.2.5. The median fluorescence (MdX) of 10,000 T-cells from each sample was recorded. For *ex vivo* determination of $[peroxide]_{cyt}$ concentration, cells were loaded with DCFH-DA immediately following purification. To examine the effect of culture and activation on $[peroxide]_{cyt}$, T-cells were cultured at a concentration of $2x10^6$/ml in RPMI 1640 supplemented with 10% FCS and 1% P/S in the presence or absence of 10μg/ml of PHA for 3 days. All incubations were performed in a humidified 95% air, 5% CO_2 humidified atmosphere. Each data point represents the DCF MdX value obtained from each individual. Bars represent the mean DCF MdX value of each group. Statistical analysis for significance between normals and rheumatoids was performed by Mann Whitney non-parametric U-test. Arbitary units, a.u.

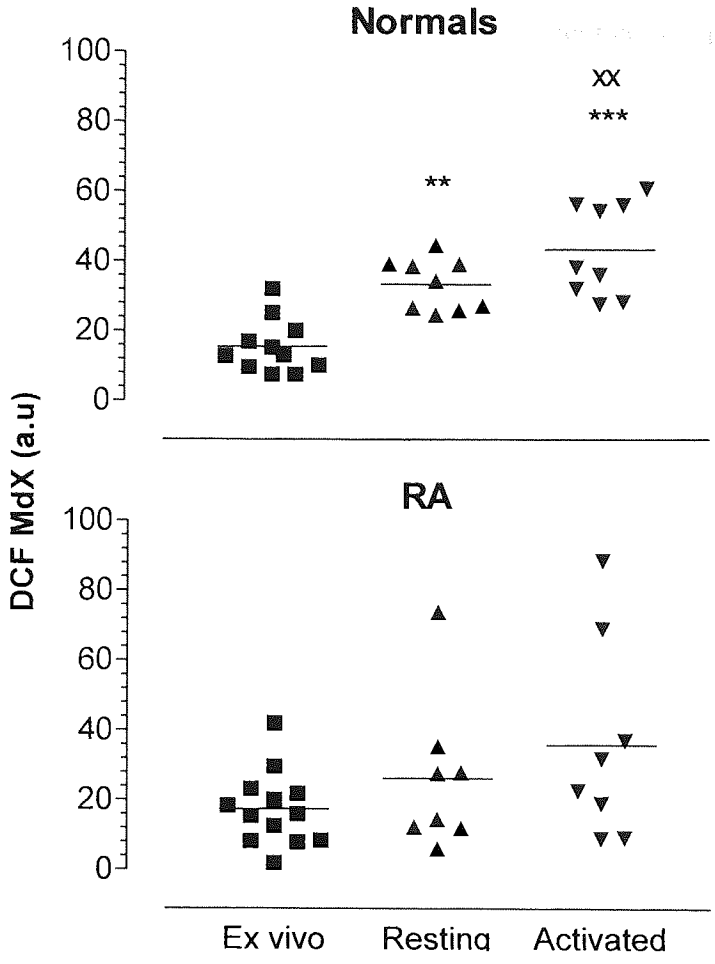

Figure 4.4. The effect of cell culture on cytosolic peroxide concentration of T-lymphocytes from peripheral whole blood of normal and rheumatoid subjects. Resting $CD3^+$ T-lymphocytes were isolated and purified from the venous blood of normal healthy volunteers or individuals with rheumatoid arthritis as described in methods 4.2.2.and 4.2.3. To examine the cytosolic peroxide concentration $[peroxide]_{cyt}$, T-cells were resuspended in serum free RPMI 1640 and incubated for 40 minutes with 50μM DCFH-DA. At the end of the incubation period, the viable T-cell population determined by forward scatter and side scatter parameters, were analysed by flow cytometry for DCF fluorescence on a single parameter histogram of log FL1 flourescence versus count. Recordings were made against a standard DCF fluorescence of Jurkat T-cells treated identically as controls and set to a DCF MdX channel of 100 as described in method 4.2.5. The median fluorescence (MdX) of 10,000 T-cells from each sample was recorded. For *ex vivo* determination of $[peroxide]_{cyt}$ concentration, cells were loaded with DCFH-DA immediately following purification. To examine the effect of culture and activation on $[peroxide]_{cyt}$, T-cells were cultured at a concentration of $2x10^6$/ml in RPMI 1640 supplemented with 10% FCS and 1% P/S in the presence or absence of 10μg/ml of PHA for 3 days. All incubations were performed in a humidified 95% air, 5% CO_2 humidified atmosphere. Each data point represents the DCF MdX value obtained from one individual. Bars represent the mean DCF MdX value of each group. ** ($p<0.01$) and ** ($p<0.001$) represent significant difference of resting T-cells and activated T-cells respectively from ex vivo T-cell by one way ANOVA followed by Dunnett's multiple comparison test. xx ($p<0.01$) represents statistical difference between resting and activated T-cells by Wilcoxon non-parametric matched pairs test. Arbitary units, a.u.

The DCF fluorescence of T-cells isolated from rheumatoid patients was not statistically different to that of normals *ex vivo* ($p>0.05$), or resting T-cells in culture ($p>0.05$) and activated T-cells in culture ($p>0.05$; see Figure 4.3). The mean DCF MdX value obtained from normal T-cells ex vivo was 15.51 ± 7.71 (mean $\pm$ s.d), $n = 11$, and was significantly increased upon culture for 3 days to 34.18 ± 7.48, $n=8$ ($p<0.01$) and elevated further following PHA activation to 44.83 ± 13.60, $n=8$ ($p<0.001$). Since T-cells from the same normal individual were cultured for 3 days with or without PHA, a Wilcoxon non-parametric matched paired T-test revealed that PHA activated T-cells *in vitro* from the same individual possessed greater DCF fluorescence than resting T-cell *in vitro* ($p<0.05$; see Figure 4.4). In the RA group, *ex vivo* T-cell DCF fluorescence was not different to either resting T-cells in culture ($p>0.05$) or PHA activated T-cell in culture ($p>0.05$). Furthermore, a Wilcoxon non-parametric matched paired T-test examining the difference between the DCF fluorescence of resting and activated T-cells *in vitro* from the same individual revealed no significant difference in $[peroxide]_{cyt}$ ($p>0.05$; see Figure 4.4).

There was no significant difference in the *ex vivo*, resting *in vitro* or PHA activated *in vitro* T-cell endogenous concentrations of ceramide or DAG between normals and rheumatoids ($p>0.05$; see Figures 4.5 & 4.6). In normals, the concentration of ceramide and DAG were the same *ex vivo* as in resting and PHA activated T-cells *in vitro* ($p>0.05$; see Figure 4.6), an observation reflected in patients with RA ($p>0.05$; see Figure 4.7).

DAG and ceramide have been suggested to mediate the opposing signal transduction pathways of proliferation and apoptosis respectively. Since these two lipids are

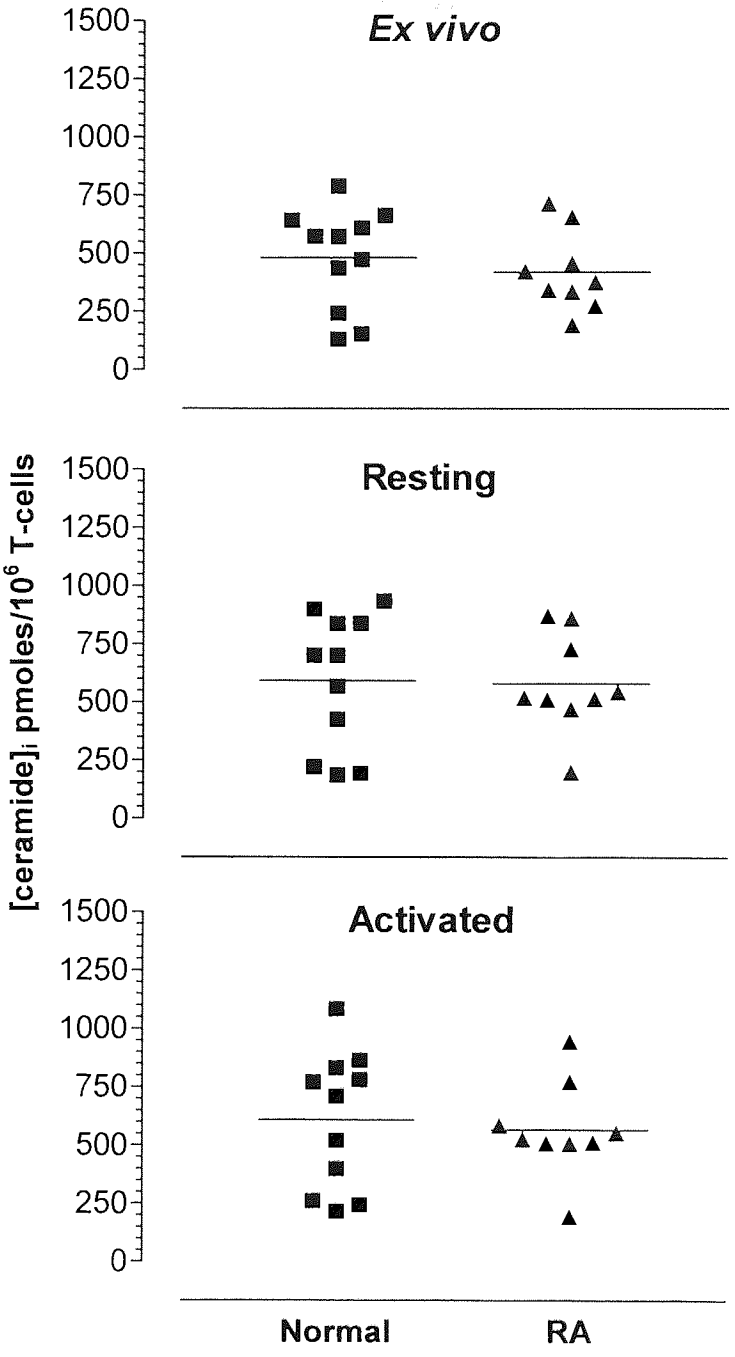

Figure 4.5. There is no difference in the endogenous ceramide and content of T-lymphocytes of normals and patients with rheumatoid arthritis (RA). Resting $CD3^+$ T-lymphocytes were isolated and purified from the venous blood of normal healthy volunteers or individuals with RA as described in methods 4.2.2 and 4.2.3. For *ex vivo* examination, lipids were extracted immediately following isolation. Lipid extraction of activated and resting T-cells was performed following 3 days of culture at a concentration of $2x10^6$/ml in RPMI 1640 supplemented with 10% FCS and 1% P/S in the presence or absence of 10μg/ml of PHA respectively. The ceramide content per 10^6 T-cells was quantified in duplicate utilising the DAGK assay as described in method 4.2.4. Each data point represents the mean ceramide content/10^6 T-cells obtained from one individual. Data were analysed for statistical significance between normals and patients with RA utilising the Mann-Whitney U test where a $p<0.05$ was considered to be significant. Bars represent the mean of each group.

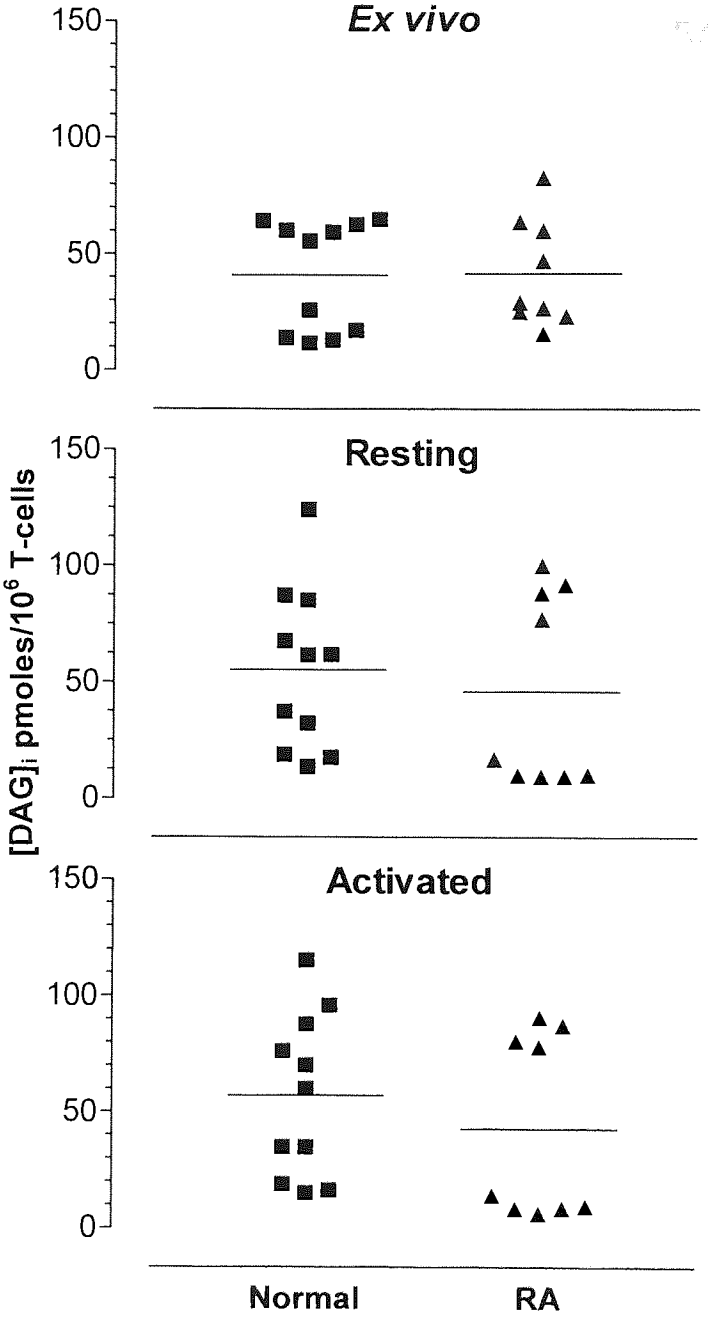

Figure 4.6. There is no difference in the endogenous diacylglycerol (DAG) and content of T-lymphocytes of normals and patients with rheumatoid arthritis (RA). Resting $CD3^+$ T-lymphocytes were isolated and purified from the venous blood of normal healthy volunteers or individuals with RA as described in methods 4.2.2 and 4.2.3. For *ex vivo* examination, lipids were extracted immediately following isolation. Lipid extraction of activated and resting T-cells was performed following 3 days of culture at a concentration of $2x10^6$/ml in RPMI 1640 supplemented with 10% FCS and 1% P/S in the presence or absence of 10μg/ml of PHA respectively. The DAG content per 10^6 T-cells was quantified in duplicate utilising the DAGK assay as described in method 4.2.4. Each data point represents the mean DAG content/10^6 T-cells obtained from one individual. Data were analysed for statistical significance between normals and patients with RA utilising the Mann-Whitney U test, where a $p<0.05$ was considered to be significant. Bars represent the mean of each group.

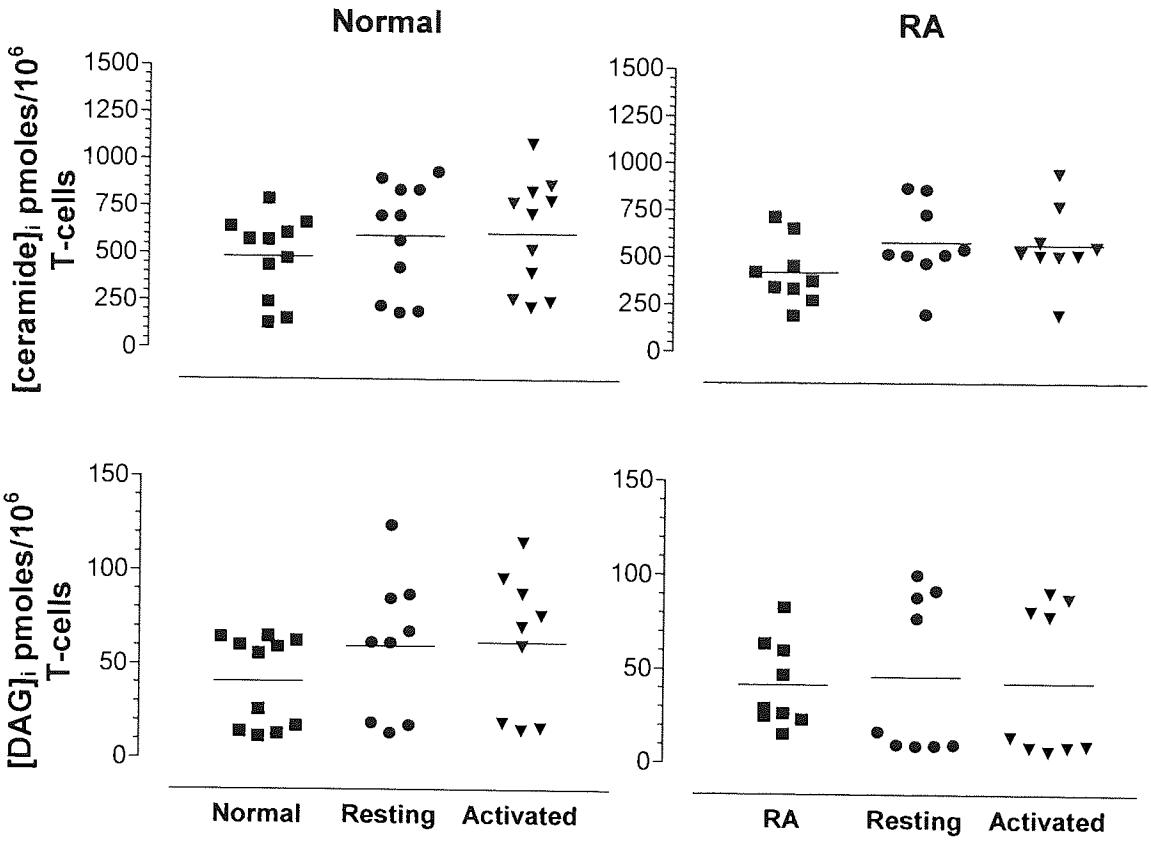

Figure 4.7. The culture of T-lymphocytes from normals or rheumatoid arthritis (RA) patients does not affect endogenous ceramide and diacylglycerol (DAG) levels. Resting $CD3^+$ T-lymphocytes were isolated and purified from the venous blood of normal healthy volunteers or individuals with RA as described in methods 4.2.2 and 4.2.3. For *ex vivo* examination, lipids were extracted immediately following isolation. Lipid extraction of activated and resting T-cell was performed following 3 days of culture at a concentration of $2x10^6$/ml in RPMI 1640 supplemented with 10% FCS and 1% P/S in the presence or absence of 10μg/ml of PHA respectively. T-cells were washed twice with serum free RPMI 1640 prior to lipid extraction. All incubations were performed in a humidified 95% air, 5% CO_2 humidified atmosphere and the ceramide or DAG content per 10^6 T-cells quantified in duplicate utilising the DAGK assay as described in method 4.2.4. Each data point represents the mean ceramide or DAG content/10^6 T-cells obtained from one individual. Statistical analysis was performed by one-way ANOVA followed by Tukey's post *hoc* test. Statistical difference between the endogenous ceramide/DAG content of resting and activated T-cells was evaluated by a Wilcoxon non-parametric matched pairs T-test was performed, where $p<0.05$ was considered significant. Bars represent the mean of each group.

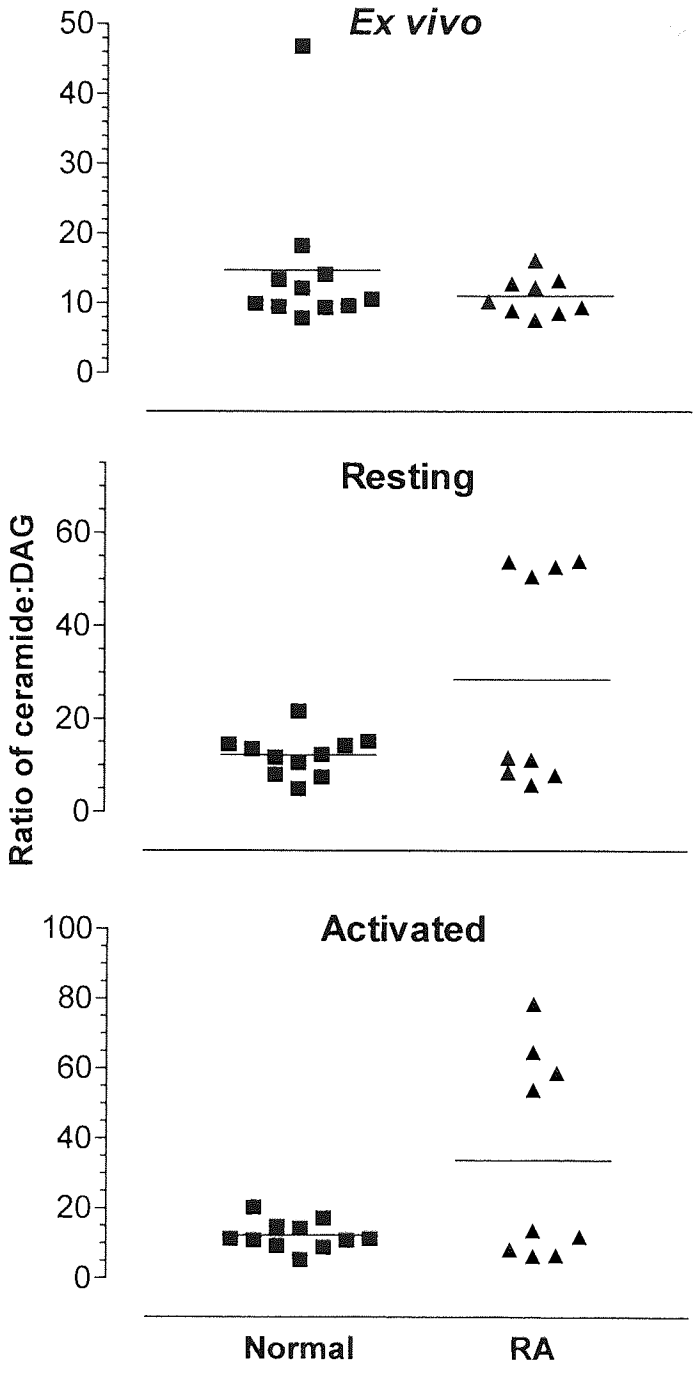

Figure 4.8. There is no difference in the ratio of endogenous ceramide to diacyglycerol (DAG) content of T-lymphocytes of normals and patients with rheumatoid arthritis (RA). Resting $CD3^+$ T-lymphocytes were purified from the venous blood of normal healthy volunteers or individuals with RA as described in methods 4.2.2.and 4.2.3. For *ex vivo* examination, lipids were extracted immediately following isolation. Lipid extraction of activated and resting T-cells was performed following 3 days of culture at a concentration of $2x10^6$/ml in RPMI 1640 supplemented with 10% FCS and 1% P/S in the presence or absence of 10μg/ml of PHA respectively. The ceramide and DAG content per 10^6 T-cells were quantified in duplicate utilising the DAGK assay as described in method 4.2.4. Each data point represents the ratio of ceramide to DAG obtained from one individual. Data were analysed for statistical significance between normals and RA patients utilising the Mann-Whitney U test. Bars represent the mean of each group.

metabolites of one another, it is the relative balance in their endogenous concentration that may dictate the ability of cells to survive or perish, rather than an elevation in one of the lipids. Consequently, the relative ratio of ceramide to DAG was analysed in T-cells from rheumatoids compared to normals. There was no significant difference in the ratio of ceramide to DAG in *ex vivo* T-cells, resting T-cells *in vitro* and PHA activated T-cells *in vitro* between normals and RA patients ($p>0.05$; see Figure 4.8)

The ages of individuals from the normal and RA groups displayed no correlation with the number of T-cells extracted from 40mls of peripheral whole blood, the T-cell DCF MdX, endogenous T-cell ceramide concentration or endogenous DAG concentration (see Figure 4.9).

Given the observations described here of synthetic short chain ceramide mediated antioxidant-like effects (see Chapter 2) and the reports by others of redox regulation in the generation of ceramide, it was hypothesised that DCF fluorescence of T-cells and endogenous T-cell ceramide or DAG concentration may be related and may differ between healthy individuals and those diagnosed with RA. However, no significant correlation existed between DCF fluorescence and endogenous ceramide or DAG concentrations of *ex vivo* T-cells from either the rheumatoid or normals group (see Figure 4.10).

Serum CRP levels and ESR are often quoted to describe the severity of inflammatory disease. The CRP score and ESR of RA patients involved in this study showed a strong positive correlation (see Figure 4.11). The DCF MdX values of T-lymphocytes *ex vivo* obtained from patients with RA negatively correlated with their

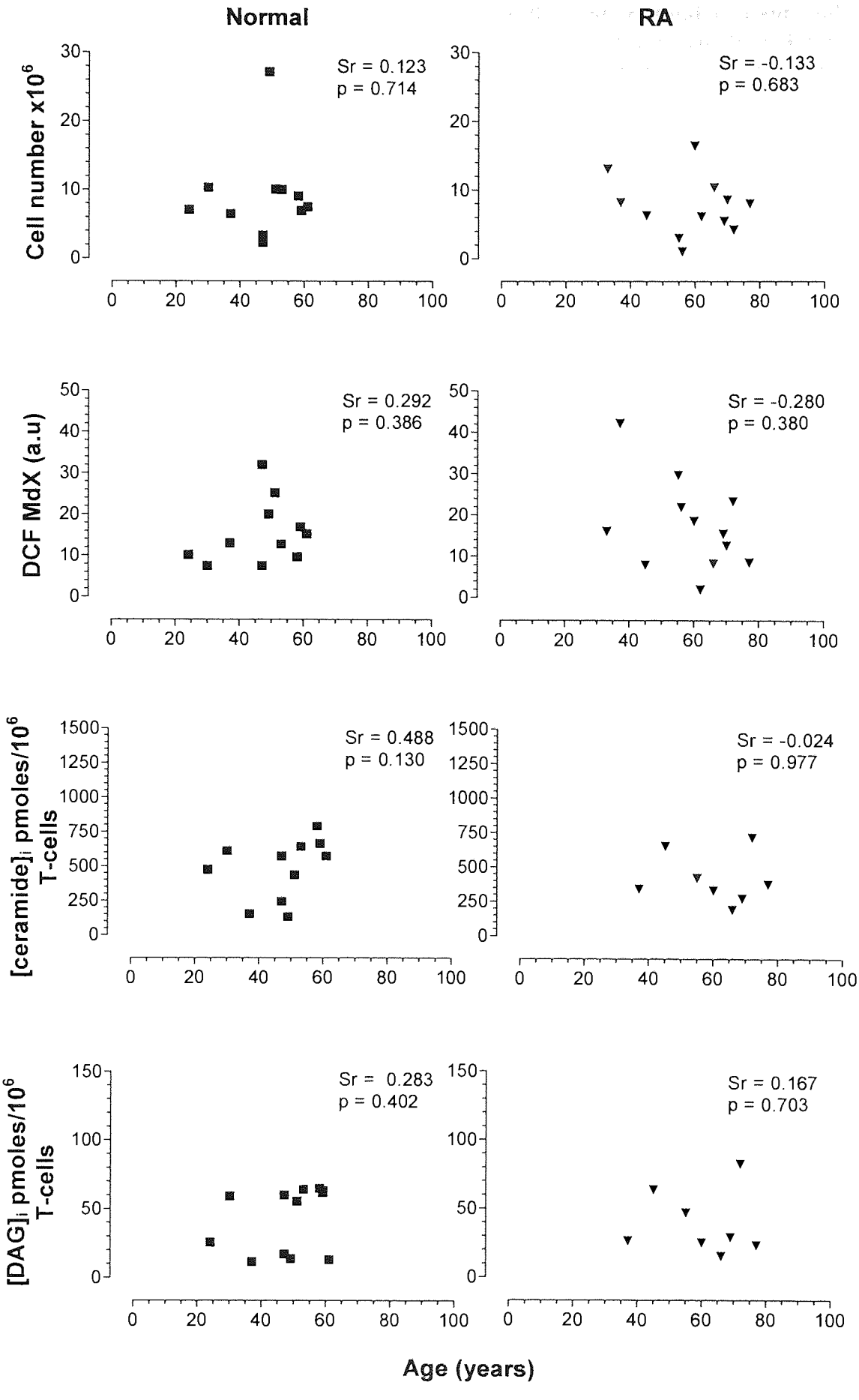
Normal
RA
Cell number x10^6
Sr = 0.123
p = 0.714
Sr = -0.133
p = 0.683
DCF MdX (a.u)
Sr = 0.292
p = 0.386
Sr = -0.280
p = 0.380
[ceramide]i pmoles/10^6 T-cells
Sr = 0.488
p = 0.130
Sr = -0.024
p = 0.977
[DAG]i pmoles/10^6 T-cells
Sr = 0.283
p = 0.402
Sr = 0.167
p = 0.703
Age (years)

Figure 4.9. Correlations between age and T-cell number, lipid content and cytosolic peroxide levels. The number of freshly isolated viable T-cells from 40mls of peripheral whole blood from consenting normals and rheumatoids were determined by trypan blue exclusion using an improved Neubauer haemocytometer (Weber Scientific International Ltd., Teddington, UK). Consequently, lipids were extracted and the ceramide and diacylglycerol (DAG) content per 10^6 T-cells quantified in duplicate by the DAGK assay as described in method 4.2.4. To examine the cytosolic peroxide concentration $[peroxide]_{cyt}$, T-cells were resuspended in serum free RPMI 1640 and incubated for 40 minutes with 50μM DCFH-DA. At the end of the incubation period, the viable T-cell population determined by forward scatter and side scatter parameters, were analysed by flow cytometry for DCF fluorescence on a single parameter histogram of log FL1 flourescence versus count. Recordings were made against a standard DCF fluorescence of Jurkat T-cells treated identically as controls and set to a DCF MdX channel of 100 as described in method 4.2.5. The median fluorescence (MdX) of 10,000 T-cells from each sample was recorded. Each data point represents a normal individual or a patient diagnosed with rheumatoid arthritis (RA). Data was analysed for correlation using Spearman's rank analysis where $p<0.05$ was considered significant. Statistical analysis was performed by GraphPad prism. Shown in each histogram are the significance value (p) and Spearman's rank correlation coefficient (Sr). Arbitary units, a.u.

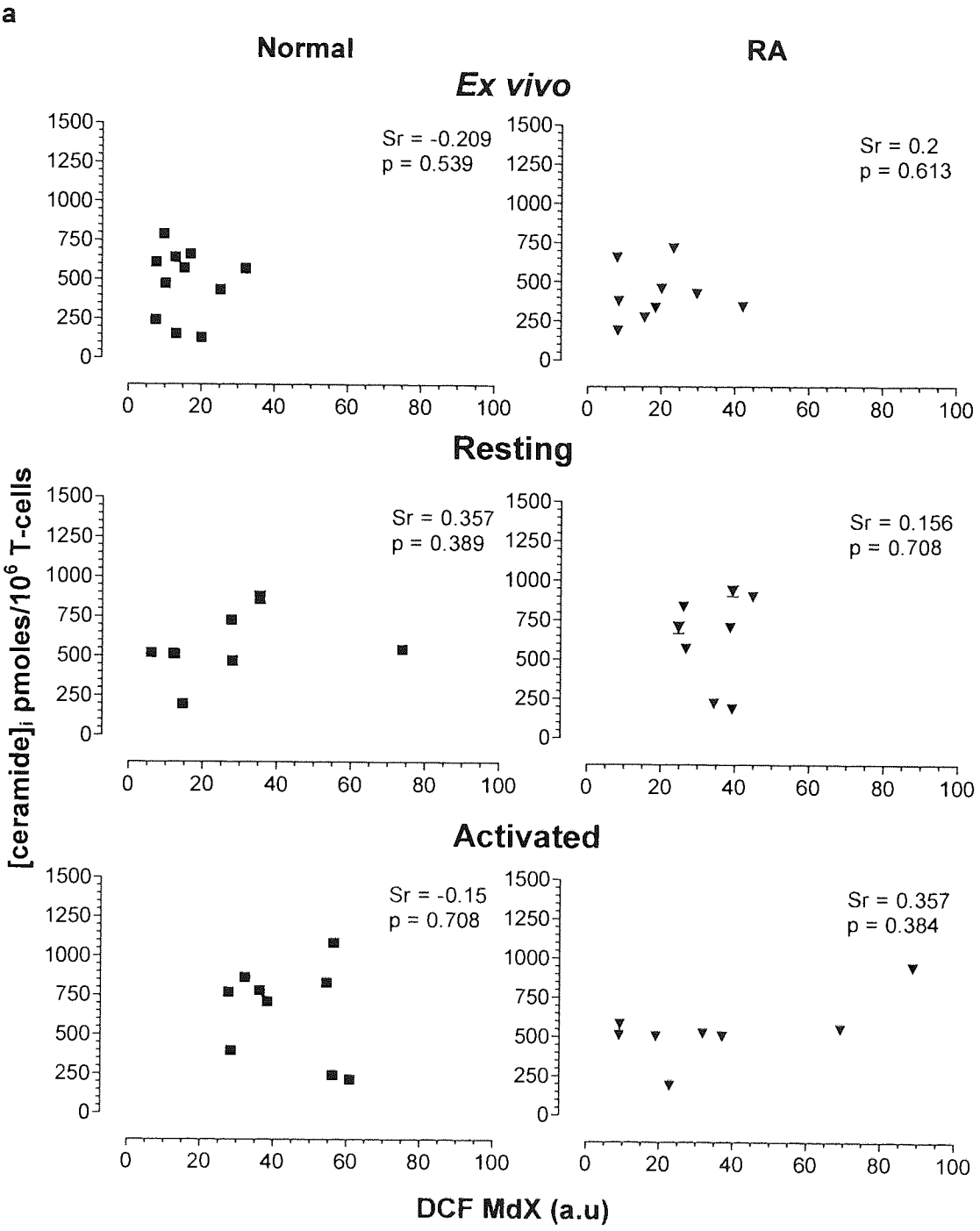

Figure 4.10. No correlation exists between the cytosolic peroxide levels and either ceramide or diacylglycerol (DAG) in T-lymphocytes from normals or individuals with rheumatoid arthritis (RA). Resting $CD3^+$ T-lymphocytes were isolated and purified from the venous blood of normal healthy volunteers or individuals with RA as described in methods 4.2.2 and 4.2.3. Lipids were extracted and the ceramide and DAG content per 10^6 T-cells quantified in duplicate utilising the DAGK assay as described in method 4.2.4. To examine the cytosolic peroxide concentration ($[peroxide]_{cyt}$), T-cells were resuspended in serum free RPMI 1640 and incubated for 40 minutes with 50μM DCFH-DA. At the end of the incubation period, the viable T-cell population determined by forward scatter and side scatter parameters, were analysed by flow cytometry for DCF fluorescence on a single parameter histogram of log FL1 flourescence versus count. Recordings were made

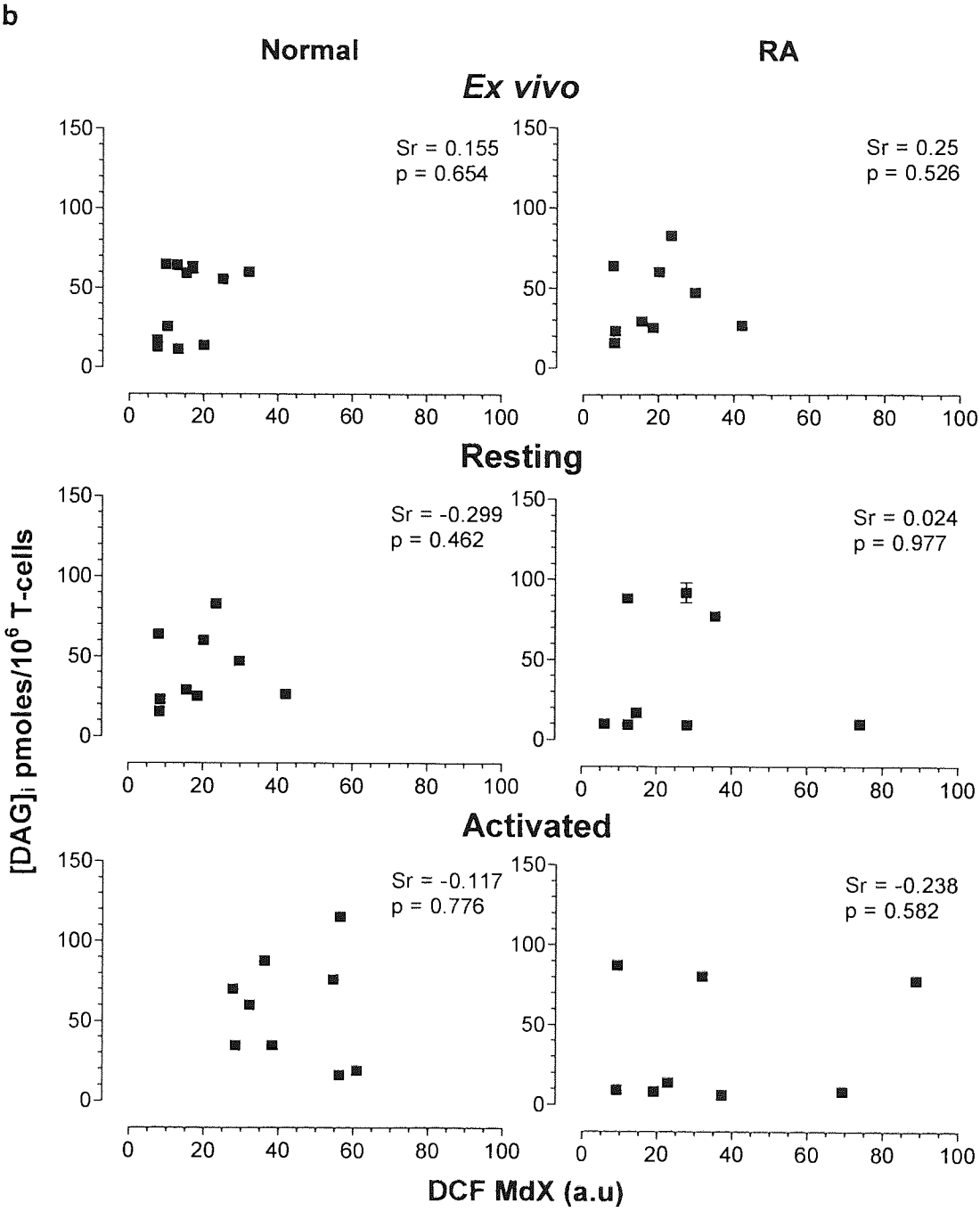

Figure 4.10 (Continued). against a standard DCF fluorescence of Jurkat T-cells treated identically to primary T-cells and set to a DCF MdX 100 as described. The median fluorescence (MdX) of 10,000 T-cells from each sample was recorded. For *ex vivo* determination of $[peroxide]_{cyt}$ concentration or endogenous DAG and ceramide levels, cells were loaded with DCFH-DA or lipids extracted immediately following purification as described in method 4.2.5. To examine the effect of culture, T-cells were cultured at a concentration of $2x10^6$/ml in RPMI 1640 supplemented with 10% FCS and 1% P/S in the presence or absence of 10μg/ml of PHA for 3 days to activate. All incubations were performed in a humidified 95% air, 5% CO_2 humidified atmosphere. Each data point represents a normal individual or a patient diagnosed with RA. Data was analysed for correlation using Spearman's rank analysis where $p<0.05$ was considered significant. Statistical analysis was performed by GraphPad prism. Shown in each histogram are the significance value (p) and Spearman's rank correlation coefficient (Sr). Arbitary units, a.u.

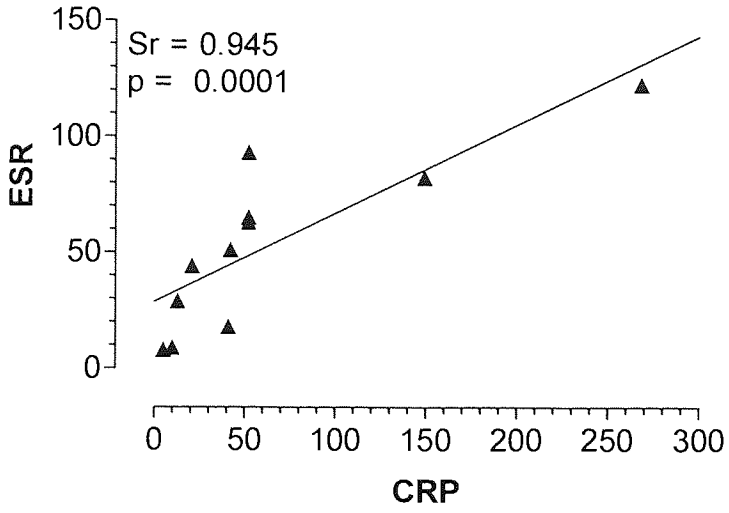

Figure 4.11. The serum C-reactive protein (CRP) score of patients with rheumatoid arthritis (RA) positively correlates with their erythrocyte sedimentation rate (ESR). Shown are the ESR and serum CRP score of 11 humans diagnosed with RA. Data was analysed for correlation using Spearman's rank analysis where a $p<0.05$ was considered significant. Statistical analysis was performed by GraphPad prism. Shown are the significance value (p) and Spearman's rank co-efficient (Sr).

ESR and CRP levels. On the other hand, there was no significant correlation between serum CRP levels or ESR levels with *ex vivo* endogenous T-cell ceramide or DAG (see Figure 4.12). Due to the small sample number, the dissection of sex from the RA and normals groups was not possible.

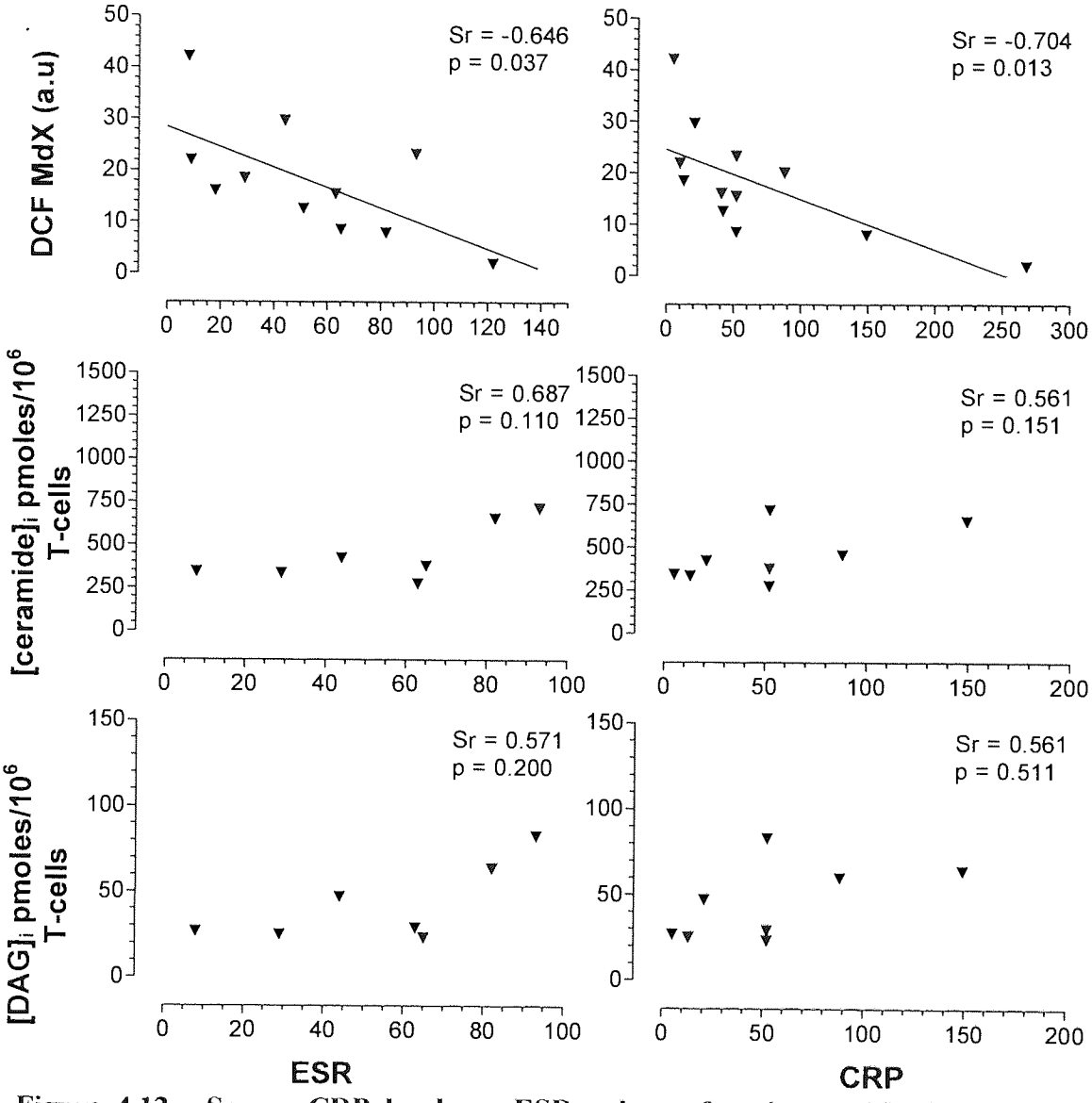

Figure 4.12. Serum CRP levels or ESR values of patients with rheumatoid arthritis (RA) correlate with *ex vivo* T-lymphocyte cytosolic peroxide concentrations but not ceramide or diaclyglcerol (DAG). Freshly isolated T-cells from the peripheral whole blood of consenting rheumatoid arthritis patients were analysed for ceramide and DAG content per 10^6 T-cells quantified utilising the DAGK assay as described in method 4.2.4. To examine the cytosolic peroxide concentration $[peroxide]_{cyt}$, T-cells were resuspended in serum free RPMI 1640 and incubated for 40 minutes with 50μM DCFH-DA. At the end of the incubation period, the viable T-cell population determined by forward scatter and side scatter parameters, were analysed by flow cytometry for DCF fluorescence on a single parameter histogram of log FL1 flourescence versus count. Recordings were made against a standard DCF fluorescence of Jurkat T-cells treated identically to primary T-cells and set to a DCF MdX of 100 as described 4.2.5. The median fluorescence (MdX) of 10,000 T-cells from each sample was recorded. Each data point represents a single individual diagnosed with RA. Data was analysed for correlation using spearman's rank analysis where $p<0.05$ (*) was considered significant. Statistical analysis was performed by GraphPad prism. Shown in each histogram are the significance value (p) and Spearman's rank correlation coefficient (Sr). Arbitary units, a.u.

4.4 Discussion.

One of the hallmarks of RA is the increase in cellularity of the synovial cavity of an affected joint. The infiltration, accumulation and persistence of one of these cell types, T-lymphocytes, indicates a defect in the ability to undergo apoptosis, a malfunction in the mechanisms that promote proliferation, or a combination of both. Moreover, a lack of synovial T-cell apoptosis *in vivo*, despite synovial T-cells expressing a phenotype that is suggestive of a susceptibility to apoptosis points to defective intracellular signalling (Salmon *et al.*, 1997). Indeed, FLIP is constitutively expressed in $CD4^+$ T-cells from BALB/c mice with PG induced arthritis. These cells fail to undergo CD3 mediated apoptosis due to inhibition of procaspase-3 and –8 by FLIP (Zhang *et al.*, 2001). Additionally, the RA exclusive T-cell subset $CD4^+CD28^-$ express enhanced levels of $Bcl\text{-}_2$ (Firestein *et al.*, 1995) whereas freshly isolated RA synovial T-cells highly express $Bcl\text{-}x_l$ allied to a lack of synovial T-cell apoptosis and contrary to that observed in synovial T-cell from gout patients (Salmon *et al.*, 1997). However, Ohshima *et al.*, (2000) speculate that the pro-apoptotic actions of CD95 are counteracted by the proliferative effects of TNFα and its preferential use of a common signalling intermediate.

ROS, the sphingolipid ceramide and DAG have been identified *in vitro* as signalling intermediates in response to stimuli associated with RA and other inflammatory diseases including CD95, TNFα, IL-1β and TCR activation (Aussel *et al.*, 1990; Andrieu *et al.*, 1994; Cifone *et al.*, 1993; Gamard *et al.*, 1997; Gulbins *et al.*, 1995; Liu *et al.*, 1998; Obeid *et al.*, 1993; Schulze-Osthoff *et al.*, 1992; Verheij *et al.*, 1996

as reviewed in; Altman *et al.*, 1992; Berridge, 1997). Consequently the basal levels of $[peroxide]_{cyt}$, and endogenous ceramide and DAG were quantified *ex vivo*, from the peripheral whole blood of apparently healthy individuals and those diagnosed with RA according to the criteria set by the American College of Rheumatology 1987 (Arnet *et al.*, 1988). Furthermore, the effects of *in vitro* culture of resting T-cell and their PHA activation *in vitro* on $[peroxide]_{cyt}$, and endogenous ceramide and DAG were determined.

The $[peroxide]_{cyt}$, and endogenous ceramide and DAG of $CD3^+$ T-cells from patients with RA was not significantly different normal T-cells. The level of activation as determined by flow cytometric evaluation of the membrane expression of CD25 was almost zero and the same between the groups. Upon culture for 72 hours with or without PHA induced activation, the endogenous and ceramide levels remained indistinguishable from that of *ex vivo* T-cells from normals or RA. T-cells from normals and RA displayed similar levels of activation with or without PHA stimulation following 3 days of culture.

DAG and ceramide are largely responsible for the modulation of proliferative and apoptotic intracellular responses respectively. Indeed they are simultaneously regulated in opposing directions of interrelated metabolic pathways (as reviewed in; Bielawska *et al.*, 2001; Ruvulo, 2001; see Figure 4.1). In the human T-cell line, Kitt 225, the addition of IL-2 led to an increase in the DAG:ceramide ratio allied to a proliferative response, which upon IL-2 withdrawal to induce apoptosis, led to a decrease in the DAG:ceramide ratio. This pattern was reflected in the DAG and ceramide precursors PC and SM respectively (Flores *et al.*, 2000). No difference in

the ceramide:DAG ratio in T-cells *ex vivo* between normals and RA patients was observed here. Furthermore, there was no difference in the mean ratio between *ex-vivo* T-cells, resting T-cells in culture or *in vitro* PHA activated T-cells irrespective of health. However, despite no significant difference in the mean ceramide:DAG ratio between resting or PHA-activated of normals and RA, the RA group was sub-divided into a group with identical ceramide:DAG ratio to normals and a group with a significantly elevated ceramide:DAG ratio. The significance of this group was not analysed due to the small number but the difference observed could not be attributed to serum CRP levels, ESR or a common regimen of medication.

Despite the lack of evidence for a difference in the endogenous ceramide and DAG levels of T-cells either directly following isolation from peripheral blood or following 72 hours in culture in a resting or PHA activated state, the involvement of these lipids as signalling intermediates early in the stimulation of the TCR can not be ruled out. It is described in this thesis that in the induction of apoptosis by CD95L in Jurkat T-cells, endogenous ceramide accumulates within one hour of exposure and returns to basal levels after 4 hours (see Chapter 2). In this regard, other authors have described similar findings (as reviewed in; Adam *et al.*, 2001). DAG is enhanced in multistep fashion at 2, 20 and 120 minutes in murine splenic lymphocytes stimulated with the T-cell specific mitogen concanavalin A (Jolly *et al.*, 1996). In this report, alterations in endogenous ceramide and DAG levels of T-cells upon PHA stimulation may have occurred in a time window that was not analysed, and occur earlier in the TCR signalling of T-cell activation. Differences in T-cell ceramide or DAG formation, or their relative ratios in response to TCR activation by PHA *in vitro* and their relevance to the T-cell pathology observed in RA require further examination.

It has previously been reported that CD28 induced A-SMase activation leads to a rapid and transient production of ceramide in resting and activated murine T-cells which was associated with proliferation (cited in; Adam *et al.*, 2002). However, in human resting T-cells, the application of synthetic ceramide for 72 hours abrogated proliferation induced by TCR or CD28 stimulation (O'Byrne & Sansom, 2000) whereas Mengubas *et al.*, (1999) reported that PHA prevented C_2-ceramide induced cell death. Furthermore, it is observed here that normal T-cells activated with PHA for 72 hours undergo apoptosis when exposed to C_2-ceramide for a further 24 hours (see Chapter 2). The ability of resting or PHA activated T-cells isolated from RA patients to undergo apoptosis *in vitro* following synthetic short chain ceramide treatment was not investigated.

A limitation to the quantification of ceramide and DAG utilising the DAGK assay is the relatively high number of cells required to extract and radioactively label enough lipids for detection. Consequently, T-cell subpopulations were not analysed and due to the limited number, neither were synovial T-cells. Further, this assay does not permit resolution of endogenous ceramide species with varying degrees of saturation and fatty acid acyl chain lengths. It is possible that certain ceramide species may mediate specific cellular responses (Watts *et al.*, 1997; 1999). The recent development of a fluorescently tagged ceramide Ab, anti-ceramide 15B4 (Alexis Biochemicals, Nottingham, UK) may allow quantification by flow cytometry of alterations in endogenous ceramide levels from specific T-cell phenotypes associated with RA that are of relatively low number or those from the synovium. Using immunofluorescence, A-SMase mobilisation from the intracellular compartment to the plasma membrane has been observed, leading to the formation of ceramide and its

fusion in to lipid rafts. This phenomona lead to the clustering of various receptors such as CD95 and CD40 (Grassmé *et al.*, 2001a & b; 2002) or the spatial separation of others such as CD28, which is excluded from rafts (Cheng *et al.*, 1999; Janes *et al.*, 1999). Further, CD28 stimulation promotes migration of intracellular lipid rafts to the membrane inducing redistribution of the TCR ligand contact site (Viola *et al.*, 1999). Analysis of T-cell lipid rafts and receptor clustering in response to cytokines and TCR activation, and their relative differences in RA patients compared to normals may help to resolve the functional T-cell defects associated with the pathophysiology of RA.

$[Peroxide]_{cyt}$ of normal resting T-cells following 72 hours of culture was significantly increased when compared to *ex vivo* T-cells and may be due to mitogens within FCS of the T-cell culture medium, although no alteration in the surface expression of CD25 was detected. The $[peroxide]_{cyt}$ of normal T-cells was enhanced further by the 72 hours culture in the presence of PHA to induce activation. Conversely, no significant difference in $[peroxide]_{cyt}$ could be identified between *ex vivo* T-cells, resting T-cells and PHA-activated T-cells isolated from RA peripheral blood. Where cell number permitted, T-cells from each disease free individual were divided in 2 for *in vitro* culture with or without PHA for 3 days. The $[peroxide]_{cyt}$ concentration of resting T-cells obtained from each individual was elevated by PHA activation *in vitro*. Conversely, T-cells from each individual RA patient failed to upregulate $[peroxide]_{cyt}$ upon activation despite possessing an identical shift in the membrane expression of the activation marker CD25. This supports the hypothesis that T-cell activation can occur independently of ROS production. Others have shown that CD28 stimulation via its natural ligand CD80 or with anti-CD28 MoAb does

synergise with PMA or anti-CD3 MoAb to increase ROS production in primary human T-cells. Furthermore, the antioxidant ascorbic acid substantially inhibits ROS production in T-cells treated with PMA or the calcium ionophore A23187 but does not affect IL-2 release or proliferation (Tatla *et al.*, 1999). Here, PHA has been used to stimulate the T-cell receptor predominately via CD2 and the ζ chain of CD3 (O'Flyn *et al.*, 1986; Kanner *et al.*, 1992) rather than anti-CD3 or CD2 MoAb in the presence of CD28 (as reviewed in; Gold and Matsuuchi, 1995). It is possible that activation of rheumatoid T-cells by anti-CD3/CD2 in combination of CD28 may induce the production of $[peroxide]_{cyt}$ not seen with PHA. Furthermore, Devades *et al.*, (2002) described that anti-CD3 MoAb treatment of the murine T-cell hybridoma 9C127 induced the rapid production of discrete species of oxidant utilising both the superoxide sensitive probe dihydroethidium and the peroxide sensitive probe DCFH-DA (as used this investigation). Simulation of the TCR induced superoxide and peroxide formation that regulated distinct signalling pathways. TCR stimulation induced peroxide formation to activate the ERK cascade which was associated with proliferation. Conversely, TCR mediated superoxide formation activated a pro-apoptotic pathway via enhanced CD95L expression. However, the kinetics in formation of each species differed. Superoxide formation was transient forming after 45 minutes and returning to baseline after 70 minutes post anti-CD3 MoAb stimulation whereas peroxide was initially enhanced after 15 minutes and remained elevated for the entire experimental period (90 minutes). The application of pharmacological agents or the use of a genetic approach to increase the intracellular levels of anti-oxidant selective for either ROS confirmed the fluorescent probe observations (Davades *et al.*, 2002). Others have demonstrated that qualitatively different ROS are produced following T-cell activation in the presence of MNC than

when alone. TCR induced ROS generation in the presence of MNC was inhibited by ascorbic acid, DMSO and desferroxamine treatment, whereas ROS generation induced by anti-CD3 MoAb alone was only inhibited by ascorbic acid. Additionally, anti-CD2 MoAb treatment of primary T-cells induced ROS without CD3 activation, but was not accompanied by proliferation and IL-2 release (Tatla *et al.*, 1999). In agreement with the described defective $[peroxide]_{cyt}$ response in RA peripheral blood T-cells in response to *in vitro* PHA activation are the observations of Carruthers *et al.*, (1996), who showed defective $[Ca^{2+}]_i$ signalling following PHA activation which correlated with reduced IL-2 production and proliferation. In a follow up study, the $[Ca^{2+}]_i$ elevation in response to PHA activation of RA synovial T-cells was found to be lower in magnitude than RA activated peripheral blood T-cells from the same patient. This was attributed to enhanced $[Ca^{2+}]$ in the thapsigargin pool within the endoplasmic reticulum (ER) suggesting a smaller proportion of Ca^{2+} is released in response to TCR stimulation with PHA (Carruthers *et al.*, 2000). However, it should be appreciated that these differences in the magnitude of Ca^{2+} signalling between RA synovial T-cells, RA peripheral blood T-cells and T-cells of normals were obtained following over a short period following stimulation with PHA and do not necessarily equate to the defective $[peroxide]_{cyt}$ observed here after 72hrs of PHA activation.

The flow cytometry methodology employed here does not allow for inter-cellular variation of $[peroxide]_{cyt}$ responses between T-cell subpopulations obtained from any individual RA patient. It is possible that the inability to enhance $[peroxide]_{cyt}$ within RA peripheral blood T-cells may be due to a subpopulation which has no enhancement of $[peroxide]_{cyt}$ thus lowering the mean $[peroxide]_{cyt}$ obtained from those which are capable of elevating $[peroxide]_{cyt}$ following PHA stimulation. The

source of $[peroxide]_{cyt}$ formation following TCR activation in normal peripheral blood T-cells and consequently the site at which there is a loss of PHA mediated elevations in $[peroxide]_{cyt}$ of RA peripheral blood T-cells has not been investigated, although possible sources include the mitochondria and ER electron transport chains, hypoxanthine/xanthine oxidase, lipoxygenase and cyclooxygenase within the cytosol, and NADPH oxidase system located within the plasma membrane (as reviewed in; Gabbita *et al.*, 2000)

Here, $[peroxide]_{cyt}$ was evaluated after long term culture of resting T-cells and PHA-activated T-cells from normals and RA patients. From the work of others it is clear that the varying mechanisms of T-cell activation have differing requirements for ROS production. Further experiments are required to determine whether the inability of RA peripheral blood T-cells to upregulate the generation of $[peroxide]_{cyt}$ following PHA activation is reflected at shorter incubation periods and whether these differences exist following T-cell activation by different means. Since superoxide formation is capable of activating different signalling intermediates to those of peroxide and consequently differential cellular responses, their relative formation in RA T-cells compared to those from normals and associated kinetics warrants investigation. The data presented here is suggestive that enhancement of $[peroxide]_{cyt}$ is not necessary for T-cell activation as observed by the enhanced membrane expression of CD25 in PHA-activated peripheral blood T-cells both from normals and rheumatoids displaying peroxide competent and incompetent phenotypes respectively. However, the inability of RA peripheral blood T-cells to upregulate $[peroxide]_{cyt}$ production may compromise a shift in the intracellular redox balance, activation of transcription factors and other signalling pathways seen in normal TCR

activated T-cells. The gene expression of proteins required for efficient cell cycle progression and cellular metabolism in T-cells may be altered in RA. It is hypothesised that this dysfunction in redox responses to TCR stimulation contributes to the enhanced survivability and hyporesponsivness of rheumatoid T-cells, and their inability to undergo apoptosis *in vivo*, instigating and propagating the RA pathology. The proliferation of *in vitro* PHA activated T-cells from the peripheral whole blood of patients with RA and their ability to secrete IL-2 compared to those of normals with respect to $[peroxide]_{cyt}$ has not been evaluated in this study. It is likely that the reduced $[peroxide]_{cyt}$ observed in PHA activated RA T-cells contributes to their reduced proliferation and IL-2 secretion described by others (Carruthers *et al.*, 1996).

The $[peroxide]_{cyt}$ of *ex vivo* T-cells did not correlate with endogenous ceramide or DAG levels in either the RA or normals group. This observation was reflected in resting T-cells in culture and PHA-activated T-cells *in vitro* from either group. It is likely that the perturbations in $[peroxide]_{cyt}$ of *ex vivo* T-cells encountered from one individual to the next are not sufficient to induce loss of GSH to relieve its negative regulation on the activity of N-SMase and hence elevate endogenous ceramide levels, unlike that induced in the human breast carcinoma cell line MCF-7 by the action of TNFα or following the cellular depletion of GSH (Liu & Hannun, 1997; Liu *et al.*, 1998). As discussed, while the possibility exists that perturbations in ceramide and DAG content of cells following 72 hours PHA activation may have been missed, these data imply that the elevation in $[peroxide]_{cyt}$ levels induced by the TCR stimulation of normal cells *in vitro* encountered are either not sufficient to remove GSH inhibition of N-SMase to induce enhancement of ceramide levels. Additionally, earlier alterations in ceramide formation following TCR stimulation may occur via a

ROS independent mechanism, via A-SMase (Sawada *et al.*, 2002) or ceramide synthase, although no reports exist discussing a role for, or against, redox regulation of ceramide synthase.

ESR and serum CRP measurements are reflections of the acute phase response where the latter is a prognostic indicator of RA progression and real time measure of its activity. While ESR is the primary inflammatory disease marker used in the USA, both ESR and CRP values are utilised within Europe, where in combination they are good indicators of radiological disease progression. Indeed as is observed here, ESR and CRP can be correlated. However, ESR is influenced by erythrocyte size, shape and number. Furthermore, ESR is dependent upon fibrinogen, albumin, globulin, age of patient and anaemia. The range in which ESR fluctuates is typically 2-3 fold whereas normal CRP concentrations are typically low, 1μg/ml, but following tissue injury or inflammation they are rapidly elevated to a circulatory concentration of up to approximately 1000 fold. Although some lymphocytes are capable of CRP synthesis via IL-6 stimulation, since the administration of anti-IL-6 MoAb to RA patients lowers serum CRP scores, CRP is primarily produced in the liver. Its synthesis is therefore a true reflection of mediators of inflammation, although a deficiency in serum CRP levels is not necessarily representational of absence disease activity. Due to its site of formation, CRP levels are higher in the circulation than in the synovium of rheumatoids, however, the function of CRP is uncertain (as reviewed in; Otterness; 1994). Here, it is shown that the no correlation exists between the endogenous T-cell ceramide or DAG concentraion *ex vivo* and CRP or ESR of rheumatoids, however, $[peroxide]_{cyt}$ of T-cell *ex vivo* obtained from the peripheral whole blood of patients diagnosed with RA negatively correlates with both serum

CRP score and ESR. In agreement with our observations, *in vitro* studies have described that the binding of CRP to normal human PBM inhibits superoxide production induced by phorbol esters (Dobrinich & Spagnolo, 1991). In contrast, in guinea pig alveolar macrophages, CRP ameliorated superoxide production alone, or that induced either by platelet aggregating factor (PAF), N-formyl-methionyl-leucyl-phenylalanine (fMLP) or the PKC activator phorbol 12-12-myristate 13-acetate (PMA). Further, CRP attenuated the elevation in $[Ca^{2+}]$ induced by PAF or fMLP with similar IC_{50} values as those obtained from the inhibition of superoxide (Földes-Filep *et al.*, 1992). CRP peptides corresponding to the amino acid sequences 27-82 and 201-206 of natural CRP molecule reduced superoxide production in neutrophils treated with opsonised zymosan. This inhibition of neutrophil function was attributed to the disruption of metabolism by inhibition of neutrophil glycolysis and ATP generation (Shephard *et al.*, 1992). In addition to this downregulation in cellular oxidative capacity, in a cell free xanthine oxidase-acetylaldehyde system, CRP inhibited the production of superoxide demonstrating (Dobrinich & Spaguolo, 1991) direct free radical scavenging potential. However, heat aggregated CRP, which on its own did not mediate alteration in ROS generation in normal peripheral blood human neutrophils or monocytes, enhanced the intracellular ROS concentration induced by heat aggregated IgG treatment without effecting the secretion of ROS into the supernatants (Zeller & Sullivan, 1992).

There is a plethora of evidence that suggests differences exist between the phenotype and signalling of T-cells from synovial fluid compared to those from PB from the same RA patient, suggesting that environmental factors unique to the synovial environment have additional roles. Oligoclonal T cells in synovial fluid accumulate

independently of the clonality of T-cell in peripheral blood. Consequently, the expansion of T-cell clones within joints of RA patients through continuous antigenic stimulation may contribute to the inflammation process and not be necessarily reflected in the peripheral blood of the same individual (as reviewed in Hasunuma *et al.*, 1998). RA synovial T-cells readily undergo apoptosis upon culture, whereas spontaneous apoptosis of PB T-cells is less (Salmon *et al.*, 1997). Indeed, differences in the extent of the apoptotic response between PBL and synovial T-cells to CD95L treatment *in vitro* suggest that T-cells do not simply home to the synovium, but undergo transformation in their phenotype to become more sensitive (Cantwell *et al.*, 1997). CD95 expression is also lower in RA PB T-cells than RA synovial T-cells, however this reflects the $CD45Rb^{dull}$ phenotype. Further, IL-2 induced some proliferation in the culture of synovial T-cells, but this proliferative effect was minimal in PBL T-cells (Salmon *et al.*, 1997). A reduction in $[Ca^{2+}]$ signalling after TCR stimulation of T-cells observed in T-cells from the peripheral blood RA patients compared to normals. A further inhibition in $[Ca^{2+}]$ signalling was observed upon TCR stimulation of rheumatoid synovial T-cells (Carruthers *et al.*, 1996, 2000). T-cell interaction with cells of varying lineage that are present in the RA synovium also contribute to their prolonged survivability and persistence. Synovial fluid antigen presenting cells possesses enhanced co-stimulatory ability to activate peptide specific human T-cells when compared to PBMNC from RA patients (Robertson *et al.*, 1997). Salmon *et al.*, (1997) suggested that loss of apoptotic function in RA T-cells *in vitro* requires at least in part the interaction with synovial fibroblasts which upregulate Bcl-x_l but not Bcl-$_2$, to mimick the synovial T-cell phenotype observed *in vivo*. It is likely that the inability of RA T-cells to upregulate $[peroxide]_{cyt}$ production in response to

PHA activation unlike that observed from healthy normals may be further accentuated in RA synovial T-cells, and requires further investigation.

In summary, the data presented here shows that there is no difference in the $[peroxide]_{cyt}$, or endogenous ceramide and DAG content of peripheral blood T-cells *ex vivo* compared to those obtained from apparently healthy individuals. Furthermore, no alteration in ceramide or DAG levels are reported after 72 hours of T-cell culture or following TCR stimulation by PHA *in vitro* for 72 hours in either the RA group or normals group. However, this data does not exclude that differences may exist between the T-cells of RA patients and normals with regards early perturbations in the endogenous ceramide and DAG levels in response to PHA, which are likely to be of transient nature. Differences in the ability of RA T-cells and normal T-cells to mobilise lipids required for the formation of lipid rafts may resolve their functional differences. The hyporesponsiveness of rheumatoid T-cells and the failure to undergo apoptosis may be a reflection of their inability to upregulate $[peroxide]_{cyt}$ compared to normal T-cells in response to TCR stimulation *in vitro*. As a consequence, redox sensitive transcription factors and signalling pathways may not be induced contributing to an altered pattern of gene expression and insufficiencies in the proteins required for normal metabolic respiration. The observation of a negative correlation between the $[peroxide]_{cyt}$ of resting $CD3^+$ T-cells *ex vivo* and serum CRP levels of patients diagnosed with RA supports an associated antioxidant-like role for this acute phase response protein.

Chapter 5.0: Essential requirement for reactive oxygen species generation in the mechanism of action of methotrexate.

Discussed within the introduction to this chapter are the current theories believed to account for mechanisms of action for the anti-folate drug methotrexate. However, these do not totally account for the immunosuppressant and anti-inflammatory actions of this agent observed clinically in the treatment of RA. A role for ROS as signalling mediators of methotrexate toxicity is proposed. Furthermore, recent advances in the molecular studies of inflammation suggest that cell-cell interactions by specific adhesion molecules may be important targets for immunosuppression, consequently it is hypothesised that methotrexate mediates functional changes in cell adhesion. The experimental evidence and ensuing discussion address these issues.

5.1 Introduction.

The folate antagonist methotrexate (MTX) is a potent cytotoxic agent, initially developed for the treatment of malignancies (Farber *et al.*, 1956) and is presently used in non-neoplastic diseases as an anti-inflammatory agent and immunosuppressant. These include chronic inflammatory disorders such including psoriasis, primary biliary cirrhosis, intrinsic asthma and, in the prophylaxis of acute graft versus host disease used either alone or with cyclosporin A and or prednisolone (as reviewed in; Alarćon, 2000; Bondeson, 1997; Genestier *et al.*, 2000). MTX is the most widely used drug in the second line treatment of rheumatoid arthritis (RA) as one of the few disease modifying antirheumatic agents available. It has a well-documented efficacy relative to toxicity profile, however, its ability to reduce radiological progression is uncertain (Rau *et al.*, 1997). In autoimmune disease or allografts, doses are normally in the range of 7.15mg/week orally or by intramuscular injection whereas in cancer chemotherapy, doses escalate up to $30g/m^2$ with subsequent administration of the antidote leucovorin (Folic acid, citrovorum factor; Coombe *et al.*, 1995; Hamilton & Krammer, 1995; Oguey *et al.*, 1992)

MTX is a weak bicarboxcylic, organic acid transported into cells by an energy dependent process suggesting active transport. A low affinity folate transmembrane carrier transports reduced folate analogues such as leucovorin and MTX with approximately the same efficacy, with poor transport of folic acid. The membrane associated folate-binding protein has a nonomolar affinity for both reduced folates

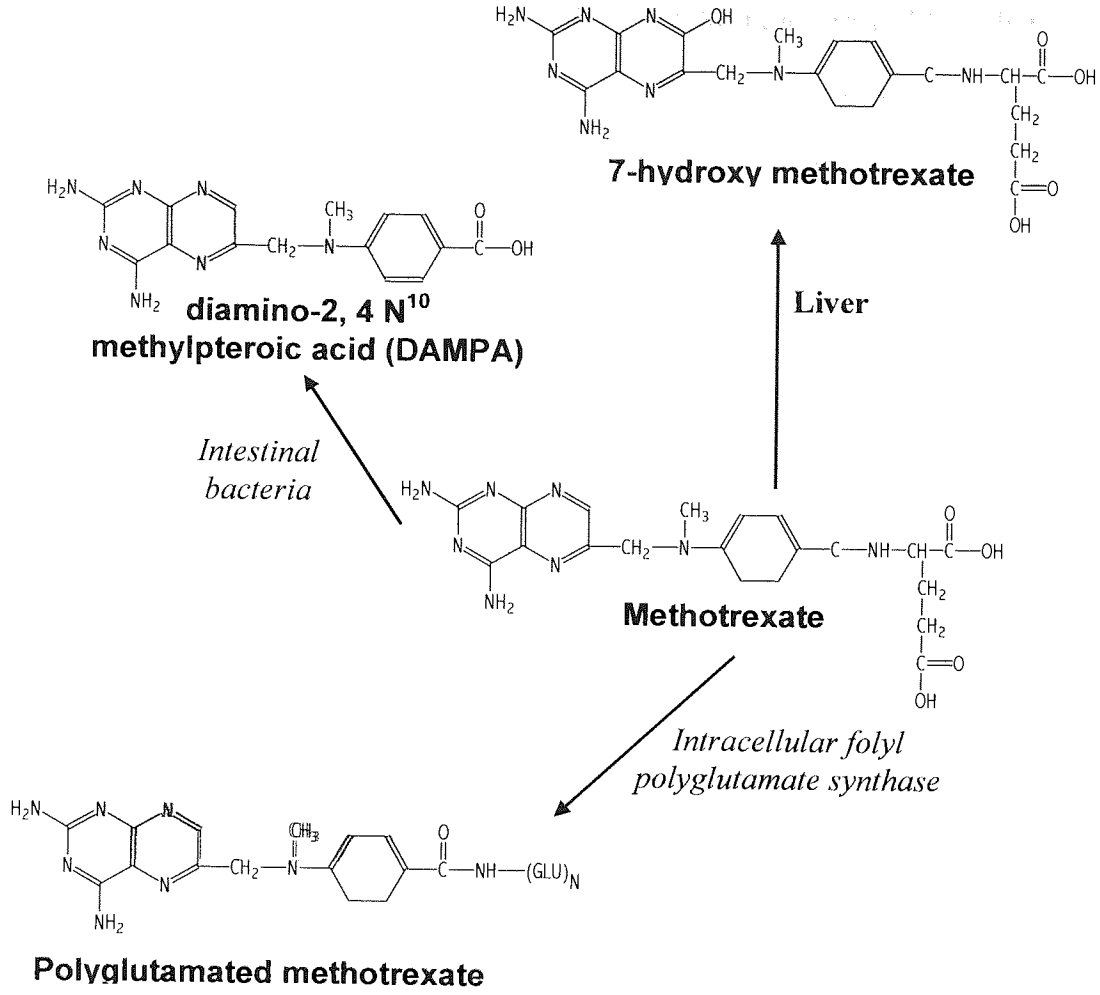

Figure 5.1. Metabolism of Methotrexate. Adapted from Genestier *et al.*, (2000).

and folic acid, however it acts as a relatively poor substrate for MTX, with a 10-30 fold lower affinity. Additionally, at high concentrations, MTX is also capable of passive diffusion across cell membranes. Like physiological folates, MTX is converted to a polyglutamate form by the binding of 2-5 polyglutamate groups, essentially trapping MTX within the cell and thereby increasing the half life of MTX. Polyglutamated MTX retention is directly proportional to the chain length. The addition of glutamate groups to MTX is mediated by the enzyme folyl polyglutamyl synthase utilising ATP. MTX may also be metabolised in liver hepatocytes to form 7-hydroxy-MTX by the aldehyde oxidase driven hydroxylation at position 7 of the pterine ring and this represents a major detoxification pathway. However, 7-hydroxy-

MTX is converted to polyglutamated MTX 2.7 fold faster than MTX but has increased affinity for folate transporters. The contribution of 7-hydroxy-MTX to the immunosuppressive and anti-inflammatory actions of MTX is unknown. Additionally, MTX is metabolised by carboxypeptidases of intestinal bacteria to diamino-2, 4-N-10-methylpteroic acid (DAMPA), potentially reducing the effective dose and is indicative of a detoxification pathway (see Figure 5.1; as reviewed in; Genestier *et al.*, 2000).

The cytotoxic actions of MTX have been attributed to its inhibition of RNA, DNA and protein synthesis, and release of adenosine. It is thought that the cytotoxicity of MTX is dependent on its property as a powerful antimetabolite for folate, competitively inhibiting dihydrofolate reductase (DHFR), preventing regeneration of tetrahydrafolate (FH4) from dihydrofolate (FH2) and thereby inhibiting *de novo* purine and pyrimidine synthesis. FH4 is used in the conversion of thymidylate (dUMP) to deoxyuridylate (dTMP) catalysed by thymidylate synthase (TS; see Figure 5.2). Consequently there is an imbalance in the oxynucleotide pool which could explain improper DNA synthesis and the subsequent apoptosis observed by others (Genestier *et al.*, 1998a; Paillot *et al.*, 1998; da Silva *et al.*, 1995). The MTX metabolite 7-hydroxy MTX is less effective as a DHFR inhibitor (Budzik *et al.*, 2000; as reviewed in Allison, 2000; Genestier *et al.*, 2000). However, the anti-inflammatory actions are unlikely to arise from this property, as supplementation with folate in RA patients to attenuate MTX toxicity does not compromise its clinical efficacy (Morgan *et al.*, 1994). Furthermore, the dosing regimen for RA is in the order of three orders of magnitude lower than for oncological disease (Coombe *et al.*, 1995; Hamilton & Krammer, 1995; Oguey *et al.*, 1992). In support of this, Fairbanks

et al., (1999) described that in activated peripheral blood lymphocytes (PBL), the immunosuppressant properties of MTX resulting in cytostasis were due to the inhibition of the enzyme amidophosphoribosyl transferase leading to elevated PP-ribose-P and stimulation of UTP synthesis but not via the inhibition of the two folate dependent enzymes (see Figure 5.2).

Conflicting evidence surrounds the effect of MTX on blockade of 5-amino-imidazole carboxamide ribonucleotide (AICAR) transformylase, an essential enzyme for the conversion of 10-formyl FH4 to FH4. Intracellular MTX is converted to the polyglutamated forms, potent inhibitors of AICAR transformylase leading to an increase in extracellular adenosine (see Figure 5.2; Baggott *et al.*, 1993; Bannwarth *et al.*, 1994). Adenosine has been reported to be a potent endogenous anti-inflammatory purine nucleotide that inhibits superoxide generation (Cronstein *et al.*, 1985; Roberts *et al.*, 1985), induces apoptosis in activated PBL (Genestier *et al.*, 1998a), neutrophil mediated damage to the endothelium and leukocyte accumulation in the inflamed hamster air pouch model (Cronstein *et al.*, 1993). In contrast, more recent work has shown that AICAR transformylase inhibition by polyglutamated forms of MTX in human T-cells, causes a dose-dependent reduction in adenosine and guanosine pools (Budzik *et al.*, 2000). Further, the contribution of adenosine production in the cytotoxic action of MTX in human or murine activated T-cells has been described as minimal (Genestier *et al.*, 1998a; Paillot *et al.*, 1998).

The immunosuppressive activities of MTX have been studied in the context of cell proliferation, and recruitment. Paillot *et al.*, (1998) and Genestier *et al.*, (1998a) describe the induction of activation dependent T-cell apoptosis by low dose MTX *in*

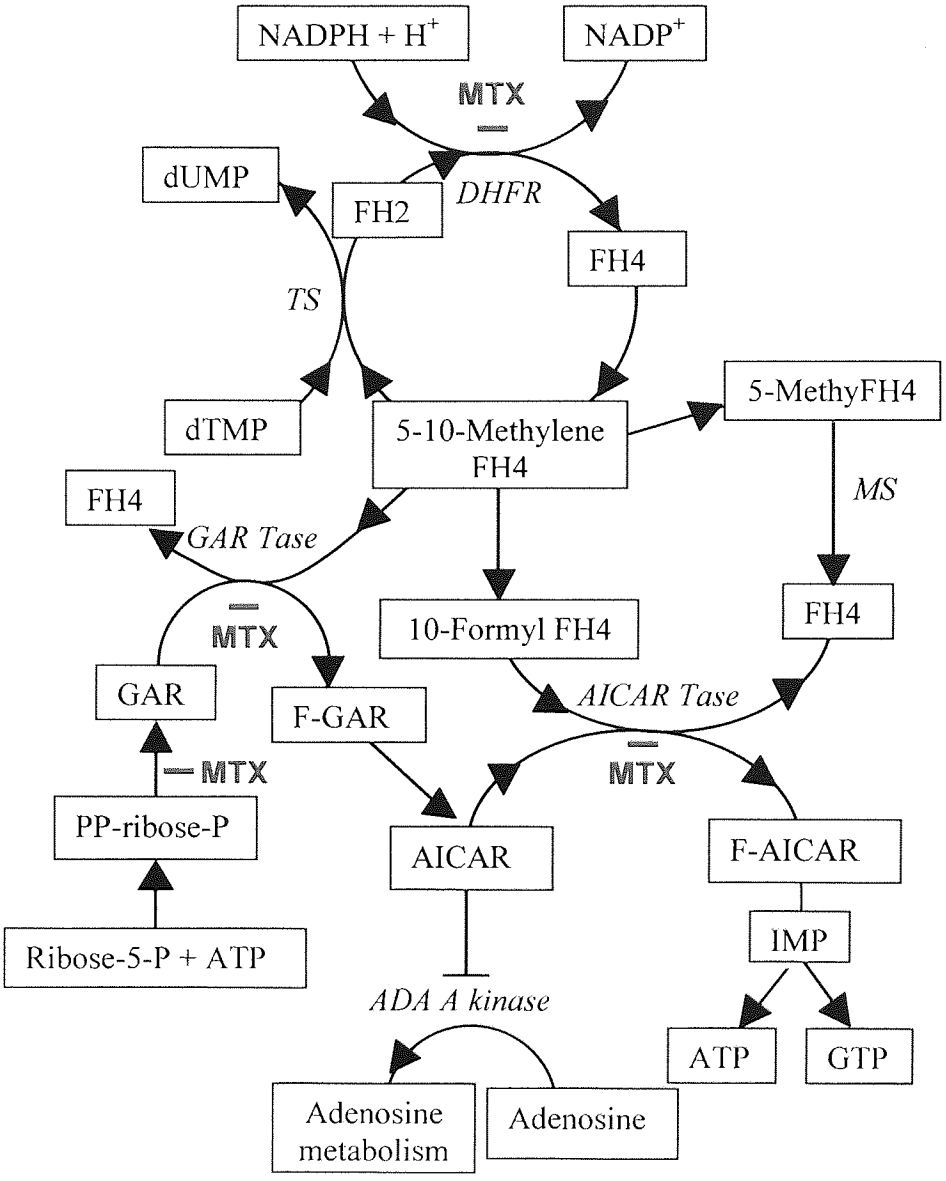

Figure 5.2. Simplified schematic representation of the folate cycle and the proposed sites of methotrexate action. Abbreviations used; ADA A; adenosine deaminase A; AICAR, 5-amino 4 carboxamide ribonucleotide; DHFR, dihydrofolate reductase; dTMP, thymidylate; dUMP, deoxyuridylate; F, Formyl; FH2, dihydrofolate; FH4, 5,10 methylenetetrahydrofolate; GAR, glycinamide ribonucleotide; MS, methylene synthase; PP-ribose-P, 5-phosphoribosyl-1-pyrophosphate; Tase, transformylase; TS, thymidylate synthase. Adapted from Fairbanks *et al.*, (1999); as reviewed in; Genestier *et al.*, (2000).

vitro. This is supported by da Silva *et al.,* (1995), who examined the cytotoxicity of several chemotherapeutic drugs and observed chromatin condensation, membrane blebbing and nuclear fragmentation, typical of apoptosis in Jurkat T cells. However, MTX inhibits growth and induces terminal differentiation of keratinocytes, indicating a cell-type specific response (Schwartz *et al.*, 1995). Recent advances in the molecular studies of inflammation suggest that cell-cell interactions by specific adhesion molecules could be important targets for immunosuppression, where down-regulation of both CD18 on mononuclear cells and ICAM-1 on endothelial cells has been described following treatment with MTX during cardiac allograft transplantation in rats (Cielski *et al.*, 1998a, 1998b).

MTX mediated modulation of pro-inflammatory cytokine secretion, particularly IL-1β, IL-6 and TNFα, and cycloxygenase and lipoxygenase activities that are associated with the aetiology of RA have been widely investigated, however there is no consistent effect observed either *in vitro* or *in vivo* (Anderson *et al.*, 2000; Bondeson & Sundler, 1995; Hawkes *et al.*, 1993, 1994; Hu *et al*, 1998; Sperling *et al.*, 1992; Williams *et al*, 1999).

The progression of RA is characterised by the development of an inflammatory pannus where expansion of the synovium, termed synovial hyperplasia, is a histological hallmark. As discussed in Chapter 3, the interaction of various adhesion molecules expressed on leukocytes and tissue facilitates migration of leukocytes from the circulatory system, through the extracellular matrix towards the inflammatory site in response to chemotactic stimuli and consequently in the case of RA, into the synovium. In addition, the attachment of synoviocytes to cartilage and bone is a

crucial step in the pathogenesis of RA (as reviewed in; Cunnane *et al.*, 1998). However, the functional ability of MTX to reduce this radiological progression is unknown.

Few redox-altering properties of MTX have been described. MTX treatment of peripheral blood neutrophils (PBN) induces a dose dependent increase in peroxide levels (Gressier *et al.*, 1994) and is associated with a loss in the cellular and mitochondrial levels of the anti-oxidant glutathione (Babiak *et al.*, 1998; Neuman *et al.*, 1999). Therefore, it is reasoned that generation of ROS is an important mechanism in the immunosuppressive and anti-inflammatory effects of MTX. To address this hypothesis, the effects of MTX on monocyte and T cell intracellular redox status, cell cycle distribution and adhesion of monocytes to endothelial cells were investigated. For the first time, it is presented here that reactive oxygen species (ROS) are generated by MTX, mediating functional changes in leukocyte adhesion, where scavengers of ROS are effective inhibitors of MTX induced cell cycle arrest, apoptosis and changes in monocyte-endothelial adhesion.

5.2 Materials and methods.

5.2.1 Materials.

All reagents were obtained from Sigma Chemical Company (Poole, UK), solvents were from Fisher (Loughborough, UK) and all gases from BOC Ltd (Guildford, UK) unless otherwise stated. RPMI 1640, foetal bovine serum, Hanks balanced salt solution (HBSS), gentamicin and penicillin (1000u/ml)/streptomycin (10,000μg/ml) were purchased from GibcoBRL (Paisley, UK

The antioxidants N-acetylcysteine (NAC) and glutathione (GSH) were made up in serum free RPMI 1640. In the assays for $[peroxide]_{cyt}$, the final cellular concentration of DMSO employed did not exceed 0.1%. LPS were reconstituted in sterile phosphate buffered saline (PBS; 0.01M Na_2HPO_4, 0.002M KH_2PO_4, 0.003M KCl, 0.137M NaCl; pH 7.4) containing 0.1% fraction V bovine serum albumin (BSA; Sigma, Poole, UK). MTX was dissolved to a concentration of 50mg/ml in 1M NaOH and further dilutions made in RPMI 1640.

5.2.2 Cell culture and stimulation.

The acute human T-cell leukaemia cell line, Jurkat and the human monocytic cell line, U937 were maintained in RPMI 1640 media, supplemented with 10% heat inactivated foetal calf serum and 1% penicillin/streptomycin. Cells were incubated at

37°C in a humidified atmosphere of 5% CO_2 and 95% air. The number of viable cells per ml was determined by trypan blue exclusion using an improved Neubauer haemocytometer (Weber Scientific International Ltd., Teddington, UK). Cells at a concentration of $2x10^6$/ml were serum starved for 4 hours in the described incubator conditions prior to treatment. Where indicated, cells were treated with methotrexate for the times and concentrations noted, incubations at 37°C in a humidified 5% CO_2/95% air incubator. To investigate the role of $[peroxide]_{cyt}$ in the cellular response to MTX, cell suspensions were pre-treated for 4 hours with 10mM NAC or GSH. Stimulation was discontinued by removing cells suspensions from culture vessels, centrifuging at 1000xg (Eppendorf centrifuge 5415D, Hamburg, Germany) for 5 minutes and washing twice with 1ml of ice cold PBS prior to further experimental manipulation.

Individual additions to cells suspensions did not exceed 1% of the total volume and were dispersed with gentle mixing by pipette. Control experiments were conducted under identical conditions as tests, employing vehicle treatment.

5.2.3 Flow cytometric DNA cell cycle analysis.

PBS washed cells were resuspended in 1ml of hypotonic fluorochrome solution and incubated in the dark at 4°C for 4-24 hours. Cell cycles were then analysed by flow cytometry and the phases of the cell cycle quantified as described in Method 2.2.9.

5.2.4 *Flow cytometric assay for [peroxide]cyt production.*

The detection of $[peroxide]_{cyt}$ by flow cytometric evaluation of the fluorescence emitted from cells incubated with the peroxide sensitive dye DCFH-DA was performed as described in Method 2.2.10.

5.2.5. Cellular GSH and protein determination.

Total cellular GSH was quantified according to the recycling assay of Tietze, (1969; see Method 2.2.14). Protein concentration was determined in quadruplicate using the BCA assay described in Method 2.2.15.

5.2.6 Adhesion assay.

Endothelial cells were isolated, cultured and treated with 1μg/ml of LPS for 5 or 24 hours and the adhesion assay performed identically as described in Methods 3.2.3 & 3.2.4.

5.2.7 Analysis of monocyte adhesion molecule expression.

The surface expression of proteins associated with adhesion on U937 monocytes was analysed by flow cytometry as described in Method 3.2.5.

5.2.8 Flow cytometric analysis of cell viability.

U937 monocytes or Jurkat T-cells were resuspended in 1ml of PI (25μg/ml) in PBS/0.1% BSA per 10^6 cells and analysed for uptake of PI by flow cytometry as described in Method 2.2.12.

5.3 Results.

Methotrexate treatment of Jurkat T-cells induced a time and dose dependent elevation in specific apoptosis. At all concentrations examined (10nM-100μM), methotrexate did not mediate any significant elevation in apoptosis following 6 hours treatment. After 16 hours exposure, methotrexate induced a concentration dependent elevation in specific apoptosis initially observed at 30nM ($p<0.05$) and was maximal at 1μM ($p<0.01$) with approximately 32% apoptosis. Increasing the methotrexate

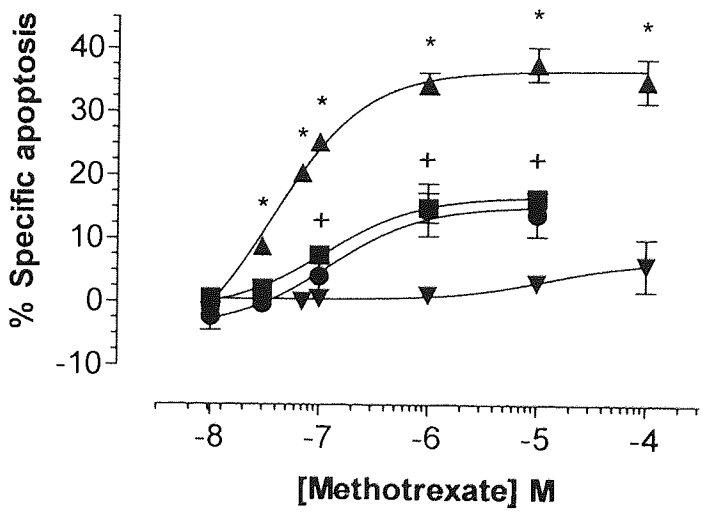

Figure 5.3. Methotrexate mediated induction of apoptosis in Jurkat T-cells is inhibited by the anti-oxidants glutathione and N-acetylcysteine. Jurkat T-cells ($2x10^6$/ml) were serum starved for 4 hours prior to the addition of methotrexate (0-$1x10^{-4}$M) for 6 hours (▼) or 16hrs (▲), and 16hrs in the presence of 10mM of the anti-oxidants N-acetylcysteine (NAC; ■) or 10mM glutathione (GSH;●). Incubations were performed at 37°C in a 95% air, 5% CO_2 humidified atmosphere and terminated by washing the cells twice with ice cold PBS. Cell pellets were resuspended in 1ml of hypotonic fluorochrome solution and incubated in the dark at 4°C overnight prior to DNA cell cycle analysis by flow cytometry. The sub-diploid DNA content of 20,000 nucleoids from each sample was analysed. The data is expressed as the mean ± s.e.m of at least 4 individual experiments, expressed as the percentage specific apoptosis where * ($p<0.05$) represents significant difference from control samples by one-way ANOVA followed by Dunnetts' multiple comparison test and + ($p<0.05$) represents significant difference of 16hrs methotrexate samples pre-treated with NAC/GSH compared to none pre-treated samples by students T-test.

concentration up to the maximum dose analysed, 100μM, did not further increase the percentage of apoptosis ($p>0.05$). A plateau in the percentage specific apoptosis induced by methotrexate was observed at 1μM (see Figure 5.3).

Pre-treatment of Jurkat T-cells with either 10mM GSH or NAC significantly reduced the specific apoptosis observed in Jurkat T-cells following 16 hours methotrexate (30nM - 10μM) treatment at all doses. When pre-treated with GSH or NAC, methotrexate-induced apoptosis in Jurkat T-cells was only observed after 1μM ($p<0.05$) and 10μM ($p<0.05$) treatment respectively which mediated a 10% elevation in apoptosis, approximately 22% lower than that observed in Jurkat T-cells with no pre-treatment (see Figure 5.3).

The presence of $[peroxide]_{cyt}$ in Jurkat T-cells following methotrexate (30nM - 10μM) exposure was analysed by flow cytometry as the fluorescence emitted by the peroxide sensitive dye DCFH-DA. The MdX fluorescence of DCF of the viable cell population, determined by the FS and SS properties of methotrexate treated Jurkat T-cells, increased as a function of time and dose. $[peroxide]_{cyt}$ production was not determined for non-apoptotic methotrexate doses (<10nM, see Figure 5.4a). Methotrexate concentrations of 1μM and 10μM produced a significant elevation in DCF fluorescence within 4hours ($p<0.05$) to approximately 20 a.u above control levels and increased dramatically up to approximately 130 a.u following 16 hours ($p<0.01$) treatment. At all incubation periods, the change in DCF fluorescence produced by 1μM and 10μM methotrexate treatment of Jurkat T-cells was not significant ($p>0.05$). After 16 hours treatment, 0.1μM methotrexate also induced a significant increase in DCF fluorescence ($p<0.01$) to approximately 75 a.u above

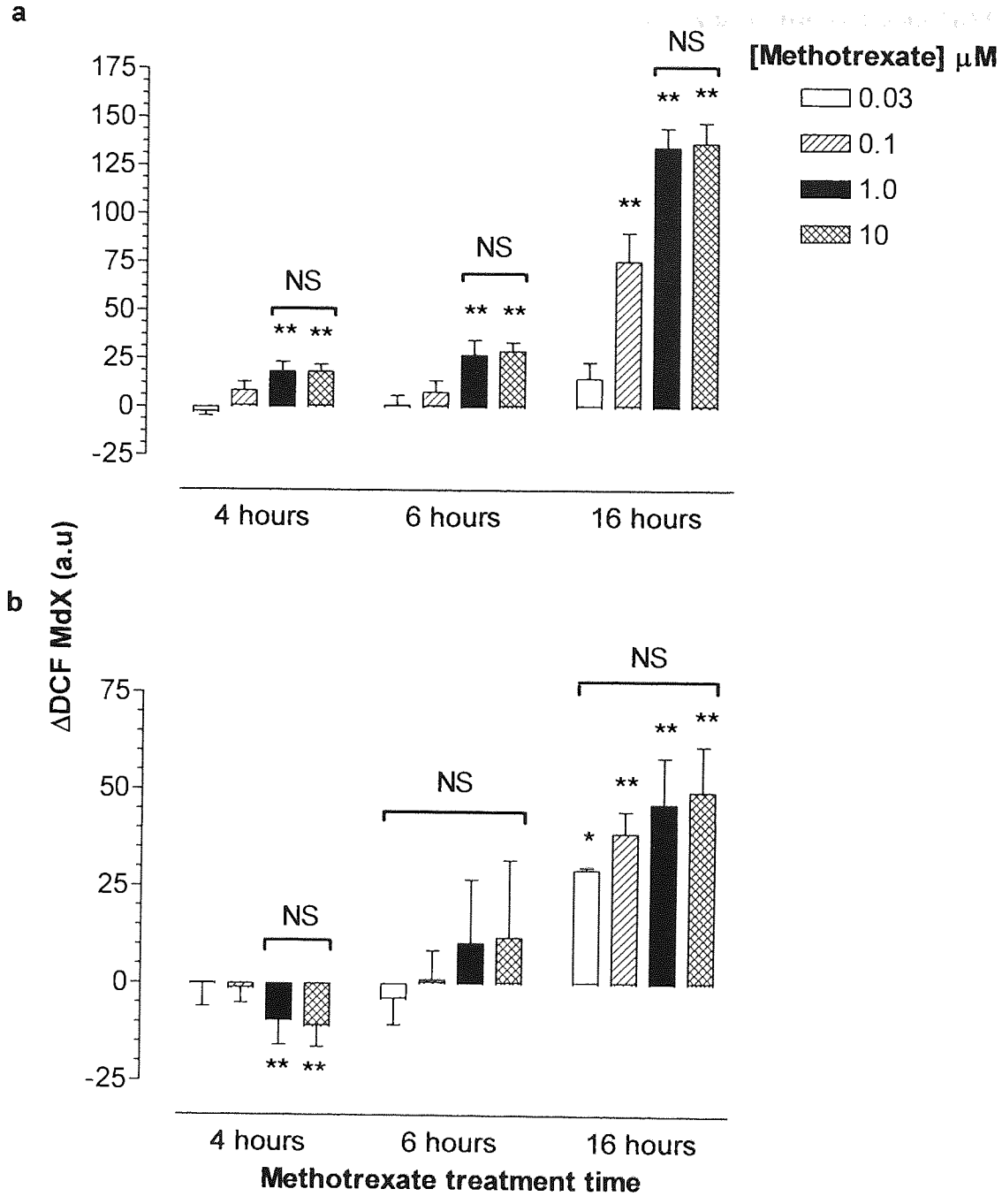

Figure 5.4. Methotrexate mediated alterations in the cytosolic peroxide levels of Jurkat T-cells and U937 monocytes: kinetics for the oxidation of DCFH to DCF. Jurkat T-cells (a) or U937 monocytes (b; $2x10^6$/ml) were serum starved in RMPI 1640 for 4 hours prior to the addition of 0-100μM methotrexate for 4,6 or 16 hours. Cells were treated with 50μM DCFH-DA as described in method 5.2.4. At the end of the treatment periods, cell samples were analysed immediately for DCF fluorescence by flow cytometry. The median X (MdX) DCF fluorescence of 10,000 cells was analysed per sample. ΔDCF represents the difference in MdX DCF of methotrexate treated cells from that of vehicle treated cells for each time point. All incubations were performed at 37°C in a humidified, 95% air, 5% CO_2 atmosphere. The data is expressed as the mean ± s.e.m of at least 4 individual experiments where * ($p<0.05$) and ** ($p<0.01$) were considered significantly different from control samples by one-way ANOVA followed by Tukey's post *hoc* test. a.u, arbitrary units.

those of control cells but was not to the same magnitude as that observed with 1μM or 10μM methotrexate ($p>0.05$; see Figure 5.4a).

Pre-treatment of Jurkat T-cells with the anti-oxidants GSH or NAC (10mM) significantly reduced the DCF fluorescence induced by 16 hours 0.1-10μM methotrexate treatment compared to cells without pre-treatment ($p<0.05$). DCF fluorescence induced by methotrexate at these doses in the presence of anti-oxidant was reduced to levels observed in control Jurkat T-cells without anti-oxidant treatment ($p>0.05$; see Figure 5.5a).

Methotrexate (10nM - 10μM) did not affect the protein content of Jurkat T-cells following 6 or 16 hours treatment (see Figures 5.6a & b). Consequently, to standardise, total cellular GSH levels were expressed per mg of protein. At low doses, 10nM and 100nM, 6 hours methotrexate treatment of Jurkat T-cells did not affect total GSH levels, although a trend towards GSH loss was observed at 1μM and 10μM ($p>0.05$; see Figure 5.7a). After 16 hours of Jurkat T-cell treatment with 30nM methotrexate, a significant elevation of total GSH levels ($p<0.05$) was observed to approximately 115% of control treated cells. On increasing the concentration of methotrexate, the total GSH levels of Jurkat T-cells were significant reduced to approximately 60% of control levels ($p<0.05$; see Figure 5.7b).

Unlike Jurkat T-cells, U937 monocytes treated with methotrexate induced an accumulation of DNA in the G0/G1 phase of the cell cycle, which is indicative of growth arrest, with corresponding loss of G2M DNA (see Figure 5.8). There were no observations of fragmented DNA, a marker of apoptosis. Methotrexate at a

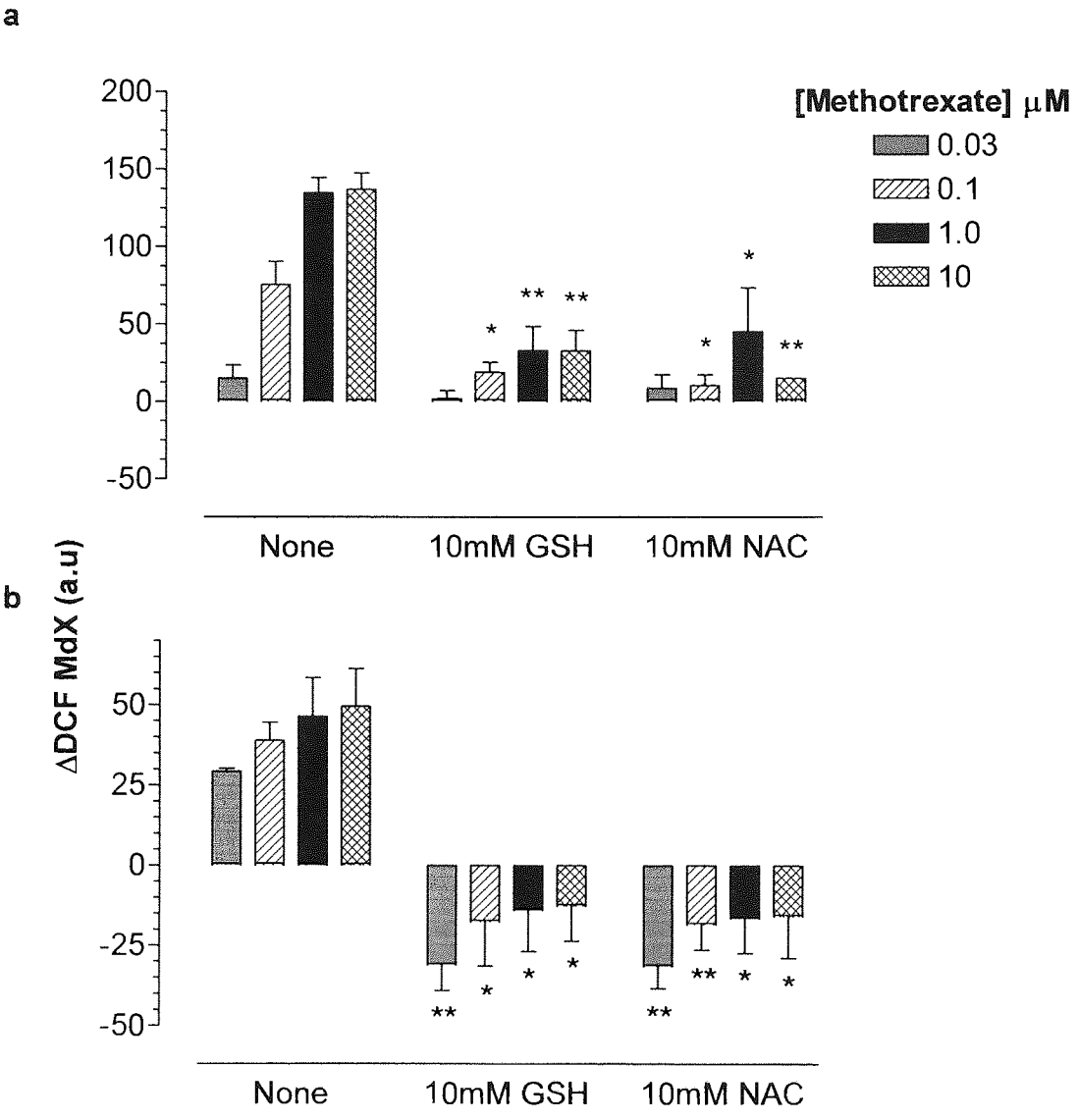

Figure 5.5. Inhibition of methotrexate induced cytosolic peroxide formation in Jurkat T-cells and U937 monocytes by anti-oxidants: kinetics for the inhibition of methotrexate mediated oxidation of DCFH to DCF. Jurkat T-cells (a) or U937 monocytes (b) ($2x10^6$/ml) were serum starved in RMPI 1640 for 4 hours in the presence or absence of 10mM glutathione (GSH) or N-acetylcysteine (NAC) prior to the addition of 0-100μM methotrexate for 16 hours. Cells were treated with 50μM DCFH-DA as described in method 5.2.4. At the end of the treatment periods, cell samples were analysed immediately for DCF fluorescence by flow cytometry. The median X (MdX) DCF fluorescence of 10,000 cells was analysed per sample. ΔDCF represents the difference in MdX DCF of methotrexate treated cells from that of vehicle treated cells for each time point. All incubations were performed at 37°C in a humidified, 95% air, 5% CO_2 atmosphere. The data is expressed as the mean ± s.e.m of at least 4 individual experiments where * ($p<0.05$) and ** ($p<0.01$) of GSH/NAC pre-treated samples were considered significantly different from samples with no pre-treatment by the students T-test. a.u, arbitrary units.

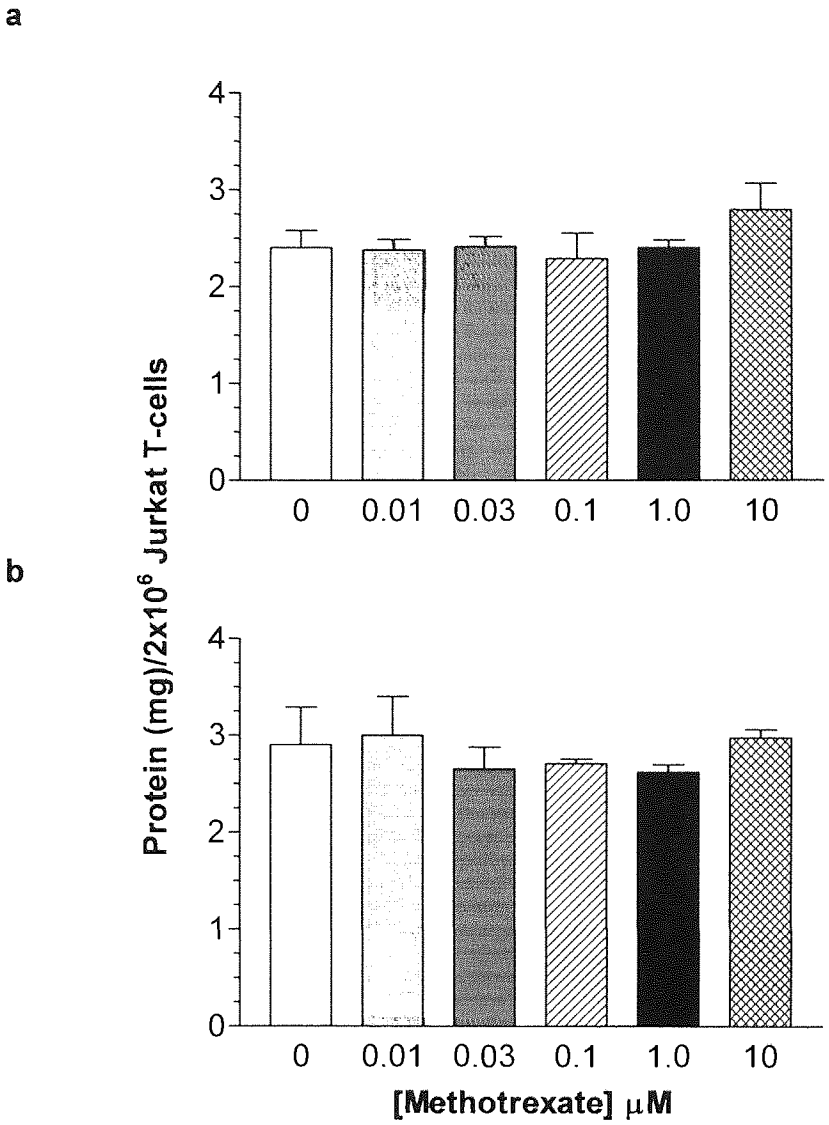

Figure 5.6. Jurkat T-cell protein content is not affected by methotrexate treatment. Jurkat T-cells ($2x10^6$/ml) were serum starved in RMPI 1640 for 4 hours prior to the addition of methotrexate (0-10μM) for 6 hours (a) or 16 hours (b). At the end of the treatment period, cells were washed twice with ice cold PBS. The total protein content analysed by spectrophotometry and quantified against a standard curve of known protein concentrations as described in method 5.2.5. Data represents the mean ± s.e.m of 4 individual experiments analysed in quadruplicate. Statistical analysis was performed by one-way ANOVA followed by Tukey's post hoc test.

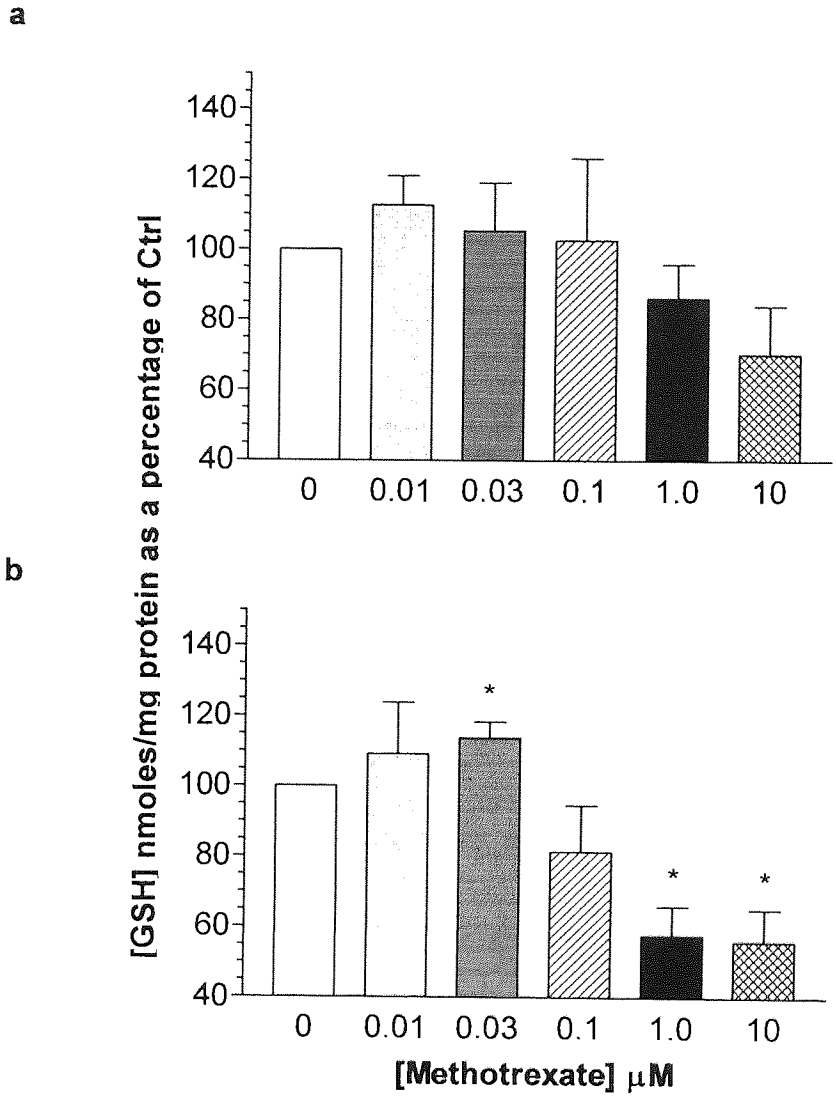

Figure 5.7. The effect of methotrexate on Jurkat T-cell total cellular glutathione levels. Jurkat T-cells ($2x10^6$/ml) were serum starved for 4 hours prior to the addition of methotrexate (0-10μM) for 6 hours (a) or 16 hours (b). At the end of the treatment period, cells were washed twice with ice cold PBS. The total glutathione (GSH) content analysed by spectrophotometric determination of reduced DNTB using a GSSG recycling assay and quantified against a standard curve of known GSH concentrations as described in method 5.2.5. Data represents the mean GSH content per mg of cellular protein ± s.e.m of 4 individual experiments analysed in quadruplicate. Statistical analysis was performed by one-way ANOVA followed by Tukey's post hoc test where * ($p<0.05$) was considered significant from vehicle control treatments.

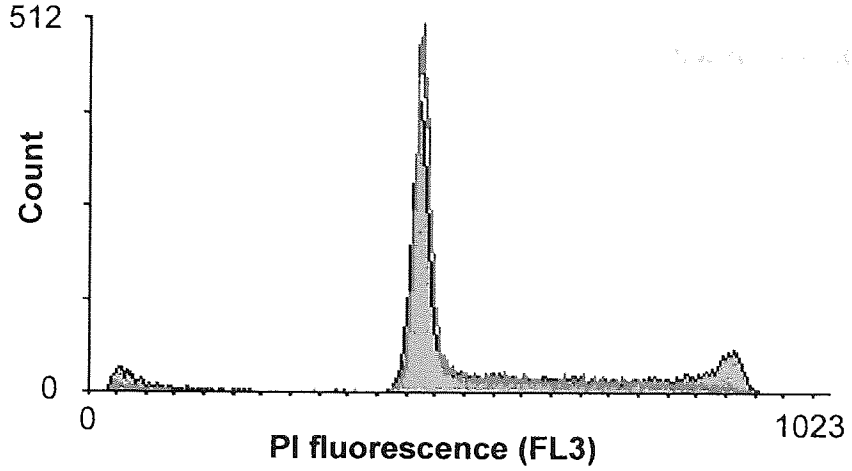

Figure 5.8. Methotrexate induces an accumulation of nucleoids in the G0/G1 phase of the cell cycle with loss of G2M DNA content in U937 monocytes. U937 monocytes ($2x10^6$/ml) were serum starved for 4 hours in RPMI 1640 prior to the addition of 0-100μM methotrexate for 16 hours. Incubations were terminated by washing the cells twice with ice cold PBS. Cell pellets were resuspended in 1ml of hypotonic fluorochrome solution and incubated in the dark at 4°C overnight prior to flow cytometric DNA cell cycle analysis of 20,000 nucleoids from each sample. Shown is a typical DNA cell cycle histogram of control treated cells (black outline, grey solid fill) overlayed with those from 0.1μM methotrexate treated cells (blue outline, no fill).

concentration greater than 1μM induced a significant increase in the G0/G1 content of approximately 15% compared to controls ($p<0.05$), to 70% from 55% after 6 hours exposure. Extending the U937 treatment period to 16 hours with concentrations greater than 1μM methotrexate did not further elevate the percentage of G0/G1 content when compared to 6 hours of treatment, although the variation between samples was reduced. Additionally, after 16 hours treatment a lower dose of methotrexate (100nM) induced a significant increase in G0/G1 DNA content compared to control cells ($p<0.01$) and to the same level, approximately 70%, as that seen with methotrexate concentrations exceeding 100nM ($p>0.05$; see Figure 5.9).

Pre-treatment of U937 monocytes with 10mM GSH/NAC caused significant abrogation of nucleoid accumulation in the G0/G1 phases at all concentrations of

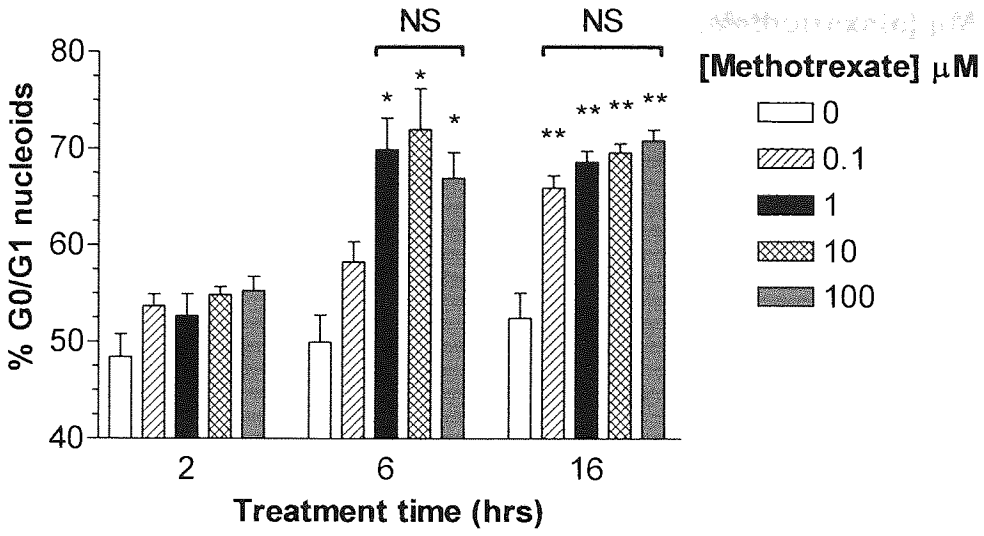

Figure 5.9. Methotrexate induces growth arrest in U937 monocytes. U937 monocytes ($2x10^6$/ml) were serum starved for 4 hours in RPMI 1640 prior to the addition of 0-100μM methotrexate for 2, 6 or 16 hours. Incubations were terminated by washing the cells twice with ice cold PBS. Cell pellets were resuspended in 1ml of hypotonic fluorochrome solution and incubated in the dark at 4°C overnight prior to DNA cell cycle analysis by flow cytometry as described in method 5.2.3. The percentage G0/G1 DNA content of 20,000 nucleoids from each sample was analysed using MultiCycle™ for Windows (Phoenix Flow Systems, San Diego, U.S.A.). The data is expressed as the mean ± s.e.m of at least 4 individual experiments, where * ($p<0.05$) and ** ($p<0.01$) were considered significantly different from control samples by one-way ANOVA followed by Tukey's multiple comparison test.

(100nM-10μM) following 16 hours treatment ($p<0.01$). The percentage of nucleoids in the G0/G1 phase following methotrexate exposure of 10mM GSH or NAC pre-treated U937 monocytes was not significantly different from controls ($p>0.05$; see Figure 5.10). Vehicle control U937 monocytes possessed identical G0/G1 content irrespective of exposure period or pre-treatment ($p>0.05$; see Figures 5.9 & 5.10).

Since apoptosis is not the exclusive form of cell death, the possibility that methotrexate treatment of U937 monocytes or Jurkat T-cells may induce necrosis was examined by dye exclusion. The uptake of the membrane impermeable dye PI,

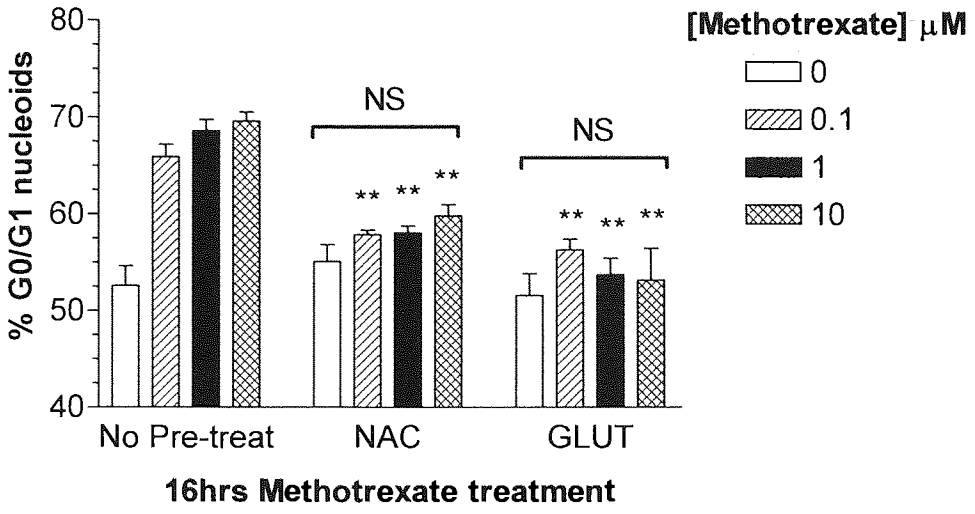

Figure 5.10. Methotrexate induced growth arrest in U937 monocytes is inhibited by the anti-oxidants glutathione and N-acetylcysteine. U937 monocytes ($2x10^6$/ml) were serum starved for 4 hours in RMPI 1640 in the presence or absence of 10mM N-acetylcysteine (NAC) or 10mM glutathione (GSH) prior to the addition of 0-100μM methotrexate for 16 hours. Incubations were terminated by washing the cells twice with ice cold PBS. Cell pellets were re-suspended in 1ml of hypotonic fluorochrome solution and incubated in the dark at 4°C overnight prior to DNA cell cycle analysis by flow cytometry as described in method 5.2.3. The percentage G0/G1 DNA content of 20,000 nucleoids from each sample was analysed using MultiCycle™ for Windows (Phoenix Flow Systems, San Diego, U.S.A.). The data is expressed as the mean ± s.e.m. of at least 4 individual experiments where ** ($p<0.01$) were considered significantly different from samples with no pre-treatment by students T-test. NS = no significant difference by one-way ANOVA followed by Tukey's post hoc test.

evaluated by flow cytometry, showed no difference between concentration of methotrexate and vehicle controls for either cell types ($p>0.05$; see Figure 5.11 and 5.12).

Contrary to the increase in DCF fluorescence observed in Jurkat T-cells upon methotrexate treatment, Figure 5.6b illustrates that an initial decrease was recorded in U937s after 4 hours exposure to concentrations of 1.0μM and 10μM ($p<0.01$). DCF fluorescence returned to control levels after 6 hours methotrexate treatment and showed a dose dependent elevation in ΔDCF after 16 hours exposure. Methotrexate

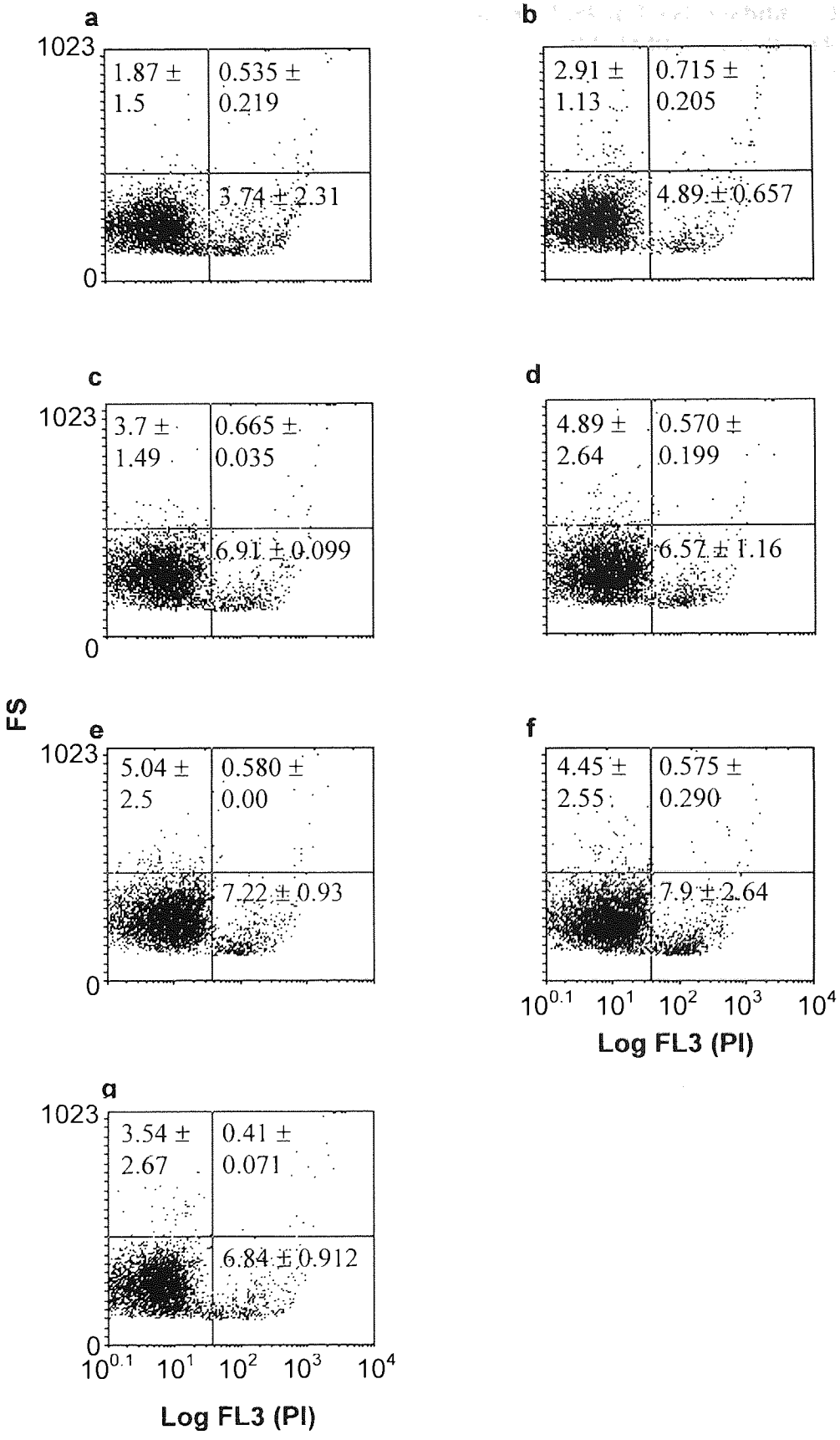
a
1023
1.87 ± 1.5
0.535 ± 0.219
3.74 ± 2.31
0
b
2.91 ± 1.13
0.715 ± 0.205
4.89 ± 0.657
c
1023
3.7 ± 1.49
0.665 ± 0.035
6.91 ± 0.099
0
d
4.89 ± 2.64
0.570 ± 0.199
6.57 ± 1.16
FS
e
1023
5.04 ± 2.5
0.580 ± 0.00
7.22 ± 0.93
0
f
4.45 ± 2.55
0.575 ± 0.290
7.9 ± 2.64
10^0.1 10^1 10^2 10^3 10^4
Log FL3 (PI)
g
1023
3.54 ± 2.67
0.41 ± 0.071
6.84 ± 0.912
0
10^0.1 10^1 10^2 10^3 10^4
Log FL3 (PI)

Figure 5.11. Methotrexate does not compromise Jurkat T-cell viability. Jurkat T-cells ($2x10^6$/ml) were serum starved for 4 hours in RPMI 1640 prior to the addition of 0 **(a)**, 0.01 (b), 0.03 (c), 0.07 (d) 0.1 (e) 1.0 (f) and 10μM (g) methotrexate for 16 hours at 37°C in a 95% air, 5%CO_2 humidified atmosphere. Incubations were terminated by washing the cells twice with ice cold PBS. Cell pellets were resuspended in 1ml of PI solution (25μg/ml in PBS containing 0.1% BSA) and incubated in the dark at room temperature for 15 minutes prior to immediate analysis of PI uptake by flow cytometry on a dual parameter histogram of log FL3 (propidium iodide, PI) versus forward scatter as described in method 5.2.8. Flow cytometry histograms shown are representational of 3 individual experiments. Data are expressed as the percentage of cells in each quadrant as the mean ± s.d of 3 individual experiments and test samples analysed for statistical significance from control by one-way ANOVA followed by Dunnett's multiple comparison test.

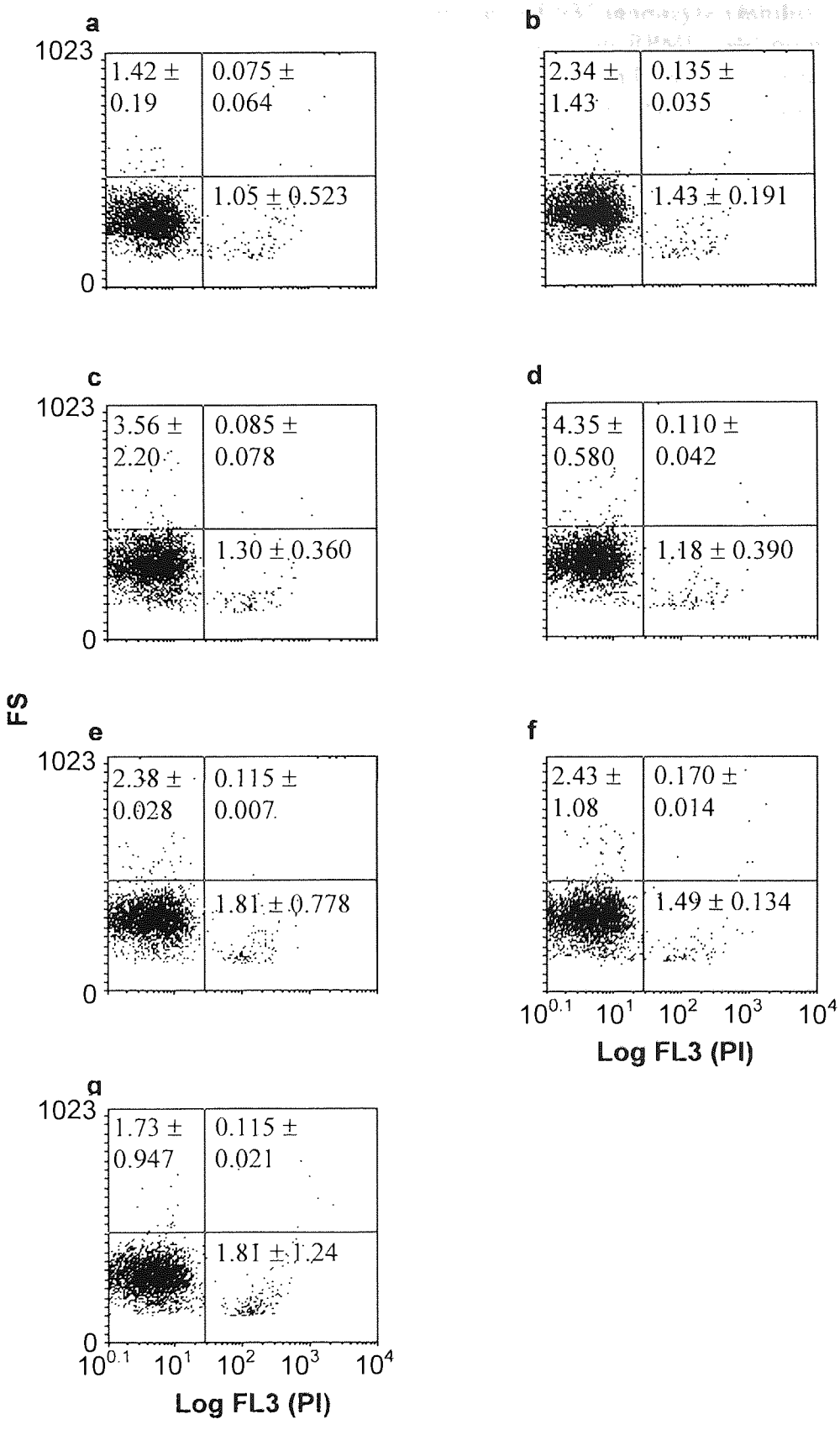
a
1023
1.42 ± 0.19
0.075 ± 0.064
1.05 ± 0.523
0
b
2.34 ± 1.43
0.135 ± 0.035
1.43 ± 0.191
c
1023
3.56 ± 2.20
0.085 ± 0.078
1.30 ± 0.360
0
d
4.35 ± 0.580
0.110 ± 0.042
1.18 ± 0.390
FS
e
1023
2.38 ± 0.028
0.115 ± 0.007
1.81 ± 0.778
0
f
2.43 ± 1.08
0.170 ± 0.014
1.49 ± 0.134
10^0.1 10^1 10^2 10^3 10^4
Log FL3 (PI)
g
1023
1.73 ± 0.947
0.115 ± 0.021
1.81 ± 1.24
0
10^0.1 10^1 10^2 10^3 10^4
Log FL3 (PI)

Figure 5.12. Methotrexate does not compromise U937 monocyte viability. U937 monocytes ($2x10^6$/ml) were serum starved for 4 hours in RPMI 1640 prior to the addition of 0 (a), 0.01 (b), 0.03 (b), 0.07 (d) 0.1 (e) 1.0 (f) and 10μM (g) methotrexate for 16 hours at 37°C in a 95% air, 5%CO_2 humidified atmosphere. Incubations were terminated by washing the cells twice with ice cold PBS. Cell pellets were resuspended in 1ml of PI solution (25μg/ml in PBS containing 0.1% BSA) and incubated in the dark at room temperature for 15 minutes prior to immediate analysis of PI uptake by flow cytometry on a dual parameter histogram of log FL3 (propidium iodide, PI) versus forward scatter as described in method 5.2.8. Flow cytometry histograms shown are representational of 3 individual experiments. Data are expressed as the percentage of cells in each quadrant as the mean ± s.d of 3 individual experiments and test samples analysed for statistical significance from control by one-way ANOVA followed by Dunnett's multiple comparison test.

concentrations of 100nM or more induced an increase in DCF fluorescence of approximately 45 a.u above controls ($p<0.01$) whereas 30nM mediated a 25 a.u rise in ΔDCF ($p<0.05$; see Figure 5.4b). Pre-treatment of U937 monocytes with 10mM of the anti-oxidants GSH or NAC significantly inhibited the elevation in ΔDCF induced by 16 hours treatment with methotrexate concentrations of 30nM - 10μM ($p<0.05$; See Figure 5.5b).

The protein content of U937 monocytes remained unchanged irrespective of methotrexate treatment or period ($p>0.05$; see Figures 5.13). The total cellular GSH content of U937 monocytes was expressed per mg of protein. No alteration in the total cellular GSH levels of U937 monocytes was observed following 6 hours MTX treatment ($p>0.05$; see Figure 14a). After 16 hours treatment, methotrexate (≥10nM) induced a significant reduction in total GSH levels compared to controls ($p<0.05$). The degree of GSH loss in U937s was statistically equivalent for all concentrations of methotrexate examined ($p>0.05$; see Figure 5.14b). The total cellular GSH concentration of control U937 monocytes (mean = 31.18 ± 1.479 nmoles of GSH/mg protein, n=6) was significantly greater than that of Jurkat T-cells (mean = 10.95 ± 2.103 nmoles of GSH/mg protein, n=6; $p<0.01$; see Figure 5.15).

The mechanism by which methotrexate modulates inflammation is widely debated, although the immunosuppressive properties of low dose methotrexate has been postulated to relate to the induction of apoptosis in activated T-cells. However, the effects of methotrexate on the activity of monocytes in the inflammatory responses are unknown. Considering that a characteristic of several inflammatory states is the recruitment and adhesion of monocytes to sites of inflammation and these data show

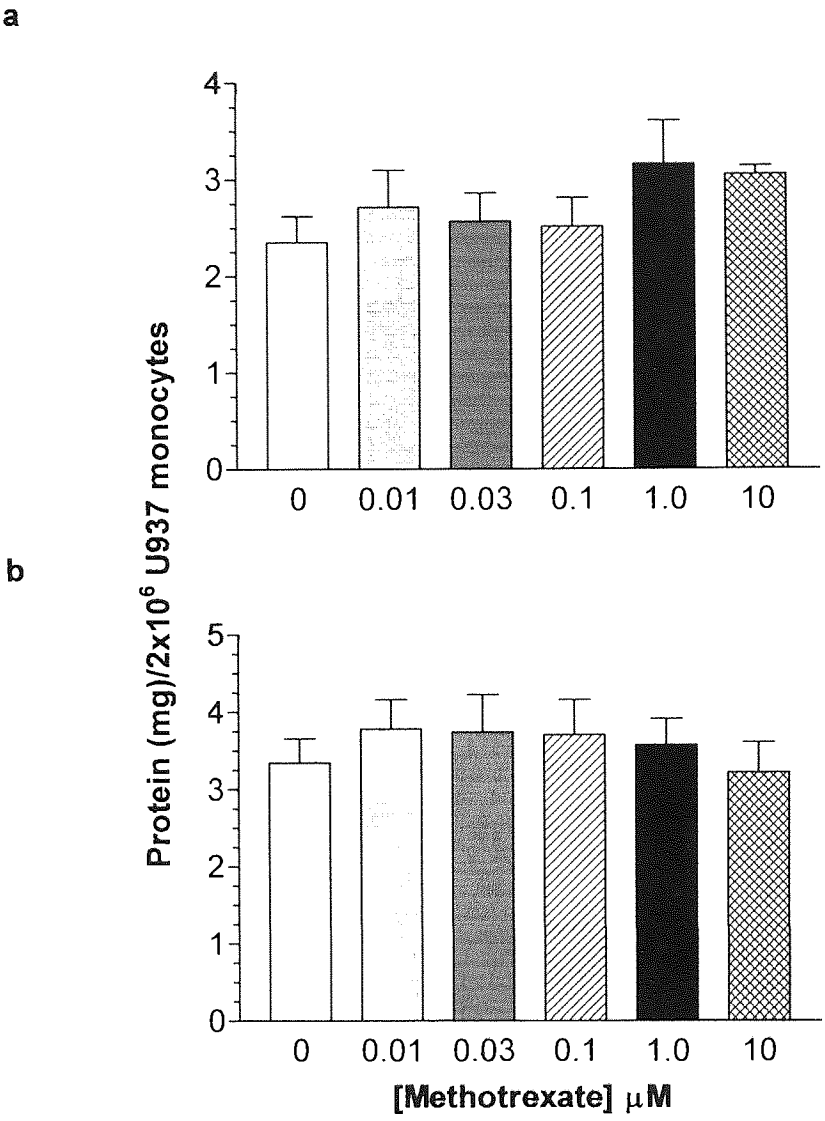

Figure 5.13. The protein content of U937 monocytes is not affected by methotrexate treatment. U937 monocytes ($2x10^6$/ml) were serum starved in RPMI 1640 for 4 hours prior to the addition of methotrexate (0-10μM) for 6 hours (a) or 16 hours (b). At the end of the treatment period, cells were washed twice with ice cold PBS. The total protein content analysed by spectrophotometry and quantified against a standard curve of known protein concentrations as described in method 5.2.5. Data represents the mean ± s.e.m of 4 individual experiments analysed in quadruplicate. Statistical analysis was performed by one-way ANOVA followed by Tukey's post hoc test.

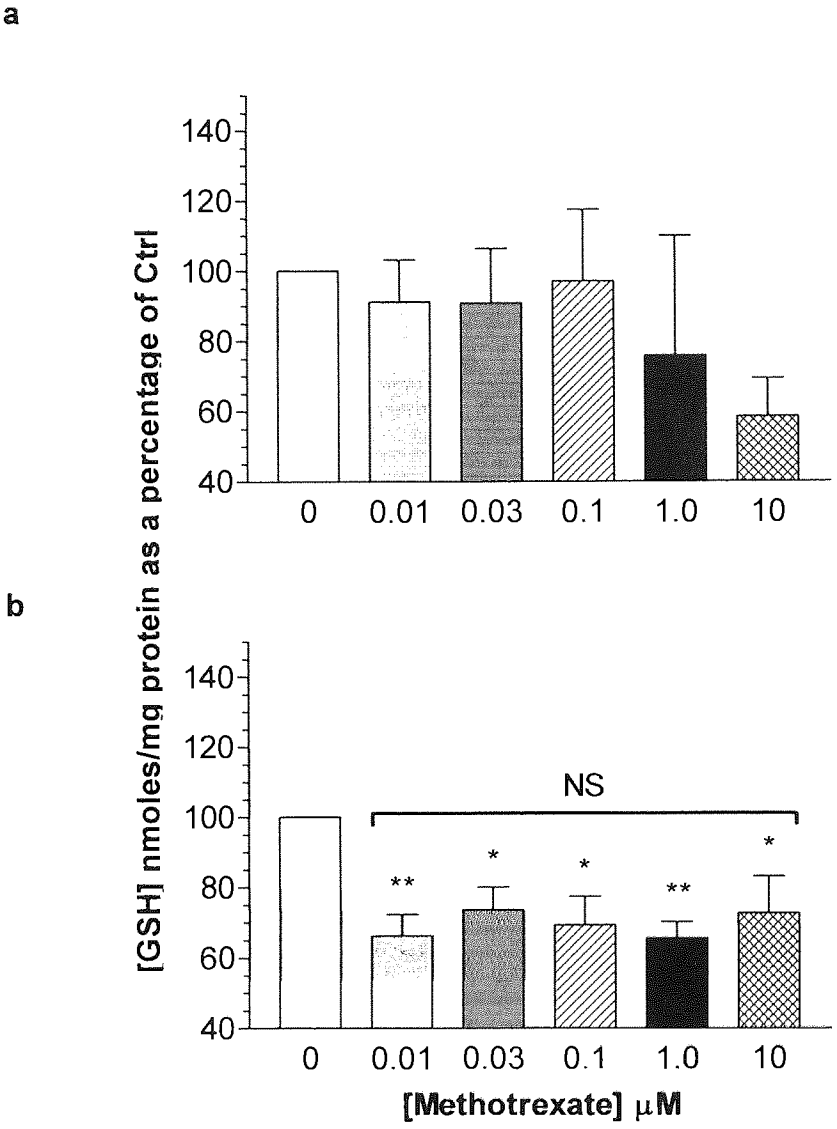

Figure 5.14. The effect of methotrexate on U937 monocyte total cellular glutathione levels. U937 monocytes ($2x10^6$/ml) were serum starved for 4 hours in RPMI 1640 prior to the addition of methotrexate (0-10μM) for 6 hours (a) or 16 hours (b). At the end of the treatment period, cells were washed twice with ice cold PBS. The total glutathione (GSH) content analysed by spectrophotometric determination of DNTB using a GSSG recycling assay and quantified against a standard curve of known GSH concentrations as described in method 5.2.5. Data represents the mean GSH content per mg of cellular protein ± s.e.m of 4 individual experiments analysed in quadruplicate. Statistical analysis was performed by one-way ANOVA followed by Tukey's post hoc test where * ($p<0.05$) and ** ($p<0.01$) represents significant difference from control samples. NS = not significant.

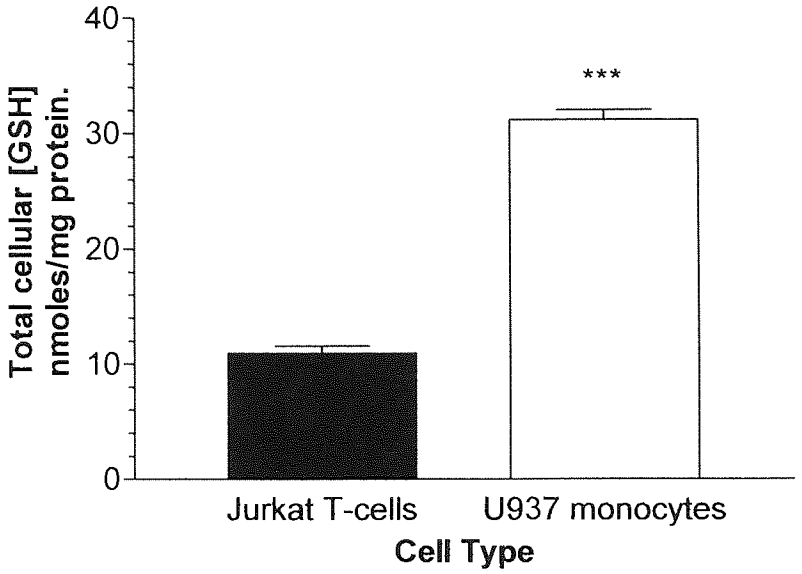

Figure 5.15. U937 monocytes possess higher endogenous levels of total cellular glutathione than Jurkat T-cells. Jurkat T-cells or U937 monocytes ($2x10^6$/ml) were serum starved for 4 hours after which cells were washed twice with ice cold PBS. The total glutathione (GSH) content analysed by spectrophotometric determination of reduced DNTB and quantified against a standard curve of known GSH concentrations as described in method 5.2.5. Data represents the mean GSH content per mg of cellular protein ± s.e.m of 6 individual experiments analysed in quadruplicate. Statistical analysis was performed by students T-test where the total cellular GSH content of U937 monocytes was considered significant from Jurkat T-cells (***; $p<0.001$).

that the treatment of U937 monocytes with methotrexate induced no evidence of cell death (see Figures 5.9 & 5.12), the effect of methotrexate on the adhesion of monocytes to endothelial cells was investigated. Methotrexate treatment of U937 monocytes with 30nM and 1.0μM did not affect their adhesion to resting HUVEC (see Figure 5.16a). However, when HUVEC monolayers were activated with LPS (1μg/ml) for 5 hours, the 30nM and 1.0μM methotrexate treated U937s showed significantly reduced adherence to approximately 60 % ($p<0.01$) and 70% ($p<0.05$) of control treated U937 monocytes respectively (see Figure 5.16b). When the HUVEC were activated with 1μg/ml of LPS for 24 hours, methotrexate treatment of U937 monocytes reduced their adhesion further to approximately 40% of that of control

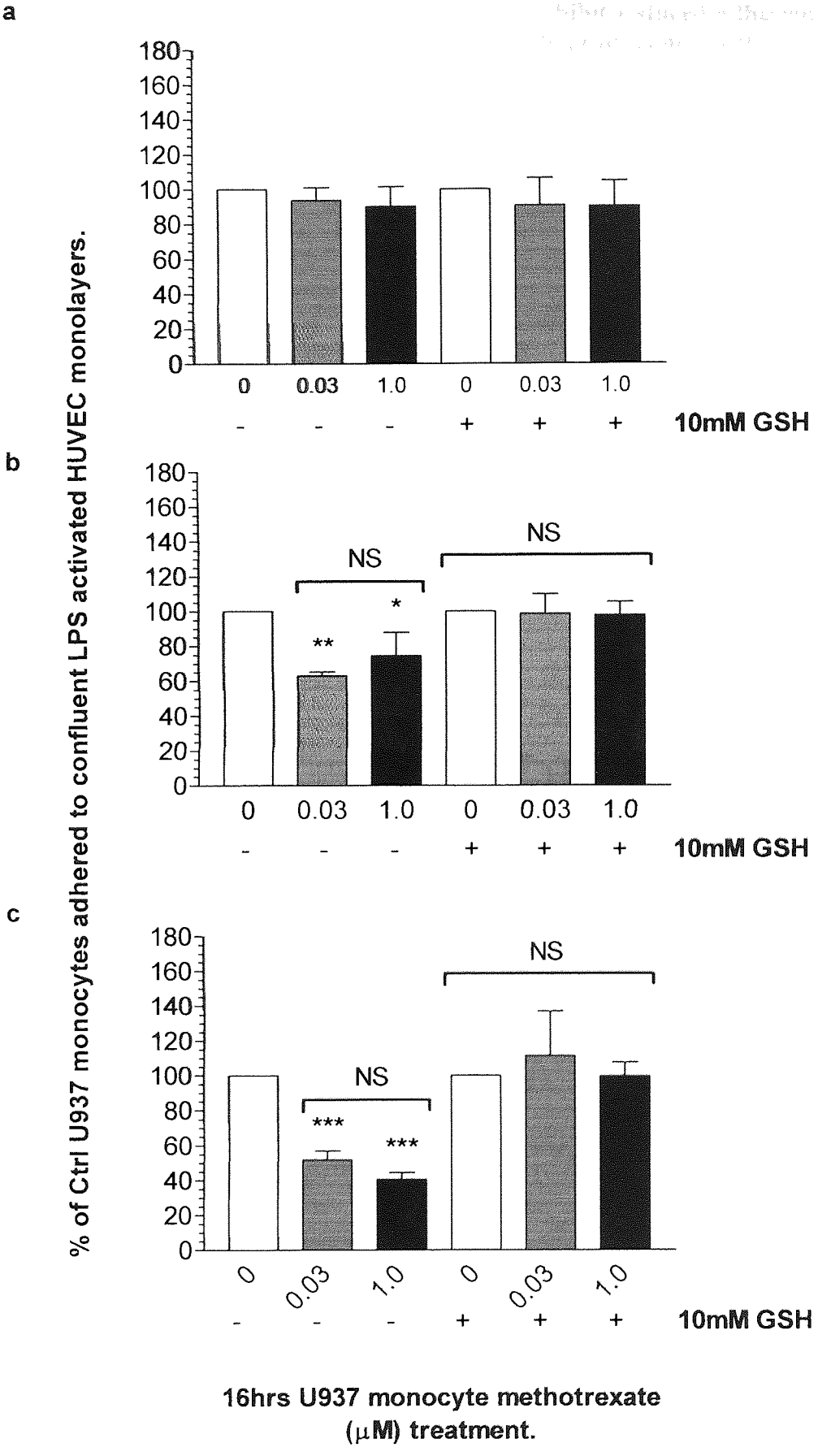
a
b
c
% of Ctrl U937 monocytes adhered to confluent LPS activated HUVEC monolayers.
180
160
140
120
100
80
60
40
20
0
0
0.03
1.0
0
0.03
1.0
-
-
-
+
+
+
10mM GSH
NS
NS
**
*
***
***
16hrs U937 monocyte methotrexate
(μM) treatment.

Figure 5.16. Methotrexate treated monocytes exhibit reduced adhesion to LPS activated HUVEC with a requirement for ROS production. U937 monocytes ($2x10^6$/ml) were serum starved for 4 hours in RPMI 1640 in the presence or absence of 10mM glutathione (GSH) prior to 0, 0.03 or 1.0μM methotrexate treatment. Treatments were terminated by centrifugation and the resulting cell pellets washed twice with ice cold PBS. Cells ($5x10^6$/ml) were loaded with 1μg/ml of BCECF-AM for 30 minutes in the dark. Cells were then washed and resuspended in M199 to a concentration of $0.5x10^6$/ml. Confluent HUVEC monolayers in 24 well plates were treated with 1μg/ml LPS for 0 (a), 5 (b) or 24 hours (c). HUVEC were washed twice prior to the addition of treated monocyte suspensions in duplicate for 30 minutes under the described incubator conditions. Their adherence was quantified against a standard curve of vehicle treated monocytes and expressed as a percentage of controls. The results are presented as the mean ± s.d of at least 4 individual experiments where * ($p<0.05$), ** ($p<0.01$) and *** ($p<0.001$) represent significant difference from controls by one-way ANOVA with Dunnett's post-test analysis. NS, no significant difference.

Treatment	Mean MdX ± St Dev	Significant Difference from Ctrl
Ctrl	12.35 ± 2.192	-
30mM	13.95 ± 1.354	No
1μM	12.65± 0.636	No

Table 5.1. Methotrexate does not interfere with the fluorescence emitted from BCECF-AM in U937 monocytes. U937 monocytes ($2x10^6$/ml) were serum starved for 4 hours in RPMI 1640 prior to 0, 0.03 or 1.0μM methotrexate treatment. Treatments were terminated by centrifugation and the resulting cell pellets washed twice with ice cold PBS. Cells ($5x10^6$/ml) were loaded with 1μg/ml of BCECF-AM for 30 minutes in the dark. Cells were then washed and resuspended in M199 to a concentration of $0.5x10^6$/ml and the fluorescence of the viable U937 monocyte population, as determined by forward scatter (FS) and side scatter (SS) properties, analysed by flow cytometry on a single parameter histogram of Log FL1 versus count. 10,000 cells were analysed per sample and the median x (MdX) of the fluorescence peak recorded. Results are presented as the arithmetic mean of 3 individual experiments and analysed for statistical difference by one way ANOVA followed by Dunnets' multiple comparison tests where $p<0.05$ was considered significantly different from vehicle treated control cells.

monocytes ($p<0.01$). There was no significant difference in the anti-adhesive properties of 30nM and 1.0μM methotrexate treatment of U937 monocyte to 24 hours LPS (1μg/ml) activated HUVEC ($p>0.05$; see Figure 5.16c).

The reduction in adhesion of monocytes treated with methotrexate to activated HUVEC was inhibited by pre-treatment of U937 monocytes with of the antioxidant GSH (10mM) and was not significantly different to control treated U937 monocytes, irrespective of the period of HUVEC activation by LPS (1μg/ml; $p>0.05$; see Figures 5.16a, b & c). U937 monocyte adherence was quantified utilising fluorophotometric analysis of the fluorescent probe BCECF-AM. Flow cytometric quantification of the fluorescence emitted from cells loaded with BCECF-AM following treatment with MTX showed no effect on the fluorescence emitted by this probe (see Table 5.1). The decrease in fluorescence observed in the adhesion assay of cells treated the MTX compared to vehicle treated controls which is consequently converted via a standard curve to a cell number is not due to quenching of BCECF-AM fluorescence by MTX.

To further evaluate the anti-adhesive properties of methotrexate treatment of U937 monocytes, the membrane expression of monocyte integrin molecules CD11a, CD11b, CD18, CD29, CD31 and CD49D, and the leukocyte associated selectin CD62L were quantified by flow cytometry. Monocytes treated with 30nM or 1.0μM methotrexate induced a significant elevation in the membrane expression of all the adhesion molecules examined of between 120-140% of that of control U937 monocytes ($p<0.05$) with no significant difference observed between MTX concentrations ($p>0.05$). Pre-treatment of U937 monocytes with 10mM GSH

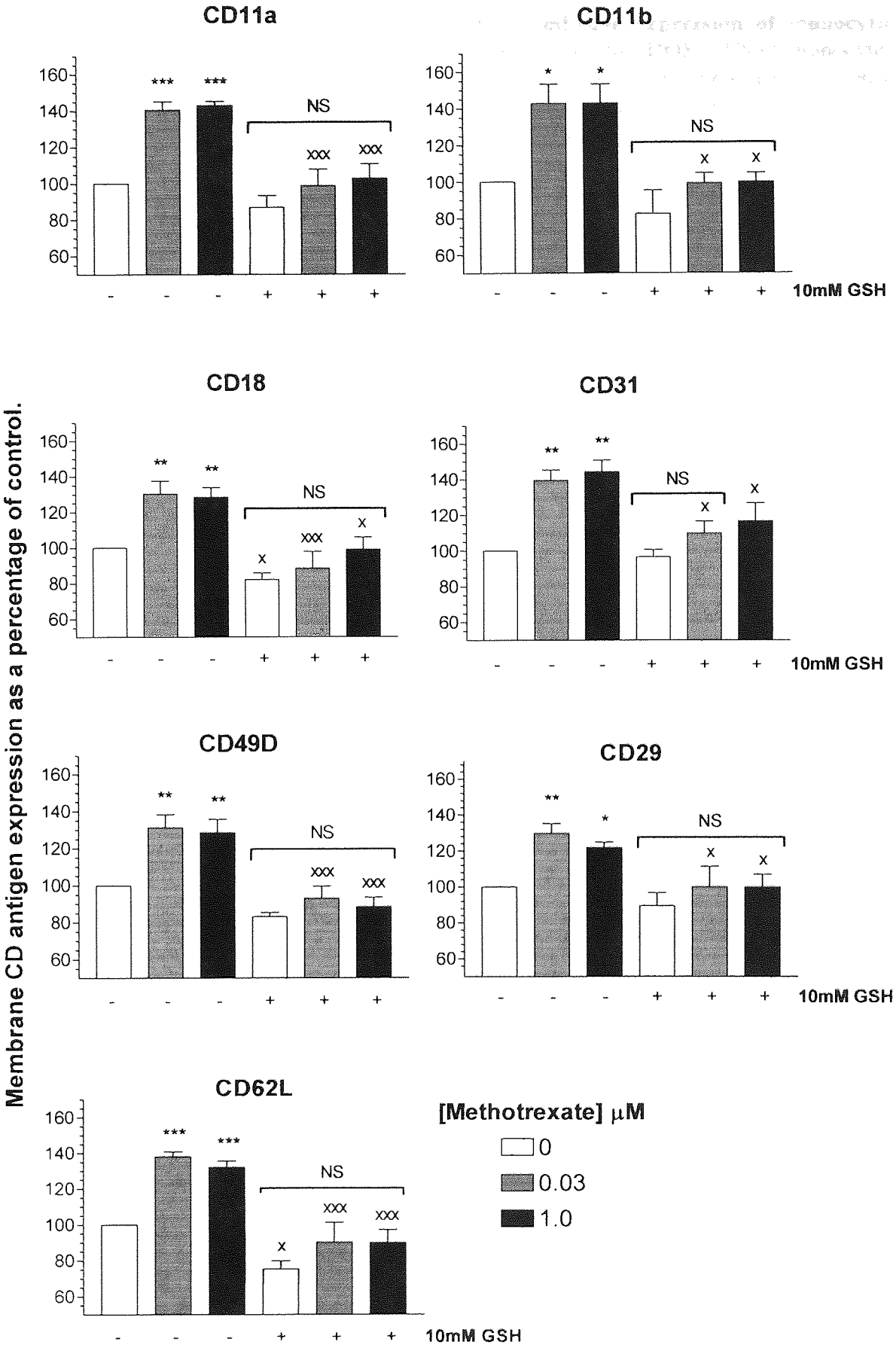
CD11a
CD11b
CD18
CD31
CD49D
CD29
CD62L
Membrane CD antigen expression as a percentage of control.
160
140
120
100
80
60
***
**
*
NS
xxx
x
- - - + + +
10mM GSH
[Methotrexate] μM
0
0.03
1.0

Figure 5.17. Methotrexate increases the membrane expression of monocytic adhesion molecules with an essential requirement for ROS. U937 monocytes ($2x10^6$/ml) were serum starved for 4 hours in RPMI 1640 in the presence or absence of 10mM glutathione (GSH) prior to 0, 0.03 or 1.0μM methotrexate treatment for 16 hours. Treatments were terminated by centrifugation and the resulting cell pellets washed twice with ice cold PBS. Cells were treated with >10μl of fluorescently tagged mouse IgG1 monoclonal antibody (MoAb) or isotype negative control per 10^6 cells for 30 minutes on ice, in the dark and fixed as described in method 5.2.7. Samples were then analysed by flow cytometry. Background fluorescence of each sample was established utilising cells stained with isotype negative controls. Positive regions were defined to contain 1% of the negatively stained cells. Samples were then analysed for MoAb membrane expression and the median X of the fluorescent peak recorded. The membrane expression of CD11a, CD11b, CD18, CD31, CD29, CD49D and CD62L were evaluated. At least 10,000 cells were analysed per sample. The results are presented as the mean ± s.d of at least 4 individual experiments where * ($p<0.05$) and ** ($p<0.01$) represent significant difference from controls by one-way ANOVA with Tukeys' post *hoc* test analysis. x ($p<0.05$) and xxx ($p<0.001$) signifies statistical difference of samples pre-treated with 10mM GSH compared to no pre-treatment by students T-test. NS, no significant difference.

inhibited the methotrexate-mediated elevation in adhesion molecule membrane expression ($p<0.05$; see Figure 5.17).

5.4 Discussion.

The neutralisation of monocyte/macrophage activity is recognised as a potential therapeutic strategy in the treatment of RA, where macrophages comprise 20% of primary cultured cells from rheumatoid synovium (Krane *et al.*, 1990). There is a wealth of data indicating that the two macrophage derived cytokines IL-1 and TNFα play a pivotal role in RA (Elliott *et al.*, 1994; Feldmann *et al.*, 1996; Plows *et al.*, 1995; Ruschen *et al.*, 1992; Van den Berg, 1995; Zangerle *et al.*, 1992) where this may arise through stimulation of matrix metalloproteinases (Krane *et al.*, 1990). Indeed, more recently developed therapeutics (e.g. etanercept) have been specifically targeted against the effects of TNFα (as reviewed; Alldred, 2001; Richard-Miceli & Dougados, 2001).

Nevertheless, there are several disease modifying antirheumatic drugs which were discovered serendipitously, and whose mechanism of action remains unknown. MTX is one such potent antiinflammatory agent, which is widely used to control the arthritic process. Furthermore, as a chemotherapeutic agent, MTX is the cornerstone of acute lymphoblastic leukaemia (ALL) treatment and has increasing use in the prevention of allograft rejection in graft versus host disease. Its therapeutic efficacy in multiple disease states is of a consequence to multiple sites of action. However, a limiting factor in the use of MTX is its associated toxicity at numerous locations including the liver and lungs (as reviewed in Alarcón, 2000). Therefore, further elucidation of the mechanism(s) of action of MTX may allow development of compounds or therapeutic regimens with improved efficacy:toxicity profiles.

Consequently, the effects of MTX on the DNA cell cycle and its capacity to generate intracellular ROS have been examined, using concentrations that encompass the plasma concentration (500nM) observed in RA subjects receiving a weekly 7.5mg oral dose of MTX (Coombe *et al.*, 1995) or in leukaemia patients (Synold *et al.*, 1994). In agreement of the effects of MTX treatment of PMN (Gressier *et al.*, 1994), the data presented here show that treatment of U937 monocytes and Jurkat T-cells induces the production of $[peroxide]_{cyt}$ in both a dose and time dependent fashion. Also, DNA fragmentation was observed in Jurkat T-cells in response to MTX to precede loss of membrane integrity and this confirms the observations of da Silva *et al.*, (1995). Furthermore, pre-treatment with the anti-oxidants GSH or NAC ameliorates the MTX induced alterations in the cell cycle. This data confirms that the elevation in $[peroxide]_{cyt}$ is essential for the adaptive cellular response of growth arrest and for apoptosis resulting from MTX exposure observed in U937 monocytes and Jurkat T-cell respectively.

The $[peroxide]_{cyt}$ production in Jurkat T-cells at concentrations which induced apoptosis was approximately two-fold greater than the $[peroxide]_{cyt}$ that induced growth arrest in U937 monocytes. The greater increase in $[peroxide]_{cyt}$ in T-cells may induce the apoptotic response rather than the adaptive response of growth arrest seen in monocytes. Moreover, the amplitude of $[peroxide]_{cyt}$ production in response to MTX at all concentrations may reflect the intrinsic, endogenous levels of antioxidant present within the cell. Indeed, monocytes possess three times the concentration of total cellular glutathione than Jurkat T-cells and hence may reduce $[peroxide]_{cyt}$ levels to those which mediate a non-deleterious response rather than the terminal cellular response of apoptosis associated with the massive production of

peroxide. The importance of the intrinsic total cellular GSH level in determining the response to MTX in different cell types requires elucidation. Inhibition of GSHpx or GSH reductase with BSO or BCNU respectively, or DEM to deplete GSH in U937 monocytes may confer an apoptotic response rather than that of the observed G0/G1 growth arrest.

Pre-treatment of Jurkat T-cells with either of the anti-oxidants GSH or NAC completely abrogated the apoptosis induced by MTX at low doses (<1μM). At higher doses (1-10μM) MTX significantly reduced the percentage specific apoptosis by approximately 20% due to incomplete detoxification by GSH/NAC of the large quantities of $[peroxide]_{cyt}$ produced, compartmentalisation of these antioxidants away from ROS generating sites or the induction of apoptosis via a peroxide independent process may explain incomplete protection. Pre-treatment of Jurkat T-cells or U937 monocytes with NAC or GSH in excess of 10mM was itself toxic (Data not shown). Conversely, the accumulation of nucleoids in the G0/G1 phase of the cell cycle in U937 monocytes in response to MTX treatment (≥100nM), which is indicative of growth arrest, was completely inhibited by NAC or GSH at all concentrations analysed implying that the growth arrest response to MTX is totally dependent on $[peroxide]_{cyt}$ production. Membrane integrity, evaluated by the flow cytometric analysis of PI uptake, was not compromised for all concentrations of MTX analysed after 16 hours exposure in both U937s and Jurkat T-cells indicating that MTX effects are independent of necrosis. Whether the arrest of MTX treated monocytes in the G0/G1 phase of the cell cycle precedes the occurrence of late apoptosis was not addressed and the effects of MTX on the cell cycle following longer incubation periods in Jurkat T-cells and U937 monocytes warrants further investigation. Dual

modes of cell death in response to DNA damaging agents exist. In response to 0.1μM daunorubicin HL-60 cells demonstrate delayed cell death with some regrowth following the formation of enlarged, polyploid cells caused by endoreduplication which is in contrast to acute apoptosis induced by concentrations of 0.5 to 1μM (Coombe *et al.*, 1995).

Previous work implicates ROS as signalling molecules in apoptotic cell death (Mansat-de Mas *et al.*, 1999; Yamauchi *et al.*, 1989). There is a plethora of evidence that is suggestive that the generation of ROS intracellularly act as signalling intermediates in their own right (Hennet *et al.*, 1993; Mansat-de Mas *et al.*, 1999' Verheij *et al.*, 1996). Additionally, their production affects the overall redox state of the cell and the consequent activity of redox sensitive signalling pathways. The requirement of $[peroxide]_{cyt}$ production and the alteration in antioxidant capacity in the cellular response to MTX observed in Jurkat T-cell and U937 monocytes is suggestive for involvement of redox sensitive signalling pathways. A reduction in the cellular GSH levels of HeLa cells in response to MTX has been reported (Babiak *et al.*, 1998). Further, the MTX mediated depletion of total cellular GSH may be necessary for initial increases in $[peroxide]_{cyt}$ (Tan *et al.*, 1998). In U937 monocytes, even at concentrations less than those that conferred growth arrest (<0.1μM), MTX reduced the total cellular concentration of GSH independently of concentration, to approximately 70% of vehicle control treated monocytes. Similarly, MTX at a concentration of 1μM or more, which induce a maximal apoptotic response, decreased total GSH levels in Jurkat T-cells. Loss of GSH can arise from formation of mixed disulfides with proteins or oxidised GSH (GSSG) which would normally be recycled by GSR. MTX has been shown to inhibit the activity of GSR supporting the

hypothesis of GSH export (Babiak *et al.*, 1998). Excess GSSG is ordinarily exported into the extracellular space, however, the translocation system is inhibited by ROS (as reviewed in; Evans *et al.*, 1997) and is therefore likely to be inhibited by MTX. An excessive intracellular accumulation of GSSG may lead to impaired protein function due to the formation of mixed disulfides (prSSG) via the interaction with free cysteine thiols, for example thiols of active protein tyrosine phosphatases (PTP; as reviewed in Gabbita *et al.*, 2000), rendering the protein inactive. Additionally, H_2O_2 generation inactivates PTP removing its inhibitory effect on the MAPK p38 (as reviewed in Gabbita *et al.*, 2000). PTP are of primary importance in mitogenesis, cell adhesion, cell differentiation, oncogenic transformation and apoptosis, regulating protein tyrosine kinase activity.

However, at a lower dose of MTX (30nM) the total GSH concentration in Jurkat T-cells was significantly elevated above control cells indicating that the $[peroxide]_{cyt}$ generated at this low MTX concentration may act in a transient signalling capacity to increase GSH synthesis related gene expression in an attempt to prevent MTX-peroxide mediated cell death via redox sensitive transcription of GCS (as reviewed in; Haddad *et al.*, 2002; Rahman, 2000). In this instance, the small accumulation of $[peroxide]_{cyt}$ may act as a protective mechanism (Tan *et al.*, 1998).

It is also likely that the redox sensitive transcription factors NFκB (Schreck *et al.*, 1991, 1992) or AP-1 (Hirota *et al.*, 1997; Nakamura *et al.*, 1997) play an essential role in the mechanisms of MTX action. The anthracycline antibiotic and chemotherapeutic agent daunorubicin induces the generation of ceramide via NSmase prior to apoptosis in Jurkat T-cells, events which are inhibitable by the antioxidants

NAC and PDTC. Furthermore, JNK, AP-1 and NFκB are activated following daunorubicin exposure and inhibited by antioxidants (Boland *et al.*, 1997; Mansat-de Mas *et al.*, 1999). It is likely that the ROS generated by daunorubicin remove the inhibition bestowed by GSH on the enzyme N-SMase to permit ceramide accumulation (Liu & Hannun, 1997; Liu *et al.*, 1998). However, Boland *et al.*, (1997) suggested that the elevation in ceramide in response to daunorubicin was due to ceramide synthase since its accumulation was inhibited by fumonsin B1. There is much controversy surrounding the intracellular targets of ceramide generation and it is suggested that ceramide generation in response to daunorubicin does not activate NFκB since its action was inhibited antioxidants and not by the ceramide synthase inhibitor fumonsin B1 (Boland *et al.*, 1997).

The present study has not evaluated the role of ceramide as a mediator of the apoptotic or growth arrest responses of Jurkat T-cells or U937 monocytes to MTX exposure. However, given that MTX induces the same response in these cell lines as C_2-/C_6-ceramide (see Chapter 2), albeit to differing magnitudes reflecting possible involvement of additional signalling pathways, and that ROS formation mediates ceramide generation following daunorubicin treatment of Jurkat T-cells, the effect of MTX on ceramide generation requires attention. Following DNA damage, the appearance of DNA strand breaks is sufficient for induction of the tumour suppressor gene p53, although the exact mechanism by which p53 senses of DNA damage remains to be determined (as reviewed in; Giaccia & Kastan, 1998). p53 may also mediate apoptosis and DNA repair. Chemotherapy induced CD95 dependent apoptosis in various cancer cell lines can involve p53 where CD95 receptor but not CD95L is upregulated in a p53 dependent manner (Muller *et al.*, 1998). Additionally,

the treatment of MCF-7 cells with doxorubicin or MTX sensitises cells to CD95 mediated apoptosis, indicating chemotherapeutic agents may lower the threshold for induction of apoptosis (Ruiz-Ruiz *et al.*, 1999). Similar observations were made in Jurkat T-cells following exposure to the tetracycline derivative doxycycline where the induction of apoptosis was associated with the elevated surface expression of CD95 receptor and ligand (Liu *et al.*, 1999). However, in activated T-cells, MTX triggered apoptosis via a CD95 independent pathway (Genestier *et al.*, 1997). A further understanding of the roles of these redox sensitive signalling pathways and transcription factors in the context of the cellular response to MTX may facilitate the development of novel therapeutic strategies in the treatment of inflammatory conditions such as RA or expand the use of MTX as a chemotherapeutic agent.

The development of cellular resistance to MTX limits its clinical efficacy. The production of peroxide by leukocytes over time may contribute the loss of cytotoxicity observed in Jurkat T-cells following long term MTX exposure through adaptive responses such as an increase in GSR gene transcription in addition to the elevated DHFR copy number described (Hall *et al.*, 1997). Other cellular antioxidant defence systems such thioredoxin, catalase or superoxide dismutase (SOD) may be upregulated in the response to MTX mediated peroxide production and their contribution in the molecular actions of MTX cannot be dismissed. The large magnitude of $[peroxide]_{cyt}$ formation in response to MTX in both U937 monocytes and Jurkat T-cells is suggestive of alternative sources of ROS production for the source of $[peroxide]_{cyt}$ other than as a result of GSH depletion. Possible MTX or polyglutamated MTX targets include the intracellular organelles of the mitochondria

and endoplasmic reticulum or the plasma membrane NADPH oxidase system (as reviewed by; Coyle & Puttfarken; 1993; Cross & Jones, 1991).

Treatment of U937 monocytes with MTX at low (30nM) and high (1μM) concentrations induced a differentiated-like phenotype with the enhanced expression of the α-integrin, CD11b as reported by Seitz *et al.*, (1998). Further, MTX induced an equivalent elevation of the β2 integrin CD18 and all other integrin adhesion molecules studied (CD11a, CD29, CD49D) in addition to the immunoglobulin CD31 and the leukocyte associated selectin, CD62L. The MTX induced elevation in adhesion molecule expression was also dependent on the production of ROS since GSH pre-treatment of monocytes inhibited these effects. MTX has been reported to alter membrane expression of a variety of functionally important antigens expressed on Jurkat T-cells (Hall *et al.*, 1997). Seitz *et al.*, (1998) postulated that MTX might inhibit the recruitment of immature and inflammatory monocytes from bone marrow into the inflammatory sites. However, expression alone (as measured by flow cytometry) does not equate to function, where changes in conformation of integrins are required for altered behaviour (Landis *et al.*, 1993; Diamond & Springer, 1993; Springer *et al.*, 1990). A ten-fold elevation in CD11b/CD18 surface expression alone of neutrophils is neither sufficient nor necessary for increased adhesion (Springer *et al.*, 1990a).

Monocytes treated with MTX did not show altered adherence to resting, quiescent endothelial cells, but MTX was effective in inhibiting monocytic adherence to 5hr activated endothelial cells and displayed greater efficacy in reducing monocyte interaction with 24hr LPS activated endothelial cells. These effects were completely

abrogated when U937 monocytes were pre-treated with the antioxidant GSH implying an essential requirement for ROS in the inhibition of monocyte adherence to activated endothelial cells. The initial attraction of leukocytes to endothelial cells is mediated by actions of chemokines, secreted by a large variety of different cell types, on chemokine receptors expressed on leukocyte membranes. Chemokine receptors can be up or down regulated and are in fact lost upon cellular differentiation (von Andrian & Mackay, 2000). The reduction in HUVEC adhesion observed in monocytes treated with MTX may be mediated by an effect on chemokine membrane receptor expression or a conformational change into an inactive state, in addition to adhesion molecule conformational changes. This possibility could be examined by treatment of U937 monocytes with Pertussis Toxin which inhibits G-protein coupled receptor dependent chemokine signalling, or with phorbol esters that activate integrins independent of chemokine receptor signalling. If the effects of MTX are mediated by reducing chemokine receptor expression on monocytes then Pertusis toxin pre-treatment should inhibit U937 monocyte adhesion to HUVEC. In contrast, phorbol ester-treatment of U937 monocytes would predictably induce elevated integrin expression and elevated adhesion to HUVEC which should not be sensitive to MTX. Furthermore, the effects of MTX on monocyte surface expression on the carbohydrate ligands for CD62E and CD62P have not been evaluated. Engagement of these receptors and their appropriate ligands are important in the initial interaction of monocytes with endothelial cells. Synovial hyperplasia is a pathological feature of RA characterised by an elevated number of inflammatory mononuclear cells within the synovial tissue. This commences with the adhesion of monocytes to the endothelium followed by their transendothelial migration and passage through the extracellular matrix into the inflamed synovium where monocytes differentiate into

tissue macrophages and type A synoviocytes Furthermore, the attachment of synoviocytes to cartilage and bone is a crucial step in the aetiology of RA (as reviewed in; Cunnane *et al.*, 1998; Müller-Ladner *et al.*, 1998). It is by inhibition of monocyte adhesion at various stages of their recruitment into the synovium that MTX may mediate the clinical observations of reduced radiological progression in RA. In light of the data presented here, it is likely that MTX treated monocytes, macrophages or type A synoviocytes possess a reduction in their efficacy to adhere to synovial tissue, tissue matrix, cartilage and bone.

The redox sensitive mechanisms of MTXs action observed in immortalised cell lines could be extended to primary normal T-lymphocytes and monocytes *ex vivo*. Given that the cytotoxic affects MTX in normal human T-cells requires their activation (Genestier *et al.*, 1998a) and that *in vitro* PHA activated purified human peripheral blood T-lymphocytes possess elevated $[peroxide]_{cyt}$ compared to resting T-lymphocytes (see Chapter 4), the probable differential effects on $[peroxide]_{cyt}$ production in resting and activated T-cells is intriguing and may further elucidate reasons for the requirement of an activated state in T-lymphocyte apoptosis mediated by MTX. Further, during RA, mononuclear cells in the synovial sublining frequently cluster in lymphocytic aggregates (as reviewed in; Müller-Ladner *et al.*, 1998), the effects of lymphocyte monocyte interaction following MTX treatment may further elucidate the anti-inflammatory action of MTX.

The observation that folate supplementation of up to 27.5mg/week administered to MTX treated RA patients reduces toxicity without compromising clinical efficacy (Morgan *et al.*, 1994) is strongly suggestive that the anti-

inflammatory/immunosuppressive actions of MTX do not directly involve the inhibition of DHFR (Budzik *et al.*, 2000). It has been postulated that the mechanism of MTX action is via the release of anti-inflammatory autocoid, adenosine (Cronstein, 1994; Merril *et al.*, 1997). In normal human primary T-cells and the human T-cell line, GEM, MTX dose dependently decreases *de novo* adenosine and guanosine pools (Budzik *et al.*, 2000). However, MTX treatment in combination with the adenosine antagonist R-P1A did not attenuate the MTX anti-rheumatic effect of MTX alone in rats with antigen induced arthritis (Anderson *et al.*, 2000), implying that the release of adenosine is not important. Further, a concentration of adensosine deaminase (2U) that completely abrogated adenosine induced apoptosis in activated PBL *in vitro*, only decreased MTX mediated apoptosis by 10-20% (Paillot *et al.*, 1998; Genestier *et al.*, 1998a). Adenosine has been described to strongly inhibit the adherence of PBN to rat mesenteric venules (Cronstein *et al.*, 1993) via A2 receptors present on PBN. Further, adenosine reduces superoxide formation (Cronstein *et al.*, 1985; Roberts *et al.*, 1985). These reports contradict the observations of elevated $[peroxide]_{cyt}$ described here which dictate the cellular responses in both U937 monocytes and Jurkat T-cells to MTX treatment, and that the functional response of reduced adherence of U937 monocytes to activated endothelial cells possesses an essential requirement for ROS production. The pronounced clinical effects of MTX cannot be ascribed to the accumulation of adenosine only and taken together, these findings add considerable weight to the scepticism of adenosine as the sole mediator in the mechanism of action of MTX. It is proposed here that MTX or its polyglutamated metabolites target free radical/ROS producing centres of the cell. The ensuing elevation in peroxide is responsible, at least in part to the cellular responses and functional consequence of MTX treatment.

In summary, it is described here for the first time that the production of peroxide is essential in the mechanism of MTX anti-inflammatory and immunosuppressive action. The stress responses of growth arrest and apoptosis in monocytes and T-cells respectively to MTX treatment is dependent on the production of peroxide. The anti-inflammatory action of MTX has been further clarified by investigating the functional consequence of the MTX treatment of monocytes with regards their recruitment to endothelial cells. MTX may affect the progression of inflammatory disease states such as RA or GVHD by inhibiting monocyte interaction with the inflamed endothelium. The cellular effects of the major liver metabolite MTX, 7-hydroxy MTX (Chladek *et al.*, 1997) and their contribution to the anti-inflammatory/immunosuppressive action of MTX *in vivo* remain to be determined.

Chapter 6.0: Final discussion.

6.0 Final discussion.

Despite inducing identical cellular responses, i.e. apoptosis in Jurkat T-cells and growth arrest in U937 monocytes, the mechanisms of action of MTX and synthetic ceramides in mediating these cellular outcomes are fundamentally different. Overall, MTX induced enhanced $[peroxide]_{cyt}$ in both cell types whereas C_2-/C_6-ceramide mediated the opposite effects. However, the magnitude of peroxide alteration appears to dictate the response, where the greater disruption in $[peroxide]_{cyt}$ was associated with the apoptotic response and the lesser disruption with growth arrest. Further, the relative potencies of these agents were different in each cell type. Significantly greater apoptosis was observed following 6 hours treatment of Jurkat T-cells with either C_2-/C_6-ceramide, although these species displayed different potencies themselves, than those mediated by MTX (0-100μM). Conversely, MTX induced growth arrest in U937 monocytes after 6 hours exposure whereas no accumulation of nucleoids in the G0/G1 phase of the cell cycle was observed following C_2-/C_6-ceramide over same period.

It is described here that synthetic short chain ceramides manipulate the generation of ROS at two sites. In agreement with much of the published data, C_2-/C_6-ceramide induces the generation of ROS from the mitochondria in a transient fashion, although at relatively low levels compared with those reported by others (Quillet-Mary *et al.*, 1997). However, contrary to these findings, it is shown here that the $[peroxide]_{cyt}$ was disrupted to a greater extent than that of the peroxide from the mitochondria. Surprisingly, C_2-/C_6-ceramide induced loss of $[peroxide]_{cyt}$ prior to the response of

Jurkat T-cells and U937 monocytes to these agents. These observations were reflected in $CD3^+$ T-cells and $CD14^+$ monocytes from peripheral whole blood treated with C_2-/C_6-ceramide and additionally in resting or PHA-activated T-cells *in vitro*. It was consequently argued that the disruption in $[peroxide]_{cyt}$ was the primary redox altering effect of synthetic ceramides. This hypothesis was based upon the inability of antioxidants to inhibit C_2-/C_6-ceramide induced cell death, and what's more, by lowering the $[peroxide]_{cyt}$ of U937 monocytes with anti-oxidants prior to synthetic ceramide treatment, a growth arrest response was switched to that of apoptosis.

Short chain synthetic ceramides are often used to investigate the consequence of enhanced cellular levels of natural endogenous ceramide to external stimuli due to their increased solubility. Due to the length of the fatty acid acyl chain and degree of saturation, natural ceramides have relatively poor solubility in aqueous solutions and therefore reduced cellular availability. It is a consequence of this physical property that the use of short chain ceramides is criticised. Various authors have proposed that due to the insolubility of endogenous natural ceramide in aqueous solutions, ceramide is compartmentalised at the site of its formation. Indeed, where ceramide is proposed to be formed in acidic lysosome compartments localised within the cytosol, it cannot escape from these organelles, unlike short chain ceramides or fluorescently tagged ceramides (Ségui *et al.*, 2000; Chatelut *et al.*, 1998; as reviewed in Augé *et al.*, 2000; Hannun & Luberto, 2000). How natural ceramides are able to access the mitochondria from its site of formation in various lipid rich membranes is unknown. However, due to the increased solubility of short chain ceramides used here and by others (Quillet-Mary *et al.*, 1997), these species can access the mitochondria and induced ROS formation at the site of the electron transport chain. Observations

obtained from isolated mitochondria are overwhelmingly in favour of the hypothesis that short chain ceramides can disrupt electron transport through the mitochondrial respiratory chain thereby promoting electron leakage and ROS formation (Gudz *et al.*, 1997; Quillet-Mary *et al.*, 1997). Here, the concentrations of synthetic short chain ceramide applied to whole cells *in vitro* encompass the fluctuation range achieved by endogenous natural ceramide in response to external stimuli. Other authors have used C_2-/C_6-ceramide levels which are in excess of 5 times the concentration /10^6 cells that we have used here and hence achieve a greater C_2-/C_6-ceramide at the mitochondria. This may in part explain the greater generation of peroxide at the mitochondria than described here and furthermore, why the growth arrest in U937 monocytes is achieved here rather than apoptosis observed in other reports (Mansat-de Mas *et al.*, 1999; Zamzami *et al.*, 1995; Quillet-Mary *et al.*, 1997). These differential redox altering effects observed here, and the contradictory reports offered by different laboratories with regards ROS formation in response to synthetic short ceramide may in part explain the widespread contradiction in the literature regarding the activation of signalling intermediates such as NFκB.

Loss in $[peroxide]_{cyt}$ was also induced by CD95 mediated elevations in endogenous natural ceramide indicating that synthetic short chain ceramides are representational for this cellular response, although the degree of $[peroxide]_{cyt}$ loss was not to the same extent as that mediated by short chain synthetic ceramides and may reflect the slower kinetics of apoptosis induction in Jurkat T-cells or the activation of ceramide independent pathways such as the caspase cascade. The effect of CD95L on $[peroxide]_m$ have not been investigated and this warrants further attention. Contradictory observations have been reported as to the involvement of ROS

generation in the intracellular signalling pathway of CD95. The effects of antioxidant pre-treatment on CD95 induced apoptosis in Jurkat T-cells have not been investigated here, although overall the literature is suggestive that the pre-treatment of cells with antioxidants does not abrogate the cellular response to CD95. Therefore, it is proposed that CD95 induce ceramide generation does not induced $[peroxide]_m$ production. It is likely that subcellular localisation of ceramide dictates its redox altering affects as wells as its ability to activate downstream signalling molecules.

Enhanced monocyte endothelial cell interaction is a key pathophysiological observation in the exacerbation of inflammatory diseases of vascular origin, with consequent migration of monocytes into tissue (as reviewed in; Lum & Roebuck, 2001; Ridley *et al.*, 2001; Ross, 1999; Springer, 1990). This process is required for the formation of athersclerotic lesions in the blood vessels of subjects with cardiovascular disease and, the elevated migration of monocytes to the synovium of patients diagnosed with RA where they differentiate into macrophage-like type A synoviocytes, or into the lung alveolar compartment contributing to the development of acute and chronic inflammatory lung disease (Lioté *et al.*, 1996; as reviewed in; Cutolo *et al.*, 1993; Carlos & Harlan, 1994; Müller-Ladner *et al.*, 1998; Ridley *et al.*, 2001). Oxidative stress is a primary mediator of vascular dysfunction observed in inflammatory conditions, participating in a positive amplification process to increase the production and secretion of pro-inflammatory cytokines from multiple different cell types. Collectively these enhance the activation status of endothelial cells and leukocytes mediating elevated adherence. Indeed, exposure of PBN with H_2O_2 or xanthine/xanthine oxidase to generate intracellular $O_2^{-\cdot}$, enhanced their adhesion to resting TNFα activated HEAC. It was hypothesised that the increase in adhesion was

due to enhanced peroxide production since the $O_2^{-\cdot}$ chelator desferroxamine did not affect adhesion of H_2O_2 or xanthine/xanthin oxidase treated PBN. Further, H_2O_2 increased the PBN membrane expression of CD11b and CD18 (Fraticelli *et al.*, 1996). Conversely, it has been hypothesised here that reducing the $[peroxide]_{cyt}$ would reduce monocyte adhesion to endothelial cells of differing activation status *in vitro*. Both the antioxidant GSH and C_2-/C_6-ceramide reduced the $[peroxide]_{cyt}$ of U937 monocyte following 16 hours treatment, and consequently their adhesion to 5 hours or 24 hours LPS activated HUVEC *in vitro*, but not resting HUVEC. This alteration in monocytes function was mediated at least in part by a reduction in the monocyte surface expression of integrins, selectins and immunoglobulin superfamily family proteins, which are associated with cell adhesion. It is also theorised that the mechanism by which ceramide reduces the adhesion of monocytes to activated HUVEC may be due to disruption in the plasma membrane lipid content of treated cells, altering the function of proteins involved with adhesion, inhibiting the clustering of integrins, and selectins on the apical surface required for efficient cell-cell interaction. It is unlikely that the induction of mild growth arrest contributes to this alteration in function since C_2-/C_6- ceramide also reduced monocyte adhesion to activated HUVEC following 2 hours treatment, 14 hours prior to the observation of G0/G1 arrest.

This thesis provides encouraging preliminary data for the prevention of monocyte adhesion to the inflamed endothelium *in vivo*, a pathology associated with disease states such as atherosclerosis, RA or acute/chronic inflammatory lung disease, by the treatment of monocytes with short chain synthetic ceramides. However, the diversity of cell types involved in these diseases of vascular origin, including multiple

circulatory cells and vascular cells, the plethora of pro-inflammatory mediators, and the observations *in vitro* of multiple differential cell type dependent responses to the application of synthetic ceramides or alterations in the relative ratios of cellular endogenous sphingolipids, complicates the potential use of short chain synthetic ceramides *in vivo*. At first glance, enhancement of the ceramide content of endothelial cells appears to be pro-inflammatory. Indeed, the additions of bacterial SMase or TNFα to induce endogenous ceramide formation or the addition of C_8-ceramide to HUVEC enhanced the CD62E dependent adhesion of resting neutrophils *in vitro* (Modur *et al.*, 1996). Furthermore, intracellularly produced ceramide and S1P can induce DNA synthesis in both endothelial and smooth muscle cells and potentiate the mitogenic activity of PDGF (as reviewed in; Levade *et al.*, 2001). Conversely, endothelial cell treatment with TNFα induced activation of sphingosine kinase with corresponding enhancement in the levels of the ceramide metabolite S1P to increase endothelial cell expression of CD62E, VCAM-1 via the NFκB and MAPK pathways, despite SM hydrolysis and ceramide formation. Here sphinosine kinase inhibition prevented TNFα mediated endothelial cell activation (Xi *et al.*, 1998, 1999). Conversely, applications of short chain synthetic ceramides have also been reported to induce apoptosis of endothelial cells. Further, the proliferation of smooth muscle cells from hypertensive rats in response to TNFα is associated with inhibition of ceramide generation and a reduction in SMase mRNA (as cited in; Levade *et al.*, 2001). Clearly, more research is required to elucidate the effects of ceramide on vascular cells and disease processes, however, collectively this data suggests that endogenous natural ceramide is metabolised to its mitogenic metabolite S1P to mediate TNFα mediated endothelial cell proliferation. The diverse cellular responses to synthetic short chain ceramide treatment suggests that to transfer our observations

in vitro to *in vivo* disease models requires targeting of ceramide specifically to circulatory monocytes. Whether the short chain ceramides used here C_2-/C_6-ceramide are metabolised to other sphingolipid metabolites in smooth muscle or endothelial cells to activate proliferative pathways requires investigation. The concentration range of C_2-/C_6-ceramide (0-20μM/10^6 cells) employed in the experimental systems here are believed not to induce fluctuations in sphingolipid metabolites (as reviewed in; Hannun & Luberto, 2000). The enhanced solubility of the short chain ceramides utilised in this work in aqueous environments may contribute to translipid bilayer movement as well as interbilayer movement which would not be observed with endogenous natural ceramides, suggesting that their functional and biochemical responses are likely to differ.

The involvement of ceramide, its sphingolipid metabolites and their association with the aetiology of RA and acute or chronic inflammatory disease is, at the point of writing, relatively unstudied. However, the role of this class of lipid and the enzymes responsible for their metabolism in the development atherosclerosis has received significant attention over the last few years (as reviewed in; Augé *et al.*, 2000; Levade *et al.*, 2001). Of note, SMase treatment of native LDL is accompanied by the elevated formation of aggregated particles, whereas atherosclerotic lesion LDL exhibits enhanced SM and ceramide when compared to serum LDL associated with enhanced levels of secreted A-SMase. Further, mildly oxidised LDL, generated by UV radiation can stimulate proliferation of bovine aortic smooth muscle cells inducing SM hydrolysis and ceramide turnover (as reviewed in Augé *et al.*, 2000). However, smooth muscle cells mitogenesis mediated by oxidised LDL also increased acidic and alkaline ceramidase activity, and sphingosine kinase activity to mediate

enhanced sphingosine and S1P levels. This was confirmed by inhibition of the mitogenic effects of oxidised LDL using inhibitors of ceramidase and sphingosine kinase (Augé *et al.*, 1999).

The accumulation, persistence, hyporesponsiveness and lack of apoptosis of T-cells within the synovial joints of patients diagnosed with RA is suggestive of aberrant intracellular signalling. Both the ceramide and the related metabolite DAG have been identified as signalling intermediates in the transduction of extracellular signals to the nucleus primarily mediating apoptosis or proliferation respectively. Herein, it is described that the endogenous ceramide and DAG content of resting $CD3^+$ T-lymphocytes *ex vivo*, *in vitro* or following mitogenic stimulation for 72 hours with PHA *in vitro* are no different to those obtained from apparently healthy individuals. What is more, T-cell ceramide and DAG concentration were not altered following culture for 3 days with or without PHA-induced activation. However, this study does not eliminate discrete, acute fluctuations in the cellular concentration these signalling lipids to differ between RA and normals immediately following PHA induced activation, or activation induced by other methods of TCR crosslinking *in vitro* and this warrants attention. Indeed acute alterations in ceramide and DAG levels have been described in primary human and murine T-cells upon activation by TCR or CD28 (Jolly *et al.*, 1996; as cited in; Adam *et al.*, 2002). Further, TCR or CD28 induced human T-cell proliferation was abrogated by synthetic ceramide (O'Byrne & Sanson, 2002). Additionally, alterations in the cellular content of ceramide and DAG related metabolites, which possess signalling capabilities in their own right or the enzymes responsible for their generation, cannot be ignored as biomolecules contributing to the aetiology of RA. These lipids represent feasible targets for

therapeutic manipulation in RA and diseases characterised by the enhanced survivability of cells.

Although the $[peroxide]_{cyt}$ of resting $CD3^+$ T-cells *ex vivo* was not significantly different between normal individuals and RA patients, significant differences in the response of T-cells from the same individual to PHA induce TCR stimulation for 72 hours *in vitro* was observed. However, this deficiency did not affect activation levels of RA T-cells compared to normals as analysed by membrane expression of CD25. Therefore, the data presented her contributes to the theory that the activation of T-cells can occur independently of ROS. Nevertheless, the overall cellular redox state of T-cells from RA patients is transformed compared to that of normal T-cells and is likely to affect levels of cellular antioxidants, manipulating the function of redox sensitive transcription factors and other signalling intermediates which in part mediates the hyporesponsivness and increased survivability of RA T-cells.

RA T-cells of a synovial source have been described to possess different phenotypes (Salmon *et al.*, 1997) and more subdued responses to TCR stimulation than those from peripheral whole blood (Carruthers *et al.*, 2000) contributing to differing functional properties (Cantwell *et al.*, 1997). The simple homing to the synovium from the periphery does not completely explain the T-cell pathology found here. The RA synovium is rich in multiple cell types with enhanced co-stimulatory ability to activate T-cells (Robertson *et al.*, 1997), which in cohort with numerous pro-inflammatory cytokines present (as reviewed in; Cunnane *et al.*, 1998), mediates transformation in T-cell phenotype increasing their persistence and hyporesponsiveness. It is therefore likely that the deficiency in RA peripheral blood

T-cells to enhance their $[peroxide]_{cyt}$ in response to PHA activation is exacerbated further by T-cells of a synovial source. There is an abundance of reports investigating sphingolipid turnover, particularly ceramide, in immortalised T-cell lines of leukemic source in response to the various cytokines found within the synovium. Whether these observations are representational of cytokine signalling in normal primary human T-cells requires elucidation. Further, the effect of normal or RA T-cell stimulation by combinations of cytokines and/or activating agents *in vitro* on their intracellular signalling intermediates is more likely to reflect responses *in vivo*.

6.1 Concluding remarks.

In conclusion, it is described here that the application of synthetic ceramides to human immortalised or primary circulatory cells induces two discrete and opposing alterations on cellular peroxide generation prior to the cellular response. By targeting the mitochondria, probably at the electron transport chain, ceramide induces a transient alteration in peroxide production. Simultaneously, the cytosolic peroxide content is reduced by an unknown mechanism. However, since antioxidants do not circumvent the ensuing short chain synthetic ceramide induced apoptosis in T-cells, and switch the mild G0/G1 growth arrest in monocytes to an apoptotic response by further lowering the peroxide levels, it is hypothesised that synthetic ceramide alterations in cytosolic peroxide rather than mitochondrial peroxide is of primary importance in dictating the cellular response. This theory was further supported by

the observation of CD95 induced endogenous ceramide accumulation also mediating cytosolic peroxide loss.

Rather than use the synthetic short chain ceramides as a biochemical tool to further investigate consequences of endogenous natural ceramide generation, this class of agents was utilised in a pharmacological perspective. For the first time, it is described here that the application of synthetic ceramides to monocytes, inhibits their enhanced adhesion to activated endothelial cells *in vitro*, in part by reducing the membrane expression of proteins associated with cell-cell interaction, in an anti-oxidant like fashion. It is proposed that the targeted delivery of short chain ceramides to monocytes *in vivo* may represent a novel therapeutic regimen for the treatment of inflammatory diseases associated with the enhanced adhesion of monocytes to the vascular endothelium, epithelium and other tissues.

The histological feature of RA of the enhanced infiltration of T-cells and consequent persistence, increased survivability and hyporesponsiveness is not due to defective endogenous levels of ceramide, DAG or cytosolic peroxide. Further, chronic PHA induced TCR activation *in vitro* does not induce alterations in DAG or ceramide levels, although this study does not dismiss their roles as signalling intermediates following short term treatment with PHA. Differences in the signalling properties of these lipids following acute stimulation with pro-inflammatory cytokines, PHA or other physiological agents within T-cells of normal individuals and patients with RA may aid elucidation of the T-cell pathology in RA. The aberrant upregulation of cytosolic levels of RA T-cells upon PHA activation compared to normal PHA activated T-cells *in vitro* is proposed to contribute RA T-cell hyporesponsiveness and

increased survivability by altering the redox state and hence the activation of signalling pathways in response to other physiological stimuli. The negative correlation observed between RA resting $CD3^+$ T-cell cytosolic peroxide concentrations *ex vivo* and serum CRP score ex vivo supports an associated anti-oxidant like property of CRP.

Investigation into the biochemical pharmacology of methotrexate, one of few clinically available therapeutic agents that induce remission of the RA pathology, has revealed an essential requirement for peroxide generation for methotrexate's anti-inflammatory and immunosuppressive action. Herein, cytostasis, cytotoxicity and inhibition of cell-cell interaction by methotrexate require the enhancement of cytosolic peroxide. Further characterisations of methotrexate's intracellular redox altering properties may aid the development of therapeutic regimens that reduces toxicity and increases efficacy, and also prevent the build up of tolerance that limits its use long term.

Chapter 7.0: References.

7.0 References.

ADAM, D., HEINRICH, M., KABELITZ, D. & SCHUTZE, S. (2002). Ceramide: does it matter for T cells? *Trends Immunol.*, **23**, 1-4.

ADAM, D., WIEGMANN, K., ADAM-KLAGES, S., RUFF, A. & KRÖNKE, M. (1996). A novel cytoplasmic domain of the p55 tumour necrosis factor receptor initiates the neutral sphingomyelinase pathway. *J. Biol. Chem.*, **271**, 14617-14622.

ADAM-KLAGES, S., ADAM, D., WIEGMANN, K., STRUVE, S., KOLANUS, W., SCHNEIDER-MERGENER, J. & KRONKE, M. (1996). FAN, a novel WD-repeat protein, couples the p55 TNF-receptor to neutral sphingomyelinase. *Cell*, **86**, 937-947.

AGGARWAL, B. & HIGUCHI, M. (1997). Role of ceramide in tumour necrosis factor-mediated apoptosis and nuclear transcription factor-κB activation. *Biochem. Soc. Trans.*, **25**, 1166-1171.

ALARCÓN, A. (2000). Methotrexate use in rheumatoid arthritis. A clinician's perspective. *Immunopharmacology*, **47**, 259-271.

ALLDRED, A. (2001). Etanercept in rheumatoid arthritis. *Expert Opin. Pharmacother.*, **2**, 1137-1148.

ALLEN, C., HIGHTON, J. & PALMER, D. (1989). Increased expression of p150,95 and CR3 leukocyte adhesion molecules by mononuclear phagocytes in rheumatoid synovial membranes. Comparison with osteoarthritic and normal synovial membranes. *Arthritis Rheum.*, **32**, 947-954.

ALLISON, A. (2000). Immunosuppresive drugs: the first 50 years and a glance forward. *Immunopharmacology*, **47**, 63-83.

ALTMAN, A., MALLY, M. & ISAKOV, N. (1992). Phorbol ester synergizes with Ca^{2+} ionophore in activation of protein kinase C (PKC)alpha and PKC beta isoenzymes in human T cells and in induction of related cellular functions. *Immunology*, **76**, 465-471.

AMARANTE-MENDES, G.P., NAEKYUNG, K.C., LIU, L., HUANG, Y., PERKINS, C., GREEN, D.R. & BHALLA, K. (1998). Bcr-Abl exerts its antiapoptotic effect against diverse apoptotic stimuli through blockage of mitochondrial release of cytochrome C and activation of caspase-3. *Blood*, **91**, 1700-1705.

ANDERSSON, S., JOHANSSON, L.H., LEXMÜLLER, K. & EKSTRÖM, G. (2000). Anti-rheumatic effect of methotrexate: is it really mediated by adenosine? *European Journal of Pharmaceutical Sciences*, **9**, 333-343.

ANDREIEU-ABADIE, N., GOUAZÉ, V., SALVAYRE, R. & LEVADE, T. (2001). Ceramide in apoptosis signaling: relationship with oxidative stress. *Free Rad. Biol. Med.*, **31**, 717-728.

ANDRIEU, N., SALVAYRE, R. & LEVADE, T. (1994). *Biochem J.*, **303**, 341-345.

ANDRIEU-ABADIE, N., GOUAZÉ, V., SALVAYRE, R. & LEVADE, T. (2001). Ceramide in apoptosis signaling: relationship with oxidative stress. *Free Rad. Biol. Med.*, **31**, 717-728.

AREND, W. (1997). The pathophysiology and treatment of rheumatoid arthritis. *Arthritis Rheum.*, **40**, 595-597.

ARNET, F., EDWORTHY, S., BLOCH, D., MCSHANE, D., FRIES, J., COOPER, N., HEALEY, L., KAPLAN, S., LIANG, M., LUTHRA, H., MEDSGER JR, T., MITCHELL, D., NEUSTADT, D., PINALS, R., SCHALLER, J., SHARP, J., WILDER, R. & HUDNER, G. (1988). The American rheumatism association 1987 revised criteria for the classification of rheumatoid arthritis. *Arthritis Rheum.*, **31**, 315-324.

AUGÉ, N., NÈGRE-SALVAYRE, A., SALVAYRE, R. & LEVADE, T. (2000). Sphingomyelin metabolites in vascular cell signaling and atherogenesis. *Prog. Lipid Res.*, **39**, 207-229. AUGÉ, N., NIKOLOVA-KARAKASHIAN, M., CARPENTIER, S., PARTHASARATHY, S., NEGRE-SALVAYRE, A., SALVAYRE, R., MERRILL JR., A. & LEVADE, T. (1999). Role of sphingosine 1-phosphate in the mitogenesis induced by oxidized low density lipoprotein in smooth muscle cells via activation of sphingomyelinase, ceramidase, and sphingosine kinase. *J. Biol. Chem.*, **274**, 21533-21538.

AUSSEL, C., PELASSY, C. & ROSSI, B. (1990). Breakdown of a phosphatidylcholine pool arising from the metabolic conversion of phosphatidylethanolamine as a novel source of diacylglycerol in activated T cells. *J. Lipid Mediat.*, **2**, 103-116.

BABIAK, R., CAMPELLO, A., CARNIERI, E. & OLIVEIRA, M. (1998). Methotrexate; pentose cycle and oxidative stress. *Cell Biochem. Funct.*, **16**, 283-293.

BAEUERLE, P. & BALTIMORE, D. (1996). NF-kappa B: ten years after. *Cell*, **87**, 13-20.

BAEURELE, P. & HENKEL, T. (1994). Function and activation of NFkB in the immune system. *Annu. Rev. Immunol.*, **12**, 141-179.

BAGGOTT, J., MORGAN, S., HA, T., ALARCÓN, G., KOOPMAN, W. & KRUMDIECK, C. (1993). Antifolates in rheumatoid arthritis: a hypothetical mechanism of action. *Clin. Exp.*

Rheumatol., **11**, S101-S105.

BANNWARTH, B., LABAT, L., MORIDE, Y. & SCHAEVERBEKE, T. (1994). Methotrexate in rheumatoid arthritis: an update. *Drugs*, **47**, 25-50.

BASS, D., PARCE, J., DECHATELET, L., SZEJDA, P., SEEDS, M. & THOMAS, M. (1983). Flow cytometric studies of oxidative product formation by neutrophils: a graded response to membrane stimulation. *J. Immunol.*, **130**, 910-917.

BASU, S. & KOLESNICK, R. (1998). Stress signals for apoptosis: ceramide and c-jun kinase. *Oncogene*, **17**, 3277-3285.

BAVEYE, S., ELASS, E., FERNIG, D., BLANQUART, C., MAZURIER, J. & LEGRAND, D. (2000). Human lactoferrin interacts with soluble CD14 and inhibits expression of endothelial adhesion molecules, E-selectin and ICAM-1, induced by the CD14-lipopolysaccharide complex. *Infect. Immun.*, **68**, 6519-6525.

BERRIDGE, M. (1997). Lymphocyte activation in health and disease. *Crit. Rev. immunol.*, **17**, 155-178.

BEUTLER, B. & BAZZONI, F. (1998). TNF, apoptosis and autoimmunity: a common thread? *Blood Cells Mol. Dis.*, **24**, 216-230.

BIELAWSKA, A., PERRY, D. & HANNUN, Y. (2001). Determination of ceramides and diglycerides by the diglyceride kinase assay. *Anal. Biochem.*, **298**, 141-150.

BLIGH, E. & DYER, W. (1959). A rapid method of total lipid extraction. *Can. Biochem. J. Phyiol.*, **37**, 911-917.

BOESEN-DE COCK, J., TEPPER, A., DE VRIES, E., VAN BLITTERSWIJK, E.J. & BORST, J. (1998). CD95 (Fas/APO-1) induces ceramide formation and apoptosis in the absence of a functional acid sphingomyelinase. *J. Biol. Chem.*, **273**, 7560-7565.

BOLAND, M., FOSTER, S. & O'NEILL, L. (1997). Daunorubicin activates NFκB and induces κB-dependent gene expression in HL-60 promyelocytic and Jurkat T lymphoma cells. *J. Biol. Chem.*, **272**, 12952-12960.

BOLAND, M. & O'NEILL, L. (1998). Ceramide activates NFκB by inducing processing of p105. *J. Biol. Chem.*, **273**, 15494-15500.

BONDESON, J. (1997). The mechanisms of action of disease-modifying anti-rheumatic drugs: a review with emphasis on macrophage signal transduction and the induction of pro-inflammatory cytokines. *Gen. Pharmac.*, **29**, 127-150.

BONDESON, J. & SUNDLER, R. (1995). Auranofin inhibits the induction of interleukin 1 and tumour necrosis factor alpha mRNA in macrophages. *Biochem. Pharmac.*, **52**, 35-42.

BONIFACE, J., RABINOWITZ, J., WÜLFING, C., HAMPL, J., REICH, Z., ALTAN, J., KANTOR, R., BEESON, C., MCCONNELL, H. & DAVIS, M. (1998). Initiation of signal transduction though the T cell receptor requires the multivalent engagement of peptide/MHC ligands. *Immunity*, **9**, 459-466.

BOSE, R., VERHEIJ, M., HAIMOVITZ-FRIEDMAN, A., SCOTTO, K., FUKS, Z. & KOLESNICK, R. (1995). Ceramide synthase mediates daunorubicin-induced apoptosis: an alternative mechanism for generating death signals. *Cell*, **82**, 405-414.

BOURGUINON, L., JY, W., MAJERCIK, M. & BOURGUINON, G. (1988). Lymphocyte activation and capping of hormone receptors. *J. Cell. Biochem.*, **37**, 131-150.

BÖHLER, T., WAISER, J., HEPBURN, H., GAEDEKE, J., LEHMANN, C., HAMBACH, P., BUDDE, K. & NEUMAYER, H.-H. (2000). TNF-alpha and IL-1alpha apoptosis in subconfluent rat mesangial cells. Evidence for the involvement of hydrogen peroxide and lipid peroxidation as second messengers. *Cytokine*, **12**, 986-991.

BRENNER, B., KOPPENHOEFFER, U., WEINSTOCK, C., LINDERKAMP, O., LANG, F. & GULBINS, E. (1997). Fas- or ceramide-induced apoptosis is mediated by a Rac1-regulated activation of Jun N-terminal kinase/p38 kinases and GADD153. *J. Biol. Chem.*, **272**, 22173-22181.

BROWN, D. & LONDON, E. (1998). Structure and origin of ordered lipid domains in biological membranes. *J. Membr. Biol.*, **164**, 103-114.

BUDZIK, G., COLLETTI, L. & FALTYNEK, C. (2000). Effects of methotrexate on nucleotide pools in normal T cells and the CEM T cell line. *Life Sciences*, **66**, 2297-2307.

BUTTKE, T. & SANDSTROM, P. (1994). Oxidative stress as a mediator of apoptosis. *Immuno. Today*, **15**, 7-10.

BÖHLER, T., WAISER, J., HEPBURN, H., GAEDEKE, J., LEHMANN, C., HAMBACH, P., BUDDE, K. & NEUMAYER, H.-H. (2000). TNF-α and IL-1α apoptosis in subconfluent rat mesangial cells. Evidence for the involvement of hydrogen peroxide and lipid peroxidation as second messengers. *Cytokine*, **12**, 986-991.

CAI, H. & HARRISON, D. (2000). Endothelial dysfunction in cardiovasclar disease. *Circ. Res.*, **87**,

840-844.

CAI, J. & JONES, D. (1998). Superoxide in apoptosis. *J. Biol. Chem.*, **273**, 11401-11404.

CANTWELL, M., HUA, T., ZVAIFLER, N. & KIPPS, T. (1997). Deficient fas ligand expression by synovial lymphocytes from patients with rheumatoid arthritis. *Arthritis Rheum.*, **40**, 1644-1652.

CARLOS, T.M. & HARLAN, J,M. (1994). Leukocyte-endothelial adhesion molecules. *Blood.*, **84**, 2068-101.

CARRUTHERS, D., ARROL, H., BACON, P. & YOUNG, S. (2000). Dysregulated intracellular Ca^{2+} stores and Ca^{2+} signaling in synovial fluid T lymphocytes from patients with chronic inflammatory arthritis. *Arthritis. Rheum.*, **43**, 1257-1265.

CARRUTHERS, D., NAYLER, W., ALLEN, M., KITAS, G., BACON, P. & YOUNG, S. (1996). Characterisation of latered calcium signaling in T lymphocytes from patients with rheumatoid arthritis (RA). *Clin. Exp. Immunol.*, **105**, 291-296.

CARTER, W., NARAYANAN, P. & ROBINSON, J. (1994). Intracellular hydrogen peroxide and superoxide anion detection in endothelial cells. *J. Leuk. Biol.*, **55**, 253-258.

CHALFANT, C., KISHIKAWA, K., MUMBY, M., KAMIBAYASHI, C., BIELAWSKA, A. & HANNUN, Y. (1999). Long chain ceramides activate protein phophatase-1 and protein phosphatase-2A. *J. Biol. Chem.*, **274**, 20313-20317.

CHAN, H. & AGGARWAL, B. (1994). Role of tumour necrosis factor receptors in the activation of nuclear factor κB in human histocytic lymphoma U-937 cells. *J. Biol. Chem.*, **269**, 31424-31429.

CHATELUT, M., LERUTH, M., HARZER, K., DAGAN, A., MARCHESINI, S., GATT, S., SALVAYRE, R., COURTOY, P. & LEVADE, T. (1998). Natural ceramide is unable to escape the lysosome, in contrast to a fluorescent analogue. *FEBS Lett.*, **426**, 102-106.

CHATTERJEE, S. (1994). Neutral sphingomyelinase action stimulates signal transduction of tumor necrosis factor-alpha in the synthesis of cholesteryl esters in human fibroblasts. *J. Biol. Chem.*, **269**, 879-882.

CHEN, C.-C. , CHOU, C.-Y. , SUN, Y.-T. & HUANG, W.-C. (2001). Tumour necrosis factor alpha-induced activation of downstream NF kappa B site of the promoter mediates epithelial ICAM-1 expression and monocyte adhesion: Involvement of PKC alpha, tryosine kinase, and IKK2, but not MAPKs, pathway. *Cell. Signal.*, **13**, 543-553.

CHENG, P., DYKSTRA, M., MITCHELL, R. & PIERCE, S. (1999). A role for lipid rafts in B cell antigen signaling and antigen targeting. *J. Exp. Med.*, **190**, 1549-1560.

CHLADEK, J., MARTINKOVA, J. & SISPERA, L. (1997). An *in vitro* study on methotrexate hydroxylation in rat and human liver. *Physiol. Res.*, **46**, 371-379.

CHULUYAN, H. & ISSEKUTZ, A. (1993). VLA-4 integrin can mediate CD11/CD18-independent transendothelial migration of human monocytes. *J. Clin. Invest.*, **92**, 2768-2777.

CIESIELSKI, C., MEI, J. & PICCININI, L. (1998). Effects of cyclosporine A and methotrexate on CD18 expression in recipients of rat cardiac allografts. *Transplant Immunology*, **6**, 122-123.

CIESIELSKI, C., PFLUG, J., MEI, J. & PICCININI, L. (1998). Methotrexate regulates ICAM-1 expression in recipients of rat cardiac allografts. *Transplant Immunology*, **6**, 111-121.

CIFONE, M., DE MARIA, R., RONCAIOLI, P., RIPPO, M., AZUMA, M., LANIER, L., SANTONI, A. & TESTI, R. (1993). Apoptotic signaling through CD95 (Fas/Apo-1) activates an acidic sphingomyelinase. *J. Exp. Med.*, **177**, 1547-1552.

CLUTTON, S. (1997). The importance of oxidative stress in apoptosis. *Br. Med. Bull.*, **53**, 662-668.

COHEN, J. (1993). Apoptosis. *Immuno. Today*, **14**, 126-130.

COLLINS, R., VELJI, R., GUEVARA, N., HICKS, M., CHAN, L. & BEAUDET, A. (2000). P-Selectin or intercellular adhesion molecule (ICAM)-1 deficiency substantially protects against atherosclerosis in apolipoprotein E-deficient mice. *J. Exp. Med.*, **191**, 189-194.

COOMBE, B., EDNO, L., LAFFORGUE, P., BOLOGNA, J., ACQUAVIVA, P., SANY, J. & BRESSOLLE, F. (1995). Total and free methotrexate pharmacokinetics, with and without piroxicam, in rheumatoid arthritis patients. *J. Rheumatol.*, **34**, 421-428.

CORDA, S., LAPLACE, C., VICAUT, E. & DURANTEAU, J. (2001). Rapid reactive oxygen species production by mitochondria in endothelial cells exposed to tumour necrosis factor-alpha is mediated by ceramide. *Am. J. Respir. Cell Mol. Biol.*, **24**, 762-768.

COSSARIZZA, A., FRANCESCHI, C., MONTI, D., SALVIOLI, S., BELLESIA, E., RIVABENE, R., BIONDO, L., RAINALDI, G., TINARI, A. & MALORNI, W. (1995). Protective effect of N-acetylcysteine in tumour necorsis factor-α-induced apoptosis in U937 cells: the role of mitochondria. *Exp. Cell Res.*, **220**, 232-240.

COYLE, J. & PUTTFARKEN, P. (1993). Oxidative stress, glutamate, and neurodegenerative disorders. *Science*, **262**, 689-695.

CREMESTI, A., PARIS, F., GRASSMÉ, H., HOLLER, N., TSCHOPP, J., FUKS, Z., GULBINS, E. &

KOLESNICK, R. (2001). Ceramide enables Fas to Cap and Kill. *J. Biol. Chem.*, **276**, 23954-23961.

CRONSTEIN, B. (1994). Adenosine, an endogenous anti-inflammatory agent. *J. Appl. Physiol.*, **76**, 5-13.

CRONSTEIN, B., NAIME, D. & OSTAD, E. (1993). The anti-inflammatory mechanism of methotrexate. Increased adenosine release at inflamed sites diminishes leukocyte accumulation in an in vivo model of inflammation. *J. Clin. Invest.*, **92**, 2675-2692.

CRONSTEIN, B., ROSENSTEIN, E., KRAMER, S., WEISSMANN, G. & HIRSCHHORN, R. (1985). Adenosine; a physiological modulator of superoxide anion generation by human neutrophils. Adenosine acts via an A2 receptor on neutorphils. *J. Immunol.*, **135**, 1366-1371.

CROSS, A. & JONES, O. (1991). Enzymatic mechanisms of superoxide production. *Biochim. Biophys. Acta*, **1057**, 281-298.

CROW, J. (1997). Dichlorofluorescein and dihydrorhodamine 123 are sensitive indicators of peroxynitrite *in vitro*: implications for intracellular measurement of reactive oxygen species. *Nitric oxide: Biol. Chem.*, **1**, 145-157.

CUNNANE, G., HUMMEL, K., MÜLLER-LADNER, U., GAY, R. & GAY, S. (1998). Mechanism of joint destruction in rheumatoid arthritis. *Arch. Immunol. Ther. Exp.*, **46**, 1-7.

CUTOLO, M., SULLI, A., BARONE, A., SERIOLO, B. & ACCARDO, S. (1993). Macrophages, synovial tissue and rheumatoid arthritis. *Clin. Exp. Rheumatol.*, **11**, 331-339.

CUVILLIER, O. & LEVADE, T. (2001). Sphingosine 1-phosphate antagonises apoptosis of human leukemia cells by inhibiting release of cytochrome c and Smac/DIABLO from mitochondria. *Blood*, **98**, 2828-2836.

CUVILLIER, O., PIRIANOV, G., KLEUSER, B., VANEK, P., COSO, O., GUTKIND, J. & SPIEGEL, S. (1996). Suppression of ceramide-mediated programmed cell death by sphingosine-1-phosphate. *Nature*, **381**, 800-803.

CUVILLIER, O., ROSENTHAL, D., SMULSON, M. & SPIEGEL, S. (1998). Sphingosine 1-phosphate inhibits activation of caspases that cleave poly(ADP-ribose) polymerase and lamins during Fas- and ceramide-mediated apoptosis in Jurkat T lymphocytes. *J. Biol. Chem.*, **273**, 2910-2916.

CYBULSKY, M. & GIMBRONE JR., M. (1991). Endothelial expression of a mononuclear leukocyte adhesion molecule during atherogenesis. *Science*, **251**, 788-789.

DA SILVA, C., DE OLIVEIRA, C. & DE LIMA, M. (1995). Apoptosis as a mechanism of cell death induced by different chemotherapeutic drugs in human leukemic T-lymphocytes. *Biochemical Pharmacology*, **51**, 1331-1340.

DAVIES, M., GORDON, J. & GEARING, A. (1993). The expression of the adhesion molecules ICAM-1, VCAM-1, PECAM, and E-selectin in human atherosclerosis. *J. Pathol.*, **171**, 223-229.

DAVIS, M., FLAWS, J., YOUNG, M., COLLINS, K. & COLBURN, N. (2000). Effect of ceramide in intracellular glutathione determines apoptotic or necrotic cell death of JB6 Tumour cells. *Toxicol. Sci.*, **53**, 48-55.

DBAIBO, G., EL-ASSAAD, W., KRIKORIAN, A., LIU, B., DIAB, K., IDRISS, N., EL-SABBAN, M., DRISCOLL, T., PERRY, D. & HANNUN, Y. (2001). Ceramide generation by two distinct pathways in tumour necrosis factor alpha-induced cell death. *FEBS Lett.*, **503**, 7-12.

DBAIBO, G., PUSHKAREVA, M., JAYADEV, S., SCHWARZ, J., HOROWITZ, J., OBEID, L. & HANNUN, Y. (1995). *Proc. Natl. Acad. Sci. U S A*, **92**, 1347-1351.

DE CLERCK, L., BRIDTS, C., MERTENS, A., MOENS, M. & STEVENS, W. (1994). Use of fluorescent dyes in the determination of adherence of human leucocytes to endothelial cells and the effect of fluorochromes on cellular function. *J. Immunol. Methods*, **172**, 115-124.

DE GANNES, G.-P. , BELAUD-ROTUREAU, M.-A. , VOISIN, P., LEDUQ, N., BELLOC, F., CANIONI, P. & DIOLEZ, P. (1998). Flow cytometric analysis of mitochondrial activity *in situ*: Application to acetylceramide-induced mitochondrial swelling and apoptosis. *Cytometry*, **33**, 333-339.

DE MARIA, R., LENTI, L., MALISAN, F., D'AGOSTINO, F., TOMASSINI, B., ZEUNER, A., RIPPO, M.R. & TESTI, R. (1997). Requirement for GD3 ganglioside in CD95- and ceramide-induced apoptosis. *Science*, 277, 1652-1655.

DE MARIA, R., RIPPO, M., SCHUCHMAN, E. & TESTI, R. (1998). Acidic sphingomyelinase (ASM) is necessary for fas-induced GD3 ganglioside accumulation and efficient apoptosis in lymphoid cells. *J. Exp. Med.*, **187**, 897-902.

DE NADAL, C., SESTI, P., CANTONI, O., LIÈVREMONT, J.-P. , SCIORATI, C., BARSACCHI, R., MONCADA, S., MELDOLESI, J. & CLEMENTI, E. (2000). Nitric oxide inhibits tumour necrosis factor-α-induced apoptosis by reducing the generation of ceramide. *Proc. Natl. Acad. Sci. U S A*, **97**, 5480-5485.

DEVADES, S., ZARITSKAYA, L., RHEE, S., OBELEY, L. & WILLIAMS, M. (2002). Discrete generation of superoxide and hydrogen peroxide by T cell receptor stimulation: selective regulation of mitogen activated protein kinase activation and Fas ligand expression. *J. Exp. Med.*, **195**, 59-70.

DIAMOND, M. & SPRINGER, T. (1993). A subpopulation of Mac-1 (CD11b/CD18) molecules mediates neutrophil adhesion to ICAM-1 and fibrinogen. *J. Cell Biol.*, **120**, 545-556.

DOBRINICH, R. & SPAGNUOLO, P. (1991). Binding of C-reactive protein to human neutrophils. *Arthritis Rheum.*, **34**, 1031-1038.

DOBROWSKY, R. (2000). Sphingolipid signaling domains floating on rafts or buried in caves? *Cell. Signal.*, **12**, 81-90.

DOBROWSKY, R., KAMIBAYASHI, C., MUMBY, M. & HANNUN, Y. (1993). Ceramide activates heterotrimeric protein phosphatase 2A. *J. Biol. Chem.*, **268**, 15523-15530.

DOLHAIN, R., VAN DER HEIDEN, A., TER HAAR, N., BREEDVELD, F. & MILTENBURG, A. (1996). Shift towards T lymphocytes with a T helper 1 cytokine secretion profile in the joints of patients with rheumatoid arthritis. *Arthritis Rheum.*, **39**, 1961-1969.

DRESSLER, K. & KOLESNICK, R. (1990). Ceramide 1-phosphate, a novel phospholipd in human leukemia (HL-60) cells: synthesis via ceramide from sphingomyelin. *J. Biol. Chem.*, **265**, 14917-14921.

DRÖGE, W., SCHULZE-OSTHOFF, K., MIHM, S., GALTER, D., SCHENK, H., ECK, H., ROTH, S. & GMUNDER, H. (1994). *FASEB J.*, **8**, 1131-1138.

DU, C., FANG, M., LI, Y., LI, L. & WANG, X. (2000). Smac, a mitochondrial protein that promotes cytochrome c-dependent caspase activation by eliminating IAP inhibition. *Cell*, **102**, 33-42.

DUDLER, J., PANG, L., DECKER, S., BRIDGES, A. & SALTIEL, A. (1995). A synthetic inhibitor of the mitogen-activated protein kinase cascade. *Proc. Natl. Acad. Sci. U S A*, **92**, 7686-7689.

DUDLER, J. & SO, K.A. (1998). T cells and related cytokines. *Curr. Opin. Rheumatol.*, **10**, 207-211.

DUMONT, A., HEHNER, S., HOFMANN, T., UEFFING, M., DRÖGE, W. & SCHMITZ, M. (1999). Hydrogen peroxide-induced apoptosis is CD95-independent, requires the release of mitochondria-derived oxygen species and the activation of NF-kB. *Oncogene*, **18**, 747-757.

EDER, J. (1997). Tumour necrosis factor alpha and iterluekin 1 signaling: do MAPK kinases connect at all? *Trends Pharmacol. Sci.*, **18**, 319-322.

EL-ASSAAD, W., EL-SABBAN, M., AWARAJI, C., ABBOUSHI, N. & DBAIBO, G. (1998). Distinct sites of action of Bcl-2 and Bcl-xl in ceramide pathway of apoptosis. *Biochem J.*, **336**, 735-741.

EL-GABALAWY, H., CANVIN, J., MA, G., VAN DER VIEREN, M., HOFFMAN, P., GALLATIN, M. & WILKINS, J. (1996). Synovial distribution of alpha d/CD18, a novel leukointegrin. Comparison with other integrins and their ligands. *Arthritis Rheum.*, **39**, 1913-1921.

ELLIOTT, M., MAINI, R., FELDMANN, M., KALDEN, J., ANTONI, C., SMOLEN, J., LEEB, B., BREEDVELD, F., MACFARLANE, J., BIJL, H. & WOODY, J. (1994). Randomized double-blind comparison of chimeric monoclonal antibody to tumour necorsis factor (cA2) versus placebo in rheumatoid arthritis. *Lancet*, **344**, 1105-1110.

ESPOSTI, M., HATSINISIRIOU, I., MCLENNAN, H. & RALPH, S. (1999). Bcl-$_2$ and mitochondrial oxygen radicals. *J. Biol. Chem.*, **274**, 29831-29837.

ESPOSTI, M. & MCLENNAN, H. (1998). Mitochondria and cells produce reactive oxygen species in virtual anaerobiosis: relevance to ceramide-induced apoptosis. *FEBS Lett.*, **338**, 338-342.

EVANS M., GRIFFITHS H. & LUNEC J. (1997). Reactive oxygen species and their cytotoxic mechanisms. In *Advances in Molecular and Cell Biology*, ed. Bittar E. & Chipman J. pp. 25-73. JAI Press Inc., London .

FAIRBANKS, L., RÜCKERMANN, K., QUI, Y., HAWRYLOWICZ, C., RICHARDS, D., SWAMINATHAN, R., KIRSCHBAUM, B. & SIMMONDS, H. (1999). Methotrexate inhibits the first committed step of purine biosynthesis in mitogen-stimulated human T-lymphocytes: a metabolic basis for efficacy in rheumatoid arthritis. *Biochemical J.*, **342**, 143-152.

FANG, W., RIVARD, J.J., GANSER, J., LEBIEN, T.W., NATH, K.A., MUELLER, D.L. & BEHRENS, T.W. (1995). Bcl-x_L rescues WEHI 231 B lymphocytes from oxidant-mediated death following diverse apoptotic stimuli. *J. Immunol.*, **155**, 66-75.

FARBER S., TOCH R., SEARS E. & PINKEL D. (1956). Advances in chemotherapy of cancer in man. In *Advances in Cancer Research*, ed. Greebstein J.-P. pp. 2-73. Academic Press, New York .

FARCSHON, D., COUTURE, C., MUSTELIN, T. & NEWMEYER, D. (1997). Temporal phases in apoptosis defined by the actions of Src homology 2 domains, ceramide, Bcl-2, interleukin-1b converting enzyme proteases, and a dense membrane fraction. *J. Cell Biol.*, **137**, 1117-1125.

FELDMANN, M. (2001). Pathogensis of arthritis: recent research progress. *Nat. Immunol.*, **2**, 771-773.

FELDMANN, M., BRENNAN, F. & MAINI, R. (1996). Role of cytokines in rheumatoid arthritis.

Annu. Rev. Immunol., **14**, 397-440.

FELDMANN, M. & MAINI, R. (1999). The role of cytokines in the pathogenesis of rheumatoid arthritis. *Rheumatology*, **38**, 3-7.

FERNÁNDEZ-CHECA, J., GARCIA-RUIZ, C., COLELL, A., MORALES, A., MARI, M., MIRANDA, M. & ARDITE, A. (1998). Oxidative stress: role of mitochondria and protection by glutathione. *Biofactors*, **8**, 7-11.

FIRESTEIN, G. (1998). Novel therapeutic strategies involving animals, arthritis, and apoptosis. *Curr. Opin. Rheumatol.*, **10**, 236-241.

FIRESTEIN, G., XU, W., TOWNSEND, K., BROID, D., ALVARO-GRACIA, J., GLASEBROOK, A. & ZVAIFLER, N. (1988). Cytokines in chronic inflammatory arthritis. I. Failure to detect T cell lymphokines (interleukin 2 and interleukin 3) and presence of macrophage colony-stimulating factor (CSF-1) and a novel mast cell growth factor in rheumatoid synovitis. *J. Exp. Med.*, **168**, 1573-1586.

FIRESTEIN, G., YEO, M. & ZVAIFLER, N. (1995). Apoptosis in the rheumatoid synovium. *J. Clin. Invest.*, **96**, 1631-1638.

FIRESTEIN, G. & ZVAIFLER, N. (1987). Peripheral blood and synovial fluid monocyte activation in inflammatory arthritis. II. Low levels of synovial fluid and synovial tissue interferon suggest the gamma-interferon is not the primary macrophage activating factor. *Arthritis Rheum.*, **30**, 864-871.

stromal cells to produce pro-inflammatory and hematopoetic cyokines. *J. Exp. Med.*, **183**, 2593-2603.

FLORES, I., JONES, D. & MÉRIDA, I. (2000). Changes in the balance between mitogenic and anti-mitogenic second messengers during proliferation, cell arrest, and apoptosis in T lymphocytes. *FASEB J.*, **14**, 1873-1875.

FLORES, I., MARTINEZ-A, C., HANNUN, Y. & MÉRIDA, I. (1998). Dual role of ceramide in the control of apoptosis following IL-2 withdrawal. *J. Immunol.*, **160**, 3528-3533.

FRATICELLI, A., SERRANO JR., C., BOCHNER, B., CAPOGROSSI, M. & ZWEIER, J. (1996). Hydrogen peroxide and superoxide modulate leukocyte adhesion molecule expression and leukocyte endothelial adhesion. *Biochim. Biophys. Acta*, **1310**, 251-259.

FÖLDES-FILEP, É., FILEP, J.G. & SIROIS, P. (1992). C-reactive protein inhibits intracellular calcium mobilisation and superoxide production by guinea pig alveolar macrophages. *J. Leukoc. Biol.*, **51**, 13-18.

GABBITA, S., ROBINSON, K., STEWART, C., FLOYD, R. & HENSLEY, K. (2000). Redox regulatory mechanisms of cellular signal transduction. *Arch. Biochem. Biophys.*, **376**, 1-13.

GABOURY, J., ANDERSON, D. & KUBES, P. (1994). Molecular mechanisms involved in superoxide-induced endothelial cell interactions in vivo. *Am. J. Physiol. Heart. Circ. Physiol.*, **266**, H637-H642.

GAMARD, C., DBAIBO, G., LIU, B., OBEID, L. & HANNUN, Y. (1997). Selective involvement of ceramide in cytokine-induced apoptosis. *J. Biol. Chem.*, **272**, 16474-16481.

GARCÍA-RUIZ, C., COLELL, A., MARI, M., MORALES, A. & FERNÁNDEZ-CHECA, J. (1997). Direct effect of ceramide in the mitochondrial electron transport chain leads to generation of reactive oxygen species. *J. Biol. Chem.*, **272**, 11369-11377.

GARCIA-RUIZ, C., COLELL, A., MORALES, A., KAPLOWITZ, N. & FERNANDEZ-CHECA, J. (1995). Role of oxidative stress generated from the mitochondrial electron transport chain and mitochondrial glutathione status in loss of mitochondrial function and activation of transcription factor nuclear factor-kappa B: studies with isolated mitochondria and. *Mol. Pharmacol.*, **48**, 825-834.

GAY, S. (1998). Rheumatoid arthritis. *Curr. Opin. Rheumatol.*, .

GERSZTEN, R., LIM, Y., DING, H., SNAPP, K., KANSAS, G., DICHEK, D., CABANAS, C., SANCHEZ-MADRID, F., GIMBRONE JR., M., ROSENZWEIG, A. & LUSCINSKAS, F. (1998). Adhesion of monocytes to vascular cell adhesion molecule-1-transduced human endothelial cells: implications for atherogenesis. *Circ. Res.*, **82**, 871-878.

GERSZTEN, R., LUSCINSKAS, F., DING, H., DICHEK, D., STOOLMAN, L., GIMBRONE JR., M. & ROSENZWEIG, A. (1996). Adhesion of memory lymphocytes to vascular cell adhesion molecule-1-transduced human vascular endothelial cells under simulated physiological flow conditions in vitro. *Circ. Res.*, **79**, 1205-1215.

GENESTIER, L., PAILLOT, R., BONNEFOY-BERARD, N., MEFFRE, G., FLACHER, M., FÈVRE, D., LIU, Y., LE BOUTEILLER, P., WALDMANN, H., ENGELHARD, V., BANCHEREAU, J. & J.-P., R. (1997). Fas independent apoptosis of activated T cells induced by antibodies to the HLA class I a1 domain. *Blood*, **90**, 3629-3639.

GENESTIER, L., PAILLOT, R., FOURNAL, S., FERRARO, C., MIOSSEC, P. & REVILLARD, J.-P. (1998a). Immunosuppressive properties of methotrexate: apoptosis and clonal deletion of activated peripheral T cells. *J. Clin. Invest.*, **102**, 322-328.

GENESTIER, L., PAILLOT, R., QUEMENEUR, L., IZERADJENE, K. & J-P., R. (2000). Mechanisms of action of methotrexate. *Immunopharmacology*, **47**, 247-257.

GENESTIER, L., PRIGENT, A.-F. , PAILLOT, R., QUEMENEUR, L., DURAND, I., BANCHEREAU, J., J-P., R. & BONNEFOY-BÉRARD, N. (1998b). Caspase-dependent ceramide production in Fas- and HLA class I-mediated peripheral T cell apoptosis. *J. Biol. Chem.*, **273**, 5060-5066.

GENESTIER, L., PRIGENT, A.-F. , PAILLOT, R., QUEMENEUR, L., DURAND, I., BANCHEREAU, J., REVILLARD, J. & BONNEFOY-BÉRARD, N. (1998). Caspase-dependent ceramide production in Fas- and HLA class I-mediated peripheral T cell apoptosis. *J. Biol. Chem.*, **273**, 5060-5066.

GHAFOURIFAR, P., KLEIN, S., SCHUCHT, O., SCHENK, U., PRUSCHY, M., ROCHA, S. & RICHTER, C. (1999). Ceramide induces cytochrome c release from isolated mitochondria: importance of mitochondrial redox state. *J. Biol. Chem.*, **274**, 6080-6084.

GHIBELLI, L., FANELLI, C., ROTILIO, G., LAFAVIA, E., COPPOLA, S., COLUSSI, C., CIVITAREALE, P. & CIRIOLO, M. (1998). Rescue of cells from apoptosis by inhibition of active GSH extrusion. *FASEB J.*, **12**, 479-486.

GIACCIA, A. & KASTAN, M. (1998). The complexity of p53 modulation: emerging patterns from divergent signals. *Gene. Dev.*, **12**, 2973-2983.

GOLD, M. & MATSUUCHI, L. (1995). Signal transduction by the antigen receptors of B and T lymphocytes. *Int. Rev. Cytol.*, **157**, 181-276.

GOLDSTONE, S., MILLIGAN, A. & HUNT, N. (1996). Oxidative signaling and gene expression during lymphocyte activation. *Biochim. Biophys. Acta*, **1314**, 175-182.

GOOSSENS, V., GROOTEN, J., DE VOS, K. & FRIERS, W. (1995). Direct evidence for tumour necrosis factor-induced mitochondrial reactive oxygen intermediates and their involvement in cytotoxicity. *Proc. Natl. Acad. Sci. USA.*, **92**, 8115-8119.

GOPALAKRISHNA, R. & JAKEN, S. (2000). Protein kinase C signaling and oxidative stress. *Free Rad. Biol. Med.*, **28**, 1349-1361.

GORONZY, J., BARTZ-BAZZANELLA, P., HU, W., JENDRO, M., WALSER-KUNTZ, D. & WEYAND, C. (1994). Dominant clonotypes in the repertoire of peripheral $CD4^+$ T cells in rheumatoid arthritis. *J. Clin. Invest.*, **94**, 2068-2076.

GOUAZÉ, V., MIRAULT, M.-E. , CARPERNTIER, S., SALVAYRE, R., LEVADE, T. & ANDREIEU-ABADIE, N. (2001). Glutathione oxidase over-expression prevents ceramide production and partially inhibits apoptosis in doxorubicin-treated human breast carcinoma cells. *Mol. Pharmacol.*, **60**, 488-496.

GOÑI, F. & ALONSO, A. (1999). Structural and functional properties of diacylglycerols in membranes. *Prog. Lipid Res.*, **38**, 1-48.

GRACIE, J., FORSEY, R., CHAN, W., GILMOUR, A., LEUNG, B., GREER, M., KENNEDY, K., CARTER, R., WEI, X.-Q. , XU, D., FIELD, M., FOULIS, A., LIEW, F. & MCINNES, I. (1999). A pro-inflammatory role for IL-18 in rheumatoid arthritis. *J. Clin. Invest.*, **104**, 1393-401.

GRASSMÉ, H., JEKLE, A., RIEHLE, A., SCHWARZ, H., BERGER, J., SANDHOFF, K., KOLESNICK, R. & GULBINS, E. (2001a). CD95 signaling via ceramide-rich rafts. *J. Biol. Chem.*, **276**, 20589-20596.

GRASSMÉ, H., JENDROSSEK, V., BOCK, J., RIEHLE, A. & GULBINS, E. (2002). Ceramide-rich membrane rafts mediate CD40 clustering. *J. Immunol.*, **168**, 298-307.

GRASSMÉ, H., SCHWARZ, H. & GULBINS, E. (2001b). Molecular mechanisms of ceramide-mediated CD95 clustering. *Biochem. Biophys. Res. Commun.*, **284**, 1016-1030.

GRAZIADEI, L., RIABOWOL, K. & BAR-SAGI, D. (1990). Co-capping of ras proteins with surface immunoglobulins in B lymphocytes. *Nature*, **347**, 396-399.

GREEN, D. & KROEMER, G. (1998). The central executioners of apoptosis: capases or mitochondria. *Trends Cell Biol.*, **8**, 267-271.

GRESSIER, B., LEBEGUE, S., BRUNET, C., LUYCKX, M., DINE, T., CAZIN, M. & CAZIN, J. (1994). Pro-oxidant properties of methotrexate: evaluation and prevention by an anti-oxidant drug. *Pharmazie*, **49**, 679-681.

GRIFFITHS HR, MOLLER L, BARTOSZ G, BAST A, BERTONI-FREDDARI C, COLLINS A, COOKE M, COOLEN S, HAENEN G, HOBERG AM, LOFT S, LUNEC J, OLINSKI R, PARRY J, POMPELLA A, POULSEN H, VERHAGEN H, ASTLEY SB. (2002). Biomarkers. *Mol. Aspects Med.*, **23**,101-208.

GUDZ, T., TSERNG, K.-Y. & HOPPEL, C. (1997). Direct inhibition of mitochondrial respiratory chain complex III by cell-permeable ceramide. *J. Biol. Chem.*,, **272**, 24154-24158.

GULBINS, E., BISSONNETTE, R., MAHBOUBI, A., MARTIN, S., NISHIOKA, W., BRUNNER,

T., BAIER, G., BAIER-BITTERLICH, G., BYRD, C., LANG, F., KOLESNICK, R., ALTMAN, A. & GREEN, D. (1995). FAS-induced apoptosis is mediated via a ceramide-initiated RAS signalling pathway. *Immunity*, **2**, 341-351.

HADDAD, J., SAADE, N. & SAFIEH-GARABEDIAN, B. (2002). Redox regulation of TNFα biosynthesis: Augmentation by irreversible inhibition of [gamma]-glutamylcysteine synthetase and the involvement of IκB-α/NF-κB-independent pathway in alveolar epithelial cells. *Cell Signal.*, **14**, 211-218.

HAIMOVITZ-FRIEDMAN, A., KOLESNICK, R. & FUKS, Z. (1997). Ceramide signaling in apoptosis. *Br. Med. Bull.*, **53**, 539-553.

HALL, M., LAWRENCE, D., LANSIEDEL, J., WALSH, A., COMSTOCK, L. & KREMER, J. (1997). Long-term exposure to methotrexate induces immunopheotypic changes, decrease methotrexate uptake and increased dihydrofolate gene number in Jurkat T cells. *Int. J. Immunophramac.*, **19**, 709-720.

HALLIWEL, B. (1995). Oxygen radicals, nitric oxide and human inflammatory joint disease. *Ann. Rheum. Dis.*, **54**, 505-510.

HALLIWELL, B. & GUTTERIDGE, J. (1990). Role of free radicals and catalytic metal ions in human disease: an overview. *Methods Enzymol..*, **186**, 1-85.

HAMILTON,R.A. & KRAMER, J. (1995). The effects of food on methotrexate absorption. *J. Rheumatol.*, **22**, 630-632.

HANNA, A., CHAN, E., XU, J., STONE, J. & BRINDLEY, D. (1999). A novel pathway for Tumour necrosis factor-α and ceramide signaling involving sequential activation of tyrosine kinase p21ras, and phosphatidylinositol 3-kinase. *J. Biol. Chem.*, **274**, 12722-12729.

HANNUN, Y. (1996). Functions of ceramide in coordinating cellular responses to stress. *Science*, **274**, 1855-1859.

HANNUN, Y., GREENBERG, C. & BELL, R. (1987). Sphingosine inhibition of agonist-dependent secretion and activation of human platelets implies that protein kinase C is a necessary and common event of the signal transduction pathways. *J. Biol. Chem.*, **262**, 13620-13626.

HANNUN, Y. & LUBERTO, C. (2000). Ceramide in the stress eukaryotic stress response. *Trends Cell Biol.*, **10**, 73-80.

HASHIMATO, H., TANAKA, M., SUDA, T., TOMITA, T., HAYASHIDA, K., TAKEUCHI, E., KANEKO, M., TAKANO, H., NAGATA, S. & OCHI, T. (1998). Soluble Fas ligand in the joints of patients with rheumatoid arthritis and osteoarthritis. *Arthritis Rheum.*, **Check**, 657-662.

HASSAN, M., HADI, R., AL-RAWI, Z., PADRON, V. & STOHS, S. (2001). The glutathione defense system in the pathogenesis of rheumatoid arthritis. *J. Appl. Toxicol.*, **21**, 69-73.

HASUNUMA, T., HOA, T., AONO, H., ASAHARA, H., YONEHARA, S., YAMAMOTO, K., SUMIDA, T., GAY, S. & NISHIOKA, K. (1996). Induction of Fas dependent apoptosis in synovial infiltrating cells in rheumatoid arthritis. *Int. Immunol.*, **8**, 1595.

HASUNUMA, T., KATO, T., KOBATA, T. & NISHIOKA, K. (1998). Molecular mechanisms of immune reponse, synovial proliferation and apoptosis in rheumatoid arthritis. *Springer Semin. Immunopathol.*, **20**, 41-52.

HASUNUMA, T., KAYAGAKI, N., ASAHARA, H., MOTOKAWA, S., KOBATA, T., YAGITA, H., AONO, H., SUMIDA, T., OKUMURA, K. & NIKIOOKA, K. (1997). Accumulation of soluble Fas in inflamed joints of patients with rheumatoid arthritis. *Arthritis Rheum.*, **40**, 80.

HAWKES, J., CLELAND, L. & JAMES, M. (1993). The effect of methotrexate in lipoxygenase metabolism in neutrophils from rats: *in vitro* and *ex vivo* studies. *Agents Actions*, **40**, 181-185.

HAWKES, J., CLELAND, L., PROUDMAN, S. & JAMES, M. (1994). The effect of methotrexate on *ex vivo* lipoxygenase metabolism in neutophils from patients with rheumatoid arthirtis. *J. Rheumatol.*, **21**, 55-58.

HEMLER, M., BRENNER, M., MCLEAN, J. & STROMINGER, J. (1984). Antigenic stimulation regulates the level of expression of interleukin 2 receptor on human T cells. *Proc. Natl. Acad. Sci. U S A*, **81**, 2172-2175.

HEMPEL, S., BUETTNER, O., Y.Q.O., WESSELS, D. & FLAHERTY, D. (1999). Dihydrofluorescein diacetate is superior for detecting intracellular oxidants: comparison with 2',7'-dichlordihydrofluorescein diacetate, 5(and 6)-carboxy-2',7'-dichlorodihydrofluorescein diacetate, and dihydrorhodamine. *Free Rad. Biol. Med.*, **27**, 146-159.

HENNET, T., RICHTER, C. & PETERHANS, E. (1993). Tumour necrosis factor-α induces superoxide anion generation in mitochondria of L929 cells. *Biochem. J.*, **289**, 587-592.

HERR, I., WILHELM, D., BÖHLER, T., ANGEL, P. & DEBATIN, K.-M. (1997). Activation of CD95 (APO-1/Fas) signaling by ceramide mediates cancer therapy-induced apoptosis. *EMBO J.*, **16**, 6200-6208.

HERRMANN, J., BRUCKHEIMER, E. & MCDONNELL, T. (1996). Cell death signal transduction and Bcl-2 function. *Biochem. Soc. Trans.*, **24**, 1059-1065.

HIGUCHI, M., HONDA, T., PROSKE, R. & YEH, E. (1998). Regulation of reactive oxygen species-induced apoptosis and necrosis by caspase 2-like proteases. *Oncogene*, **17**, 2753-2760.

HILDEMAN, D.A., H., MITCHELL, T., TEAGUE, T., HENSON, P., DAY, B., KAPPLER, J. & MARRACK, P. (1999). Reactive oxygen species regulate activation-induced T cell apoptosis. *Immunity*, **10**, 735-744.

HIROTA, K., MATSUI, M., IWATA, S., NISHIYAMA, A., MORI, K. & YODOI, J. (1997). AP-1 transcriptional activity is regulated by a direct association between thioredoxin and Ref-1. *Proc. Natl. Acad. Sci. USA*, **94**, 3633-3638.

HOA, T., HASUNUMA, T., AONO, H., MASUKO, K., KOBATA, T., YAMAMOTO, K., SUMIDA, T. & NISHIOKA, K. (1996). Novel mechanisms of selective apoptosis in synovial T cells of patients with rheumatoid arthritis. *J. Rheumatol.*, **23**, 1332-1337.

HOCKENBERY, D., OLTVAI, Z., YIN, X., -M., MILLMAN, C. & KORSMEYER, S. (1993). Bcl-2 functions in an antioxidant pathway to prevent apoptosis. *Cell*, **75**, 241-251.

HOFMAN, K. & DIXIT, V. (1998). Ceramide in apoptosis - does it really matter? *Trends Biochem. Sci.*, **23**, 374-377.

HOFMANN, K. & DIXIT, V. (1998). *Trends Biochem. Sci.*, **23**, 374-377.

HOLOPAINEN, J., SUBRAMANIAN, M. & KINNUNEN, P. (1998). Sphingomyelinase induces lipid microdomain formation in phospatidylcholine/sphingomyelin membrane. *Biochemistry*, **37**, 17562-17570.

HORINOUCHI, K., ERLICH, S., PERL, D., FERLINZ, K., BISAIER, C., SANDHOFF, K., DESNICJ, R., STEWART, C. & SCHUCHMAN, E. (1995). Acid sphingomyelinase deficient mice: a model of types A and B Niemann-Pick disease. *Nat. Genet.*, **10**, 288-293.

HU, S., MITCHKO, Y., ORONSKY, A. & KERWAR, S. (1998). Studies on the effect of methotrexate on macrophage function. *J. Rheumatol.*, **15**, 206-209.

HUANG, H.-W. , GOLDBERG, E. & ZIDOVETZKI, R. (1998). Ceramide perturb the structure of phospatidylcholine bilayers and modulate the activity of phospolipase A2. *Eur. Biophys. J.*, **27**, 361-366.

HUANG, H.-W. , GOLDBERG, E. & ZIDOVETZKI, R. (1996). Ceramide induces structural defects into phosphatidylcholine bilayers and activates phospholipase A2. *Biochem. Biophys. Res. Commun.*, **220**, 834-838.

HUG, H., ENARI, M. & NAGATA, S. (1994). No requirement of reactive oxygen intermediates in Fas-mediated apoptosis. *FEBS Lett.*, **351**, 311-313.

HUO, Y. & LEY, K. (2001). Adhesion molecules and atherogenesis. *Acta Physiol. Scand.*, **173**, 35-43.

HUWILER, A., BRUNNER, J., HUMMEL, R., VERVOORDELDONK, M., STABEL, S., VAN DEN BOSCH, H. & PFEILSCHIFTER, J. (1996). Ceramide-binding and activation defines protein kinase c-Raf as a ceramide-activated protein kinase. *Proc. Natl. Acad. Sci. U S A*, **93**, 6959-6963.

HUWILER, A., BRUNNER, J., HUMMEL, R., VERVOORDELDONK, M., STABEL, S., VAN DEN BOSCH, H. & PFEILSCHIFTER, J. (1996). Ceramide-binding and activation defines protein kinase c-Raf as a ceramide-activated protein kinase. *Proc. Natl. Acad. Sci. USA.*, **93**, 6959-6963.

HUWILER, A., FABBRO, D. & PFEILSCHIFTER, J. (1998). Selective ceramide binding to protein kinase C-alpha and -delta isoenzymes in renal mesangial cells.Selective ceramide binding to protein kinase C-alpha and -delta isoenzymes in renal mesangial cells.. *Biochemsitry*, **37**, 14556-14562.

JACKSON, M., PAPA, S., BOLANOS, J., BRUCKDORFER, R., CARLSEN, H., ELLIOTT, R.M., FLIER, J., GRIFFITHS, H., HEALES, S., HOLST, B., LORUSSO, M., LUND, E., OIVIND MOSKAUG, J., MOSER, U., DI PAOLA, M. POLIDORI, C.M, SIGNORILE, A., STAHL, W. & VINA-RIBES (2002). Antioxidants, reactive oxygen and nitrogen species, gene induction and mitochondrial function. *Mol. Aspects Med.*, **23**, 209-285.

JACOBSON, M. (1996). Reactive oxygen species and programmed cell death. *Trends Biochem. Sci.*, **21**, 83-86.

JAFFE, E., NACHMAN, R., BECKER, C. & MINICK, C. (1973). Culture of human endothelial cells derived from umbilical veins. *J. Clin. Invest.*, **52**, 2745-2756.

JAFFRÉZOU, J., LEVADE, T., BETTAIEB, A., ANDRIEU, N., BEZOMBES, C., MAESTRE, N., VERMEERSCH, S., ROUSSE, A. & LAURENT, G. (1996). Daunorubicin-induced apoptosis: triggering of ceramide generation through sphingomyelin hydrolysis. *EMBO J.*, **15**, 2417-2424.

JAFFRÉZOU, J.-P. , MAESTRE, N., MANSAT-DE MAS, V., BEZOMES, C., LEVADE, T. & LAURENT, G. (1998). Positive feedback control of neutral sphingomyelinase activity by ceramide. *FASEB J.*, **12**, 999-1006.

JANES, P., LEY, S. & MAGEE, A. (1999). Aggregation of lipid rafts accompanies signaling via the T

cell antigen receptor. *J. Cell Biol.*, **147**, 447-461.

JARVIS, W., FORNARI, F.J., BROWNING, J., GEWIRTZ, D., KOLESNICK, R. & GRANT, S. (1994a). Attenuation of ceramide-induced apoptosis by diglyceride in human myeloid leukemia cells. *J. Biol. Chem.*, **269**, 31685-31692.

JARVIS, W., KOLESNICK, R., FORNARI, F., TRAYLOR, R., GEWIRTZ, D. & GRANT, S. (1994b). Induction of apoptotic DNA damage and cell death by activation of the sphingomyelin pathway. *Proc. Natl. Acad. Sci. U S A*, **91**, 73-77.

JARVIS, W., TURNER, A., POVIRK, L., TRAYLOR, R. & GRANT, S. (1994). Induction of apoptotic DNA fragmentation and cell death in HL-60 human promyelocytic leukemia cells by pharmacological inhibitors of protein kinase C. *Cancer Res.*, **54**, 1707-1714.

JAYADEV, S., LIU, B., BIELAWSKA, A., LEE, J., NAZAIRE, F., PUSHKAREVA, M., OBEID, L. & HANNUN, Y. (1995). Role of ceramide in cell cycle arrest. *J. Biol. Chem.*, **270**, 2047-2052.

JAYANTHI, S., ORDONEZ, S., MCCOY, M. & CADET, J. (1999). Duel mechanism of Fas-induced cell death in neuroglioma cells: a role for reactive oxygen species. *Brain Res. Mol. Brain Res.*, **72**, 158-165.

JI, L., ZHANG, G., UENATSU, S., AKAHORI, Y. & HIRABAYASHI, Y. (1995). Induction of apoptotic DNA fragmentation and cell death by natural ceramide. *FEBS Lett.*, **358**, 211-214.

JIKIMOTO, T., NISHIKUBO, Y., KOSHIBA, M., KANAGAWA, S., MORINOBU, S., MORINOBU, A., SAURA, R., MIZUNO, K., KONDO, S., TOYOKUNI, S., NAKAMURA, H., YODOI, J. & KUMAGAI, S. (2001). Thioredoxin as a biomarker for oxidative stress in patients with rheumatoid arthritis. *Mol. Pharmacol.*, **38**, 765-772.

JOLLY, C., LAURENZ, J., MCMURRAY, D. & CHAPKIN, R. (1996). Diacylglycerol and ceramide kinetics in primary cultures of activated T-lymphocytes. *Immunol. Lett.*, **49**, 43-48.

JONES, S. & KAZLAUSKAS, A. (2001). Growth factor-dependent signalling in cell cycle progression. *FEBS Lett.*, **490**, 110-116.

KALOGERIS, T., KEVIL, C., LAROUX, F., COE, L., PHIFER, T. & ALEXANDER, J. (1999). Differential monocyte adhesion and adhesion molecule expression in venous and arterial endothelial cells. *Am. J. Physiol.*, **276**, L9-L19.

KANNER, S., DAMLE, N., BLAKE, J., ARUFFO, A. & LEDBETTER, J. (1992). CD2/LFA-3 ligation induces phospholipase C gamma 1 tyrosine phosphorylation and regulates CD3 signalling. *J. Immunol.*, **148**, 2023-2029.

KANOH, H., SAKANE, F., IMAI, S.-I. & WADA, I. (1993). Diacylglycerol kinase and phosphatidic acid phosphatase-enzymes metabolising lipid second messengers. *Cell Signal.*, **5**, 495-503.

KARASAVAS, N. & ZAKERI, Z. (1999). Relationships of apoptotic signaling mediated by ceramide and TNF-α in U937 cells. *Cell Death Diff.*, **6**, 115-123.

KASAMA, T., SHIOZAWA, F., KOBAYASHI, K., YAJIMA, N., HANYUDA, M., TAKEUCHI, H., MORI, Y., NEGISHI, M., IDE, H. & ADACHI, M. (2001). Vascular endothelial growth factor expression by activated synovial leukocytes in rheumatoid arthritis. *Arthritis Rheum.*, **44**, 2512-2524.

KERR, J., WYLLIE, A. & CURRIE, A. (1972). Apoptosis: a big biological phenomenon with wide ranging implications in tissue kinetics. *Br. J. Cancer*, **26**, 239-257.

KEVIL, C., PATEL, R. & BULLARD, D. (2001). Essential role of ICAM-1 in mediating monocyte adhesion to aortic endothelial cells. *Am. J. Physiol. Cell Physiol.*, **281**, C1442-C1447.

KINNUNENE, P. & HOLOPAINEN, J. (2002). Sphingomyelinase activity of LDL: a link between atherosclerosis, ceramide, and apoptosis? *Trends Cardiovasc. Med.*, **12**, 37-42.

KNEBEL, A., RAHMSDORF, H., ULLRICH, A. & HERRLICH, P. (1996). Dephosphorylation of receptor tyrosine kinases as target of regulation by radiation, oxidants or alkylating agents. *EMBO J.*, **15**, 5314-5325.

KOBAYASHI, T., OKAMOTO, K., KOBATA, T., HASUMUNA, T. & NISHIOKA, K. (1999). Apomodulation as a novel therapeutic concept for the regulation of apoptosis in rheumatoid synoviocytes. *Curr. Opin. Rheumatol.*, **11**, 188-193. KOCH, A., BURROWS, J., HAINES, G., CARLOS, T., HARLAN, J. & LEIBOVICH, S. (1991). Immunolocalisation of endothelial and leukocyte adhesion molecules in human rheumatoid and osteoarthritic synovial tissues. *Lab. Invest.*, **64**, 313-320.

KOCH, A., KUNKEL, S. & STRIETER, R. (1995). Cytokines in rheumatoid arthritis. *J. Clin. Invest.*, **43**, 28-38.

KOHNO, K & KURIMOTO, M. (1998). Interleukin 18, a cytokine which resembles IL-1 structurally and IL-12 functionally but exerts its effect independently of both. *Clin. Immunol. Immunopatho.l*, **86**, 11-15.

KOKURA, S., WOLF, R., YOSHIKAWA, T., GRANGER, D. & AW, T. (1999). Molecular

mechanisms of neutrophil-endothelial cell adhesion induced by redox imbalance. *Circ. Res.*, **84**, 516-524.

KOLESNICK, R. & KRÖNKE, M. (1998). Regulation of ceramide production and apoptosis. *Annu. Rev. Immunol.*, **60**, 643-665.

KORLIPARA, L., LEON, M., RIX, D., DOUGLAS, M., GIBBS, P., BASSENDINE, M. & KIRBY, J. (1996). Development of a flow cytometric assay to quantify lymphocyte adhesion to cytokine-stimulated human endothelial and bilary epithelial cells. *J. Immunol. Methods*, **191**, 121-130.

KRAMMER, P.B., I., DANIEL, P., DHEIN, J. & DEBATIN, K.-M. (1994). Regulation of apoptosis in the immune system. *Curr. Opin. Immunol.*, **6**, 279-289.

KRANE, S., CONCA, W., STEPHENSON, M., AMENTO, E. & GOLDRING, M. (1990). Mechanisms of matrix degradation in rheumatoid arthritis. *Ann. N. Y. Acad. Sci.*, **580**, 340-354.

KREMER, J. & PHELPS, T. (1992). A long-term prospective study of the use of methotrexate in rheumatoid arthritis: update after a mean of 90 months. *Arthritis Rheum.*, **35**, 138-145.

KRENN, V., SCHEDEL, J., DÖRING, A., HUPPERTZ, H.-I. , GOHLKE, F., TONY, H.-P. , VOLLMERS, H. & MÜLLER-HERMELINK, H. (1997). Endothelial cells are the major sources of sICAM-1 in rheumatoid synovial tissue. *Rheumatol. Int.*, 17-27.

KRÖNKE, M. (1999). Biophysics of ceramide signaling: interaction with proteins and phase transition of membranes. *Chem. Phys. Lipids*, **101**, 109-121.

KUROHORI, Y., SATO, K., SUZUKI, S. & KASHIWAZAKI, S. (1995). Adhesion molecule expression on peripheral blood mononuclear cells in rheumatoid arthritis: positive correlation between the proportion of L-selectin an disease activity. *Clin. Rheumatol.*, **14**, 335-341.

LANDIS, R., BENNETT, R. & HOGG, N. (1993). A novel LFA-1 activation epitope maps to the I domain. *J. Cell Biol.*, **120**, 1519-1527. LANE, T., LAMKIN, G. & WANCEWICZ, E. (1989). Modulation of endothelial cell expression of intercellular adhesion molecule 1 by protein kinase C activation. *Biochem. Biophys. Res. Commun.*, **161**, 945-952.

LAOUAR, A., GLESNE, D. & HUBERMAN, E. (1999). Involvement of protein kinase C-β and ceramide in tumour necrosis factor-α-induced but not Fas-induced apoptosis of human myeloid leukeamia cells. *J Biol Chem.*, **274:23526-34.**, 23526-23534.

LEE, B. & UM, H.-D. (1999). Hydrogen peroxide suppresses U937 cell death by two different mechanisms depending on its concentration. *Exp. Cell Res.*, **248**, 430-438.

LEVADE, T., AUGÉ, N., VELDMANN, R., CUVILLIER, O., NÈGRE-SALVAYRE, A. & SALVAYRE, R. (2001). Sphingolipid mediators in cardiovascular cell biology and pathology. *Circ. Res.*, **89**, 957-968.

LEVADE, T. & JAFFRÉZOU, J.-P. (1999). Signaling sphingomyelinases: which, where, how, why? *Biochim. Biophys. Acta*, **1438**, 1-7.

LEY, K. & BROOKE, A. (2000). hsc.virginia.edu/medicine/basic-sci/ biomed/ley/map.gif.

LIEBERTHAL, W., TRIACA, V., KOH, J.S., PAGANO, P.J. & LEVINE, J.S. (1998). Role of superoxide in apoptosis induced by growth factor withdrawal. *Am J. Pathol.*, **275**, 691-702.

LIOTÉ, F., BOVAL-BOIZARD, B., WEILL, D., KUNTZ, D. & WAUTIER, J.-L. (1996). Blood monocyte activation in rheumatoid arthritis: increased monocyte adhesiveness, integrin expression, and cytokine release. *Clin. Exp. Immunol.*, **106**, 13-19.

LI, H., CYBULSKY, M., GIMBRONE JR., M. & LIBBY, P. (1993). An atherogenic diet rapidly induces VCAM1, a cytokine-regulatable mononuclear leukocyte adhesion molecule, in rabbit aortic endothelium. *Arterioscler. Thromb.*, **13**, 197-204.

LIU, B., ANDREIEU-ABADIE, N., LEVADE, T., ZHANG, P., OBEID, L. & HANNUN, Y. (1998). Glutathione regulation of neutral sphingomyelinase in Tumour necrosis factor-a induced cell death. *J. Biol. Chem.*, **273**, 11313-11320.

LIU, P. & ANDERSON, R. (1995). Compartmentalized production of ceramide at the cell surface. *J. Biol. Chem.*, **270**, 27179-27185.

LIU, B. & HANNUN, Y. (1997). Inhibition of neutral magnesium-dependent sphingomyelinase by glutathione. *J. Biol. Chem.*, **272**, 16281-16287.LIU,P. & ANDERSON (1995). Compartmentalised production of ceramide at the cell surface. *J. Biol. Chem.*, 27179-27185.

LIU, J., KUSZYNSKI, C. & BAXTER, B. (1999). Doxycycline induces Fas/Fas ligand-mediated apoptosis in Jurkat T lymphocytes. *Biochem. Biophys. Res. Commun.*, **260**, 562-567.

LIZARD, G., FOURNAL, S., GENESTIER, L., DHEDIN, N., CHAPUT, C., FLACHER, M., MUTIN, M., PANAYE, G. & J.-P., R. (1995). Kinetics of plasma membrane and mitochondrial alterations in cells undergoing apoptosis. *Cytometry*, **21**, 275-283.

LO, S., JANAKIDEVI, K., LAI, L. & MALIK, A. (1993). Hydrogen peroxide-induced increase in endothelial adhesiveness is dependent on ICAM-1 activation. *Am. J. Physiol.*, **264**, L406-L412.

LOKESH, B. & CUNNINGHAM, M. (1986). Further studies on the formation of oxygen radicals by

potassium superoxide in aqueous medium for biochemical investigations. *Toxicol. Lett.*, **34**, 75-84.

LOS, M., DRÖGE, W., STRICKER, K., BAEUERLE, P. & SCHULZE-OSTHOFF, K. (1995). Hydrogen peroxide as a potent activator of T lymphocyte functions. *Eur. J. Immunol.*, **25**, 159-165.

LOZANO, J., BERRA, E., MUNICIO, M., DIAZ-MECO, M., DOMINGUEZ, I., SANZ, L. & MOSCAT, J. (1994). Protein kinase C ζ isoform is critical for κB-dependent promoter activation by sphingomyelinase. *J. Biol. Chem.*, **269**, 19200-19202.

LUBERTO, C. & HANNUN, Y. (1999). Sphingolipid metabolism in the regulation of bioactive molecules. *Lipids*, **34**, S5-S11.

LUM, H. & ROEBUCK, K. (2001). Oxidant stress and endothelial cell dysfunction. *Am. J. Physiol. Cell Physiol.*, **280**, C719-C741.

MACKICHAN, M. & DEFRANCO, A. (1999). Role of ceramide in lipopolysacharide (LPS)-induced signalling. *J. Biol. Chem.*, **274**, 1767-1775.

MADRI, J. & GRAESSER, D. (2000). Cell migration in the immune system: the evolving inter-related roles of adhesion molecules and proteinases. *Dev. Immunol.*, **7**, 103-116.

MAKAROV, S. (2001). NF-kappa B in rheumatoid arthritis: a pivotal regulator of inflammation, hyperplasia, and tissue destruction. *Arthritis Res.*, **3**, 200-206.

MANGAN, D., TAICHMAN, N., LALLY, E. & WAHL, S. (1991). Lethal effects of Actinobacillus actinomycetemcomitans leukotoxin on human T lymphocytes. *Infect. Immun.*, **59**, 3267-2.

MANNA, S., GAD, Y., MUKHOPADHYAY, A. & AGGARWAL, B. (1999). Overexpression of manganese superoxide dismutase suppresses tumour necrosis factor-induced apoptosis and activation of nuclear transcription factor-κB and activater protein-1. *J. Biol. Chem.*, **273**, 13245-13254.

MANSAT-DE MAS, V., BEZOMBES, C., QUILLET-MARY, A., BETTAIEB, A., DE THONEL D'ORGEIX, A., LAURENT, G. & JAFFRÉZOU, J.-P. (1999). Implication of radical oxygen species in ceramide generation, c-Jun terminal kinase activation and apoptosis induced by daunorubicin. *Molecular Pharmacology*, **56**, 867-874.

MANSAT-DE MAS, V., LAURENT, G., LEVADE, T., BETTAIEB, A. & JAFFREZOU, J. (1997). The protein kinase C activators phorbol esters and phosphatidylserine inhibit neutral sphingomyelinase activation, ceramide generation, and apoptosis triggered by daunorubicin. *Cancer Res.*, **57**, 5300-5304.

MATHENY, H., DEEM, T. & COOK-MILLS, J. (2000). Lymphocyte migration through monolayers of endothelial cell lines involves VCAM-1 signaling via endothelial cell NADPH oxidase. *J. Immunol.*, **164**, 6550-6559.

MATHIAS, S., PEÑA, L. & KOLESNICK, R. (1998). Signal transduction of stress via ceramide. *Biochem J.*, **335**, 465-480.

MATSUBARA, T. & ZIFF, M. (1986). Increased superoxide anion release from human endothelial cells in response to cytokines. *J. Immunol.*, **137**, 3295-3298.

MATTHEWS, N., EMERY, P., PILING, D., AKBAR, A. & SALMON, M. (1993). Sub-populations of primed T helper cells in rheumatoid arthritis. *Arthritis Rheum.*, **36**, 603-607.

MAURICE, M., NAKAMURA, H., VAN DER VOORT, E., VAN VLIET, A., STAAL, F., TAK, P.-P. , BREEDVELD, F. & VERWEIJ, C. (1997). Evidence for the role of an altered redox state in hyporesponsiveness of synovial T cells in rheumatoid arthritis. *J. Immunol.*, **158**, 1458-1465.

MCINNES, I., LEUNG, B., STURROCK, R., FIELD, M. & LIEW, F. (1997). interleukin-15 mediates T cell-dependent regulation of tumour necrosis factor-alpha production in rheumatoid arthritis. *Nat. Med.*, **3**, 189-195.

MCINNES, I., AL-MUGHALES, J., FIELD, M., LEUNG, B., HUANG, F., DIXON, R., STURROCK, R., WILKINSON, P. & LIEW, F. (1996). The roles of interleukin-15 in T-cell migration and activation in rheumatoid arthritis. *Nat. Med.*, **2**, 175-182.

MEERSCHAERT, J. & FURIE, M.B. (1995). The adhesion molecules used by monocytes for migration across endothelium include CD11a/CD18, CD11b/CD18, and VLA-4 on monocytes and ICAM-1, VCAM-1, and other ligands on endothelium. *J. Immunol.*, **154**, 4099-4112.

MEERSCHAERT, J. & FURIE, M. (1994). Monocytes use either CD11/CD18 or VLA-4 to migrate across human endothelium in vitro. *J. Immunol.*, **152**, 1915-1926.

MENGUBAS, K., FAHEY, A., LEWIN, J., MEHTA, A., HOFFBRAND, A. & WICKREMASINGHE, R. (1999). Killing of T lymphocytes by synthetic ceramide is by a nonapoptotic mechanism and is abrogated following mitogenic activation. *Exp. Cell Res.*, **249**, 116-122.

MERCURIO, F., ZHU, H., MURRA,Y.B.W., SHEVCHENKO, A., BENNETT, B., LI, J., YOUNG, D., BARBOSA, M., MANN, M., MANNING, A. & RAO, A. (1997). IKK-1 and IKK-2: cytokine-activated IkappaB kinases essential for NF-kappaB activation. *Science*, **278**, 860-866.

MEREDITH, M., CUSICK, C., SOLTANINASSAB, S., SEKHAR, K., LU, S. & FREEMAN, M. (1998). Expression of Bcl-2 increases intracellular glutathione by inhibiting methionine-dependent GSH efflux. *Biochem. Biophys. Res. Commun.*, **248**, 458-463.

MERRIL, J., SHEN, C., SCHREIBMAN, D., COFFEY, D., ZAKJARENKO, O., FISHER, R., LAHITA, R., SALMON, J. & CRONTSTEIN, B. (1997). Adenosine A1 receptor promotion of multinucleated giant cell formation by human monocytes: a mechanism for methotrexate-induced nodulosis in rheumatoid arthritis. *Arthritis & Rheumatism*, **40**, 1308-1315.

MERRILL, A., SCHMELZ, M., DILLEHAY, D., SPEIGEL, S., SHAYMAN, J., SCHROEDER, J., RILEY, R., VOSS, K. & WANG, E. (1997). Sphingolipids - The enigmatic lipid class: biochemistry, physiology and pathophysiology. *Toxicol. Appl. Pharm.*, **142**, 208-225.

MIAGKOV, A., KOVALENKO, D., BROWN, C., DIDSBURY, J., COGSWELL, J., STIMPSON, S., BALDWIN, A. & MAKAROV, S. (1998). NF-κB activation provides the potential link between inflammation and hyperplasia in the arthritic joint. *Proc. Natl. Acad. Sci. U S A*, **95**, 13859-13864.

MIESEL, R., MURPHY, M. & KROGER, H. (1996). Enhanced mitochondrial radical production in patients which rheumatoid arthritis correlates with elevated levels of tumour necrosis factor alpha in plasma. *Free Rad. Biol. Med.*, **25**, 161-169.

MIGNOTTE, B. & VAYSSIERE, J.-L. (1998). Mitochondria and apoptosis. *Eur. J. Biochem.*, **252**, 1-15.

MODUR, V., ZIMMERMAN, G., PRESCOTT, S. & MCINTYRE, T. (1996). Endothelial cell inflammatory responses to tumour necrosis factor-α. *J. Biol. Chem.*, **271**, 13094-13102.

MOJCIK, C. & SHEVACH, E. (1997). Adhesion molecules: a rheumatologic perspective. *Arthritis Rheum.*, **40**, 991-1004.

MONKS, C., FREIBERG, B., KUPFER, H., SCIAKY, N. & KUPFER, A. (1998). Three dimensional segregation of supramolecular activation clusters in T cells. *Nature*, **395**, 82-86.

MORGAN, S., BAGGOTT, J., VAUGHN, W., AUSTIN, J., VEITCH, T., LEE, J., KOOPMAN, W., KRUMDIECK, C. & ALARCÓN, G. (1994). Supplementation with folic acid during methotrexate therapy for rheumatoid arthritis. A double-blind, placebo controlled trial. *Ann. Int. Med.*, **121**, 833-841.

MULLER, M., WILDER, S., BANNASCH, D., ISRAELI, D., LEHLBACH, K. & LI-WEBER, M. (1998). P53 activates the CD95 (APO-1/Fas) gene in response to DNA damage by anticancer drugs. *J. Exp. Med.*, **188**, 2033-2045.

MULLER, W., WEIGL, S., DENG, X. & PHILLIPS, D. (1993). PECAM-1 is required for transendothelial migration of leukocytes. *J. Exp. Med.*, **178**, 449-460.

MÜLLER, G., AYOUB, M., STORZ, P., RENNECKE, J., FABBRO, D. & PFIZENMAIER, K. (1995). PKCζ is a molecular switch in signal transduction of TNF-a, bifunctionally regulated by ceramide and arachidonic acid. *EMBO J.*, **14**, 1961-1969.

MÜLLER-LADNER, U., GAY, R. & GAY, S. (1998). Molecular biology of cartilage and bone destruction. *Curr. Opin. Rheumatol.*, **10**, 212-219.

MURPHY, M., PACKER, M., SCARLETT, J. & MARTIN, S. (1998). Peroxynitrite: a biological significant oxidant. *Gen. Pharmac.*, **31**, 179-186.

NAGATA, S. (1998). Human autoimmune lymphoproliferative syndrome, a defect in the apoptosis-inducing Fas receptor: a lesson from the mouse model. *J. Hum. Genet.*, **43**, 2-8.

NAGATA, S. (1994). Fas and Fas ligand: a death factor and its receptor. *Adv. Immunol.*, **57**, 129-144.

NAGATA, S. & SUDA, T. (1995). Fas and Fas ligand: lpr and gld mutations. *Immunol. Today*, **16**, 39-43.

NAGEH, M., SANDBERG, E., MAROTTI, K., LIN, A., MELCHIOR, E., BULLARD, D. & BEAUDET, A. (1997). Deficiency of inflammatory cell adhesion molecules protects against atherosclerosis in mice. *Arterioscler. Thromb. Vasc. Biol.*, **17**, 1517-1520.

NAKAJIMA, T., AONO, H., HASUNUMA, T., YAMAMOTO, K., SHIRAI, T., HIROHATA, K. &
NAKAMURA, H., NAKAMURA, K. & YODOI, J. (1997). Redox regulation of cellular activation. *Annu. Rev. Immunol.*, **15**, 351-369.

NAKASHIMA, Y., RAINES, E., PLUMP, A., BRESLOW, J. & ROSS, R. (1998). Upregulation of VCAM-1 and ICAM-1 at atherosclerosis-prone sites on the endothelium in the apoe-deficient mouse. *Arterioscler Thrombosis Vascular Biol.*, **18**, 945-951.

NAPOLI, C., DE NIGRIS, F. & PALINSKI, W. (2001). Multiple role of reactive oxygen species in the arterial wall. *Agents Actions*, 682.

NASH, R.A., PEPE, M., STORB, R., LONGTON, G., PETTINGER, M., ANASETTI, C., APPELBAUM, F., BOWDEN, R., DEEG, H., DONEY, K., MARTIN, P., SULLIVAN, K., Sanders, J. & WITHERSPOON, R. (1992). Acute graft-vs.-host disease; analysis of risk facotrs after allogeneic marrow transplanation and prophylaxis with cyclosporine and methotrexate. *Blood*, **80**,

1838-1845.
NATOLI, G., COSTANZO, A., GUIDO, F., MORETTI, F. & LEVERO, M. (1998). Apoptotic, non-apoptotic, and anti-apoptotic pathways of tumour necrosis factor signaling. *Biochem. Pharmacol.*, **56**, 915-920.
N'CHO, M. & BRAHMI, Z. (1999). Fas-mediated apoptosis in T cells involves the dephophorylation of the retinoblastoma protein by type 1 protein phosphatases. *Human Immunol.*, **60**, 1183-1194.
NEUMAN, M., CAMERON, R., HABER, J., KATZ, G., MALKIEWICZ, I. & SHEAR, N. (1999). Inducers of cytochrome P450 2E1 enhance methotrexate-induced hepatotoxixity. *Clin. Biochem.*, **32**, 519-536.
NEWMAN, P. (1997). The biology of PECAM-1. *J. Clin. Invest.*, **11** (Suppl 1), S25-S29.
NICOLLETTI, I., MIGLIORATI,G, PAGLIACCII, M., GRIGNANI, F. & RICCARDI, C. (1991). A rapid and simple method for measuring thymocyte apoptosis by propidium iodide staining and flow cytometry. *J. Immunol. Methods*, **139**, 271-279.
NIE, Q., FAN, J., HARAOKA, S., SHIMOKAMA, T. & WATANABE, T. (1997). Inhibition of monomuclear cell recruitment in aortic intima by treatment with anti-ICAM-1 and anti-LFA-1 monoclonal antibodies in hypercholesterolemic rats: implication of the ICAM-1 and LFA-1 pathway in atherogenesis. *Lab. Invest.*, **77**, 469-488.
NISHIOKA, K. (1995). Apoptosis and functional Fas antigen in rheumatoid arthritis. *Arthritis Rheum.*, **38**, 485-491.
OBEID, L., LINARDIC, C., KAROLAK, L. & HANNUN, Y. (1993). Programmed cell death induced by ceramide. *Science*, **259**, 1769-1771.
O'BRIEN, K., ALLEN, M. & MCDONALD, T. (1993). Vascular cell adhesion molecule-1 is expressed in human coronary atherosclerotic plaques. Implications for the mode of progression of advanced coronary atherosclerosis. *J. Clin. Invest.*, **92**, 945-951.
O'BRIEN, K., MCDONALD, T., CHAIT, A., ALLEN, M. & ALPERS, C. (1996). Neovasculartur expression of E-selectin, intercellular adhesion molecule-1, and vascular cell adhesion molecule-1 in human atherosclerosis and their relation to intimal leukocyte content. *Circulation*, **93**, 672-682.
O'BYRNE, D. & SANSOM, D. (2000). Lack of costimulation by both sphingomyelinase and C_2 ceramide in resting human T cells. *Immunology*, **100**, 225-230.
O'CONNOR, L., HARRIS, A. & STRASSER, A. (2000). CD95 (Fas/APO-1) and p53 signal apoptosis independently in diverse cell types. *Cancer Res.*, **60**, 1217-1220.
ODEH, M. (1997). New insights into the pathogensis and treatment of rheumatoid arthritis. *Immunopharmacology*, **83**, 103-113.
O'FLYNN, K., RUSSEL-SAIB, M., ANDO, I., WALLACE, D., BEVERLEY, P., BOYLSTON, A. & LYNCH, D. (1986). Different pathways of human T-cell activation revealed by PHA-P and PHA-M. *Immunology*, **57**, 55-60.
OGRETMEN, B., PETTUS, B., ROSSI, M., WOOD, R., USTA, J., SZULC, Z., BIELAWSKA, A., OBEID, L. & HANNUN, Y. (2002). Biochemical mechanism of the generation of endogenous long chain ceramide in response to exogenous short chain ceramide in the A549 human lung adenocarcinoma cell line: role for endogenous ceramide in mediating the action of exogenous ceramide. *J. Biol. Chem.*, 277, 12690-12699.
OGUEY, D., KOLLIKER, F., GERBER, N. & REICHEN, J. (1992). Effect of food on the bioavailability of low dose methotrexate in patients with rheumatoid arthritis. *Arthritis & Rheumatism*, **35**, 611-614.
OH, W., KIM, W., KANG, K., KIM, T., KIM, M. & CHOI, K. (1998). Induction of p21 during ceramide-mediated apoptosis in human hepatocarcinoma cells. *Cancer Lett.*, **129**, 215-222.
OHSHIMA, S., MIMA, T., SASAI, M., NISHIOKA, K., SHIMIZU, M., MURATA, N., YOSHIKAWA, H., NAKANISHI, K., SUEMURA, M., MCCLOSKEY, R., KISIMOTO, T. & SAEKI, Y. (2000). Tumour necorsis factor alpha (TNFα) interferes with Fas-mediated apoptotic cell death on rheumatoid arthritis (RA) synovial cells: a possible mechanism of rheumatoid synovial hyperplasia and a clinical benefit of anti-TNFα therapy for RA. *Cytokine*, **12**, 281-288.
OKAMURA, H., KASHIWAMURA, S., TSUTSUI, H., YOSHIMOTO, T. & NAKANISHI, K. (1998). Regulation of interferon-gamma production by IL-12 and IL-18. *Curr. Opin. Immunol.*, **10**, 259-264.
OKAZAKI, T., BELL, R. & HANNUN, Y. (1989). Sphingomyelin turnover induced by vitamin D3 in HL-60 cells. Role in cell differentiation. *J. Biol. Chem.*, **264**, 19076-19080.
OKAZAKI, T., KONDO, T., KITANO, T. & TASHIMA, M. (1998). Diversity and complexity of ceramide signaling in apoptosis. *Cell Signal.*, **10**, 685-692.
ORMEROD, M. (1999). Flow Cytometry, 2nd edition. Bios, Oxford.
OSTRAKHOVITCH, E. & AFANAS'EV, I. (2001). Oxidative stress in rheumatoid arthritis

leukocytes: suppression by rutin and other antioxidants and chelators. *Biochem. Pharmac.*, **62**, 743-746.

OTTERNESS, I. (1994). The value of C-reactive protein measurement in rheumatoid arthritis. *Semin. Arth. Rheum.*, **24**, 91-104.

PAHAN, K., DOBASHI, K., HOSH, B. & SINGH, I. (1999). Induction of the manganese superoxide dismutase gene by sphingomyelinase and ceramide. *J. Neurochem*, **73**, 513-520.

PAILLOT, R., GENESTIER, L., FOURNEL, S., FERRARO, C., MIOSSEC, P. & REVILLARD, J. (1998). Activation-dependent lymphocyte apoptosis induced by methotrexate. *Transplantation Proceedings*, **30**, 2348-2350.

PATRA, S., ALONSO, A., ALONSO, J. & GONI, F. (1999). *J. Liposome Res.*, **9**, 263-270.

PAUMEN, M., ISHIDA, Y., HAN, H., EGUCHI, Y., TSUJIMOTO, Y. & HONJO, T. (1997). Direct interaction of the mitochondrial membrane protein cartine palmitoyltransferase I with Bcl-2. *Biochem. Biophys. Res. Commun.*, **231**, 523-525.

PELASSY, C., MARY, D. & AUSSEL, C. (1991). Diacylglycerol production in Jurkat T-cells: differences between CD3; CD2 and PHA activation pathways. *Cell Signal.*, **3**, 35-40.

PEÑA, L., FUKS, Z. & KOLESNICK, R. (1997). Stress-induced apoptosis and the sphingomyelin pathway. *Biochem. Pharmac.*, **53**, 615-321.

PERERA, C., ST. CLAIR, D. & MCCLAIN, C. (1995). Differntial regulation of manganese superoxide dismutase activity by alcohol and TNF in human hepatoma cells. *323nts Actions*, **2**, 476.

PERRY, D. & HANNUN, Y. (1999). The use of diglyceride kinase for quantifying ceramide. *Trends Biochem. Sci.*, **24**, 226-227.

PETIT, P., GENDRON, M.-C. , SCHRANTZ, N., MÉTIVIER, D., KROEMER, G., MACIOROWSKA, Z., SUREAU, F. & KOESTER, S. (2001). Oxidation of pyridine nucleotides during Fas- and ceramide-induced apoptosis in Jurkat cells: correlation with changes in mitochondria. glutathione depletion, intracellular acidification and caspase 3 activation. *Biochem J.*, **353**, 357-367.

PFIZENMAIER K., HIMMLER A., SCHÜTZE S., SCHEURICH P. & KRÖNKE M. (1991). TNF receptors and TNF signal transduction. In *Tumour Necrosis Factors: The molecules and their Emerging Role in Medicine.*, ed. Beutler B. pp. 439-470. Raven Press, Ltd., N.Y., U.S.A. .

PLOWS, D., PROBERT, L., GEORGOPOULOS, S., ALEXOPOULOU, L. & KOLLIAS, G. (1995). The role of tumour necorsis factor (TNF) in arthritis: studies in transgenic mice. *Rheumatol. Eur.*, **24**, 51-54.

POBER, J., GIMBRONE JR., M., LAPIERRE, L., MENDRICK, D., FIERS, W., ROTHLEIN, R. & SPRINGER, T. (1986). Overlapping patterns of activation of human endothelial cells by interleukin-1 tumour necrosis factor, and immune interferon. *J. Immunol.*, **137**, 1893-1896.

POSTON, R., HASKARD, D., COUCHER, J., GALL, N. & JOHNSON-TIDEY, R. (1992). Expression of intracellular adhesion molecule-1 in atherosclerotic plaques. *Am. J. Pathol.*, **140**, 665-673.

PREISS, J., LOOMIS, C., BISHOP, W., STEIN, R., NIEDEL, J. & BELL, R. (1986). Quantitative measurement of sn-1,2-diacylglcerols present in platelets, hepatocytes, and ras- and sis-transformed normal rat kidney cells. *J. Biol. Chem.*, **261**, 8597-8600.

QUILLET-MARY, A., JAFFRÉZOU, J.-P. , MANSAT, V., BORDIER, C., NAVAL, J. & LAURENT, G. (1997). Implication of mitochondrial hydrogen peroxide generation in ceramide-induced apoptosis. *J. Biol. Chem.*, **272**, 21388-21395.

RAGG, S., KAGA, S., BERG, K. & OCHI, A. (1998). The Mitogen-activated protein kinases pathway inhibits ceramide-induced terminal differentiation of a human monoblastic leukemia cell line, U937. *J. Immunol.*, **161**, 1390-1398.

RAHA, S. & ROBINSON, B. (2000). Mitochondria, oxygen free radicals, disease and ageing. *Trends Biochem. Sci.*, **25**, 502-508.

RAHAMAN, A., BANDO, M., KEFER, J., ANWAR, K. & MALIK, A. (1999). Protein kinase C-activated oxidant generation in endothelial cells signals intercellular adhesion molecule-1 gene transcription. *Mol. Pharmacol.*, **55**, 575-583.

RAHMAN, I. (2000). Regulation of nucelar factor-kappa B, activator protein-1, and glutathione levels by tumour necrosis factor-alpha and dexamethasone in aveolar epithelial cells. *Biochem. Pharmac.*, **60**, 1041-1049.

RAHMAN, I. & MACNEE, W. (2000). Regulation of redox glutathione levels and gene transcription in lung inflammation: therapeutic approaches. *Free Radic. Biol. Med.*, **28**, 1405-1420.

RATTAN, V., SULTANA, C., SHEN, Y. & KALRA, V. (1997). Oxidant stress-induced transendothelial migration of monocytes is linked to phosphorylation of PECAM-1. *Am. J. Physiol.*, **273**, E453-E461.

RAU, R., SCHLEUSSER, B., HERBORN, G. & KARGER, T. (1997). Long term treatment of destructive rheumatoid arthritis with methotrexate. *J. Rheumatol.*, **24**, 1881-1889.

REEDQUIST, K., ROSS, E., KOOP, E., WOLTHUIS, R., ZWARTKRUIS, F., VAN KOOYK, Y., SALMON, M., BUCKLEY, C. & BOS, J. (2000). The small GTPase, Rap1, mediates CD31-induced integrin adhesion. *J. Cell. Biol.*, **148**, 1151-1158.

RICHARD-MARCELI, C. & DOUGADOS, M. (2001). Tumour necrosis factor-alpha blockers in rheumatoid arthritis: review of the clinical experience. *BiodDrugs*, **15**, 251-259.

RIDGWAY, N., LAGACE, T., COOK, H. & BYERS, D. (1998). Differential effects of sphingomyelin hydrolysis and cholesterol transport on oxysterol-binding protein phosphorylation and Golgi localization. *J. Biol. Chem.*, **273**, 31621-31628.

RIDLEY, A. (2001). Rho proteins, PI 3-kinases, and monocyte/macrophage motility. *FEBS Lett.*, **498**, 168-171.

ROBERTS, P., NEWBY, A., HALLET, M. & CAMPBELL, A. (1985). Inhibition of adenosine by reactive oxygen metabolite production by human polymorphonuclear leukocytes. *Biochemical J.*, **227**, 669-674.

ROBERTSON, S., YOUNG, S., VINER, N. & BACON, P. (1997). Enhanced co-stimulatory ability of synovial fluid accessory cells in rheumatoid arthritis. *Br. J. Rheumatol.*, **36**, 413-419.

ROEBUCK, K. & FINNEGAN, A. (1999). Regulation of intracellular adhesion molecule (CD54) gene expression. *J. Leukoc. Biol.*, **66**, 876-888.

ROEBUCK, K., RAHMAN, A., LAKSHMINARAYANAN, V., JANAKIDEVI, K. & MALIK, A. (1995). H_2O_2 and tumour necrosis factor-alpha activate intercellular adhesion molecule 1 (ICAM-1) gene transcription through distinct cis-regulatory elements within the ICAM-1 promoter. *J . Biol. Chem.*, **270**, 18966-18974.

ROKUTAN, K., TESHIMA, S., MIYOSHI, M., KAWAI, T., NIKAWA, T. & KISHI, K. (1998). Glutathione depletion inhibits oxidant-induced activation of nuclear factor-κB, AP-1, and c-Jun/ATF2 in cultured guinea-pig gastric epithelial cell. *J. Gastroenterol.*, **33**, 646-655.

ROSENMAN, S., GANJI, A., Tedder, T.F. & GALLATIN, W. (1993). Syn-capping of human T lymphocyte adhesion/activation molecules and their redistribution during interaction with endothelial cells. *J. Leuk. Biol.*, **53**, 1-10.

ROSS, R. (1999). Atherosclerosis-an inflammatory disease. *New Engl. J. Med.*, **340**, 115-126.

ROSSEAU, S., SELHORST, J., WIECHMANN, K., LEISSNER, K., MAUS, U., MAYER, K., GRIMMINGER, F., SEEGER, W. & LOHMEYER, J. (2000). Monocyte migration through the aveloar epithelial barrier: adhesion molecule mechanisms and impact of chemokines. *J. Immunol.*, **164**, 427-435.

ROSSEAU, S., SELHORST, J., WIECHMANN, K., LEISSNER, K., MAUS, U., MAYER, K., GRIMMINGER, F.S., W. & LOHMEYER, J. (2000). Monocyte migration through the alveolar epithelial barrier: adhesion molecule mechanisms and impact of chemokines. *J. Immunol.*, **164**, 427-435.

ROTHE, G., EMMENDORFFER, A., OSER, A., ROESLER, J. & VALET, G. (1991). Flow cytometric measurement of the respiratory burst activity of phagocytes using dihydrorhodamine 123. *J. Immunol. Methods*, **138**, 133-135.

ROTS, M., Pieters, R., KASPERS, G.-J. , VAN ZANTWIJK, C., NOORDHUIS, P., MAURITZ, R., VEERMAN, A., JANSEN, G. & PETERS, G. (1999). Differential methotrexate resistance in childhood T- versus commmon/preB-acute lymphoblastic leukemia can be measured by an *in situ* thymidylate synthase inhibition assay, but not by the MTT assay. *Blood*, **93**, 1067-1074.

ROYAL, J. & ISCHIROPOULOS, H. (1993). Evaluation of 2',7'-dichlorofluoroscin and dihydrorhodamine 123 as fluorescent probes for intracellular H_2O_2 in cultured endothelial cells. *Arch. Biochem. Biophys.*, **302**, 348-355.

RUIZ-RUIZ, M.D.C. & LOPEZ-RIVAS, A. (1999). P53-mediated up-regulation of CD95 is not involved in genotoxic drug-induced apoptosis of human breast tumour cells. *Cell Death Diff.*, **6**, 271-280.

RUSCHEN, S., STELLBERG, W. & WARNATZ, H. (1992). Kinetics of cytokine secretion by mononuclear cells of the blood from rheumatoid patients are different from those from healthy controls. *Clin. Exp. Immunol.*, **89**, 32-37.

RUVOLO, P. (2001). Ceramide regulates cellular homeostastis via diverse stress signalling pathways. *Leukemia*, **15**, 1153-1160.

RUVOLO, P., DENG, X., ITO, T., CARR, B. & MAY, W. (1999). Ceramide induces $Bcl\text{-}_2$ dephosphorlation via a mechanism involving mitochondrial PP2A. *J . Biol. Chem.*, **274**, 20296-20300.

SAKATA, K., VELA-ROCH, N., ESPINOSA, R., ESCALANTE, A., KONG, L., NAKABAYASHI,

T., CHENG, J., TALAL, N. & DANG, H. (1998). Fas (CD95)-transduced signal preferentially stimulates lupus peripheral T lymphocytes. *Eur. J. Immunol.*, **28**, 2648-2660.

SALMON, M. & GASTON, J. (1995). The role of T-lymphocytes in rheumatoid-arthritis. *Br. Med. Bull.*, **51**, 332-345.

SALMON, M., SCHEEL-TOELLNER, D., HUISSOON, A., PILLING, D., SHAMSADEEN, N., HYDE, H., D'ANGEAC, A., BACON, P., EMERY, P. & AKBAR, A. (1997). Inhibition of T cell apoptosis in the rheumatoid synovium. *J.Clin. Invest.*, **99**, 439-446.

SANT, M., LYONS, S., PHILLIPS, L. & CHRISTOPHERSON, R. (1992). Antifolates induce inhibition of amido phosphoribosyltransferase in leukemia cells. *J. Biol. Chem.*, **267**, 11038-11045.

SANTANA, P., PEÑA, L., HAIMOVITZ-FRIEDMAN, A., MARTIN, S., GREEN, D., MCLOUGHLIN, M., CORDON-CARDO, C., SCHUCHMAN, E., FUKS, Z. & KOLESNICK, R. (1996). Acid sphingomyelinase-deficient human lymphoblasts and mice are defective in radiation-induced apoptosis. *Cell*, **86**, 189-199.

SAWADA, M., NAKASHIMA, S., KIYONO, T., YAMADA, J., HARA, S., NAKAGAWA, M., SHINODA, J. & SAKAI, N. (2002). Acid sphingomyelinase activation requires caspase-8 but not p53 nor reactive oxygen species during Fas-induced apoptosis in human glioma cells. *Exp. Cell Res.*, **273**, 157-168.

SAUER, H., WATENBERG, M. & HESCHELER, J. (2001). Reactive oxygen species as intracellular messengers during cell growth and differentiation. *Cell Physiol. Biochem.*, **11**, 173-186.

SCALIA, R. & LEFER, A. (1998). In vivo regulation of PECAM-1 activity during acute endothelial dysfunction in the rat messenteric microvasculature. *J. Leukoc. Biol.*, **64**, 163-169.

SCHIRMER, M., VALLEJO, A., WEYAND, C. & GORONZY, J. (1998). Resistance if apoptosis and elevated expression of Bcl-$_2$ in clonally expanded CD4+CD28- T cells from rheumatoid arthritis patients. *J. Immunol.*, **161**, 1018-1025.

SCHNEIDER, P., HOLLER, N., BODMER, J., HAHNE, M., FREI, K., FONTANA, A. & TSCHOPP, J. (1998). Conversion of membrane bound Fas (CD95) ligand to its soluble form is associated with downregulation of its proapoptotic activity and loss of liver toxicity. *J. Exp. Med.*, **187**, 1205-1213.

SCHRECK, R., ALBERMANN, K. & BAEUERLE, P. (1992). Nuclear factor kappa B: an oxidative stress-responsive transcription factor of eukaryotic cells (a review). *Free Rad. Res. Commun.*, **17**, 221-227.

SCHRECK, R., MEIER, B. & BAEUERLE, P. (1991). Kappa B transcription factor and HIV-1. *EMBO J.*, **10**, 2247-2258.

SCHUCHMAN, E. (1995). Two new mutations in the acid sphingomyelinase gene causing type a Niemann-pick disease: N389T and R441X. Two new mutations in the acid sphingomyelinase gene causing type a Niemann-pick disease: N389T and R441X. *Hum. Mat.*, **6**, 352-354.

SCHUCHMANN, E., LEVRAN, O., PEREIRA, L. & DESNICK, R. (1992). Structural organisation and complete nucleotide sequence of the gene encoding human acid sphingomyelinase (SMPD1). *Genomics*, **12**, 197-205.

SCHULZE-OSTHOFF, K., BAKKER, A., VANHAESEBROECK, B., BEYAERT, R., JACOB, W. & FRIERS, W. (1992). Cytotoxic activity of tumour necrosis factor is mediated by early damage of mitochondrial functions. *J. Biol. Chem.*, **267**, 5317-5323.

SCHULZE-OSTHOFF, K., BEYAERT, R., VANDEVOORDE, V., HAEGEMAN, G. & FIERS, W. (1993). Depletion of the mitochondrial electron transport abrogates the cytotoxic and gene-inductive effects of TNF. *EMBO J.*, **12**, 3095-3104.

SCHULZE-OSTHOFF, K., KRAMMER, P. & DRÖGE, W. (1994). Divergent signaling via APO-1/Fas and the TNF receptor two homologous molecules involved in physiological cell death. *EMBO J.*, **13**, 4587-4596.

SCHWANDNER, R., WIEGMANN, K., BERNARDO, K., KREDER, D. & KRÖNKE, M. (1998). TNF receptor death-domain-associated proteins TRADD and FADD activation of acid sphingomyelinase. *J. Biol. Chem.*, **273**, 5916-5922.

SCHWARTZ, P., BARNETT, S. & MILSTONE, L. (1995). Karatinocytes differentiate in response to inhibitors of deoxyribonucleotide synthesis. *Journal of Dermatological Science*, **9**, 129-135.

SCHÜTZE, S., POTTHOFF, K., MACHLEIDT,T., BERKOVIC, D., WIEGMANN, K. & KRÖNKE, M. (1992). TNF activates NFκB by phosphatidylcholine-specific phospholipase C-induced "acidic" sphingomyelin breakdown. *Cell*, **71**, 765-776.

SEGUI, B., BEZOMBES, C., URO-COSTE, E., MEDIN, J.A., N., AUGE, N., BROUCHET, A., LAURENT, G., SALVAYRE, R., JAFFREZOU, J.P. & LEVADE, T. (2000). Stress-induced apoptosis is not mediated by endolysosomal ceramide. *FASEB J.*, **14**, 36-47.

SEITZ, M., ZWICKER, M. & LOETSCHER, P. (1998). Effects of methotrexate on differentiation of monocytes and production of cytokine inhibitors by monocytes. *Arthritis & Rheumatism*, **41**, 2032-

2038.

SELLACK, F., E., HAKIM, J. & PASQUIER, C. (1994). Reactive oxygen species rapidly increase endothelial ICAM-1 ability to bind neutrophils without detectable upregulation. *Blood*, **83**, 2669-2677.

SEWELL, K. & TRENTHAM, D. (1993). Pathogenesis of rheumatoid arthritis. *Lancet*, **341**, 283-286.

SHARMA, K. & SHI, Y. (1999). The yins and yangs of ceramide. *Cell Res.*, **9**, 1-10.

SHEPHARD, E., ANDERSON, R., ROSEN, O. & FRIDKIN, M. (1992). C-reactive protein (CRP) peptides inactivate enolase in human neutrophils leading to depletion of intracellular ATP and inhibition of superoxide. *Immunology*, **76**, 79-85.

SILLENCE, D. & ALLAN, D. (1997). Evidence against an early signaling role for ceramide in Fas-mediated apoptosis. *Biochem J.*, **324**, 29-32.

SIMON JR., C. & GEAR, A. (1998). Membrane-destabilising properties of C_2-ceramide may be responsible for it ability to inhibit platelet aggregation. *Biochemistry*, **37**, 2059-2069.

SIMONS, K. & IKONEN, E. (1997). Functional rafts in cell membrane. *Nature*, **387**, 569-572.

SISKIND, L. & COLOMBINI, M. (2000). The lipids C_2- and C_{16}-ceramide form large stable channels. *J. Biol. Chem.*, **275**, 38640-38644.

SMITH, R., SMITH, T., BLIEDEN, T. & PHIPPS, R. (1997). Fibroblasts as sentinel cells: synthesis of chemokines and regulation of inflammation. *Am. J. Pathol.*, **151**, 317-322.

SPERLING, R., BENINCASO, A., ANDERSON, COBLYN, J., K.F., A. & WEINBLATT, M. (1992). Acute and chronic suppression of leukotriene B4 synthesis ex vivo in neutrophils from patients with rheumatoid arthritis beginning treatment with methotrexate. *Arthritis & Rheumatism*, **35**, 376-384.

SPRANG S. & ECK M. (1991). The 3-D structure of TNF. In *Tumour Necrosis Factors: The molecules and their Emerging Role in Medicine.*, ed. Beutler B. pp. 11-32. Raven Press, Ltd., N.Y., U.S.A.

SPERTINI, O., LUSCINSKAS, F., GIMBRONE JR., M. & TEDDER, T. (1992). Monocyte attachment to activated human vascular endothelium in vitro is mediated by leukocyte adhesion molecule-1 (L-selectin) under nonstatic conditions. *J. Exp. Med.*, **175**, 1789-1792.

SPERTINI, O., LUSCINSKAS, F., KANSAS, G., MUNRO, J., GRIFFIN, J., GIMBRONE JR., M. & TEDDER, T. (1991). Leukocyte adhesion molecule-1 (LAM-1, L-selectin) interacts with an inducible endothelial cell ligand to support leukocyte adhesion. *J. Immunol.*, **147**, 2565-2573.

SPRINGER, T. (1994). Traffic signals for lymphocyte recirculation and leukocyte emigration: the multistep paradigm. *Cell*, **76**, 301-314.

SPRINGER, T. (1990). Adhesion receptors in the immune system. *Nature*, **346**, 425-433.

STEWART, C., MIHAI, R. & HOLLY, J. (1999). Increased tyrosine kinase activity but not calcium mobilisation is required for ceramide-induced apoptosis. *Exp. Cell Res.*, **250**, 329-338.

STORB, R., DEEG, H., WHITEHEAD, J., APPELBAUM, F., BEATTY, P., BENSINGER, W., BUCKNER, D., CLIFT, R., DONEY, K., FAREWELL, V., HANSEN, J., STEWART, P., SULLIVAN, K., WITHERSPOON, R. & YEE, G., Thomas, E.D. (1986). Methotrexate and cyclosporine compared with cyclosporine alone for prophylaxis of acute graft-vs.-host disease after marrow transplantation for leukemia. *N. Engl. J. Med.*, **314**, 729-735.

SUMIDA, T., HOA, T., ASAHARA, H., HASUNUMA, T. & NISHIOKA, K. (1997). T cell receptor of Fas-sensative T cells in rheumatoid synovium. *J. Immunol.*, **158**, 1965-1970.

SUNG, J.-Y. , HONG, J.-H. , KANG, H.-S. , CHOI, I., LIM, S.-D. , LEE, J.-K. , SEOK, J.-H. , LEE, J.-H. & HUR, G.-M. (20000). Methotrexate suppresses the interleukin-6 induced generation of reactive oxygen species in the synoviocytes of rheum. *Immunopharmacology*, **47**, 44.

SUSIN, S., ZAMZAMI, N., CASTEDO, M., DAUGAS, E., WANG, H.-G. , GELEY, S., FASSY, F., REED, J. & KROEMER, G. (1997). The central executioner of apoptosis: multiple connections between protease activation and mitochondria in Fas/APO-1/CD95 and ceramide-induced apoptosis. *J. Exp. Med.*, **186**, 25-37.

SUZUKI, Y. & ONO, Y. (1999). Involvement of reactive oxygen species produced via NADPH oxidase in tyrosine phosphorylation in human B- and T-lineage lymphoid cells. *Biochem. Biophys. Res. Commun.*, **255**, 262-267.

SUZUKI, Y., ONO, Y. & HIRABAYASHI, Y. (1998). Rapid and specific reactive oxygen species generation via NADPH oxidase activation during Fas-mediated apoptosis. *FEBS Lett.*, **425**, 209-212.

SYNOLD, T., RELLING, M., BOYETT, J., RIVERA, G., SANDLUND, J., MAHMOUD, M., CRIST, W., PUI, C. & EVANS, W. (1994). Blast cell methotrexate-polyglutamate accumulation *in vivo* differs by lineage, ploidy and methotrexate does in acute lymphoblastic leukemia. *J. Clin. Invest.*, **94**, 1996-2001.

TAK, P., ZVAIFLER, N., GREEN, D. & FIRESTEIN, G. (2000). Rheumatoid arthritis and p53: how oxidative stress might alter the course of inflammatory diseases. *Imunol. Today*, **21**, 78-82.

TAKEDA, K., TSUTSUI, H., YOSHIMOTO, T., ADACHI, O., YOSHIDA, N., KISHIMOTO, T., OKAMURA, H.N., K. & AKIRA, S. (1998). Defective NK cell activity and Th1 response in IL-18-deficient mice. *Immunity*, **8**, 383-390.

TAN, S., SAGARA, Y., LIN, Y., MAHER, P. & SCHUBERT, D. (1998). The regulation of reactive oxygen species production during programmed cell death. *J. Cell Biol.*, **141**, 1423-1432.

TARAZA, C., MOHORA, M., VĂRGOLICI, B. & DINU, V. (1997). Importance of reactive oxygen species in rheumatoid arthritis. *Rev. Roum. Méd. Int.*, **35**, 89-98.

TATLA, S., WOODHEAD, V., FOREMAN, J. & CHAIN, B. (1999). The role of reactive oxygen species in triggering proliferation and IL-2 secretion in T cells. *Free Rad. Biol. Med.*, **26**, 14-24.

TAYSI, S., POLAT, F., GUL, M., SARI, R. & BAKAN, E. (2002). Lipid peroxidation, some extracellular antioxidants, and antioxidant enzymes in serum of patients with rheumatoid arthritis. *Rheumatol. Int.*, **21**, 200-204.

TEPPER, A., BOESEN-DE COCK, J.G.R., DE VRIES, E., BORST, J. AND VAN BLITTERSWIJK, W.J. (1997). CD95/Fas-induced ceramide formation proceeds with slow kinetics and is not blocked by caspase-3/CPP32 inhibition. *J. Biol. Chem.*, **272**, 24308-24312.

TEPPER, A., DE VRIES, E., VAN BLITTERSWIJK, W.J. & BORST, J. (1999). Ordering of ceramide formation, caspase activation, and mitochondrial changes during CD95- and DNA damage-induced apoptosis. *J. Clin. Invest.*, **103**, 971-978.

THOMPSON, C. (1995). Apoptosis in the pathogenesis and treatment of disease. *Science*, **267**, 1456-1462.

TIETZE, F. (1969). Enzymic Methods for Quantitative Determination of Nanogram Amounts of Total and Oxidized Glutathione: Applications to Mammalian Blood and Other Tissues. *Analyitical Biochemistry*, **27**, 502-522.

TOSI, M., STARK, J., SMITH, C., HAMEDANI, A., GRUENERT, D. & INFELD, M. (1992). Induction of ICAM-1 expression on human airway epithelial cells by inflammatory cytokines: effects on neutrophil-epithelial cell adhesion. *Am. J. Respir. Cell Mol. Biol.*, **7**, 214-221.

TSUBOI, H., ANDO, J., KORENAGA, R., TAKADA, Y. & KAMIYA, A. (1995). Flow stimulates ICAM-1 expression time and shear stress dependently in cultured human endothelial cells. *Biochem. Biophys. Res. Commun.*, **206**, 988-996.

UM, H.-D. , ORENSTEIN, J. & WAHL, S. (1996). Fas mediated apoptosis in human monocytes by a reactive oxygen intermediate dependent pathway. *J. Immunol.*, **156**, 3469-3477.

VAN DEN BERG, W. (1995). Uncoupling of inflammation and joint destruction in arthritis; pivitol role of interleukin 1 in destruction. *Trends Cell Biol.*, **5**, 392-399.

VAN DER GOES, A., WOUTERS, D., VAN DER POL, S., HUIZINGA, R., RONKEN, E., ADAMSON, P., GREENWOOD, J., DIJKSTRA, C. & DE VRIES, H. (2001). Reactive oxygen species enhance the migration of monocytes across the blood brain barrier in vitro. *The FASEB Journal*, **15**, 1852-1854.

VENABLE, M., LEE, J., SMYTH, M., BIELAWSKA, A. & OBEID, L. (1995). *J. Biol. Chem.*, **270**, 30701-30708.

VENKATARAMAN, K. & FUTERMAN, A. (2000). Ceramide as a second messenger: sticky solutions to sticky problems. *Trends Cell Biol.*, **10**, 408-412.

VERHEIJ, M., BOSE, R., LIN, X., YAO, B., JARVIS, W., GRANT, S., BIRRER, M., SZABO, E., ZON, L., KYRIAKIS, J., HAIMOVITZ-FRIEDMAN, A., FUKS, Z. & KOLESNICK, R. (1996). Requirement for ceramide initiated SAPK/JNK signaling in stress-induced apoptosis. *Nature*, **380**, 75-79.

VIOLA, A., SCHROEDER, S., SAKAKIBARA, Y. & LANZAVECCHIA, A. (1999). T lymphocyte costimulation mediated by reorganization of membrane microdomains. *Science*, **283**, 680-682.

VOEHRINGER, D. & MEYN, R. (2000). Redox aspects of Bcl-2 function. *Antiox. Redox Signal.*, **2**, 537-550.

VON ANDRIAN, U. & MACKAY, C. (2000). T-cell function and migration. Two sides of the same coin. *N. Engl. J. Med.*, **343**, 1020-1034.

WAGNER, S., FRITZ, P., EINSELE, H., SELL, S. & SAAL, J. (1997). Evaluation of synovial cytokine patterns in rheumatoid arthritis and osteoarthritis by quantitative reverse transcriptase polymerase chain reaction. *Rheumatol. Int.*, **16**, 191-196.

WAKISAKA, S., SUZUKI, N., TAKEBA, Y., SHIMOYAMA, Y., NAGAFUCHI, H., TAKENO, M., SAITO, N., YOKOE, T., KANEKO, A., ASAI, T. & SAKANE, T. (1998). Modulation by proinflammatory cytokines of Fas/Fas ligand-mediated apoptotic cell death of synovial cells in patients with rheumatoid arthritis (RA). *J. Clin. Invest.*, **114**, 119-128.

WANG, H., RAPP, U. & REED, J. (1996). Bcl-2 targets the protein kinase Raf-1 to mitochondria. *Cell*, **87**, 679-638.

WATANABE, T. & FAN, J. (1998). Atherosclerosis and inflammation: mononuclear cell recruitment and adhesion molecules with reference to the implication of ICAM-1/LFA-1 pathway in atherogenesis. *Int. J. Cardiol.*, **66**, S45-S53.

WATTS, J., GU, M., PATTERSON, S., AEBERSOLD, R. & POLVERINO, A. (1999). On the complexities of ceramide changes in cells undergoing apoptosis: lack of evidence for a second messenger function in apoptotic induction. *Cell Death Diff.*, **6**, 105-114.

WATTS, J., GU, M. & POLVERINO, A.P., S.D. Aebersold, R. (1997). Fas-induced apoptosis of T cells occurs independently of ceramide generation. *Proc. Natl. Acad. Sci. U S A*, **94**, 7292-7296.

WAYNER, E., GARCIA-PARDO, A., HUMPHRIES, M., MCDONALD, J. & CARTER, W. (1989). Identification and characterization of the T lymphocyte adhesion receptor for an alternative cell attachment domain (CS-1) in plasma fibronectin. *J. Cell Biol.*, **109**, 1321-1330.

WEBER, C., ERL, W., WEBER, K. & WEBER, P. (1996). Increased adhesiveness of isolated monocytes to endotheluim is prevented by vitamin C intake in smokers. *Circulation*, **93**, 1488-1492.

WESTWICK, J., BIELAWSKA, A., DBAIBO, G., HANNUN, Y. & BRENNER, D. (1995). Ceramide activates the stress-activated protein kinases. *J. Biol. Chem.*, **270**, 22689-22692.

WIEGMANN, K., SCHÜTZE, S., MACHLEIDT, T., WITTE, D. & KRÖNKE, M. (1994). Functional dichotomy of neutral and acidic sphingomyelinases in tumour necrosis factor signaling. *Cell 78, 1005-1015.*, **78**, 1005-1015.

WILLIAMS, A., JONES, S., GOODFELLOW, R., ARMOS, N. & WILLIAMS, B. (1999). Interluekin-1beta (IL-1β) inhibition: a possible mechanism for the anti-inflammatory potency of liposomally conjugated methotrexate formulation in arthritis. *B. J. Pharmacol.*, **128**, 234-240.

WOOLLARD, K., LORYMANM, C., MEREDITH, E., BEVANM, R., SHAW, J., LUNEC, J. & GRIFFITHS, H. (2002). Effects of oral vitamin C on monocyte: endothelial cell adhesion in healthy subjects. *Biochem. Biophys. Res. Commun.*, **294**, 1161-1168.

WONG, G., ELWELL, J., OBERLEY, L. & GOEDDEL, D. (1989). Manganous superoxide dismutase is essential for cellular resistance to cytotoxicity of tumor necrosis factor. *Cell*, **58**, 923-931.

WYLIE, A. (1980). Glucocorticoid-induced thymocyte apoptosis is associated with endonuclease activation. *Nature*, **284**, 554-556.

XIA, P., GAMBLE, J., RYE, K.-A. , WANG, L., HII, C., COCKERILL, P., KHEW-GOODALL, Y., BERT, A., BARTER, P. & VADAS, M. (1998). Tumour necrosis factor-alpha induces adhesion molecule expression through the sphingosine pathway. *Proc. Natl. Acad. Sci. U S A*, **95**, 14196-14201.

XIA, P., WANG, L., GAMBLE, J. & VADAS, M. (1999). Activation of sphingosine kinase by tumour necrosis factor-alpha inhibits apoptosis in human endothelial cells. *J. Biol. Chem.*, **274**, 34499-34505.

YAMAUCHI, N., KURIYAMA, H., WATANABE, N., NEDA, H., MAEDA, M. & NIITSU, Y. (1989). Intracellular hydroxyl radical production induced by recombinant human tumour necrosis factor and its implication in the killing of tumour cells *in vitro*. *Cancer Res.*, **49**, 1671-1675.

YANG, X., KHOSRAVI-FAR, R., CHANG, H. & BALTIMORE, D. (1997). Daxx, a novel Fas-binding protein that activates JNK and apoptosis. *Cell*, **89**, 1067-1076.

YEH, C., HIS, B. & FAULK, W. (1981). Propidium iodide as a molecular marker in immunofluorescence. II. Use with cellular identification and viability studies. *J. Immunol. Methods*, **43**, 275.

ZAMZAMI, N., MARCHETTI, P., CASTEDO, M., DECAUDIN, D., MACHO, A., HIRST, T., SUSIN, S., PETIT, P., MIGNOTTE, B. & KROEMER, G. (1995). Sequential reduction in mitochondrial transmembrane potential and generation of reactive oxygen species in early programmed cell death. *J. Exp. Med.*, **182**, 367-377.

ZANGERLE, P., DE GROOTE, D., LOPEZ, M., R.J., M., VRINDTS, Y., FAUCHET, F., DEHART, I., JADOUL, M., RADOUX, D. & FRANCHIMONT, P. (1992). Direct stimulation of cytokines (IL-1 beta, TNF-alpha, IL-6, IL-2, IFN-gamma and GM-CSF) in whole blood II: application to rheumatoid arthritis and osteoarthritis. *Cytokines*, **4**, 568-575.

ZELLER, J. & SULLIVAN, B. (1992). C-reactive protein selectively enhances the intracellular generation of reactive oxygen products by IgG-stimulated monocytes and neutrophils. *J. Leukoc. Biol.*, **52**, 449-455.

ZHANG, J., ALTER, N., REED, J., BORNER, C., OBEID, L. & HANNUN, Y. (1996). Bcl-2 interrupts the ceramide-mediated pathway of cell death. *Proc. Natl. Acad. Sci. U S A*, **93**, 5325-5328.

ZHANG, J., BÁRDOS, T., MIKECZ, K., FINNEGAN, A. & GLANT, T. (2001). Impaired Fas signaling pathway is involved in defective T cell apoptosis in autoimmune murine arthritis. *J. Immunol.*, **166**, 4981-4986.

ZHANG, P., LIU, B., KANG, S., SEO, M., RHEE, S. & OBEID, L. (1997). Thioredoxin peroxidase is

a novel inhibitor of apoptosis with a mechanism distinct from that of Bcl-2. *J. Biol. Chem.*, **272**, 30615-30618.

ZHU, H., BANNENBERG, G., MOLDEUS, P. & SHERTZER, H. (1994). Oxidation pathways for the intracellular probe 2',7'-dichlorofluorescein. *Arch. Toxicol.*, **68**, 582-587.

ZIMMERMAN, R., CHAN, A. & LEADON, S. (1989). Oxidative damage in murine tumour cells treated *in vitro* by recombinant human tumour necrosis factor. *Cancer Res.*, **49**, 1644-1648.

ZU, H., BANNENBERG, G., MOLDEUS, P. & SHERTZER, H. (1994). Oxidation pathways for intracellular probe 2',7'-dichlorofluoroscein. *Arch. Toxicol.*, **68**, 582-587.

ZUMBANSEN, M. & STOFFEL, W. (1997). Tumour necrosis factor alpha activates NFκB in acid sphingomyelinase-deficient mouse embryonic fibroblasts. *J. Biol. Chem.*, **272**, 10904-10909.

ZUNDEL, W.a.G., A. (1998). Inhibition of the anti-apoptotic PI(3)K/Akt/Bad pathway by stress. *Genes. Dev.*, **12**, 1941-1946.

ZUNDEL, W., SWIERSZ, L. & GIACCIA, A. (2000). Caveolin 1-mediated regulation of receptor tyrosine kinase-associated phospatidylinosi tol 3-kinase activity by ceramide. *Mol. Cell. Biol.*, **20**, 1507-1514.

Chapter 8.0: Appendix.

DESCRIPTION OF RESEARCH PROJECT FOR SUBMISSION TO THE DUDLEY LOCAL RESEARCH ETHICS COMMITTEE

INVITATION TO PARTICIPATE IN A STUDY EXAMINING THE MECHANISMS OF INFLAMMATION IN RHEUMATOID ARTHRITIS

Study Title:
An investigation into aberrant signaling in T cells during rheumatoid inflammation.

We would like to invite you to take part in a study which looks into the mechanisms that cause continuous inflammation and joint damage in rheumatoid arthritis. We would be grateful if you read the information below before you decide whether you wish to take part or not. Your participation is entirely voluntary, and whatever you decide will not affect your current or future follow up and treatment in any way. It is unlikely that you will benefit directly from this study, but the knowledge gained, may help treat rheumatoid arthritis more effectively in the future. The findings from this study will be published in scientific journals with the anonymity of volunteers guaranteed.

Rheumatoid arthritis is characterised by continuous inflammation of the joints, which can cause permanent joint damage if it is not controlled. Inflammation is the result of several mechanisms which occur due to abnormal function of several different cell types. One of the most important cell types is the T cells. In rheumatoid arthritis, these cells are known to behave in an unusual way, in that they live longer than normal T cells and continue to cause inflammation in circumstances that they would normally have died. This study will investigate specifically the mechanisms within the cells that decide whether T cells continue to live or die.

To show whether these mechanisms are normal or abnormal, we need to study them in 25 patients who have rheumatoid arthritis, and compare them with 25 patients who have a different type of arthritis which is not due to inflammation, i.e. osteoarthritis.

You will be asked to give 40mls of blood ONCE ONLY. This is a bit more than double the amount you usually give for routine blood tests in the rheumatology clinic. You will not need to come back specifically for this study, the blood can be taken during your routine visit to the hospital. Some information about you will be recorded, including your age, sex, medical conditions, habits (diet, smoking, alcohol intake), height, weight, and blood pressure. This will not require tests or measurements over and

above those you have when you attend clinic, and the information will be anonymised.

You will be given this information sheet to read. Any questions you may have will be discussed and answered. If you agree to take part, we will ask you to sign the consent form at the bottom of this sheet, in front of a witness. Only then will we collect the blood, assign a number to the blood test tubes (different to your hospital number) and record the information described above in a single sheet with the same number. No other particulars will be recorded, so you will remain anonymous.

If you have any concerns or wish to ask any questions for this study, please contact

Aston University

Content has been removed for copyright reasons

CONSENT FORM

Study Title: An investigation into aberrant signaling in T cells during rheumatoid inflammation.

- I have read and understood this information sheet.
- I have had the opportunity to discuss any questions about the study, and these have been answered to my satisfaction.
- I understand that I am under no obligation to take part in this study.
- I agree to take part in this study as it is outlined above.

Volunteer:

Name..... Signature..... Date:.....

Witness:

Name..... Signature..... Date:.....

ASTON UNIVERSITY

Volunteer bloods from RA/OA patients

Exclusion criteria for RA = those on cytotoxics (MTX or azathioprine), or with reactive arthritis

Patient ID sticker (age ,sex)	
Seropositive ?	Yes / no Details;
CRP or ESR ?	
NSAIDs?	Yes/no Which one ? Dose ?
Prednisolone?	Yes / no
Chloroquine?	Yes / no
Sulphasalazine?	Yes / no
Penicillamine?	Yes / no
Gold?	Yes / no
Comorbidity?	
Smoker ?	Yes/ no

UNIVERSITY OF BIRMINGHAM
School of Medicine
Edgbaston, Birmingham

ASTON UNIVERSITY

DONOR INFORMATION SHEET

Title: RESEARCH INTO THE IMPORTANCE OF ENDOTHELIAL CELLS IN VASCULAR PATHOLOGY

Professor Gerard Nash, Dept. Physiology, University of Birmingham